



EMERGING FRONTIERS IN THE FORMATION OF VIABLE BUT NON-CULTURABLE MICROORGANISMS AND BIOFILMS DURING FOOD PROCESSING

EDITED BY: Yang Deng, Zhenbo Xu, Viduranga Y. Waisundara, Xihong Zhao
and Nguyen Thi Thanh Hanh
PUBLISHED IN: *Frontiers in Microbiology*



frontiers

Frontiers eBook Copyright Statement

The copyright in the text of individual articles in this eBook is the property of their respective authors or their respective institutions or funders. The copyright in graphics and images within each article may be subject to copyright of other parties. In both cases this is subject to a license granted to Frontiers.

The compilation of articles constituting this eBook is the property of Frontiers.

Each article within this eBook, and the eBook itself, are published under the most recent version of the Creative Commons CC-BY licence.

The version current at the date of publication of this eBook is CC-BY 4.0. If the CC-BY licence is updated, the licence granted by Frontiers is automatically updated to the new version.

When exercising any right under the CC-BY licence, Frontiers must be attributed as the original publisher of the article or eBook, as applicable.

Authors have the responsibility of ensuring that any graphics or other materials which are the property of others may be included in the CC-BY licence, but this should be checked before relying on the CC-BY licence to reproduce those materials. Any copyright notices relating to those materials must be complied with.

Copyright and source acknowledgement notices may not be removed and must be displayed in any copy, derivative work or partial copy which includes the elements in question.

All copyright, and all rights therein, are protected by national and international copyright laws. The above represents a summary only. For further information please read Frontiers' Conditions for Website Use and Copyright Statement, and the applicable CC-BY licence.

ISSN 1664-8714

ISBN 978-2-88971-313-4

DOI 10.3389/978-2-88971-313-4

About Frontiers

Frontiers is more than just an open-access publisher of scholarly articles: it is a pioneering approach to the world of academia, radically improving the way scholarly research is managed. The grand vision of Frontiers is a world where all people have an equal opportunity to seek, share and generate knowledge. Frontiers provides immediate and permanent online open access to all its publications, but this alone is not enough to realize our grand goals.

Frontiers Journal Series

The Frontiers Journal Series is a multi-tier and interdisciplinary set of open-access, online journals, promising a paradigm shift from the current review, selection and dissemination processes in academic publishing. All Frontiers journals are driven by researchers for researchers; therefore, they constitute a service to the scholarly community. At the same time, the Frontiers Journal Series operates on a revolutionary invention, the tiered publishing system, initially addressing specific communities of scholars, and gradually climbing up to broader public understanding, thus serving the interests of the lay society, too.

Dedication to Quality

Each Frontiers article is a landmark of the highest quality, thanks to genuinely collaborative interactions between authors and review editors, who include some of the world's best academicians. Research must be certified by peers before entering a stream of knowledge that may eventually reach the public - and shape society; therefore, Frontiers only applies the most rigorous and unbiased reviews.

Frontiers revolutionizes research publishing by freely delivering the most outstanding research, evaluated with no bias from both the academic and social point of view. By applying the most advanced information technologies, Frontiers is catapulting scholarly publishing into a new generation.

What are Frontiers Research Topics?

Frontiers Research Topics are very popular trademarks of the Frontiers Journals Series: they are collections of at least ten articles, all centered on a particular subject. With their unique mix of varied contributions from Original Research to Review Articles, Frontiers Research Topics unify the most influential researchers, the latest key findings and historical advances in a hot research area! Find out more on how to host your own Frontiers Research Topic or contribute to one as an author by contacting the Frontiers Editorial Office: frontiersin.org/about/contact

EMERGING FRONTIERS IN THE FORMATION OF VIABLE BUT NON-CULTURABLE MICROORGANISMS AND BIOFILMS DURING FOOD PROCESSING

Topic Editors:

Yang Deng, Qingdao Agricultural University, China

Zhenbo Xu, University of Tennessee Health Science Center (UTHSC),
United States

Viduranga Y. Waisundara, Australian College of Business and Technology,
Sri Lanka

Xihong Zhao, Wuhan Institute of Technology, China

Nguyen Thi Thanh Hanh, Seoul National University, South Korea

Citation: Deng, Y., Xu, Z., Waisundara, V. Y., Zhao, X., Hanh, N. T. T., eds. (2021).
Emerging Frontiers in the Formation of Viable but Non-Culturable
Microorganisms and Biofilms During Food Processing. Lausanne: Frontiers Media
SA. doi: 10.3389/978-2-88971-313-4

Table of Contents

- 06 Editorial: Emerging Frontiers in the Formation of Viable but Non-culturable Microorganisms and Biofilms During Food Processing**
Zhenbo Xu, Yang Deng, Xihong Zhao, Nguyen Thi Thanh Hanh and Viduranga Y. Waisundara
- 08 Comparative Evaluation of Different Sanitizers Against *Listeria monocytogenes* Biofilms on Major Food-Contact Surfaces**
Zi Hua, Ahmed Mahmoud Korany, Saadia Helmy El-Shinawy and Mei-Jun Zhu
- 16 Graphene-Based Steganographic Aptasensor for Information Computing and Monitoring Toxins of Biofilm in Food**
Qi Wang, Qingli Yang and Wei Wu
- 27 Stress Response of *Vibrio parahaemolyticus* and *Listeria monocytogenes* Biofilms to Different Modified Atmospheres**
Hui Qian, Wei Li, Linxia Guo, Ling Tan, Haiquan Liu, Jingjing Wang, Yingjie Pan and Yong Zhao
- 42 Progress on Structured Biosensors for Monitoring Aflatoxin B1 From Biofilms: A Review**
Qi Wang, Qingli Yang and Wei Wu
- 57 Detection and Quantification Methods for Viable but Non-culturable (VBNC) Cells in Process Wash Water of Fresh-Cut Produce: Industrial Validation**
Pilar Truchado, Maria I. Gil, Mar Larrosa and Ana Allende
- 67 Stress Tolerance of Yeasts Dominating Reverse Osmosis Membranes for Whey Water Treatment**
Eirini Vitzilaiou, Stina D. Aunsbjerg, N. A. Mahyudin and Susanne Knøchel
- 83 Insights Into the Role of Extracellular DNA and Extracellular Proteins in Biofilm Formation of *Vibrio parahaemolyticus***
Wei Li, Jing Jing Wang, Hui Qian, Ling Tan, Zhaohuan Zhang, Haiquan Liu, Yingjie Pan and Yong Zhao
- 97 Formation and Control of the Viable but Non-culturable State of Foodborne Pathogen *Escherichia coli* O157:H7**
Yanmei Li, Teng-Yi Huang, Congxiu Ye, Ling Chen, Yi Liang, Kan Wang and Junyan Liu
- 106 The Characterization of Two-Component System *PmrA/PmrB* in *Cronobacter sakazakii***
Jingjing Hua, Xiangyin Jia, Liang Zhang and Yanyan Li
- 116 Isolation of Antibacterial, Nitrosylmyoglobin Forming Lactic Acid Bacteria and Their Potential Use in Meat Processing**
Yinglian Zhu and Qingli Yang
- 128 Reduction, Prevention, and Control of *Salmonella enterica* Viable but Non-culturable Cells in Flour Food**
Yanmei Li, Tengyi Huang, Caiying Bai, Jie Fu, Ling Chen, Yi Liang, Kan Wang, Jun Liu, Xiangjun Gong and Junyan Liu

- 139 ***Flagellar Motility is Critical for Salmonella enterica Serovar Typhimurium Biofilm Development***
Feiying Wang, Le Deng, Fangfang Huang, Zefeng Wang, Qiujuan Lu and Chenran Xu
- 151 ***Development and Application of a Simple “Easy To Operate” Propidium Monoazide-Crossing Priming Amplification on Detection of Viable and Viable But Non-culturable Cells of O157 Escherichia coli***
Wenqu Zhou, Kan Wang, Wei Hong, Caiying Bai, Ling Chen, Xin Fu, Tengyi Huang and Junyan Liu
- 158 ***Effect of Environmental Conditions on the Formation of the Viable but Nonculturable State of Pediococcus acidilactici BM-PA17927 and Its Control and Detection in Food System***
Yanmei Li, Teng-Yi Huang, Yuzhu Mao, Yanni Chen, Fan Shi, Ruixin Peng, Jinxuan Chen, Caiying Bai, Ling Chen, Kan Wang and Junyan Liu
- 167 ***Distinct Roles for Bacterial and Fungal Communities During the Curing of Vanilla***
Fei Xu, Yonggan Chen, Yingying Cai, Fenglin Gu and Kejing An
- 176 ***Antibacterial Activity and Mechanism of Lacidophilin From Lactobacillus pentosus Against Staphylococcus aureus and Escherichia coli***
Yinglian Zhu and Shuang Zhang
- 187 ***Study on the Viable but Non-culturable (VBNC) State Formation of Staphylococcus aureus and Its Control in Food System***
Yanmei Li, Teng-Yi Huang, Yuzhu Mao, Yanni Chen, Fan Shi, Ruixin Peng, Jinxuan Chen, Lei Yuan, Caiying Bai, Ling Chen, Kan Wang and Junyan Liu
- 196 ***Inactivation Efficacy of 405 nm LED Against Cronobacter sakazakii Biofilm***
Yixiao Huang, Quanwei Pei, Ruisha Deng, Xiaoying Zheng, Jialu Guo, Du Guo, Yanpeng Yang, Sen Liang and Chao Shi
- 208 ***First Report on the Rapid Detection and Identification of Methicillin-Resistant Staphylococcus aureus (MRSA) in Viable but Non-culturable (VBNC) Under Food Storage Conditions***
Aifen Ou, Kan Wang, Yanxiong Mao, Lei Yuan, Yanrui Ye, Ling Chen, Yimin Zou and Tengyi Huang
- 215 ***Inhibition of Biofilm Formation and Related Gene Expression of Listeria monocytogenes in Response to Four Natural Antimicrobial Compounds and Sodium Hypochlorite***
Yunge Liu, Lina Wu, Jina Han, Pengcheng Dong, Xin Luo, Yimin Zhang and Lixian Zhu
- 227 ***Direct Detection of Viable but Non-culturable (VBNC) Salmonella in Real Food System by a Rapid and Accurate PMA-CPA Technique***
Aifen Ou, Kan Wang, Yanrui Ye, Ling Chen, Xiangjun Gong, Lu Qian and Junyan Liu
- 234 ***Pathogenic and Virulence Factor Detection on Viable but Non-culturable Methicillin-Resistant Staphylococcus aureus***
Hua Jiang, Kan Wang, Muxia Yan, Qian Ye, Xiaojing Lin, Ling Chen, Yanrui Ye, Li Zhang, Junyan Liu and Tengyi Huang

242 Pressure and Temperature Combined With Microbial Supernatant Effectively Inactivate *Bacillus subtilis* Spores

Jingyu Li, Yaxin Sun, Fang Chen, Xiaosong Hu and Li Dong

253 Development of a Direct and Rapid Detection Method for Viable but Non-culturable State of *Pediococcus acidilactici*

Yu Guan, Kan Wang, Yang Zeng, Yanrui Ye, Ling Chen and Tengyi Huang



Editorial: Emerging Frontiers in the Formation of Viable but Non-culturable Microorganisms and Biofilms During Food Processing

Zhenbo Xu^{1,2*}, Yang Deng³, Xihong Zhao⁴, Nguyen Thi Thanh Hanh⁵ and Viduranga Y. Waisundara⁶

¹ Guangdong Key Laboratory for Green Processing of Natural Products and Product Safety, School of Food Science and Engineering, Engineering Research Center of Starch and Vegetable Protein Processing Ministry of Education, South China University of Technology, Guangzhou, China, ² Department of Civil and Environmental Engineering, University of Maryland, College Park, MD, United States, ³ College of Food Science and Engineering, Qingdao Agricultural University, Qingdao, China, ⁴ Research Center for Environmental Ecology and Engineering, School of Environmental Ecology and Biological Engineering, Wuhan Institute of Technology, Wuhan, China, ⁵ Institutes of Green Bio Sciences and Technology, Seoul National University, Pyeongchang, South Korea, ⁶ Australian College of Business and Technology, Kandy, Sri Lanka

Keywords: viable but nonculturable state, biofilm, food microbiology, food safety and control, formation

Editorial on the Research Topic

Emerging Frontiers in the Formation of Viable but Non-culturable Microorganisms and Biofilms During Food Processing

This Research Topic, led by myself and Dr. Yang Deng, together with an editorial team including Dr. Xihong Zhao, Dr. Nguyen Thi Thanh Hanh, and Dr. Viduranga Y. Waisundara, contains a total of 24 excellent manuscripts. As the background of this topic was concerned, a viable but non-culturable (VBNC) state, a unique state in which a number of bacteria respond to adverse circumstances, was first discovered in 1982 (Xu et al., 1982), and has been extensively studied in bacteria, characterized by an inability of the cells to grow on culture media, even though they are still viable and maintain a detectable metabolic activity. Various environmental factors including temperature, the physiological age of the culture, salinity, the oxygen content, light, and ventilation can induce the entry of bacterial cells into a VBNC state.

All submitting authors had made an important contribution to this Research Topic. Exceptionally and importantly, as far as our knowledge can reach, this is the first time that researchers have validated the “Control” of the VBNC state, which represents a milestone and breakthrough in the field of VBNC. In a few articles in this Research Topic, relevant studies had been conducted on *Staphylococcus aureus*, *Escherichia coli*, *Salmonella*, and *Pediococcus acidilactici*. First, investigating the key conditions of the VBNC formation of the above organisms, the authors further based their research on key conditions to prevent, reduce, or even eliminate the VBNC state formation within such microbes. The VBNC state has been a leading concern in the field of microbiology, as a major methodology microbiologists have been employing for decades to study microbes is culturing. Via streaking on a medium plate and further obtaining colonies, microbiologists are thus able to conduct a large variety of experiments on microbes. However, one important issue raised here is that the culturing methodology relies on the formation of colonies which is designated as culturability, and once lost, it is incapable of obtaining colonies from medium plates. VBNC is a state when microbial cells are not culturable but still viable and potentially capable of resuscitating to being culturable. As a large proportion of microbiological routine detections are based on the culturing methodology, capability in acquisition of colonies,

OPEN ACCESS

Edited by:

Julio Parra-Flores,
University of the Bío Bío, Chile

Reviewed by:

Ariadna Cruz-Córdova,
Federico Gómez Children's
Hospital, Mexico

*Correspondence:

Zhenbo Xu
zhenbo.xu@hotmail.com

Specialty section:

This article was submitted to
Food Microbiology,
a section of the journal
Frontiers in Microbiology

Received: 16 June 2021

Accepted: 30 June 2021

Published: 08 September 2021

Citation:

Xu Z, Deng Y, Zhao X, Hanh NTT and
Waisundara VY (2021) Editorial:
Emerging Frontiers in the Formation of
Viable but Non-culturable
Microorganisms and Biofilms During
Food Processing.
Front. Microbiol. 12:726348.
doi: 10.3389/fmicb.2021.726348

number, and type of colonies, have determined the test results as positive and negative. As a critical gap between culturable (positive) and dead (negative), the VBNC state is an exceptionally important and eventually unavoidable topic for microbiologists, but also commonly underestimated and even controversial. Just lately in 2021, an opinion article entitled “Viable but non-culturable cells’ are dead,” had been published (Song and Wood, 2021b). Not surprisingly, a few opposing comments/opinions had been posed subsequently, as firstly a correspondence entitled “How dead is dead? Viable but non-culturable vs. persister cells” by Kirschner et al. (2021), with a later response from the original authors entitled “Waiting for Godot: response to ‘How dead is dead? Viable but non-culturable vs. persister cells’” (Song and Wood, 2021c); secondly another correspondence entitled “What do we mean by viability in terms of ‘viable but non-culturable’ cells?” by Mu et al. (2021), with a later response from the original authors entitled “Mostly dead and all dead: response to ‘what do we mean by viability in terms of ‘viable but non-culturable cells’” (Song and Wood, 2021a). Definitely, VBNC cells are not dead. However, seen from the aforementioned opinions, the VBNC field has drawn wide attention and great interest from microbiologists. Our opinions are as follows. Firstly, what should the definitions of VBNC and persister cells be? The term VBNC has perfectly described a specific microbial cellular state when a cell is not culturable but still viable which is metabolically alive and has potential to resuscitate back to culturable. We strongly agree with Kirschner et al. (2021) on the definition of VBNC, which was firstly proposed by Oliver (2010), as “A bacterial cell in the VBNC state may be defined as one which fails to grow at the routine bacteriological cultivation conditions under which it would normally grow, but which in fact is alive and has still metabolic activity.” Song et al. had argued that “By inactivating their ribosomes, persister cells sleep through stress and resuscitate once (i) the stress is removed, (ii) nutrients are presented, and (iii) ribosome content reaches a threshold... it is the persister (always-viable) cell population that revives, rather

than the cell husks, which are dead,” however, firstly the authors had not provided the definition of persister cells (or they had, but assumably it is similar to VBNC) and then secondly why not use “VBNC” as this term literally and perfectly describes the cellular state. Secondly, Song and Wood (2021a,b,c), had provided considerable evidence that the determination of VBNC had been conducted in an incorrect way which we strongly agree with. Unfortunately, a large number of microbiologists have still been following such procedure to study VBNC cells, for which the opinion article of Song et al. is very helpful. Remarkably, it is noteworthy to point out that, in this Research Topic, the idea and progress in control of VBNC, including prevention, reduction, or even elimination of VBNC cells based on changes in the critical conditions of VBNC formation, contains profound importance and particular interests.

As concluded, the articles in this Research Topic have made contributions to the relevant field, however, a few opinions have been proposed as controversial in this topic. It should not be surprising as in the VBNC field, more studies had been conducted and previously unclear questions had been better documented. In contrast, seen from the accepted articles in this Research Topic and several opinions articles in the relevant field, the VBNC field has drawn wide attention and great interest from microbiologists. Based on the intrinsic importance of the VBNC state, confusion in the definitions between VBNC and persister cells, as well as the standardization of accurate determination of VBNC cells, we strongly suggest an urgent need for a comprehensive article from microbiologists with expertise in VBNC, to answer essential questions such as “what is the definition of VBNC and what is the difference between VBNC and persister cells” and “how to standardly and accurately determine VBNC cells.”

AUTHOR CONTRIBUTIONS

ZX wrote the editorial. All authors approved the manuscript.

REFERENCES

- Kirschner, A. K. T., Vierheilg, J., Flemming, H. C., Wingender, J., and Farnleitner, A. H. (2021). How dead is dead? Viable but non-culturable versus persister cells. *Environ. Microbiol. Rep.* 13, 243–245. doi: 10.1111/1758-2229.12949
- Mu, D. S., Du, Z. J., Chen, J., Austin, B., and Zhang, X. H. (2021). What do we mean by viability in terms of ‘viable but non-culturable’ cells? *Environ. Microbiol. Rep.* 13, 248–252. doi: 10.1111/1758-2229.12953
- Oliver, J. D. (2010). Recent findings on the viable but nonculturable state in pathogenic bacteria. *FEMS Microbiol. Rev.* 34, 415–425. doi: 10.1111/j.1574-6976.2009.00200.x
- Song, S., and Wood, T. K. (2021a). Mostly dead and all dead: response to ‘what do we mean by viability in terms of ‘viable but non-culturable cells’’. *Environ. Microbiol. Rep.* 13, 253–254. doi: 10.1111/1758-2229.12952
- Song, S., and Wood, T. K. (2021b). ‘Viable but non-culturable cells’ are dead. *Environ. Microbiol.* 23, 2335–2338. doi: 10.1111/1462-2920.15463
- Song, S., and Wood, T. K. (2021c). Waiting for Godot: response to ‘How dead is dead? Viable but non-culturable versus persister cells’. *Environ. Microbiol. Rep.* 13, 246–247. doi: 10.1111/1758-2229.12951
- Xu, H.-S., Roberts, N., Singleton, F. L., Attwell, R. W., Grimes, D. J., and Colwell, R. R. (1982). Survival and viability of nonculturable *Escherichia coli* and *Vibrio*

cholerae in the estuarine and marine environment. *Microb. Ecol.* 8, 313–323. doi: 10.1007/BF02010671

Conflict of Interest: The authors declare that the research was conducted in the absence of any commercial or financial relationships that could be construed as a potential conflict of interest.

Publisher’s Note: All claims expressed in this article are solely those of the authors and do not necessarily represent those of their affiliated organizations, or those of the publisher, the editors and the reviewers. Any product that may be evaluated in this article, or claim that may be made by its manufacturer, is not guaranteed or endorsed by the publisher.

Copyright © 2021 Xu, Deng, Zhao, Hanh and Waisundara. This is an open-access article distributed under the terms of the Creative Commons Attribution License (CC BY). The use, distribution or reproduction in other forums is permitted, provided the original author(s) and the copyright owner(s) are credited and that the original publication in this journal is cited, in accordance with accepted academic practice. No use, distribution or reproduction is permitted which does not comply with these terms.



Comparative Evaluation of Different Sanitizers Against *Listeria monocytogenes* Biofilms on Major Food-Contact Surfaces

Zi Hua^{1†}, Ahmed Mahmoud Korany^{1,2†}, Saadia Helmy El-Shinawy² and Mei-Jun Zhu^{*†}

¹School of Food Science, Washington State University, Pullman, WA, United States, ²Food Hygiene and Control Department, Faculty of Veterinary Medicine, Beni-Suef University, Beni Suef, Egypt

OPEN ACCESS

Edited by:

Viduranga Y. Waisundara,
Australian College of Business and
Technology, Sri Lanka

Reviewed by:

Kihwan Park,
Chung-Ang University,
South Korea
Xuetong Fan,
United States Department of
Agriculture, United States

*Correspondence:

Mei-Jun Zhu
meijun.zhu@wsu.edu

[†]These authors have contributed
equally to this work

Specialty section:

This article was submitted to
Food Microbiology,
a section of the journal
Frontiers in Microbiology

Received: 22 July 2019

Accepted: 14 October 2019

Published: 07 November 2019

Citation:

Hua Z, Korany AM, El-Shinawy SH
and Zhu M-J (2019) Comparative
Evaluation of Different Sanitizers
Against *Listeria monocytogenes*
Biofilms on Major
Food-Contact Surfaces.
Front. Microbiol. 10:2462.
doi: 10.3389/fmicb.2019.02462

Contaminated food-contact surfaces are recognized as the primary reason for recent *L. monocytogenes* outbreaks in caramel apples and cantaloupes, highlighting the significance of cleaning and sanitizing food-contact surfaces to ensure microbial safety of fresh produce. This study evaluated efficacies of four commonly used chemical sanitizers at practical concentrations against *L. monocytogenes* biofilms on major food-contact surfaces including stainless steel, low-density polyethylene (LDPE), polyvinyl chloride (PVC), polyester (PET), and rubber. In general, efficacies against *L. monocytogenes* biofilms were enhanced by increasing concentrations of quaternary ammonium compound (QAC), chlorine, and chlorine dioxide, or extending treating time from 1 to 5 min. The 5-min treatments of 400 ppm QAC, 5.0 ppm chlorine dioxide, and 200 ppm chlorine reduced 3.0–3.7, 2.4–2.7, and 2.6–3.8 log₁₀ CFU/coupon *L. monocytogenes* biofilms depending on surfaces. Peroxyacetic acid (PAA) at 160 and 200 ppm showed similar antimicrobial efficacies against biofilms either at 1- or 5-min contact. The 5-min treatment of 200 ppm PAA caused 4.0–4.5 log₁₀ CFU/coupon reduction of *L. monocytogenes* biofilms on tested surfaces. Surface material had more impact on the efficacies of QAC and chlorine, less influence on those of PAA and chlorine dioxide, while organic matter soiling impaired sanitizer efficacies against *L. monocytogenes* biofilms independent of food-contact surfaces. Data from this study provide practical guidance for effective disinfection of food-contact surfaces in food processing/packing facilities.

Keywords: biofilm, *L. monocytogenes*, sanitizers, food-contact surfaces, organic matter, peroxyacetic acid

INTRODUCTION

As a critical foodborne pathogen, *Listeria monocytogenes* causes approximately 1,600 cases of infection and 260 cases of death annually in the United States (Scallan et al., 2011). It has been implicated in multi-state outbreaks on fresh produce including cantaloupes (CDC, 2012), prepackaged caramel apples (CDC, 2015a), bean sprouts (CDC, 2015b), frozen vegetables (CDC, 2016a), and packaged salads (CDC, 2016b) since 2011. Contaminated food-contact surfaces, packing lines, and environment are incriminated as the primary reasons linked to *L. monocytogenes* outbreaks in fresh produce (McCollum et al., 2013; Angelo et al., 2017).

Therefore, it is vital to sanitize food-contact surfaces along produce production lines effectively to ensure microbial safety of fresh produce.

Stainless steel (SS) and plastics are preferably used in the fresh produce industry due to their anti-fouling ability (FDA, 2008). SS, a corrosion-resistant metal, is an excellent material for food processing/packing equipment and extensively used in food industries such as fresh apple packing facilities (Jellesen et al., 2006). A conveyor belt, one of the most prevalent food-contact surfaces, directly contacts fresh produce and transports it to further processing or packing during post-harvest handling. Polyvinyl chloride (PVC), low-density polyethylene (LDPE), and rubber are FDA-approved food-contact substances that are extensively used as important components of conveyor belts (FDA, 2017). The conveyor belts around the optical sorting lines have been determined to be the major contamination sites in a minimally processed vegetable plant (Meireles et al., 2017). The brush bed, mostly made of polyester (PET), is an important and essential processing tool of the packing lines of fresh apples and other fruits. The contaminated brush-bed spray bar system was implicated in a recent caramel apple *L. monocytogenes* outbreak (Angelo et al., 2017). *L. monocytogenes* form biofilms on SS, PVC, LDPE, PET, and rubber surfaces (Krysinski et al., 1992; Beresford et al., 2001; Takahashi et al., 2010; Doijad et al., 2015; Papaioannou et al., 2018), exerting enhanced resistances to acid and sanitizer treatments (Ibusquiza et al., 2011; van der Veen and Abee, 2011), which makes routine disinfection in a food processing facility more difficult.

Food-contact surfaces are cleaned and disinfected daily with different chemical sanitizers in fresh produce processing plants and apple packing facilities. Peroxyacetic acid (PAA) is an environment-friendly sanitizer that decomposes and produces no harmful by-product (Dell'Erba et al., 2007). Quaternary ammonium compound (QAC) and chlorine are the most commonly used sanitizers for surface disinfections (Robbins et al., 2005; Olszewska et al., 2016; Dhowlaghar et al., 2018). Chlorine dioxide is considered as an alternative for chlorine due to its high oxidizing capacity (~2.5 times higher than that of chlorine) (Benarde et al., 1965). The bactericidal effects of the aforementioned sanitizers against *L. monocytogenes* biofilms on polystyrene surfaces were compromised in the presence of organic matter or when biofilm was aged (Korany et al., 2018). Different food-contact surfaces have unique physicochemical properties and hydrophobicity, which may provide unique harbor sites for *L. monocytogenes* during sanitizer intervention. Therefore, the objective of this study was to evaluate antimicrobial efficacies of four FDA-approved sanitizers against aged *L. monocytogenes* biofilms on major food-contact surfaces in the absence or presence of organic matter.

MATERIALS AND METHODS

L. monocytogenes Strains and Cocktail Preparation

Listeria monocytogenes strain NRRL B-33069, NRRL B-57618, NRRL B-33006, NRRL B-33466, NRRL B-33071, and NRRL

B-33385 were obtained from USDA-ARS culture collection of National Center (NRRL) for Agricultural Utilization Research (Peoria, IL, United States) and were stored at -80°C in Trypticase Soy Broth with 0.6% Yeast Extract (TSBYE, Fisher Scientific, Fair Lawn, NJ, United States) and 20% (v/v) glycerol. Each frozen culture was activated in TSBYE at $35 \pm 2^{\circ}\text{C}$ for 24 ± 2 h statically, then sub-cultured in TSBYE for additional 24 ± 2 h at $35 \pm 2^{\circ}\text{C}$. The six-strain *L. monocytogenes* cocktail was prepared by mixing equal volumes of each activated strain, then centrifuged at $8,000 \times g$ for 5 min at room temperature (22°C , RT). The resulting pellet was re-suspended in Modified Welshimer's Broth (MWB, HiMedia, West Chester, PA, United States) to have a final population level of $\sim 10^8$ CFU/ml.

Surface Selection, Preparation, and Conditioning

The SS (AISI 316, No. 4 brushed finish) was obtained from the Washington State University Engineering Shops (Pullman, WA, United States). PVC, LDPE, and PET sheets were purchased from Interstate Plastics (Sacramento, CA, United States), and silicone rubber sheet was purchased from Rubber Sheet Warehouse (Los Angeles, CA, United States). All surface materials were cut into coupons of 15 mm \times 7.5 mm at the Washington State University Engineering Shops.

To clean coupons, the prepared surface coupons were immersed in 100% methanol (Fisher Scientific) for 1 h, rinsed with sterile water three times, then immersed for 1 h in 70% ethanol (Fisher Scientific). The treated coupons were air dried under a biosafety cabinet overnight, which were ready for biofilm growth. To condition surface coupon with organic matter, the above cleaned surface coupons were immersed in 1:10 diluted apple juice or milk for 1 h at RT (Brown et al., 2014). After removing conditioning solution, coupons were air dried for 1 h at RT under a biosafety cabinet.

L. monocytogenes Biofilm Formation

The above prepared coupons were subjected to a 15-min UV treatment in the biosafety hood to surface decontamination before inoculation with 2.0 ml of *L. monocytogenes* cocktail suspension in MWB ($\sim 10^8$ CFU/ml). The inoculated coupons in 24-well plates were incubated statically at RT for 7 days to grow *L. monocytogenes* biofilms without agitation (Abeyesundara et al., 2018).

Sanitizer Intervention Against *L. monocytogenes* Biofilms

Bioside HS (EnviroTech, Modesto, CA, United States) containing 15% PAA was used to prepare 160 and 200 ppm PAA solutions using sterile water. STOPIT (Pace International, Wapato, WA, United States) was diluted with sterile water to prepare 200 and 400 ppm QAC solutions. Chlorine solutions at 100 and 200 ppm were made from Accu-Tab (Pace International, Wapato, WA, United States), while 2.5 and 5.0 ppm chlorine dioxide solutions were generated on-site using chlorine dioxide generator donated by Pace International (Wapato, WA, United States). Concentration of PAA was verified using a AquaPhoenix Preacetic Acid test kit (Hanover, PA, United States), levels of

QAC and chlorine were confirmed by the QAC and Chlorine test kits from LaMotte (Chestertown, MD, United States), and the concentration of chlorine dioxide solutions were measured by a HACH Chlorine Dioxide test kit (Loveland, CO, United States).

To evaluate the antimicrobial efficacy of sanitizers, 7-day-old *L. monocytogenes* biofilms on each surface coupon were washed with 2.0 ml of sterile phosphate buffered saline (PBS) three times and then immersed in 2.0 ml of each sanitizer solution for 1 or 5 min at RT. Coupons were first rinsed with 2.0 ml of Dey-Engley Neutralizing Broth (Oxoid, United States), then 2.0 ml sterile PBS immediately after sanitizer treatment. Four replicates were used for each surface material and sanitizer treatment, and triple independent experiments were conducted for each treatment combination.

Biofilm Detachment and Enumeration

To detach and enumerate the *L. monocytogenes* cells in biofilm on the above treated coupons, the coupon in the respective well was transferred to 2-ml microtube containing 1.0 ml of sterile PBS and 3~4 glass beads. The tubes containing coupons were vigorously vortexed for 2 min using a benchtop mixer at the maximal speed. The detached bacterial suspension was 10-fold serially diluted with sterile PBS, and appropriate dilution was plated on TSAYE plates in duplicate. The plates were incubated at $35 \pm 2^\circ\text{C}$ for 48 h before enumeration.

Statistical Analysis

Data were analyzed by uncorrected Fisher's Least Significant Difference (LSD) to determine significant difference among groups at $p \leq 0.05$ using Prism (Version 7.0, San Diego, CA, United States).

Each experiment was repeated three times independently. Data were presented as an average from three independent studies and mean \pm standard error mean (SEM) was reported.

RESULTS

Efficacy of Quaternary Ammonium Compound Against *L. monocytogenes* Biofilms on Food-Contact Surfaces

In general, increasing the QAC concentration from 200 to 400 ppm improved its efficacy against *L. monocytogenes* biofilms on different food-contact surfaces except LDPE surface for both 1- and 5-min exposures (Figure 1). A 5-min exposure of QAC at 200 or 400 ppm showed a similar efficacy against *L. monocytogenes* biofilms on SS coupons (Figure 1A). Except for rubber surface, the efficacy of QAC against *L. monocytogenes* biofilms on different surfaces was enhanced when exposure time increased from 1 to 5 min (Figure 1). Among all surfaces, QAC at 5 min exposure was the most effective against *L. monocytogenes* biofilms on SS (Figure 1A), least effective against *L. monocytogenes* biofilms on rubber (Figure 1E), while exhibiting a comparable efficacy against *L. monocytogenes* biofilms on LDPE and PET (Figures 1B–D). For *L. monocytogenes* biofilms on PVC surface, the 5-min exposure of 400 ppm QAC showed a similar efficacy as those of LDPE and PET; however, 200 ppm QAC for 5 min of exposure was less effective on PVC surface than those of LDPE and PET (Figures 1B–D). QAC at the FDA-approved concentration of 400 ppm for 5 min caused 3.7, 3.2, 3.7, 3.6, and 3.0 \log_{10} CFU/coupon reductions of *L. monocytogenes* biofilms on SS, LDPE, PVC, PET, and rubber surface, respectively (Figure 1).

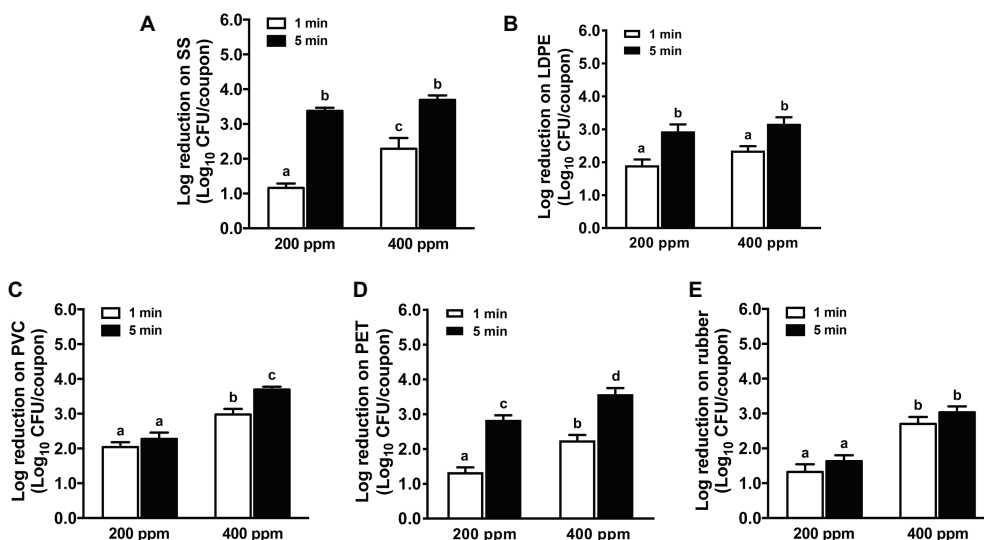


FIGURE 1 | Antimicrobial efficacy of quaternary ammonium compound (QAC) against *L. monocytogenes* biofilms on food-contact surfaces. (A) Stainless steel (SS); (B) low-density polyethylene (LDPE); (C) polyvinyl chloride (PVC); (D) polyester (PET); (E) rubber. The 7-day-old biofilms on different surface coupons (15 mm \times 7.5 mm) were treated with 200 or 400 ppm QAC for 1 or 5 min at 22°C . The surviving bacteria were shown as means \pm SEMs, $n = 3$. ^{a-d}Bars topped with the different letters are significantly different at $p \leq 0.05$.

Efficacies of Chlorine and Chlorine Dioxide Against *L. monocytogenes* Biofilms on Food-Contact Surfaces

Chlorine dioxide solution at 2.5 ppm exhibited a limited efficacy against *L. monocytogenes* biofilms on all surfaces tested; 1-min treatments only reduced ~1.1, 0.6, 0.9, 1.1, and 0.9 log₁₀ CFU/coupon *L. monocytogenes* biofilms on SS, LDPE, PVC, PET, and rubber surfaces, respectively (Figure 2). Though the efficacy of chlorine dioxide was enhanced with increased concentration and contact time, it displayed limited potency to inactivate *L. monocytogenes* biofilms on food-contact surfaces. A 5-min treatment of 5.0 ppm chlorine dioxide caused similar bactericidal efficacy against *L. monocytogenes* biofilms on all surfaces with 2.4–2.7 log₁₀ CFU/coupon reductions (Figure 2).

The efficacy of chlorine against *L. monocytogenes* biofilms on the tested surfaces was enhanced at increased concentration and extended contact time except LDPE surface (Figure 3). A 1-min treatment of 100 ppm chlorine showed a similar efficacy against *L. monocytogenes* biofilms as 1-min exposure of 200 ppm QAC (Figure 1) and was more effective than 1-min treatment of 2.5 ppm chlorine dioxide (Figure 2), causing 1.0–2.0 log₁₀ CFU/coupon reductions of biofilms on all surfaces tested. Chlorine at 200 ppm for 5.0-min exposure caused 3.8, 2.7, 3.3, 3.6, and 3.0 log₁₀ CFU/coupon reductions of *L. monocytogenes* biofilms on SS, LDPE, PVC, PET, and rubber surfaces, respectively (Figure 3).

Efficacy of Peroxyacetic Acid Against *L. monocytogenes* Biofilms on Food-Contact Surfaces

Among all selected sanitizers, PAA was the most effective against *L. monocytogenes* biofilms on all food-contact surfaces

(Figure 4). One min treatment of 160 ppm PAA reduced ~4.3, 3.5, 3.8, 4.1, and 3.7 log₁₀ CFU/coupon *L. monocytogenes* biofilms on SS, LDPE, PVC, PET, and rubber surfaces, respectively (Figure 4). In general, the bactericidal effects of PAA against *L. monocytogenes* biofilms on all surfaces was not improved when the PAA concentration increased from 160 to 200 ppm or when the treatment time increased from 1 to 5 min (Figure 4). The 5-min treatment of 200 ppm PAA caused 4.5, 4.0, 4.4, 4.3, and 4.4 log₁₀ CFU/coupon reductions of *L. monocytogenes* biofilms on SS, PET, PVC, LDPE, and rubber, respectively (Figure 4).

Effects of Organic Matter on Sanitizer's Efficacy

The anti-*Listeria* efficacies of all sanitizers were compromised by organic matter regardless of surfaces tested; food residues from apple juice or milk comparably impacted QAC efficacy (Figure 5). Soiling has a greater influence on the antimicrobial efficacy of QAC against biofilms on SS and rubber than those on LDPE, PET, and PVC (Figure 5A). Among all tested surfaces, the anti-*Listeria* efficacy of chlorine on SS is the most impacted by organic matter. Chlorine at 200 ppm and 5-min contact time showed a similar anti-*Listeria* efficacy on soiled SS, LDPE and rubber surfaces regardless of organic matter type (Figure 5B). The bactericidal effect of chlorine dioxide against *L. monocytogenes* biofilms was compromised by organic matter regardless of surface materials or food residue source. Chlorine dioxide at 5.0 ppm for 5 min caused 1.0–2.0 log₁₀ CFU/coupon reduction depending on surface material (Figure 5C). Though the PAA efficacy against *L. monocytogenes* biofilms on all surfaces was impaired by organic soiling as much as other sanitizers, it was still the most effective sanitizer, which caused 3.0–3.7 log₁₀ CFU/coupon reductions of *L. monocytogenes* biofilms on different surfaces (Figure 5D).

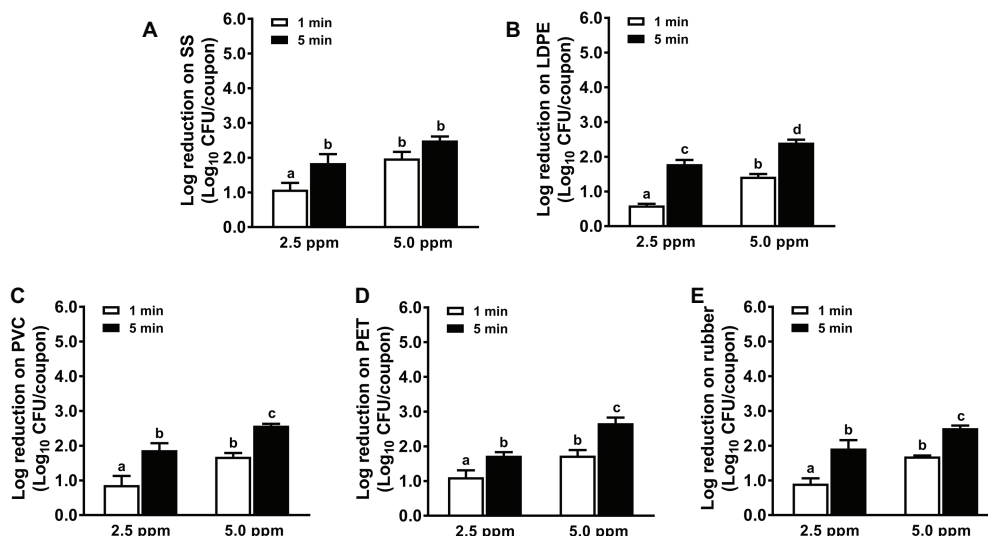


FIGURE 2 | Antimicrobial efficacy of chlorine dioxide against *L. monocytogenes* biofilms on food-contact surfaces. (A) Stainless steel (SS); (B) low-density polyethylene (LDPE); (C) polyvinyl chloride (PVC); (D) polyester (PET); (E) rubber. The 7-day-old biofilms on different surface coupons (15 mm × 7.5 mm) were treated with 2.5 or 5.0 ppm chlorine dioxide solution for 1 or 5 min at 22°C. The remaining bacteria post-sanitizer treatment were shown as means ± SEMs, *n* = 3. ^{a-d}Bars topped with the different letters are significantly different at *p* ≤ 0.05.

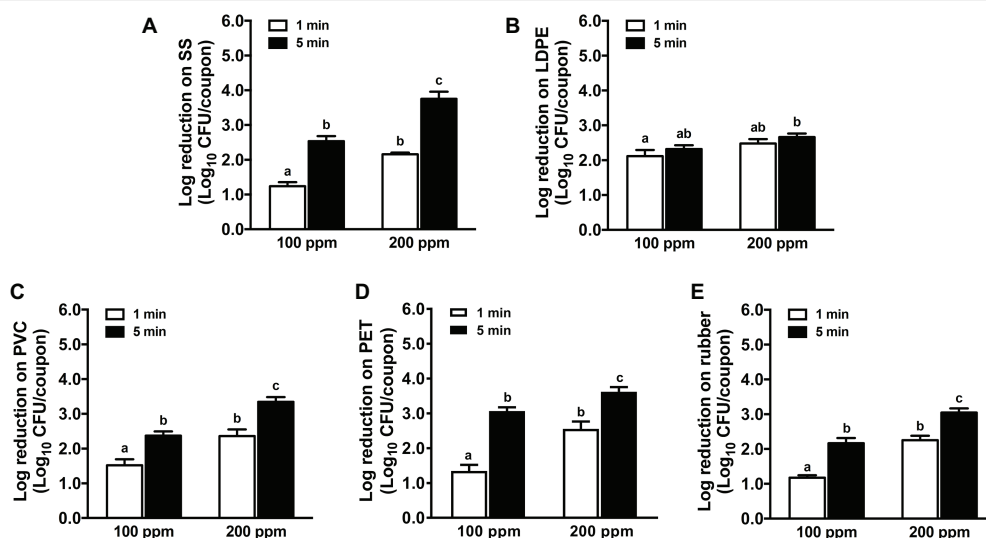


FIGURE 3 | Antimicrobial efficacy of chlorine against *L. monocytogenes* biofilms on food-contact surfaces. (A) Stainless steel (SS); (B) low-density polyethylene (LDPE); (C) polyvinyl chloride (PVC); (D) polyester (PET); (E) rubber. The 7-day-old biofilms on different surface coupons (15 mm × 7.5 mm) were treated with 100 or 200 ppm chlorine solution for 1 or 5 min at 22°C. The survivors post-chlorine treatment were enumerated and shown as means ± SEMs, $n = 3$. ^{a-c}Bars topped with the different letters are significantly different at $p \leq 0.05$.

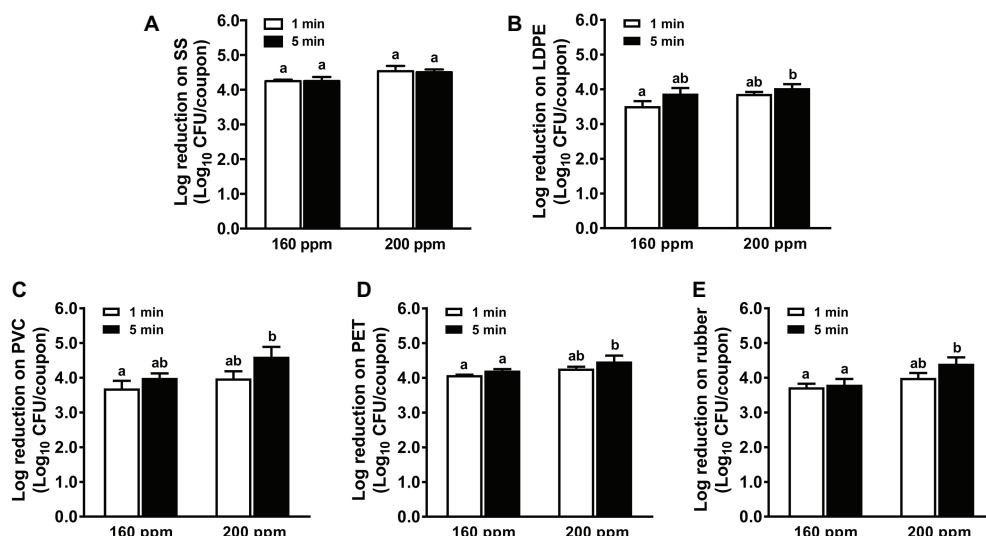


FIGURE 4 | Antimicrobial efficacy of peroxyacetic acid (PAA) against *L. monocytogenes* biofilms on food-contact surfaces. (A) Stainless steel (SS); (B) low-density polyethylene (LDPE); (C) polyvinyl chloride (PVC); (D) polyester (PET); (E) rubber. The 7-day-old biofilms on different surface coupons (15 mm × 7.5 mm) were treated with 160 or 200 ppm PAA for 1 or 5 min at 22°C. The surviving bacteria were shown as means ± SEMs, $n = 3$. ^{a,b}Bars topped with the different letters are significantly different at $p \leq 0.05$.

DISCUSSION

The Effect of Concentration, Contacting Time of Sanitizers on Inactivation of *L. monocytogenes*

The concentrations of QAC, chlorine dioxide, chlorine and PAA against *L. monocytogenes* biofilms on common food-contact surfaces were selected complying with FDA regulation (FDA, 2017). The 200 ppm QAC, 2.5 ppm chlorine dioxide, or 100 ppm chlorine

interventions showed limited efficacies against aged *L. monocytogenes* biofilms on different food-contact surfaces, but their efficacies were enhanced with increased concentrations, which was consistent with our previous findings on polystyrene surface (Korany et al., 2018) and other studies on SS surface (Robbins et al., 2005; Trinetta et al., 2012; Dhowlaghar et al., 2018). The antimicrobial efficacies of QAC, chlorine dioxide, and chlorine at selected concentrations were improved when increasing contact time from 1 to 5 min, which is supported by a recent

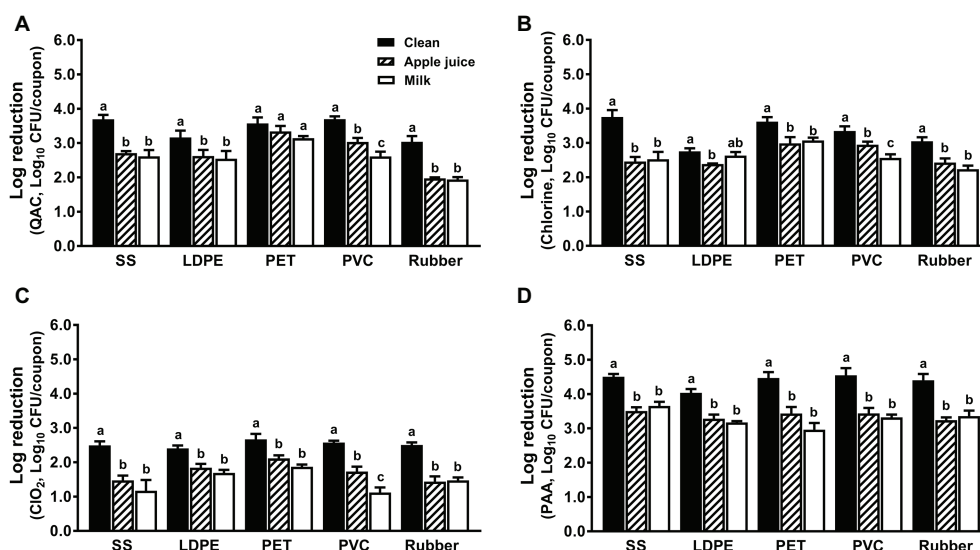


FIGURE 5 | Efficacy of four commonly used sanitizers against *L. monocytogenes* biofilms on food-contact surfaces conditioned with organic matters. **(A)** Quaternary ammonium compound (QAC, 400 ppm); **(B)** chlorine (200 ppm); **(C)** chlorine dioxide (ClO_2 , 5.0 ppm); **(D)** peroxyacetic acid (PAA, 200 ppm); stainless steel (SS); low-density polyethylene (LDPE); polyester (PET); polyvinyl chloride (PVC). Apple juice: food-contact surfaces were conditioned with apple juice; milk: food-contact surfaces were conditioned with milk. The 7-day-old biofilms on different surface coupons (15 mm × 7.5 mm) were treated with the respective sanitizers for 5 min, then survivors were enumerated and shown as means ± SEMs, $n = 3$. ^{a-c}Bars topped with the different letters are not significantly different at $p \leq 0.05$.

report of QAC and chlorine against *L. monocytogenes* biofilms on SS surface (Dhowlaghar et al., 2018). Similarly, the efficacy of chlorine dioxide in aqueous and gaseous phase against *L. monocytogenes* biofilms on food contact surfaces increased with extended contact time (Vaid et al., 2010; Trinetta et al., 2012; Park and Kang, 2017). Increasing PAA concentration from 160 to 200 ppm or extending the contacting time from 1 to 5 min at selected concentration did not improve its efficacy in general. A similar result was obtained for *L. monocytogenes* biofilms on polystyrene surfaces (Korany et al., 2018). Compared with QAC, chlorine, and chlorine dioxide, PAA tested in the present study was the most effective sanitizer against aged *L. monocytogenes* biofilms on all surfaces, which was consistent with findings on polystyrene (Korany et al., 2018), SS (Dhowlaghar et al., 2018), and PVC (Berrang et al., 2008). It could be due to its high reactivity, oxidizing capacity, decomposition rate, and low molecular weight, which together allow PAA to penetrate biofilm matrix, thus accomplishing bactericidal activity (Ibusquiza et al., 2011).

Effects of Surface Materials on Efficacy of Different Sanitizers Against *L. monocytogenes*

The efficacies of sanitizers against aged *L. monocytogenes* biofilms varied on different surfaces. The 1-min treatment of QAC or chlorine at selected concentrations caused comparative efficacies against *L. monocytogenes* biofilms on SS, PET, and rubber, which is supported by a previous report on polystyrene surface (Korany et al., 2018). Compared with rubber and LDPE, 400 ppm QAC and 200 ppm chlorine at 5-min exposure were more effective against *L. monocytogenes* biofilms on SS and other surfaces. In support of our finding, *L. monocytogenes*

on rubber surface was more difficult to remove by chlorine, QAC, and chlorine dioxide than that on SS surface (Ronner and Wong, 1993; Park and Kang, 2017). Different from QAC and chlorine, the anti-*Listeria* effects of PAA and chlorine dioxide were minimally influenced by surface material at different concentration and time combinations. Regardless of surfaces, chlorine dioxide at 5.0 ppm showed a 2.5 log reduction after 5-min treatment, which is a very limited efficacy in contrast to 4.0 or more reduction caused by 200 ppm PAA at 5-min contact. Similar to our results, the aerosolized PAA exhibited similar antimicrobial efficacy against *L. monocytogenes* biofilms on SS and PVC surfaces, though the efficacy was lower than our finding (Park et al., 2012). Each type of surface material has different topography and roughness that provide unique microcracks/harbor sites for *L. monocytogenes* and protect the entrapped cells from antimicrobial agents (Chaturongkasumrit et al., 2011; Schlisselberg and Yaron, 2013), which might explain the difference in efficacy against biofilms on different surfaces. In support, 20 ppm gaseous chlorine dioxide was more effective against attached *L. monocytogenes* on glossy SS than coarse SS, and *Salmonella* biofilms on smooth SS were more susceptible to 50 ppm chlorine treatment than those on a rough surface (Schlisselberg and Yaron, 2013). Surface materials with different hydrophobicity and hydration levels lead to various sanitizing efficacy; hydrophobic surface was more difficult to clean than hydrophilic surface (Park and Kang, 2017).

The Antimicrobial Efficacy of Sanitizers in the Presence of Organic Matter

Food residues established on food-contact surfaces alter the physicochemical property of these surfaces and impact sanitizer

efficacy (Abban et al., 2012; Brown et al., 2014). The present study indicated that organic soiling, regardless of sources, impaired efficacies of all sanitizers against biofilms on all food-contact surfaces, which is consistent with the finding on polystyrene surface (Korany et al., 2018). In agreement with our findings, protein and fat residues on SS reduced the efficacies of chlorine dioxide (Vandekinderen et al., 2009), hydrogen peroxide (Moretro et al., 2019), acidic electrolyzed water and sodium hypochlorite (Ayebeh et al., 2006), QAC, chlorine, and PAA (Aarnisalo et al., 2000; Somers and Wong, 2004; Kuda et al., 2008) against *L. monocytogenes* biofilms. Besides attracting bacterial cells as an adhesive layer, protein coating reduced water contact angle, leading to decreased hydrophobicity of food-contact surface (Abban et al., 2012; Park and Kang, 2017). In addition, sanitizers may have difficulty reaching bacterial cells due to the physical and chemical barriers built up by exopolysaccharide substance of biofilm matrix together with food residues (Fernandes et al., 2015).

CONCLUSION

The type of surface material has more dramatic effects on anti-*Listeria* efficacy of QAC and chlorine than those treated with chlorine dioxide and PAA. Food residue soiling, regardless of sources, reduced anti-*Listeria* efficacies of all sanitizers against biofilms on surfaces in general. Among all sanitizers, PAA was the most effective sanitizer against *L. monocytogenes* biofilms on different surfaces. A 5-min treatment of 200 ppm PAA resulted in 3.0–3.7 log₁₀ reductions of aged multi-strain *L. monocytogenes* biofilms on major food contact surfaces in the presence of organic matter. Data once again highlight the importance of thorough cleaning of food-contact surfaces prior

to sanitizer interventions and provide useful information for food industries in selecting appropriate sanitizers for food-contact surfaces' decontamination.

DATA AVAILABILITY STATEMENT

The datasets generated for this study are available on request to the corresponding author.

AUTHOR CONTRIBUTIONS

ZH and AK conducted the experiments. ZH wrote the manuscript. M-JZ designed the study. M-JZ and SE-S revised the manuscript.

FUNDING

This study was supported by Washington Tree Fruit Research Commission.

ACKNOWLEDGMENTS

We acknowledge Pace International Inc. for their generous donations of Accu-Tab, Bioside HS, STOP-IT, and the Chlorine Dioxide Generator. We would like to express our gratitude to Dr. Ines Hanrahan at Washington Tree Fruit Research for her input from a practical industry perspective. We thank Mrs. Tonia Green for her assistance in preparation of experimental materials and Mr. Mike Taylor for his critical reading of the manuscript.

REFERENCES

- Aarnisalo, K., Salo, S., Miettinen, H., Suihko, M. L., Wirtanen, G., Autio, T., et al. (2000). Bactericidal efficiencies of commercial disinfectants against *Listeria monocytogenes* on surfaces. *J. Food Saf.* 20, 237–250. doi: 10.1111/j.1745-4565.2000.tb00302.x
- Abban, S., Jakobsen, M., and Jespersen, L. (2012). Attachment behaviour of *Escherichia coli* K12 and *Salmonella typhimurium* P6 on food contact surfaces for food transportation. *Food Microbiol.* 31, 139–147. doi: 10.1016/j.fm.2012.04.003
- Abeyundara, P. D. A., Dhowlaghar, N., Nannapaneni, R., Schilling, M. W., Mahmoud, B., Sharma, C. S., et al. (2018). *Salmonella enterica* growth and biofilm formation in flesh and peel cantaloupe extracts on four food-contact surfaces. *Int. J. Food Microbiol.* 280, 17–26. doi: 10.1016/j.ijfoodmicro.2018.04.042
- Angelo, K. M., Conrad, A. R., Saupe, A., Dragoo, H., West, N., Sorenson, A., et al. (2017). Multistate outbreak of *Listeria monocytogenes* infections linked to whole apples used in commercially produced, prepackaged caramel apples: United States, 2014–2015. *Epidemiol. Infect.* 145, 848–856. doi: 10.1017/S0950268816003083
- Ayebeh, B., Hung, Y. C., Kim, C., and Frank, J. F. (2006). Efficacy of electrolyzed water in the inactivation of planktonic and biofilm *Listeria monocytogenes* in the presence of organic matter. *J. Food Prot.* 69, 2143–2150. doi: 10.4315/0362-028X-69.9.2143
- Benarde, M. A., Israel, B. M., Olivieri, V. P., and Granstrom, M. L. (1965). Efficiency of chlorine dioxide as a bactericide. *Appl. Environ. Microbiol.* 13, 776–780.
- Beresford, M. R., Andrew, P. W., and Shama, G. (2001). *Listeria monocytogenes* adheres to many materials found in food-processing environments. *J. Appl. Microbiol.* 90, 1000–1005. doi: 10.1046/j.1365-2672.2001.01330.x
- Berrang, M. E., Frank, J. F., and Meinersmann, R. J. (2008). Effect of chemical sanitizers with and without ultrasonication on *Listeria monocytogenes* as a biofilm within polyvinyl chloride drain pipes. *J. Food Prot.* 71, 66–69. doi: 10.4315/0362-028X-71.1.66
- Brown, H. L., Reuter, M., Salt, L. J., Cross, K. L., Betts, R. P., and van Vliet, A. H. M. (2014). Chicken juice enhances surface attachment and biofilm formation of *Campylobacter jejuni*. *Appl. Environ. Microbiol.* 80, 7053–7060. doi: 10.1128/AEM.02614-14
- CDC (2012). Multistate outbreak of listeriosis linked to whole cantaloupes from Jensen farms, Colorado (final update). Available at: <https://www.cdc.gov/listeria/outbreaks/cantaloupes-jensen-farms/index.html> (Accessed July 20, 2019).
- CDC (2015a). Multistate outbreak of listeriosis linked to commercially produced, prepackaged caramel apples made from Bidart bros, apples (final update). Available at: <https://www.cdc.gov/listeria/outbreaks/caramel-apples-12-14/index.html> (Accessed July 20, 2019).
- CDC (2015b). Wholesome soy products, Inc. sprouts and investigation of human listeriosis cases (final update). Available at: <https://www.cdc.gov/listeria/outbreaks/bean-sprouts-11-14/index.html> (Accessed July 20, 2019).
- CDC (2016a). Multistate outbreak of listeriosis linked to frozen vegetables (final update). Available at: <https://www.cdc.gov/listeria/outbreaks/frozen-vegetables-05-16/index.html> (Accessed July 20, 2019).
- CDC (2016b). Multistate outbreak of listeriosis linked to packaged salads produced at Springfield, Ohio dole processing facility (final update). Available at: <https://www.cdc.gov/listeria/outbreaks/bagged-salads-01-16/index.html> (Accessed July 20, 2019).
- Chaturongkasumrit, Y., Takahashi, H., Keeratipibul, S., Kuda, T., and Kimura, B. (2011). The effect of polyesterurethane belt surface roughness on *Listeria*

- monocytogenes* biofilm formation and its cleaning efficiency. *Food Control* 22, 1893–1899. doi: 10.1016/j.foodcont.2011.04.032
- Dell'Erba, A., Falsanisi, D., Liberti, L., Notarnicola, M., and Santoro, D. (2007). Disinfection by-products formation during wastewater disinfection with peracetic acid. *Desalination* 215, 177–186. doi: 10.1016/j.desal.2006.08.021
- Dhowlaghar, N., Abeysundara, P. D., Nannapaneni, R., Schilling, M. W., Chang, S., Cheng, W. H., et al. (2018). Growth and biofilm formation by *Listeria monocytogenes* in catfish mucus extract on four food contact surfaces at 22 and 10°C and their reduction by commercial disinfectants. *J. Food Prot.* 81, 59–67. doi: 10.4315/0362-028X.JFP-17-103
- Doijad, S. P., Barbuddhe, S. B., Garg, S., Poharkar, K. V., Kalorey, D. R., Kurkure, N. V., et al. (2015). Biofilm-forming abilities of *Listeria monocytogenes* serotypes isolated from different sources. *PLoS One* 10:e0137046. doi: 10.1371/journal.pone.0137046
- FDA (2008). Guidance for industry: guide to minimize microbial food safety hazards of fresh-cut fruits and vegetables. Available at: <https://www.fda.gov/food/guidanceregulation/ucm064458.htm> (Accessed July 20, 2019).
- FDA (2017). CFR-code of federal regulations title 21. Available at: <https://www.accessdata.fda.gov/scripts/cdrh/cfdoh/cfcltr/cfrsearch.cfm> (Accessed July 20, 2019).
- Fernandes, M. D., Kabuki, D. Y., and Kuaye, A. Y. (2015). Behavior of *Listeria monocytogenes* in a multi-species biofilm with *Enterococcus faecalis* and *Enterococcus faecium* and control through sanitation procedures. *Int. J. Food Microbiol.* 200, 5–12. doi: 10.1016/j.ijfoodmicro.2015.01.003
- Ibusquiza, P. S., Herrera, J. J. R., and Cabo, M. L. (2011). Resistance to benzalkonium chloride, peracetic acid and nisin during formation of mature biofilms by *Listeria monocytogenes*. *Food Microbiol.* 28, 418–425. doi: 10.1016/j.fm.2010.09.014
- Jellessen, M. S., Rasmussen, A. A., and Hilbert, L. R. (2006). A review of metal release in the food industry. *Mater. Corros.* 57, 387–393. doi: 10.1002/maco.200503953
- Korany, A. M., Hua, Z., Green, T., Hanrahan, I., El-Shinawy, S. H., El-Kholy, A., et al. (2018). Efficacy of ozonated water, chlorine, chlorine dioxide, quaternary ammonium compounds and peroxyacetic acid against *Listeria monocytogenes* biofilm on polystyrene surfaces. *Front. Microbiol.* 9:2296. doi: 10.3389/fmicb.2018.02296
- Krysinski, E., Brown, L., and Marchisello, T. (1992). Effect of cleaners and sanitizers on *Listeria monocytogenes* attached to product contact surfaces. *J. Food Prot.* 55, 246–251. doi: 10.4315/0362-028X-55.4.246
- Kuda, T., Yano, T., and Kuda, M. T. (2008). Resistances to benzalkonium chloride of bacteria dried with food elements on stainless steel surface. *LWT Food Sci. Technol.* 41, 988–993. doi: 10.1016/j.lwt.2007.06.016
- McCollum, J. T., Cronquist, A. B., Silk, B. J., Jackson, K. A., O'Connor, K. A., Cosgrove, S., et al. (2013). Multistate outbreak of listeriosis associated with cantaloupe. *New Engl. J. Med.* 369, 944–953. doi: 10.1056/NEJMoa1215837
- Meireles, A., Fulgencio, R., Machado, I., Mergulhao, F., Melo, L., and Simoes, M. (2017). Characterization of the heterotrophic bacteria from a minimally processed vegetables plant. *LWT Food Sci. Technol.* 85, 293–300. doi: 10.1016/j.lwt.2017.01.038
- Moretro, T., Fanebust, H., Fagerlund, A., and Langsrud, S. (2019). Whole room disinfection with hydrogen peroxide mist to control *Listeria monocytogenes* in food industry related environments. *Int. J. Food Microbiol.* 292, 118–125. doi: 10.1016/j.ijfoodmicro.2018.12.015
- Olszewska, M. A., Zhao, T., and Doyle, M. P. (2016). Inactivation and induction of sublethal injury of *Listeria monocytogenes* in biofilm treated with various sanitizers. *Food Control* 70, 371–379. doi: 10.1016/j.foodcont.2016.06.015
- Papaioannou, E., Giaouris, E. D., Berillis, P., and Boziaris, I. S. (2018). Dynamics of biofilm formation by *Listeria monocytogenes* on stainless steel under mono-species and mixed-culture simulated fish processing conditions and chemical disinfection challenges. *Int. J. Food Microbiol.* 267, 9–19. doi: 10.1016/j.ijfoodmicro.2017.12.020
- Park, S. H., Cheon, H. L., Park, K. H., Chung, M. S., Choi, S. H., Ryu, S., et al. (2012). Inactivation of biofilm cells of foodborne pathogen by aerosolized sanitizers. *Int. J. Food Microbiol.* 154, 130–134. doi: 10.1016/j.ijfoodmicro.2011.12.018
- Park, S. H., and Kang, D. H. (2017). Influence of surface properties of produce and food contact surfaces on the efficacy of chlorine dioxide gas for the inactivation of foodborne pathogens. *Food Control* 81, 88–95. doi: 10.1016/j.foodcont.2017.05.015
- Robbins, J. B., Fisher, C. W., Moltz, A. G., and Martin, S. E. (2005). Elimination of *Listeria monocytogenes* biofilms by ozone, chlorine, and hydrogen peroxide. *J. Food Prot.* 68, 494–498. doi: 10.4315/0362-028X-68.3.494
- Ronner, A. B., and Wong, A. C. L. (1993). Biofilm development and sanitizer inactivation of *Listeria monocytogenes* and *Salmonella typhimurium* on stainless steel and Buna-N rubber. *J. Food Prot.* 56, 750–758. doi: 10.4315/0362-028X-56.9.750
- Scallan, E., Hoekstra, R. M., Angulo, F. J., Tauxe, R. V., Widdowson, M. A., Roy, S. L., et al. (2011). Foodborne illness acquired in the United States—major pathogens. *Emerg. Infect. Dis.* 17, 7–15. doi: 10.3201/eid1701.P11101
- Schlisselberg, D. B., and Yaron, S. (2013). The effects of stainless steel finish on *Salmonella typhimurium* attachment, biofilm formation and sensitivity to chlorine. *Food Microbiol.* 35, 65–72. doi: 10.1016/j.fm.2013.02.005
- Somers, E. B., and Wong, A. C. L. (2004). Efficacy of two cleaning and sanitizing combinations on *Listeria monocytogenes* biofilms formed at low temperature on a variety of materials in the presence of ready-to-eat meat residue. *J. Food Prot.* 67, 2218–2229. doi: 10.4315/0362-028X-67.10.2218
- Takahashi, H., Suda, T., Tanaka, Y., and Kimura, B. (2010). Cellular hydrophobicity of *Listeria monocytogenes* involves initial attachment and biofilm formation on the surface of polyvinyl chloride. *Lett. Appl. Microbiol.* 50, 618–625. doi: 10.1111/j.1472-765X.2010.02842.x
- Trinetta, V., Vaid, R., Xu, Q., Linton, R., and Morgan, M. (2012). Inactivation of *Listeria monocytogenes* on ready-to-eat food processing equipment by chlorine dioxide gas. *Food Control* 26, 357–362. doi: 10.1016/j.foodcont.2012.02.008
- Vaid, R., Linton, R. H., and Morgan, M. T. (2010). Comparison of inactivation of *Listeria monocytogenes* within a biofilm matrix using chlorine dioxide gas, aqueous chlorine dioxide and sodium hypochlorite treatments. *Food Microbiol.* 27, 979–984. doi: 10.1016/j.fm.2010.05.024
- van der Veen, S., and Abee, T. (2011). Mixed species biofilms of *Listeria monocytogenes* and *Lactobacillus plantarum* show enhanced resistance to benzalkonium chloride and peracetic acid. *Int. J. Food Microbiol.* 144, 421–431. doi: 10.1016/j.ijfoodmicro.2010.10.029
- Vandekinderen, I., Devlieghere, F., Van Camp, J., Kerkaert, B., Cucu, T., Ragaert, P., et al. (2009). Effects of food composition on the inactivation of foodborne microorganisms by chlorine dioxide. *Int. J. Food Microbiol.* 131, 138–144. doi: 10.1016/j.ijfoodmicro.2009.02.004

Conflict of Interest: The authors declare that the research was conducted in the absence of any commercial or financial relationships that could be construed as a potential conflict of interest.

Copyright © 2019 Hua, Korany, El-Shinawy and Zhu. This is an open-access article distributed under the terms of the Creative Commons Attribution License (CC BY). The use, distribution or reproduction in other forums is permitted, provided the original author(s) and the copyright owner(s) are credited and that the original publication in this journal is cited, in accordance with accepted academic practice. No use, distribution or reproduction is permitted which does not comply with these terms.



Graphene-Based Steganographic Aptasensor for Information Computing and Monitoring Toxins of Biofilm in Food

Qi Wang, Qingli Yang* and Wei Wu*

College of Food Science and Engineering, Qingdao Agricultural University, Qingdao, China

OPEN ACCESS

Edited by:

Zhenbo Xu,
University of Maryland, Baltimore,
United States

Reviewed by:

Zhong Zhang,
Shaanxi Normal University, China
Junhua Chen,
Guangdong Institute of
Eco-environmental Science and
Technology, China

*Correspondence:

Qingli Yang
rice407@163.com
Wei Wu
wuweiouc@126.com

Specialty section:

This article was submitted to
Food Microbiology,
a section of the journal
Frontiers in Microbiology

Received: 02 December 2019

Accepted: 27 December 2019

Published: 04 February 2020

Citation:

Wang Q, Yang Q and Wu W (2020)
Graphene-Based Steganographic
Aptasensor for Information Computing
and Monitoring Toxins of Biofilm in
Food. *Front. Microbiol.* 10:3139.
doi: 10.3389/fmicb.2019.03139

Fungi-forming biofilm would produce various toxins in food. The toxin contamination will cause great harm to food and human health. Herein, a novel graphene-based steganographic aptasensor was assembled for multifunctional applications, which depended on the specific recognition and information encoding ability of DNA aptamers [mycotoxins, including zearalenone (ZEN) and ochratoxin A (OTA) aptamers, as models] and the selective absorption and fluorescence quenching capacities of graphene oxide (GO). The graphene-based steganographic aptasensor can be regarded as an information encryption and steganographic system using GO as a cover, aptamers for specific target recognition as information carriers and dual targets (ZEN and OTA) as special keys. In our work, the fluorescence of capture probes (Cy3 aptamer and Alexa Fluor 488 aptamer) was quenched by GO to realize information encryption. In the presence of dual targets in the GO–APT solution, Cy3 aptamer (APT1), and Alexa Fluor 488 aptamer (APT2) were released from the surface of GO, decrypting the hidden information. In addition, our work offers a sensor for rapid and sensitive simultaneous fluorescence determination of ZEN and OTA. The detection limit of the aptasensor was 1.797 ng/ml for ZEN and 1.484 ng/ml for OTA. In addition, the graphene-based steganographic aptasensor can be used to construct a molecular logic gate system in which GO, aptamers, and mycotoxins are employed as the input and compounds and fluorescence signals were used as the output. This would be helpful to control the biofilm toxin in the future.

Keywords: aptasensor, graphene oxide, mycotoxin, fluorescence, encryption, steganography

INTRODUCTION

Biofilm is an extracellular matrix (including toxin) secreted by biological flora, which is easy to adhere to a biological or non-biological surface (Galié et al., 2018; Xu et al., 2019). In other words, biofilm is a self-protection mechanism of bacteria and fungi. Once biofilm is formed, it is difficult to remove. Fungi can avoid being damaged by high temperature and pressure in the closed environment formed by a biofilm. In these circumstances, fungi will produce more mycotoxins to be discharged outside the biofilm. Mycotoxins are a kind of low-molecular-weight natural secondary metabolites that possesses strong toxicities to humans and animals (Rong et al., 2019). Therefore, the existence of biofilms will aggravate food pollution and other safety problems. Mycotoxins should be detected before biofilm formation to reduce food pollution.

Mycotoxin toxicity is mainly manifested as the following: damage to liver and kidney, teratogenicity, cancer, and mutation (Hussein and Brasel, 2001). Worst of all, mycotoxins not only lessen crop yield and quality but also cause significant economic losses (Turner et al., 2009; Sun X. D. et al., 2017). So far, the traditional detection methods of ochratoxin A (OTA) and zearalenone (ZEN) mainly include thin-layer chromatography (TLC), high-performance liquid chromatography (HPLC), gas chromatography (GC), capillary electrophoresis (CE), and enzyme-linked immunosorbent assay (ELISA) (Li et al., 2013; Zhang et al., 2018b; Wu et al., 2019a). These detection approaches face challenges due to their time-consuming, high-cost, and low-sensitivity methods. Moreover, there is a great possibility that foods and animal feeds will be contaminated simultaneously with several mycotoxins. However, a single detection pattern will not provide comprehensive monitoring for food safety. Thus, it is necessary to strengthen the simultaneous detection technology for mycotoxins in food and feed. Moreover, it is essential to develop a novel, rapid, low-cost, sensitive, simultaneous detection biosensor for mycotoxins.

In this internet era of information (text, audio, video, and image data), information storage and cryptography have crucial roles for countries and enterprises. To ensure information security and prevent information leakage, the universally used methods are information encryption and information concealment (Zhu et al., 2019). However, the safety level of these methods is low. Consequently, it is essential to improve information security and exploit a novel encryption and steganographic approach for information security. More interestingly, the processes of molecular interactions and chemical reactions can allow operation and transmission of information. Inspired by nature, DNA-based information encryption and concealment have emerged. In addition, due to DNA-specific molecular recognition, information encoding and ultrahigh-information-density capabilities, DNA-based biosensors, information storage, computing, encryption, and steganography have received increasing attention (Ejike et al., 2017; Zhang et al., 2017; Zhou et al., 2018; Lopez et al., 2019). Moreover, the development of conventional logic circuits based on semiconductors has reached a bottleneck development stage because the heat capacity, volume, and operational speed of semiconductor materials are difficult to further improve. However, the above issues can be solved perfectly by DNA molecules. Therefore, traditional logic circuits will give way to molecular logic gates, and DNA is an optimum alternative to silicon (Liu et al., 2012; Zhu et al., 2019).

Aptamers are short oligonucleotide sequences, and the ones used in this study were selected from a nucleic acid random library using systematic evolution of ligands by exponential enrichments (SELEX) *in vitro* (Jayasena, 1999; Wu et al., 2019b). The three-dimensional structure of an aptamer depends on the base sequence, the length of the nucleotide sequence, and the environmental conditions (Hermann and Patel, 2000). Due to their three-dimensional structure, aptamers possess high specificity and affinity for targets. Therefore, aptamers are usually assembled with nanomaterials as biomolecular recognition components in aptasensors (Pehlivan et al., 2019). Optical

aptamer sensors are the most common aptamer sensors because the optical signal of the reaction process can be easily detected. A GO fluorescence resonance energy transfer (FRET) platform is constructed by fluorescent-modified aptamers and GO, which can be an ideal candidate for mycotoxin detection (Yugender Goud et al., 2017). In recent years, GO has attracted much interest due to its superior fluorescence quenching property relative to other quenchers (Wu et al., 2012; Kim et al., 2017). According to the FRET principle, a fluorophore was used as a fluorescence donor, GO was used as a fluorescence acceptor, and the fluorescence was blocked by GO. GO-based fluorescence biosensors have been extensively applied in a variety of detection fields. In addition, the different measured targets include metal ions (Qian et al., 2015; Wu et al., 2019c), cells (Wang et al., 2010), proteins (Zhou et al., 2015), pathogens (Zhu et al., 2019), mycotoxins (Sun A. L. et al., 2017; Yugender Goud et al., 2017), and DNA and other small molecules (Wang et al., 2018; Zhao et al., 2019). It is interesting to note that GO has different adsorption capacities for single-stranded DNA (ssDNA), double-stranded DNA (dsDNA), and G-quadruplex (Sun A. L. et al., 2017). GO has an extraordinary adsorption capacity for single-stranded oligonucleotides because of π - π stacking. According to this property, a fluorescence switch-on detection system has a theoretical basis.

In our work, a graphene-based steganographic aptasensor was designed for multifunctional applications, simultaneous fluorescence detection of mycotoxins (ZEN and OTA), and information computing, encryption, and concealing. The graphene-based steganographic aptasensor mentioned here can also be utilized to construct a simple DNA molecule logic gate system in which materials are the input and the compounds and fluorescence produced by the material interactions act as dual outputs. Moreover, graphene-based steganographic aptasensors will offer a novel model for molecular information encrypting and concealing technology.

MATERIALS AND METHODS

Reagents and Materials

OTA and ZEN were purchased from Pribolab Co., Ltd. (Qingdao, China, <http://www.pribolab.com>). GO was purchased from Xianfeng Nanomaterials Tech Co., Ltd. (Nanjing, China). The oligonucleotide sequences of aptamer 1 (APT1, for ZEN) and aptamer 2 (APT2, for OTA) were taken from previously reported literature (McKeague et al., 2014; Zhang et al., 2018b). Two aptamers were purchased from Sangon Biotechnology Co., Ltd. (Shanghai, China). DNA probes were modified with the fluorescence dyes (Cy3 and Alexa Fluor 488) on their 5'-end. The oligonucleotide sequences of APT1 and APT2 are shown in **Table 1**. The methanol used in the experiment was analytically pure reagent. Ultrapure water (18.25 M Ω /cm) was used in all experiments.

All fluorescence spectra were scanned using a Hitachi F-2700 fluorescence spectrophotometer (Hitachi Ltd., Japan). The slit width was 5 nm, and the voltage of the photomultiplier tube was 700 V. Fluorescence emission spectra were collected at an excitation wavelength of 512 nm for APT1 and 499 nm for

APT2. The height trace images of the atomic force microscope (AFM) were scanned using an SPM-9700 AFM (Shimadzu, Japan). The dried samples on mica sheets were scanned in phase imaging mode.

All experiments were repeated at least three times.

Operation Process of Detecting Dual Targets of Biofilm

Freeze-dried powder of the aptamers was diluted to working concentration (1 μM) in phosphate buffer saline (PBS) (containing NaCl 136.89 mM, KCl 2.67 mM, Na₂HPO₄ 8.1 mM, KH₂PO₄ 1.76 mM, pH = 7.4). Then, 30-μl GO nanosheets (250 μg/ml) were homogeneously mixed separately with 20 μl of APT1, APT2, and APT 1&2 at room temperature for 5 min. Subsequently, different concentrations of ZEN and OTA (0, 1, 5, 10, 50, 100, and 500 ng/ml) were dropped in the GO-aptamer mixed solution, and the ultimate volume of the solution of 1 ml was achieved by adding PBS. The final liquid was incubated at 45°C for 1 h (reaction temperature optimization shown in Figure 4). The most important thing was that the whole experiment was conducted under dark conditions. Fluorescence intensity was measured using an F2700 fluorescence spectrophotometer. Samples (GO, GO-APT1, GO-APT2, GO-APT1-ZEN, and GO-APT2-OTA) after incubation in a water bath were centrifuged for 10 min at 8,000 × g to

obtain GO nanosheets. Then, GO nanosheets were diluted to an appropriate concentration (5 μg/ml) with ultrapure water and dispersed by ultrasonication for 10 min. The height trace image was scanned using an SPM-9700 AFM. Each sample was parallel scanned 20 times.

Detection of ZEN and OTA in Real Samples

To confirm the practicality of the graphene-based steganographic aptasensor, wine samples were used for testing in our study. The wine sample was purchased from a local market (RT-Mart). First, the sediment was removed by centrifugation for 10 min. In addition, the supernatant was adjusted to pH 7.4 and diluted 20-fold with PBS buffer. Then, ZEN and OTA at known concentrations were spiked in pretreated samples. According to the above operation process, wine samples were quantitatively detected using a fluorescence aptasensor.

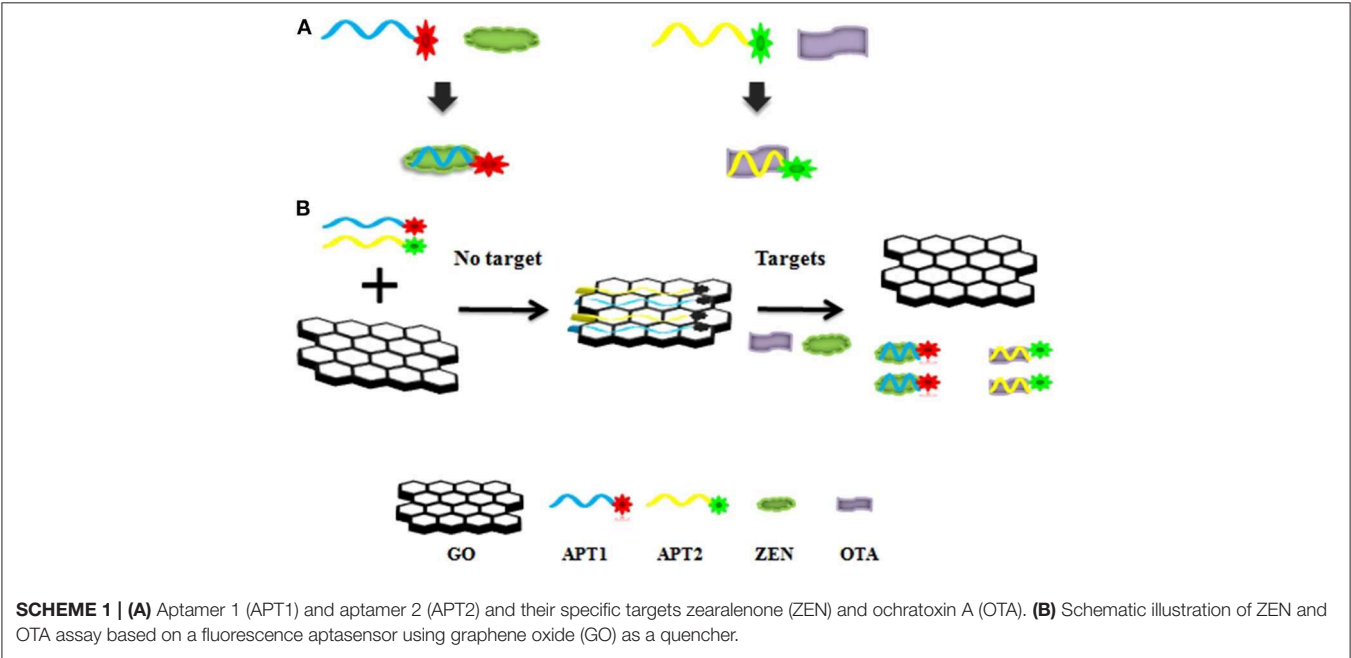
RESULTS AND DISCUSSION

The Principle of a Fluorescence Aptasensor to Simultaneously Detect OTA and ZEN of Biofilm

The graphene-based steganographic aptasensor was composed of a ssDNA aptamer and GO. It depends on the high affinity and specific molecular recognition and information

TABLE 1 | Oligonucleotides used in this study.

	Modification	Sequences (5'-3')
APT1	5' Cy3 (for ZEN)	CTACCAGCTTTGAGGCTCGATCCAGCTTATTCAATTATACCAGCTTATTCAATTATACCAGC
APT2	5' Alexa Fluor 488 (for OTA)	AGCCTCGTCTGTTCTCCCGGCGCATGATCATTCGGTGGGTAAGGTGGTGGTAACGTTGGGGAAGACAAGCAGACGT



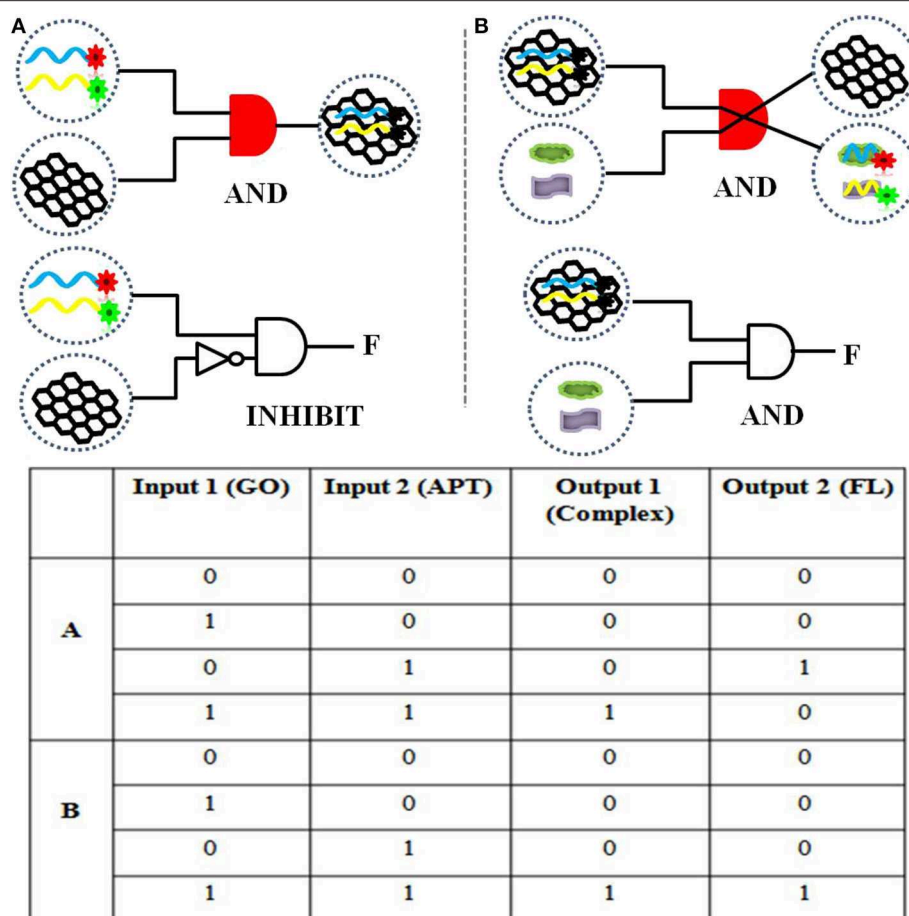


FIGURE 1 | (A) The logical symbol diagram and truth table of the (aptamer “AND” GO) material gate and the “INHIBIT” (aptamer “AND” “NOT” GO) fluorescence gate. **(B)** The logical symbol diagram and truth table of the (aptamer–GO “AND” targets) matter gate and the (aptamer–GO “AND” targets) fluorescence gate.

carrier abilities of the ssDNA aptamer and the fluorescence quenching and ssDNA adsorption capability of GO. The strategy of simultaneous detection of mycotoxins based on switch-on fluorescence aptasensors is shown in **Scheme 1**. Dual aptamers were regarded as prototypes, where APT1 can specifically recognize T1 (ZEN) and APT2 can specifically recognize T2 (OTA) (**Scheme 1A**, sequences in **Table 1**). In the simultaneous detection aptasensor system, APT1 and APT2 were adsorbed by GO due to the presence of oxygen-containing functional groups and conjugated structures on the GO surface. In addition, hydrogen bonds and π - π bonds formed between GO and APT1 and APT2. Accompanying the appearance of non-covalent bonds, the distance between GO and the aptamers decreased. In addition, the fluorescence of the aptamers was quenched by FRET. The GO-FRET platform was assembled by aptamers and GO. In the absence of the dual targets from the previous solution, the simultaneous detection system for mycotoxin was in the switch-off state. Upon the addition of targets, APT1, APT2, and their specific targets combine due to hydrogen bonding and electrostatic and hydrophobic interactions. The interaction forces of the aptamer target were more powerful than

those of the GO aptamer (Zhang et al., 2018a). Subsequently, the aptamer target was released from GO, recovering the prominent fluorescence of APT1 and APT2. At this time, the simultaneous detection system of mycotoxin was in a switch-on state. Accordingly, with the increased concentration of targets, the fluorescence intensity recovery value increased. The target concentration and the restored fluorescence intensity show a good proportional relationship.

Construction of a Logic Gate

To realize information computing, the feasibility of constructing a DNA logic gate was verified first. Our constructed APT–GO FRET platform can implement “AND” and “INHIBIT” logic gates by using changes in materials and energy. For the truth table of logic gates, 0 and 1 indicate the absence and presence of input and output, respectively. On the basis of the principle of the “AND” logic gate, the simultaneous existence of all the inputs induces the appearance of the output. This means that when the input is (1, 1), the output is 1. The output of an “INHIBIT” gate happens for one and only one specific input. In **Figure 1**, the materials (GO, APT, target, and compound) were regarded as the

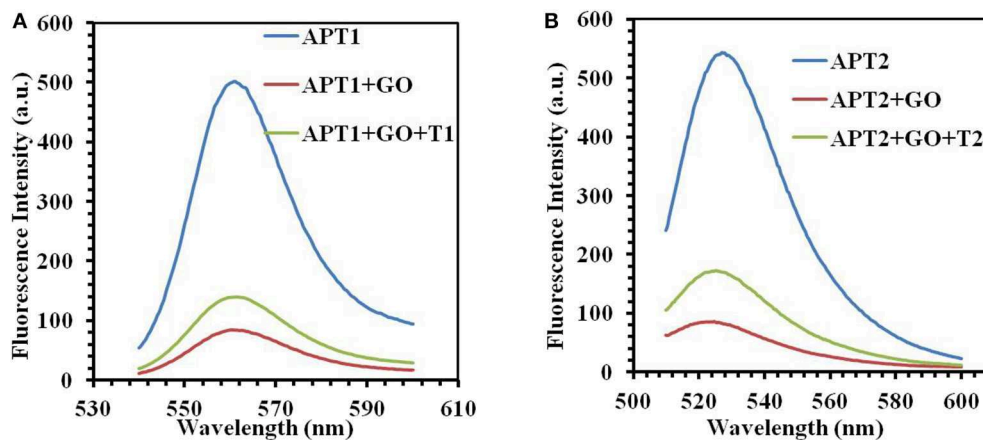


FIGURE 2 | (A) The fluorescence emission spectra of APT1 for T1 (ZEN). (B) The fluorescence emission spectra of APT2 for T2 (OTA).

inputs and outputs of the integration circuit. The interaction of GO and APT (APT1/APT2/APT1&2) can be used to construct an “AND” logic gate. The GO–APT complex was present only when GO and APT simultaneously appeared in solution. When both inputs were 1, we marked the output as 1. In other cases, the output was 0. Simultaneous appearances of the dual targets (ZEN and OTA) and the GO–APT complex interacted with each other. Then, the transfer of the aptamer was accomplished from the surface of GO to the target, outputting the GO and APT target. Clearly, there is an “AND” logic gate for material exchange. On the basis of all cases in the truth table, the output was 1 when both inputs were 1. The interaction of matter leads to a change in fluorescence in the system. Therefore, fluorescence was deemed as the output. For the fluorescence signal, the self-construction of GO and aptamer can be understood as an “INHIBIT” logic gate. According to all cases of the truth table, fluorescence was outputted only when there were aptamers and no GO. In other words, when the inputs were (0, 1), the output was 1. With the combination of the GO–APT complex and dual targets, an “AND” logic gate will be formed, and fluorescence will be the output when both the GO–APT complex and dual targets exist.

The change of matter and energy can be used to realize molecular logical operation based on binaries 1 and 0. There is a close association between the biosensor and the logic gate. It is essential to further explore molecular logic gates with more complex combinations. Only in this way can molecular computing and molecular information technology be quickly realized.

Verification of Experimental Feasibility

The next work tested and verified whether the principle of the switch-on fluorescence aptasensor was justified. The feasibility of the fluorescence aptasensor using GO as a quencher is demonstrated in **Figure 2**. The relationship among the fluorescence intensity of the aptamer, aptamer–GO, and aptamer–GO–target is shown clearly in **Figure 2**. The fluorescence intensity was stronger when there were aptamers alone (APT1 or APT2) in the solution (blue curves in **Figures 2A,B**). When the fluorescent aptamer

was incubated with GO, the fluorescence intensity dropped sharply (blue and red curves in **Figures 2A,B**). The results showed that the fluorescence of the aptamers was blocked by GO. When the targets appeared in the aqueous solution, the aptamers (APT1 or APT2) combined with the special targets and were released from the GO surface, restoring the prominent fluorescence of the aptamers (red and green curves in **Figures 2A,B**). This phenomenon illustrated that the targets showed a stronger affinity than GO for the aptamers, resulting in APT1 and APT2 being released from GO and combining with the target. Therefore, the restored fluorescence intensity of the aptamer–target complexes was measured by fluorescence spectroscopy.

An AFM was also used to test the accuracy of the concept design. The height trace and size of GO were scanned by AFM. As shown in **Figure 3**, the average height of the GO sheets was approximately 1.28 ± 0.01 nm (**Figure 3A**). This result is consistent with the theory that GO is a single atomic layer. Then, the height of the aptamer–GO complexes was 1.80 ± 0.007 nm (**Figure 3B**) and 1.87 ± 0.034 nm (**Figure 3D**). The increased thickness demonstrated that aptamers were successfully adsorbed on the surface of GO. Finally, when the GO–APT complex was incubated with targets, its thickness significantly decreased to 1.58 ± 0.005 nm (**Figure 3C**) and 1.51 ± 0.008 nm (**Figure 3E**). This phenomenon confirmed that the aptamer was released from the surface of GO because the interaction forces of the aptamer target were stronger than those of the GO aptamer. Both of the above methods showed that the experimental design is correct.

Temperature Optimization for Detection

To improve the efficiency of fluorescence recovery after adding targets, temperature optimization measures were taken. At room temperature, the fluorescence intensity did not recover significantly after adding the target. The interaction of GO and the aptamer was weakened by increasing the temperature, and the APT target desorbed. Thus, to enhance the fluorescence restoration, increasing the temperature is an ideal method. At the same time, excessively high temperatures will destroy the binding

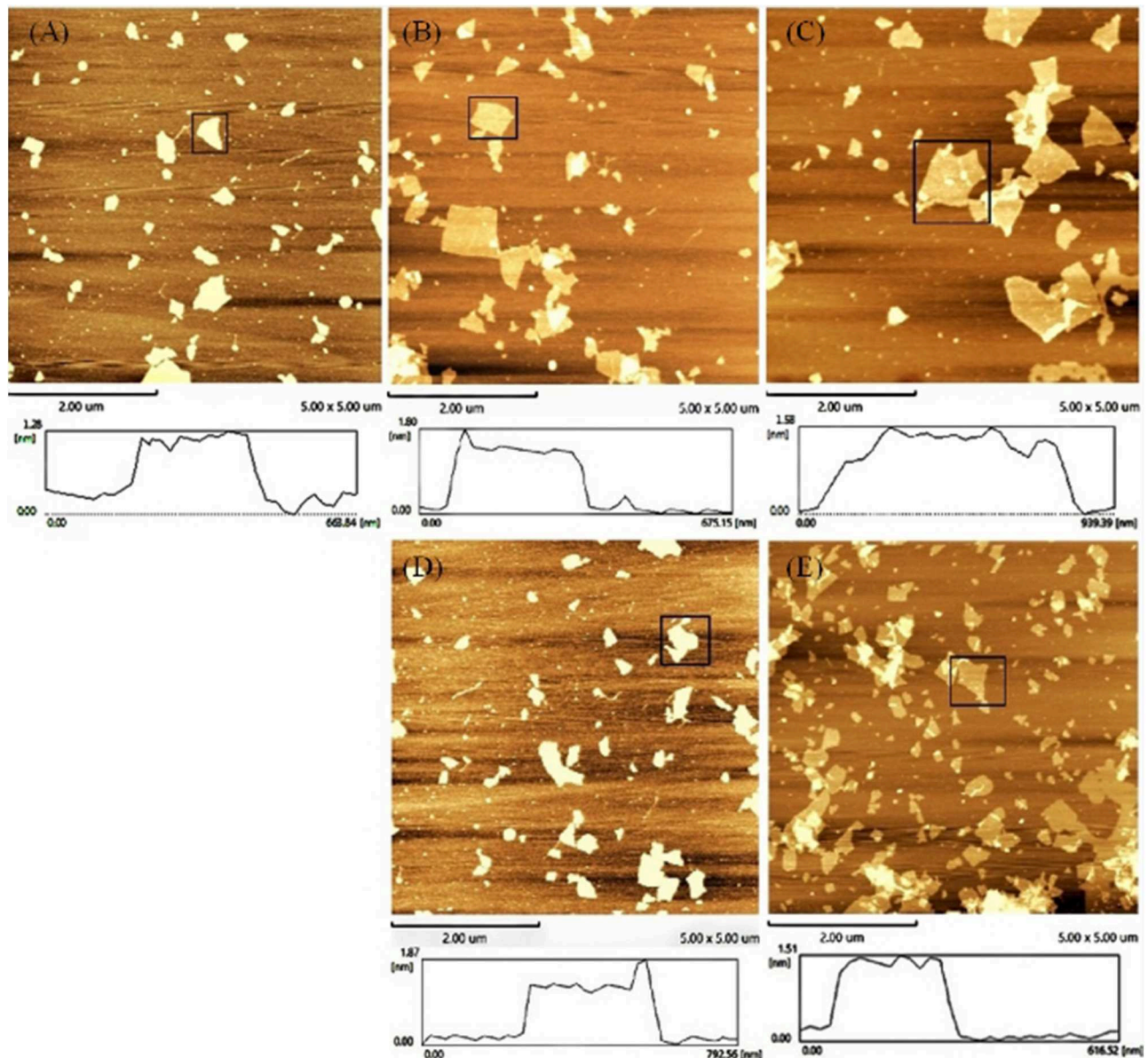


FIGURE 3 | Atomic force microscope images of (A) GO, (B) GO-APT1, (C) GO-APT1-T1, (D) GO-APT2, and (E) GO-APT2-T2.

between the aptamer and the target. It is important to optimize the temperature.

The fluorescence intensity restoration increased with increasing temperature (30, 35, 40, 45, and 50°C) in general when there was no target (blue bars in **Figure 4**). This phenomenon confirmed the previous theory that high temperature accelerates the release of the aptamer from the GO surface. However, the phenomenon was different when targets were added to the GO-APT compound. The fluorescence signal increased regularly below 45°C (red bars in **Figure 4**). When the temperature exceeded 45°C, the fluorescence intensity restoration was weakened. Thus, 45°C is the critical point of the fluorescence intensity restoration.

Sensitivity Test of the Fluorescence Aptasensor

To prove the sensitivity of the fluorescence-switch aptasensor, the targets (ZEN and OTA) at different concentrations (0, 1, 5, 10, 50, 100, and 500 ng/ml) were incubated with the GO-APT complex. The fluorescence intensity increased, as shown in **Figure 5**. With both increasing concentrations of ZEN and OTA, the fluorescence intensity increased from 83.97 to 139.6 (a.u.) for the GO-APT1 mixed solution and from 85.07 to 172.6 (a.u.) for the GO-APT2 mixed solution. As shown in **Figure 5**, the regression equation of ZEN was $y = 8.9712 \ln(x) + 84.532$, $R^2 = 0.9986$, and that of OTA was $y = 13.352 \ln(x) + 88.132$, $R^2 = 0.9886$. Hence, a conclusion was drawn that

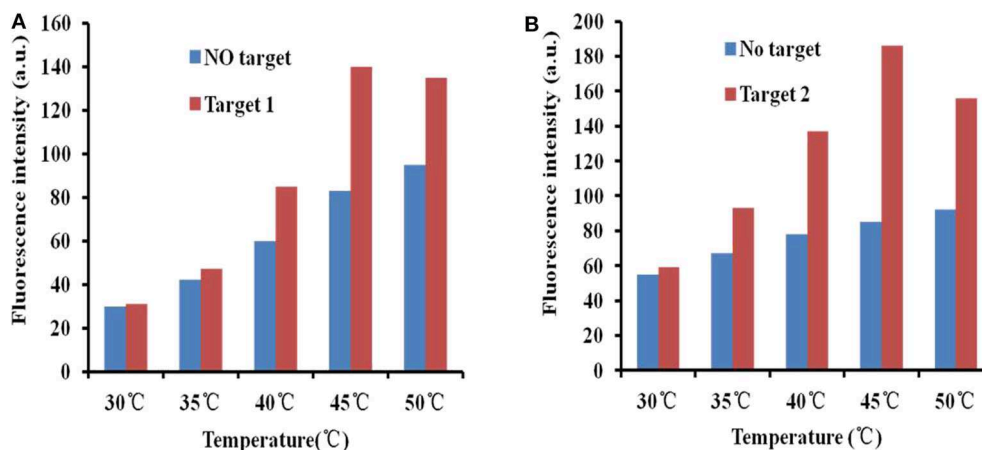


FIGURE 4 | (A) Fluorescence desorption of the GO-APT complex in the presence and absence of T1 (500 ng/ml) at different temperatures (30–50°C). **(B)** Fluorescence desorption of the GO-APT complex in the presence and absence of T2 (500 ng/ml) at different temperatures (30–50°C).

the target concentration and the restored value of fluorescence intensity have a good proportional relationship. The limit of detection (LOD) of this aptasensor is the target concentration responding to the fluorescence intensity of the mean blank value plus 3 standard deviations (SD). For ZEN, the mean fluorescent intensity of 20 blank experiments was 84.95, and the SD was 1.612. The responding fluorescence intensity of LOD was 89.786. According to standard equation (Figure 5B), LOD was 1.796 ng/ml. For OTA, the mean fluorescent intensity of 20 blank experiments was 87.37, and the SD was 2.01. The responding fluorescence intensity of LOD was 93.4. According to standard equation (Figure 5D), LOD was 1.484 ng/ml. The quenching and recovery of fluorescence illustrated that GO played a crucial role in the fluorescence switch aptasensor. A comparison of the many sensors for ZEN and OTA detection with the detection limits is summarized in Table S1.

Specificity Test of the Fluorescence Aptasensor

The specificity of the fluorescence aptasensor was further checked using other possible interfering mycotoxins, such as aflatoxin B1 (AFB1), aflatoxin M1 (AFM1), fumonisin B1 (FB1), and patulin. ZEN, OTA, AFB1, AFM1, FB1, and patulin were added separately to the GO-APT1&2 complex at a concentration of 100 ng/ml each. The value of the fluorescence recovery is shown in Figure 6. The fluorescence recovery value of interfering mycotoxins was negligible, as shown in this bar chart. In comparison, the fluorescence recovery values of ZEN and OTA were apparent. The results strongly illustrated that APT1&2 possesses a higher specificity for ZEN and OTA, respectively, than other mycotoxins.

Monitor of Dual Targets in Real Samples

Three different concentrations of ZEN and OTA were monitored by a fluorescence aptasensor. Reliability was further evaluated by recovery experiments in real samples using the standard spiking experiment. The concentrations of ZEN and OTA were

determined using the method described above and calculated by using the linear equation. The result is shown in Table 2. The recoveries ranged from 89 to 99.89% for ZEN and from 91.75 to 103.56% for OTA. This method can be used to simultaneously check ZEN and OTA in real food samples.

Information Steganography of the Fluorescence Aptasensor Based on GO

In this era of increasing information, the safety of messages has a crucial role. Information steganography is the method of hiding information (text, audio, video, and image data) within other information (text, audio, video, and image data). Moreover, information steganography is analogous to the natural camouflage of animals. There is no doubt that information steganography is a brilliant approach for the process of information transfer. It is very difficult to find hidden information within abundant information and to further remove the cover. Therefore, the information receiver must have the right key to decode hidden information. To further explore novel information steganography technology, DNA molecules and traditional steganography technology were combined in our work.

The steganographic analysis relied mostly on the adsorption and release ability of GO for the ssDNA aptamer. The basic components of the steganography system (Scheme 2) included three parts: APT, GO, and dual targets (ZEN and OTA). The aptamer not only was an excellent information carrier (A, T, G, and C) but also bore a high specific recognition ability. In addition, GO could be recognized as a cover that could hide the information of an aptamer. Moreover, dual targets (ZEN and OTA) could be used as special keys that could decode the hidden information. In Scheme 1, the fluorescence quenching and ssDNA adsorption capability of GO were previously confirmed. This characteristic was applied to hide the information of the aptamer. Meanwhile, the quenched fluorescence signal could be used as an indicator signal that the aptamer information was

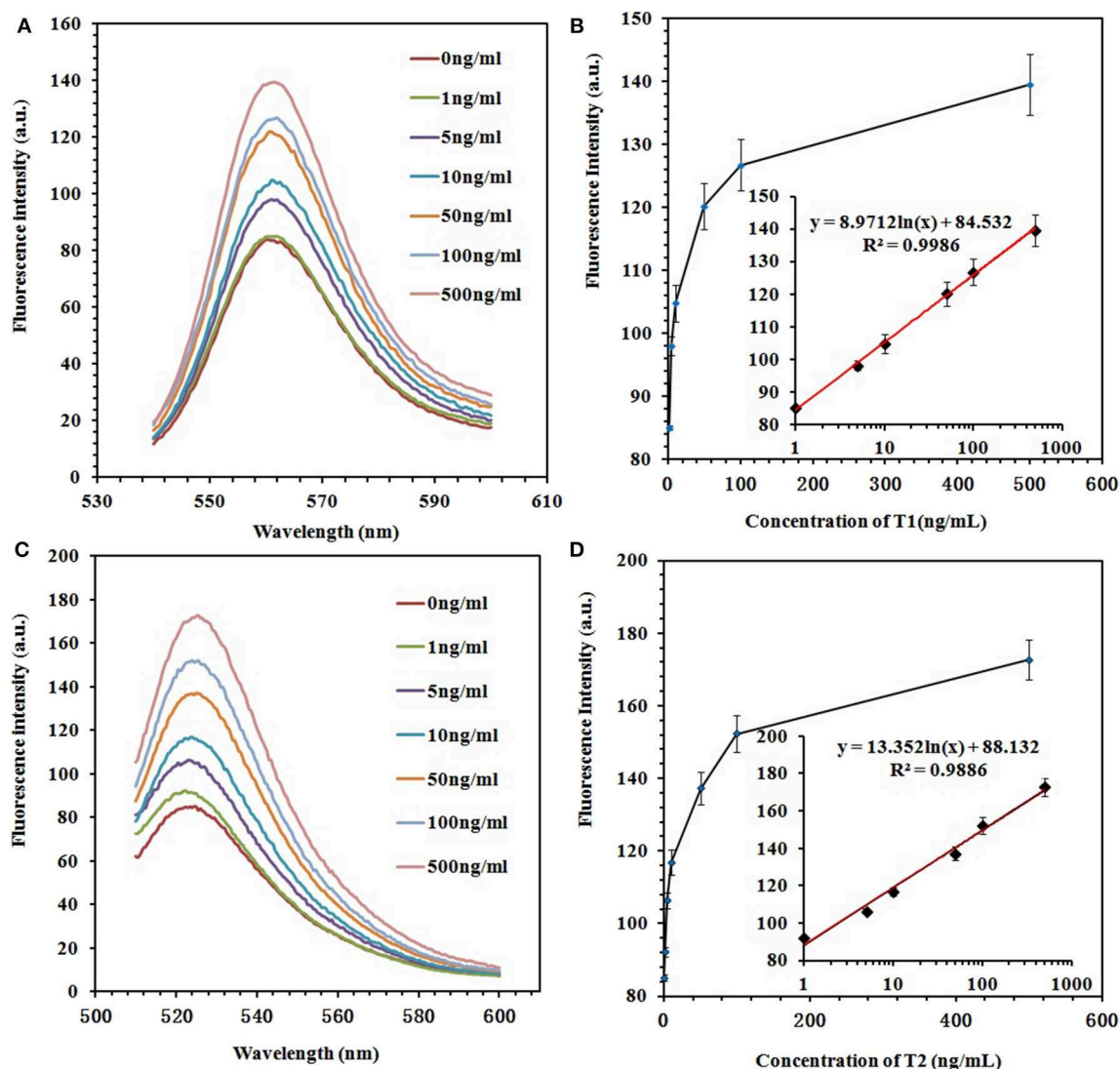


FIGURE 5 | (A) Fluorescence emission spectra of the GO-APT1 complex (30 μg/ml; 20 nM) in the presence of ZEN (0, 1, 5, 10, 50, 100, and 500 ng/ml). **(B)** Calibration plot of ZEN with a concentration range of 1–500 ng/ml. **(C)** Fluorescence emission spectra of the GO-APT2 complex (30 μg/ml; 20 nM) in the presence of OTA (0, 1, 5, 10, 50, 100, and 500 ng/ml). **(D)** Calibration plot of OTA with a concentration range of 1–500 ng/ml.

successfully hidden by GO. In this procedure, GO played a role as a two-dimensional monoatomic layer platform and information cover. As we all know, a lock can only be opened by the correct key. In other words, the state of encrypted information would not change if there is no key or the correct key. Then, APT1 could specifically recognize ZEN, and APT2 could specifically recognize OTA. Therefore, the dual targets could be defined as the key to release the aptamer from GO and obtain the hidden information. The hidden information of APT1 could only be recovered by ZEN. Similarly, the hidden information of APT2 could only be recovered by OTA. The hidden double information of APT1 and APT2 could be recovered by ZEN and OTA. Thus, the key possessed high specificity for revealing the concealed information due to the high specificity of the aptamer to the target.

On a steganography foundation, the base sequences of the aptamer were further encrypted using complicated cipher texts. There are four possibilities (A, T, G, and C) for each DNA base position: the more bases of DNA there are, the higher the information density. We can use a few adjacent bases to represent letters or numbers and to further express the true information behind complicated cipher texts. Therefore, we can utilize information steganography and encryption technology to develop a dual-insurance method for information security.

CONCLUSION

We designed a graphene-based steganographic aptasensor for multifunctional applications, simultaneous fluorescence detection of toxins (ZEN and OTA) of biofilm, and information

computing, encryption, and concealment. Our constructed easy-to-use and efficient sensing platform for the simultaneous detection of ZEN and OTA may have wide application value in

food and feed security monitoring. According to the change in materials and fluorescence, this graphene-based steganographic aptasensor can be utilized as a DNA-based encryption and concealment system for strengthening information security. This information steganographic system used an aptamer as an information carrier, GO as a cover, and targets as special keys. In summary, not only does our work offer a convenient simultaneous detection prototype for varied mycotoxins in foodstuff and feed safety monitoring, but our proposed model of

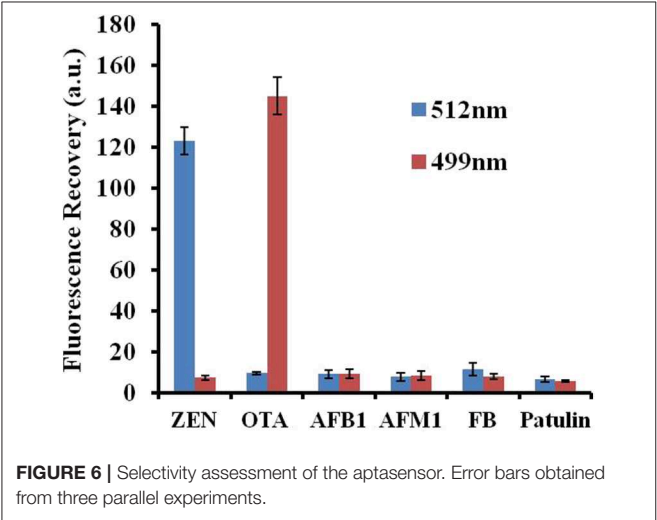
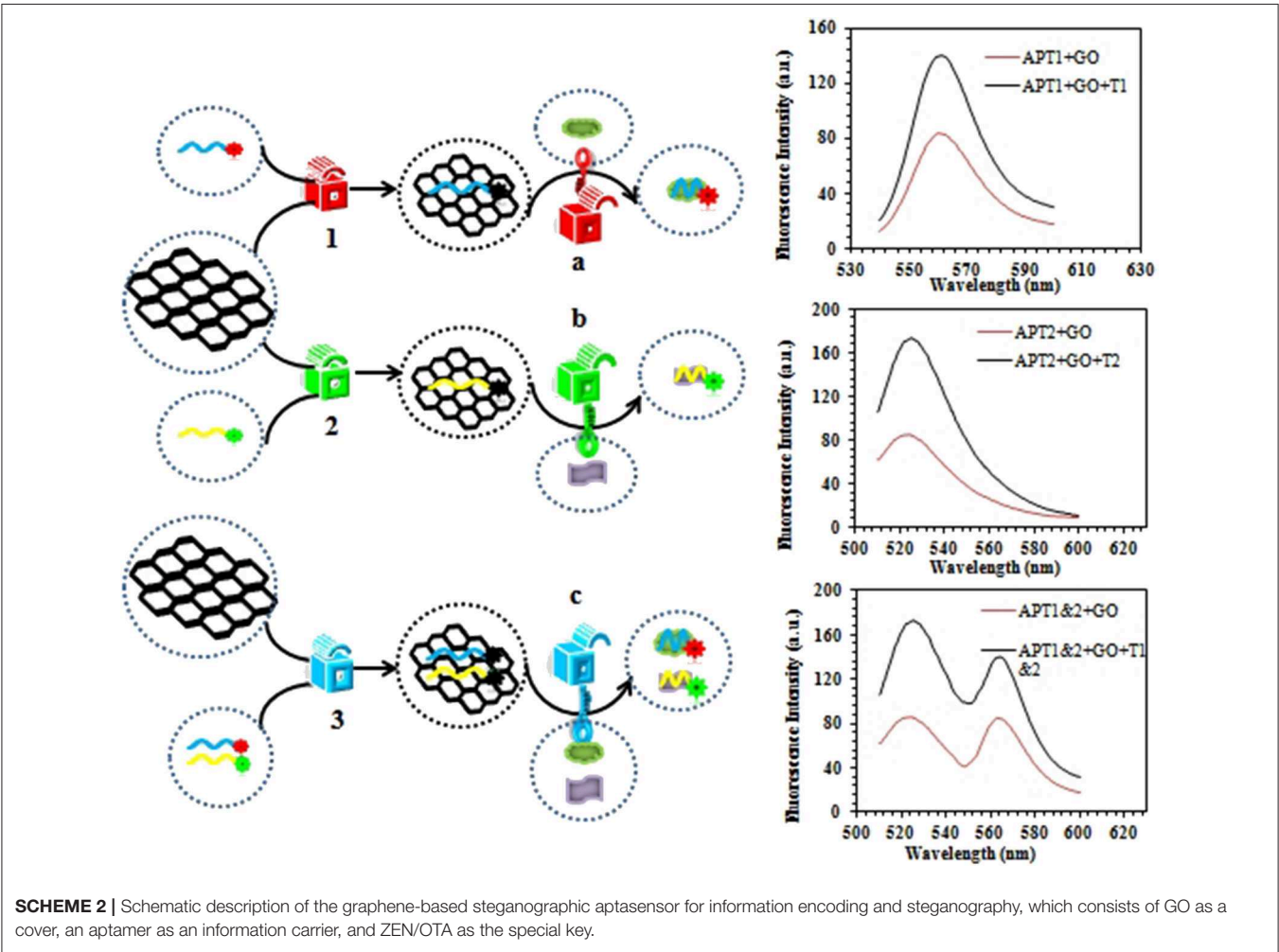


TABLE 2 | Real measurements of ZEN and OTA at different concentrations in wine samples.

Wine sample	Added (ng/ml)	Founded (ng/ml)	Recovery (%)
ZEN	1	0.89 ± 0.003	89
	4	3.85 ± 0.010	96.25
	16	15.95 ± 0.027	99.89
OTA	1	0.92 ± 0.007	92
	4	3.67 ± 0.015	91.75
	16	16.57 ± 0.039	103.56



a graphene-based steganographic aptasensor is also helpful for developing a molecular computer and information encryption and concealment technology.

DATA AVAILABILITY STATEMENT

The raw data supporting the conclusions of this article will be made available by the authors, without undue reservation, to any qualified researcher.

AUTHOR CONTRIBUTIONS

WW and QY were responsible for the conceptualization of the study, funding acquisition and the original draft. QW was responsible for the method, data acquisition, curation and analysis.

REFERENCES

- Ejike, C. E. C. C., Collins, S. A., Balasuriya, N., Swanson, A. K., Mason, B., and Udenigwe, C. C. (2017). DNA Fountain enables a robust and efficient storage architecture. *Trends Food Sci. Technol.* 355, 950–954. doi: 10.1126/science.aaj2038
- Galié, S., García-Gutiérrez, C., Miguélez, E. M., Villar, C. J., and Lombó, F. (2018). Biofilms in the food industry: health aspects and control methods. *Front. Microbiol.* 9:898. doi: 10.3389/fmicb.2018.00898
- Hermann, T., and Patel, D. J. (2000). Adaptive recognition by nucleic acid aptamers. *Science* 287, 820–825. doi: 10.1126/science.287.5454.820
- Hussein, H. S., and Brasel, J. M. (2001). Toxicity, metabolism, and impact of mycotoxins on humans and animals. *Toxicology* 167, 101–134. doi: 10.1016/S0300-483X(01)00471-1
- Jayasena, S. D. (1999). Aptamers: an emerging class of molecules that rival antibodies in diagnostics. *Clin. Chem.* 45, 1628–1650.
- Kim, J., Park, S. J., and Min, D. H. (2017). Emerging approaches for graphene oxide biosensor. *Anal. Chem.* 89, 232–248. doi: 10.1021/acs.analchem.6b04248
- Li, P., Zhang, Z., Hu, X., and Zhang, Q. (2013). Advanced hyphenated chromatographic-mass spectrometry in mycotoxin determination: current status and prospects. *Mass Spectrom. Rev.* 32, 420–452. doi: 10.1002/mas.21377
- Liu, X. Q., Aizen, R., Freeman, R., Yehezkeili, O., and Willner, I. (2012). Multiplexed aptasensors and amplified DNA sensors using functionalized graphene oxide: application for logic gate operations. *ACS Nano* 6, 3553–3563. doi: 10.1021/nn300598q
- Lopez, R., Chen, Y. J., Dumas, S., Yekhanin, A. S., Makarychev, K., Rac, M. Z., et al. (2019). DNA assembly for nanopore data storage readout. *Nat. Commun.* 10:2933. doi: 10.1038/s41467-019-10978-4
- McKeague, M., Velu, R., Hill, K., Bardóczy, V., Mészáros, T., and DeRosa, M. C. (2014). Selection and characterization of a novel DNA aptamer for label-free fluorescence biosensing of ochratoxin A. *Toxins* 6, 2435–2452. doi: 10.3390/toxins6082435
- Pehlivan, Z. S., Torabfām, M., Kurt, H., Ow-Yang, C., Hildebrandt, N., and Yüce, M. (2019). Aptamer and nanomaterial based FRET biosensors: a review on recent advances (2014–2019). *Microchim. Acta* 186, 563–585. doi: 10.1007/s00604-019-3659-3
- Qian, Z., Shan, X., Chai, L., Chen, J., and Feng, H. (2015). A fluorescent nanosensor based on graphene quantum dots-aptamer probe and graphene oxide platform for detection of lead (II) ion. *Biosens. Bioelectron.* 68, 225–231. doi: 10.1016/j.bios.2014.12.057
- Rong, X., Sun-Waterhouse, D., Wang, D., Jiang, Y., Li, F., Chen, Y., et al. (2019). The significance of regulatory microRNAs: their roles in toxicodynamics of mycotoxins and in the protection offered by dietary therapeutics against mycotoxin-induced toxicity. *Compr. Rev. Food Sci. Food Saf.* 18, 48–66. doi: 10.1111/1541-4337.12412

FUNDING

This work was supported by the National Key Research and Development Programme under grant no. 2016YFD0400105, Breeding Plan of Shandong Provincial Qingchuang Research Team (2019), National Natural Science Foundation of China under grant no. 81703228, National Science Foundation of Shandong Province under grant no. ZR2016CQ10, and China Postdoctoral Science Foundation under grant no. 2019M652320.

SUPPLEMENTARY MATERIAL

The Supplementary Material for this article can be found online at: <https://www.frontiersin.org/articles/10.3389/fmicb.2019.03139/full#supplementary-material>

- Sun, A. L., Zhang, Y. F., Sun, G. P., Wang, X. N., and Tang, D. (2017). Homogeneous electrochemical detection of ochratoxin A in foodstuff using aptamer-graphene oxide nanosheets and DNase I-based target recycling reaction. *Biosens. Bioelectron.* 89(Pt 1), 659–665. doi: 10.1016/j.bios.2015.12.032
- Sun, X. D., Su, P., and Shan, H. (2017). Mycotoxin contamination of maize in China. *Compr. Rev. Food Sci. Food Saf.* 16, 835–849. doi: 10.1111/1541-4337.12286
- Turner, N. W., Subrahmanyam, S., and Piletsky, S. A. (2009). Analytical methods for determination of mycotoxins: a review. *Anal. Chim. Acta* 632, 168–180. doi: 10.1016/j.aca.2008.11.010
- Wang, S. Y., Wang, C. F., Lv, Y. K., and Shen, S. G. (2018). Fabrication of fluorescent biosensing platform based on graphene oxide-DNA and their application in biomolecule detection. *TrAC Trends Anal. Chem.* 106, 53–61. doi: 10.1016/j.trac.2018.07.004
- Wang, Y., Li, Z., Hu, D., Lin, C. T., and Lin, Y. (2010). Aptamer/graphene oxide nanocomplex for *in situ* molecular probing in living cells. *J. Am. Chem. Soc.* 132, 9274–9276. doi: 10.1021/ja103169v
- Wu, S., Duan, N., Ma, X., Xia, Y., Wang, H., Wang, Z., et al. (2012). Multiplexed fluorescence resonance energy transfer aptasensor between upconversion nanoparticles and graphene oxide for the simultaneous determination of mycotoxins. *Anal. Chem.* 84, 6263–6270. doi: 10.1021/ac301534w
- Wu, W., Jing, Z., Yu, X., Yang, Q., Sun, J., Liu, C., et al. (2019a). Recent advances in screening aquatic products for *Vibrio* spp. *TrAC Trends Anal. Chem.* 111, 239–251. doi: 10.1016/j.trac.2018.11.043
- Wu, W., Yu, C., Chen, J., and Yang, Q. (2019c). Fluorometric detection of copper ions using click chemistry and the target-induced conjunction of split DNzyme fragments. *Int. J. Environ. Anal. Chem.* 1–9. doi: 10.1080/03067319.2019.1636977
- Wu, W., Yu, C. D., Wang, Q., Zhao, F. Y., He, H., Liu, C. Z., et al. (2019b). Research advances of DNA aptasensors for foodborne pathogen detection. *Crit. Rev. Food Sci. Nutr.* doi: 10.1080/10408398.2019.1636763. [Epub ahead of print].
- Xu, Y., Dhaouadi, Y., Stoodley, P., and Ren, D. (2019). Sensing the unreachable: challenges and opportunities in biofilm detection. *Curr. Opin. Biotechnol.* 64, 79–84. doi: 10.1016/j.copbio.2019.10.009
- Yugender Goud, K., Hayat, A., Satyanarayana, M., Sunil Kumar, V., Catanante, G., Vengatajalabathy Gobi, K., et al. (2017). Aptamer-based zearalenone assay based on the use of a fluorescein label and a functional graphene oxide as a quencher. *Microchim. Acta* 184, 4401–4408. doi: 10.1007/s00604-017-2487-6
- Zhang, S., Ma, L., Ma, K., Xu, B., Liu, L. J., and Tian, W. J. (2018a). Label-free aptamer-based biosensor for specific detection of chloramphenicol using AIE probe and graphene oxide. *ACS Omega* 3, 12886–12892. doi: 10.1021/acsomega.8b01812
- Zhang, Y., Lu, T., Wang, Y., Diao, C., Zhou, Y., Zhao, L., et al. (2018b). Selection of a dna aptamer against zearalenone and docking analysis for highly sensitive

- rapid visual detection with a label-free aptasensor. *J. Agric. Food Chem.* 66:12102–12110. doi: 10.1021/acs.jafc.8b03963
- Zhang, Y., Wang, Z., Wang, Z., Liu, X., and Yuan, X. (2017). A DNA-based encryption method based on two biological axioms of DNA chip and polymerase chain reaction (PCR) amplification techniques. *Chemistry* 23, 13387–13403. doi: 10.1002/chem.201701411
- Zhao, Y., Zheng, F., Ke, W., Zhang, W., Shi, L., and Liu, H. (2019). Gap-Tethered Au@AgAu raman tags for the ratiometric detection of MC-LR. *Anal. Chem.* 91, 7162–7172. doi: 10.1021/acs.analchem.9b00348
- Zhou, C., Zou, H., Sun, C., Ren, D., Chen, J., and Li, Y. (2018). Signal amplification strategies for DNA-based surface plasmon resonance biosensors. *Biosens. Bioelectron.* 117, 678–689. doi: 10.1016/j.bios.2018.06.062
- Zhou, Z. M., Feng, Z., Zhou, J., Fang, B. Y., Qi, X. X., Ma, Z. Y., et al. (2015). Capillary electrophoresis-chemiluminescence detection for carcino-embryonic antigen based on aptamer/graphene oxide structure. *Biosens. Bioelectron.* 64, 493–498. doi: 10.1016/j.bios.2014.09.050
- Zhu, Q. Y., Zhang, F. R., Du, Y., Zhang, X. X., Lu, J. Y., Yao, Q. F., et al. (2019). Graphene-based steganographically aptasensing system for information computing, encryption and hiding, fluorescence sensing and *in vivo* imaging of fish pathogens. *ACS Appl. Mater. Interfaces* 11, 8904–8914. doi: 10.1021/acsami.8b22592
- Conflict of Interest:** The authors declare that the research was conducted in the absence of any commercial or financial relationships that could be construed as a potential conflict of interest.
- Copyright © 2020 Wang, Yang and Wu. This is an open-access article distributed under the terms of the Creative Commons Attribution License (CC BY). The use, distribution or reproduction in other forums is permitted, provided the original author(s) and the copyright owner(s) are credited and that the original publication in this journal is cited, in accordance with accepted academic practice. No use, distribution or reproduction is permitted which does not comply with these terms.



Stress Response of *Vibrio parahaemolyticus* and *Listeria monocytogenes* Biofilms to Different Modified Atmospheres

Hui Qian¹, Wei Li¹, Linxia Guo¹, Ling Tan¹, Haiquan Liu^{1,2,3,4}, Jingjing Wang^{1,2,3*}, Yingjie Pan^{1,2,3} and Yong Zhao^{1,2,3*}

¹ College of Food Science and Technology, Shanghai Ocean University, Shanghai, China, ² Laboratory of Quality and Safety Risk Assessment for Aquatic Products on Storage and Preservation (Shanghai), Ministry of Agriculture, Shanghai, China, ³ Shanghai Engineering Research Center of Aquatic-Product Processing and Preservation, Shanghai, China, ⁴ Engineering Research Center of Food Thermal-Processing Technology, Shanghai Ocean University, Shanghai, China

OPEN ACCESS

Edited by:

Zhenbo Xu,
University of Maryland, Baltimore,
United States

Reviewed by:

Huhu Wang,
Nanjing Agricultural University, China
Qingli Dong,
University of Shanghai for Science
and Technology, China

*Correspondence:

Jingjing Wang
jjwang@shou.edu.cn
Yong Zhao
yzhao@shou.edu.cn

Specialty section:

This article was submitted to
Food Microbiology,
a section of the journal
Frontiers in Microbiology

Received: 20 October 2019

Accepted: 07 January 2020

Published: 20 February 2020

Citation:

Qian H, Li W, Guo L, Tan L, Liu H,
Wang J, Pan Y and Zhao Y (2020)
Stress Response of *Vibrio*
parahaemolyticus and *Listeria*
monocytogenes Biofilms to Different
Modified Atmospheres.
Front. Microbiol. 11:23.
doi: 10.3389/fmicb.2020.00023

The sessile biofilms of *Vibrio parahaemolyticus* and *Listeria monocytogenes* have increasingly become a critical threat in seafood safety. This study aimed to evaluate the effects of modified atmospheres on the formation ability of *V. parahaemolyticus* and *L. monocytogenes* biofilms. The stress responses of bacterial biofilm formation to modified atmospheres including anaerobiosis (20% carbon dioxide, 80% nitrogen), micro-aerobiosis (20% oxygen, 80% nitrogen), and aerobiosis (60% oxygen, 40% nitrogen) were illuminated by determining the live cells, chemical composition analysis, textural parameter changes, expression of regulatory genes, etc. Results showed that the biofilm formation ability of *V. parahaemolyticus* was efficiently decreased, supported by the fact that the modified atmospheres significantly reduced the key chemical composition [extracellular DNA (eDNA) and extracellular proteins] of the extracellular polymeric substance (EPS) and negatively altered the textural parameters (biovolume, thickness, and bio-roughness) of biofilms during the physiological conversion from anaerobiosis to aerobiosis, while the modified atmosphere treatment increased the key chemical composition of EPS and the textural parameters of *L. monocytogenes* biofilms from anaerobiosis to aerobiosis. Meanwhile, the expression of biofilm formation genes (*luxS*, *aphA*, *mshA*, *oxyR*, and *opaR*), EPS production genes (*cpsA*, *cpsC*, and *cpsR*), and virulence genes (*vopS*, *vopD1*, *vcrD1*, *vopP2β*, and *vcrD2β*) of *V. parahaemolyticus* was downregulated. For the *L. monocytogenes* cells, the expression of biofilm formation genes (*flgA*, *flgU*, and *degU*), EPS production genes (*lmo2554*, *lmo2504*, *inlA*, *rmlB*), and virulence genes (*vopS*, *vopD1*, *vcrD1*, *vopP2β*, and *vcrD2β*) was upregulated during the physiological conversion. All these results indicated that the modified atmospheres possessed significantly different regulation on the biofilm formation of Gram-negative *V. parahaemolyticus* and Gram-positive *L. monocytogenes*, which will provide a novel insight to unlock the efficient control of Gram-negative and Gram-positive bacteria in modified-atmosphere packaged food.

Keywords: stress response, *Vibrio parahaemolyticus*, *Listeria monocytogenes*, modified atmospheres, biofilms, extracellular polymeric substance, gene expression

INTRODUCTION

Vibrio parahaemolyticus and *Listeria monocytogenes* are important facultative and food-borne pathogens in the food industry (Xu et al., 2015; Vazquez-Boland et al., 2017; Chimalapati et al., 2018). In 2014, 605 cases of *V. parahaemolyticus* infections in the United States were reported according to the Cholera and Other Vibrio Illness Surveillance (Centers for Disease Control and Prevention [CDC], 2014). Meanwhile, 675 listeriosis cases were reported in 47 states and the District of Columbia (Centers for Disease Control and Prevention [CDC], 2014). In China, 71 outbreaks of *V. parahaemolyticus* in Zhejiang Province were monitored from 2010 to 2014, resulting in 933 illnesses and 117 hospitalizations (Chen et al., 2017). For listeriosis, 253 invasive cases are reported from 2011 to 2016 in 19 provinces (Li W. et al., 2018).

In natural environments, the formation of bacterial biofilms is the prevailing microbial lifestyle (Watnick and Kolter, 2000). Biofilms are complex communities of microorganisms attached to surfaces and enclosed in firm three-dimensional, multicellular, complex, and self-assembled extracellular polymeric substances (EPS) [exopolysaccharides, proteins, extracellular DNA (eDNA), etc.] (Lamas et al., 2016; Han et al., 2017). EPS immobilizes biofilm cells, which facilitates their intense interactions including intercellular communication, horizontal gene transfer, and the formation of synergistic microconsortia (Flemming and Wingender, 2010). In addition, EPS contributes to the initial attachment and nutrient capture of bacteria and the integrity of the biofilm structures (Han et al., 2017; Tan et al., 2018). Meanwhile, EPS has been demonstrated to have good resistance to different environmental stresses including disinfectants, desiccation, salinity, temperature, heavy metal pollution, etc. (Xue et al., 2012; Blanco et al., 2019).

During recent decades, there is increasing evidence indicating that biofilms are involved in contaminating food processing equipment and food products (Brooks and Flint, 2008), including *V. parahaemolyticus* and *L. monocytogenes*. For *V. parahaemolyticus*, it can form biofilms on various biotic or abiotic surfaces such as oysters, stainless steel (SS), etc. (Mizan et al., 2016). Moreover, the pathogenic strains of *V. parahaemolyticus*, on average, formed more biofilm than non-pathogenic strains at all tested temperatures (Song et al., 2016). Additionally, *V. parahaemolyticus* formed the highest amount of biofilms at 2% NaCl and the least biofilm at 5% NaCl (Mizan et al., 2018). For *L. monocytogenes*, when bacteriocin from *L. plantarum* ST8SH, vancomycin (antimicrobial), propolis (a natural antimicrobial product), and EDTA (chelating agent) are used individually or combined, the formation of bacterial biofilms will be inhibited in different degrees (Todorov et al., 2018). Different strains differ in their biofilm formation ability, which is closely linked with the resistance of *L. monocytogenes* to antimicrobials in food processing environments (Pan et al., 2009; van der Veen and Abee, 2010). The study suggests that EDTA influences biofilm formation by affecting the initial adherence of *L. monocytogenes* onto abiotic surfaces (Chang et al., 2012).

For *Vibrio*, extracellular nucleases (Xds and Dns) control the level of eDNA and are involved in multiple processes including

the development of a typical three-dimensional biofilm structure (Seper et al., 2011). The exogenous addition of extracellular flagellin-homologous proteins (rFHPs) significantly increased the biofilm formation of *V. parahaemolyticus*, reaching ~3.8-fold compared to control (Jung et al., 2019). For timely expression of EPS under specific conditions, bacterial cells utilize diverse signal recognition systems and subsequent regulatory mechanisms, such as quorum sensing and cyclic di-GMP (c-di-GMP) (Jung et al., 2019). CpsQ is a c-di-GMP-binding transcription factor that activates the expression of capsular polysaccharide (CPS) genes, thereby inducing biofilm development in *V. parahaemolyticus* (Zhou et al., 2013). For *L. monocytogenes*, all genes of the *pssA-E* operon and a separately located *pssZ* gene are required for exopolysaccharide production. Under environmental conditions, eDNA of *L. monocytogenes* is released by lysate bacteria, which enhances the initial attachment and formation of biofilm (Colagiorgi et al., 2016). Meanwhile, the bacterial surface or extracellular proteins have been shown to be responsible for the induction of biofilm formation (Kayal and Charbit, 2006; Franciosa et al., 2009; Colagiorgi et al., 2016).

The expression of genes related to bacterial biofilm plays a key role in biofilm formation. Flagella and other filamentous structures regulated by related genes have clearly been shown to contribute to the initial approach, attachment, and efficient biofilm formation on surfaces (Kirov, 2003). The bacterial gene expression regulated by quorum sensing is caused by small molecules called autoinducers, allowing bacteria to adapt efficiently to environmental conditions during growth (Lamas et al., 2016). For *V. parahaemolyticus*, the quorum-sensing genes including *opaR* and *luxS* play a critical role in the biofilm formation. Additionally, the *cpsA* and *cpsC* gene-regulated secretion of CPS is associated with the adhesion ability of *V. parahaemolyticus* (Hsieh et al., 2003).

The stress response (such as oxygen starvation stress, etc.) is an adaptive strategy for bacteria, which allows them to rapidly cope with changing environmental conditions and ensure their survival (Schimel et al., 2007; Alvarez-Ordóñez et al., 2015). When the modified atmospheres act on bacteria, they are able to maintain viability by regulating certain genes (Alvarez-Ordóñez et al., 2015). Previous studies found that *V. parahaemolyticus* and *L. monocytogenes* could grow under aerobic and anaerobic conditions (Gomez-Gil et al., 2003; Valimaa et al., 2015). However, the modified atmosphere packaging (MAP) also dramatically reduced the growth of Gram-negative bacteria including *Vibrio* spp. (Paludan-Müller et al., 1998). In addition, the Gram-positive *L. monocytogenes* were inhibited under all MAP compositions [(1): 40% CO₂/55% N₂/5% O₂, (2): 60% CO₂/40% N₂, and (3): 50% CO₂/50% N₂] (Arvanitoyannis et al., 2011). Therefore, the modified atmospheres are an important way of affecting the growth of Gram-negative and Gram-positive bacteria.

The biofilm formation ability of *V. parahaemolyticus* and *L. monocytogenes* in multiple conditions (temperatures, nutrients, contact surface, or pH) has been well studied in previous studies (Di Bonaventura et al., 2008; Nilsson et al., 2011; Bonsaglia et al., 2014; Song et al., 2016). However, few studies paid attention to the stress responses of the biofilm

formation of *V. parahaemolyticus* and *L. monocytogenes* to the modified atmospheres. On this basis, the aim of this study was to evaluate the biofilm formation of *V. parahaemolyticus* and *L. monocytogenes* under the stress of different modified atmospheres including anaerobiosis (20% carbon dioxide, 80% nitrogen), micro-aerobiosis (20% oxygen, 80% nitrogen), and aerobiosis (60% oxygen, 40% nitrogen), by determining the changes in the EPS, structural parameters, and the related regulatory genes. The present study will provide a novel insight to unlock the efficient control of Gram-negative and Gram-positive bacteria in modified-atmosphere packaged food.

MATERIALS AND METHODS

Bacterial Strains and Culture Conditions

Four-strain cocktails of *V. parahaemolyticus* strains (VP-S36, VP-39, VP-49, and VP-54) were used (Li et al., 2017). Meanwhile, four-strain cocktails of *L. monocytogenes* strains (NO.12, NO.14, NO.51, and NO.66) were used. All of the genotypes and origins of each strain are listed in **Table 1**. Strains of *V. parahaemolyticus* were stored at -80°C in tryptic soy broth (TSB, Land Bridge Technology, China) with 50% (v/v) glycerol. And the four *L. monocytogenes* strains in Brain Heart Infusion (BHI) with 50% glycerol were stored at -80°C . Before every experiment, frozen cells of *V. parahaemolyticus* were streaked on thiosulfate citrate bile salts sucrose agar (TCBS agar, Land Bridge Technology, Beijing, China), and *L. monocytogenes* were streaked on PALCAM medium base (Land Bridge Technology, Beijing, China). After that, the working solutions of *V. parahaemolyticus* and *L. monocytogenes* were incubated in TSB (Beijing Land Bridge Technology Company Ltd., Beijing, China) at 37°C for approximately 12 h and with shaking at 200 r/min. Subsequently, the cultures of *V. parahaemolyticus* and *L. monocytogenes* were diluted by TSB to acquire a bacteria population of 8 log CFU/ml.

TABLE 1A | The genotype and origins of *Vibrio parahaemolyticus* used in this study.

Strains	Genotype	Origin
VP-S36	<i>tdh</i> ⁻ / <i>trh</i> ⁻ / <i>tli</i> ⁺	Shrimp
VP-C39	<i>tdh</i> ⁺ / <i>trh</i> ⁺ / <i>tli</i> ⁺	CDC
VP-C49	<i>tdh</i> ⁺ / <i>trh</i> ⁺ / <i>tli</i> ⁺	Clinical isolation
VP-C54	<i>tdh</i> ⁺ / <i>trh</i> ⁺ / <i>tli</i> ⁺	Clinical isolation

TABLE 1B | The genotype and origins of *Listeria monocytogenes* used in this study.

Strains	Genotype	Origin	Number
NO.12	1/2a	Raw pork	4bLM
NO.14	1/2a	Human	ATCC 7644
NO.51	4b	Spinal fluid of child with meningitis	ATCC 13932
NO.66	4b	Human	ATCC 19115

Biofilm Formation in Different Modified Atmosphere Conditions

Biofilm formation of *V. parahaemolyticus* and *L. monocytogenes* cocktails was carried out as described previously (Song et al., 2016; Han et al., 2017) with minor modifications. Static biofilms were grown in 24-well polystyrene microtiter plates (Sangon Biotech Co., Ltd., Shanghai, China). Ten microliters of the obtained *V. parahaemolyticus* and *L. monocytogenes* solutions was added into 990 μl fresh TSB medium, respectively. And then, the OD_{600nm} values of these two mixtures were determined to be 0.061 and 0.053, respectively. Finally, the bacterial solutions were employed to form biofilms. And each 24-well polystyrene microtiter plate was transferred to sterile sampling bags (32*20 cm) with poor atmosphere permeability (Qingdao Hope Bio-Technology Co., Ltd., Qingdao, China), which were packed by an external vacuum inflatable packaging machine (Qingpa Food Packaging Machinery Co., Ltd., Shanghai, China) under three different atmosphere conditions: anaerobiosis (20% carbon dioxide, 80% nitrogen), micro-aerobiosis (20% oxygen, 80% nitrogen), and aerobiosis (60% oxygen, 40% nitrogen), and then sealed with thermoplastic, respectively. Subsequently, the 24-well plates of *V. parahaemolyticus* cocktail were incubated at 25°C statically to form biofilms for 48 h, and the *L. monocytogenes* cocktail was incubated at 37°C statically to form biofilms for 72 h.

Crystal Violet Staining Method

Biofilm production was quantified by using the crystal violet staining method as described previously (Han et al., 2017; Tan et al., 2018) with some modifications. After incubation, the supernatant of the plates' wells was discarded, these plates were gently washed three times with 1 ml of 0.01 M phosphate buffer (PBS, pH 7.4) to remove planktonic cells, and then the microtiter plates were put into the electric blast drying oven for about 20 min and stained with 1 ml of 0.1% (w/v) crystal violet (Sangon Biotech Co., Ltd., Shanghai, China) for 30 min at room temperature. The plates were then gently washed three times with PBS (Sangon Biotech Co., Ltd., Shanghai, China) to remove excess crystal violet. The next step was to dissolve the crystal violet-stained biofilm with 1 ml 95% ethanol for 30 min. Biofilm was solubilized using 1 ml of 95% ethanol (Sinopharm Chemical Reagent Co., Ltd., Shanghai, China) for 30 min. The optical density of each well was measured at a wavelength of 600 nm (Han et al., 2017). All assays were performed in triplicate in three independent experiments. And at least 12 wells were tested in each experiment.

Visualization of the Biofilms Using Confocal Laser Scanning Microscopy

Before the experiment of cultivating biofilm, a sterile glass slide (1.4 cm in diameter) also needed to be placed into the wells of the 24-well microtiter plates. The culture process of biofilms is as described above. The biofilms of *V. parahaemolyticus* and *L. monocytogenes* cocktails for confocal laser scanning microscopy (CLSM) were pre-treated based on the method of Han et al. (2017). Subsequently, the next step is to add the corresponding bacterial solution and fresh culture medium and

then incubate them following the previous experiment of biofilm formation conditions. After static incubation, the biofilms of *V. parahaemolyticus* and *L. monocytogenes* formed on the sterile glass, and then the plates were washed three times with 1 ml of 0.01 M PBS. Next, the plates were fixed with 4% glutaraldehyde (Sangon Biotech Co., Ltd., Shanghai, China) at 4°C for 30 min. Then, the biofilms were gently rinsed three times with 1 ml of 0.01 M PBS. Therefore, after the above operation, SYBR Green I (Sangon Biotech Co., Ltd., Shanghai, China) was used to stain the biofilms at room temperature and dark conditions for 30 min. Before removing the sterile glass from the plate, the plate needs to be washed three times with 1 ml of 0.01 M PBS. It may take about 20 min to air-dry the sterile glass before the end of the experiment. All microscopy images were captured and acquired using the CLSM machine (LSM710, Carl Zeiss AG, Germany). A 40 × objective was used to monitor SYBR Green I fluorescence excited at 488 nm and emitted at 500–550 nm. Then the most representative place was scanned to provide a stack of horizontal planar images with a z-step of 1 μm. In order to compare the change of the biofilms under different modified atmospheres, the CLSM images were performed by using the ISA-2 software (Professor Haluk Beyenal, Montana State University, United States) to determine the structural parameters [such as biovolume, mean thickness, bio-roughness, and textural entropy (TE)] of biofilms (Beyenal et al., 2004b). For each sample, the representative images of nine separate sites on the glass slide were randomly acquired.

Visualization of the Biofilms Using Scanning Electron Microscopy

The method of culturing bacterial biofilms is similar to that described above. The biofilms of *V. parahaemolyticus* and *L. monocytogenes* cocktails for CLSM were pre-treated based on the method of Han et al. (2017). Next, the plates were incubated to form bacterial biofilms. After static incubation, the biofilms were washed three times with 1 ml of 0.01 M PBS and then were fixed overnight with 2.5% glutaraldehyde at 4°C. Next, the biofilms were gently washed three times with 1 ml of sterile 0.01 M PBS. Then, the biofilms were dehydrated in an ascending acetonitrile series (30, 50, 70, 80, 90, and 100% twice for 10 min each). Samples were then dried and finally coated with a turbomolecular pumped sputter coater (Q150T ES PLUS, Quorum, United Kingdom). Subsequently, extreme-resolution analytical field emission SEM (JEOL JSM-7800F Prime, Japan) was used to observe the biofilms. The images were acquired for three independent replicates.

EPS Extraction and Chemical Analysis

Extracellular polymeric substance, which consists of bacterial biofilms, was extracted using the sonication method (Liu et al., 2007; Gong et al., 2009; Han et al., 2017). Firstly, the density of the planktonic cells of the suspended cultures was measured by a BioTek microplate reader at OD_{595nm}. Then, the planktonic cells were removed and discarded after washing three times with 1 ml of 0.01 M PBS. Afterward, the mature biofilms were collected and scrapped in 1 ml 0.01 M KCl solution.

The cells were sonicated by a sonicator (VCX 500, SONICS, Newtown, CT, United States) for four cycles of 5 s of run and 5 s of pause at a power level of 3.5 Hz. Afterward, the sonicated suspensions were centrifuged at 4°C, 4000 × g for 10 min, and the supernatant was then filtered through a 0.22 mm membrane filter (Sangon Biotech Co., Ltd., Shanghai, China). The amounts of protein, carbohydrate, and eDNA in the filtrate were analyzed. The eDNA was quantified by the Quanti-iT™ PicoGreen® dsDNA Reagent and Kits (Life Technologies, Shanghai, China) according to the manufacturer's instructions (Grande et al., 2015). For extracellular protein, it was quantified by the Stable Lowry Protein Assay Kit (Sangon Biotech Co., Ltd., Shanghai, China), and bovine serum albumin (BSA) was used as a protein standard to perform the calibration curve, which contains slightly more modifications compared with the Lowry method. A certain amount of extracellular polysaccharide in the filtrate was quantified by the phenol-sulfuric acid method (Kim and Park, 2013) and expressed as OD_{490nm}/OD_{595nm}. Each experiment was carried out at least three times.

Expression of Biofilm Formation, EPS, and Virulence-Related Genes

After the treatment of *V. parahaemolyticus* and *L. monocytogenes* biofilm under three modified atmospheric conditions, the total RNA was extracted using the Bacteria RNA Extraction Kit (Vazyme Biotech Co., Ltd., Nanjing, China) and quantified using a BioTek microplate reader. Total RNA was then resuspended in 50 μl of diethyl pyrocarbonate (DEPC)-treated water. RNA purity and integrity were assessed according to a previous study (Kim et al., 2016). Complementary DNA (cDNA) was reversely transcribed from 2 μl of total RNA using a HiScript® III RT SuperMix for qPCR (+ gDNA wiper) (Vazyme Biotech Co., Ltd., Nanjing, China). The qRT-PCR reactions were executed via a ChamQ™ Universal SYBR® qPCR Master Mix and carried out by a 7500 Fast Real-Time PCR system (Applied Biosystems, Waltham, MA, United States). All the primers were synthesized by Sangon Biotech (Shanghai, China). All qPCR reactions were performed in a total volume of 20 μl containing 10 μl of 2 × ChamQ Universal SYBR qPCR Master Mix (Vazyme Biotech Co., Ltd., China), 0.4 μl of 10 μM forward primer, 0.4 μl of 10 μM reverse primer, 2 μl of cDNA, and 7.2 μl of deionized water. Cycling parameters for qPCR included an initial denaturation at 95°C for 5 min, followed by 35 cycles of 95°C for 30 s, 58°C for 30 s, and primer extension at 72°C for 30 s. The fluorescent products were detected after the extension step of each cycle. The changes in relative gene expression were calculated with the $2^{-\Delta\Delta CT}$ method. Primers used in this study for the detection of *V. parahaemolyticus* and *L. monocytogenes* are listed in Table 2. Genes 1–14 in Table 2 belong to *V. parahaemolyticus*, and genes 15–26 belong to *L. monocytogenes*. Each experiment was carried out at least three times.

Statistical Analysis

The experimental data were expressed as the mean ± standard deviation. Analysis of one-way ANOVA was used to compare the

TABLE 2 | Primer sequences of the RT-qPCR assay.

Number	Gene	Primer name	Primer sequence (5'-3')	References
1.	<i>recA</i>	<i>recA</i> -F	GCTAGTAGAA AAAGCGGGTG	Ma et al., 2015
		<i>recA</i> -R	GCAGGTGCTTC TGGTTGAG	
2.	<i>oxyR</i>	<i>oxyR</i> -F	TCGTGAGCT AGAGGAAGG	Chung et al., 2016
		<i>oxyR</i> -R	TGGTCGCGT AAGCAATGC	
3.	<i>aphA</i>	<i>aphA</i> -F	ACACCCAACCGT TCGTGATG	Wang et al., 2013
		<i>aphA</i> -R	GTTGAAGGCG TTGCGTAGTAAG	
4.	<i>luxS</i>	<i>luxS</i> -F	GATGGGATGTC GCACTGGTTT	Wang et al., 2014
		<i>luxS</i> -R	ACTTGCTGTT CAGAAGGCGTA	
5.	<i>opaR</i>	<i>opaR</i> -F	TGTCTACCAAC CGCACTAACC	Zhang et al., 2016
		<i>opaR</i> -R	GCTCTTTCAAC TCGGCTTCAC	
6.	<i>mshA</i>	<i>mshA</i> -F	GGTTTCGT TTAGGTCACG	Shime-Hattori et al., 2006
		<i>mshA</i> -R	CGTCGAAATG TCGGCGG	
7.	<i>cpsA</i>	<i>cpsA</i> -F	GCGCACAACGAAG AATATCG	This study
		<i>cpsA</i> -R	CCATCTTATC GAGCGTGTCG	
8.	<i>cpsC</i>	<i>cpsC</i> -F	TCGACCAGGACT GACGATAGAA	This study
		<i>cpsC</i> -R	AACCGTGCGC TGCATACTTA	
9.	<i>cpsR</i>	<i>cpsR</i> -F	CCAATATGCG AACGGACTCA	This study
		<i>cpsR</i> -R	AGCACGCCAAG AGACGGTAT	
10.	<i>vcrD1</i>	<i>vcrD1</i> -F	AAGGTAGGGC AACGCAAAGA	Ding et al., 2016
		<i>vcrD1</i> -R	AGCAGCACGAC AGCAATACT	
11.	<i>vopS</i>	<i>vopS</i> -F	TAGAACGCGATTA CCGTGGG	Ding et al., 2016
		<i>vopS</i> -R	TTACCGAGGT CTTTGTCCGC	
12.	<i>vopD1</i>	<i>vopD1</i> -F	GCGGGTGCACT AAAAAGCAA	Ding et al., 2016
		<i>vopD1</i> -R	AAGCTCACCCA TCAGTTTCG	
13.	<i>vcrD2β</i>	<i>vcrD2β</i> -F	AGAGAGTTTGGGG ACAAGCG	Ding et al., 2016
		<i>vcrD2β</i> -R	CCTTCAGCCG AGCTTTGAGA	
14.	<i>vopP2β</i>	<i>vopP2β</i> -F	AGAAGGCGGG GTAAATGCT	Ding et al., 2016
		<i>vopP2β</i> -R	ACCTCCGCAACC TAAGTTCA	

(Continued)

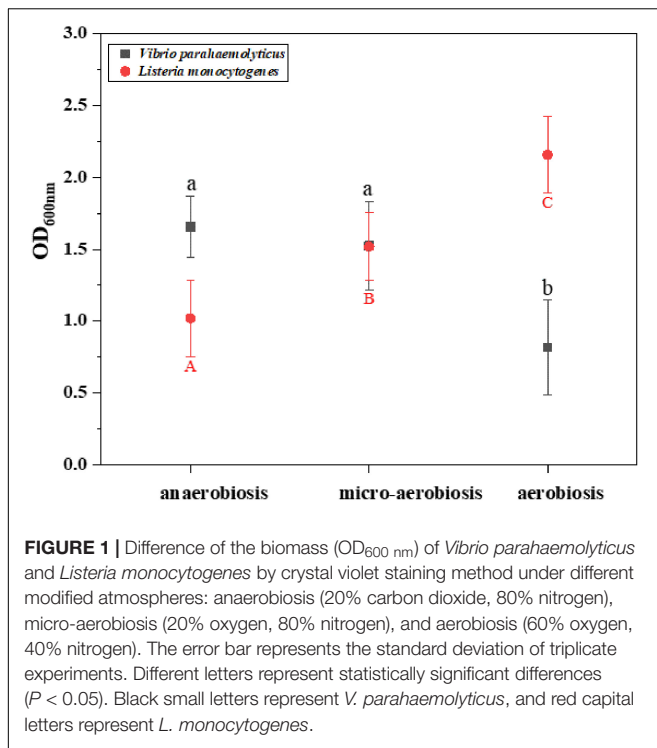
TABLE 2 | Continued

Number	Gene	Primer name	Primer sequence (5'-3')	References
15.	<i>Gap</i>	<i>Gap</i> -F	AAAGCTGGCGCTA AAAAAGTTG	Mattila et al., 2011
		<i>Gap</i> -R	TTCATGGTTTACATT GTAACGATTG	
16.	<i>flaA</i>	<i>flaA</i> -F	GAAGGCATGACTC AAGCGCA	This study
		<i>flaA</i> -R	GCAAGACCAGCAG CGTCATC	
17.	<i>flgE</i>	<i>flgE</i> -F	CAGCAGGTTCC CCGACTTC	This study
		<i>flgE</i> -R	CGGCCTTGTA GTGCTGCAT	
18.	<i>degU</i>	<i>degU</i> -F	GGAGGAGTAGTCA TTATGGC	This study
		<i>degU</i> -R	ACTTCTGGTTG TTGGTAGCC	
19.	<i>inlA</i>	<i>inlA</i> -F	AAGTGACGTAAGCT CACTTGC	This study
		<i>inlA</i> -R	TGTTGGTGGTG TAGGTTCTTG	
20.	<i>plcA</i>	<i>plcA</i> -F	TTAGCGAGAAC GGGACCAT	This study
		<i>plcA</i> -R	CCTTCAGCCG AGCTTTGAGA	
21.	<i>lmo2504</i>	<i>lmo2504</i> -F	CGCTAAGAGTGTC CGCTGTTG	This study
		<i>lmo2504</i> -R	TGGCCTCCACCGG AACTTAC	
22.	<i>lmo2554</i>	<i>lmo2554</i> -F	AAAGGCGACGAT GGTCTGTC	This study
		<i>lmo2554</i> -R	ACATTTGCGAC ACACAGGGT	
23.	<i>rmlB</i>	<i>rmlB</i> -F	TATTTCTGTGGAAGC GGGTGT	This study
		<i>rmlB</i> -R	CTTTGCGCGTGAT TTTAGTGG	
24.	<i>actA</i>	<i>actA</i> -F	GGCGAAAGAGT CACTTGC	This study
		<i>actA</i> -R	GTTGGAGGCGGT GGAAAT	
25.	<i>prfA</i>	<i>prfA</i> -F	TAACCAATGGGAT CCACAAG	This study
		<i>prfA</i> -R	TGCTAACAGCTG AGCTATGTG	
26.	<i>hly</i>	<i>hly</i> -F	TGTAACTTCGGC GCAATC	This study
		<i>hly</i> -R	TAAGCAATGGG AACTCCTG	

value differences ($P < 0.05$) using SPSS 17.0 (SPSS Inc., Chicago, IL, United States).

RESULTS

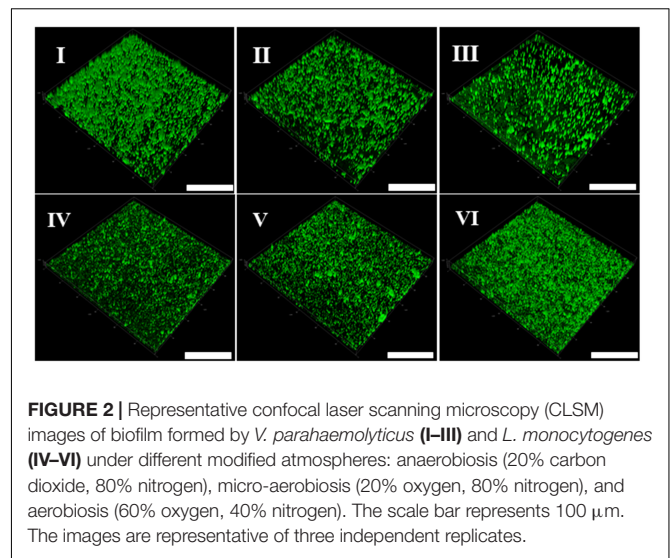
The effects of different modified atmospheres against the biofilm formation of *V. parahaemolyticus* and *L. monocytogenes* cocktails



are shown in **Figure 1**. The crystal violet staining assay indicated that the biofilms of *V. parahaemolyticus* were reduced from 1.66 (OD_{600nm}) under anaerobiosis to 1.52 (OD_{600nm}) under micro-aerobiosis, and further significantly ($P < 0.05$) decreased to 0.82 (OD_{600nm}) under aerobiosis. However, the biofilms of *L. monocytogenes* treated by modified atmospheres were significantly ($P < 0.05$) increased from 1.12 (OD_{600nm}) under anaerobiosis to 1.52 (OD_{600nm}) under micro-aerobiosis, and further significantly ($P < 0.05$) increased to 2.15 under aerobiosis. All these facts implied that the modified atmospheres produced completely opposite effects on the biofilm formation of *V. parahaemolyticus* and *L. monocytogenes*.

In addition, the CLSM was used to perform *in situ* characterization of *V. parahaemolyticus* and *L. monocytogenes* biofilms under different modified atmospheres. As shown in **Figure 2I**, the biofilms of *V. parahaemolyticus* presented a compact and structured biofilm architecture under anaerobiosis. However, the biofilms became slightly loose and presented unevenly dispersed structures under micro-aerobiosis (**Figure 2II**). Much sparser and lower amounts of biofilms were observed under aerobiosis (**Figure 2III**). For the biofilms of *L. monocytogenes*, they displayed sparser and looser biofilms with a patchy coverage on the contact surface under anaerobiosis (**Figure 2IV**). Nevertheless, the biofilms presented an increased amount and compact structures under micro-aerobiosis (**Figure 2V**). Furthermore, the biofilms displayed more compact and dense structures under aerobiosis (**Figure 2VI**).

Scanning electron microscopy (SEM) is used to directly observe biofilms (Pan et al., 2016). As shown in **Figure 3I**, a layer of mature biofilms of *V. parahaemolyticus* with well-organized



network structures was observed under anaerobic conditions, and bacterial biofilm cells were closer to each other. However, few bacterial cells aggregated, and the ordered biofilm structures were not found under micro-aerobiosis (**Figure 3II**). Even much fewer cells were sporadically scattered on the contact surface under aerobiosis (**Figure 3III**). The biofilms of *L. monocytogenes* also exhibited an opposite trend of structure changes compared with *V. parahaemolyticus* (**Figures 3IV–VI**). Based on above results, the modified atmospheres especially for aerobiosis significantly inhibited the biofilm formation of *V. parahaemolyticus*, while the anaerobiosis greatly restrained the biofilm formation of *L. monocytogenes*.

The effects of modified atmospheres on the production of EPS including eDNA, protein, and polysaccharide were examined in the biofilms of *V. parahaemolyticus* and *L. monocytogenes* (**Figure 4**). Overall, the eDNA and protein of *V. parahaemolyticus* biofilms were greatly reduced from anaerobic to aerobic conditions. However, the extracellular polysaccharide was increased. In detail, the eDNA of EPS was significantly ($P < 0.05$) decreased from 0.75 μ g/ml under anaerobiosis to 0.08 μ g/ml (89%) under aerobiosis (**Figure 4A**). Meanwhile, the extracellular protein of EPS was markedly ($P < 0.05$) reduced from 14.3 μ g/ml under anaerobiosis to 5.0 μ g/ml (65%) under aerobiosis (**Figure 4B**). Conversely, the extracellular polysaccharide of EPS in *V. parahaemolyticus* biofilms was slightly increased from 1.02 to 1.60 (OD_{490nm}/OD_{595nm}) (**Figure 4C**).

For the biofilms of *L. monocytogenes*, the eDNA and protein were dramatically elevated from anaerobic to aerobic conditions. However, the extracellular polysaccharide was reduced from anaerobic to aerobic conditions. In **Figure 4A**, the eDNA content of EPS was significantly ($P < 0.05$) increased from 0.32 μ g/ml under anaerobiosis to 0.93 μ g/ml (73%) under aerobiosis. Similarly, the extracellular protein of EPS was markedly ($P < 0.05$) increased from 6.42 μ g/ml under anaerobiosis to 24 μ g/ml (66%) under aerobiosis. Conversely, the extracellular polysaccharide of EPS in *L. monocytogenes* biofilms was gradually reduced from 1.53 under anaerobiosis to 0.93

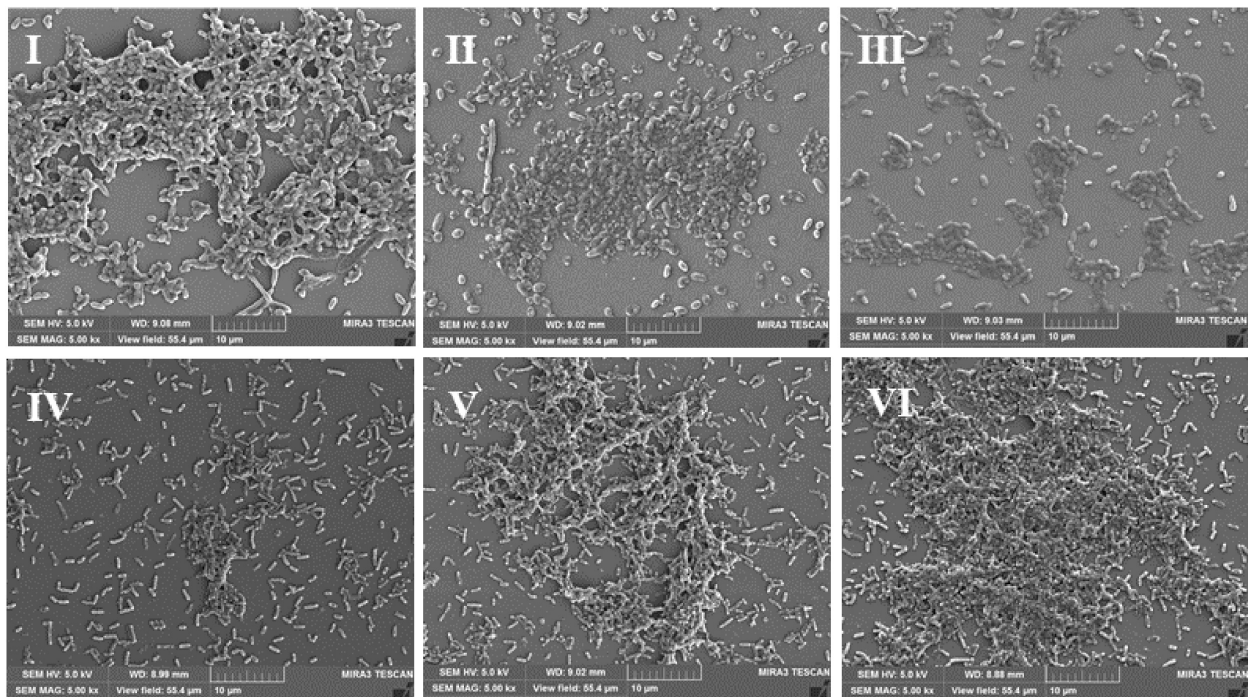


FIGURE 3 | Representative scanning electron microscopy (SEM) images of biofilms formed by *V. parahaemolyticus* (I–III) and *L. monocytogenes* (IV–VI) under different modified atmospheres: anaerobiosis (20% carbon dioxide, 80% nitrogen), micro-aerobiosis (20% oxygen, 80% nitrogen), and aerobiosis (60% oxygen, 40% nitrogen). The scale bar represents 10 μm . The images are representative of three independent replicates.

under aerobiosis ($\text{OD}_{490\text{nm}}/\text{OD}_{595\text{nm}}$). It was concluded that the modified atmosphere treatment inhibited the biofilm formation of *V. parahaemolyticus*, and the inhibition degree values could be ranked as eDNA > extracellular proteins > extracellular polysaccharide; however, the modified atmosphere treatment enhanced the biofilm formation of *L. monocytogenes*, and the enhancement degree values could be ranked as extracellular proteins > eDNA > extracellular polysaccharide.

Subsequently, the morphological and structural changes of the biofilms of *V. parahaemolyticus* and *L. monocytogenes* were analyzed by ISA software (Figure 5). The quantitative image analysis (QIA) of *V. parahaemolyticus* biofilms revealed that the biovolume of biofilms was greatly ($P < 0.05$) decreased from $13.49 \times 10^5 \mu\text{m}^3$ under anaerobiosis to $8.62 \times 10^5 \mu\text{m}^3$ under aerobiosis (Figure 5A). The biofilm thickness was significantly ($P < 0.05$) reduced from $16.72 \mu\text{m}$ under anaerobiosis to $9.65 \mu\text{m}$ under aerobiosis (Figure 5B). Meanwhile, the bio-roughness was significantly ($P < 0.05$) increased from 0.46 under anaerobiosis to 1.00 under aerobiosis (Figure 5C). Meanwhile, the TE was slowly increased from 7.16 under anaerobiosis to 7.40 under aerobiosis (Figure 5D).

For *L. monocytogenes*, the biovolume of its biofilms was significantly ($P < 0.05$) increased from 11.41×10^5 to $20.58 \times 10^5 \mu\text{m}^3$ during the physiological conversion from anaerobiosis to aerobiosis (Figure 5A). The biofilm thickness was dramatically ($P < 0.05$) increased from 11.63 to $19.63 \mu\text{m}$ (Figure 5B). Meanwhile, its bio-roughness was markedly ($P < 0.05$) improved from 0.49 under anaerobiosis to 0.27 under

aerobiosis (Figure 5C). The TE was gradually decreased from 7.82 under anaerobiosis to 7.59 under aerobiosis (Figure 5D).

Vibrio parahaemolyticus possesses the ability to form biofilms and secrete endotoxin, which can lead to serious diseases, and *L. monocytogenes* can also form biofilms and cause terrible listeriosis by secreting exotoxin such as listeriolysin O (LLO) (Gekara et al., 2008; Hamon et al., 2012; Wang et al., 2015). In this study, the regulatory genes of biofilm formation (*luxS*, *aphA*, *mshA*, *oxyR*, and *opaR*) and EPS production genes (*cpsA*, *cpsC*, and *cpsR*) of *V. parahaemolyticus* were selected to determine the effects of the modified atmospheres on their transcriptional levels. In Figure 6A, the expression levels of the biofilm formation genes and EPS production genes were slightly downregulated by aerobiosis; however, all the genes were significantly ($P < 0.05$) upregulated under anaerobiosis. For the *L. monocytogenes* cells, the gene expression levels of the biofilm formation (*flgA*, *flgE*, and *degU*) and EPS production (*Imo2554*, *Imo2504*, *inlA*, *rmlB*) were significantly ($P < 0.05$) downregulated under the anaerobiosis, except *inlA* and *rmlB* (Figure 6C). However, all the above genes were slightly upregulated by aerobiosis, except the obviously upregulated *flgA*.

To investigate the effects of modified atmospheres on the expression levels of virulence genes, the genes including *vopS*, *vopD1*, *vcrD1*, *vopP2 β* , and *vcrD2 β* of *V. parahaemolyticus* and *actA*, *plfA*, *hly*, and *plcA* of *L. monocytogenes* were evaluated by RT-qPCR. For *V. parahaemolyticus* (Figure 7A), the expression levels of all the virulence genes were downregulated under aerobiosis, reaching 1.88, 1.30, 1.96, 1.14, and 1.10

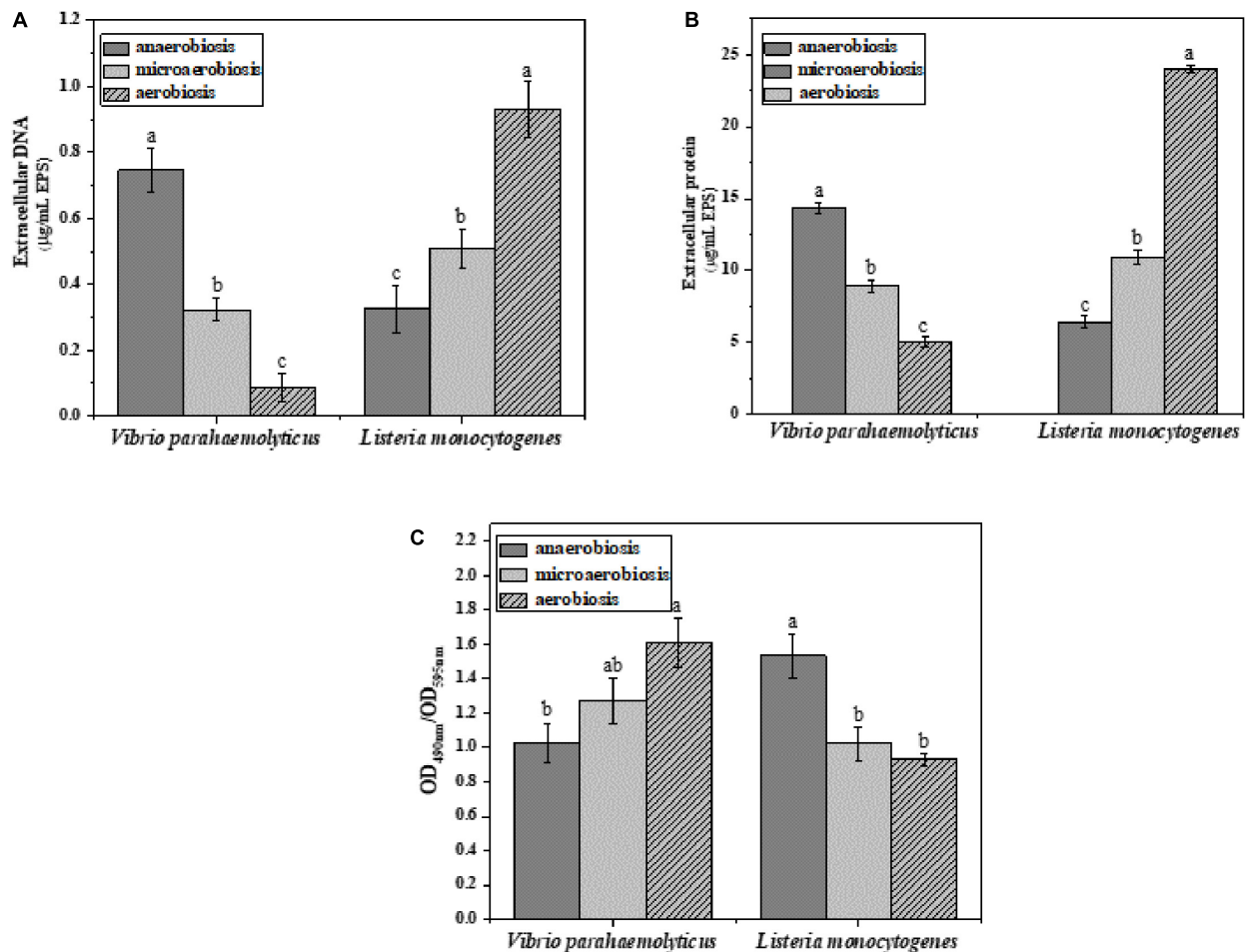


FIGURE 4 | Chemical composition and contents of EPS in *V. parahaemolyticus* and *L. monocytogenes* biofilms under different modified atmospheres: anaerobiosis (20% carbon dioxide, 80% nitrogen), micro-aerobiosis (20% oxygen, 80% nitrogen), and aerobiosis (60% oxygen, 40% nitrogen). **(A)** Extracellular DNA ($\mu\text{g/mL}$), **(B)** extracellular protein ($\mu\text{g/mL}$), and **(C)** polysaccharide ($\text{OD}_{490\text{nm}}/\text{OD}_{595\text{nm}}$) in EPS of *V. parahaemolyticus* and *L. monocytogenes* biofilms. Error bars represent the standard error. And the same letter represents no significant difference ($P < 0.05$).

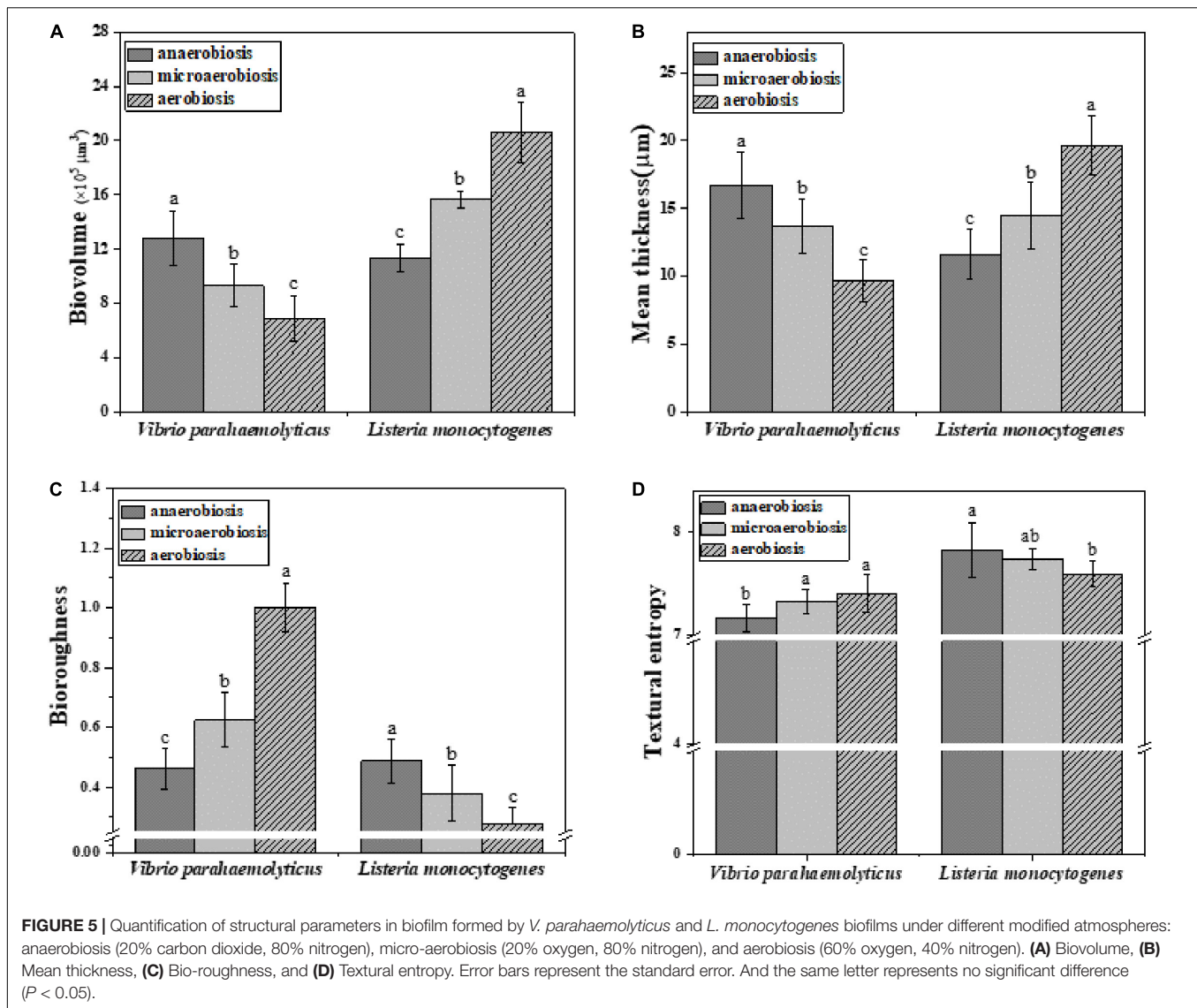
times, separately; but all the genes were upregulated under anaerobiosis, reaching 1.84, 1.36, 1.46, 5.30, and 1.31 times, respectively. However, the expression levels of all virulence genes of *L. monocytogenes* were downregulated under anaerobiosis, reaching 2.09, 3.58, 1.76, and 1.66 times, respectively; however, all the genes were upregulated under aerobiosis, reaching 1.37, 1.44, 1.14, and 1.21 times, separately (Figure 7B).

DISCUSSION

Previous studies showed that all the tested modified atmospheres were effective in reducing *V. parahaemolyticus* in sea bream fillets compared with air-packaged samples (Provincial et al., 2013a). Meanwhile, Provincial et al. (2013b) found that the modified atmospheres were more effective in decreasing the *Listeria* spp. with the increase of CO_2 concentrations from 20% to 30%. Rutherford et al. (2007) also found differences in the amount of *Listeria* on shrimp which were stored in air,

vacuum, and map packaging (100% CO_2) at 3, 7, and 10°C. Moreover, *V. parahaemolyticus* and *L. monocytogenes* could form bacterial biofilms to survive on food processing surfaces under anaerobiosis or aerobiosis (Voidarou et al., 2011; Valimaa et al., 2015; Perez-Ibarreche et al., 2016; Song et al., 2016). In an early study, the biofilm formation of *Vibrio vulnificus* was reduced due to the lack of oxygen (Phippen and Oliver, 2015). However, *Salmonella* spp. produced the highest amount of biofilm under a CO_2 -rich atmosphere (Stepanovic et al., 2003). In food products, Wang et al. (2017) reported that the MAP inhibited the growth of *Pseudomonas fragi* strains in meat, and more loose and less bound EPS were produced by *P. fragi* in the modified-atmosphere packaged samples. The present study demonstrated that *V. parahaemolyticus* possessed a stronger ability to develop biofilms under anaerobic conditions in comparison with microaerobiosis and aerobiosis (Figure 1).

For Gram-positive bacteria, compared to the increased CO_2 atmosphere and anaerobic condition, the aerobic atmosphere of methicillin-resistant *Staphylococcus aureus* was not efficient

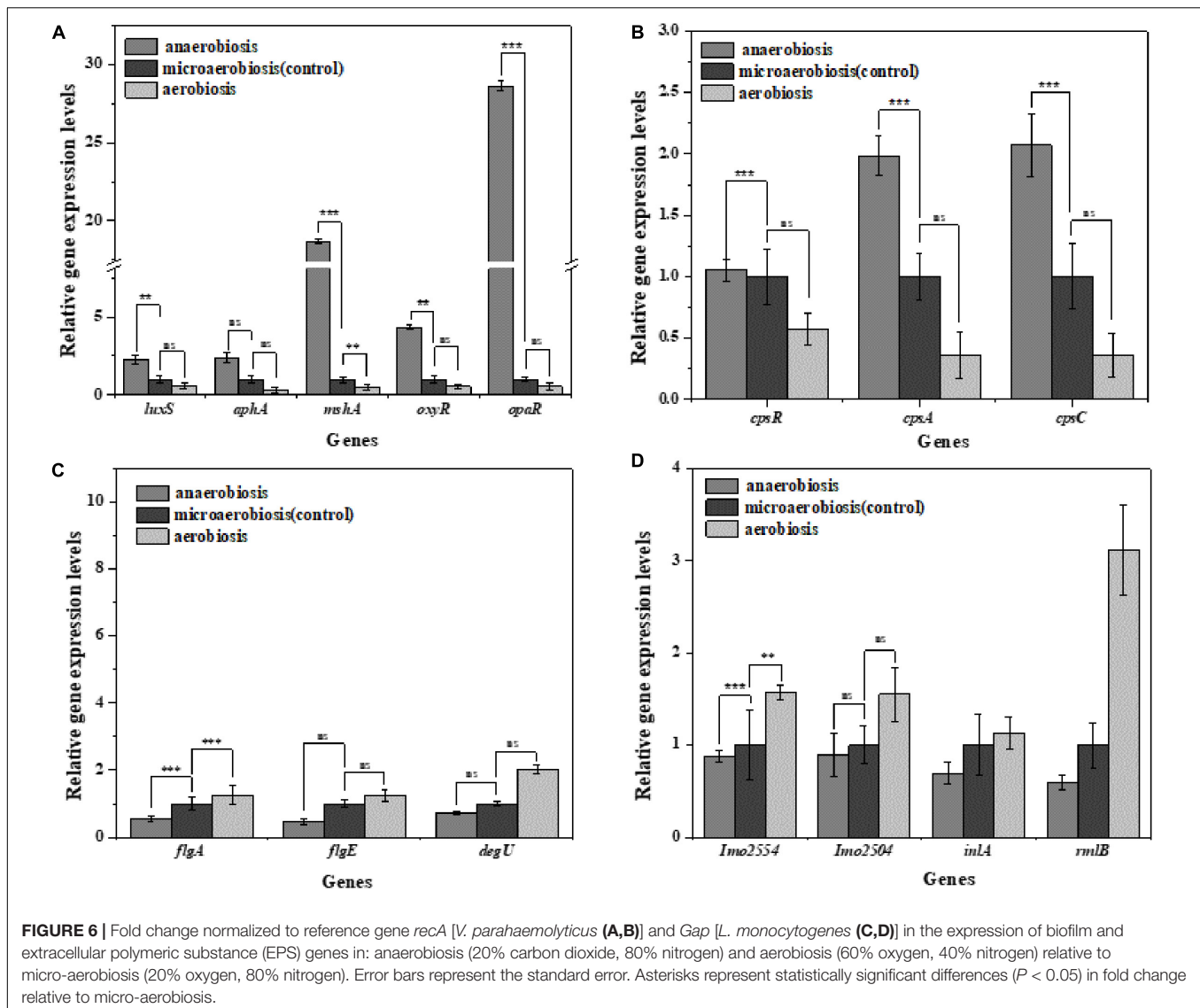


in promoting the biomass of biofilms (Ursic and Tomic, 2008). However, the aerobic biofilms of wild-type *S. aureus* were more robust than that under anaerobic conditions (Hess et al., 2013). Our results showed that the *L. monocytogenes* biofilms were increased from 1.01 (OD_{600nm}) under anaerobiosis to 2.02 (OD_{600nm}) under aerobiosis (Figure 1). In addition, the biofilms formed by different Gram-negative *Salmonella* strains ($n = 30$) exhibited a different stress response to the modified atmospheres, indicating the heterogeneity of the biofilm formation ability of *Salmonella* strains under the modified atmospheres (Stepanovic et al., 2003).

It is widely reported that high fluorescence intensities observed by CLSM are caused by the aggregation of biofilms in different layers and depths (Webster et al., 2005; Han et al., 2017). Moreover, SEM images can also be used to describe the biofilm morphotypes (Simões et al., 2007). In our study, the results of CLSM and SEM clearly showed that the biofilm cells of *V. parahaemolyticus* displayed more compact

aggregates and well-organized structures under anaerobiosis compared to micro-aerobiosis and aerobiosis (Figures 2, 3). However, it was observed that few aggregated cells and sparser structures of *L. monocytogenes* biofilms formed with a lower fluorescence intensity under anaerobiosis (Figures 2, 3). Overall, the results of the CLSM and SEM confirmed the results of crystal violet staining.

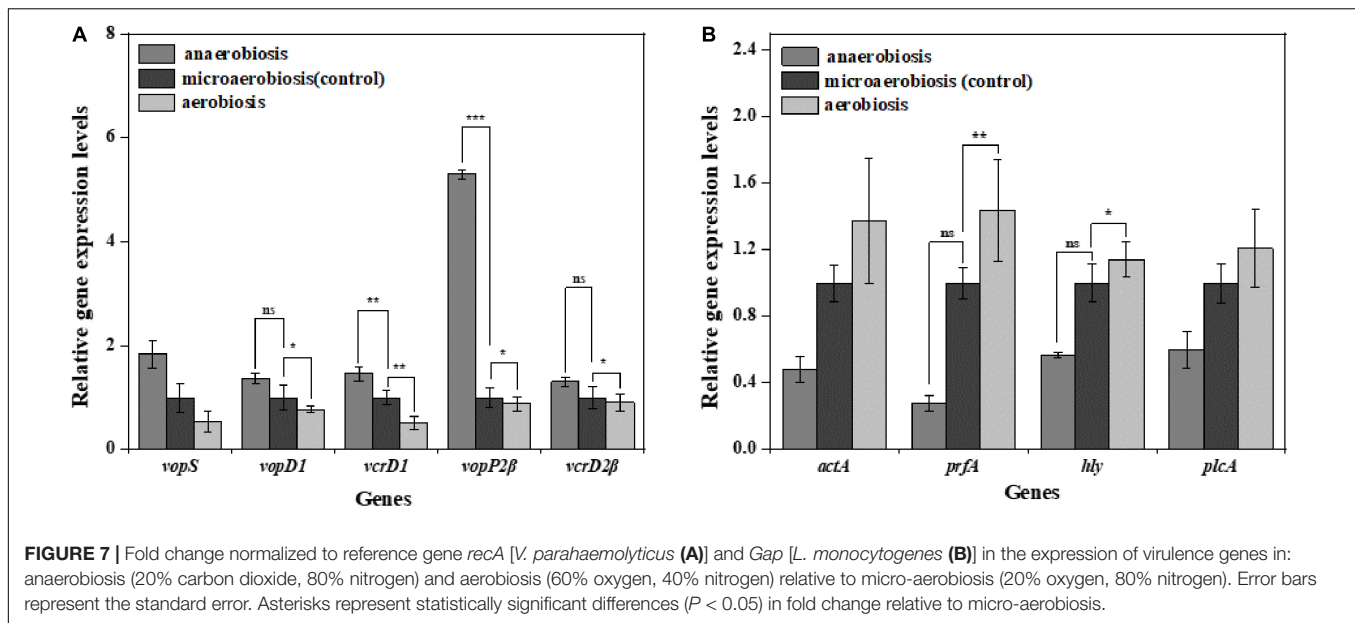
The EPS consists of about 80% dry mass of the biofilms, mainly including extracellular proteins (3–37%), nucleic acids (9–50%), and polysaccharides (3–21%) (Andersson et al., 2009), which plays a major role in mediating biofilm formation (Liu et al., 2007). It was concluded that the eDNA was essential in the initial establishment of *Pseudomonas aeruginosa* biofilms and perhaps biofilms formed by other bacteria (Whitchurch et al., 2002). Besides, three matrix proteins contributing to biofilm stability were identified in *Vibrio cholerae*, which involved in cell-cell and cell-surface adhesion (Yildiz et al., 2014). Up to now, the most descriptive matrix protein was extracellular adhesin



CdrA, which promoted the aggregate formation through the interaction of extracellular polysaccharide Psl under planktonic conditions and helped to stabilize the matrix and maintain the structural integrity of aggregates (da Silva et al., 2019). In **Figure 4**, the eDNA and extracellular proteins of the *V. parahaemolyticus* biofilms were significantly ($P < 0.05$) reduced from anaerobiosis to aerobiosis, but the extracellular polysaccharides were gradually increased. However, our results showed that the eDNA and extracellular proteins of the *L. monocytogenes* biofilms were dramatically ($P < 0.05$) increased from anaerobiosis to aerobiosis; conversely, the extracellular polysaccharides were decreased (**Figure 4**). Our results were supported by the fact that anaerobic incubation decreased the production of extracellular polysaccharide in Gram-negative *Escherichia coli* 0157:H7 (Dewanti and Wong, 1995). It showed that the extracellular proteins and eDNA of Gram-positive *S. aureus* were significantly decreased under anaerobic conditions (Hess et al., 2013). The results demonstrated that the anaerobic

conditions induced the highest levels of carbohydrates in biofilms compared to aerobic conditions (Yang et al., 2006). The reported results were highly coincident with the changes of EPS of Gram-positive *L. monocytogenes* in this study.

Quantitative image analysis was used to characterize the structure of the biofilms (Tan et al., 2018). The variation of the textural parameters reflects the changes of biofilm structure and biofilm adhesion ability (**Figures 5A–C**). The biovolume represented the total volume of cells (μm^3) in the biofilms (Bridier et al., 2010). Meanwhile, the mean thickness (μm) of biofilms was also determined directly from the confocal stack images. In **Figures 5A,B**, the decrease in biovolume and thickness of biofilms suggested that the total volume of adherent cells was reduced from anaerobiosis to aerobiosis. Bio-roughness offered a metric of variations in biofilm thickness and was an indicator of the superficial biofilm-interface heterogeneity, so the significantly increased bio-roughness suggested that a high variation of biofilm thickness



means a high superficial biofilm-interface heterogeneity (Bridier et al., 2010) (Figure 5C). It is now widely accepted that the texture entropy (TE) is positively correlated with the heterogeneity of biofilms (Beyenal et al., 2004a), but the changes of TE of these two bacterial biofilms were not obvious, indicating that the heterogeneity of biofilms did not exhibit obvious alteration under modified atmosphere treatment (Figure 5D). However, the increase in biovolume and thickness of *L. monocytogenes* biofilms indicated the increased total volume of adherent cells from anaerobiosis to aerobiosis. The bio-roughness, an indicator of variation of biofilm thickness, was significantly ($P < 0.05$) decreased, implying the low superficial heterogeneity of biofilm interface from anaerobiosis to aerobiosis (Bridier et al., 2010). It was concluded that the modified atmospheres could highly shape the biofilm formation of *V. parahaemolyticus* and *L. monocytogenes* cocktails. Based on the above analysis, this study was the first one to evaluate the potential effects of the modified atmospheres on bacterial biofilms by monitoring the changes of biofilm architectures, chemical compositions, etc.

The biofilm formation of *V. parahaemolyticus* and *L. monocytogenes* was regulated by a variety of genes. For *V. parahaemolyticus*, the *oxyR* has been known to regulate the formation of cell appendages and biofilm formation (Chung et al., 2016). The expression of quorum-controlled genes *aphA* was necessary for the biofilm formation of *V. parahaemolyticus* (Wang et al., 2013). Meanwhile, it has been shown that quorum-controlled genes *opaR* directly or indirectly regulated 5.2% of genes in the genome of *V. parahaemolyticus* which were pertinent to social activities of bacteria such as biofilm formation (Gode-Potratz and McCarter, 2011). Additionally, biofilm formation was also regulated by the *luxS*-dependent quorum-sensing system in *V. parahaemolyticus* (Guo et al., 2018). From anaerobiosis to aerobiosis, our study showed that the expression levels of *oxyR*, *aphA*, *opaR*, and *luxS* were

downregulated. Such facts indicated that the bacteria decreased their physiological activity and mitigated the expression of essential genes to cut down the energy costs of cells to adapt the changes of environmental conditions (Bayramoglu et al., 2017). Therefore, the results suggested a relationship between the biofilm formation and expression of biofilm and quorum-sensing genes in *V. parahaemolyticus* (Lamas et al., 2016).

MshA is a type IV pilin subunit gene that mediates the adhesion of *V. parahaemolyticus* to the surface through pili (Shime-Hattori et al., 2006; Agesen and Hase, 2012). The expression of *mshA* significantly increased ($P < 0.05$) under anaerobic conditions but obviously decreased under aerobic conditions, which might suggest decreased functions of type IV pili in the adhesion of *V. parahaemolyticus*. Meanwhile, the *cpsA* and *cpsC* regulated the production and transportation of CPS, and *cpsR* was required for the exopolysaccharide production of *V. parahaemolyticus* biofilm (Guvener and McCarter, 2003; Zhang et al., 2018). The downregulation of these genes (*cpsA*, *cpsC*, and *cpsR*) suggested that the aerobic conditions inhibited the production of CPS and exopolysaccharide, which would reduce the adhesion ability and biofilm formation of *V. parahaemolyticus* on the target surfaces. Likewise, the virulence genes of *V. parahaemolyticus* are also affected by the modified atmospheres. *VcrD1*, *vopS*, and *vopD1* are the main virulence factors of the *V. parahaemolyticus* type III secretory system 1 (T3SS1). *VcrD1*, an inner membrane protein, is a component of T3SS1 in *V. parahaemolyticus* (Kwon-Sam et al., 2004; Noh et al., 2015). *VopS* is an effector secreted by T3SS1 during infection and can inhibit actin assembly (Yarbrough et al., 2009). *VopD1* is the essential component of the translocation of T3SS1 (Shimohata et al., 2012). *VopP2β* and *vcrD2β* are the main virulence factors of *V. parahaemolyticus* type III secretory system 2 (T3SS2). *VopP2β* inhibits mitogen-activated protein kinases (MAPK) signal transduction and prevents ATP binding in T3SS2 (Trosky et al., 2007; Tsai et al., 2013). And *vcrD2β* encodes an

inner membrane protein of T3SS2 (Kwon-Sam et al., 2004; Tsai et al., 2013). The type III secretion system (T3SS), which consists of T3SS1 (*vcrD1*, *vopS*, *vopD1*) and T3SS2 (*vopP2β*, *vcrD2β*), is considered to be an important virulence factor for delivering effectors into host cells (Noh et al., 2015). The downregulation of these genes (*VcrD1*, *vopS*, *vopD1*, *VopP2β*, *vcrD2β*) suggested that the aerobic conditions inhibited the expression of these virulence genes, but the anaerobic conditions conversely improved the expression of virulence genes.

For *L. monocytogenes*, *flgA* and *flgE* are flagellum-related genes associated with biofilm formation (Li R. et al., 2018). The *degU* gene-encoded DegU is essential for flagellar synthesis and bacterial motility in *L. monocytogenes* (Gueriri et al., 2008; Pieta et al., 2014). It is well known that flagellum-mediated motility plays a predominant role in biofilm formation of *L. monocytogenes* (Renier et al., 2011). The upregulation of *flgA*, *flgE*, and *degU* ($P < 0.05$) implied that the aerobic conditions facilitated the initial biofilm formation of *L. monocytogenes*. However, the downregulation of *flgA*, *flgE*, and *degU* indicated that anaerobic conditions caused a decrease in the ability of biofilm formation. L-rhamnose is widely found in cell walls and capsules of many pathogenic bacteria including *L. monocytogenes*, which can be regulated by *rmlB* (Giraud and Naismith, 2000; Eugster et al., 2015). *Imo2554* is confirmed to be involved in the glycolipid synthesis of *L. monocytogenes*, an important cell wall polymer in Gram-positive bacteria (Webb et al., 2009). *Imo2504* encodes the binding protein of the cell wall which participates in the biofilm formation (Lourenco et al., 2013). *InlA* encodes InlA (the bacterial surface protein), which gains invasiveness and invades the *L. monocytogenes* cells (Pizarro-Cerda et al., 2012). The anaerobic downregulation of *rmlB*, *Imo2554*, *Imo2504*, and *inlA* indicated that the synthesis of these key proteins was inhibited, indicating the highly decreased physiological activity of *L. monocytogenes*. Conversely, the aerobic upregulation of these genes suggested the enhanced expression of key proteins and physiological activity of *L. monocytogenes* which finally strengthened the biofilm formation. For the virulence genes, it was concluded that the pathogenesis was mainly related to the expression of virulence genes (LIPI-1) (Stelling et al., 2010). The virulence genes were located in the virulence island, which is a 9-KB-long gene cluster mainly containing *hly*, *plcA*, *prfA*, and *actA* (Stelling et al., 2010). In this study, the anaerobic downregulation of *hly*, *plcA*, *prfA*, and *actA* suggested that the toxicity of *L. monocytogenes* was decreased, while the aerobic upregulation of these genes indicated the increased toxicity of *L. monocytogenes*.

REFERENCES

- Aagesen, A. M., and Hase, C. C. (2012). Sequence analyses of type IV Pili from *Vibrio cholerae*, *Vibrio parahaemolyticus*, and *Vibrio vulnificus*. *Microb. Ecol.* 64, 509–524. doi: 10.1007/s00248-012-0021-2
- Alvarez-Ordóñez, A., Broussolle, V., Colin, P., Nguyen-The, C., and Prieto, M. (2015). The adaptive response of bacterial food-borne pathogens in the environment, host and food: implications for food safety. *Int. J. Food Microbiol.* 213, 99–109. doi: 10.1016/j.ijfoodmicro.2015.06.004
- Andersson, S., Dalhammar, G., Land, C. J., and Kuttuva Rajarao, G. (2009). Characterization of extracellular polymeric substances from denitrifying organism *Comamonas denitrificans*. *Appl. Microbiol. Biotechnol.* 82, 535–543. doi: 10.1007/s00253-008-1817-3
- Arvanitoyannis, I. S., Kargaki, G. K., and Hadjichristodoulou, C. (2011). Effect of several MAP compositions on the microbiological and sensory properties of Graviera cheese. *Anaerobe* 17, 310–314. doi: 10.1016/j.anaerobe.2011.04.013
- Bayramoglu, B., Toubiana, D., and Gillor, O. (2017). Genome-wide transcription profiling of aerobic and anaerobic *Escherichia coli* biofilm and planktonic cultures. *Fems Microbiol. Lett.* 364:fnx006. doi: 10.1093/femsle/fnx006

CONCLUSION

The modified atmospheres significantly reduced the eDNA and proteins of EPS and negatively altered the biofilm structures of *V. parahaemolyticus* during the physiological conversion from anaerobiosis to aerobiosis. The modified atmospheres also downregulated the expression of biofilm formation genes (*luxS*, *aphA*, *mshA*, *oxyR*, and *opaR*) and EPS production genes (*cpsA*, *cpsC*, and *cpsR*) and virulence genes (*vopS*, *vopD1*, *vcrD1*, *vopP2β*, and *vcrD2β*) of *V. parahaemolyticus*. Conversely, the expressions of biofilm formation genes (*flgA*, *flgU*, and *degU*), EPS production genes (*Imo2554*, *Imo2504*, *inlA*, *rmlB*) and virulence genes (*vopS*, *vopD1*, *vcrD1*, *vopP2β*, and *vcrD2β*) of *L. monocytogenes* were upregulated during the same physiological conversion. Therefore, the modified atmospheres showed significantly different regulation on the biofilm formation of Gram-negative *V. parahaemolyticus* and Gram-positive *L. monocytogenes*. The generated knowledge will facilitate our understanding of the stress response of Gram-negative and Gram-positive pathogens to the modified atmosphere treatment and hence provide an efficient way to control the pathogens in modified-atmosphere packaged food.

DATA AVAILABILITY STATEMENT

All datasets generated for this study are included in the article.

AUTHOR CONTRIBUTIONS

YZ, JW, YP, and HL conceived and supervised the study. HQ and WL designed and performed the experiments. HQ analyzed the data. LG, LT, JW, and YZ revised the manuscript. HQ wrote the manuscript.

FUNDING

This research was supported by the National Natural Science Foundation of China (31571917 and 31671779), National Key R&D Program of China (2018YFC1602205 and 2018YFC1602200), Shanghai Agriculture Applied Technology Development Program (T20170404), and Innovation Program of Shanghai Municipal Education Commission (2017-01-07-00-10-E00056).

- Beyenal, H., Donovan, C., Lewandowski, Z., and Harkin, G. (2004a). Three-dimensional biofilm structure quantification. *J. Microbiol. Methods* 59, 395–413. doi: 10.1016/j.mimet.2004.08.003
- Beyenal, H., Lewandowski, Z., and Harkin, G. (2004b). Quantifying biofilm structure: facts and fiction. *Biofouling* 20, 1–23. doi: 10.1080/0892701042000191628
- Blanco, Y., Rivas, L. A., Gonzalez-Toril, E., Ruiz-Bermejo, M., Moreno-Paz, M., Parro, V., et al. (2019). Environmental parameters, and not phylogeny, determine the composition of extracellular polymeric substances in microbial mats from extreme environments. *Sci. Total Environ.* 650, 384–393. doi: 10.1016/j.scitotenv.2018.08.440
- Bonsaglia, E. C. R., Silva, N. C. C., Fernandes Júnior, A., Araújo Júnior, J. P., Tsunemi, M. H., and Rall, V. L. M. (2014). Production of biofilm by *Listeria monocytogenes* in different materials and temperatures. *Food Control* 35, 386–391. doi: 10.1016/j.foodcont.2013.07.023
- Bridier, A., Dubois-Brissonnet, F., Boubetra, A., Thomas, V., and Briandet, R. (2010). The biofilm architecture of sixty opportunistic pathogens deciphered using a high throughput CLSM method. *J. Microbiol. Methods* 82, 64–70. doi: 10.1016/j.mimet.2010.04.006
- Brooks, J. D., and Flint, S. H. (2008). Biofilms in the food industry: problems and potential solutions. *Int. J. Food Sci. Technol.* 43, 2163–2176. doi: 10.1111/j.1365-2621.2008.01839.x
- Centers for Disease Control and Prevention [CDC] (2014). *National Enteric Disease Surveillance: COVIS Annual Summary*. Available at: <https://www.cdc.gov/national-surveillance/pdfs/covis-annual-summary-2014-508c.pdf> (accessed January, 2015).
- Chang, Y. H., Gu, W. M., and McLandsborough, L. (2012). Low concentration of ethylenediaminetetraacetic acid (EDTA) affects biofilm formation of *Listeria monocytogenes* by inhibiting its initial adherence. *Food Microbiol.* 29, 10–17. doi: 10.1016/j.fm.2011.07.009
- Chen, J., Zhang, R. H., Qi, X. J., Zhou, B., Wang, J. K., Chen, Y., et al. (2017). Epidemiology of foodborne disease outbreaks caused by *Vibrio parahaemolyticus* during 2010–2014 in Zhejiang Province. *China. Food Control* 77, 110–115. doi: 10.1016/j.foodcont.2017.02.004
- Chimalapati, S., de Souza Santos, M., Servage, K., De Nisco, N. J., Dalia, A. B., and Orth, K. (2018). Natural transformation in *Vibrio parahaemolyticus*: a rapid method to create genetic deletions. *J. Bacteriol.* 200:e00032–18. doi: 10.1128/JB.00032-18
- Chung, C. H., Fen, S. Y., Yu, S. C., and Wong, H. C. (2016). Influence of oxyR on growth, biofilm formation, and mobility of *Vibrio parahaemolyticus*. *Appl. Environ. Microbiol.* 82, 788–796. doi: 10.1128/aem.02818-15
- Colagiorgi, A., Di Ciccio, P., Zanardi, E., Ghidini, S., and Ianieri, A. (2016). A look inside the *Listeria monocytogenes* biofilms extracellular matrix. *Microorganisms* 4:22. doi: 10.3390/microorganisms4030022
- da Silva, D. P., Matwichuk, M. L., Townsend, D. O., Reichhardt, C., Lamba, D., Wozniak, D. J., et al. (2019). The *Pseudomonas aeruginosa* lectin LecB binds to the exopolysaccharide Psl and stabilizes the biofilm matrix. *Nat. Commun.* 10:2183. doi: 10.1038/s41467-019-10201-4
- Dewanti, R., and Wong, A. C. L. (1995). Influence of culture conditions on biofilm formation by *Escherichia coli* O157:H7. *Int. J. Food Microbiol.* 26, 147–164.
- Di Bonaventura, G., Piccolomini, R., Paludi, D., D'Orto, V., Vergara, A., Conter, M., et al. (2008). Influence of temperature on biofilm formation by *Listeria monocytogenes* on various food-contact surfaces: relationship with motility and cell surface hydrophobicity. *J. Appl. Microbiol.* 104, 1552–1561. doi: 10.1111/j.1365-2672.2007.03688.x
- Ding, X. Y., Ling-Yun, Q. U., Wang, C., Tian, X. X., Sun, C. J., and Wang, M. Q. (2016). Effect of temperature on T3SS Gene Expression of *Vibrio parahaemolyticus*. *Adv. Mar. Sci.* 34, 250–259.
- Eugster, M. R., Morax, L. S., Huls, V. J., Huwiler, S. G., Leclercq, A., Lecuit, M., et al. (2015). Bacteriophage predation promotes serovar diversification in *Listeria monocytogenes*. *Mol. Microbiol.* 97, 33–46. doi: 10.1111/mmi.13009
- Flemming, H. C., and Wingender, J. (2010). The biofilm matrix. *Nat. Rev. Microbiol.* 8, 623–633. doi: 10.1038/nrmicro2415
- Franciosa, G., Maugliani, A., Scalfaro, C., Floridi, F., and Aureli, P. (2009). Expression of internalin a and biofilm formation among *Listeria monocytogenes* clinical isolates. *Int. J. Immunopathol. Pharmacol.* 22, 183–193. doi: 10.1177/039463200902200121
- Gekara, N. O., Groebe, L., Viegas, N., and Weiss, S. (2008). *Listeria monocytogenes* desensitizes immune cells to subsequent Ca²⁺ signaling via listeriolysin O-induced depletion of intracellular Ca²⁺ stores. *Infect. Immun.* 76, 857–862. doi: 10.1128/iai.00622-07
- Giraud, M. F., and Naismith, J. H. (2000). The rhamnose pathway. *Curr. Opin. Struct. Biol.* 10, 687–696.
- Gode-Potratz, C. J., and McCarter, L. L. (2011). Quorum sensing and silencing in *Vibrio parahaemolyticus*. *J. Bacteriol.* 193, 4224–4237. doi: 10.1128/jb.00432-11
- Gomez-Gil, B., Thompson, F. L., Thompson, C. C., and Swings, J. (2003). *Vibrio rotiferianus* sp. nov., isolated from cultures of the rotifer *Brachionus plicatilis*. *Int. J. Syst. Evol. Microbiol.* 53(Pt 1), 239–243. doi: 10.1099/ijs.0.02430-0
- Gong, A. S., Bolster, C. H., Benavides, M., and Walker, S. L. (2009). Extraction and analysis of extracellular polymeric substances: comparison of methods and extracellular polymeric substance levels in *Salmonella pullorum* SA 1685. *Environ. Eng. Sci.* 26, 1523–1532.
- Grande, R., Marcantonio, M. C. D., Robuffo, I., Pompilio, A., Celia, C., Marzio, L. D., et al. (2015). *Helicobacter pylori* ATCC 43629/NCTC 11639 Outer Membrane Vesicles (OMVs) from Biofilm and Planktonic Phase Associated with Extracellular DNA (eDNA). *Front. Microbio.* 6:1369. doi: 10.3389/fmicb.2015.01369
- Guerri, I., Cyncynatus, C., Dubrac, S., Arana, A. T., Dussurget, O., and Msadek, T. (2008). The DegU orphan response regulator of *Listeria monocytogenes* autorepresses its own synthesis and is required for bacterial motility, virulence and biofilm formation. *Microbiology* 154(Pt 8), 2251. doi: 10.1099/mic.0.2008/017590-0
- Guo, M. H., Fang, Z. J., Sun, L. J., Sun, D. F., Wang, Y. L., Li, C., et al. (2018). Regulation of thermostable direct hemolysin and biofilm formation of *Vibrio parahaemolyticus* by quorum-sensing genes luxM and luxS. *Curr. Microbiol.* 75, 1190–1197. doi: 10.1007/s00284-018-1508-y
- Guvener, Z. T., and McCarter, L. L. (2003). Multiple regulators control capsular polysaccharide production in *Vibrio parahaemolyticus*. *J. Bacteriol.* 185, 5431–5441. doi: 10.1128/jb.185.18.5431-5441.2003
- Hamon, M. A., Ribet, D., Stavru, F., and Cossart, P. (2012). Listeriolysin O: the Swiss army knife of *Listeria*. *Trends Microbiol.* 20, 360–368. doi: 10.1016/j.tim.2012.04.006
- Han, Q., Song, X., Zhang, Z., Fu, J., Wang, X., Malakar, P. K., et al. (2017). Removal of foodborne pathogen biofilms by acidic electrolyzed water. *Front. Microbiol.* 8:988. doi: 10.3389/fmicb.2017.00988
- Hess, D. J., Henry-Stanley, M. J., Luszczek, E. R., Beilman, G. J., and Wells, C. L. (2013). Anoxia inhibits biofilm development and modulates antibiotic activity. *J. Surgical Res.* 184, 488–494. doi: 10.1016/j.jss.2013.04.049
- Hsieh, Y. C., Liang, S. M., Tsai, W. L., Chen, Y. H., Liu, T. Y., and Liang, C. M. (2003). Study of capsular polysaccharide from *Vibrio parahaemolyticus*. *Infect. Immun.* 71, 3329–3336. doi: 10.1128/iai.71.6.3329-3336.2003
- Jung, Y. C., Lee, M. A., and Lee, K. H. (2019). Role of flagellin-homologous proteins in biofilm formation by pathogenic *Vibrio* Species. *Mbio* 10:e01793-19. doi: 10.1128/mBio.01793-19
- Kayal, S., and Charbit, A. (2006). Listeriolysin O: a key protein of *Listeria monocytogenes* with multiple functions. *Fems Microbiol. Rev.* 30, 514–529. doi: 10.1111/j.1574-6976.2006.00021.x
- Kim, H. S., and Park, H. D. (2013). Ginger extract inhibits biofilm formation by *Pseudomonas aeruginosa* PA14. *Plos One* 8:e76106. doi: 10.1371/journal.pone.0076106
- Kim, M. J., Miks-Krajnik, M., Kumar, A., and Yuk, H. G. (2016). Inactivation by 405 +/- 5 nm light emitting diode on *Escherichia coli* O157:H7, *Salmonella Typhimurium*, and *Shigella sonnei* under refrigerated condition might be due to the loss of membrane integrity. *Food Control* 59, 99–107. doi: 10.1016/j.foodcont.2015.05.012
- Kirov, S. M. (2003). Bacteria that express lateral flagella enable dissection of the multifunctional roles of flagella in pathogenesis. *Fems Microbiol. Lett.* 224, 151–159. doi: 10.1016/s0378-1097(03)00445-2
- Kwon-Sam, P., Ono, T., Rokuda, M., Myoung-Ho, J., Okada, K., Iida, T., et al. (2004). Functional characterization of two type III secretion systems of *Vibrio parahaemolyticus*. *Infect. Immun.* 72, 6659–6665. doi: 10.1128/iai.72.11.6659-6665.2004
- Lamas, A., Miranda, J. M., Vazquez, B., Cepeda, A., and Franco, C. M. (2016). Biofilm formation, phenotypic production of cellulose and gene expression in

- Salmonella enterica* decrease under anaerobic conditions. *Int. J. Food Microbiol.* 238, 63–67. doi: 10.1016/j.ijfoodmicro.2016.08.043
- Li, H., Tang, R., Lou, Y., Cui, Z., Chen, W., Hong, Q., et al. (2017). A Comprehensive Epidemiological Research for clinical *Vibrio parahaemolyticus* in Shanghai. *Front. Microbiol.* 8:1043. doi: 10.3389/fmicb.2017.01043
- Li, R., Du, W., Yang, J., Liu, Z., and Yousef, A. E. (2018). Control of *Listeria monocytogenes* biofilm by paenibacterin, a natural antimicrobial lipopeptide. *Food Control* 84, 529–535. doi: 10.1016/j.foodcont.2017.08.031
- Li, W., Bai, L., Fu, P., Han, H., Liu, J., and Guo, Y. (2018). The epidemiology of *Listeria monocytogenes* in China. *Foodborne Pathog. Dis.* 15, 459–466. doi: 10.1089/fpd.2017.2409
- Liu, Y., Li, J., Qiu, X., and Burda, C. (2007). Bactericidal activity of nitrogen-doped metal oxide nanocatalysts and the influence of bacterial extracellular polymeric substances (EPS). *J. Photochem. Photobiol. A Chem.* 190, 94–100.
- Lourenco, A., de Las Heras, A., Scotti, M., Vazquez-Boland, J., Frank, J. F., and Brito, L. (2013). Comparison of *Listeria monocytogenes* Exoproteomes from Biofilm and Planktonic State: Lmo2504, a Protein Associated with Biofilms. *Appl. Environ. Microbiol.* 79, 6075–6082. doi: 10.1128/aem.01592-13
- Ma, Y. J., Sun, X. H., Xu, X. Y., Zhao, Y., Pan, Y. J., Hwang, C. A., et al. (2015). Investigation of reference genes in *Vibrio parahaemolyticus* for gene expression analysis using quantitative RT-PCR. *PLoS One*. 10:e0144362. doi: 10.1371/journal.pone.0144362
- Mattila, M., Lindström, M., Somervuo, P., Markkula, A., and Korkeala, H. (2011). Role of flhA and motA in growth of *Listeria monocytogenes* at low temperatures. *Int. J. Food Microbiol.* 148, 177–183. doi: 10.1016/j.ijfoodmicro.2011.05.022
- Mizan, M. F. R., Ashrafudoulla, M., Sadekuzzaman, M., Kang, I., and Ha, S. D. (2018). Effects of NaCl, glucose, and their combinations on biofilm formation on black tiger shrimp (*Penaeus monodon*) surfaces by *Vibrio parahaemolyticus*. *Food Control* 89, 203–209. doi: 10.1016/j.foodcont.2017.12.004
- Mizan, M. F. R., Jahid, I. K., Kim, M., Lee, K. H., Kim, T. J., and Ha, S. D. (2016). Variability in biofilm formation correlates with hydrophobicity and quorum sensing among *Vibrio parahaemolyticus* isolates from food contact surfaces and the distribution of the genes involved in biofilm formation. *Biofouling* 32, 497–509. doi: 10.1080/08927014.2016.1149571
- Nilsson, R. E., Ross, T., and Bowman, J. P. (2011). Variability in biofilm production by *Listeria monocytogenes* correlated to strain origin and growth conditions. *Int. J. Food Microbiol.* 150, 14–24. doi: 10.1016/j.ijfoodmicro.2011.07.012
- Noh, H. J., Nagami, S., Kim, M. J., Kim, J., Lee, N. K., Lee, K.-H., et al. (2015). Role of VcrD1 protein in expression and secretion of flagellar components in *Vibrio parahaemolyticus*. *Arch. Microbiol.* 197, 397–410. doi: 10.1007/s00203-014-1069-9
- Paludan-Müller, C., Dalgaard, P., Huss, H. H., and Gram, L. (1998). Evaluation of the role of *Carnobacterium piscicola* in spoilage of vacuum- and modified-atmosphere-packed cold-smoked salmon stored at 5 degrees C. *Int. J. Food Microbiol.* 39, 155–166. doi: 10.1016/s0168-1605(97)00133-5
- Pan, M., Zhu, L., Chen, L., Qiu, Y., and Wang, J. (2016). Detection techniques for extracellular polymeric substances in biofilms: a review. *Bioresources* 11, 8092–8115. doi: 10.15376/biores.11.3.8092-8115
- Pan, Y., Breidt, F., and Kathariou, S. (2009). Competition of *Listeria monocytogenes* Serotype 1/2a and 4b Strains in Mixed-Culture Biofilms. *Appl. Environ. Microbiol.* 75, 5846–5852. doi: 10.1128/AEM.00816-09
- Perez-Ibarreche, M., Castellano, P., Leclercq, A., and Vignolo, G. (2016). Control of *Listeria monocytogenes* biofilms on industrial surfaces by the bacteriocin-producing *Lactobacillus sakei* CRL1862. *Fems Microbiol. Lett.* 363, fnw118. doi: 10.1093/femsle/fnw118
- Phippen, B. L., and Oliver, J. D. (2015). Role of anaerobiosis in capsule production and biofilm formation in *Vibrio vulnificus*. *Infect. Immun.* 83, 551–559. doi: 10.1128/IAI.02559-14
- Pieta, L., García, F. B., Riboldi, G. P., de Oliveira, L. A., Frazzon, A. P. G., and Frazzon, J. (2014). Transcriptional analysis of genes related to biofilm formation, stress-response, and virulence in *Listeria monocytogenes* strains grown at different temperatures. *Ann. Microbiol.* 64, 1707–1714. doi: 10.1007/s13213-014-0814-2
- Pizarro-Cerda, J., Kuhbacher, A., and Cossart, P. (2012). Entry of *Listeria monocytogenes* in mammalian epithelial cells: an updated view. *Cold Spring Harbor Perspect. Med.* 2:a010009. doi: 10.1101/cshperspect.a010009
- Provincial, L., Guillen, E., Alonso, V., Gil, M., Roncales, P., and Beltran, J. A. (2013a). Survival of *Vibrio parahaemolyticus* and *Aeromonas hydrophila* in sea bream (*Sparus aurata*) fillets packaged under enriched CO2 modified atmospheres. *Int. J. Food Microbiol.* 166, 141–147. doi: 10.1016/j.ijfoodmicro.2013.06.013
- Provincial, L., Guillen, E., Gil, M., Alonso, V., Roncales, P., and Beltran, J. A. (2013b). Survival of *Listeria monocytogenes* and *Salmonella Enteritidis* in sea bream (*Sparus aurata*) fillets packaged under enriched CO2 modified atmospheres. *Int. J. Food Microbiol.* 162, 213–219. doi: 10.1016/j.ijfoodmicro.2013.01.015
- Renier, S., Hebraud, M., and Desvaux, M. (2011). Molecular biology of surface colonization by *Listeria monocytogenes*: an additional facet of an opportunistic gram-positive foodborne pathogen. *Environ. Microbiol.* 13, 835–850. doi: 10.1111/j.1462-2920.2010.02378.x
- Rutherford, T. J., Marshall, D. L., Andrews, L. S., Coggins, P. C., Schilling, M. W., and Gerard, P. (2007). Combined effect of packaging atmosphere and storage temperature on growth of *Listeria monocytogenes* on ready-to-eat shrimp. *Food Microbiol.* 24, 703–710. doi: 10.1016/j.fm.2007.03.011
- Schimel, J., Balser, T. C., and Wallenstein, M. (2007). Microbial stress-response physiology and its implications for ecosystem function. *Ecology* 88, 1386–1394. doi: 10.1890/06-0219
- Seper, A., Fengler, V. H. I., Roier, S., Wolinski, H., Kohlwein, S. D., Bishop, A. L., et al. (2011). Extracellular nucleases and extracellular DNA play important roles in *Vibrio cholerae* biofilm formation. *Mol. Microbiol.* 82, 1015–1037. doi: 10.1111/j.1365-2958.2011.07867.x
- Shime-Hattori, A., Iida, T., Arita, M., Park, K. S., Kodama, T., and Honda, T. (2006). Two type IV pili of *Vibrio parahaemolyticus* play different roles in biofilm formation. *Fems Microbiol. Lett.* 264, 89–97. doi: 10.1111/j.1574-6968.2006.00438.x
- Shimohata, T., Mawatari, K., Iba, H., Hamano, M., Negoro, S., Asada, S., et al. (2012). VopB1 and VopD1 are essential for translocation of type III secretion system 1 effectors of *Vibrio parahaemolyticus*. *Can. J. Microbiol.* 58, 1002–1007. doi: 10.1139/w2012-081
- Simões, M., Pereira, M. O., Sillankorva, S., Azeredo, J., and Vieira, M. J. (2007). The effect of hydrodynamic conditions on the phenotype of *Pseudomonas fluorescens* biofilms. *Biofouling* 23, 249–258.
- Song, X., Ma, Y., Fu, J., Zhao, A., and Yong, Z. (2016). Effect of temperature on pathogenic and non-pathogenic *Vibrio parahaemolyticus* biofilm formation. *Food Control* 73, 485–491. doi: 10.1016/j.foodcont.2016.08.041
- Stelling, C. R. L., Orsi, R. H., and Wiedmann, M. (2010). Complementation of *Listeria monocytogenes* Null mutants with selected *Listeria seeligeri* virulence genes suggests functional adaptation of Hly and PrfA and considerable diversification of prfA Regulation in *L. seeligeri*. *Appl. Environ. Microbiol.* 76, 5124–5139. doi: 10.1128/aem.03107-09
- Stepanovic, S., Cirkovic, I., Mijac, V., and Svabic-Vlahovic, M. (2003). Influence of the incubation temperature, atmosphere and dynamic conditions on biofilm formation by *Salmonella* spp. *Food Microbiol.* 20, 339–343. doi: 10.1016/s0740-0020(02)00123-5
- Tan, L., Zhao, F., Han, Q., Zhao, A., Malakar, P. K., Liu, H., et al. (2018). High correlation between structure development and chemical variation during biofilm formation by *Vibrio parahaemolyticus*. *Front. Microbiol.* 9:1881. doi: 10.3389/fmicb.2018.01881
- Todorov, S. D., de Paula, O. A. L., Camargo, A. C., Lopes, D. A., and Nero, L. A. (2018). Combined effect of bacteriocin produced by *Lactobacillus plantarum* ST8SH and vancomycin, propolis or EDTA for controlling biofilm development by *Listeria monocytogenes*. *Rev. Argentina Microbiol.* 50, 48–55. doi: 10.1016/j.ram.2017.04.011
- Trosky, J. E., Li, Y., Mukherjee, S., Keitany, G., Ball, H., and Orth, K. (2007). VopA inhibits ATP binding by acetylating the catalytic loop of MAPK kinases. *J. Biol. Chem.* 282, 34299–34305. doi: 10.1074/jbc.M706970200
- Tsai, S. E., Jong, K. J., Tey, Y. H., Yu, W. T., Chiou, C. S., Lee, Y. S., et al. (2013). Molecular characterization of clinical and environmental *Vibrio parahaemolyticus* isolates in Taiwan. *Int. J. Food Microbiol.* 165, 18–26. doi: 10.1016/j.ijfoodmicro.2013.04.017
- Ursic, V., and Tomic, V. M. (2008). Effect of different incubation atmospheres on the production of biofilm in methicillin-resistant *Staphylococcus aureus* (MRSA) grown in nutrient-limited medium. *Curr. Microbiol.* 57, 386–390. doi: 10.1007/s00284-008-9211-z
- Valimaa, A. L., Tilsala-Timisjärvi, A., and Virtanen, E. (2015). Rapid detection and identification methods for *Listeria monocytogenes* in the food

- chain - A review. *Food Control* 55, 103–114. doi: 10.1016/j.foodcont.2015.02.037
- van der Veen, S., and Abee, T. (2010). Mixed species biofilms of *Listeria monocytogenes* and *Lactobacillus plantarum* show enhanced resistance to benzalkonium chloride and peracetic acid. *Int. J. Food Microbiol.* 144, 421–431. doi: 10.1016/j.ijfoodmicro.2010.10.029
- Vazquez-Boland, J. A., Kryptou, E., and Scotti, M. (2017). *Listeria* placental infection. *MBio* 8:e00949-17. doi: 10.1128/mBio.00949-17
- Voidarou, C., Alexopoulos, A., Plessas, S., Noussias, H., Stavropoulou, E., Fotou, K., et al. (2011). Microbiological quality of grey-mullet roe. *Anaerobe* 17, 273–275. doi: 10.1016/j.anaerobe.2011.03.008
- Wang, G. Y., Ma, F., Wang, H. H., Xu, X. L., and Zhou, G. H. (2017). Characterization of EXTRACELLULAR POLYMERIC SUBSTANCES Produced by *Pseudomonas fragi* under air and modified atmosphere packaging. *J. Food Sci.* 82, 2151–2157. doi: 10.1111/1750-3841.13832
- Wang, J. F., Qiu, J. Z., Tan, W., Zhang, Y., Wang, H. S., Zhou, X., et al. (2015). Fisetin Inhibits *Listeria monocytogenes* virulence by interfering with the oligomerization of listeriolysin O. *J. Infect. Dis.* 211, 1376–1387. doi: 10.1093/infdis/jiu520
- Wang, L., Ling, Y., Jiang, H., Qiu, Y., Qiu, J., Chen, H., et al. (2013). AphA is required for biofilm formation, motility, and virulence in pandemic *Vibrio parahaemolyticus*. *Int. J. Food Microbiol.* 160, 245–251. doi: 10.1016/j.ijfoodmicro.2012.11.004
- Wang, Y., Zhu, S., Zhang, C., and Zeng, M. (2014). Detection of quorum sensing in *Vibrio parahaemolyticus* Isolated from *Macrobrachium rosenbergii*. *Biotechnol. Bull.* 3, 146–150. doi: 10.13560/j.cnki.biotech.bull.1985.2014.03.030
- Watnick, P., and Kolter, R. (2000). Biofilm, city of microbes. *J. Bacteriol.* 182, 2675–2679. doi: 10.1128/jb.182.10.2675-2679.2000
- Webb, A. J., Karatsa-Dodgson, M., and Grundling, A. (2009). Two-enzyme systems for glycolipid and polyglycerolphosphate lipoteichoic acid synthesis in *Listeria monocytogenes*. *Mol. Microbiol.* 74, 299–314. doi: 10.1111/j.1365-2958.2009.06829.x
- Webster, P., Wu, S., Webster, S., Rich, K. A., and McDonald, K. (2005). Ultrastructural preservation of biofilms formed by non-typeable *Hemophilus influenzae*. *Biofilms* 1, 165–182. doi: 10.1017/s1479050504001425
- Whitchurch, C. B., Tolker-Nielsen, T., Ragas, P. C., and Mattick, J. S. (2002). Extracellular DNA Required for Bacterial Biofilm Formation. *Am. Assoc. Adv. Sci.* 295:1487.
- Xu, X. J., Sang, B. H., Chen, W. B., Yan, Q. P., Xiong, Z. Y., Su, J. B., et al. (2015). Intracellular survival of virulence and low-virulence strains of *Vibrio parahaemolyticus* in *Epinephelus awoara* macrophages and peripheral leukocytes. *Genet. Mol. Res.* 14, 706–718. doi: 10.4238/2015.January.30.14
- Xue, Z., Sendamangalam, V. R., Gruden, C. L., and Seo, Y. (2012). Multiple Roles of Extracellular Polymeric Substances on Resistance of Biofilm and Detached Clusters. *Environ. Sci. Technol.* 46, 13212–13219. doi: 10.1021/es3031165
- Yang, Y., Sreenivasan, P. K., Subramanyam, R., and Cummins, D. (2006). Multiparameter assessments to determine the effects of sugars and antimicrobials on a polymicrobial oral biofilm. *Appl. Environ. Microbiol.* 72, 6734–6742. doi: 10.1128/aem.0101306
- Yarbrough, M. L., Li, Y., Kinch, L. N., Grishin, N. V., Ball, H. L., and Orth, K. (2009). AMPylation of Rho GTPases by *Vibrio* VopS disrupts effector binding and downstream signaling. *Science* 323, 269–272. doi: 10.1126/science.1166382
- Yildiz, F., Fong, J., Sadovskaya, I., Grard, T., and Vinogradov, E. (2014). Structural characterization of the extracellular polysaccharide from *Vibrio cholerae* O1 El-Tor. *PLoS One* 9:e86751. doi: 10.1371/journal.pone.0086751
- Zhang, L. L., Weng, Y. W., Wu, Y., Wang, X. Y., Yin, Z., Yang, H. Y., et al. (2018). H-NS is an activator of exopolysaccharide biosynthesis genes transcription in *Vibrio parahaemolyticus*. *Microb. Pathogen.* 116, 164–167. doi: 10.1016/j.micpath.2018.01.025
- Zhang, Y., Zhang, L., Hou, S., Huang, X., Sun, F., and Gao, H. (2016). the master quorum-sensing Regulator OpaR is activated Indirectly by H-NS in *Vibrio parahaemolyticus*. *Curr. Microbiol.* 73, 71–76. doi: 10.1007/s00284-016-1018-18
- Zhou, D. S., Yan, X. J., Qu, F., Wang, L., Zhang, Y. Q., Hou, J., et al. (2013). Quorum sensing modulates transcription of cpsQ-mfpABC and mfpABC in *Vibrio parahaemolyticus*. *Int. J. Food Microbiol.* 166, 458–463. doi: 10.1016/j.ijfoodmicro.2013.07.008

Conflict of Interest: The authors declare that the research was conducted in the absence of any commercial or financial relationships that could be construed as a potential conflict of interest.

Copyright © 2020 Qian, Li, Guo, Tan, Liu, Wang, Pan and Zhao. This is an open-access article distributed under the terms of the Creative Commons Attribution License (CC BY). The use, distribution or reproduction in other forums is permitted, provided the original author(s) and the copyright owner(s) are credited and that the original publication in this journal is cited, in accordance with accepted academic practice. No use, distribution or reproduction is permitted which does not comply with these terms.



Progress on Structured Biosensors for Monitoring Aflatoxin B1 From Biofilms: A Review

Qi Wang, Qingli Yang* and Wei Wu*

College of Food Science and Engineering, Qingdao Agricultural University, Qingdao, China

OPEN ACCESS

Edited by:

Zhenbo Xu,
University of Maryland, Baltimore,
United States

Reviewed by:

Omar Mukama,
University of Rwanda, Rwanda
Zhiyuan Fang,
Guangdong University of Technology,
China

*Correspondence:

Qingli Yang
rice407@163.com
Wei Wu
wuweiouc@126.com

Specialty section:

This article was submitted to
Food Microbiology,
a section of the journal
Frontiers in Microbiology

Received: 15 December 2019

Accepted: 27 February 2020

Published: 27 March 2020

Citation:

Wang Q, Yang Q and Wu W
(2020) Progress on Structured
Biosensors for Monitoring Aflatoxin
B1 From Biofilms: A Review.
Front. Microbiol. 11:408.
doi: 10.3389/fmicb.2020.00408

Aspergillus exists commonly in many crops and any process of crop growth, harvest, storage, and processing can be polluted by this fungus. Once it forms a biofilm, *Aspergillus* can produce many toxins, such as aflatoxin B1 (AFB1), ochratoxin, zearalenone, fumonisin, and patulin. Among these toxins, AFB1 possesses the highest toxicity and is labeled as a group I carcinogen in humans and animals. Consequently, the proper control of AFB1 produced from biofilms in food and feed has long been recognized. Moreover, many biosensors have been applied to monitor AFB1 in biofilms in food. Additionally, in recent years, novel molecular recognition elements and transducer elements have been introduced for the detection of AFB1. This review presents an outline of recent progress made in the development of biosensors capable of determining AFB1 in biofilms, such as aptasensors, immunosensors, and molecularly imprinted polymer (MIP) biosensors. In addition, the current feasibility, shortcomings, and future challenges of AFB1 determination and analysis are addressed.

Keywords: aflatoxin B1, detection, aptasensors, aptamers, immunosensor, biosensors

INTRODUCTION

A biofilm is an extracellular matrix secreted by biological flora and easily adheres to biological or non-biological surfaces (Srey et al., 2013; Xu et al., 2019). Biofilm formation represents a self-protection mechanism of bacteria and fungi. Moreover, the biofilms formed by *Aspergillus* intensively produce many toxins in food. It is commonly accepted that the infection and proliferation of biofilm mycotoxins may occur in any field, harvest, and storage process (Siegel and Babuscio, 2011). Mycotoxins are low-molecular-weight natural secondary metabolites produced by certain fungi (Krittayavathananon and Sawangphruk, 2017). AFB1 is the most toxic among all mycotoxins, posing teratogenic, carcinogenic, and mutagenic risks to humans, and has been labeled as a group I carcinogen in humans by the International Agency for Research on Cancer (IARC) (IARC, 2002; Abnous et al., 2017a). In addition, AFB1 commonly exists in many crops such as grain, peanut, corn, and feed. AFB1 production and pollution can occur during all processes along the food chain. Because AFB1 results in significant health and economic problems in many countries, AFB1 contamination is one of the most serious problems threatening food safety (Uludag et al., 2016; Xue et al., 2019). Therefore, it is necessary to exploit novel, low-cost, and fast on-site detection technology as well as miniaturized instruments for real-time monitoring of AFB1 and prevention of AFB1 contamination.

Traditionally, aflatoxin B1 (AFB1) detection is performed by thin-layer chromatography (TLC) (Var et al., 2007; Casoni et al., 2017), enzyme-linked immunosorbent assay (ELISA) (Lee et al., 2004), mass spectrometry (MS), gas chromatography (GC), liquid chromatography (LC) (Jin and Choi, 2007; Fan et al., 2015), and high-performance LC (HPLC) (Ghali et al., 2009). These

detection assays benefit from having a high sensitivity and mature technology. However, these methods require high-cost instruments and equipment, long test times, and skilled lab researchers for the detection process. These shortcomings have limited the development of these methods for mycotoxin detection to a certain extent. Moreover, biological sensors are a new, emerging technology for the determination of mycotoxins.

A biosensor is a kind of detection method used to convert biological signals into electrical signals. This detection method offers an excellent performance, as it is easy-to-use, inexpensive, very specific, and highly sensitive. Generally, a biosensor includes three main parts: a bio-recognition component, a signal converter, and a signal measurement system (**Figure 1A**). The bio-recognition element is the core part of a biosensor, and common bio-recognition elements include aptamers (Alizadeh et al., 2018; Danesh et al., 2018), antibodies (Eivazzadeh et al., 2017), molecularly imprinted polymers (MIPs; Ton et al., 2015), and enzymes (Ricard and Buc, 2005). These bio-recognition elements possess a high selectivity and specificity for specific target substances, and only in this way can biological sensors achieve better selectivity. In addition, the signal converter is closely connected to the biological recognition component. First, the target molecules are captured by the biological recognition component. Then, the signal converter converts the biological signals into physical signals, including electrical signals, fluorescence signals, magnetic signals, and so on. Finally, these signals are detected by the detection system. Sometimes, the signal generated by the signal converter will be amplified by the signal amplifier before reaching the detection system. To date, biosensors have been used in many fields, including pathogen (Khansili et al., 2018) toxin and pesticide residue (Shang et al., 2011) detection in food, bio-marker detection for medical diagnostics, detection in water (Han et al., 2013), and detection in the atmosphere. In recent years, the combination of biosensors and nanomaterials [quantum dots (QDs), carbon nanomaterials, noble metal nanoparticles, and magnetic nanoparticles] has attracted the attention of researchers (Farka et al., 2017; Xue et al., 2019).

Based on the differences between the bio-recognition elements, biosensors have been classified as aptasensors, immunosensors, and MIP-based biosensors (**Figure 1B**). Herein, this review focuses on biosensors developed for AFB1 detection in the past 5 years. We aim to evaluate the superiority and limitations of the reported biosensors in overcoming the challenges and drawbacks of their applications.

APTASENSORS FOR AFLATOXIN B1 FROM BIOFILM

An aptasensor is a biosensor that uses aptamers as the recognition element. Aptamers are short, single-stranded oligonucleotide sequences (DNA, RNA, or nucleic acid analogs) selected from a nucleic acid molecular library using the *in vitro* systematic evolution of ligands by exponential enrichment (SELEX) method (Stoltenburg et al., 2007; Abnous et al., 2017b; Alizadeh et al., 2018). Owing to their dimensional folded configurations,

aptamers possess a high specificity and affinity for specific targets, including mycotoxins, pathogens, metal ions, pesticides, and cells (Meng et al., 2015; Danesh et al., 2018; Liu et al., 2019; Wu et al., 2019c,d; Yu S.H. et al., 2019). In contrast to antibodies, aptamers possess a superior sensitivity and stronger stability toward various pH values, temperatures, and ions, can be easily synthesized *in vitro* and modified, and are inexpensive (Rothlisberger and Hollenstein, 2018; Wu et al., 2019c). Therefore, the latent recognition ability of aptasensors for use as biosensors is better than that of immunosensors. So far, aptasensors have attracted a great deal of attention and have created new approaches for the sensitive and selective detection of toxins (Yugender Goud et al., 2017; Qian et al., 2018; Ma et al., 2019; Wang J. et al., 2019; Wu et al., 2019b). Additionally, various aptasensors have been utilized for AFB1 detection, including chemiluminescent aptasensors, fluorescent aptasensors, surface-enhanced Raman scattering (SERS)-based aptasensors, colorimetric aptasensors, and electrochemical aptasensors. Herein, we classified and comprehensively evaluated the reported aptasensors for monitoring AFB1. In addition, aptamer sequence, LOD and linear range of various aptasensors were listed in **Table 1**.

Fluorescent Aptasensors

Fluorescence spectrometry is a practical method for the sensitive determination of samples with low quantitative amounts (Gao et al., 2018; Yang Y. et al., 2018). In recent years, coupling with fluorescent nanomaterials, such as carbon dots (CDs), fluorescence dyes, up-conversion nanoparticles (UCNPs), QDs, metal nanoparticles [e.g., gold nanoparticles (AuNPs) and silver nanoparticles (AgNPs)], has become a trend in fluorescent aptasensors (Huang et al., 2018; Yang C.Y. et al., 2018; Li Z. et al., 2019; Wang Y.J. et al., 2019; Zhang M.M. et al., 2019). The most commonly used strategy of fluorescent aptasensors is the *signal-on* method, except for some cases that typically apply the theory of fluorescence resonance energy transfer (FRET). On the other hand, *signal-off* fluorescent aptasensors usually cannot eliminate the potential experimental uncertainties and false positives caused by the fluorescence source itself. According to FRET, fluorophores are used as fluorescence donors, and quenchers are used as fluorescence acceptors. First, fluorescence is blocked by the quencher, forming a detection platform in the fluorescence *signal-off* state. When the target analytes are added, the fluorophore-modified aptamer would release from the quencher surface due to the binding affinity of the aptamer and target being stronger than that of the aptamer and quencher, and the aptamer would subsequently combine with the targets and yield a significant fluorescence intensity. In addition, metal nanoparticles, humic acid (HA) (Guo M. et al., 2019), graphene oxide (GO) (Wang et al., 2020), and a quenching group have frequently been used as fluorescence quenchers.

Metal nanoparticles (AuNPs or AgNPs) are usually used as fluorescence acceptors due to their high extinction coefficient and powerful quenching ability (Farka et al., 2017; Xue et al., 2019). Recently, Lu et al. (2019) employed fluorescence switch-on aptasensors for the determination of AFB1 based

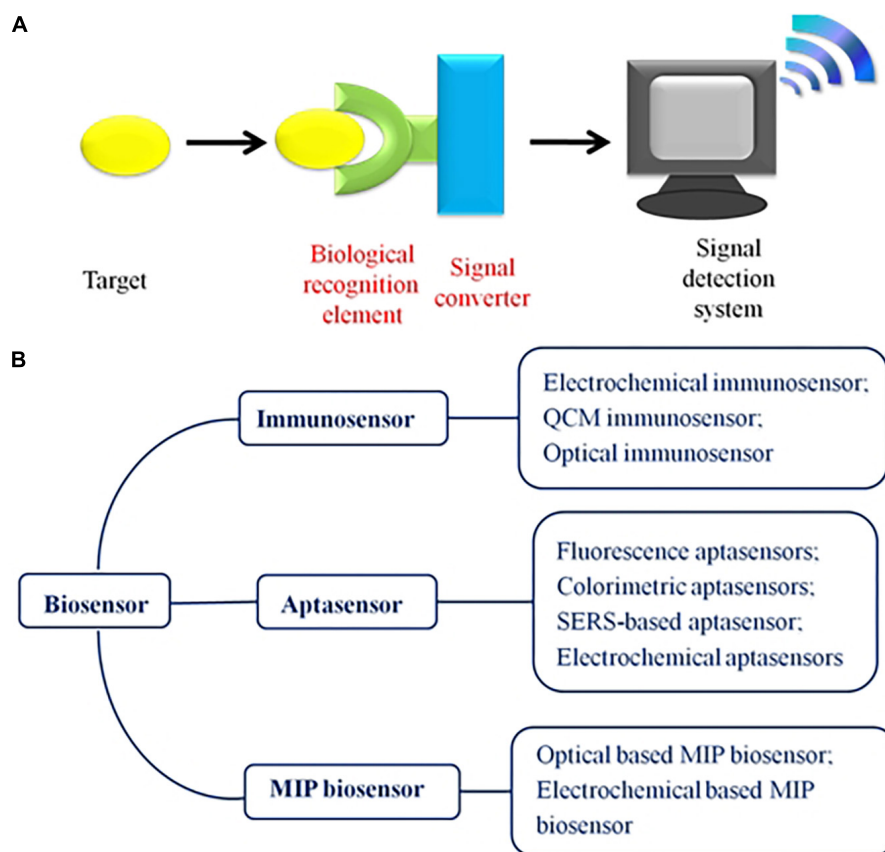


FIGURE 1 | (A) Schematic illustration of the biosensor, including the following three parts: the bio-recognition element, the signal converter, and the signal measurement system. **(B)** Outline of the biosensors used for monitoring AFB1. According to the bio-recognition element, the biosensor is divided into aptasensors, immunosensors, and MIP biosensors in this review.

on the FRET mechanism between CdZnTe QDs and AuNPs (**Figure 2A**). Therein, highly fluorescent ternary CdZnTe QDs were successfully prepared. After incubation of the CdZnTe QDs-aptamer and AuNPs-cDNA, the fluorescence of the QDs was blocked by the AuNPs because of the DNA hybridization that occurred between the aptamer and cDNA. When the target was added, the aptamer preferred to combine with AFB1 because the aptamer had a higher affinity for AFB1 than for the target, resulting in the fluorescence recovery of the CdZnTe QDs and detachment of cDNA-AuNPs. In addition, the LOD of this work was shown to be 50 pg/mL. Different metal nanoparticles have been used for AFB1 detection. For instance, Nasirian et al. (2017) established a FRET platform for the ultrasensitive determination of AFB1 that depended on the adsorption and fluorescence quenching ability of AgNPs-cDNA to a polymer dots-aptamer. Interestingly, the LOD of that work was shown to be 0.3 pg/mL.

A material with a strong affinity for single-stranded DNA (ssDNA), such as HA and GO, can also be employed to construct FRET platforms. The former, HA, possesses abundant quinoid units, aromatic rings, and sugar moieties. The latter, GO, possesses a large amount of oxygen-containing functional groups on its surface. Owing to π - π stacking, the aptamer is adsorbed

on the GO surfaces. Li et al. developed a novel fluorescence aptasensor using CD-modified aptamers as the capture probes and HA as the quencher for AFB1 detection, and the LOD was 70 pg/mL (Guo M. et al., 2019). Compared with conventional metal QDs, CDs have the following benefits: they are easy to synthesize, environmentally friendly, green, non-toxic, derived from abundant sources, inexpensive, biodegradable, and so on. In addition, Poda's group assembled a GO-FRET platform by utilizing a QD-aptamer and GO for AFB1 detection, and the LOD was 0.004 $\mu\text{g}/\mu\text{L}$ (Kumar et al., 2018).

A quencher group, such as black hole quencher 1 (BHQ1) and tetramethyl-6-carboxyrhodamine (TAMRA), has also been used in the quenching system. Generally, fluorophores, such as FAM (carboxyfluorescein), are modified with an aptamer, and the quencher group is modified with cDNA. In the absence of a target, the fluorescence is blocked due to the base complementary condition of the aptamer and cDNA. When a target is added, fluorescence is recovered and cDNA is detached. Taking advantage of these properties, Xia et al. (2019) constructed a dual-terminal proximity structure detection platform by utilizing the FAM-aptamer and anti-aptamer-labeled BHQ1. In this aptasensor, AFB1 competitively combines with the aptamers, resulting in

TABLE 1 | Selected examples of aptasensors for detection of AFB1.

Detection methods	Aptamer sequence (5'–3')	LOD	Linear range	References
Fluorescence	GTT GGG CAC GTG TTG TCT CTC TGT GTC TCG TGC CCT TCG CTA GGCCC	20 pg/mL	0.05–100 ng/mL	Lu et al., 2019
	GT TGG GCA CGT GTT GTC TCT CTG TGT CTC GTG CCC TTC GCT AGG CCC ACA	0.3 pg/mL	5–1000 pg/mL	Nasirian et al., 2017
	AAA AAA AAG TTG GGC ACG TGT TGT CTC TCT GTG TCT CGT GCC CTT CGC TAG GCC CAC AC	70 pg/mL	0.1–0.8 ng/mL	Li Z. et al., 2019
	ATA TCT TTT CCT ACT CAT CTT TGA ATA ACT ACC GGG CAT TAC TTT CTG GCC TCC CTG CCT CCT AAA TCA CCA ATT AAT TCG CGG CCC CCC G	4 ng/mL	0.002–0.2 µg/mL	Kumar et al., 2018
	GTT GGG CAC GTG TTG TCT CTC TGT GTC TCG TGC CCT TCG CTA GGC CC	1 pM	–	Wu et al., 2019a
SERS	GTTGG GCA CGT GTT GTC TCT CTG TGT CTC GTG CCC TTC GCT AGG CCC	3.6 pg/mL	0.01–100 ng/mL	Chen et al., 2018
	GTTGG GCA CGT GTT GTC TCT CTG TGT CTC GTG CCC TTC GCT AGG CCC	0.54 pg/mL	0.001–10 ng/mL	Yang et al., 2017
SPR	TGG GCA CGT GTT GTC TCT CTG TGT CTC GTG CCC T	0.4 nM	0.4–200 nM	Sun et al., 2017
	GTT GGG CAC GTG TTG TCT CTC TGT GTC TCG TGC CCT TCG CTA GGC CCA CA	0.19 ng/mL	1.5–50 ng/mL	Wu et al., 2018
Electrochemistry	GTT GGG CAC GTG TTG TCT CTC TGT GTC TCG TGC CCT TCG CTA GGC CCA CA	0.01 fg/mL	0.1 fg/mL–0.1 µg/mL	Peng et al., 2018
	GTT GGG CAC GTG TTG TCT CTC TGT GTC TCG TGC CCT TCG CTA GGC CCA CA	86 fg/mL	0.1–10 ng/mL	Selvolini et al., 2019
	GTT GGG CAC GTG TTG TCT CTC TGT GTC TCG TGC CCT TCG CTA GGC CCA CA	0.13 ng/mL	1–20 ng/mL	Mo et al., 2018

the destruction of the dual-terminal proximity structure. Additionally, the aptasensor can be used to implement ultrafast determination in one minute. Therefore, this work produced an immensely successful aptasensor for the rapid determination of AFB1.

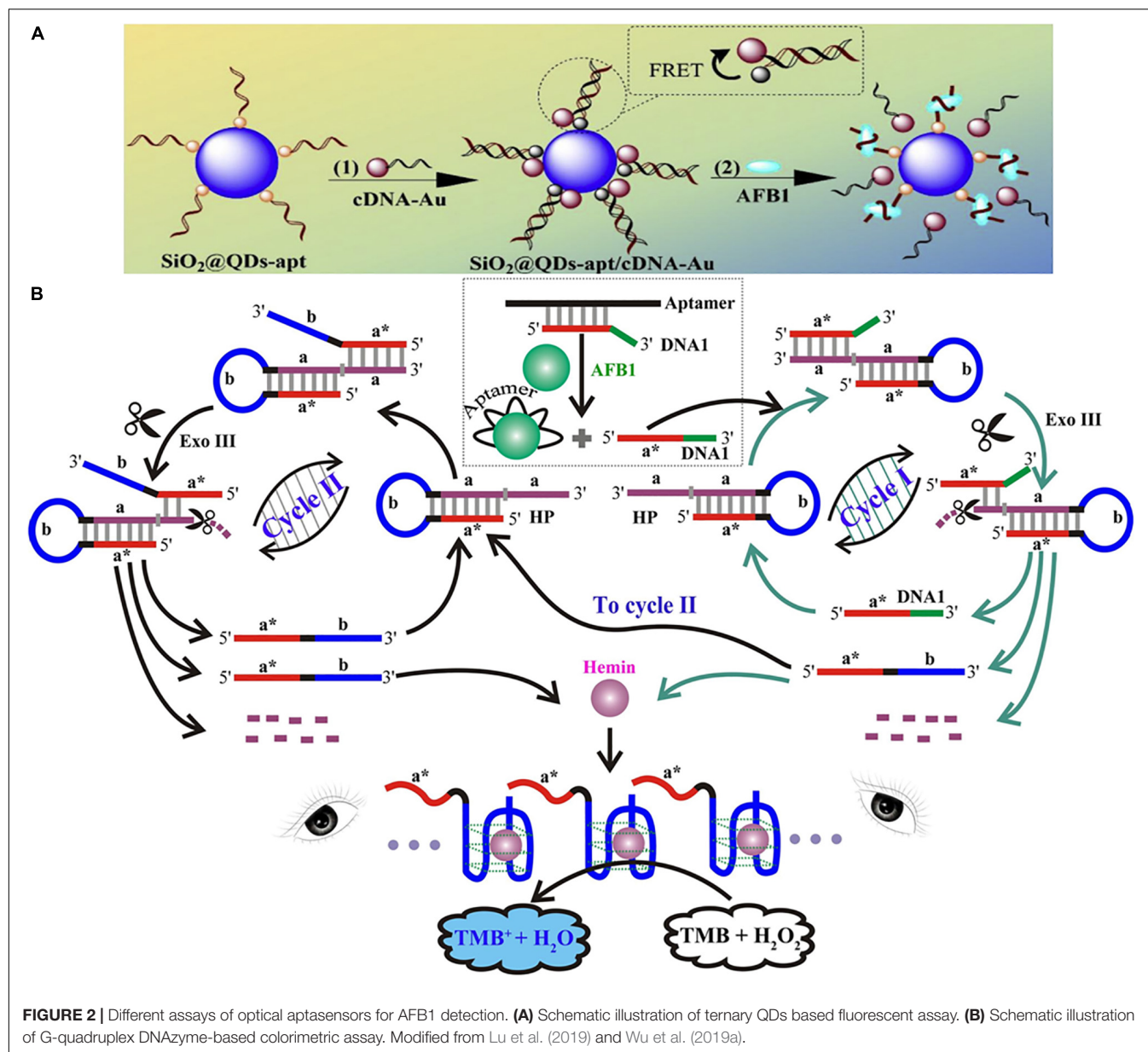
A label-free method can obtain direct evidence by detecting analytes without a label. Thus, label-free biosensors are one of the most widely used detection methods. In fact, most of the reported aptasensors were designed using the label-free approach. Jia et al. (2019) reported a new label-free fluorescent aptasensor for monitoring AFB1 in food samples by employing aggregation-induced emission (AIE) molecules and GO. Jia et al. considered the possibility of traditional fluorescence dye self-quenching in an aggregated state. Therefore, quaternized tetraphenylethene salt (TPE-Z), a kind of AIE molecule, was used as the label-free fluorescence dye. In this work, the LOD was 0.25 ng/mL.

Colorimetric Aptasensors

Colorimetry is a convenient method for *in situ* detection because the detection results can be observed by the naked eye without using an instrument. When the targets are added, the colorimetric aptasensors can convert the target signal into a color change. To improve the sensitivity, the signal amplification strategy has been employed in increasingly more widespread applications in colorimetric biosensors for detecting low analyte concentrations (Taghdisi et al., 2018; Li C. et al., 2019). In the colorimetric aptasensor system, noble metal nanoparticles are usually applied as signal indicators due to their ability to change color when changing from a dispersion

state to an aggregation state (Danesh et al., 2018; Zhang et al., 2018). Enzyme catalysis is another common method used to change the color.

A colorimetric biosensor based on the nuclease-assisted signal amplification strategy was fabricated for the naked-eye detection of AFB1 (**Figure 2B**) (Wu et al., 2019a). In this work, the domain a* of DNA1 and the AFB1 aptamer were hybridized together in the absence of AFB1, preventing the combination of DNA1 and the hairpin DNA probe (HP). The HP included the stem region (domains a, which was the recognition unit, and a*, which was complementary to a), and a surrounded the G-rich sequence lying in the loop domain (domain b). The aptamer preferred to combine with AFB1 in the presence of this toxin, releasing DNA1. Then, DNA1 and HP combined based on the principle of base complementarity, forming the blunt or recessed 3' termini of the HP. At this time, Exo III could cleave duplex DNA, liberating DNA 1 to re-enter the above-mentioned cycle (cycle I). Moreover, a new DNA fragment (domains a* and b of DNA 2) could participate in the next cycle (cycle II), in which HP catalyzed the cleavage of mononucleotides to form DNA 2 by Exo III. At the end of the cleavage reaction of cycles I and II, the G-rich oligomer of the exponentially growing DNA 2 and co-factor hemin could assemble into active DNazyme. Then, the G-quadruplex DNazyme could catalyze the oxidation reaction of H₂O₂ and TMB, and the color of the system would change from colorless to blue. Note that this work represented a brilliantly designed colorimetric aptasensor based on the signal amplification principle. In addition, the new DNA fragment (DNA 2) played a crucial role in the recycling process.



Another example employed enzyme-free amplified colorimetric aptasensors based on AuNPs for AFB1 determination (Chen et al., 2016). The signal amplification system was assembled by three biotinylated hairpin DNA probes (H1, H2, and H3). In the absence of AFB1, the aptamer-based T-DNA combined with DNA (B). However, the aptamer-AFB1 complex would activate the signal amplification device when AFB1 was added. T-DNA subsequently opened the hairpin structure of H1, H2, and H3, further forming the T-H1-H2-H3 complex. However, T-DNA would dissociate from the T-H1-H2-H3 complex, continuing to open the left hairpins. In this aptasensor, streptavidin functionalized AuNPs were used as colorimetric indicators. Then, biotinylated H1-H2-H3 complexes would combine with AuNPs via streptavidin-biotin interaction, forming a crosslinked network of AuNPs. The

ultimate red-to-blue color variation can be distinguished by the naked eye.

SERS Aptasensors

Surface enhanced Raman scattering (SERS) is an extension of the spectroscopic method developed on the basis of Raman spectra and metal nanoparticles (AuNPs or AgNPs) (Lee et al., 2019; Yu B.R. et al., 2019). Because metal nanoparticles possess an excellent signal amplification effect, the sensitivity level of SERS can be equivalent to that of fluorescence (Ding et al., 2017). The SERS aptasensors not only provide a label-free approach, which simplifies the steps and saves costs, but also possess an ultrahigh sensitivity, even down to the single-molecule level.

Due to the stability and sensitivity of the SERS signal, core-shell nanoparticles have been widely employed in SERS sensors. One SERS aptasensor was assembled by aptamer-CS-Fe₃O₄ and AFB1-complementary aptamer-AuNR@DNTB@Ag nanorods (ADANRs) (**Figure 3A**) (Chen et al., 2018). ADANRs are SERS reporter nanoprobe with a core-shell structure and produce a very sensitive SERS signal. When AFB1 was added, this compound preferred to combine with the aptamer, leading to the dissociation of the aptamer-CS-Fe₃O₄ and cDNA-ADANRs. In addition, the SERS signal at 1331 cm⁻¹ decreased, and the ADANRs were released. Using this SERS aptasensor, AFB1 was monitored at concentrations as low as 0.0036 ng/mL. Chen et al. also employed novel core-shell nanoparticles [gold nanotriangles (GNTs)-DTNB@Ag-DTNB nanotriangles] as reporters for AFB1 determination (Yang et al., 2017). The Raman characteristic peak of AFB1 is 1331 cm⁻¹. The LOD was 0.54 pg mL⁻¹, and the linear range was from 0.001 to 10 ng/mL.

Electrochemical Aptasensors

Due to their outstanding advantages, which include fast detection, easy operation, and low cost, electrochemical biosensors have been widely utilized in medical, food, and environmental fields (Wu et al., 2018). There is growing interest in employing electrochemical aptasensors that combine aptamers with electrochemical analysis technology for analyte detection.

A novel AFB1 electrochemical aptasensor based on a stereoscopic regulated macroporous MoS₂-AuNP film (SRM MoS₂-AuNPs) was constructed and used as a horseradish peroxidase (HRP)-modified electrode (**Figure 3B**) (Peng et al., 2018). In this work, the AFB1 aptamer could hybridize tetrahedral DNA nanostructures (TDNs), which were immobilized on the modified electrode. In the presence of AFB1, the aptamer preferentially combined with the toxin, forming base vacant TDNs. Thus, the TDNs could bind with the complex of the helper strand (H1)/HRP-modified nanospheres due to the base complementarity of H1 and the TDNs. HRP could catalytically reduce H₂O₂ to produce one electron. There was a linear relationship between the current response and the AFB1 concentration. Moreover, the detection limit of this brilliantly designed aptasensor was 0.01 fg/mL.

Selvolini et al. (2019) reported novel electrochemical aptasensors based on competitive approaches using AFB1 and bovine serum albumin (AFB1-BSA). The AFB1-BSA complex was coupled on the surface of graphite screen-printed electrodes. In addition, free and immobilized AFB1 molecules competed to combine with the aptamer, and the streptavidin-alkaline phosphatase enzyme conjugate monitored this process. The LOD of AFB1 was 0.086 ng/mL.

A porous anodized alumina (PAA) membrane can be used to construct nanostructured arrays. Nanochannel sensors are sensitive to electric charge change. Mo et al. (2018) developed novel sandwich structures of electrochemical aptasensors using a PAA membrane, aptamer, and GO to monitor AFB1. In the presence of AFB1, GO detached from the nanochannel surfaces, causing a decrease in the steric effect and charge density.

Therefore, the current response increased as Fe(CN)₆³⁻ passed through the nanochannels.

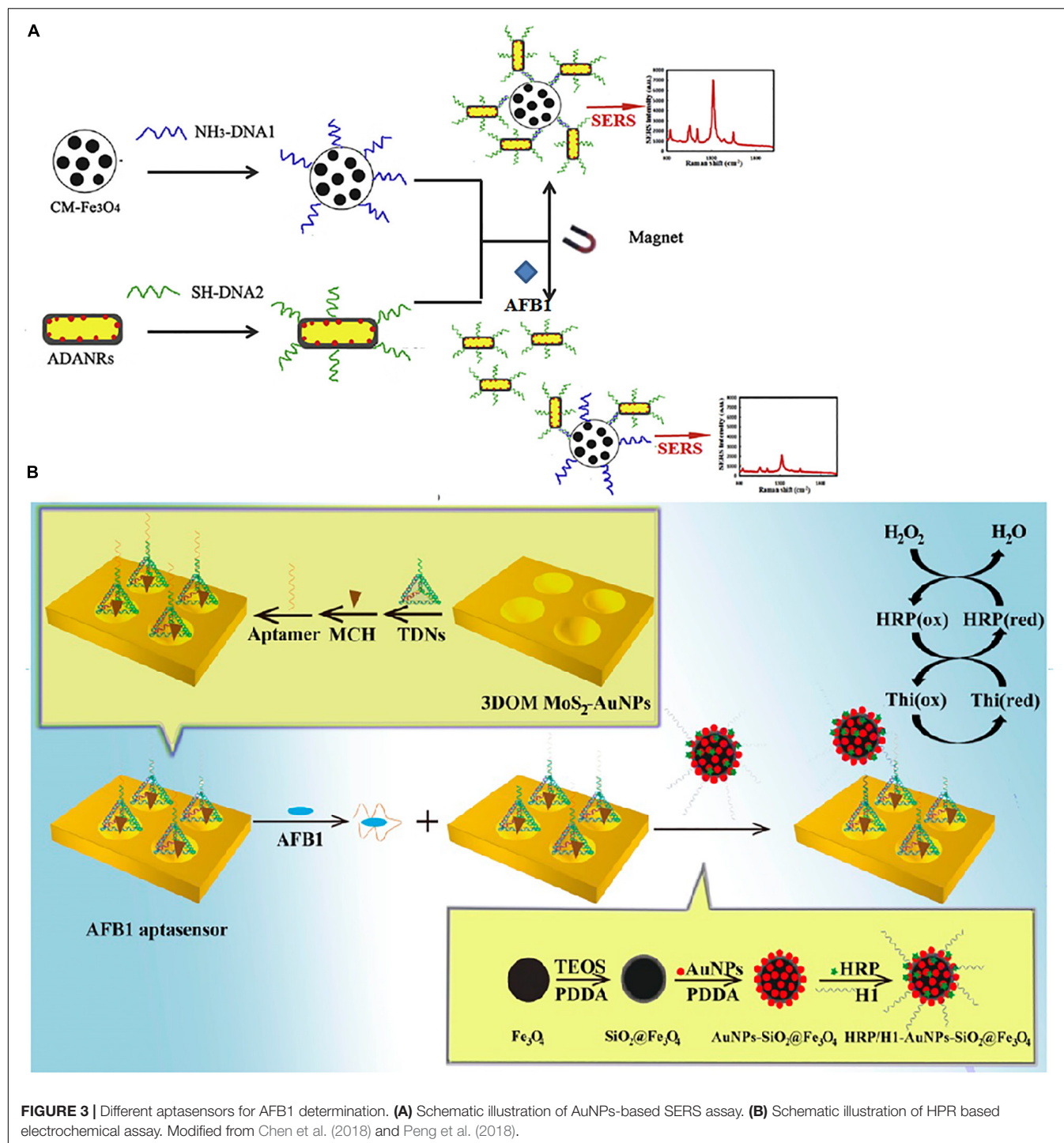
IMMUNOSENSORS

Immunosensors are the most mature monitoring method for rapid detection and combine immunoassays and biosensor technology. Immunosensors can convert the recognition of an antibody toward a specific antigen into a detection signal. Normally, the antibody is an immunoglobulin secreted by B lymphocytes in the immune system when the body is infected by antigens. Although other recognition elements have been applied in the detection field, classic antibodies, as the most popular recognition components, still dominate most markets in the field of study and commercial affinity assays.

Electrochemical Immunosensors

In electrochemical biosensors, the recognition element is mostly immobilized on the surface of electrodes. Therefore, electrochemical immunosensors can convert the recognition of an antibody toward a specific target into a detectable electrochemical signal (current, resistance, and potential). In this part of the review, electrochemical techniques, including electrochemical impedance spectroscopy (EIS), cyclic voltammetry (CV), and photoelectrochemical (PEC) methods, are discussed.

We found that EIS and CV were frequently used together in these studies. EIS measures the ratio of voltage to current at a specific frequency. In this way, it is easier to analyze the data. EIS is a detection method of the frequency domain, and this technique can monitor a wide frequency range. CV is one of the most popular electrochemical techniques and measures the current response. In addition, the sensitivity of the biosensor is determined by the sensitivity of the electrode to a change in the material. To improve the sensitivity of electrodes, nanomaterials—such as AuNPs, QDs, magnetic beads, and carbon nanomaterials—are increasingly applied to electrochemical immunoassays. Among these nanomaterials, AuNPs are commonly used as signal amplification labels due to their excellent catalytic, electrical, optical, and chemical properties. Bhardwaj et al. (2019) described an approach in which graphene QDs (GQDs) and AuNP-based electrochemical immunosensors were used to detect AFB1. Here, antibodies against AFB1 were immobilized on the surface of an ITO glass electrode coated with the GQD-AuNP composite. CV and EIS techniques were both used to evaluate the electrochemical response of this immunosensor. The edge effects of the GQDs dramatically increased the rate of heterogeneous electron transport of the composite GQDs-AuNPs. Moreover, the electrocatalytic activity of the AuNPs improved the electronic properties of the composite GQDs-AuNPs. In this study, there was a linear relationship between the concentration of AFB1 and the current signal. In addition, the linear range was 0.1–3.0 ng/mL. Similarly, Li et al. (2017) constructed a label-free impedimetric immunosensor based on Au three-dimensional nanotube ensembles (3DTNEs) and the AFB1 antibody. The



AFB1 antibodies were immobilized on the 3DTNEEs using a staphylococcus protein A layer. In this study, the particular tube-like structure and the high surface areas of the 3DTNEEs effectively improved the sensitivity of the immunosensor. The LOD of AFB1 was 1 pg/mL. In another example, Costa's group reported an impedimetric immunosensor based on carbon nanotubes and an Au electrode for monitoring AFB1 (Costa et al., 2017). In this immunosensor, the carbon nanotubes

exhibited an exceptional surface/volume ratio and excellent electrical properties.

PEC can not only translate chemical energy produced by light into electrical energy but also provide high sensitivity and a low background signal. In addition, illumination electrodes play a crucial role in PEC biosensors. $\text{Zn}_3(\text{OH})_2\text{V}_2\text{O}_7 \cdot 2\text{H}_2\text{O}$, a photoelectrochemically active material, can produce a photocurrent under UV light due to its wide band gap, but this

TABLE 2 | Selected examples of optical immunosensors for detection of AFB1.

Optical strategies	Nanomaterials	LOD	Linear range	References
Fluorescence	Magnetic fluorescent beads	27 ± 3 pg/mL	5–150 pg/mL	Guo M. et al., 2019
	CdTe/CdS/ZnS quantum dot	0.01 ng/mL	0.08–1.25 ng/mL	Zhang M.M. et al., 2019
	–	0.21 ng/mL	1.0–1000 ng/mL	Shu et al., 2019
	Porous g-C3N4 nanosheets	2 pg/mL	0.01–0.5 ng/mL	Xie et al., 2019
SPR	AuNPs	0.003 nM	0.01–50 nM	Bhardwaj et al., 2020
	–	0.59 ng/mL	–	Wei et al., 2019
	–	2.51 ppb	–	Moon et al., 2018
SERS	AuNPs	0.06 g/kg	–	Li et al., 2018
	Silica-encapsulated hollow AuNPs	0.1 ng/mL	1–10 ⁵ ng/mL	Ko et al., 2015
	Gold nanobipyramids	0.5 µg/L	–	Lin et al., 2020
PL	Gold-coated porous silicon nanocomposite	2.5 pg/ml	0.01–10 ng/ml	Myndrul et al., 2017

characteristic is very weak for visible light absorption. Lin et al. (2017) synthesized novel composites with doped transition metal ions to improve the performance of $\text{Zn}_3(\text{OH})_2\text{V}_2\text{O}_7 \cdot 2\text{H}_2\text{O}$. Moreover, dopamine-loaded liposomes were utilized to upgrade the photocurrent of Mn^{2+} -doped composites. Considering the abovementioned advantages, Lin et al. developed a novel on-site PEC immunosensor based on signal amplification for monitoring AFB1. Importantly, the LOD of this PEC immunosensor was 0.3 pg/mL.

Optical Immunosensors

Optical immunosensors used for AFB1 detection have been fabricated by fluorescence, SERS, surface plasmon resonance (SPR), and photoluminescence (PL) assays. Nanoparticles play vital roles in optical immunosensors. The core reasons might be due to the excellent optical properties of the nanomaterials and the sensitivity of the immunosensors. In this part, we compared various immunosensors based on optical monitoring assays. Optical immunosensors reported for monitoring AFB1 are reviewed in **Table 2**.

Fluorescence Immunosensors

Guo L. et al. (2019) synthesized bi-functional magnetic fluorescent beads (MFBs) with a core/shell structure by using iron oxide nanoparticles and CdSe/ZnS QDs (**Figure 4A**). Anti-AFB1 antibody-labeled MFBs (MFB-mAbs) were used to fabricate MFB strips. MFBs were first reported as dual-functional probes for pre-concentrating the target and increasing the response of the competitive sensor. Under the optimal detection conditions, the detection of the biosensor reported in this work ranged from 5 to 150 pg/mL. In another example, Zhang F. et al. (2019) also employed CdTe/CdS/ZnS QDs for conjugation with an artificial antigen. Based on a one-step fluorescence immunoassay (FLISA), this immunosensor was developed for the accurate detection of AFB1.

SPR Immunosensors

Surface plasmon resonance is a practical and label-free optical sensing technology based on the differential refractive index changes of the molecular surface. In essence, SPR is generated from the resultant force of free charge oscillations and

electromagnetic waves at the interface of the medium and metal (Zhao et al., 2019). Thus far, SPR biosensors have been employed in the fields of food (food allergens and mycotoxins), medicine (biomarkers and genes), and so on (Breveglieri et al., 2019; Jena et al., 2019; Wei et al., 2019; Zhou et al., 2019).

A new type of SPR immunosensor used for AFB1 determination using nanoparticles integrated into a gold chip was reported by Bhardwaj et al. (2020). Lipoic acid and cystamine could form a self-assembled monolayer (SAM) on the gold chip surface. AuNPs were immobilized on the SAM gold chip surface by an amine linkage. The SAM gold chip was carboxylated by EDC-NHS, combined with protein-A, and finally coupled with AFB1 antibodies. Using this approach, the linear range for monitoring AFB1 was 0.01–50 nM, with an LOD as low as 3 pM. In another example, Tao et al. established an SPR sensor chip based on a SAM for the simultaneous determination of AFB1, deoxynivalenol, zearalenone, and ochratoxin A in wheat and corn (Wei et al., 2019). The four antigens were immobilized on the SAM-SPR chip through a hydrazone linkage. Upon antibody addition, the binding index of the antibody and antigen was indicated by the SPR signal. Cross-reaction is a serious problem for many biosensors applied to simultaneously detect multiple targets. However, the low cross-reaction rate of antibodies demonstrates the high selectivity of the antibody to the antigen in this immunosensor. In addition, the ability to simultaneously detect multiple targets will become the development trend of biosensors.

SERS Immunosensors

Surface-enhanced Raman scattering assays have an advantage in that SERS signals do not exhibit self-quenching. In addition, Au/Ag nanoparticles are constantly used in SERS sensors. Li et al. (2018) explored an immunosensor based on SERS for the multiplexing determination of mycotoxins. In this study, AuNPs were applied as Raman labels and were combined with anti-mycotoxin antibodies by 5,5-dithiobis(succinimidyl-2-nitrobenzoate) (DSNB). The AuNP-DSNB-antibody complexes were used as SERS nanoprobes in which the Raman intensity of the DSNBs was greatly improved by AuNPs. The results showed a negative correlation between the concentration of AFB1 and the characteristic peak intensity in all spectra. In

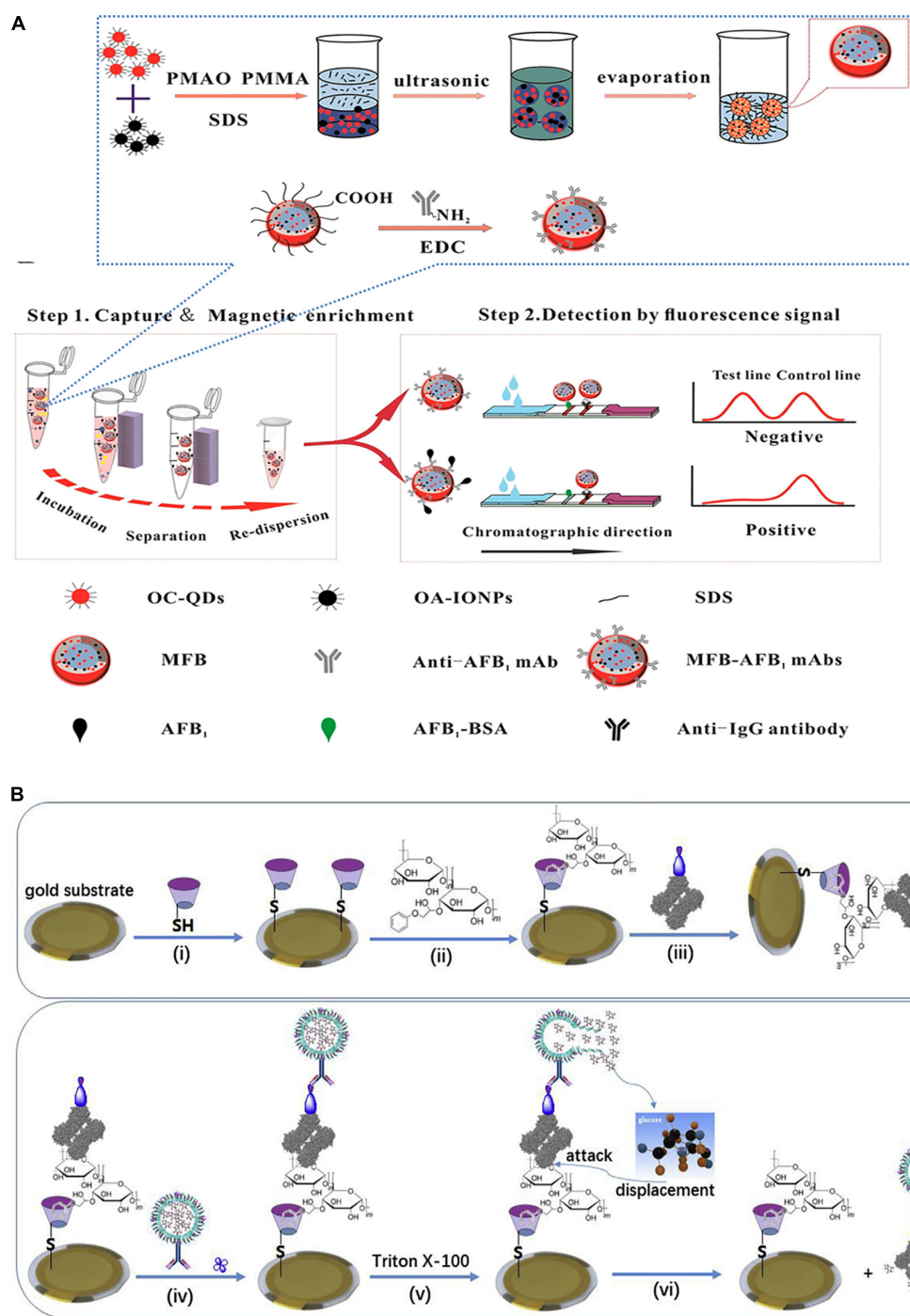


FIGURE 4 | Different immunosensor for AFB1 detection. **(A)** Schematic illustration of magnetic QDs fluorescence-based assay. **(B)** Schematic illustration of QCM-based immunoassay. Modified from Tang et al. (2018) and Guo L. et al. (2019).

another example, a SERS immunosensor based on a sandwich approach was reported by Ko et al. (2015). Anti-AFB1-modified magnetic beads were used as the fixation material, and anti-AFB1-conjugated silica-encapsulated hollow AuNPs were employed to provide the SERS signal in this immunosensor; when AFB1 was added, the toxin combined with those

two materials, forming a sandwich structure. The LOD of AFB1 was 0.1 ng/mL.

PL Immunosensors

Due to their portability and low cost, PL immunosensors are also very popular. Myndrul et al. (2017) applied a PL immunosensor

based on macroporous silicon (PSi) blanketed by a thin gold (Au) layer to detect AFB1. The PSi/Au structures showed excellent PL properties. Here, protein A played a key role in coupling the PSi/Au structures and antibodies against AFB1. The linear range of the PSi/Au/protein-A/antibody-based immunosensors for AFB1 detection was from 0.001 to 100 ng/mL.

Quartz Crystal Microbalance Immunosensors

A quartz crystal microbalance (QCM) is a quality testing instrument with a high sensitivity and has often been used as the conduction element in piezoelectric biosensors. The key technology for QCM immunosensors is to utilize the piezoelectric characteristics of quartz crystal resonators.

Tang et al. (2018) utilized a signal-on competitive QCM immunosensor for monitoring AFB1 in food (**Figure 4B**). In this method, a complex of AFB1-BSA and Con A was immobilized on the surface of an Au substrate modified with thiolated β -cyclodextrin. Anti-AFB1 antibody-marked nanoliposomes were combined with AFB1-functionalized QCM probes. When Triton X-100 was added, the encapsulated glucose molecules would be lysed and released from the nanoliposomes and would combine with Con A owing to the powerful affinity of glucose for Con A. Subsequently, anti-AFB1-labeled Con A dissociated from the QCM probe, leading to an alteration in the QCM frequency. In the presence of AFB1, the toxin and the immobilized AFB1-BSA on the probe competed for the anti-AFB1 antibody marked on the nanoliposome. The more AFB1 that was present, the more nanoliposomes that could detach from the QCM, thus causing an increase in the QCM frequency. With the optimal factors, the LOD of this immunosensor could be as low as 0.83 ng/kg, and the linear range was 1.0 ng/kg–10 mg/kg. In another example, Chauhan et al. (2015) introduced a novel electrochemical piezoelectric immunosensor functionalized with a SAM. The SAM of 4-aminothiophenol (4-ATP) was modified on an Au-coated quartz crystal (6 MHz). The AFB1 antibody (aAFB1) was immobilized on the surface of the quartz crystal by the amide linkage between aAFB1 and 4-ATP. The change in the QCM frequency indicated the mass of AFB1. This immunosensor exhibited a linear range of 0.1–4.0 ng/mL. In addition, this immunoelectrode could be reused up to five or six times.

BIOSENSORS BASED ON MIPs

An MIP is a synthetic polymer with a specific recognition function for a specific target (Ahmad et al., 2019). The polymer is self-assembled by a template molecule and functional monomers via the polymerization of crosslinkers. When the template molecule is removed, there are holes with multiple active sites that match the spatial configuration of the template molecule in the polymer. In this situation, the polymer selectively identifies the template molecule and its analogs. Therefore, MIPs can be employed as recognition elements in biosensors based on MIPs. Conventional MIPs have many advantages, such as high specificity and sensitivity, ease of operation, and inexpensiveness. However, incomplete template elimination and

a lower utilization of binding sites are undeniable limitations. Therefore, developing improved MIPs is attracting growing interest. The key to the success of an MIP sensor is whether the MIP is fixed on the converter effectively. At present, there are three common fixing methods: *in situ* polymerization, physical coating, and electropolymerization. In addition, the number of applications of MIP sensors in mycotoxin detection is limited, and only two kinds of MIP sensors are introduced in this section.

Fluorescence Biosensors Based on MIPs

Fluorescence analyses have the advantages of being highly sensitive and selective and thus are broadly used in biological sensing systems. Chmangui et al. (2019) constructed a fluorescent probe for aflatoxin (AF) recognition based on MIP-QDs (Chmangui et al., 2019). MIPs were synthesized by applying methacrylic acid (MAA) as a unit and 5,7-dimethoxycoumarin (DMC) as an artificial template. Mn-doped ZnS QDs, template, and monomer were mixed together, forming a fluorescent MIP by the self-assembly method. Therefore, the MIPs were coated with Mn-doped ZnS QDs, which successfully transformed the signal of the target into a fluorescence signal. This biosensor showed a high sensitivity to AF, with an LOD of 0.016 mg/L.

In recent years, the research hotspots of biosensor designs have been focused on on-site detection methods and technology. Due to their advantages of easy operation and detection capability in the field, smartphone-based biosensors have been reported on many times in the literature. Biosensors combining novel materials have been well received because this method avoids tedious instrument operation. Sergeyeve et al. (2019) reported an MIP biosensor based on a smartphone for AFB1 detection. MIP membranes with binding sites were constructed by *in situ* polymerization with acrylamide (AA) and 2-(diethylamino)ethylmethacrylate (AMPSA) as functional monomers. Under UV irradiation, AFB1 binding with MIPs could emit fluorescence, and the AFB1 concentration was directly proportional to the fluorescence intensity. In addition, the fluorescence signal was recorded by obtaining photographs with a cell phone camera and was analyzed using image analysis software. Moreover, the LOD of this smartphone-based optical biomimetic sensor was 20 ng/mL.

QCM Biosensors Based on MIPs

QCM sensing systems consist of a quartz crystal and metal thin layer electrodes. The combined application of QCM and MIPs has received much attention in recent years (Baek et al., 2018; Battal et al., 2018; Gu et al., 2019; Zeilinger et al., 2019). Gu et al. (2019) developed a QCM-based biosensor for the determination of AFB1, which was fabricated by AuNPs by doping a molecularly imprinted layer on an AuNP-modified electrode (**Figure 5**). In this biosensor, an MIP membrane was synthesized by an electropolymerization method on the surface of the electrode. In addition, the MIP membrane synthesized in this way showed controllable film thickness and strong adhesion. The crosslink formed between the AuNPs and MIPs overcame the shortcomings of the MIPs because the AuNPs exhibited excellent electrochemical properties, favorable biocompatibility, and good chemical stabilization. Many recognition sites were

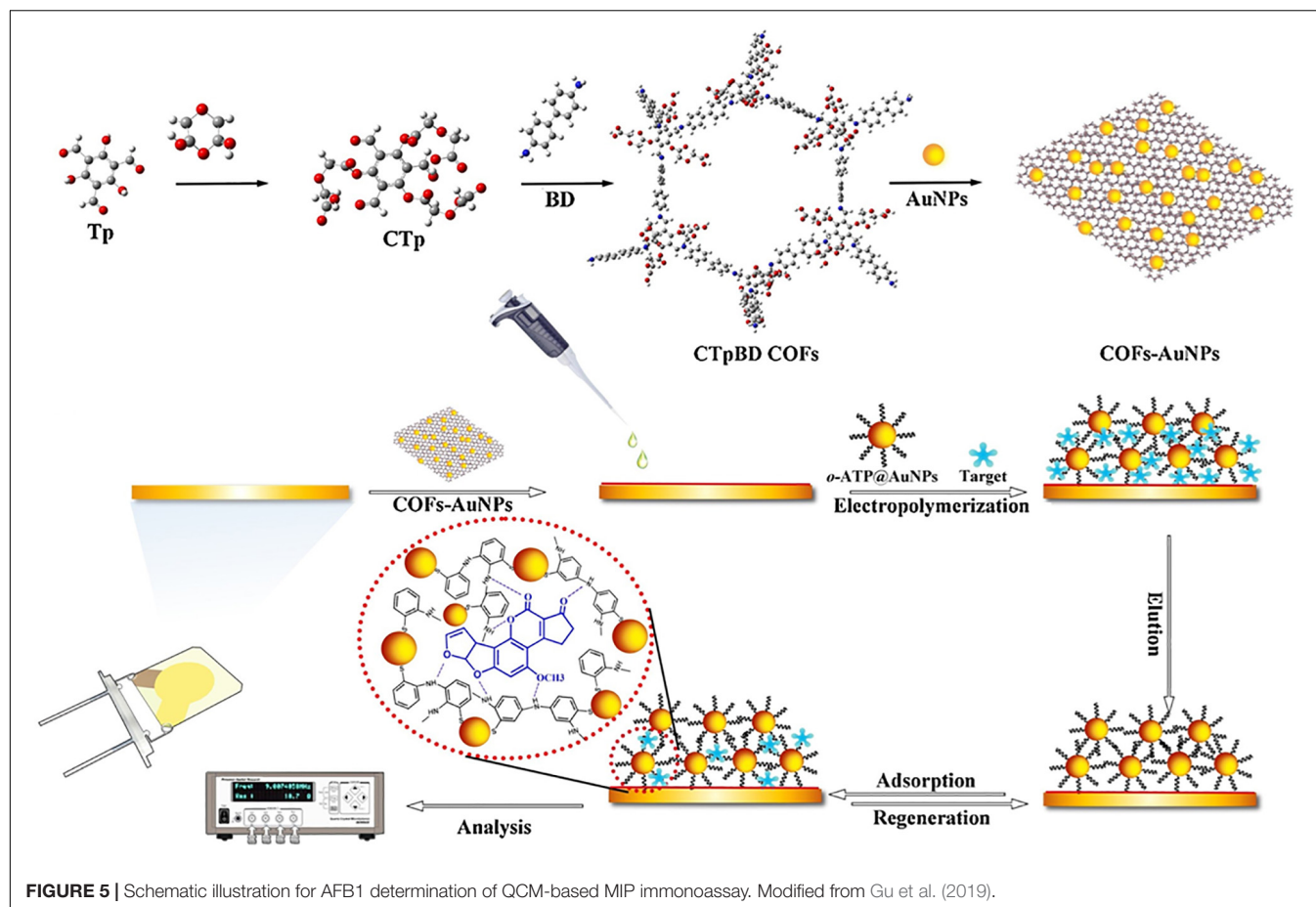


FIGURE 5 | Schematic illustration for AFB1 determination of QCM-based MIP immunoassay. Modified from Gu et al. (2019).

established on the biosensor owing to the stereoscopic structure of the imprinted polymer and the large specific surface area of the AuNP base layer. When AFB1 was added, the mass changed, leading to a change in the crystal resonance frequency. Under optimal conditions, a low limit of detection of 2.8 pg/mL was achieved.

CONCLUSION AND FUTURE OUTLOOK

In the past decades, toxin contamination produced by biofilms has resulted in many negative effects. Moreover, mycotoxin contamination has become a serious challenge for preserving food and environmental safety and has received increasing attention worldwide. Therefore, diverse biosensors have been established for the detection of different low-concentration mycotoxins. In this review, the applications of biosensors for monitoring AFB1 from biofilms in the food field have been highlighted. Compared to other biosensors, optical biosensors possess a high selectivity for monitoring analytes with low concentrations. Moreover, electrochemical biosensors have received much attention because of their simplicity, ease of operation, and high selectivity.

In addition, we noticed a strong interest in the use of nanomaterials (noble metal nanoparticles, QDs, magnetic

nanoparticles, and carbon-based nanoparticles) in biosensors due to the excellent optical, catalytic, and electrical properties of these nanomaterials. With the development of nanotechnology, novel nanomaterials, nanostructures, and the unique properties characteristic of these nanomaterials have been gradually discovered. Although the methods used to synthesize nanomaterials and the ability to control their sizes have attracted great interest, the above-mentioned factors remain a challenge. Moreover, the signal amplification strategy of biosensors is commonly used to detect analytes, specifically, low-concentration mycotoxins. Common signal amplifiers include hybridization chain reaction (HCR), the nuclease-assisted signal amplification strategy, AuNPs, the toehold-mediated DNA strand displacement reaction, and enzyme (e.g., HRP)-catalyzed amplification.

To date, the field of mycotoxin detection has achieved outstanding progress as more rapid, sensitive, and accurate methods have been developed. However, challenges and drawbacks remain in the application of biosensors for monitoring mycotoxins from biofilms. So far, researchers in related research fields seem to focus on constructing highly sensitive and selective biosensors, seeking simpler equipment and more rapid detection methods. However, researchers have overlooked an important detail: the reproducibility of biosensors. It is undeniable that large-scale instruments have great advantages in this respect. With the development of miniaturized portable instruments,

the accuracy and reproducibility of biosensors are facing increased scrutiny. On the other hand, green detection methods and systems should be considered to avoid contributing to further contamination. For example, traditional metal QDs (CdS/CdTe/CuInS₂ QDs) have a few drawbacks, such as strong toxicity of the metals to cells and difficult recovery. However, the above-mentioned issues can be avoided by using CDs as fluorescence probes, as CDs have the advantages of being non-toxic, environmentally friendly, widely available, and inexpensive. In addition, it is complicated and tedious to enrich low concentrations of mycotoxins in multicomponent food samples. This is a crucial step during the separation of AFB1 from small-molecule impurities in biofilms and could take a long time. In practical applications, the extraction process of mycotoxins from biofilms is still the greatest obstacle to achieving rapid on-site detection of mycotoxins. Developing multifunctional biosensors for simultaneous enrichment, separation, and detection will become an inevitable trend for on-site detection applications. Moreover, the degradation of AFB1 produced by biofilms after the end of the sample detection process is not a negligible task. Microbial fermentation and enzymolysis can reduce the toxicity of AFB1 in biofilms.

The combination of biosensors and nanomaterials will continue to expand with further development of this research field. Owing to the unique electrical, catalytic, and optical properties and other unknown properties of nanomaterials, biosensors based on nanomaterials will continue to be a research

hotspot. Regarding the detection of mycotoxins in biofilms, on-site detection methods, especially dipstick test strip assays, have attracted the most attention. Biosensors based on dipstick test strips have many advantages, such as ease of use, user friendliness, inexpensiveness, and high sensitivity. Moreover, most biosensors based on dipstick test strips could be used to produce results observable by the naked eye, achieving qualitative measurements without large-scale instruments. Therefore, in these processes, there is much room for improving the sensitivity and accuracy from the lab to practical applications.

AUTHOR CONTRIBUTIONS

QW and WW drafted the manuscript. WW and QY designed the concept and revised the manuscript.

FUNDING

This work was financially supported by the National Key Research and Development Program under Grant No. 2016YFD0400105, the National Natural Science Foundation of China under Grant No. 81703228, Breeding Plan of Shandong Provincial Qingchuang Research Team (2019), and China Postdoctoral Science Foundation under Grant No. 2019M652320.

REFERENCES

- Abnous, K., Danesh, N. M., Alibolandi, M., Ramezani, M., Sarreshtehdar Emrani, A., Zolfaghari, R., et al. (2017a). A new amplified pi-shape electrochemical aptasensor for ultrasensitive detection of aflatoxin B1. *Biosens. Bioelectron.* 94, 374–379. doi: 10.1016/j.bios.2017.03.028
- Abnous, K., Danesh, N. M., Alibolandi, M., Ramezani, M., Taghdisi, S. M., Emrani, A. S., et al. (2017b). A novel electrochemical aptasensor for ultrasensitive detection of fluoroquinolones based on single-stranded DNA-binding protein. *Sens. Actuators B Chem.* 240, 100–106. doi: 10.1016/j.snb.2016.08.100
- Ahmad, O. S., Bedwell, T. S., Esen, C., Garcia-Cruz, A., and Piletsky, S. A. (2019). Molecularly imprinted polymers in electrochemical and optical sensors. *Trends Biotechnol.* 37, 294–309. doi: 10.1016/j.tibtech.2018.08.009
- Alizadeh, N., Memar, M. Y., Mehramuz, B., Abibiglou, S. S., Hemmati, F., and Kafil, H. S. (2018). Current advances in aptamer-assisted technologies for detecting bacterial and fungal toxins. *J. Appl. Microbiol.* 124, 644–651. doi: 10.1111/jam.13650
- Baek, I. H., Han, H. S., Baik, S., Helms, V., and Kim, Y. (2018). Detection of acidic pharmaceutical compounds using virus-based molecularly imprinted polymers. *Polymers* 10:974. doi: 10.3390/polym10090974
- Battal, D., Akgonullu, S., Yalcin, M. S., Yavuz, H., and Denizli, A. (2018). Molecularly imprinted polymer based quartz crystal microbalance sensor system for sensitive and label-free detection of synthetic cannabinoids in urine. *Biosens. Bioelectron.* 111, 10–17. doi: 10.1016/j.bios.2018.03.055
- Bhardwaj, H., Pandey, M. K., Rajesh, and Sumana, G. (2019). Electrochemical Aflatoxin B1 immunosensor based on the use of graphene quantum dots and gold nanoparticles. *Mikrochim. Acta* 186:592. doi: 10.1007/s00604-019-3701-5
- Bhardwaj, H., Sumana, G., and Marquette, C. A. (2020). A label-free ultrasensitive microfluidic surface Plasmon resonance biosensor for Aflatoxin B1 detection using nanoparticles integrated gold chip. *Food Chem.* 307:125530. doi: 10.1016/j.foodchem.2019.125530
- Breveglieri, G., D'Aversa, E., Cosenza, L. C., Boutou, E., Balassopoulou, A., Voskaridou, E., et al. (2019). Detection of the sickle hemoglobin allele using a surface plasmon resonance based biosensor. *Sens. Actuators B Chem.* 296:126604. doi: 10.1016/j.snb.2019.05.081
- Casoni, D., Badea, M., Bros, I., and Cobzac, S. C. A. (2017). Investigation on image processing parameters for plate evaluation in TLC analysis of mycotoxins. *Stud. Univ. Babeş Bolyai Chem.* 62, 89–102. doi: 10.24193/subbchem.2017.3.07
- Chauhan, R., Solanki, P. R., Singh, J., Mukherjee, I., Basu, T., and Malhotra, B. D. (2015). A novel electrochemical piezoelectric label free immunosensor for aflatoxin B1 detection in groundnut. *Food Control* 52, 60–70. doi: 10.1016/j.foodcont.2014.12.009
- Chen, J., Wen, J., Zhuang, L., and Zhou, S. (2016). An enzyme-free catalytic DNA circuit for amplified detection of aflatoxin B1 using gold nanoparticles as colorimetric indicators. *Nanoscale* 8, 9791–9797. doi: 10.1039/c6nr01381c
- Chen, Q., Yang, M., Yang, X., Li, H., Guo, Z., and Rahma, M. H. (2018). A large Raman scattering cross-section molecular embedded SERS aptasensor for ultrasensitive Aflatoxin B1 detection using CS-Fe₃O₄ for signal enrichment. *Spectrochim. Acta A Mol. Biomol. Spectrosc.* 189, 147–153. doi: 10.1016/j.saa.2017.08.029
- Chmangui, A., Driss, M. R., Touil, S., Bermejo-Barrera, P., Bouabdallah, S., and Moreda-Pineiro, A. (2019). Aflatoxins screening in non-dairy beverages by Mn-doped ZnS quantum dots – molecularly imprinted polymer fluorescent probe. *Talanta* 199, 65–71. doi: 10.1016/j.talanta.2019.02.057
- Costa, M. P., Frías, I. A. M., Andrade, C. A. S., and Oliveira, M. D. L. (2017). Impedimetric immunoassay for aflatoxin B1 using a cysteine modified gold electrode with covalently immobilized carbon nanotubes. *Microchim. Acta* 184, 3205–3213. doi: 10.1007/s00604-017-2308-y
- Danesh, N. M., Bostan, H. B., Abnous, K., Ramezani, M., Youssefi, K., Taghdisi, S. M., et al. (2018). Ultrasensitive detection of aflatoxin B1 and its major metabolite aflatoxin M1 using aptasensors: a review. *Trends Analyt. Chem.* 99, 117–128. doi: 10.1016/j.trac.2017.12.009
- Ding, S. Y., You, E. M., Tian, Z. Q., and Moskovits, M. (2017). Electromagnetic theories of surface-enhanced Raman spectroscopy. *Chem. Soc. Rev.* 46, 4042–4076. doi: 10.1039/c7cs00238f

- Eivazzadeh, K. R., Pashazadeh, P., Hejazi, M., Miguel, d. I. G., and Mokhtarzadeh, A. (2017). Recent advances in Nanomaterial-mediated Bio and immune sensors for detection of aflatoxin in food products. *Trends Analyt. Chem.* 87, 112–128. doi: 10.1016/j.trac.2016.12.003
- Fan, S., Li, Q., Sun, L., Du, Y., Xia, J., and Zhang, Y. (2015). Simultaneous determination of aflatoxin B1 and M1 in milk, fresh milk and milk powder by LC-MS/MS utilising online turbulent flow chromatography. *Food Addit. Contam.* 32, 1175–1184. doi: 10.1080/19440049.2015.1048311
- Farka, Z., Jurik, T., Kovar, D., Trnkova, L., and Skladal, P. (2017). Nanoparticle-based immunochemical biosensors and assays: recent advances and challenges. *Chem. Rev.* 117, 9973–10042. doi: 10.1021/acs.chemrev.7b00037
- Gao, Y. Y., Ma, T. T., Ou, Z. Z., Cai, W. J., Yang, G. Q., Li, Y., et al. (2018). Highly sensitive and selective turn-on fluorescent chemosensors for Hg²⁺ based on thioacetal modified pyrene. *Talanta* 178, 663–669. doi: 10.1016/j.talanta.2017.09.089
- Ghali, R., Belouaer, I., Hdiri, S., Ghorbel, H., Maaroufi, K., Hedilli, A., et al. (2009). Simultaneous HPLC determination of aflatoxins B1, B2, G1 and G2 in Tunisian sorghum and pistachios. *J. Food Compos. Anal.* 22, 751–755. doi: 10.1016/j.jca.2010.01.039
- Gu, Y., Wang, Y., Wu, X., Pan, M., Hu, N., Wang, J., et al. (2019). Quartz crystal microbalance sensor based on covalent organic framework composite and molecularly imprinted polymer of poly(o-aminothiophenol) with gold nanoparticles for the determination of aflatoxin B1. *Sens. Actuators B Chem.* 291, 293–297. doi: 10.1016/j.snb.2019.04.092
- Guo, L., Shao, Y., Duan, H., Ma, W., Leng, Y., Huang, X., et al. (2019). Magnetic quantum dot nanobead-based fluorescent immunochromatographic assay for the highly sensitive detection of Aflatoxin B1 in dark soy sauce. *Anal. Chem.* 91, 4727–4734. doi: 10.1021/acs.analchem.9b00223
- Guo, M., Hou, Q., Waterhouse, G. I. N., Hou, J., Ai, S., and Li, X. (2019). A simple aptamer-based fluorescent aflatoxin B1 sensor using humic acid as quencher. *Talanta* 205:120131. doi: 10.1016/j.talanta.2019.120131
- Han, C., Doepke, A., Cho, W., Likodimos, V., and Dionysiou, D. D. (2013). A multiwalled-carbon-nanotube-based biosensor for monitoring microcystin-LR in sources of drinking water supplies. *Adv. Funct. Mater.* 23, 1807–1816. doi: 10.1002/adfm.201201920
- Huang, Q. T., Li, Q., Chen, Y. F., Tong, L. L., Lin, X. F., Zhu, J. J., et al. (2018). High quantum yield nitrogen-doped carbon dots: green synthesis and application as “off-on” fluorescent sensors for the determination of Fe³⁺ and adenosine triphosphate in biological samples. *Sens. Actuators B Chem.* 276, 82–88. doi: 10.1016/j.snb.2018.08.089
- IARC (2002). Some traditional herbal medicines, some mycotoxins, naphthalene and styrene. *IARC Monogr. Eval. Carcinog. Risks Hum.* 82, 1–556.
- Jena, S. C., Shrivastava, S., Saxena, S., Kumar, N., Maiti, S. K., Mishra, B. P., et al. (2019). Surface plasmon resonance immunosensor for label-free detection of BIRC5 biomarker in spontaneously occurring canine mammary tumours. *Sci. Rep.* 9:13485. doi: 10.1038/s41598-019-49998-x
- Jia, Y., Wu, F., Liu, P., Zhou, G., Yu, B., Lou, X., et al. (2019). A label-free fluorescent aptasensor for the detection of Aflatoxin B1 in food samples using AIEgens and graphene oxide. *Talanta* 198, 71–77. doi: 10.1016/j.talanta.2019.01.078
- Jin, H. D., and Choi, D. K. (2007). Aflatoxins: detection, toxicity, and biosynthesis. *Biotechnol. Bioprocess Eng.* 12, 585–593. doi: 10.1007/bf02931073
- Khansili, N., Rattu, G., and Krishna, P. M. (2018). Label-free optical biosensors for food and biological sensor applications. *Sens. Actuators B Chem.* 265, 35–49. doi: 10.1016/j.snb.2018.03.004
- Ko, J., Lee, C., and Choo, J. (2015). Highly sensitive SERS-based immunoassay of aflatoxin B1 using silica-encapsulated hollow gold nanoparticles. *J. Hazard. Mater.* 285, 11–17. doi: 10.1016/j.jhazmat.2014.11.018
- Krittayavathananon, A., and Sawangphruk, M. (2017). Impedimetric sensor of ss-HSDNA/reduced graphene oxide aerogel electrode toward Aflatoxin B1 detection: effects of redox mediator charges and hydrodynamic diffusion. *Anal. Chem.* 89, 13283–13289. doi: 10.1021/acs.analchem.7b03329
- Kumar, A. Y. V. V., Renuka, R. M., Achuth, J., Mudili, V., and Poda, S. (2018). Development of a FRET-based fluorescence aptasensor for the detection of aflatoxin B1 in contaminated food grain samples. *RSC Adv.* 8, 10465–10473. doi: 10.1039/c8ra00317c
- Lee, J. u., kim, w. h., lee, h. s., park, k. h., and sim, s. j. (2019). Quantitative and specific detection of exosomal miRNAs for accurate diagnosis of breast cancer using a surface-enhanced raman scattering sensor based on plasmonic head-flocked gold nanopillars. *Small* 15: 1804968. doi: 10.1002/sml.201804968
- Lee, N. A., Shuo, W., Allan, R. D., and Kennedy, I. R. (2004). A rapid aflatoxin B1 ELISA: development and validation with reduced matrix effects for peanuts, corn, pistachio, and Soybeans. *J. Agric. Food Chem.* 52, 2746–2755. doi: 10.1021/jf0354038
- Li, C., Hai, J., Fan, L., Li, S.-l., Wang, B.-d., and Yang, Z.-y. (2019). Amplified colorimetric detection of Ag⁺ based on Ag⁺-triggered peroxidase-like catalytic activity of ZIF-8/GO nanosheets. *Sens. Actuators B Chem.* 284, 213–219. doi: 10.1016/j.snb.2018.12.137
- Li, X., Cao, L., Zhang, Y., Yan, P., and Kirk, D. W. (2017). Fabrication and modeling of an ultrasensitive label free impedimetric immunosensor for Aflatoxin B1 based on Protein A self-assembly modified gold 3D nanotube electrode ensembles. *Electrochim. Acta* 247, 1052–1059. doi: 10.1016/j.electacta.2017.07.088
- Li, Y., Chen, Q., Xu, X., Jin, Y., Wang, Y., Zhang, L., et al. (2018). Microarray surface enhanced Raman scattering based immunosensor for multiplexing detection of mycotoxin in foodstuff. *Sens. Actuators B Chem.* 266, 115–123. doi: 10.1016/j.snb.2018.03.040
- Li, Z., Mao, G. B., Du, M. Y., Tian, S. B., Niu, L. Q., Ji, X. H., et al. (2019). A fluorometric turn-on aptasensor for mucin 1 based on signal amplification via a hybridization chain reaction and the interaction between a luminescent ruthenium(II) complex and CdZnTeS quantum dots. *Microchim. Acta* 186:233. doi: 10.1007/s00604-019-3347-3
- Lin, B., Kannan, P., Qiu, B., Lin, Z., and Guo, L. (2020). On-spot surface enhanced Raman scattering detection of Aflatoxin B1 in peanut extracts using gold nanobipyramids evenly trapped into the AAO nanoholes. *Food Chem.* 307:125528. doi: 10.1016/j.foodchem.2019.125528
- Lin, Y., Zhou, Q., and Tang, D. (2017). Dopamine-loaded liposomes for in-situ amplified photoelectrochemical immunoassay of AFB1 to enhance photocurrent of Mn(2+)-Doped Zn3(OH)2V2O7 nanobelts. *Anal. Chem.* 89, 11803–11810. doi: 10.1021/acs.analchem.7b03451
- Liu, M., Khan, A., Wang, Z. F., Liu, Y., Yang, G. J., Deng, Y., et al. (2019). Aptasensors for pesticide detection. *Biosens. Bioelectron.* 130, 174–184. doi: 10.1016/j.bios.2019.01.006
- Lu, X., Wang, C., Qian, J., Ren, C., An, K., and Wang, K. (2019). Target-driven switch-on fluorescence aptasensor for trace aflatoxin B1 determination based on highly fluorescent ternary CdZnTe quantum dots. *Anal. Chim. Acta* 1047, 163–171. doi: 10.1016/j.aca.2018.10.002
- Ma, L. Y., Bai, L. J., Zhao, M., Zhou, J., Chen, Y. J., and Mu, Z. D. (2019). An electrochemical aptasensor for highly sensitive detection of zearalenone based on PEI-MoS2-MWCNTs nanocomposite for signal enhancement. *Anal. Chim. Acta* 1060, 71–78. doi: 10.1016/j.aca.2019.02.012
- Meng, H., Fu, T., Zhang, X., and Tan, W. (2015). Cell-SELEX-based aptamer-conjugated nanomaterials for cancer diagnosis and therapy. *Natl. Sci. Rev.* 2, 71–84. doi: 10.1093/nsr/nwv001
- Mo, R., He, L., Yan, X., Su, T., Zhou, C., Wang, Z., et al. (2018). A novel aflatoxin B1 biosensor based on a porous anodized alumina membrane modified with graphene oxide and an aflatoxin B1 aptamer. *Electrochem. Commun.* 95, 9–13. doi: 10.1016/j.elecom.2018.08.012
- Moon, J., Byun, J., Kim, H., Lim, E. K., Jeong, J., Jung, J., et al. (2018). On-site detection of Aflatoxin B1 in grains by a palm-sized surface plasmon resonance sensor. *Sensors (Basel)* 18, 598–606. doi: 10.3390/s18020598
- Myndrul, V., Viter, R., Savchuk, M., Koval, M., Starodub, N., Silamikelis, V., et al. (2017). Gold coated porous silicon nanocomposite as a substrate for photoluminescence-based immunosensor suitable for the determination of Aflatoxin B1. *Talanta* 175, 297–304. doi: 10.1016/j.talanta.2017.07.054
- Nasirian, V., Chabok, A., Barati, A., Rafienia, M., Arabi, M. S., and Shamsipur, M. (2017). Ultrasensitive aflatoxin B1 assay based on FRET from aptamer labelled fluorescent polymer dots to silver nanoparticles labeled with complementary DNA. *Microchim. Acta* 184, 4655–4662. doi: 10.1007/s00604-017-2508-5
- Peng, G., Li, X., Cui, F., Qiu, Q., Chen, X., and Huang, H. (2018). Aflatoxin B1 electrochemical aptasensor based on tetrahedral DNA nanostructures functionalized three dimensionally ordered macroporous MoS2-AuNPs Film. *ACS Appl. Mater. Interfaces* 10, 17551–17559. doi: 10.1021/acsami.8b01693
- Qian, J., Ren, C. C., Wang, C. Q., Chen, W., Lu, X. T., Li, H. A., et al. (2018). Magnetically controlled fluorescence aptasensor for simultaneous

- determination of ochratoxin A and aflatoxin B1. *Anal. Chim. Acta* 1019, 119–127. doi: 10.1016/j.aca.2018.02.063
- Ricard, J., and Buc, J. (2005). Enzymes as biosensors. 1. Enzyme memory and sensing chemical signals. *Eur. J. Biochem.* 176, 103–109. doi: 10.1111/j.1432-1033.1988.tb14256.x
- Rothlisberger, P., and Hollenstein, M. (2018). Aptamer chemistry. *Adv. Drug Deliv. Rev.* 134, 3–21. doi: 10.1016/j.addr.2018.04.007
- Selvolini, G., Lettieri, M., Tassoni, L., Gastaldello, S., Grillo, M., Maran, C., et al. (2019). Electrochemical enzyme-linked oligonucleotide array for aflatoxin B1 detection. *Talanta* 203, 49–57. doi: 10.1016/j.talanta.2019.05.044
- Sergeyeva, T., Yarynka, D., Piletska, E., Linnik, R., Zaporozhets, O., Brovko, O., et al. (2019). Development of a smartphone-based biomimetic sensor for aflatoxin B1 detection using molecularly imprinted polymer membranes. *Talanta* 201, 204–210. doi: 10.1016/j.talanta.2019.04.016
- Shang, Z. J., Xu, Y. L., Gu, Y. X. Z., Wang, Y., Wei, D. X., and Zhan, L. L. (2011). A rapid detection of pesticide residue based on piezoelectric biosensor. *Proc. Eng.* 15, 4480–4485. doi: 10.1016/j.proeng.2011.08.842
- Shu, Q., Wu, Y., Wang, L., and Fu, Z. (2019). A label-free immunoassay protocol for aflatoxin B1 based on UV-induced fluorescence enhancement. *Talanta* 204, 261–265. doi: 10.1016/j.talanta.2019.05.109
- Siegel, D., and Babuscio, T. (2011). Mycotoxin management in the European cereal trading sector. *Food Control* 22, 1145–1153. doi: 10.1016/j.foodcont.2011.02.022
- Srey, S., Jahid, I. K., and Ha, S. D. (2013). Biofilm formation in food industries: a food safety concern. *Food Control* 31, 572–585. doi: 10.1016/j.foodcont.2012.12.001
- Stoltenburg, R., Reinemann, C., and Strehlitz, B. (2007). SELEX—A (r)evolutionary method to generate high-affinity nucleic acid ligands. *Biomol. Eng.* 24, 381–403. doi: 10.1016/j.bioeng.2007.06.001
- Sun, L., Wu, L., and Zhao, Q. (2017). Aptamer based surface plasmon resonance sensor for aflatoxin B1. *Mikrochim. Acta* 184, 2605–2610. doi: 10.1007/s00604-017-2265-5
- Taghdisi, S. M., Danesh, N. M., Ramezani, M., Emrani, A. S., and Abnous, K. (2018). Novel colorimetric aptasensor for zearalenone detection based on nontarget-induced aptamer walker, gold nanoparticles, and exonuclease-assisted recycling amplification. *ACS Appl. Mater. Interfaces* 10, 12504–12509. doi: 10.1021/acsami.8b02349
- Tang, Y., Tang, D., Zhang, J., and Tang, D. (2018). Novel quartz crystal microbalance immunodetection of aflatoxin B1 coupling cargo-encapsulated liposome with indicator-triggered displacement assay. *Anal. Chim. Acta* 1031, 161–168. doi: 10.1016/j.aca.2018.05.027
- Ton, X. A., Acha, V., Bonomi, P., Tse Sum Bui, B., and Haupt, K. (2015). A disposable evanescent wave fiber optic sensor coated with a molecularly imprinted polymer as a selective fluorescence probe. *Biosens. Bioelectron.* 64, 359–366. doi: 10.1016/j.bios.2014.09.017
- Uludag, Y., Esen, E., Kokturk, G., Ozer, H., Muhammad, T., Olcer, Z., et al. (2016). Lab-on-a-chip based biosensor for the real-time detection of aflatoxin. *Talanta* 160, 381–388. doi: 10.1016/j.talanta.2016.07.060
- Var, I., Kabak, B., and Gk, F. (2007). Survey of aflatoxin B1 in helva, a traditional Turkish food, by TLC. *Food Control* 18, 59–62. doi: 10.1016/j.foodcont.2005.08.008
- Wang, J., Wang, Y., Liu, S., Wang, H. W., Zhang, X., Song, X. L., et al. (2019). Primer remodeling amplification-activated multisite-catalytic hairpin assembly enabling the concurrent formation of Y-shaped DNA nanotorches for the fluorescence assay of ochratoxin A. *Analyst* 144, 3389–3397. doi: 10.1039/c9an00316a
- Wang, Q., Yang, Q., and Wu, W. (2020). Graphene-based steganographic aptasensor for information computing and monitoring toxins of biofilm in food. *Front. Microbiol.* 10:3139. doi: 10.3389/fmicb.2019.03139
- Wang, Y. J., Wei, Z. K., Luo, X. D., Wan, Q., Qiu, R. L., and Wang, S. Z. (2019). An ultrasensitive homogeneous aptasensor for carcinoembryonic antigen based on upconversion fluorescence resonance energy transfer. *Talanta* 195, 33–39. doi: 10.1016/j.talanta.2018.11.011
- Wei, T., Ren, P., Huang, L., Ouyang, Z., Wang, Z., Kong, X., et al. (2019). Simultaneous detection of aflatoxin B1, ochratoxin A, zearalenone and deoxynivalenol in corn and wheat using surface plasmon resonance. *Food Chem.* 300:25176. doi: 10.1016/j.foodchem.2019.125176
- Wu, J., Zeng, L., Li, N., Liu, C., and Chen, J. (2019a). A wash-free and label-free colorimetric biosensor for naked-eye detection of aflatoxin B1 using G-quadruplex as the signal reporter. *Food Chem.* 298:125034. doi: 10.1016/j.foodchem.2019.125034
- Wu, K., Ma, C., Zhao, H., Chen, M., and Deng, Z. (2019b). Sensitive aptamer-based fluorescence assay for ochratoxin A based on RNase H signal amplification. *Food Chem.* 277, 273–278. doi: 10.1016/j.foodchem.2018.10.130
- Wu, W., Yu, C., Chen, J., and Yang, Q. (2019c). Fluorometric detection of copper ions using click chemistry and the target-induced conjunction of split DNAzyme fragments. *Int. J. Environ. Anal. Chem.* 100, 324–332. doi: 10.1080/03067319.2019.1636977
- Wu, W., Zhu, Z., Li, B., Liu, Z., Jia, L., Zuo, L., et al. (2018). A direct determination of AFBs in vinegar by aptamer-based surface plasmon resonance biosensor. *Toxicol.* 146, 24–30. doi: 10.1016/j.toxicol.2018.03.006
- Wu, W., Yu, C., Wang, Q., Zhao, F., Hong, H., Chunzhao, L., et al. (2019d). Research advances of DNA aptasensors for foodborne pathogen detection. *Crit. Rev. Food Sci. Nutr.* 43, 1–16. doi: 10.1080/10408398.2019.1636763
- Xia, X., Wang, Y., Yang, H., Dong, Y., Zhang, K., Lu, Y., et al. (2019). Enzyme-free amplified and ultrafast detection of aflatoxin B1 using dual-terminal proximity aptamer probes. *Food Chem.* 283, 32–38. doi: 10.1016/j.foodchem.2018.12.117
- Xie, H., Dong, J., Duan, J., Hou, J., Ai, S., and Li, X. (2019). Magnetic nanoparticles-based immunoassay for aflatoxin B1 using porous g-C₃N₄ nanosheets as fluorescence probes. *Sens. Actuators B Chem.* 278, 147–152. doi: 10.1016/j.snb.2018.09.089
- Xu, Y., Dhauadi, Y., Stoodley, P., and Ren, D. (2019). Sensing the unreachable: challenges and opportunities in biofilm detection. *Curr. Opin. Biotechnol.* 64, 79–84. doi: 10.1016/j.copbio.2019.10.009
- Xue, Z., Zhang, Y., Yu, W., Zhang, J., Wang, J., Wan, F., et al. (2019). Recent advances in aflatoxin B1 detection based on nanotechnology and nanomaterials-A review. *Anal. Chim. Acta* 1069, 1–27. doi: 10.1016/j.aca.2019.04.032
- Yang, C. Y., Bie, J. X., Zhang, X. M., Yan, C. Y., Li, H. J., Zhang, M. H., et al. (2018). A label-free aptasensor for the detection of tetracycline based on the luminescence of SYBR Green I. *Spectrochim. Acta A Mol. Biomol. Spectrosc.* 202, 382–388. doi: 10.1016/j.saa.2018.05.075
- Yang, M., Liu, G., Mehedi, H. M., Ouyang, Q., and Chen, Q. (2017). A universal SERS aptasensor based on DTNB labeled GNTs/Ag core-shell nanotriangle and CS-Fe₃O₄ magnetic-bead trace detection of Aflatoxin B1. *Anal. Chim. Acta* 986, 122–130. doi: 10.1016/j.aca.2017.07.016
- Yang, Y., Shen, R., Wang, Y. Z., Qiu, F. Z., Feng, Y., Tang, X. L., et al. (2018). A selective turn-on fluorescent sensor for Hg (II) in living cells and tissues. *Sens. Actuators B Chem.* 255, 3479–3487. doi: 10.1016/j.snb.2017.09.180
- Yu, B. R., Ge, M. H., Li, P., Xie, Q. W., and Yang, L. B. (2019). Development of surface-enhanced Raman spectroscopy application for determination of illicit drugs: towards a practical sensor. *Talanta* 191, 1–10. doi: 10.1016/j.talanta.2018.08.032
- Yu, S. H., Lee, C. S., and Kim, T. H. (2019). Electrochemical detection of ultratrace lead ion through attaching and detaching DNA aptamer from electrochemically reduced graphene oxide electrode. *Nanomaterials* 9:817. doi: 10.3390/nano9060817
- Yugender Goud, K., Hayat, A., Satyanarayana, M., Sunil Kumar, V., Catanante, G., Vengatajalabathy Gobi, K., et al. (2017). Aptamer-based zearalenone assay based on the use of a fluorescein label and a functional graphene oxide as a quencher. *Microchim. Acta* 184, 4401–4408. doi: 10.1007/s00604-017-2487-6
- Zeilinger, M., Sussitz, H., Cuypers, W., Jungmann, C., and Lieberzeit, P. (2019). Mass-sensitive sensing of melamine in dairy products with molecularly imprinted polymers: matrix challenges. *Sensors* 19:2366. doi: 10.3390/s19102366
- Zhang, F., Liu, B., Zhang, Y., Wang, J., Lu, Y., Deng, J., et al. (2019). Application of CdTe/CdS/ZnS quantum dot in immunoassay for aflatoxin B1 and molecular modeling of antibody recognition. *Anal. Chim. Acta* 1047, 139–149. doi: 10.1016/j.aca.2018.09.058
- Zhang, M. M., Gao, G., Ding, Y. L., Deng, C. Y., Xiang, J., and Wu, H. Y. (2019). A fluorescent aptasensor for the femtomolar detection of epidermal growth factor receptor-2 based on the proximity of G-rich sequences to Ag nanoclusters. *Talanta* 199, 238–243. doi: 10.1016/j.talanta.2019.02.014
- Zhang, Z., Wang, H., Chen, Z., Wang, X., Choo, J., and Chen, L. (2018). Plasmonic colorimetric sensors based on etching and growth of noble metal nanoparticles:

- strategies and applications. *Biosens. Bioelectron.* 114, 52–65. doi: 10.1016/j.bios.2018.05.015
- Zhao, Y., Tong, R. J., Xia, F., and Peng, Y. (2019). Current status of optical fiber biosensor based on surface plasmon resonance. *Biosens. Bioelectron.* 142:111505. doi: 10.1016/j.bios.2019.111505
- Zhou, J., Qi, Q., Wang, C., Qian, Y., Liu, G., Wang, Y., et al. (2019). Surface plasmon resonance (SPR) biosensors for food allergen detection in food matrices. *Biosens. Bioelectron.* 142:111449. doi: 10.1016/j.bios.2019.111449

Conflict of Interest: The authors declare that the research was conducted in the absence of any commercial or financial relationships that could be construed as a potential conflict of interest.

Copyright © 2020 Wang, Yang and Wu. This is an open-access article distributed under the terms of the Creative Commons Attribution License (CC BY). The use, distribution or reproduction in other forums is permitted, provided the original author(s) and the copyright owner(s) are credited and that the original publication in this journal is cited, in accordance with accepted academic practice. No use, distribution or reproduction is permitted which does not comply with these terms.



Detection and Quantification Methods for Viable but Non-culturable (VBNC) Cells in Process Wash Water of Fresh-Cut Produce: Industrial Validation

Pilar Truchado^{1*}, Maria I. Gil¹, Mar Larrosa² and Ana Allende¹

¹ Research Group on Quality, Safety and Bioactivity of Plant Foods, The Centre of Edafology and Applied Biology of Segura, Spanish National Research Council (CEBAS-CSIC), Murcia, Spain, ² Faculty of Biomedical and Health Sciences, Nutrition, Microbiota and Health Group, Universidad Europea de Madrid, Villaviciosa de Odón, Madrid, Spain

OPEN ACCESS

Edited by:

Nguyen Thi Thanh Hanh,
Seoul National University,
South Korea

Reviewed by:

Dimitris Tsaltas,
Cyprus University of Technology,
Cyprus
Xiaomei Su,
Zhejiang Normal University, China

*Correspondence:

Pilar Truchado
ptruchado@cebas.csic.es

Specialty section:

This article was submitted to
Food Microbiology,
a section of the journal
Frontiers in Microbiology

Received: 16 January 2020

Accepted: 24 March 2020

Published: 04 May 2020

Citation:

Truchado P, Gil MI, Larrosa M and
Allende A (2020) Detection
and Quantification Methods for Viable
but Non-culturable (VBNC) Cells
in Process Wash Water of Fresh-Cut
Produce: Industrial Validation.
Front. Microbiol. 11:673.
doi: 10.3389/fmicb.2020.00673

The significance of viable but non-culturable (VBNC) cells in the food industry is not well known, mainly because of the lack of suitable detection methodologies to distinguish them from dead cells. The study aimed at the selection of the method to differentiate dead and VBNC cells of *Listeria monocytogenes* in process wash water (PWW) from the fruit and vegetable industry. Different methodologies were examined including (i) flow cytometry, (ii) viability quantitative polymerase chain reaction (v-qPCR) using an improved version of the propidium monoazide (PMAxx) dye as DNA amplificatory inhibitor, and (iii) v-qPCR combining ethidium monoazide (EMA) and PMAxx. The results showed that the flow cytometry, although previously recommended, was not a suitable methodology to differentiate between dead and VBNC cells in PWW, probably because of the complex composition of the water, causing interferences and leading to an overestimation of the dead cells. Based on results obtained, the v-qPCR combined with EMA and PMAxx was the most suitable technique for the detection and quantification of VBNC cells in PWW. Concentrations of 10 μ M EMA and 75 μ M PMAxx incubated at 40°C for 40 min followed by a 15-min light exposure inhibited most of the qPCR amplification from dead cells. For the first time, this methodology was validated in an industrial processing line for shredded lettuce washed with chlorine (10 mg/L). The analysis of PWW samples allowed the differentiation of dead and VBNC cells. Therefore, this method can be considered as a rapid and reliable one recommended for the detection of VBNC cells in complex water matrixes such as those of the food industry. However, the complete discrimination of dead and VBNC cells was not achieved, which led to a slight overestimation of the percentage of VBNC cells in PWW, mostly, due to the complex composition of this type of water. More studies are needed to determine the significance of VBNC cells in case of potential cross-contamination of fresh produce during washing.

Keywords: flow cytometry, quantitative PCR, microbial inactivation, food safety, *Listeria monocytogenes*

INTRODUCTION

Several studies have evidenced that many bacterial species, including foodborne pathogenic bacteria, develop stress resistance mechanisms that enable them to enter into a temporary state of low metabolic activity (Oliver, 2010). Under these conditions, cells can persist for extended periods without division, called dormancy or a viable but non-culturable (VBNC) state. The VBNC state has been defined as a survival strategy, where bacteria cannot grow on routine culture media but are alive and capable of renewing metabolic activity (Zhao et al., 2017; Dong et al., 2020). Recently, Dong et al. (2020) demonstrated that cells in the VBNC state go through different changes, including morphological and compositional variations, which allow them to have a higher resistance to chemical and physical stresses. Viable but non-culturable cells maintain their intact cell membrane and are metabolically active, to continue gene expression, having the ability to become culturable once resuscitated (Fida et al., 2017; Su et al., 2019). The occurrence of VBNC bacterial pathogens in food has been identified as a public risk concern (Makino et al., 2000). The presence of VBNC enterohemorrhagic *Escherichia coli* in salmon has been linked to a food poisoning incident (Dong et al., 2020). However, the significance of VBNC cells in the food industry related to cross-contamination during processing has not been elucidated, mostly because the available methodologies cannot differentiate dead and VBNC cells correctly in different matrixes. Therefore, there is a need to optimize the detection and quantification methods in different matrixes. Process wash water (PWW) has been recognized as one of the relevant vectors of microbial cross-contamination in the agro-food industries (Gil and Allende, 2018). Cross-contamination occurs when a contaminated product is washed and the pathogens are transferred from the contaminated product to the water and from the water to the clean product. Sanitizers are needed to maintain the microbiological quality of PWW, avoiding cross-contamination (Gombas et al., 2017). Chlorine is the most common sanitizer in the fresh produce industry. Generally, the efficacy of the sanitizers has been evaluated using plate counts (López-Gálvez et al., 2019). However, recently, Highmore et al. (2018) have demonstrated that chlorine induces the VBNC state of the foodborne pathogens *Listeria monocytogenes* and *Salmonella enterica*. Optimized quantification methods are required to determine the significance of the presence of VBNC cells in PWW.

The most popular methods to determine the presence and concentration of VBNC cells are staining techniques (Zhao et al., 2017). These techniques are based on the cell membrane integrity to differentiate between dead and VBNC cells, assuming that dead cells have the membrane damaged while VBNC and viable cells have an intact membrane (Oliver, 2010). However, as not all the dead cells have their cell membrane compromised, these methods can lead to an overestimation in the number of VBNC cells. The combination of dyes and flow cytometry has been widely used to determine the cell viability of foodborne pathogenic bacteria (Léonard et al., 2016), but it is not suitable for all the matrixes. Instead, viability quantitative polymerase chain

reaction (v-qPCR) has been widely adopted to detect and quantify the presence of viable bacteria in specific food matrixes and water (Truchado et al., 2016; Dorn-In et al., 2019). The quantitative real-time PCR (qPCR) methodology has been combined with the use of photoreactive dyes such as propidium monoazide (PMA) and ethidium monoazide (EMA), as PMA-qPCR in food matrix and water (Codony et al., 2015). This technique is based on the ability of PMA to penetrate the dead cells which compromised membrane integrity and bind covalently to the DNA and free DNA after photoactivation, thus preventing subsequent PCR amplification (Nocker et al., 2006). On the other hand, EMA can diffuse across cell membranes using efflux pumps (Codony et al., 2015). However, these methodologies have to be validated for each type of matrix to avoid overestimation of the VBNC cells due to the presence of dead cells with an intact membrane (Nocker and Camper, 2009).

The objective of the present study was to optimize a suitable detection and quantification method of VBNC cells in PWW and the food safety significance for the agro-food industry. Different methodologies were examined, including (i) combination of dyes and flow cytometry; (ii) v-qPCR using PMAxx, an improved version of the PMA dye; and (iii) v-qPCR combining EMA and PMAxx. Additionally, the selected methodology was validated for the first time under industrial settings for PWW treated with chlorine. These studies were performed using *L. monocytogenes* as a model foodborne pathogen, which has been described to enter into the VBNC state (Highmore et al., 2018) and linked to listeriosis outbreaks in fresh produce (European Food Safety Authority [EFSA], 2018).

MATERIALS AND METHODS

Bacterial Strains and Cocktail Preparation

For the inoculation of PWW, a six-strain cocktail of *L. monocytogenes* was used in this study. Strains were isolated from leafy vegetables, as previously described (Truchado et al., 2020). The *L. monocytogenes* strains were reconstituted in Brain Heart Infusion (BHI) broth (Oxoid, Basingstoke, United Kingdom) and consecutively subcultured twice in 10 ml of BHI, the first time at 37°C for 24 h and the second time at 37°C for 16 h. After the second incubation, 1 ml of each strain was combined to obtain a six-strain cocktail of *L. monocytogenes* (10^9 cfu/ml).

To assay the suitability of detection methods to differentiate dead and VBNC cells, bacterial suspensions of dead and viable cells (10^9 cfu/ml) were prepared as follows:

1. Heat treatment: The *L. monocytogenes* cocktail was exposed at 85°C for 20 min using a laboratory standard heat block.
2. Sanitizing treatment: Sodium hypochlorite was added to the six-strain cocktail of *L. monocytogenes* until a residual of 10 mg/l of free chlorine was reached to guarantee the complete inactivation of the cells. After a 1-min exposure time, 0.3 M of sodium thiosulfate pentahydrate (Scharlau, Barcelona, Spain) was added to quench the residual chlorine.

Free chlorine concentration was measured with a digital chlorine colorimeter kit (DPD method; LaMotte model DC 1100, Chestertown, MD).

The cell inactivation after the treatments was confirmed by plating serial suspension dilutions of the treated *L. monocytogenes* cocktail in buffered peptone water (BPW, 2 g/l; Oxoid, Basingstoke, United Kingdom) on Oxford agar (Scharlau, Barcelona, Spain) followed by incubation at 37°C for 24 h. To inoculate PWW, the initial six-strain cocktail of *L. monocytogenes* (10^9 cfu/ml) was centrifuged at 2,500 g for 5 min, and the supernatant was eliminated. The obtained pellet was washed twice with 18 ml of phosphate-buffered saline (PBS; Scharlau, Barcelona, Spain) using the same conditions as above. The cocktail was added to PWW to reach the desired concentration of approximately 10^5 cfu/ml. The final concentration of the inoculum in the PWW was confirmed by plating duplicate serial suspension dilutions on ALOA/OCLA agar (Scharlau, Barcelona, Spain) followed by incubation at 37°C for 24 h.

PWW Generated at Laboratory Scale

Process wash water from washing shredded lettuce was generated in the laboratory, mimicking the industrial conditions previously described (Tudela et al., 2019). Organic matter was measured as chemical oxygen demand (COD) determined by the standard photometric method (APHA, 1998) using the Spectroquant NOVA 60 photometer. The COD of the PWW was 1,700 mg/l.

Live/Dead Flow Cytometry Analysis

Cell viability was determined by flow cytometry (LSRFortessa X-20 system) using the Live/Dead BacLight® bacterial viability kit (Invitrogen, Waltham, United States) that contains two nucleic acid stains with different abilities to penetrate the bacterial cells: SYTO 9 and propidium iodine (PI). SYTO 9 is a cell-permeant green fluorescent dye that enters both live and dead cells. Propidium iodine is a membrane-impermeant dye that penetrates only in damaged or dead cells and emits red fluorescence upon intercalation with double-stranded DNA. When both dyes are used simultaneously, SYTO 9 is replaced by PI due to its higher affinity to bind DNA, quenching SYTO 9 fluorescence signal (Stiefel et al., 2015). As a result, red signals from cells are considered as “dead,” green signals as “alive,” and the double-staining cells as an intermediate state of membrane-compromised cells. The staining procedure was performed according to the manufacturer’s instructions.

Flow cytometry was used for measuring the viability of *L. monocytogenes* cells inoculated in PWW after treatment with chlorine. Untreated inoculated samples of PWW (50 ml) were used as controls and compared with inoculated PWW treated with 10 mg/l of free chlorine. This treatment reproduces the conditions found in industrial washing tanks. One milliliter of each PWW was mixed with 3 μ l of both dyes (5 μ M SYTO 9 and 30 μ M PI) incubated for 15 min at room temperature in the dark. The green fluorescence emission of live bacteria was detected in the cytometer at 520 nm (FL1 channel), while the red fluorescence emission of compromised (double-stained) or dead bacteria was detected at 630 nm (FL4 channel). During data acquisition, all

parameters were collected in the log mode, and data analysis was performed with the EC800 software version 1.3.6. (Sony Biotechnology Inc., Champaign, IL, United States). Forward and side scatter gates were established to exclude debris. Unstained and stained untreated live *L. monocytogenes* and isopropanol 70% dead *L. monocytogenes* were used as controls for gating the different regions and fluorescence adjustment.

PMAxx v-qPCR

PMAxx (Biotium, Hayward, CA, United States), an improved version of the PMA dye for the selective detection of live bacteria by qPCR, was used as follows. PMAxx was diluted in sterile water to obtain a 2 mM stock solution and stored at -20°C in the dark until used. Separate flasks of PWW (50 ml) were inoculated with a cocktail of *L. monocytogenes* containing live (exponential phase), heat-treated, and chlorine-treated cells to approximately 10^4 cfu/ml. From each flask, 10 ml of PWW was centrifuged at 4,000 rpm for 10 min at 4°C. The supernatant was removed, and the cell pellets resuspended in PBS at a final volume of 1,000 μ l supplemented with PMAxx to obtain a final dye concentration of 50, 75, and 100 μ M. After PMAxx addition, the samples were incubated at 200 rpm in the dark at room temperature or 40°C for 10–60 min. Stained samples were subsequently exposed to blue-light PMA-Lite LED photolysis (Interchim, Montluçon, France) for 15 min. In parallel, 10 ml of inoculated PWW was taken from each flask to determine the level of total bacteria by qPCR. Bacteria cells were concentrated by centrifugation (4,000 rpm, 4°C, 10 min). The supernatant was discarded, and untreated and PMAxx-treated pellets were kept at -20°C until DNA genomic extraction.

EMA + PMAxx v-qPCR

Ethidium monoazide (Biotium, Hayward, CA, United States) was dissolved in sterile water to obtain 2 mM stock solution and stored at -20°C in the dark until used. Following the same procedure as previously described, three separate flasks of PWW (50 ml) were inoculated with a *L. monocytogenes* cocktail of live, heat-treated, and chlorine-treated cells. Ten milliliters from each flask was centrifuged, the supernatants discarded, and the pellets treated with a combination of 10 μ M EMA and 75 μ M PMA, incubated at room temperature and 40°C and activated with blue-light PMA-Lite LED photolysis as previously described. The total bacteria were also determined by qPCR, as described above.

Culturable Bacteria

The concentration of *L. monocytogenes* (cfu/ml) in each of the different assays was confirmed by plating. Serial 10-fold dilutions were made in BPW (2 g/l; Oxoid) and plated in Oxford agar (Scharlau). Colonies were counted after 24 h of incubation at 37°C.

PWW From an Industrial Setting

Samples of PWW were taken in an industrial processing line (Cuenca, Spain) of shredded iceberg lettuce washed in a large washing tank containing about 3,000 l of PWW. A residual concentration of 10 mg/l of chlorine was set to maintain

TABLE 1 | Physicochemical and microbiological characteristics of the process wash water (PWW) at different sampling times including free chlorine (10 mg/l), pH, chemical oxygen demand (COD), temperature (T^a), oxidation-reduction potential (ORP), and total counts (log cfu/100 ml).

Sampling time	Free chlorine (mg/l)	pH	COD (mg/l)	T ^a	ORP	Total count (log cfu/100 ml)
8:00	12.6	6.6	537 ± 11	4.0	818	2.4
10:00	14.6	6.5	503 ± 10	3.8	821	2.3
10:30	10.9	6.6	382 ± 20	3.8	807	2.6
11:00	9.0	6.5	469 ± 19	4.3	783	2.5

the microbiological quality of the water. The washing was performed by immersion of cut lettuce for 30 s in the chlorinated water followed by a shower rinse with tap water for 30 s. The physicochemical and microbiological characteristics of the PWW were monitored each hour over 4 h (Table 1). The physicochemical analysis included pH, organic matter measured as COD, temperature, and oxidation-reduction potential (ORP) as well as free chlorine measurements determined as previously described (Tudela et al., 2019).

For microbiological analyses, three water samples (1 l each) per sampling time were taken. Samples were collected and processed, and levels of culturable bacterial populations enumerated as previously described (Tudela et al., 2019). For viable total bacteria, qPCR of EMA + PMAXx-treated samples was performed following the protocol previously described. Water samples (200 ml each) were vacuum filtered through sterile cellulose nitrate filters (0.45 µm). Filters were placed in falcon tubes (50 ml) containing 20 ml of PBS + Tween 80 (1 ml/l; Sigma-Aldrich, Saint Louis, United States) and shaken in a vortex for 2 min. After that, the filters were discarded and the tubes centrifuged for 10 min at 4,000 rpm. Then, the pellet was resuspended in sterile distilled water (1 ml) and transferred to clear transparent microtubes (2 ml). Then, the v-qPCR procedure was carried out as previously described. Cell pellets were stored at -20°C until DNA analysis.

DNA Extraction and qPCR Procedure

Genomic DNA was extracted using the MasterPure™ complete DNA and RNA Purification Kit (Epicentre, Madison, United States), according to the manufacturer's indications. The quality and concentration of DNA extracts were determined by spectrophotometric measurement at 260/280 and 260/230 nm using a NanoDrop® ND-1000 UV-Vis spectrophotometer (Thermo Fisher Scientific, Inc., Waltham, MA, United States). Quantitative real-time PCR and data analysis were performed using an ABI 7500 Sequence Detection System (ABI, Applied Biosystems, Madrid, Spain). For *L. monocytogenes*, the primer and probe concentrations as well as the cycling parameters and conditions for reactive quantification were as previously reported (Rodríguez-Lázaro et al., 2004). In the case of total bacteria, prime concentrations, cycling parameters, and amplification and detection conditions were as previously described (Truchado et al., 2019). The limit of detection (LOD) was based on the cycle threshold (Ct) value of the last detectable standard.

The samples with Ct values higher than LOQ were classified as non-determined, while Ct values lower than LOQ were classified as positive. LOD was determined to be Ct = 37

(23 cfu per reaction) for *L. monocytogenes* and Ct = 34 (85 cfu per reaction) for total bacteria.

Statistical Analysis

All experiments were performed at least in duplicate. Calculation and graphical representation of the median and interquartile range (IQR) of Ct values were performed using Sigma Plot 13 Systat Software, Inc. (Addlink Software Scientific, S.L. Barcelona, Spain). Total bacteria levels evaluated by plate count and molecular techniques were log10 transformed. IBM SPSS Statistics 25 was used for statistical analyses. Except when stated otherwise, *P* values below 0.05 were considered statistically significant. Shapiro-Wilk test was performed to assess the normality of the data (*P* > 0.05). Mann-Whitney *U* test was used to examine the differences among treatments.

RESULTS AND DISCUSSION

Viability of *L. monocytogenes* Cells Using Flow Cytometry

Flow cytometry was used to determine the proportions of *L. monocytogenes* cells at different states (dead, viable, and intermediate) in untreated and chlorine-treated PWW. Flow cytometry analysis allows the detection of VBNC cells that appear as double-stained cells, indicating that they are still alive but their cell membranes are compromised (Stiefel et al., 2015). This double staining allowed us to establish clearly the population of VBNC cells as shown in Figure 1, in which the potential VBNC cells can be visualized in the Q2 quadrant.

To compare the results obtained by the flow cytometry method with the plate count method, the values obtained by the plate count method were transformed into a percentage. As expected, 100% of culturable cells were obtained for the untreated PWW samples while in the treated PWW samples, it was estimated that 99.9% of the treated cells were dead and not able to grow in the culture medium. However, the flow cytometry methodology estimated that only 65.7% of the cells in the treated PWW were dead, 6.9% were VBNC, and 27.4% of bacteria were completely viable (Table 2). These results could indicate that by the flow cytometry method, bacteria that are not viable are estimated as cultivable. Our results are similar to those obtained by Nocker et al. (2016) with pure cultures of *E. coli*, in which a loss of cultivability of the bacteria with the use of chlorine was detected before any damage in their cell membrane was shown. This is probably because other cellular components were affected by chlorine besides the membrane,

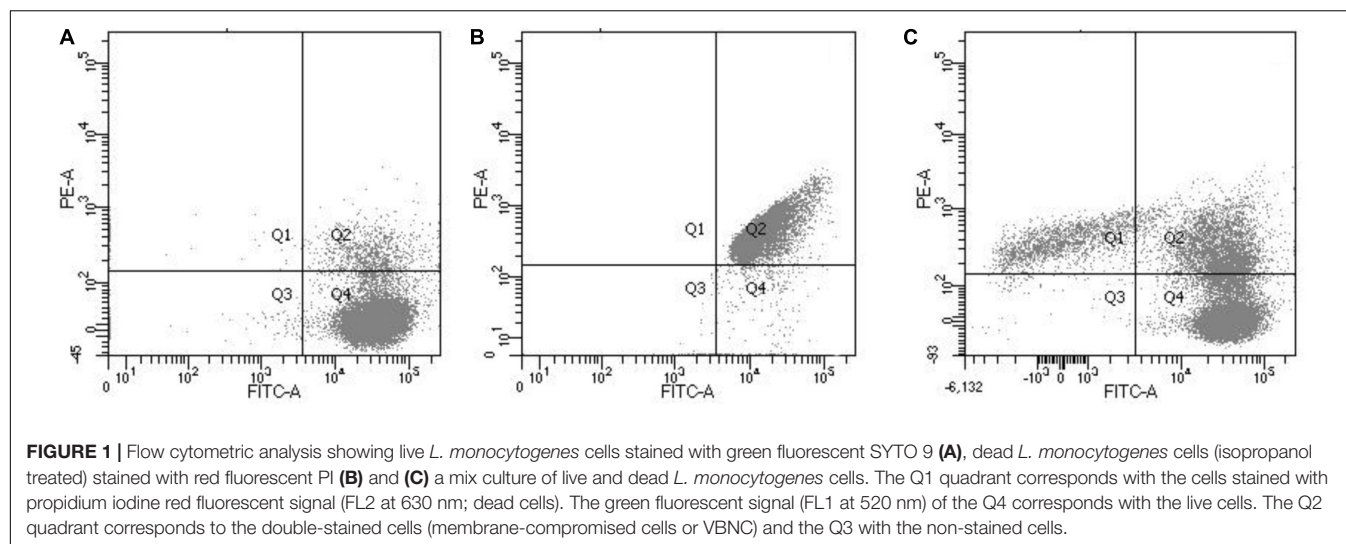


TABLE 2 | Percentage of viable, viable but non-culturable (VBNC), and dead cells of a six-strain cocktail of *Listeria monocytogenes* untreated and treated with chlorine (10 mg/L) determined by plate count and flow cytometry methods.

Methodology	Treatments	Physiological Cell Stage (%)		
		Viable	VBNC	Dead
Plate Count	Untreated	100.0		0.0
	Treated	0.0		99.9
Flow cytometry	Untreated	89.6 ± 2.3	7.8 ± 1.0	2.6 ± 1.2
	Treated	27.4 ± 3.3	6.9 ± 0.1	65.7 ± 3.3

such as proteins and lipids (Ersoy et al., 2019), which already make the cells non-viable even if their membranes were not affected. When the two methodologies were compared, the percentage of viable detected cells was higher in the flow cytometry method, which could indicate that flow cytometry could overestimate the percentage of viable cells. For the use of the flow cytometry method to determine VBNC cells, it could be necessary to use other markers of cell damage (DNA, proteins, and lipids) than the membrane. Nocker et al. (2016) observed that in samples of drinking water from a water treatment plant, there were cultivable bacteria that appeared as dead or VBNC by the flow cytometry method, in disagreement with our results. As these authors indicated, this fact could be due to the more heterogeneous natural microbiota with different susceptibilities to the disinfectant in water samples. In our study, due probably to the differences in the natural microbiota from lettuce, the results differed.

Taking into account the complex composition of the PWV, with high organic matter content and interfering compounds, the fluorescent dyes were not able to differentiate among the physiological stage of the different bacteria species. Based on the results obtained, the flow cytometry was not a suitable methodology to distinguish between viable and dead cells in PWV. Several studies have suggested the use of flow cytometry as an accurate analytical tool to determine the viability against sanitizers of the foodborne pathogenic bacteria (Nocker et al., 2016; Ersoy et al., 2019). However, these studies were

mostly performed using tap water or pure cultures, without considering the complex composition of PWV in industrial settings (Gombas et al., 2017).

Viability of *L. monocytogenes* Cells Using v-qPCR Techniques Combined With PMAxx

In general, PMA concentrations of 50 μM have been reported to be the optimal concentration for the efficient differentiation between live and dead cells without affecting the viability of *L. monocytogenes* cells (Kragh et al., 2020). However, when complex matrixes, such as PWV, are used, the concentration of PMAxx needs to be optimized to avoid any impact on cell viability. Preliminary experiments performed to determine the optimal concentration of PMAxx showed that when 50 μM of PMAxx was added to PWV, the PCR signal of dead cells was not fully discriminative (data not shown). One reason could be the presence of organic matter in the PWV, which might interfere with the photoreactive DNA dye, reducing its ability to bind to the DNA of the dead cells. Based on these results, two higher concentrations of PMAxx (75 and 100 μM) were tested. The quantitative PCR Ct values of heat-killed *L. monocytogenes* treated with 75 and 100 μM PMAxx concentrations were not significantly different (**Figure 2A**). However, a toxicity effect was observed in the live cells when a higher concentration of the dye was used (**Figure 2B**). Therefore, to avoid any impact on the

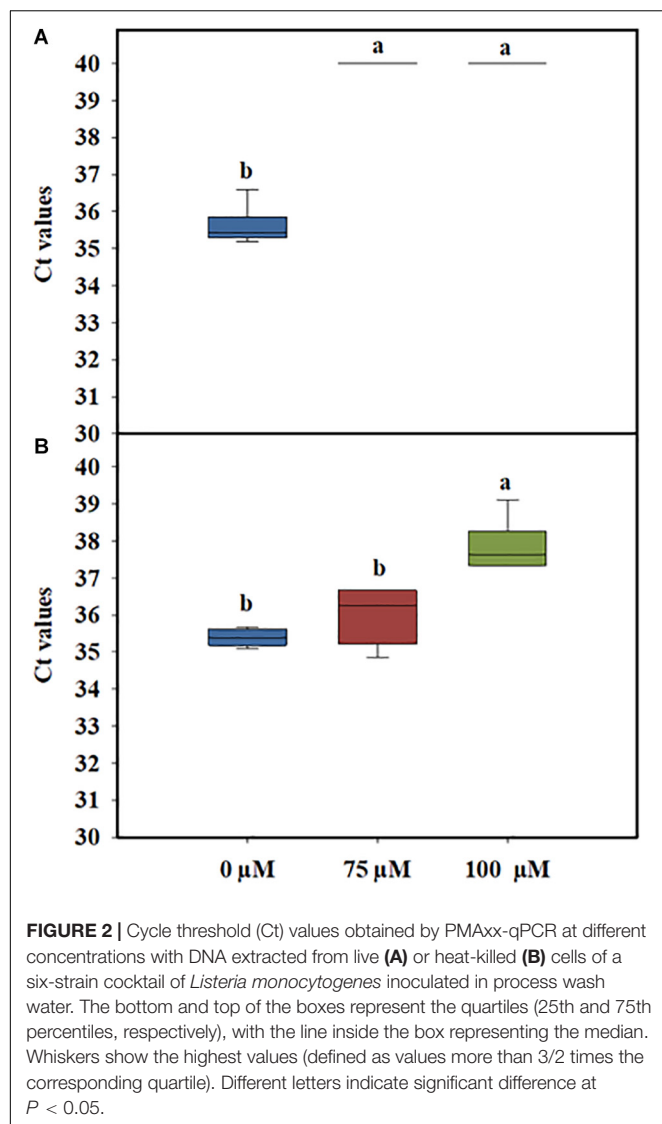


FIGURE 2 | Cycle threshold (Ct) values obtained by PMAxx-qPCR at different concentrations with DNA extracted from live (A) or heat-killed (B) cells of a six-strain cocktail of *Listeria monocytogenes* inoculated in process wash water. The bottom and top of the boxes represent the quartiles (25th and 75th percentiles, respectively), with the line inside the box representing the median. Whiskers show the highest values (defined as values more than 3/2 times the corresponding quartile). Different letters indicate significant difference at $P < 0.05$.

viability of the *L. monocytogenes* cells, the lowest concentration (75 µM) of PMAxx was selected for further analysis.

Several studies have focused on the optimization of methodologies able to discriminate between live and dead cells of pathogenic bacteria such as *Xylella fastidiosa*, *Vibrio parahaemolyticus*, and *Clavibacter michiganensis* ssp. *michiganensis* in complex matrixes such as plants, shrimp, and seed tomato, respectively (Han et al., 2018; Cao et al., 2019b; Sicard et al., 2019). Most of these studies evidence the good discriminative effect of PMAxx when compared to PMA between live and dead cells in complex matrixes. However, as far as we know, differentiation between live and dead *L. monocytogenes* in PWW has not been accomplished.

v-qPCR Combined With PMAxx + EMA

Laboratory-scale experiments were performed to study the mode of action by which chlorine killed *L. monocytogenes*

cells and whether or not the membrane integrity of the cells was affected. It has been accepted that chlorine and other chemical sanitizers usually inactivate the bacterial cell by the disruption of the cytoplasmic membrane (Venkobachar et al., 1997; Nocker et al., 2007). However, it is essential to determine the suitability of PMAxx to differentiate between live and dead cells when chlorine treatments are applied. In these experiments, PCR amplification of dead *L. monocytogenes* cells killed by heat treatment was compared with those killed by chlorine. The initial conditions used for this comparison were those previously recommended to discriminate dead *L. monocytogenes*, including 30 min of dye incubation at 40°C (Nkuipou-Kenfack et al., 2013). As expected, *L. monocytogenes* DNA activated with PMAxx (75 µM) and isolated from heat-treated *L. monocytogenes* did not show amplification in the qPCR. However, the PCR signal of *L. monocytogenes* DNA activated with PMAxx (75 µM) obtained from chlorine-treated cells was not completely inactivated, showing a Ct value below the LOD (Figure 3). Our results agree with a previous study that observed that PMA-qPCR assay (PMA at 50 µM for 20 min of incubation at 37°C) did not reduce the signal of chlorine-killed cells of *E. coli* O:157 H7 (10⁴ cfu/ml) artificially inoculated in drinking water (Cao et al., 2019a). Based on these results, new experiments were performed under different conditions of time/temperature for the incubation of the DNA with the dye. However, none of the tested combinations improved previous results obtained (data not shown).

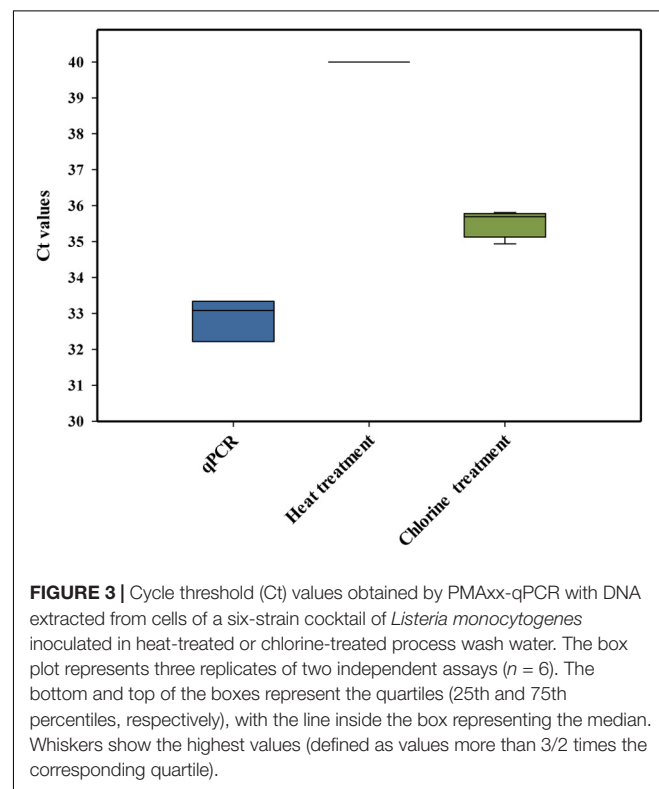
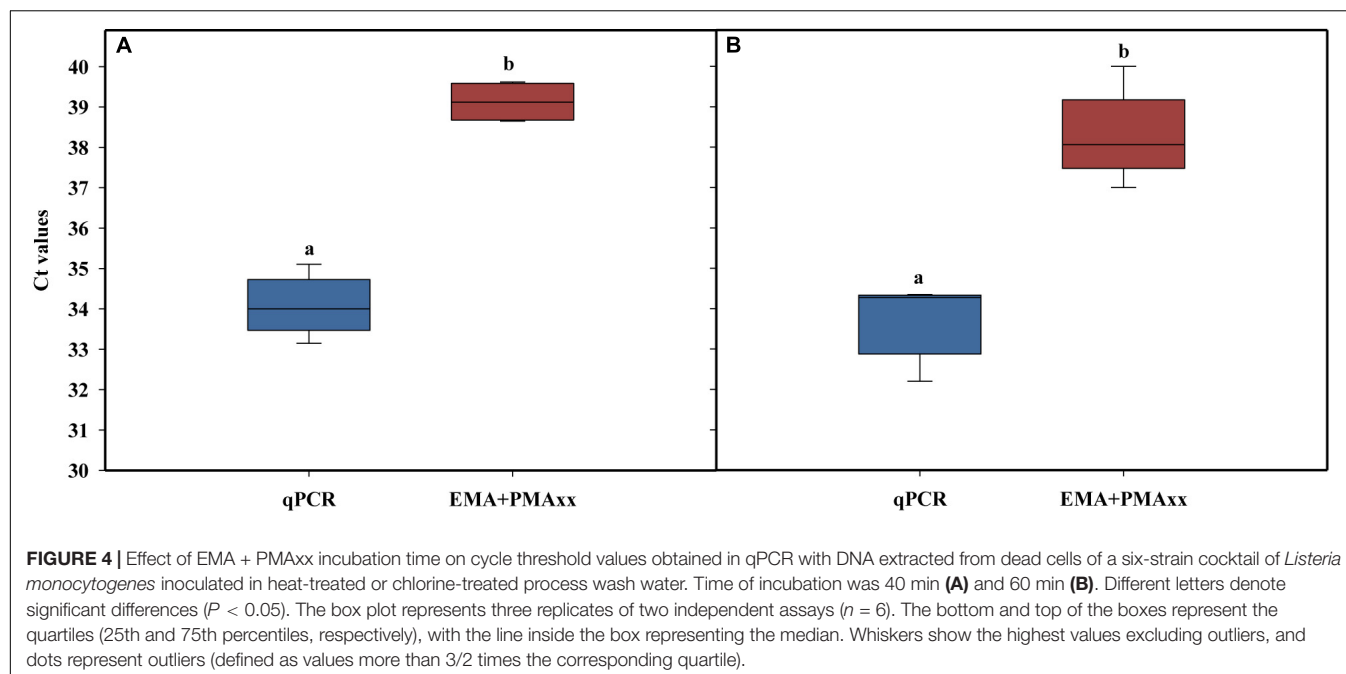


FIGURE 3 | Cycle threshold (Ct) values obtained by PMAxx-qPCR with DNA extracted from cells of a six-strain cocktail of *Listeria monocytogenes* inoculated in heat-treated or chlorine-treated process wash water. The box plot represents three replicates of two independent assays ($n = 6$). The bottom and top of the boxes represent the quartiles (25th and 75th percentiles, respectively), with the line inside the box representing the median. Whiskers show the highest values (defined as values more than 3/2 times the corresponding quartile).



The results indicated that there was an overestimation of the live cells because some dead cells could still be quantified (false-positive results) after the chlorine treatment, mostly due to the presence of an intact membrane. A similar conclusion was also achieved by Virto et al. (2005) who observed that membrane damage is not the only event involved in the inactivation of bacteria by chlorine. These authors also highlighted that the presence of organic matter could play an important role in the accessibility of chlorine to the bacteria, influencing their resistance. Based on these findings, the PMAxx-qPCR method was not considered a suitable approach to differentiate between live and dead *L. monocytogenes* cells present in PWW treated with chlorine.

The alternative method studied was EMA combined with PMAxx, to detect both membrane integrity and active metabolism (Codony, 2014; Codony et al., 2015; Agustí et al., 2017). Several authors have suggested that cell viability should include cells that have intact, functional, and active membranes (Codony et al., 2015). Some studies related to membrane integrity reported that the combination of EMA and PMA reduced the DNA signal from dead cells (intact and damage

membrane) and live cells with inactive membranes (Codony et al., 2015). This method is based on the EMA properties, which accumulate in dormant cells that lack the metabolic ability to offset its uptake using active mechanisms such as efflux pumps. Concentrations of 75 μM of PMAxx and 10 μM of EMA were used followed by incubation at 40°C at two incubation times

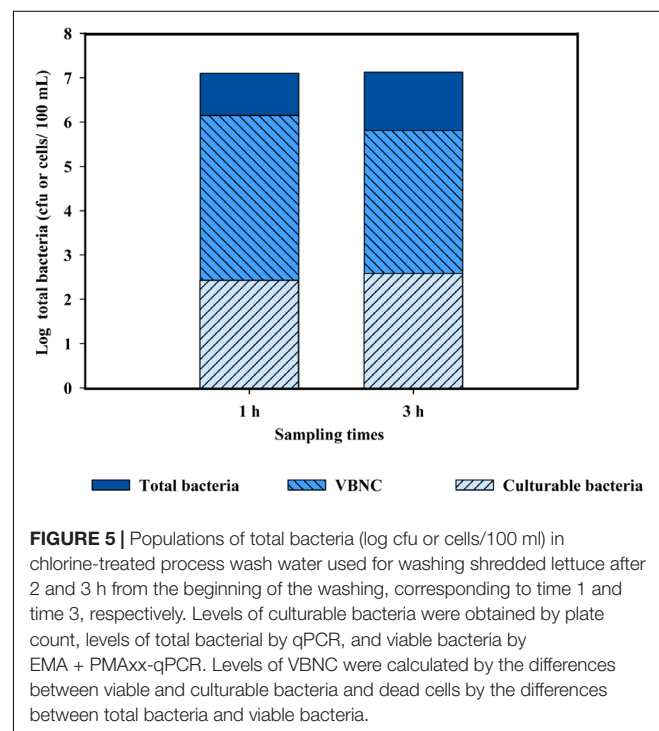


TABLE 3 | *Listeria monocytogenes* counts inoculated in process wash water detected by qPCR combined or not with EMA + PMAxx at two incubation times.

Time of incubation (min)	<i>L. monocytogenes</i> (log cfu/ml)	
	qPCR	EMA + PMAxx-qPCR
40	4.14 \pm 0.10a	3.83 \pm 0.11a
60	4.34 \pm 0.02a	3.29 \pm 0.06b

Values represent the mean \pm standard deviations for three independent replicates.

(40 and 60 min) and a 15-min light exposure. The results showed that, independently of incubation time, the combination of the two photoreactive dyes (PMAxx and EMA) reduced the amplification of dead cells after chlorine treatment above the LOD (Ct value > 37; **Figure 4**). When the two incubation times were compared, a slight increase in the Ct values was observed when 60 min was applied versus 40 min (Ct value = 39 and 37, respectively). However, it should be considered that a long incubation time might have a negative effect on the viability of *L. monocytogenes* cells inoculated in PWW. The differences between the levels of *L. monocytogenes* enumerated by qPCR and EMA + PMAxx-qPCR are shown in **Table 3**. Based on these results, an incubation time of 40 min was selected. The latest studies demonstrated that the commercial PEMA reagent (a new commercial reagent that combines both EMA and PMA) is suitable in food matrixes and complex environmental samples, avoiding the overestimation of the most common methodologies (Agustí et al., 2017; Daranas et al., 2018).

Validation of the Detection and Quantification Method for VBNC Cells

The detection method selected, EMA + PMAxx-qPCR, was validated in PWW samples obtained in an industrial processing line where shredded lettuce was washed with chlorine. Based on the results obtained, no significant changes in the concentration of free chlorine and pH were observed along with the sampling interval that was able to control the accumulation of bacteria in the PWW, maintaining a total count below 3 log units (**Table 1**). Similar results have been previously described in several industrial washing lines (López-Gálvez et al., 2019; Tudela et al., 2019).

When the levels of total bacteria present in PWW were quantified, the results obtained by cultivation-based methods were very different than those based by molecular-based techniques (both qPCR and EMA + PMAxx-qPCR). Several studies have reported that the use of plate count methods leads to an underestimation of the total bacterial levels in environmental samples, mostly due to the presence of cells in the VBNC state (Rastogi et al., 2010; Truchado et al., 2019). The results obtained indicate that chlorine (10 mg/l) induced bacteria into a VBNC state (**Figure 5**). Only slight differences were observed between the two sampling points (1 and 3 h). These results agree with those of Highmore et al. (2018) who demonstrated that the use of chlorine induced cells of *Salmonella enteritidis* and *L. monocytogenes* into a VBNC state. However, the conditions applied in this referenced study (Highmore et al., 2018) did not represent real conditions of a fresh-cut processing line, which include the presence of high concentrations of organic matter and background microbiota in the PWW. This is the first study showing the induction of the VBNC state of bacteria cells present in PWW when water was disinfected with chlorine in industrial settings.

CONCLUSION

The v-qPCR combined with the two DNA amplificatory inhibitors (EMA and PMAxx) represents the optimization technique for the detection and quantification of cells in the VBNC state. The use of these photoreactive DNA-dye combinations (EMA and PMAxx) yields a more accurate estimation of the *L. monocytogenes* viable cells present in PWW than other methodologies tested, such as flow cytometry and PMAxx-qPCR. Concentrations of 10 μ M EMA and 75 μ M PMAxx and incubation at 40°C for 40 min followed by a 15-min light exposure allowed the inactivation of most of the dead cells. The validation of the method in an industrial setting showed that the methodology optimized could significantly distinguish dead and VBNC cells in PWW treated with chlorine. This method can be considered as a rapid and reliable one recommended for the detection of VBNC cells in complex water matrixes such as those of the food industry. However, complete discrimination between dead and VBNC cells was not achieved, which led to a slight overestimation on the percentage of VBNC cells in the PWW, mostly due to the complex composition of this type of wash water. The verification of the methodology optimized with different sanitizers is worthy of being investigated.

DATA AVAILABILITY STATEMENT

The raw data supporting the conclusions of this article will be made available by the authors, without undue reservation, to any qualified researcher.

AUTHOR CONTRIBUTIONS

PT, MG, and AA designed this experiment. PT conducted the molecular lab work and data analysis. ML conducted the cytometry flow lab work and data analysis. PT drafted the manuscript under the advisement of AA. All authors met to develop methods used for conducting the study and read the draft and provided feedback.

ACKNOWLEDGMENTS

The authors are thankful for the financial support from the Center for Produce Safety Grant Agreement (Projects 2018 RFP), the MINECO (Project AGL2016-75878-R), and the Fundación Séneca (19900/GERM/15). The technical assistance of Silvia Andújar and Natalia Hernández was very much appreciated. The authors acknowledge support of the publication fee by the CSIC Open Access Publication Support Initiative through its Unit of Information Resources for Research (URICI).

REFERENCES

- Agustí, G., Fittipaldi, M., and Codony, F. (2017). False-Positive viability PCR results: an association with microtubes. 2017. *Curr. Microbiol.* 74, 377–380. doi: 10.1007/s00284-016-1189-3
- American Public Health Association [APHA] (1998). *Standard Methods for Examination of Water and Wastewater*, 20th Edn. Washington, DC: American Public Health Association.
- Cao, Y., Zhou, D., Li, R., Yu, Y., Xiau, X., Zhou, A., et al. (2019a). Molecular monitoring of disinfection efficacy of *Escherichia coli* O157:H7 in bottled purified drinking water by quantitative PCR with a novel dye. *J. Food Process Preserv.* 43:e13875. doi: 10.1111/jfpp.13875
- Cao, X., Zhao, L., Zhang, J., Chen, X., Shi, L., Famg, X., et al. (2019b). Detection of viable but nonculturable *Vibrio parahaemolyticus* in shrimp samples using improved real-time PCR and real-time LAMP methods. *Food Control* 103, 145–115.
- Codony, F. (2014). *Procedimiento Para la Detección de Células Vivas, Con las Membranas Celulares Íntegras y Funcionales, Mediante Técnicas de Amplificación de Ácidos Nucleicos*. Spanish patent, N° ES2568527B1.
- Codony, F., Agustí, G., and Allué-Guardia, A. (2015). Cell membrane integrity and distinguishing between metabolically active and inactive cells as a means of improving viability PCR. *Mol. Cell Probes.* 29, 190–192. doi: 10.1016/j.mcp.2015.03.003
- Daranas, N., Bonater, A., Francés, J., Cabrefiga, J., Montesinos, E., and Badosa, E. (2018). Monitoring viable cells of the biological control agent *Lactobacillus plantarum* PM411 in aerial plant surfaces by means of a strain-specific viability quantitative PCR method. *Appl. Environ. Microbiol.* 84, e107–e118. doi: 10.1128/AEM.00107-18
- Dong, K., Pan, H., Yang, D., Rao, L., Zhao, L., Wang, Y., et al. (2020). Induction, detection, formation, and resuscitation of viable but non-culturable state microorganisms. *Compr. Rev. Food Sci. Food Safety* 19, 149–183. doi: 10.3389/fmicb.2018.02728
- Dorn-In, S., Gareis, M., and Schwaiger, K. (2019). Differentiation of live and dead *Mycobacterium tuberculosis* complex in meat samples using PMA-qPCR. *Food Microbiol.* 84:103275. doi: 10.1016/j.fm.2019.103275
- Ersoy, Z. G., Dinc, O., Cinar, B., Gedik, S. T., and Dimoglo, A. (2019). Comparative evaluation of disinfection mechanism of sodium hypochlorite, chlorine dioxide and electroactivated water on *Enterococcus faecalis*. *LWT* 102, 205–213. doi: 10.1016/j.lwt.2018.12.041
- European Food Safety Authority [EFSA] (2018). *Listeria monocytogenes* contamination of ready to eat foods and the risk for human health in the EU. *EFSA J.* 16, 5134–5307.
- Fida, T. T., Moreno-Forero, S. K., Breugelmans, P., Heipieper, H. J., Röling, W. F., and Springael, D. (2017). Physiological and transcriptome response of the polycyclic aromatic hydrocarbon degrading *Novosphingobium* sp. LH128 after inoculation in soil. *Environ. Sci. Technol.* 51, 1570–1579. doi: 10.1021/acs.est.6b03822
- Gil, M. I., and Allende, A. (2018). “Water and wastewater use in the fresh produce industry: food safety and environmental implications,” in *Quantitative Methods for Food Safety and Quality in the Vegetable Industry*. Food Microbiology and Food Safety, eds F. Pérez-Rodríguez, P. Skandamis, and V. Valdramidis, (Switzerland: Springer), 59–77.
- Gombas, D., Luo, Y., Brennan, J., Shergill, G., Petran, R., Walsh, R., et al. (2017). Guidelines to validate control of cross-contamination during washing of fresh-cut leafy vegetables. *J. Food Protect.* 80, 312–330. doi: 10.4315/0362-028X.JFP-16-258
- Han, S., Jiang, N., Lv, Q., Kan, Y., Hao, J., Li, J., et al. (2018). Detection of *Clavibacter michiganensis* subsp. *michiganensis* in viable but nonculturable state from tomato seed using improved qPCR. *PLoS One* 13:e0196525. doi: 10.1371/journal.pone.0196525
- Highmore, C. J., Warner, J. C., Rothwell, S. D., Wilks, S. A., and Keevil, C. W. (2018). Viable-but nonculturable *Listeria monocytogenes* and *Salmonella enterica* serovar thompson induced by chlorine stress remain infectious. *mBio* 9:e00540-18. doi: 10.1128/mBio.00540-18
- Kragh, M. L., Thykier, M., and Truelstrup Hansen, L. (2020). A long-amplicon quantitative PCR assay with propidium monoazide to enumerate viable *Listeria monocytogenes* after heat and desiccation treatments. *Food Microbiol.* 86:103310. doi: 10.1016/j.fm.2019.103310
- Léonard, L., Bouarab Chibane, L., Ouled Bouhedda, B., Degraeve, P., and Oulahal, N. (2016). Recent advances on multi-parameter flow cytometry to characterize antimicrobial treatments. *Front. Microbiol.* 7:1225. doi: 10.3389/fmicb.2016.01225
- López-Gálvez, F., Tudela, J. A., Allende, A., and Gil, M. I. (2019). Microbial and chemical characterization of commercial washing lines of fresh produce highlights the need for process water control. *Innov. Food Sci. Emerg. Technol.* 51, 211–219. doi: 10.1016/j.ifset.2018.05.002
- Makino, S. I., Kii, T., Asakura, H., Shirahata, T., Ikeda, T., Takeshi, K., et al. (2000). Does enterohemorrhagic *Escherichia coli* O157:H7 enter the viable but nonculturable state in salted salmon roe? *Appl. Environ. Microbiol.* 66, 5536–5539. doi: 10.1128/aem.66.12.5536-5539.2000
- Nkuiopou-Kenfack, E., Engel, H., Fakih, S., and Nocker, A. (2013). Improving efficiency of viability-PCR for selective detection of live cells. *J. Microbiol. Method* 93, 20–24. doi: 10.1016/j.mimet.2013.01.018
- Nocker, A., and Camper, A. K. (2009). Novel approaches toward preferential detection of viable cells using nucleic acid amplification techniques. *FEMS Microbiol. Lett.* 291, 137–142. doi: 10.1111/j.1574-6968.2008.01429.x
- Nocker, A., Cheswick, R., de la Rochere, P. M. D., Denis, M., Leziart, T., and Jarvis, P. (2016). When are bacteria dead? A step towards interpreting flow cytometry profiles after chlorine disinfection and membrane integrity staining. *Environ. Technol.* 38, 891–900. doi: 10.1080/09593330.2016.1262463
- Nocker, A., Cheung, C. Y., and Camper, A. K. (2006). Comparison of propidium monoazide with ethidium monoazide for differentiation of live vs. dead bacteria by selective removal of DNA from dead cells. *J. Microbiol. Method* 67, 310–320. doi: 10.1016/j.mimet.2006.04.015
- Nocker, A., Sossa, K., and Camper, A. K. (2007). Molecular monitoring of disinfection efficacy using propidium monoazide in combination with quantitative PCR. *J. Microbiol. Methods* 70, 252–260. doi: 10.1016/j.mimet.2007.04.014
- Oliver, J. D. (2010). Recent findings on the viable but nonculturable state in pathogenic bacteria. *FEMS Microbiol. Rev.* 34, 415–425. doi: 10.1111/j.1574-6976.2009.00200.x
- Rastogi, G., Tech, J. J., Coaker, G. L., and Leveau, J. H. (2010). A PCR-based toolbox for the culture-independent quantification of total bacterial abundances in plant environments. *J. Microbiol. Method* 83, 127–132. doi: 10.1016/j.mimet.2010.08.006
- Rodríguez-Lázaro, D., Hernández, M., Scotti, M., Esteve, T., Vázquez-Boland, J. A., and Pla, M. (2004). Quantitative detection of *Listeria monocytogenes* and *Listeria innocua* by real-time PCR: assessment of hly, iap and lin02483 targets and AmpliFluor™ technology. *Appl. Environ. Microbiol.* 70, 1366–1377. doi: 10.1128/aem.70.3.1366-1377.2004
- Sicard, A., Merfa, M. V., Voeltz, M., Zeilinger, A. R., De La Fuente, L., and Almeida, R. P. P. (2019). Discriminating between viable and membrane damaged cells of the plant pathogen *Xylella fastidiosa*. *PLoS One* 14:e0221119. doi: 10.1371/journal.pone.0221119
- Stiefel, P., Schmidt-Emrich, S., Maniura-Weber, K., and Ren, Q. (2015). Critical aspects of using bacterial cell viability assays with the fluorophores SYTO9 and propidium iodide. *BMC Microbiol.* 15:36. doi: 10.1186/s12866-015-0376-x
- Su, X., Xue, B., Wang, Y., Hashmi, M. Z., Lin, H., Chen, J., et al. (2019). Bacterial community shifts evaluation in the sediments of Puyang River and its nitrogen removal capabilities exploration by resuscitation promoting factor. *Ecotoxicol. Environ. Safety* 179, 188–197. doi: 10.1016/j.ecoenv.2019.04.067
- Truchado, P., Elsser-Gravesen, A., Gil, M. I., and Allende, A. (2020). Post-process treatments are effective strategies to reduce *Listeria monocytogenes* on the surface of leafy greens: a pilot study. *Int. J. Food Microbiol.* 313:108390. doi: 10.1016/j.ijfoodmicro.2019.108390
- Truchado, P., Gil, M. I., Kostic, T., and Allende, A. (2016). Optimization and validation of a PMA qPCR method for *Escherichia coli* quantification in primary production. *Food Control* 62, 150–156. doi: 10.1016/j.foodcont.2015.10.014
- Truchado, P., Gil, M. I., Moreno-Candel, M., and Allende, A. (2019). Impact of weather conditions, leaf age and irrigation water disinfection on the major epiphytic bacterial genera of baby spinach grown in an open field. *Food Microbiol.* 78, 46–52. doi: 10.1016/j.fm.2018.09.015
- Tudela, J. A., López-Gálvez, F., Allende, A., and Gil, M. I. (2019). Chlorination management in commercial fresh produce processing lines. *Food Control.* 106:106760. doi: 10.1016/j.foodcont.2019.106760

- Venkobachar, C., Iyengar, L., and Rao, A. V. S. P. (1997). Mechanism of disinfection: effect of chlorine on cell membrane functions. *Water Res.* 11, 727–729. doi: 10.1016/0043-1354(77)90114-2
- Virto, R., Mañas, P., Álvarez, I., Condon, S., and Raso, J. (2005). Membrane damage and microbial inactivation by chlorine in the absence and presence of a chlorine-demanding substrate. *Appl. Environ. Microbiol.* 71, 5022–5028. doi: 10.1128/aem.71.9.5022-5028.2005
- Zhao, X., Zhong, J., Wei, C., Lin, C. W., and Ding, T. (2017). Current perspectives on viable but non-culturable state in foodborne pathogens. *Front. Microbiol.* 12:580. doi: 10.3389/fmicb.2017.00580

Conflict of Interest: The authors declare that the research was conducted in the absence of any commercial or financial relationships that could be construed as a potential conflict of interest.

Copyright © 2020 Truchado, Gil, Larrosa and Allende. This is an open-access article distributed under the terms of the Creative Commons Attribution License (CC BY). The use, distribution or reproduction in other forums is permitted, provided the original author(s) and the copyright owner(s) are credited and that the original publication in this journal is cited, in accordance with accepted academic practice. No use, distribution or reproduction is permitted which does not comply with these terms.



Stress Tolerance of Yeasts Dominating Reverse Osmosis Membranes for Whey Water Treatment

Eirini Vitzilaou^{1*}, Stina D. Aunbjerg¹, N. A. Mahyudin² and Susanne Knøchel¹

¹ Laboratory of Microbiology and Fermentation, Department of Food Science, University of Copenhagen, Copenhagen, Denmark, ² Department of Food Service and Management, Faculty of Food Science and Technology, Universiti Putra Malaysia, Serdang, Malaysia

OPEN ACCESS

Edited by:

Zhenbo Xu,
University of Maryland, Baltimore,
United States

Reviewed by:

Giacomo Zara,
University of Sassari, Italy
Agustin Aranda,
Instituto de Biología Integrativa
de Sistemas (UV-CSIC), Spain

*Correspondence:

Eirini Vitzilaou
eirini@food.ku.dk

Specialty section:

This article was submitted to
Food Microbiology,
a section of the journal
Frontiers in Microbiology

Received: 20 December 2019

Accepted: 06 April 2020

Published: 05 May 2020

Citation:

Vitzilaou E, Aunbjerg SD,
Mahyudin NA and Knøchel S (2020)
Stress Tolerance of Yeasts
Dominating Reverse Osmosis
Membranes for Whey Water
Treatment. *Front. Microbiol.* 11:816.
doi: 10.3389/fmicb.2020.00816

Filamentous yeast species belonging to the closely related *Saprochaete clavata* and *Magnusiomyces spicifer* were recently found to dominate biofilm communities on the retentate and permeate surface of Reverse Osmosis (RO) membranes used in a whey water treatment system after CIP (Cleaning-In-Place). Microscopy revealed that the two filamentous yeast species can cover extensive areas due to their large cell size and long hyphae formation. Representative strains from these species were here further characterized and displayed similar physiological and biochemical characteristics. Both strains tested were able to grow in twice RO-filtrated permeate water and metabolize the urea present. Little is known about the survival characteristics of these strains. Here, their tolerance toward heat (60, 70, and 80°C) and Ultraviolet light (UV-C) treatment at 255 nm using UV-LED was assessed as well as their ability to form biofilm and withstand cleaning associated stress. According to the heat tolerance experiments, the $D_{60^\circ\text{C}}$ of *S. clavata* and *M. spicifer* is 16.37 min and 7.24 min, respectively, while a reduction of 3.5 to >4.5 log (CFU/mL) was ensured within 5 min at 70°C. UV-C light at a dose level 10 mJ/cm² had little effect, while doses of 40 mJ/cm² and upward ensured a ≥ 4 log reduction in a static laboratory scale set-up. The biofilm forming potential of one filamentous yeast and one budding yeast, *Sporopachydermia lactativora*, both isolated from the same biofilm, was compared in assays employing flat-bottomed polystyrene microwells and peg lids, respectively. In these systems, employing both nutrient rich as well as nutrient poor media, only the filamentous yeast was able to create biofilm. However, on RO membrane coupons in static systems, both the budding yeast and a filamentous yeast were capable of forming single strain biofilms and when these coupons were exposed to different simulations of CIP treatments both the filamentous and budding yeast survived these. The dominance of these yeasts in some filter systems tested, their capacity to adhere and their tolerance toward relevant stresses as demonstrated here, suggest that these slow growing yeasts are well suited to initiate microbial biofouling on surfaces in low nutrient environments.

Keywords: filamentous yeast, biofilm, CIP, reverse osmosis, heat tolerance, UV tolerance

INTRODUCTION

Filamentous yeasts are emerging as highly potent biofilm-forming microorganisms in water distribution systems (Doggett, 2000; Babič et al., 2017), residential dishwashers (Zalar et al., 2011; Döğen et al., 2013; Gümrall et al., 2016; Zupančič et al., 2016) and in food industrial equipment (Tang et al., 2009; Tarifa et al., 2013; Stoica et al., 2018; Vitzilaoui et al., 2019). These findings indicate that filamentous yeasts can disperse efficiently, attach strongly to different surfaces and create robust hyphal networks capable of surviving several stresses. According to the study of Paramonova et al. (2009), an increase in hyphae content will strengthen the fungal biofilm and the resistance to such stresses as compression, vortexing and sonication. It has also been shown that filamentous yeasts can develop synergistic relationships with bacteria, leading to vigorous polymicrobial biofilm structures (Shirtliff et al., 2009; De Brucker et al., 2015; Zupančič et al., 2018).

Spiral wound RO membranes are widely used in the food industry and the recovered watery permeate may be used for different purposes. The membranes offer high filtration efficiency, but they are susceptible to biofouling causing flux reduction and shortening of membrane life (Herzberg and Elimelech, 2007; Tang et al., 2009; Anand et al., 2012, 2013; Stoica et al., 2018). Biofouling may also become an issue for final product quality, if microbial cells from the biofilms are capable of proliferating further down the processing line or in the water permeate during storage, since the water may be used for cleaning or for direct/indirect product contact processes (Casani and Knöchel, 2002; Casani et al., 2005).

Over the last decades, there has been an increasing interest in spiral wound RO membrane biofouling in the food processing industry (Tang et al., 2009; Hassan et al., 2010; Anand et al., 2012, 2013; Sánchez, 2018; Stoica et al., 2018; Vitzilaoui et al., 2019). Up to now, research has been mainly focused on bacterial contamination. In 2009, however, a filamentous yeast isolate was observed among the bacterial isolates on RO membranes from a dairy industry in New Zealand. It was isolated from the retentate side of RO elements used for processing casein water permeate and identified as the filamentous yeast *Blastoschizomyces capitatus* (Tang et al., 2009), later renamed *Magnusiomyces capitatus* (Sybren De Hoog and Smith, 2011a).

We have recently documented that filamentous yeasts belonging to the closely related species *Saprochaete clavata* and *Magnusiomyces spicifer* may dominate biofilms found after CIP treatment on both sides of RO membranes filtering whey water (Stoica et al., 2018; Vitzilaoui et al., 2019). Although these biofilms may have a great impact on RO filtration efficiency, little is known about these isolates and their response to the stress encountered. Here, our aim is to characterize two representative strains of these filamentous yeasts (*S. clavata* and *M. spicifer*) isolated from RO elements (Stoica et al., 2018; Vitzilaoui et al., 2019) with focus on properties of importance for survival and growth in the processing environment. Morphological and physiological–biochemical tests were conducted and the heat and UV-C (255 nm) light tolerance of the filamentous yeasts was investigated. The ability of one of the filamentous yeasts to create

biofilms on polystyrene flat-bottomed microwells and on peg lids, respectively, was assessed and compared to that of a budding yeast strain, *Sporopachydermia lactativora*, found on the same biofilm structures. The tolerance of biofilms on RO membrane coupons was tested toward different industrial CIP-mimicking treatments in lab-scale experiments to broaden our knowledge about these RO membrane biofouling agents and facilitate future development of targeted cleaning operations.

MATERIALS AND METHODS

Yeast Strains' Isolation

The filamentous yeast strains belonging to *S. clavata* and *M. spicifer* and the budding yeast strain belonging to *S. lactativora*, investigated here, are representative strains from the total number of yeast species previously isolated from a RO membrane filtration line for water reuse in a dairy industry (Stoica et al., 2018; Vitzilaoui et al., 2019). *S. clavata* and *M. spicifer* found to be the dominant yeast species and *S. lactativora* the most commonly found budding yeast in the detected biofilm structures. In the set up investigated, the whey was up-concentrated through Ultrafiltration (UF) and the permeate solution further subjected to two consecutive RO filtrations and two UV-C (Ultraviolet) light steps before reuse. Sampling, isolation and sequencing procedures are described in Stoica et al. (2018) and Vitzilaoui et al. (2019).

Macroscopic and Microscopic Characterization

Phase-contrast microscopy using the upright microscope Olympus BX43 (Olympus Scientific Solutions Americas Corp.) was used to observe the yeast cells grown in YPG broth (20 g/L Glucose, 20 g/L Peptone, 10 g/L Yeast Extract, pH 5.6 ± 0.2) at 25°C with shaking at 225 rpm (orbital shaker: IKA KS 130 control) and Malt Extract Agar (MEA) at 25°C (CM0059/Oxoid).

Strains Used for Physiological–Biochemical Tests

An isolate from each of the two dominant filamentous yeast species was selected for physiological–biochemical tests. These isolates will be referred to as *SC*, for *Saprochaete clavata* and *MS*, for *Magnusiomyces spicifer*, throughout the rest of the paper. Growth at different temperatures (5, 25, 30, 35, 37, 40, and 45°C) without shaking was assessed in 10 mL YPG broth tubes, inoculated with an individual colony (MEA agar plates/25°C) with triplicates for each isolate and temperature. Fermentation of carbohydrates (D-glucose, D-galactose, sucrose, maltose, lactose, raffinose, and trehalose) and assimilation of carbon compounds (D-glucose, D-galactose, sucrose, maltose, lactose, raffinose, trehalose, D-xylose, L-sorbose, cellobiose, salicin, DL-lactate, succinate, citrate) and nitrate were tested in tubes, in triplicates, incubated at 25°C without shaking, according to the experimental procedure of Kurtzman et al. (2011). Growth at different temperatures and results of fermentation and assimilation experiments were assessed after 1, 2, 3, and

4 weeks of incubation, respectively, using the Wickerham card. Urease activity was tested using Christensen's urea broth (Kurtzman et al., 2011).

Growth in Twice RO-Filtrated Water

The ability of *SC* and *MS* to grow in the twice RO-filtrated permeate water was assessed. One individual colony from *SC* and *MS*, respectively, was inoculated in tubes containing 10 mL of twice RO-filtrated permeate water from the same line (stored in the fridge/4°C). After inoculation, the tubes were incubated for 3 days at 25°C with shaking at 225 rpm. These tubes and the non-inoculated control sample (twice RO-filtrated permeate water) were analyzed to determine the urea and ammonia concentration using an enzyme assay as described by the manufacturer (Megazymes, United Kingdom).

Heat Tolerance Assay

Planktonic cell suspensions of *SC* and *MS* in Saline Peptone Solution (SPS) [1 g/L Bacto Peptone (Difco 211677), 8.5 g/L sodium chloride, pH 7.2 ± 0.2] were exposed to 60, 70, and 80°C for 5, 10, 15, and 20 min, and the CFU/mL determined on MYPG agar (10 g/L glucose, 5 g/L peptone, 3 g/L yeast extract, 3 g/L malt extract, 20 g/L agar, pH 5.6 ± 0.1) in order to assess the heat tolerance. For the inocula, the two filamentous yeast isolates (*SC* and *MS*) were incubated separately on MYPG agar plates at 25°C for 3 days. For each of them, material from an individual colony was inoculated into 20 mL YPG broth tubes and incubated with shaking at 25°C for 2 days. Cells were harvested from the liquid cultures by centrifugation (3,000 g/5 min/4°C). The supernatant was removed, cold (4°C) SPS added, and the pellet washed by vortexing, followed by centrifugation. This procedure was repeated twice, and the pellet was re-suspended in 20 mL SPS and vortexed. The Neubauer counting chamber was used to create a 10^7 cells/mL inoculum in SPS. For each temperature-time interval, 1.5 mL sterile eppendorf tubes with 990 μ L SPS were inserted in the pre-heated heating blocks and the temperature monitored in a control tube. When the solution reached the desired temperature, 10 μ L from the initial inoculum was added to the eppendorf tubes for a final concentration of 10^5 cells/mL. Triplicates were made for each isolate and temperature-time interval. After each designated temperature-time interval, tubes were placed in ice and serial dilutions made in SPS followed by spread plating on MYPG agar plates. Initial inocula were also validated on MYPG agar. Colonies were counted after 10 days of incubation at 25°C, to allow for growth of injured cells. *D*-values for 60°C for *SC* and *MS* were calculated using linear regression analysis (Murphy et al., 2000, 2002; McCormick et al., 2003).

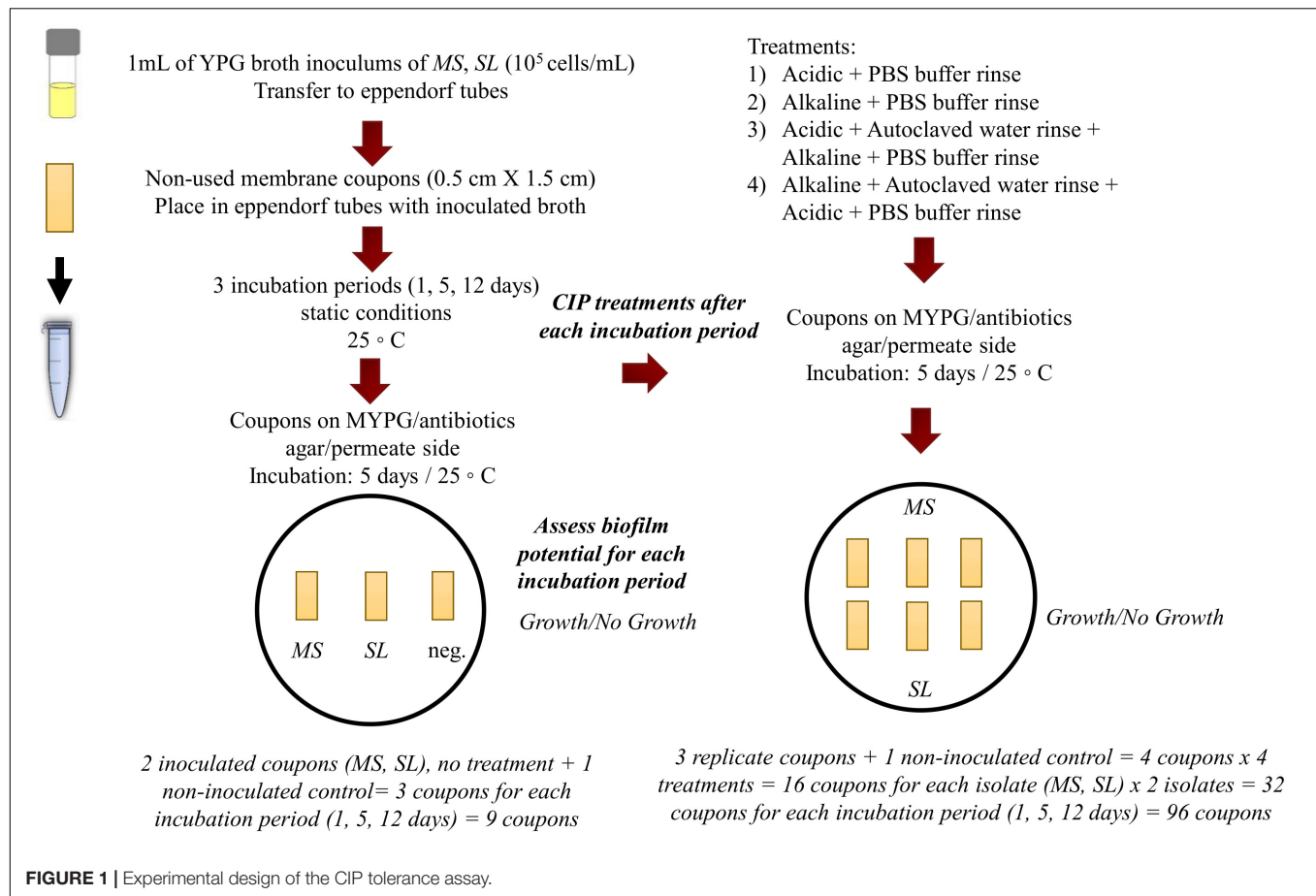
UV-C Light Treatment

UV-C light treatment at 254 nm of 40 mJ/cm² is commonly applied to RO permeate water in the finishing steps before storage and reuse. The tolerance of the two filamentous yeast isolates to UV-C light treatment was investigated, using PearlLab Beam Device from AquiSense Technologies (Kentucky, United States), a compact Collimated Beam Device employing UV-LEDs and emitting UV-C irradiation at 255 nm, following the Bolton and Linden (2003) and Bolton et al. (2015) protocols. The inoculum

was prepared as described in Section "Heat Tolerance Assay" and the inoculum concentration set at 10^6 cells/mL. The (%) UV transmittance of the SPS microbial suspension at 255 nm (UV-Vis 1800 spectrophotometer, Shimadzu) was measured to calculate the water factor. The center point irradiance [E_0 , (mW/cm²)] of the UV-C LED device was determined (radiometer ILT2400, International Light Technologies) and used together with the water factor, petri factor, divergence factor, and sensor factor to calculate the average germicidal fluence rate (E'_{avg}). To obtain the exposure time (sec) for a desired UV dose, this dose (mJ/cm²) was divided by the average fluence rate (mW/cm²). The selected UV doses were 10, 20, 40, 60, and 100 mJ/cm². The exposure time (sec) needed to achieve the desired UV-doses was calculated according to the protocol. Four individual trials were conducted with two replicates within each trial. For each UV dose, 20 mL inoculum (4°C) were transferred to a 50 mm sterile petri dish and exposed to UV-C light for specific time (sec) to achieve the desired dose. The cell suspensions were continuously stirred during the experiments. UV doses were applied in a random order. For each trial, there was a control UV-untreated sample. UV treated and untreated samples were spread-plated in MYPG agar and incubated up to 10 days at 25°C. CFU/mL were counted and survival graphs were made. Two Sample Welch *t*-test was applied with a significance level of 0.05 ($P < 0.05$), using R studio software (Version 3.6.1), to assess the differences between the two strains' inactivation profile for the same UV dose. One-way analysis of variance (ANOVA) and *post hoc* Tukey test with a significance level of 0.001 ($P < 0.001$) were conducted to assess the differences among the different doses in microbial population reduction for both strains, using R studio software (Version 3.6.1).

Cleaning-In-Place (CIP) Tolerance Assay

The tolerance of the filamentous yeast strain *MS* toward CIP treatments was compared to that of the budding yeast strain, *S. lactativora*, *SL*, both isolated from the RO membrane biofilms, by forming biofilms of single cultures on RO membrane coupons and exposing them to the different industrial CIP treatments on a lab-scale experiment. The coupons of 0.5×1.5 cm were aseptically cut from an unused RO membrane, which had been stored at 4°C in sodium metabisulfite solution (1.0% w/w). The coupons were flushed by pipetting three times from each side with autoclaved water to remove chemical traces and placed into sterile 1.5 mL eppendorf tubes. Inocula of 10^5 cells/mL were prepared for each strain with YPG broth as the suspension solution (see section "Heat Tolerance Assay"). For each isolate, 1 mL of the inoculum was poured into a tube, covering the coupon, and incubated for 1, 5, or 12 days at 25°C. For each incubation period, a positive (inoculated) and a negative control (non-inoculated) were made for the two isolates (*MS* and *SL*) (Figure 1). In order to mimic a CIP program, the operating cleaning agents and time-temperature combinations from industrial CIP programs were used (Figure 1 and Table 1). The experiment consisted of four different treatments. The first involved only the application of the acidic solution and the second only the alkaline. The third treatment applied the acidic solution before the alkaline, while the fourth applied the alkaline



first, followed by the acidic. In the third and fourth treatment, there was a rinsing step by pipetting 1 mL of autoclaved water from each side of each coupon three times between the acidic and alkaline solution. At the end of all the treatments, there was a rinsing step by pipetting 1 mL of Phosphate Buffer Solution from each side of the coupon three times in a standardized manner before placing on agar (PBS: 8.00 g/L NaCl, 0.20 g/L KCl, 1.44 g/L Na_2HPO_4 and 0.24 g/L of KH_2PO_4 , pH 7.4 ± 0.2). The CIP solutions were prepared according to the protocol of the producer using autoclaved water for dilution (**Figure 1** and **Table 1**). For each treatment, three replicate coupons in inoculated YPG broth and one coupon in non-inoculated YPG broth (control) were made for each isolate (*MS* and *SL*) and for each incubation period (1, 5, and 12 days) (**Figure 1**).

The biofilm formation on the coupons was assessed by placing the inoculated coupons from each incubation period and isolate on MYPG/antibiotics agar along with the non-inoculated control with the permeate side facing downward. For the CIP tolerance assay, the triplicate coupons tested for each incubation period and isolate combination as well as the non-inoculated controls were exposed to the four different treatments (**Figure 1**). Eppendorf tubes were filled with 1 mL of the appropriate CIP solutions, corresponding to the treatment, and pre-heated to 50°C in heating blocks to mimic the temperature of the cleaning solutions during industrial CIP. The incubated RO

membrane coupons were placed in these tubes and exposed to the various treatments. After each treatment the coupons were placed on MYPG/antibiotics agar supplemented with 0.1 g/L chloramphenicol (Sigma C0378) and 0.5 g/L chlortetracycline (Sigma C4881) with the permeate side facing downward. For both the biofilm forming potential and the CIP tolerance assays, the coupons were removed from the agar after 1 day and the plates were further incubated at 25°C for 5 days. Growth/no growth was macroscopically assessed on the agar plates after 5 days of incubation (**Figure 1** and **Table 1**).

Biofilm Formation on Polystyrene Microtiter Plates and Peg Lids

Biofilm formation on flat-bottomed polystyrene microtiter plates (Thermo Scientific™ Nunc™ MicroWell™) was assessed using 0.1% Crystal Violet (CV) staining, indicative of biomass level, and tetrazolium salt (XTT) (Sigma, cat.no.X4251) staining with 1 μM menadione (Sigma, cat.no.M5625), indicative of metabolic activity. Inocula of the filamentous yeast *SC* and the budding yeast *SL* were prepared (10^5 cells/mL) as in Section “Heat Tolerance Assay.” Three different broth media were used for the final suspension: a low nutrient broth (R2B) containing 0.5 g/L yeast extract, 0.5 g/L proteose peptone, 0.5 g/L casein hydrolysate, 0.5 g/L glucose, 0.5 g/L starch, 0.5 g/L di-potassium

TABLE 1 | The four different CIP treatments applied in the lab-scale experiment for the filamentous and budding yeast biofilm removal.

CIP treatments				
1	Acidic cleaning solution (nitric acid and citric acid) 45 min/50°C pH 1.8–2.0		PBS buffer rinse	
2	Alkaline cleaning solution (potassium hydroxide, EDTA, and sodium hydroxide) 35 min/50°C pH 11.0–11.5		PBS buffer rinse	
3	Acidic cleaning solution (nitric acid and citric acid) 45 min/50°C pH 1.8–2.0	Autoclaved water rinse	Alkaline cleaning solution (potassium hydroxide, EDTA, and sodium hydroxide) 35 min/50°C pH 11.0–11.5	PBS buffer rinse
4	Alkaline cleaning solution (potassium hydroxide, EDTA, and sodium hydroxide) 35 min/50°C pH 11.0–11.5	Autoclaved water rinse	Acidic cleaning solution (nitric acid and citric acid) 45 min/50°C pH 1.8–2.0	PBS buffer rinse

phosphate, 0.024 g/L magnesium sulfate, 0.3 g/L sodium pyruvate (pH 7.2 ± 0.2); R2B + with 100 mg/L urea and lactose, respectively (approx. concentrations found in the twice filtered RO membrane permeate samples), and a high nutrient broth, YPG. Three incubation periods were applied: 1, 4, and 7 days. For each isolate, incubation period and staining method, a microtiter plate was inoculated with the three different media (200 μ L/triplicate rows/eight wells). After 1, 4, and 7 days of incubation with shaking (25°C, 140 rpm), broth media were aspirated from the microplates, where after the microplates were washed (200 μ L PBS/three times) and stained with 0.1% CV [protocol of Kirchhoff et al. (2017)] and 1 μ M XTT/menadione [protocol of Pierce et al. (2008)]. For the 0.1% CV assay, 125 μ L of 0.1% CV solution were poured into each well and the microplates were incubated for 20 min in room temperature (RT). After three additional washing steps with 200 μ L PBS, the microplates were air-dried in inverted position at room temperature (RT) (22°C) for 3 h and 200 μ L 30% (v/v) acetic acid were added in each well. After 30 min incubation at RT, 150 μ L from each well were transferred to new microplates for each yeast strain and OD was measured at 600 nm. For the XTT/menadione assay, 100 μ L of the prepared 1 μ M XTT/menadione solution were added to the microplates after draining. After incubation for 3 h at 25°C/dark conditions, 80 μ L from each well were transferred to new microplates for each yeast strain and the OD was measured at 490 nm. OD was measured using the microtiter plate reader BioTeck ELx808. For both assays, the average OD value for each of the inoculated media wells was calculated by subtraction of the average OD value from the non-inoculated media wells. Student's paired *t*-test was conducted with a significance level of 0.001 ($P < 0.001$) to assess the differences for each medium between the different incubation

periods. R studio software (Version 3. 6. 1) was used for the statistical analysis.

Biofilm formation was also assessed on peg lids (MBEC™ P&G Assay/Innovotech) for both single and dual SC and SL yeast suspensions, applying three sonication times (10, 15, and 20 min). The method was adapted from Harrison et al. (2010). Inocula of 10^5 cells/mL were prepared for the single yeast and dual yeast biofilms, using YPG broth for the final suspension (see section “Heat Tolerance Assay”). For each sonication time: a microplate was prepared for the single yeast biofilm by inoculation of columns 1–6 with 150 μ L of SC inoculum and of columns 7–12 with 150 μ L of SL inoculum (48 wells for each strain). For the dual yeast biofilm, 75 μ L of SC and SL inocula, respectively, were added to a microplate (final volume: 150 μ L, columns 1–12, 96 wells). The peg lids were inserted into the two inoculated microplates and incubated for 48 h at 25°C with shaking (140 rpm). After incubation, the peg lids were removed from the single and dual yeast microplates and rinsed by submerging subsequently for 1 min in two microplates containing Rinse Solution (PBS: 200 μ L/well), then submerged into microplates containing Recovery Solution (YPG broth: 200 μ L/well) and sonicated for 10 min (sonicator: Branson 2210R-MT Ultrasonic Cleaner, frequency: 40 kHz). The same procedure was repeated for the 15- and 20- min sonication time. After each sonication time, 20 μ L from 12 wells of the single SC sonicated microplate were diluted into the first row of a microplate for dilutions, containing 180 μ L of Recovery solution. Four dilutions were made in total (A–D/columns 1–12). Control wells were also prepared, using non-inoculated YPG broth. 10 μ L from each well (rows A–D) and from the control wells were spotted on YPG agar. The same procedure was repeated for SL and for the dual biofilm microplate. The YPG agar plates were incubated at 25°C for 2–3 days. Log₁₀ (CFU/mL) was calculated for the single and dual biofilms for the three different sonication times, by calculating the average of 12 wells from the colonies of countable dilutions. Student's paired *t*-test was conducted to assess individually the differences for the SC single and the dual SC&SL biofilm cultures for the different sonication times with a significance level of 0.001 ($P < 0.001$). Two Sample Welch *t*-test was applied to assess the differences between SC single and the dual SC&SL biofilm cultures for the same sonication time with a significance level of 0.001 ($P < 0.001$). R studio software (Version 3. 6. 1) was used for the statistical analysis.

RESULTS

Macroscopic and Microscopic Analysis of the Filamentous Yeast Isolates

On MEA agar, after 12 days incubation at 25°C, SC colonies were circular with a 2–7 mm diameter, glassy, tough, hirsute, white, convex, and filiform with 1–4 mm mycelium length, while MS colonies were circular with a 1–3 mm diameter, butyrous, glistening, soft, whitish, convex, and filiform with 1 mm mycelium. Overall, MS developed a much shorter mycelium than SC. On MEA agar, after 4 days of incubation at 25°C, the budding yeast SL strain formed circular, glistening, butyrous,

creamy colonies without mycelium and approx. 2 mm in diameter (Table 2). Microscopically, SC and MS developed septate branching hyphae that elongated by continuous growth of the hyphal tip followed by formation of septa after 6 days of incubation in YPG broth. Septa were refractive and thick with little or no constriction and arthroconidia were rectangular-rounded. They both had large vacuoles, while MS developed swollen terminal cells or semi-circle cells (Figure 2). Cell size was measured for at least 20 cells for each yeast strain in the microscope and the minimum-maximum values were 10 and 350 μm in length and 3 and 7.5 μm in width. SL cells were ovoid-ellipsoid with minimum-maximum cell values of 4 and 6 μm in length and 2 and 4 μm in width. Multilateral budding on a narrow base was observed for SL (Table 2).

Physiological and Biochemical Tests

Both SC and MS grew at all temperatures tested in YPG broth. They could not ferment the sugars tested (glucose, sucrose, lactose, galactose, raffinose, trehalose, and maltose), but they assimilated several carbon compounds, corresponding to the species' definition of Sybren De Hoog and Smith (2011b) for

S. clavata and of Sybren De Hoog and Smith (2011a) for *M. spicifer*. Christensen's urea broth reaction for urease activity was negative for both isolates (Table 3).

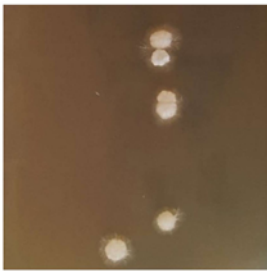
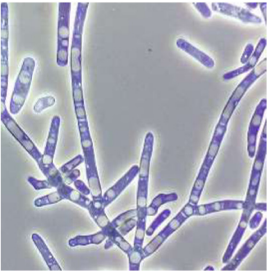

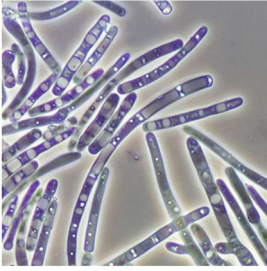

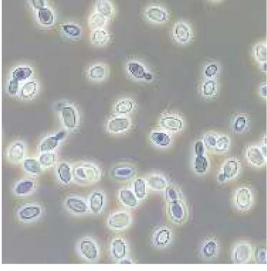
Growth in Twice Filtrated-RO Permeate Water

Although both filamentous yeast isolates were negative for the Christensen's urea broth reaction, they both grew in the twice RO-filtrated permeate water containing urea and decreased the level of urea by more than 50 mg/L while producing ammonia (Table 4).

Heat Tolerance Assay

The initial inoculum for SC (*S. clavata*) and MS (*M. spicifer*) was approx. 10^5 cells/mL (Figure 3). The cell suspensions of SC and MS were tolerant to heat treatment at 60°C, being reduced less than 2 and 3 log₁₀ (CFU/mL), respectively, after 20 min SC was still detectable after exposure at 70°C for up to 10 min, while MS became undetectable after 5 min. At 80°C, SC also became undetectable within 5 min. The D-value for SC

TABLE 2 | The selected strains for the different physiological-biochemical tests and stress tolerance assays.

Isolates	Colony morphology	Colony morphology	Cell morphology 1,000x magnification	Cell morphology
SC <i>Saprochaete clavata</i> Synonym: <i>Geotrichum clavatum</i> (Sybren De Hoog and Smith, 2011b)		Circular Glassy Convex Tough White Mycelium		Anamorph of <i>Magnusiomyces</i> spp. Asexual reproduction: True hyphae branched, disarticulating into arthroconidia.
MS <i>Magnusiomyces spicifer</i> Synonym: <i>Dipodascus spicifer</i> (Sybren De Hoog and Smith, 2011a)		Circular Butyrous Convex Soft Whitish Mycelium		Teleomorph Asexual reproduction: True hyphae branched, disarticulating into arthroconidia.
SL <i>Sporopachydermia lactativora</i> Synonym: <i>Cryptococcus lactativorus</i> (Lachance, 2011)		Circular Butyrous Glistening Convex Creamy		Teleomorph Asexual reproduction: multilateral budding on a narrow base, ovoid-ellipsoid cells, single, in pairs or clusters. No true or pseudohyphae.

S. clavata and *M. spicifer*: colonies in MEA agar/12 days incubation/25°C, cells in YPG broth/12 days incubation/25°C/shaking at 225 rpm, *Sporopachydermia lactativora*: colonies and cells in MEA agar/4 days/25°C.

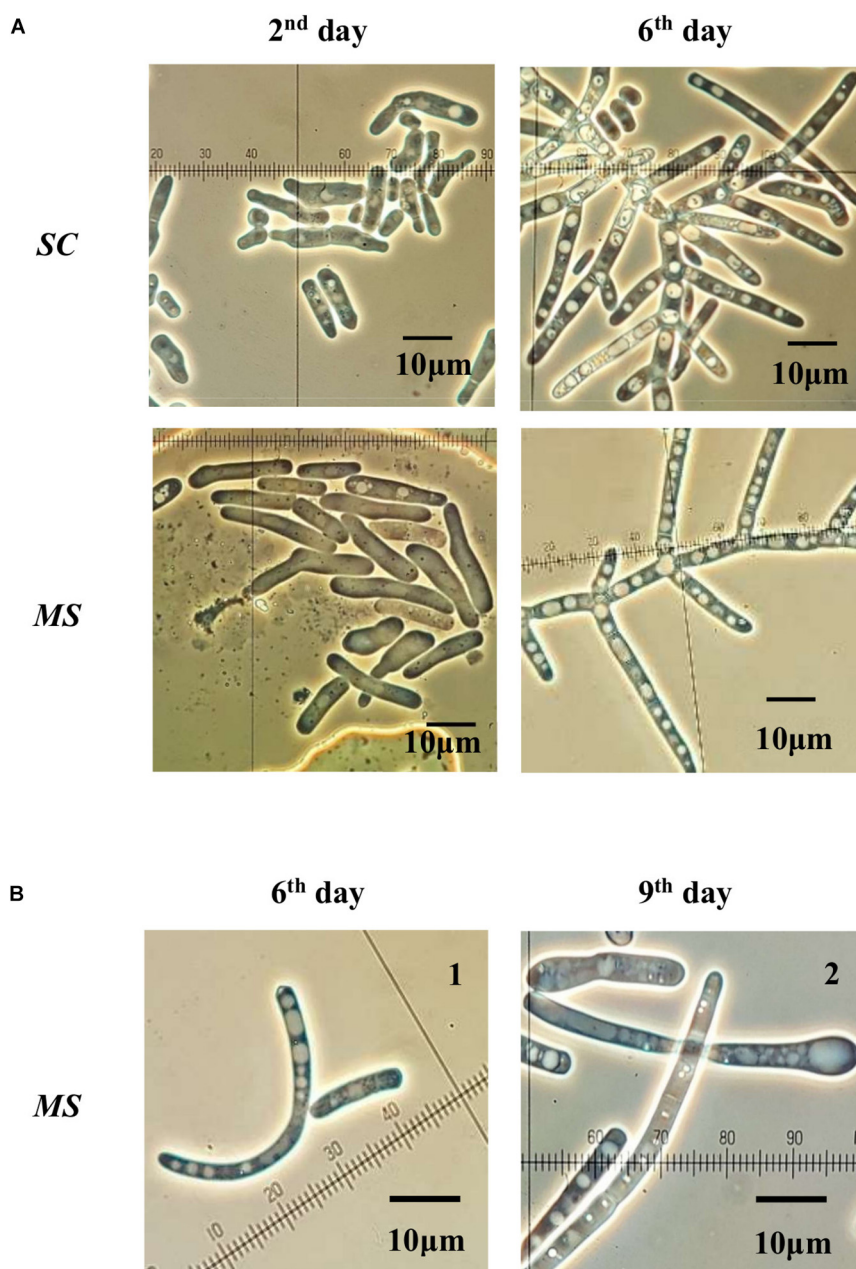


FIGURE 2 | (A) *Saprochaete clavata* (SC) and *Magnusiomyces spicifer* (MS) cells incubated in YPG broth for 2 and 6 days. **(B)** Characteristic cell structures found in MS isolate. 1: semi-circle cell structure observed after 6 days in YPG broth. 2: Swollen cells at the apex of the filament, observed after 9 days in YPG broth. Incubation at 25°C with shaking at 225 rpm.

at 60°C was $D_{60^\circ\text{C}} = 16.37 \text{ min}$, while the D -value of MS was $D_{60^\circ\text{C}} = 7.24 \text{ min}$.

UV-C Light Treatment

The survival bars in \log_{10} (CFU/mL) for MS and SC, respectively, for the different UV doses are presented in **Figure 4**. Both isolates exhibited high tolerance to UV-C treatment. Exposure to 10 mJ/cm² resulted in less than 1.00 \log_{10} (CFU/mL) and exposure to 20 mJ/cm² in less than 4.00 \log_{10} (CFU/mL)

reduction. A UV dose of 40 mJ/cm², usually applied in the industrial UV-C water treatment lines, resulted in approx. 4.00 \log_{10} (CFU/mL) reduction for MS and 5.00 \log_{10} (CFU/mL) reduction for SC. Exposure to 60 mJ/cm² resulted in approx. 1 \log_{10} (CFU/mL) further reduction for both strains. There was no higher decrease in population by applying 100 mJ/cm². After doses of 200 and 400 mJ/cm², applied in two of the trials, sporadic survivors were found (Data not shown). Two Sample Welch t -test with a significance level of 0.05 showed that the differences in

TABLE 3 | Assimilation of carbon compounds and nitrate*, urease activity** and sugar fermentation*** for *S. clavata* and *M. spicifer*.

Strains	Assimilation of carbon compounds				Sugar fermentation				
	<i>S. clavata</i> (This study)	<i>S. clavata</i> (Sybren De Hoog and Smith, 2011b)	<i>M. spicifer</i> (This study)	<i>M. spicifer</i> (Sybren De Hoog and Smith, 2011a)	<i>S. clavata</i> (This study)	<i>S. clavata</i> (Sybren De Hoog and Smith, 2011b)	<i>M. spicifer</i> (This study)	<i>M. spicifer</i> (Sybren De Hoog and Smith, 2011a)	<i>S. clavata</i> (This study)
2-5 Glucose	+	+	+	+	—	—	—	—	—
Sucrose	—	—	—	—	—	—	—	—	—
Lactose	—	—	—	—	—	—	—	—	—
Galactose	+	+	+	+	—	—	—	—	—
Raffinose	—	—	—	—	—	—	—	—	—
Trehalose	—	—	—	—	—	—	—	—	—
Maltose	—	—	—	—	—	—	—	—	—
D-Xylose	Weak	—	+	+					
L-Sorbose	Slow	+	Slow	+					
Cellobiose	+	+	Slow	+					
Salicin	+	+	Slow	+					
DL-Lactate	Weak	+ / Weak	Weak	+					
Succinate	Weak	+	Weak	+					
Citrate	Weak	+	Weak	+					
Nitrate	—	—	—	—					
Urease activity (Christensen's urea broth)	—	—	—	—					

Triplicates were made for each compound and strain ($n = 3$). *Tubes were assessed after 1, 2, 3, and 4 weeks with the Wickerham card. +: growth after 1–2 weeks. Slow: growth after 3 weeks. Weak: growth after 4 weeks. —: no growth during incubation. **Although negative for urease activity, the strains may metabolize urea through other pathways. ***Inverted Durham tubes were assessed for gas accumulation after 1, 2, 3, and 4 weeks. —: no accumulation of gas.

population level reduction between the two strains for each dose applied were no significant ($P > 0.05$). One-way ANOVA and *post hoc* Tukey test conducted, showed that for both strains, there was significant reduction in microbial population after 20 and 40 mJ/cm^2 ($P < 0.001$), compared to dose 0. However, there was not significant difference in the reduction among the doses of 40, 60, and 100 mJ/cm^2 ($P > 0.001$).

CIP Tolerance Assay

Biofilms developed already after the 1st day on the membrane coupons for both the filamentous (*MS*) and the budding (*SL*) yeast isolate, and later increased further in biomass, as seen in the upper row of **Table 5**. Exposure to individual and combined treatments with the alkaline and the acidic cleaning solution did not eliminate the biofilms of neither *SL* nor *MS* strain. However, the combined treatments were more effective than the individual ones in biofilm removal, especially after 1 day of

coupon incubation while the more mature biofilms were difficult to eradicate. This was especially true for the *SL*. Changing the succession of the acidic and alkaline solution during CIP did not seem to improve biofilm removal.

Biofilm Formation on Polystyrene Microplates

Saprochaete clavata created strong biofilm in the flat-bottomed polystyrene microtiter well assay in all the different media, according to both staining methods used (**Figure 5**). The biomass (CV) increased significantly from the first to the fourth day of incubation in all the different media (**Figures 5A,C,D**) ($P < 0.001$), while at the same time the metabolic activity (XTT) decreased significantly in R2B + and R2B (**Figures 5B,D**) ($P < 0.001$). In XTT/YPG, there were no statistically significant differences found throughout incubation (**Figure 5F**) ($P < 0.001$). From Days 4 to 7, both biomass (CV) and metabolic activity (XTT) decreased, indicating cell death. *SL* did not attach and create biofilms on polystyrene. OD was between 0.000–0.092 in 0.1% CV and between 0.000–0.058 in XTT/menadione for the different media and incubation days.

The biofilm formation on peg lids also supported that the filamentous *SC* had the ability to form biofilm, while no biofilm formation was detected for the tested budding yeast *SL* (**Table 6**). The filamentous yeast *SC* biofilm had high recovery numbers for all tested sonication times, while *SL* was below the detection limit of the method (100 cells/mL). The biofilm recovery numbers

TABLE 4 | Urea reduction and ammonia production in twice RO-filtrated permeate water by growth of the two filamentous species.

	Control (not inoculated RO water)	<i>Saprochaete clavata</i> in RO water	<i>Magnusiomyces spicifer</i> in RO water
Urea* (mg/L)	130.7	78.2	66.9
Ammonia* (mg/L)	0.0	24.7	35.2

*Detection limit: ammonia: 2.8 ppm, urea: 5.1 ppm.

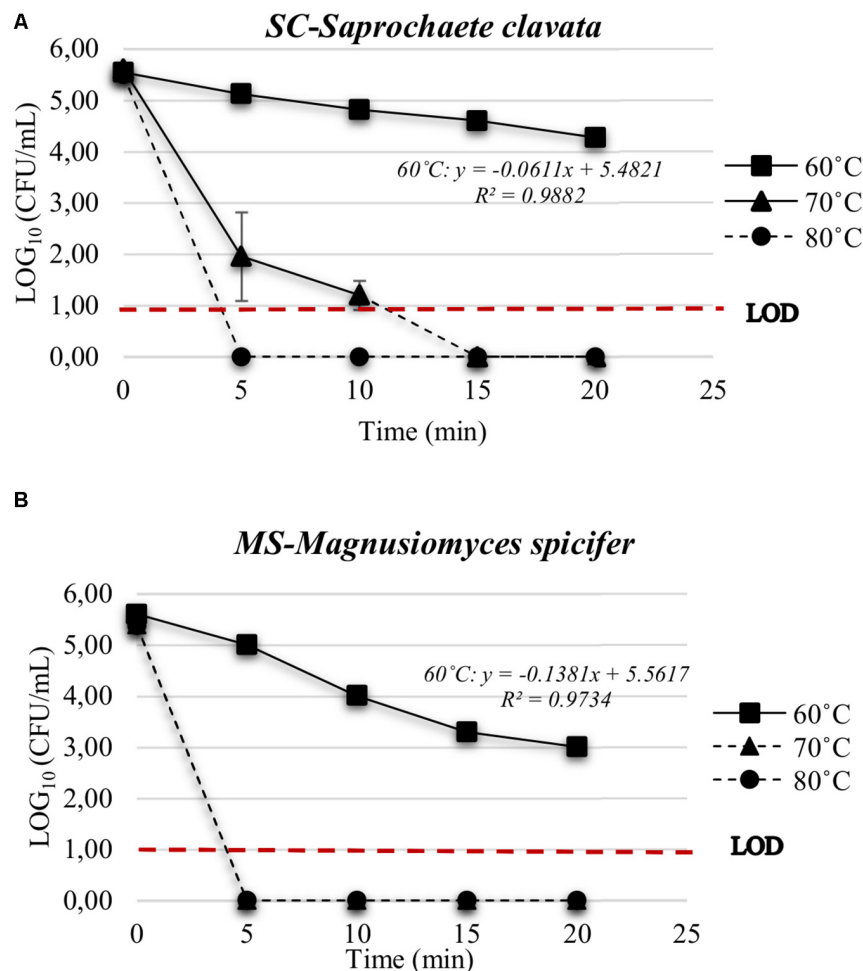


FIGURE 3 | Heat inactivation of **(A)** *S. clavata* (SC) and **(B)** *M. spicifer* (MS) in SPS at 60, 70, and 80°C for 5, 10, 15, and 20 min. Phantom lines indicate that population level was below the LOD (10 cells/mL). Mean value and standard deviation were calculated from three technical replicates for each temperature-time interval and strain ($n = 3$). Medium: MYPG agar. Incubation: 10 days/25°C.

were statistically significantly lower in the dual SC&SL biofilm compared to the single SC biofilm for 10 and 15 min ($P < 0.001$). However, no differences were observed between the single and the dual biofilm after 20 min ($P > 0.001$). Regarding the different sonication times, 15 min were more efficient in biofilm cell recovery numbers. The decrease in cell recovery numbers after 20 min could be due to inactivation of the yeast after prolonged sonication at 40 kHz.

DISCUSSION

Isolation and Characterization of the Filamentous Yeast Isolates

The filamentous yeast species *S. clavata* and *M. spicifer* dominated the biofilm communities on the retentate and permeate side of RO membranes used in a dairy operation line for treating whey water. These filamentous yeasts were isolated after CIP application on several occasions from elements having been in

use for 6 months and up to 4 years. Interestingly, the biofilms on the permeate side of most of these elements, consisted exclusively of the filamentous yeast strains. Since biofouling can interfere with flux and may potentially affect the quality of the retentate and permeate, there is clearly an interest in characterizing these yeasts and obtain an understanding of their persistence and role. It has already been established that they may cover large areas and still go relatively unnoticed unless selective media are used for their detection, since they are often present in lower numbers and grow slower than bacteria, causing them to be out-grown on non-selective media (Stoica et al., 2018; Vitzilaiou et al., 2019).

The yeasts *S. clavata* and *M. spicifer* have a high degree of similarity in physiology, cell-colony morphology and biochemical profile. They both developed mycelium on agar after long incubation and their cells elongated and created septate branching hyphae. They had the same temperature growth range and assimilated the same carbon compounds, while they did not assimilate nitrate. According to taxonomy, they are closely related species. *Saprochaete* and *Magnusiomyces*

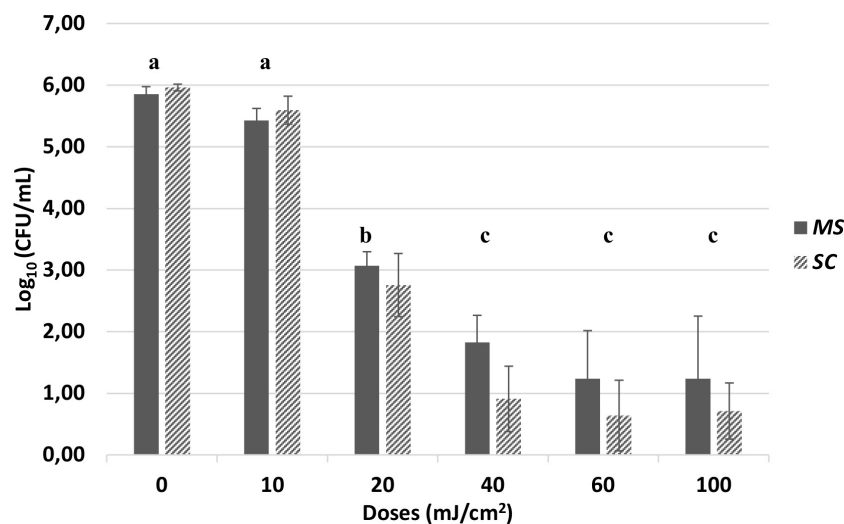


FIGURE 4 | Population level in Log₁₀ [CFU/mL] of *M. spicifer* (MS) and *S. clavata* (SC) after exposure to UV doses of 0, 10, 20, 40, 60, and 100 mJ/cm². Inoculation level: 10⁶ cells/mL. LOD: 1 CFU/mL. The average and standard deviation has been calculated from four different trials with two replicates within each trial ($n = 8$). Sporadic survivors were found when applying 200 and 400 mJ/cm² (Data not shown). No significant differences were found ($P > 0.05$) between the two strains for each dose. The different letters indicate the significant differences in microbial reduction among the different doses for both isolates ($P < 0.001$). Agar medium: MYPG, 10 days incubation at 25°C.

genera belong to the same phylum, class and order (Ascomycota, Saccharomycetes, and Saccharomycetales). *Saprochaete* is the anamorph of *Magnusiomyces* and *Magnusiomyces* and *Saprochaete* are sister genera to *Galactomyces*, *Dipodascus* and their anamorph *Geotrichum* (Sybren De Hoog and Smith, 2004, 2011a,b). The differentiation between *Saprochaete* and *Magnusiomyces* is difficult as also reported by Del Principe et al. (2016). The identification results in the NCBI Database, based on 26S and ITS rRNA sequencing, were often giving similar matches in terms of (%) coverage, (%) similarity rates and *E*-values for *M. spicifer* and *S. clavata*. Thus, we believe that there is a need to increase the diversification of the existing databases on fungal species, as well as to develop new methods for fungal species identification.

Urea Metabolism

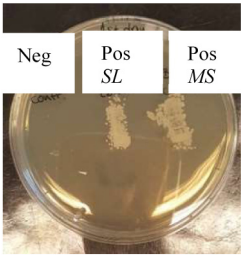
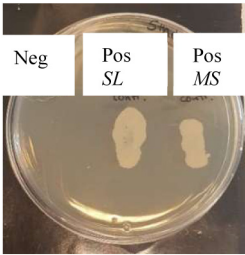
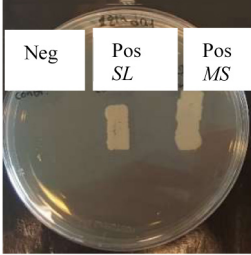
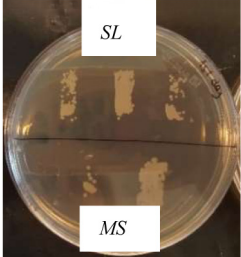
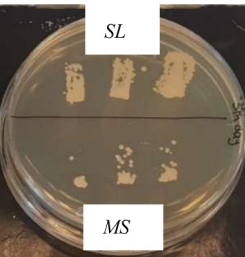
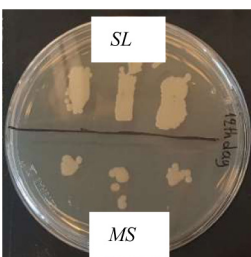
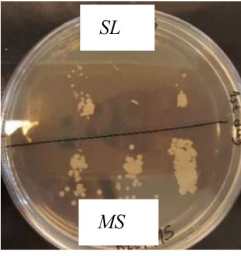
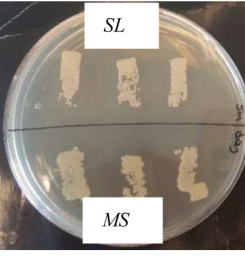
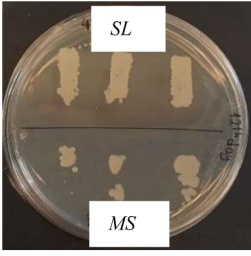
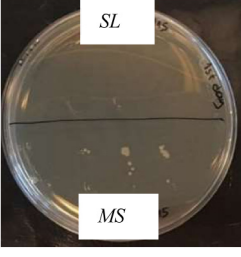
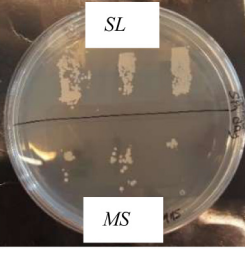
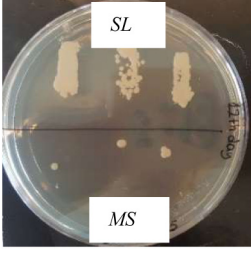
Ultrafiltration followed by RO membrane filtration will, in theory, remove the fouling agents and microbial cells, while small molecules may pass through the membrane pores. Urea from whey can pass the RO membranes (Skou et al., 2017, 2018) and may therefore be a source of nitrogen and energy for some microorganisms in the low-nutrient RO permeate. The filamentous yeast strains, *S. clavata* and *M. spicifer*, were initially tested for urease using Christensen's Urea Broth assay. The principle is based on the presence of urease, which converts urea in a one-step reaction producing ammonia thereby increasing the pH of the broth resulting in a color change. Rapid urease-positive organisms can change the medium's color to pink within 2–4 h (Kurtzman et al., 2011). Both the filamentous yeast strains tested were negative in this assay. However, when grown in the twice RO-filtrated permeate water, they both metabolized urea and produced ammonia. Both *M. spicifer* and

S. clavata belong to Hemiascomycetes, which include one class and order (Saccharomycetes and Saccharomycetales). It has been observed that yeasts belonging to Hemiascomycetes contain urea amidolyase, instead of urease (Souciet et al., 2000; Sybren De Hoog and Smith, 2004, 2011a,b; Strobe et al., 2011). Urea amidolyase is an enzyme that breaks down urea into ammonia and carbon dioxide through a two-step process. Although a slower mechanism of urea metabolism, it may be advantageous in some settings, since urea amidolyase, in contrast to urease, is not dependent on the concentration of Ni²⁺ and Co²⁺ (Booth and Vishniac, 1987; Navarathna et al., 2010; Strobe et al., 2011).

Heat Tolerance Assay in Saline Peptone Solution

The *D*-values can be affected by several parameters such as strain differences, growth phase and conditions prior to heating as well as the matrix and recovery methods (Doyle et al., 2001) and comparison between different experiments should therefore be done with caution. Nevertheless, if the *D*-values of the *S. clavata* strain ($D_{60^\circ\text{C}} = 16.37$ min) and the *M. spicifer* ($D_{60^\circ\text{C}} = 7.24$ min) are compared with previously published average values for common bacterial foodborne pathogens such as *Listeria monocytogenes* ($D_{60^\circ\text{C}} = 4.56$ min) and *E. coli* O157:H7 ($D_{60^\circ\text{C}} = 3.37$ min) (Buzrul and Alpas, 2007) in a similar matrix (1% peptone solution), both filamentous yeast strains seem markedly more tolerant to heat treatment. The more heat resistant *S. clavata* has three to four times higher $D_{60^\circ\text{C}}$ than the strains of *L. monocytogenes* and four times or more than the strains of *E. coli* O157:H7 reported by Buzrul and Alpas (2007). Although the two yeasts were very close in taxonomy, morphology and physiology, *S. clavata*

TABLE 5 | Tolerance toward different CIP treatments at 50°C of single filamentous and budding yeast biofilms, formed on RO membrane coupons.

Coupon incubation period	1st day			5th day			12th day		
Control (no treatment)	Neg	Pos SL	Pos MS	Neg	Pos SL	Pos MS	Neg	Pos SL	Pos MS
Acidic agent pH 1.8–2.0 (50°C/45 min)									
Alkaline agent pH 11.0–11.5 (50°C/35 min)									
Acidic (50°C/45 min) followed by alkaline agent (50°C/35 min)									
Alkaline (50°C/ 35 min) followed by acidic agent (50°C/45 min)									

Neg, negative coupon-control in non-inoculated YPG broth/no treatment. Pos, positive coupon-control in inoculated YPG broth/no treatment. SL, budding yeast (*S. lactivor*); MS, filamentous yeast (*M. spicifer*). Triplicates were made for each CIP treatment and strain. Initial inoculum: 10⁵ cells/mL. Agar plates' incubation: MYPG/antibiotics, 12 days, 25°C. Negative controls for CIP treatments for rows 2–5 not shown.

was markedly more heat tolerant, indicating that important functional characteristics may vary considerably.

In terms of the CIP programs applied in this type of food industry, cleaning solutions and water flushes are often applied at a temperature of 50°C for 35–45 min for each step (Table 1), since most of the RO membrane elements used in these lines cannot stand higher temperatures (Stoica et al., 2018; Vitzilaiou et al., 2019). Although the CIP cleaning may last more than 2 h, our results indicate that a temperature of 50°C will not ensure inactivation of biofilms containing these yeasts. According to the assay, temperatures of 70°C and higher for more than 10 min ensured at least 4 log reductions. This could explain previously

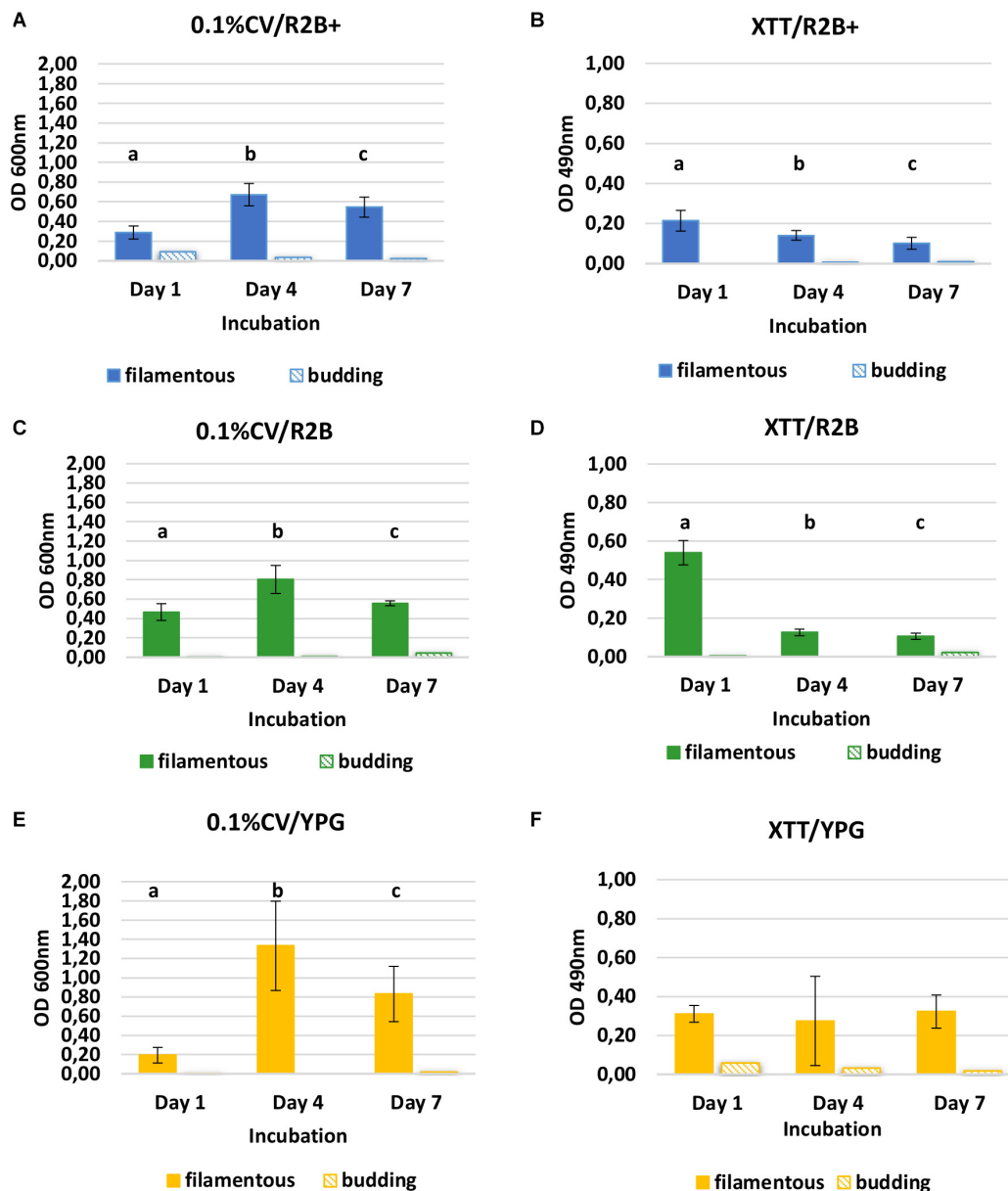


FIGURE 5 | Biofilm quantification of the filamentous yeast *S. clavata* and budding yeast *S. lactativora* using 0.1% CV and XTT/menadione stains in R2B + with urea and lactose (A,B), R2B (C,D), and YPG broth (E,F) after 1, 4, and 7 days of incubation (25°C, shaking at 140 rpm). Mean value and standard deviation are calculated from 24 replicate wells for each medium. Significant differences for the filamentous yeast are presented for each graph with the different letters (a, b, c) ($P < 0.001$).

reported observations (Stoica et al., 2018; Vitzilaiou et al., 2019) from some heat tolerant elements being exposed to high heat (78°C/20 min) where no filamentous yeasts were detected.

UV-C Tolerance

A UV dose of 40 mJ/cm², usually applied in industrial scale water treatment, reduced the population of both *S. clavata* and *M. spicifer* by approx. 4 log₁₀ (CFU/mL), but not below the LOD of the method. Moreover, higher doses of 60 and 100 mJ/cm², did not result in significantly higher inactivation, according to one way ANOVA conducted ($P > 0.001$). Bowker

et al. (2011), using a similar UV-C LED set-up at 255 nm and phosphate buffer, needed a dose of 9 mJ/cm² to decrease a 10⁸ cells/mL inoculum of *E. coli* by 2.7 log₁₀ (CFU/mL). In this study, doses of 20–40 mJ/cm² were needed to obtain the same decrease in the filamentous yeast isolates. UV-C is a well-recognized treatment for water and there is extensive information available for bacteria and viruses as summarized in several reviews (Song et al., 2016; Li et al., 2019). However, there is limited knowledge on fungal tolerance toward UV treatments and the results reported here expands our knowledge of the sensitivity of filamentous yeast.

TABLE 6 | Biofilm cell counts on peg lids obtained from Recovery Solution (YPG) at 10-, 15-, and 20-min sonication time for *S. clavata* (SC), *S. lactativora* (SL) single biofilms, and SC/SL dual biofilms.

Sonication time (min)	10	15	20
	Log ₁₀ (CFU/ml)		
SC (Single biofilm)	4.73 ± 0.17 ^a	5.25 ± 0.22 ^b	4.16 ± 0.20 ^c
SL (Single biofilm)	<LOD	<LOD	<LOD
SC&SL (Dual biofilm)	4.33 ± 0.11 ^d	4.45 ± 0.12 ^d	3.90 ± 0.34 ^c

Data from control wells was negative (not shown). Mean values and standard deviation were calculated from 12 replicates. Significant differences within SC and SC&SL biofilms for the different sonication times and between SC and SC&SL biofilms for the same sonication time are indicated with different letters (a, b, c, d) ($P < 0.001$). LOD was 100 cells/mL.

Biofilm Tolerance to CIP Assay

The budding yeast strain *S. lactativora* (SL) was found in some of the biofilm structures on the RO membrane elements together with the filamentous yeasts, but in lower numbers. When this strain and the filamentous strain, *M. spicifer* (MS), were tested for their tolerance toward CIP treatments, by forming biofilms on RO membrane coupons and exposing them to the industrial CIP solutions, they both displayed a considerable tolerance. Combination treatments inactivated more cells than acid or alkaline solutions individually. No difference in survival was found due to the order of application of the acidic and the alkaline solution. In production lines, the chemically dependent effect of the CIP solutions will only be exerted on the retentate side of the RO. According to our previous work examining RO elements from production, filamentous yeasts were detected on both the retentate and the permeate side when CIP treatments applied the acidic solution first, followed by the alkaline while yeasts were only detected on the retentate surface of one RO element in which the alkaline solution was applied first and the acidic at the end (Stoica et al., 2018; Vitzilaiou et al., 2019). Since the inactivating effect of the combinations seems to be similar, it could indicate that the membranes become more prone to hyphae breakthrough when the treatment finishes with alkali and it has been suggested that alkaline solutions can lead to membrane pore expansion (Simon et al., 2013). This merits further investigation.

The biofilm of the budding yeast isolate during the membrane coupon experiments was less affected by the CIP treatment in the laboratory-based experiments. However, the filamentous yeasts found to be the dominant microorganisms on the retentate side of RO membrane elements from industry and the only biofilm former on the RO permeate surfaces after CIP. When the individual cultures of the filamentous and the budding yeast isolate were tested for biofilm formation on polystyrene flat-bottomed microplates with high and low nutrient broth, only the filamentous yeast was able to attach and form biofilm. This was also evident when biofilm formation was assessed on peg lids. The budding yeast biofilm was hardly noticeable and recovery cell numbers after sonication were below detection level. It is likely that the filamentous yeasts may survive shear and chemical stress better due to a tighter adhesion, greater coverage and potential for making mature biofilms and they may use their hyphae to exploit temporarily induced changes of the membranes.

The recent reports on the isolation of *Saprochaete* and *Magnusiomyces* genera from household dishwashers in multi-genera biofilms (Zalar et al., 2011; Döğen et al., 2013; Gümrall et al., 2016; Zupančič et al., 2016) confirm their ability to colonize and persist on surfaces exposed to extreme conditions like heat, and periods of desiccation. They also suggest that these yeasts are commonly found in the general environment and it may be speculated that they are spread by a water transmission route. Although they may be common contaminants, *S. clavata* and species belonging to *Magnusiomyces* genera are sometimes referred to as opportunistic pathogens, since they have been associated with nosocomial outbreaks in immunocompromised patients (Gurgui et al., 2011; Birrenbach et al., 2012; Camus et al., 2014; Picard et al., 2014; Vaux et al., 2014; Ulu-Kilic et al., 2015; Del Principe et al., 2016; Favre et al., 2016; Durán Graeff et al., 2017). An association with hospital vacuum flasks was found in one outbreak, but in general, little is known about the occurrence, ecology and routes of transmission.

The data obtained from this study can serve as a new insight to understand the role that filamentous yeast may play in dual or multispecies biofilms and points toward a harboring role of the filamentous yeast species within some biofilm structures, potentially having an impact on the presence and survival of other species. In the specific setting investigated, both the retentate and the permeate were subjected to further treatment downstream before being used and in this environment the role is likely limited to occasional flux problems. However, there could be many membrane processes where these yeasts play a role and it is suggested that future investigations of biofouling should include methods targeting fungal contamination in order to clarify their relevance in different systems.

CONCLUSION

Filamentous yeast species identified as the closely related species *S. clavata* and *M. spicifer*, found to dominate biofilms on whey water associated CIP treated RO membrane retentate and permeate surfaces, were characterized by physiological/biochemical tests, stress tolerance assays and biofilm formation potential. These yeasts develop long hyphae and may cover large areas on the RO membranes compared with bacteria and budding yeasts, although they grow much slower than bacteria. Physiological and biochemical tests showed that they share similar colony and cell morphology and biochemical characteristics. The tested isolates of *S. clavata* and *M. spicifer* were found to be tolerant to heat with less than 1 log₁₀ (CFU/mL) reductions of *S. clavata* at 60°C after 15 min. Temperatures above 70°C ensured a substantial reduction of both filamentous yeasts. UV-C light at a dose level of 10 mJ/cm² had little effect, while doses of 40 mJ/cm² and upward ensured a 4 log or higher reduction in a static laboratory scale set-up. Both filamentous isolates were able to metabolize urea and grew in the low nutrient twice RO-filtrated permeate.

Magnusiomyces spicifer and *S. lactativora* formed robust biofilms on RO membrane coupons that survived sanitizing

treatments applied in lab-scale experiments, mimicking industrial CIP treatments. When a filamentous *S. clavata* isolate and a budding yeast *S. lactativora* isolate, both isolated from a RO membrane, were tested for biofilm formation on polystyrene microtiter plates, the filamentous yeast formed a copious biofilm according to 0.1% CV and XTT/menadione staining, as well as on peg lids, while the budding yeast *S. lactativora* isolate did not. When both yeasts were combined, a robust mixed biofilm was formed on peg lids indicating that the filamentous yeast can act as a harbor for the attachment and proliferation of other microorganisms. There has previously been little focus on these filamentous yeasts and the existing sequencing databases reflect the current limitations regarding taxonomy. Their ability, demonstrated here, to attach and proliferate in stressful, nutrient poor environments helps to explain how they persist on membrane surfaces despite regular CIP treatments and is thus a step towards understanding their role in membrane biofouling and flux as well as a potential impact on the quality of retentates and permeates.

DATA AVAILABILITY STATEMENT

The datasets generated for this study are available on request to the corresponding author.

REFERENCES

- Anand, S., Hassan, A., and Avadhanula, M. (2012). The effects of biofilms formed on whey reverse osmosis membranes on the microbial quality of the concentrated product. *Int. J. Dairy Technol.* 65, 451–455. doi: 10.1111/j.1471-0307.2012.00848.x
- Anand, S., Singh, D., Avadhanula, M., and Marka, S. (2013). Development and control of bacterial biofilms on dairy processing membranes. *Compr. Rev. Food Sci. Food Saf.* 13, 18–33. doi: 10.1111/1541-4337.12048
- Babič, M. N., Gunde-Cimerman, N., Vargha, M., Tischner, Z., Magyar, D., Verissimo, C., et al. (2017). Fungal contaminants in drinking water regulation? A tale of ecology, exposure, purification and clinical relevance. *Int. J. Environ. Res. Public Health* 14:636. doi: 10.3390/ijerph14060636
- Birrenbach, T., Bertschy, S., Aebersold, F., Mueller, N. J., Achermann, Y., Muehlethaler, K., et al. (2012). Emergence of *Blastoschizomyces capitatus* yeast infections, Central Europe. *Emerg. Infect. Dis.* 18, 98–101. doi: 10.3201/eid1801.111192
- Bolton, J., Beck, S., and Linden, K. (2015). *Protocol for the Determination of Fluence (UV Dose) Using A Low-Pressure or Low-Pressure High-Output UV Lamp in Bench-Scale Collimated Beam Ultraviolet Experiments*. Boulder, CO: University of Colorado at Boulder.
- Bolton, J. R., and Linden, K. G. (2003). Standardization of methods for Fluence (UV Dose) determination in Bench-Scale UV experiments. *J. Environ. Eng.* 129, 209–215. doi: 10.1061/(ASCE)0733-93722003129:3(209)
- Booth, J. L., and Vishniac, H. S. (1987). Urease testing and yeast taxonomy. *Can. J. Microbiol.* 33, 396–404. doi: 10.1139/m87-069
- Bowker, C., Sain, A., Shatalov, M., and Ducoste, J. (2011). Microbial UV fluence-response assessment using a novel UV-LED collimated beam system. *Water Res.* 45, 2011–2019. doi: 10.1016/j.watres.2010.12.005
- Buzrul, S., and Alpas, H. (2007). Modeling inactivation kinetics of food borne pathogens at a constant temperature. *LWT Food Sci. Technol.* 40, 632–637. doi: 10.1016/j.lwt.2006.02.019
- Camus, V., Thibault, M.-L., David, M., Gargala, G., Compagnon, P., Lamoureux, F., et al. (2014). Invasive *Geotrichum clavatum* fungal infection in an acute Myeloid Leukaemia patient: a case report and review. *Mycopathologia* 177, 319–324. doi: 10.1007/s11046-014-9746-9744
- Casani, S., and Knöchel, S. (2002). Application of HACCP to water reuse in the food industry. *Food Control* 13, 315–327. doi: 10.1016/S0956-7135(02)00037-33
- Casani, S., Rouhany, M., and Knöchel, S. (2005). A discussion paper on challenges and limitations to water reuse and hygiene in the food industry. *Water Res.* 39, 1134–1146. doi: 10.1016/j.watres.2004.12.015
- De Brucker, K., Tan, Y., Vints, K., De Cremer, K., Braem, A., Verstraeten, N., et al. (2015). Fungal β -1,3-glucan increases ofloxacin tolerance of *Escherichia coli* in a polymicrobial *E. coli/Candida albicans* biofilm. *Antimicrob. Agents Chemother.* 59, 3052–3058. doi: 10.1128/AAC.04650-4614
- Del Principe, M. I., Sarmati, L., Cefalo, M., Fontana, C., De Santis, G., Buccisano, F., et al. (2016). A cluster of *Geotrichum clavatum* (*Saprochaete clavata*) infection in haematological patients: a first Italian report and review of literature. *Mycoses* 59, 594–601. doi: 10.1111/myc.12508
- Dögen, A., Kaplan, E., Öksüz, Z., Serin, M. S., Ilkit, M., and Sybren de Hoog, G. (2013). Dishwashers are a major source of human opportunistic yeast-like fungi in indoor environments in Mersin. *Turkey. Med. Mycol.* 51, 493–498. doi: 10.3109/13693786.2012.738313
- Doggett, M. S. (2000). Characterization of fungal biofilms within a municipal water distribution system. *Appl. Environ. Microbiol.* 66, 1249L–1251L. doi: 10.1128/aem.66.3.1249-1251.2000
- Doyle, M. E., Mazzotta, A. S., Wang, T., Wiseman, D. W., and Scott, V. N. (2001). Heat Resistance of *Listeria monocytogenes*. *J. Food Prot.* 64, 410–429. doi: 10.4315/0362-028X-64.3.410
- Durán Graeff, L., Seidel, D., Vehreschild, M. J. G. T., Hamprecht, A., Kindo, A., Racil, Z., et al. (2017). Invasive infections due to *Saprochaete* and *Geotrichum* species: report of 23 cases from the FungiScope Registry. *Mycoses* 60, 273–279. doi: 10.1111/myc.12595

AUTHOR CONTRIBUTIONS

EV conceptualized and designed the work, acquired, analyzed and interpreted the data, wrote and reviewed the manuscript. SA contributed to the initial acquisition of data and review of the manuscript. NM acquired the data and reviewed the manuscript. SK conceptualized the work, supervised the project, interpreted the data and reviewed the manuscript. All authors read and approved the final manuscript.

FUNDING

This work was supported by the REUse of WAtER in the Food and Bioprocessing Industries consortium (REWARD: 1308-00027B) funded by the Danish Council for Strategic Research, Programme Commission on Health Food and Welfare and a Ph.D. scholarship for EV co-funded by the Danish Partnership for Resource and Water Efficient Industrial Food Production (DRIP: j.nr. 152-2014-10), and University of Copenhagen.

ACKNOWLEDGMENTS

We gratefully acknowledge Peter Baek Skou for conducting the urea/ammonia analysis.

- Favre, S., Rougeron, A., Levoir, L., Pérard, B., Milpied, N., Accoceberry, I., et al. (2016). *Saprochaete clavata* invasive infection in a patient with severe aplastic anemia: efficacy of voriconazole and liposomal amphotericin B with adjuvant granulocyte transfusions before neutrophil recovery following allogeneic bone marrow transplantation. *Med. Mycol. Case Rep.* 11, 21–23. doi: 10.1016/j.mmcr.2016.03.001
- Gümral, R., Özhak-Baysan, B., Tümgör, A., Saraçlı, M. A., Yıldırım, S. T., İlkit, M., et al. (2016). Dishwashers provide a selective extreme environment for human-opportunistic yeast-like fungi. *Fungal Divers.* 76, 1–9. doi: 10.1007/s13225-015-0327-328
- Gurgui, M., Sanchez, F., March, F., Lopez-Contreras, J., Martino, R., Cotura, A., et al. (2011). Nosocomial outbreak of *Blastoschizomyces capitatus* associated with contaminated milk in a hematological unit. *J. Hosp. Infect.* 78, 274–278. doi: 10.1016/j.jhin.2011.01.027
- Harrison, J. J., Stremick, C. A., Turner, R. J., Allan, N. D., Olson, M. E., and Ceri, H. (2010). Microtiter susceptibility testing of microbes growing on peg lids: a miniaturized biofilm model for high-throughput screening. *Nat. Protoc.* 5:1236. doi: 10.1038/nprot.2010.71
- Hassan, A. N., Anand, S., and Avadhanula, M. (2010). Microscopic observation of multispecies biofilm of various structures on whey concentration membranes. *J. Dairy Sci.* 93, 2321–2329. doi: 10.3168/jds.2009-2800
- Herzberg, M., and Elimelech, M. (2007). Biofouling of reverse osmosis membranes: role of biofilm-enhanced osmotic pressure. *J. Memb. Sci.* 295, 11–20. doi: 10.1016/j.memsci.2007.02.024
- Kirchhoff, L., Olsowski, M., Zilmans, K., Dittmer, S., Haase, G., Sedlacek, L., et al. (2017). Biofilm formation of the black yeast-like fungus *Exophiala dermatitidis* and its susceptibility to anti-infective agents. *Sci. Rep.* 7:42886. doi: 10.1038/srep42886
- Kurtzman, C. P., Fell, J. W., Boekhout, T., and Robert, V. (2011). “Chapter 7 - methods for isolation, phenotypic characterization and maintenance of yeasts,” in *The Yeasts*, 5TH Edn, eds C. P. Kurtzman, and J. W. Fell (London: Elsevier), 87–110. doi: 10.1016/B978-0-444-52149-1.00007-0
- Lachance, M.-A. (2011). “Chapter 69 - Sporopachydermia Rodrigues de Miranda (1978),” in *The Yeasts*, eds C. P. Kurtzman, J. W. Fell, and T. B. T.-T. Y. F. E. Boekhout (London: Elsevier), 799–803. doi: 10.1016/B978-0-444-52149-1.00069-0
- Li, X., Cai, M., Wang, L., Niu, F., Yang, D., and Zhang, G. (2019). Evaluation survey of microbial disinfection methods in UV-LED water treatment systems. *Sci. Total Environ.* 659, 1415–1427. doi: 10.1016/j.scitotenv.2018.12.344
- McCormick, K., Han, I. Y., Acton, J. C., Sheldon, B. W., and Dawson, P. L. (2003). D and z-values for *Listeria monocytogenes* and *Salmonella typhimurium* in packaged low-fat ready-to-eat turkey bologna subjected to a surface pasteurization treatment. *Poult. Sci.* 82, 1337–1342. doi: 10.1093/ps/82.8.1337
- Murphy, R. Y., Duncan, L. K., Berrang, M. E., Marcy, J. A., and Wolfe, R. E. (2002). Thermal inactivation D- and Z-values of *Salmonella* and *Listeria innocua* in fully cooked and vacuum packaged chicken breast meat during postcook heat treatment. *Poult. Sci.* 81, 1578–1583. doi: 10.1093/ps/81.10.1578
- Murphy, R. Y., Marks, B. P., Johnson, E. R., and Johnson, M. G. (2000). Thermal Inactivation Kinetics of *Salmonella* and *Listeria* in Ground Chicken Breast Meat and Liquid Medium. *J. Food Sci.* 65, 706–710. doi: 10.1111/j.1365-2621.2000.tb16076.x
- Navarathna, D. H., Harris, S. D., Roberts, D. D., and Nickerson, K. W. (2010). Evolutionary aspects of urea utilization by fungi. *FEMS Yeast Res.* 10, 209–213. doi: 10.1111/j.1567-1364.2010.00602.x
- Paramonova, E., Krom, B. P., van der Mei, H. C., Busscher, H. J., and Sharma, P. K. (2009). Hyphal content determines the compression strength of *Candida albicans* biofilms. *Microbiology* 155, 1997–2003. doi: 10.1099/mic.0.021568-21560
- Picard, M., Cassaing, S., Letocart, P., Verdeil, X., Protin, C., Chauvin, P., et al. (2014). Concomitant cases of disseminated *Geotrichum clavatum* infections in patients with acute myeloid leukemia. *Leuk. Lymphoma* 55, 1186–1188. doi: 10.3109/10428194.2013.820290
- Pierce, C. G., Uppuluri, P., Tristan, A. R., Wormley, F. L., Mowat, E., Ramage, G., et al. (2008). A simple and reproducible 96-well plate-based method for the formation of fungal biofilms and its application to antifungal susceptibility testing. *Nat. Protoc.* 3, 1494–1500. doi: 10.1038/nprot.2008.141
- Sánchez, O. (2018). Microbial diversity in biofilms from reverse osmosis membranes: a short review. *J. Memb. Sci.* 545, 240–249. doi: 10.1016/j.memsci.2017.09.082
- Shirliff, M. E., Peters, B. M., and Jabra-Rizk, M. A. (2009). Cross-kingdom interactions: *Candida albicans* and bacteria. *FEMS Microbiol. Lett.* 299, 1–8. doi: 10.1111/j.1574-6968.2009.01668.x
- Simon, A., Price, W. E., and Nghiem, L. D. (2013). Influence of formulated chemical cleaning reagents on the surface properties and separation efficiency of nanofiltration membranes. *J. Memb. Sci.* 432, 73–82. doi: 10.1016/j.memsci.2012.12.029
- Skou, P. B., Berg, T. A., Aunsbjerg, S. D., Thaysen, D., Rasmussen, M. A., and van den Berg, F. (2017). Monitoring process water quality using near infrared spectroscopy and partial least squares regression with prediction uncertainty estimation. *Appl. Spectrosc.* 71, 410–421. doi: 10.1177/0003702816654165
- Skou, P. B., Khakimov, B., Hansen, T. H., Aunsbjerg, S. D., Knöchel, S., Thaysen, D., et al. (2018). Chemical characterization by gas chromatography-mass spectrometry and inductively coupled plasma-optical emission spectroscopy of membrane permeates from an industrial dairy ingredient production used as process water. *J. Dairy Sci.* 101, 135–146. doi: 10.3168/jds.2017-12950
- Song, K., Mohseni, M., and Taghipour, F. (2016). Application of ultraviolet light-emitting diodes (UV-LEDs) for water disinfection: a review. *Water Res.* 94, 341–349. doi: 10.1016/j.watres.2016.03.003
- Souciet, J.-L., Aigle, M., Artiguenave, F., Blandin, G., Bolotin-Fukuhara, M., Bon, E., et al. (2000). Genomic exploration of the *Hemiascomycetous* Yeasts: 1. A set of yeast species for molecular evolution studies. *FEBS Lett.* 487, 3–12. doi: 10.1016/S0014-5793(00)02272-2279
- Stoica, I. M., Vitzilaiou, E., Lyng Røder, H., Burmølle, M., Thaysen, D., Knöchel, S., et al. (2018). Biofouling on RO-membranes used for water recovery in the dairy industry. *J. Water Process Eng.* 24, 1–10. doi: 10.1016/j.jwpe.2018.05.004
- Strope, P. K., Nickerson, K. W., Harris, S. D., and Moriyama, E. N. (2011). Molecular evolution of urea amidolyase and urea carboxylase in fungi. *BMC Evol. Biol.* 11:80. doi: 10.1186/1471-2148-11-80
- Sybren De Hoog, G., and Smith, M. (2004). Ribosomal gene phylogeny and species delimitation in *Geotrichum* and its teleomorph. *Stud. Mycol.* 50, 489–515. doi: 10.1016/j.funbio.2010.01.007
- Sybren De Hoog, G., and Smith, M. (2011a). “Chapter 45 - *Magnusiomyces Zender* (1977),” in *The Yeasts*, 5th Edn, eds C. P. Kurtzman, and J. W. Fell (London: Elsevier), 565–574. doi: 10.1016/B978-0-444-52149-1.00045-8
- Sybren De Hoog, G., and Smith, M. (2011b). “Chapter 97 - *Saprochaete Coker & Shanor* ex D.T.S. Wagner & Dawes (1970),” in *The Yeasts*, 5th Edn, eds C. P. Kurtzman, and J. W. Fell (London: Elsevier), 1317–1327. doi: 10.1016/B978-0-444-52149-1.00097-5
- Tang, X., Flint, S. H., Brooks, J. D., and Bennett, R. J. (2009). Factors affecting the attachment of micro-organisms isolated from ultrafiltration and reverse osmosis membranes in dairy processing plants. *J. Appl. Microbiol.* 107, 443–451. doi: 10.1111/j.1365-2672.2009.04214.x
- Tarifa, M. C., Brugnoli, L. I., and Lozano, J. E. (2013). Role of hydrophobicity in adhesion of wild yeast isolated from the ultrafiltration membranes of an apple juice processing plant. *Biofouling* 29, 841–853. doi: 10.1080/08927014.2013.808628
- Ulu-Kilic, A., Atalay, M. A., Metan, G., Cevahir, F., Koç, N., Eser, B., et al. (2015). *Saprochaete capitata* as an emerging fungus among patients with hematological malignancies. *Mycoses* 58, 491–497. doi: 10.1111/myc.12347
- Vaux, S., Criscuolo, A., Desnos-Ollivier, M., Diancourt, L., Tarnaud, C., Vandenbogaert, M., et al. (2014). Multicenter outbreak of infections by *Saprochaete clavata*, an unrecognized opportunistic fungal pathogen. *mBio* 5, 1–10. doi: 10.1128/mBio.02309-2314
- Vitzilaiou, E., Stoica, I. M., and Knöchel, S. (2019). Microbial biofilm communities on Reverse Osmosis membranes in whey water processing before and after cleaning. *J. Memb. Sci.* 587:117174. doi: 10.1016/j.memsci.2019.117174
- Zalar, P., Novak, M., Sybren de Hoog, G., and Gunde-Cimerman, N. (2011). Dishwashers – A man-made ecological niche accommodating human

- opportunistic fungal pathogens. *Fungal Biol.* 115, 997–1007. doi: 10.1016/j.funbio.2011.04.007
- Zupančič, J., Novak Babič, M., Zalar, P., and Gunde-Cimerman, N. (2016). The Black Yeast *Exophiala dermatitidis* and other selected opportunistic human fungal pathogens spread from dishwashers to kitchens. *PLoS One* 11:e0148166. doi: 10.1371/journal.pone.0148166
- Zupančič, J., Raghupathi, P. K., Houf, K., Burmølle, M., Sørensen, S. J., and Gunde-Cimerman, N. (2018). Synergistic interactions in microbial biofilms facilitate the establishment of opportunistic pathogenic fungi in household dishwashers. *Front. Microbiol.* 9:21. doi: 10.3389/fmicb.2018.00021

Conflict of Interest: The authors declare that the research was conducted in the absence of any commercial or financial relationships that could be construed as a potential conflict of interest.

Copyright © 2020 Vitzilaïou, Aunsbjerg, Mahyudin and Knochel. This is an open-access article distributed under the terms of the Creative Commons Attribution License (CC BY). The use, distribution or reproduction in other forums is permitted, provided the original author(s) and the copyright owner(s) are credited and that the original publication in this journal is cited, in accordance with accepted academic practice. No use, distribution or reproduction is permitted which does not comply with these terms.



Insights Into the Role of Extracellular DNA and Extracellular Proteins in Biofilm Formation of *Vibrio parahaemolyticus*

Wei Li¹, Jing Jing Wang^{1,2,3}, Hui Qian¹, Ling Tan¹, Zhaohuan Zhang¹, Haiquan Liu^{1,2,3,4}, Yingjie Pan^{1,2,3} and Yong Zhao^{1,2,3*}

¹ College of Food Science and Technology, Shanghai Ocean University, Shanghai, China, ² Laboratory of Quality and Safety Risk Assessment for Aquatic Products on Storage and Preservation, Ministry of Agriculture, Shanghai, China, ³ Shanghai Engineering Research Center of Aquatic-Product Processing and Preservation, Shanghai, China, ⁴ Engineering Research Center of Food Thermal-Processing Technology, Shanghai Ocean University, Shanghai, China

OPEN ACCESS

Edited by:

Xihong Zhao,
Wuhan Institute of Technology, China

Reviewed by:

Ruiyong Zhang,
Federal Institute for Geosciences
and Natural Resources, Germany
Yiquan Zhang,
Jiangsu University, China

*Correspondence:

Yong Zhao
yzhao@shou.edu.cn

Specialty section:

This article was submitted to
Food Microbiology,
a section of the journal
Frontiers in Microbiology

Received: 31 December 2019

Accepted: 06 April 2020

Published: 19 May 2020

Citation:

Li W, Wang JJ, Qian H, Tan L,
Zhang Z, Liu H, Pan Y and Zhao Y
(2020) Insights Into the Role
of Extracellular DNA and Extracellular
Proteins in Biofilm Formation of *Vibrio*
parahaemolyticus.
Front. Microbiol. 11:813.
doi: 10.3389/fmicb.2020.00813

The extracellular polymeric substances (EPS) construct the three-dimensional (3-D) structure of biofilms, but their respective roles are still not clear. Therefore, this study aimed to illuminate the role of key chemical components [extracellular DNA (eDNA), extracellular proteins, and carbohydrates] of EPS in biofilm formation of *Vibrio parahaemolyticus*. The correlations between each key chemical component and biofilm formation were first determined, showing that the biofilm formation of *V. parahaemolyticus* was strongly positively correlated with both eDNA and protein content ($P < 0.01$), but not with carbohydrates. Subsequently, individual DNase I or protease K treatment markedly reduced the initial adhesion and structural stability of the formed biofilms by hydrolyzing the eDNA or extracellular proteins, but did not induce significant dispersion of mature biofilms. However, the combination of DNase I and protease K treatment induced the obvious dispersion of the mature biofilms through the concurrent destruction of eDNA and extracellular proteins. The analysis at a structural level showed that the collapse of biofilms was mainly attributed to the great damage of the loop configuration of eDNA and the secondary structure of proteins caused by the enzyme treatment. Therefore, this study provides a deep understanding of the role of key chemical components of EPS in biofilm development of *V. parahaemolyticus*, which may give a new strategy to develop environmentally friendly methods to eradicate the biofilms in food industry.

Keywords: *Vibrio parahaemolyticus*, biofilm, eDNA, extracellular proteins, EPS

INTRODUCTION

Vibrio parahaemolyticus is recognized as a leading cause of seafood-derived food poisoning worldwide (Raszl et al., 2016), and it is ubiquitous in coastal waters or estuarine environments (Urmersbach et al., 2015; Mizan et al., 2016). *V. parahaemolyticus* has the high capacity to adhere to food-contact surfaces (aquaculture equipment, aquatic products, and food processing facilities) and forms biofilm (Han et al., 2016; da Rosa et al., 2018; Mougin et al., 2019). Biofilms are complex

communities of microorganisms, which provides the encased microbial cells higher ability to tolerate environmental stresses such as antibiotics and disinfectants compared to planktonic cells (Costerton et al., 1999; Costa et al., 2013; Elexson et al., 2014; DeFrancesco et al., 2017). All these properties are attributed to bacterial cells embedded in firm three-dimensional (3D), multicellular, self-assembled structures that contain extracellular polymeric substances (EPS) (Costa et al., 2013; Flemming et al., 2016). EPS are the primary ingredient in bacterial biofilms, which typically accounts for greater than 90% dry mass of the biofilm (Brown et al., 2015). Of which, the key matrix components—DNA, proteins, and exopolysaccharides—are crucial for maintaining the structural integrity of biofilms providing a shelter for cells (Flemming and Wingender, 2010; Dragos and Kovacs, 2017).

Recent studies have shown that exopolysaccharides appear to be important for initiating and maintaining cell–cell interactions in biofilms, as well as protecting encased bacterial cells (Ophir and Gutnick, 1994; Colvin et al., 2011; Cugini et al., 2019). Proteins can provide 3D architectural integrity and surface adhesion for various bacterial biofilms, such as *Escherichia coli*, *Vibrio cholerae*, *Bacillus subtilis*, and *Vibrio vulnificus* (Hobley et al., 2015; Jin et al., 2016). More importantly, the groundbreaking discovery of extracellular DNA (eDNA) by Whitchurch et al. (2002) showed that eDNA is required for the initial establishment of *Pseudomonas aeruginosa* biofilms. Since this report, the roles of eDNA in biofilm formation, structural integrity, and tolerance to antibiotics have been widely described in other species (Okshevsky and Meyer, 2013; Rose et al., 2015; Ibanez de Aldecoa et al., 2017). Moreover, eDNA can be used as a source of nutrients for live cells and facilitate the spread of genetic traits in the biofilm and the planktonic populations (Chimileski et al., 2014; Brown et al., 2015). However, the chemical composition of EPS varies greatly depending on the bacterial species and the environment that the biofilm formed.

During the last decades, many studies mainly investigated the roles of exopolysaccharides and capsular polysaccharide (CPS) in the *V. parahaemolyticus* biofilm. Thereinto, Guvener and McCarter (2003) found that the mutants of *V. parahaemolyticus*, failing to produce CPS, formed defective biofilms. Nevertheless, Chen et al. (2010) proposed that the mutants mentioned above were related to exopolysaccharide production rather than CPS. Furthermore, they revealed the genes responsible for exopolysaccharide production in *V. parahaemolyticus* were located on chromosome II, that is, the VPA1403-1412 (*cpsA-J*) operon, whereas the loci VP0219-0237 in chromosome I was the capsule genes (K-antigen). Subsequently, Wang et al. (2013) showed that exopolysaccharides-deficient mutant of *V. parahaemolyticus* stained with much less crystal violet than wild type. Therefore, it can be concluded that the importance of exopolysaccharides and CPS in *V. parahaemolyticus* biofilm formation needs to be further clarified. Meanwhile, the exogenous addition of extracellular recombinant proteins significantly increased the biofilm formation of *V. parahaemolyticus* reaching ~3.8-fold compared to control (Jung et al., 2019). However, the role of eDNA in the biofilm formation of *V. parahaemolyticus* is rarely

reported. In addition, the role of chemical components of EPS in the biofilm formation of *V. parahaemolyticus* is still controversial.

In this study, *V. parahaemolyticus* was selected as a model organism to investigate the role of key chemical components (eDNA, extracellular proteins, and carbohydrates) of EPS in the biofilm development. To achieve this purpose, the dynamic process of biofilm formation was monitored by crystal violet staining, confocal laser scanning microscopy (CLSM) and scanning electron microscopy (SEM). The respective importance of chemical components of EPS in biofilm formation was revealed by Pearson correlation analysis and enzymatic hydrolysis treatment. Furthermore, the ISA-2 software analysis and Raman spectroscopy were used to characterize the structure changes of the biofilm treated by DNase I, proteinase K, and the combination of DNase I and proteinase K (DNase I–proteinase K). This study will reveal the role of chemical components of EPS in the biofilm formation of *V. parahaemolyticus* and hence provide effective strategy to design environmental-friendly, non-chemical methods to control biofilm formation in food industry.

MATERIALS AND METHODS

Bacterial Strains and Cultivation

Vibrio parahaemolyticus ATCC17802 was used in this study and maintained in 50% (vol/vol) glycerol at -80°C . The single colony was inoculated in 9 mL tryptic soy broth (TSB; Beijing Land Bridge Technology Company Ltd., Beijing, China) supplemented with 3% (wt/vol) NaCl and incubated at 37°C for 12 h with shaking at 200 revolutions/min. After incubation, the broth culture was adjusted to $\text{OD}_{600} = 0.4$ corresponding to 4.1×10^7 colony-forming units/mL, which was used for subsequent experiments.

Biofilm Formation

Biofilm formation was performed according to the protocol previously described by Song et al. (2016) and Han et al. (2017). In detail, 24-well plates were filled with 990 μL of fresh TSB medium (3% NaCl) and then inoculated with 10 μL of the bacterial cultures ($\text{OD}_{600} = 0.4$). Then, the 24-well plates were incubated at 25°C statically to form biofilms under different times (2, 6, 12, 24, 36, and 48 h), and the wells containing TSB without inoculation were used as blank control. All plates were sealed with plastic self-sealing bags to prevent evaporation of water.

Enzyme Treatment of Biofilms

Biofilms incubated at different times (2, 12, 24, 36, and 48 h) were washed once with 1 mL of $1 \times$ phosphate-buffered saline (PBS). Subsequently, the biofilm samples were treated with DNase I (Roche), proteinase K (Sigma-Aldrich Co. LLC, Louis, United States), and the combination of DNase I and proteinase K at 37°C for 30 min. After static incubation, the wells were washed twice with $1 \times$ PBS and stained with crystal violet to quantify the biofilm. For the experiments of enzyme treatment, all DNase I, proteinase K, and DNase I–proteinase K were used at a final concentration of 100 $\mu\text{g/mL}$ unless otherwise stated. The biofilm without addition of enzymes was selected

as control. All the experiments were repeated in at least three independent experiments.

Crystal Violet Staining Assay

Biofilms of *V. parahaemolyticus* were quantified by crystal violet staining method (Crofts et al., 2018). Following static incubation, planktonic cells were removed from the wells before washing with $1 \times$ PBS gently. After drying at 60°C for 15 min, the biofilms were stained with 1 mL of 0.1% (wt/vol) crystal violet (Sangon Biotech Co., Ltd., Shanghai, China) for 30 min at room temperature. The staining solution was removed via pipette, and then $1 \times$ PBS was used to remove the non-bound dye at least three times. Stained and washed biofilms were air dried for 30 min, and then 1 mL of 95% ethanol was added to dissolve the bound crystal violet for 30 min. The optical density of each well was measured at wavelength of 600 nm using the BioTek Synergy 2 (Winooski, VT, United States).

Visualization and Structural Analysis of the Biofilms Using Confocal Laser Scanning Microscopy

The *V. parahaemolyticus* biofilms were observed by CLSM. The biofilms on sterile glass were rinsed with $1 \times$ PBS to remove loosely attached bacterial populations before fixed in 4% glutaraldehyde for 30 min at 4°C . Afterward, the staining solution of SYBR Green I (Sangon Biotech Co., Ltd.) was added to the well to completely submerge the glass, and then the biofilm was incubated for 30 min in the dark at room temperature. After that, all excessive staining solution was removed and air dried.

The confocal laser scanning microscope (TCS SP8; Leica Biosystems AG, Wetzlar, Germany) was employed to acquire biofilms images with $40 \times$ objective. Excitation at 488 nm with an argon laser in combination with a 525 ± 25 nm band-pass emission filter was used for SYBR Green I signal visualization. Then, the volumetric parameters and textural parameters (biovolume, mean thickness, biofilm roughness, and porosity) were calculated from 3D CLSM images by the ISA-2 software to quantify the structural characteristics of *V. parahaemolyticus* biofilms (Beyenal et al., 2004a). The biovolume represents the overall volume of the biofilm in the observation field. Mean thickness provides a measure of the spatial size of the biofilm and is the common variable used in biofilm research. Roughness is calculated from the thickness distribution of the biofilm and gives a measurement of the variations in biofilm thickness and is an indicator of the superficial biofilm interface heterogeneity (Heydorn et al., 2000). Porosity is defined as the ratio of void area to total area (Beyenal et al., 2004b). For each sample, the image stacking was acquired with a $1\text{-}\mu\text{m}$ thickness at six random sites.

Visualization of the Microstructure of the Biofilms Using Scanning Electron Microscopy

Biofilm samples formed on glass were washed by immersing in 1 mL of $1 \times$ PBS and then mixed with 2.5% glutaraldehyde for overnight at 4°C (Tan et al., 2018; Chen et al., 2020). Subsequently, biofilm samples were dehydrated with increasing concentrations of ethanol at 30, 50, 70, and 90% for 10 min,

respectively, followed by twice immersion in 100% ethanol for 10 min each (Liao et al., 2014). After air drying, biofilm samples were covered by using gold-palladium in an automatic sputter coater (Polaron SC7640 sputter coater; VG Microtech, East Sussex, United Kingdom) and visualized with the extreme-resolution analytical field emission scanning electron microscope (SM-7800F Prime; JEOL, Tokyo, Japan). The length of the biofilm cells was quantified by the ImageJ software (Rasband, W.S., ImageJ, US National Institutes of Health, Bethesda, MD, United States¹, 1997–2014).

Extraction and Chemical Components Analysis of EPS

The EPS of *V. parahaemolyticus* biofilms were extracted using the sonication method (DeFrancesco et al., 2017; Tan et al., 2018). Briefly, the medium was aspirated, and the remaining adherent cells were washed with sterile PBS. Biofilms were then resuspended in 1 mL 0.01M KCl solution and collected by vortexing and scraping. Next, *V. parahaemolyticus* biofilm cell clumps were dispersed with a Scientz-IID sonicator (Ningbo Scientz, Ningbo, Zhejiang, China) for six cycles of 5 s of operation and 5 s of pause at a power level of 20k Hz (45w) (Ding et al., 2019; Chen et al., 2020). The sonicated suspension was pelleted by centrifugation for 10 min at $7000 \times g$ at 4°C , and then the supernatant was removed and filtered by using a 0.22-mm membrane filter (Sangon Biotech Co., Ltd.). The amounts of DNA, proteins, and carbohydrates in the filtrate were analyzed. DNA was detected by using the Quant-iTTM PicoGreen[®] dsDNA Assay Kit (InvitrogenTM Ltd., Paisley, United Kingdom) according to manufacturer's instructions (Grande et al., 2015). The protein content was determined using Lowry method by Stable Lowry Protein Assay Kit (Sangon Biotech Co., Ltd.). The concentration of carbohydrate was quantified by the phenol-sulfuric acid method using glucose as a stand (Kim and Park, 2013). After that, the correlation analysis was created based on the OD₆₀₀ value versus the content of three chemical components after the biofilm was incubated at different times (2, 6, 12, 24, 36, and 48 h). Meanwhile, the correlation analysis between the contents of three different chemical components was also performed. Per experiment was tested in at least three replicates.

Raman Spectroscopy Analysis

The EPS of mature biofilms after DNase I, proteinase K, and DNase I–proteinase K treatment were extracted as described in the extraction and chemical component analysis of EPS. Additionally, the EPS of mature biofilms without enzyme treatment were used as control. The Raman spectra of four EPS samples were recorded with a Senterra R200-L Dispersive Raman Microscope (Bruker Optics, Ettlingen, Germany) at room temperature. A diode laser at 633 nm and $50 \times$ objective with a laser power of 3 mW was used for all Raman experiments. The Raman spectrum of each sample was calculated as the average of five measurements at different arbitrary sites on the biofilm. All Raman measurements were recorded with an accumulation time of 60 s in the range of $400\text{--}1520\text{ cm}^{-1}$. The acquisition of Raman

¹<http://imagej.nih.gov/ij/>

spectrum and preprocessing of preliminary data were conducted using the Bruker OPUS software.

Statistical Analysis

The experimental data were expressed as the mean \pm standard deviation. Statistical analysis was carried out by one-way analysis of variance using SPSS version 21.0 (SPSS Inc., Chicago, IL, United States) to compare the value differences ($P < 0.05$).

RESULTS

The Dynamic Process of Biofilm Formation

The dynamic process of *V. parahaemolyticus* biofilm formation was monitored in terms of the absorbance of the dissolved crystal violet dye from microtiter plates (**Figure 1A**). In the initial attachment phase (2–6 h), the biofilm formation was not obvious, and then a rapid increase in biofilm formation was tested in 6–12 h. After 12 h, the development of biofilms slowed down gradually. Subsequently, the biofilms further developed and reached the maximum at 24 h with an OD₆₀₀ of 2.44. After 24 h, the biofilms entered the dispersion stage leading to a sharp decrease of biomass.

The changes of *V. parahaemolyticus* biofilms were visualized using CLSM (**Figure 1B**), and their structural parameters were quantified in **Table 1**. Almost all cells were distributed as a single cell at 2 h, and then the biofilm cells gradually increased and formed scattered aggregates from 2 to 6 h, indicating the ongoing colonization of bacterial cells on the surfaces. At 6 h, the surface was covered by a slightly dense biofilm, with its biovolume and mean thickness being only $4.38 \times 10^5 \mu\text{m}^3$ and $2.47 \mu\text{m}$. When the time was prolonged to 12 h, the cells formed large clusters; furthermore, the architectures of biofilm developed from a single-layer planar structure to a multilayer 3D structure. Accordingly, the biovolume and mean thickness of the biofilm significantly increased to $6.57 \times 10^5 \mu\text{m}^3$ and $5.32 \mu\text{m}$. Conversely, the biofilm roughness and porosity were greatly reduced to 0.96 and 0.82, respectively. Mature biofilm with minimum roughness and porosity (0.89 and 0.77) was detected at 24 h. Meanwhile, the biovolume and mean thickness of biofilm reached the maximum, values of $9.36 \times 10^5 \mu\text{m}^3$ and $8.44 \mu\text{m}$, respectively. After 36 h of cultivation, the biofilm appeared disaggregated morphology where its biovolume and mean thickness decreased to $5.24 \times 10^5 \mu\text{m}^3$ and $4.10 \mu\text{m}$. After 48 h, further disaggregation of the biofilm led to a reduction in the biovolume and mean thickness, indicating the low concentration of microorganisms on the surface. Therefore, the biofilm roughness and porosity markedly increased compared to mature biofilm.

Scanning electron microscopy was used to observe the changes of microstructures during the biofilm development (**Figure 1C**), and the length of biofilm cells is shown in **Table 2**. In the initial adhesion stage, the biofilm was mainly composed of individual cells, and the morphology of cells became filamentous shape to better colonize on the contact surfaces. Simultaneously, the mean length and maximum length

of biofilm cells increased to 2.64 and $15.50 \mu\text{m}$ at 6 h, respectively. The cells further elongated themselves toward the center of microcommunity to form large aggregates after 12-h incubation. Likewise, the maximum length exhibited a great increase ranging from 15.50 to $34.23 \mu\text{m}$, and the mean length decreased slightly from 2.64 to $2.36 \mu\text{m}$. The mature biofilm with dense and complex 3D structures was acquired at 24 h, and most of the cells adhered closely and were held together by EPS, and therefore, the mean length and maximum length were not measurable. At 36 h, the 3D structures of the *V. parahaemolyticus* biofilms dissipated releasing individual cells. Obviously, the mean length and maximum length of biofilm cells decreased dramatically to 2.01 and $6.81 \mu\text{m}$. The dynamic processes of biofilm development characterized by CLSM and SEM were consistent with the results of crystal violet staining.

Correlation Between EPS and *Vibrio parahaemolyticus* Biofilm Formation

The relationship between biofilm formation and EPS was investigated using Pearson correlation analysis. The contents of eDNA, extracellular proteins, and carbohydrates were determined in **Figure 2A**. The results showed that the extracellular proteins and carbohydrates were the main components of EPS of the mature biofilm, followed by eDNA, which accounted for 72, 26, and 2% by mass, respectively. Interestingly, the three major components in EPS showed different changes during biofilm development. Of which, the amount of eDNA and extracellular proteins presented positively linear correlation with the biofilm formation, and the corresponding Pearson correlation coefficients (r_p) reached 0.99 ($R^2 = 0.9805$) and 0.983 ($R^2 = 0.9664$), respectively. However, no linear correlation was observed for carbohydrate content and biofilm formation (**Figures 2B–D**). Meanwhile, there was a strong positive correlation between eDNA and extracellular proteins ($r_p = 0.972$, $P < 0.01$) (**Figure 3A**). However, there was no correlation between carbohydrates and eDNA ($r_p = -0.387$, $P > 0.05$), as well as extracellular proteins ($r_p = -0.436$, $P > 0.05$) (**Figures 3B,C**). These results suggested that there should be collaborative functions of eDNA and extracellular proteins on the biofilm formation of *V. parahaemolyticus*.

Effect of eDNA and Extracellular Proteins on Biofilm Formation of *V. parahaemolyticus*

To determine the role of eDNA and extracellular proteins in biofilm formation of *V. parahaemolyticus*, DNase I, proteinase K, and their combination were added to the biofilms incubated at different times (2, 12, 24, 36, and 48 h). The amount of biofilm after DNase I, proteinase K, and DNase I–proteinase K treatment was determined by crystal violet staining (**Figure 4**), and their eradication efficiency is listed in **Table 3**. At the early stage (2 and 12 h), the addition of DNase I or proteinase K greatly decreased the initial attachment and destroyed the stability of formed biofilms ($P < 0.05$), proving that the eDNA and extracellular proteins were important for both initial attachment

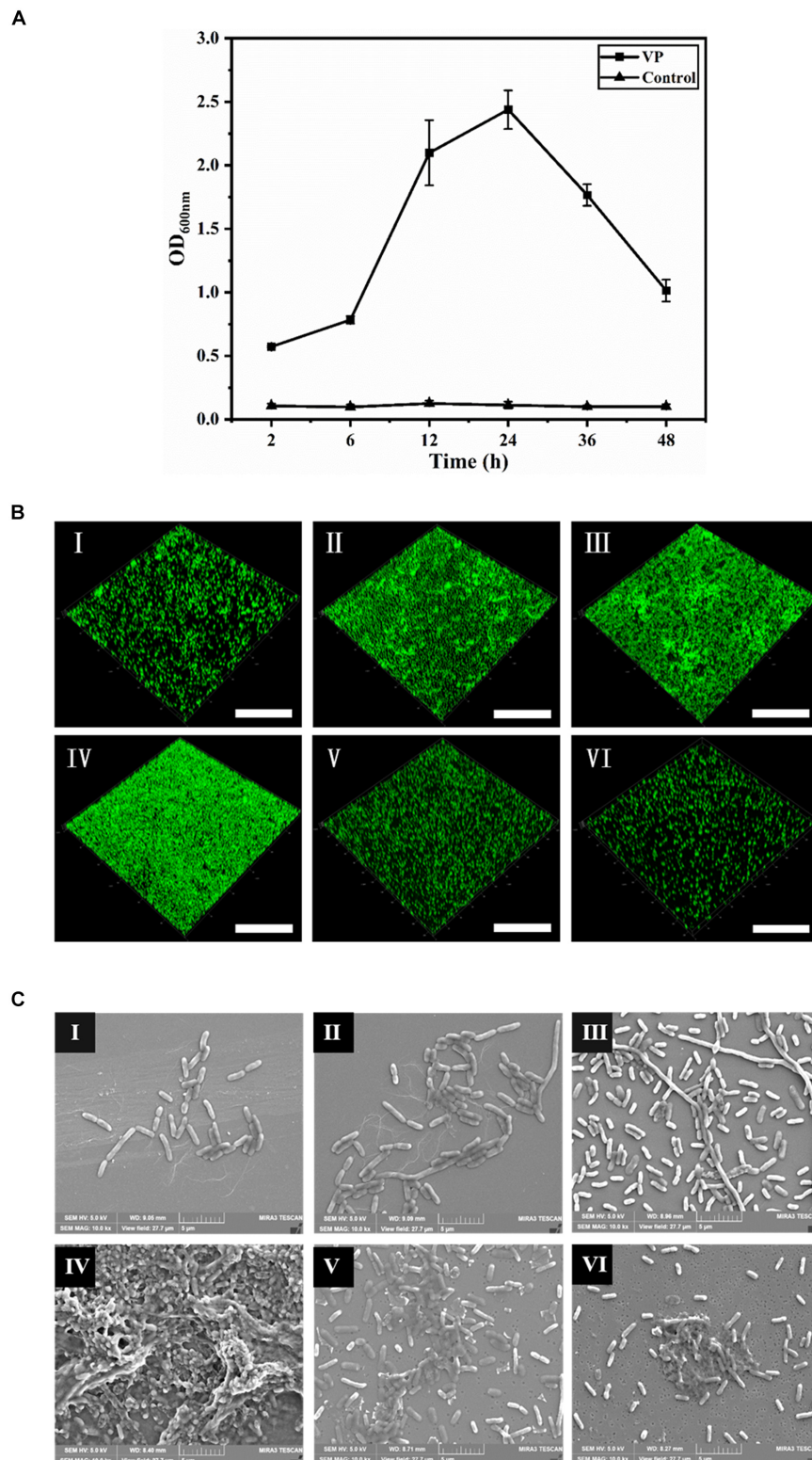


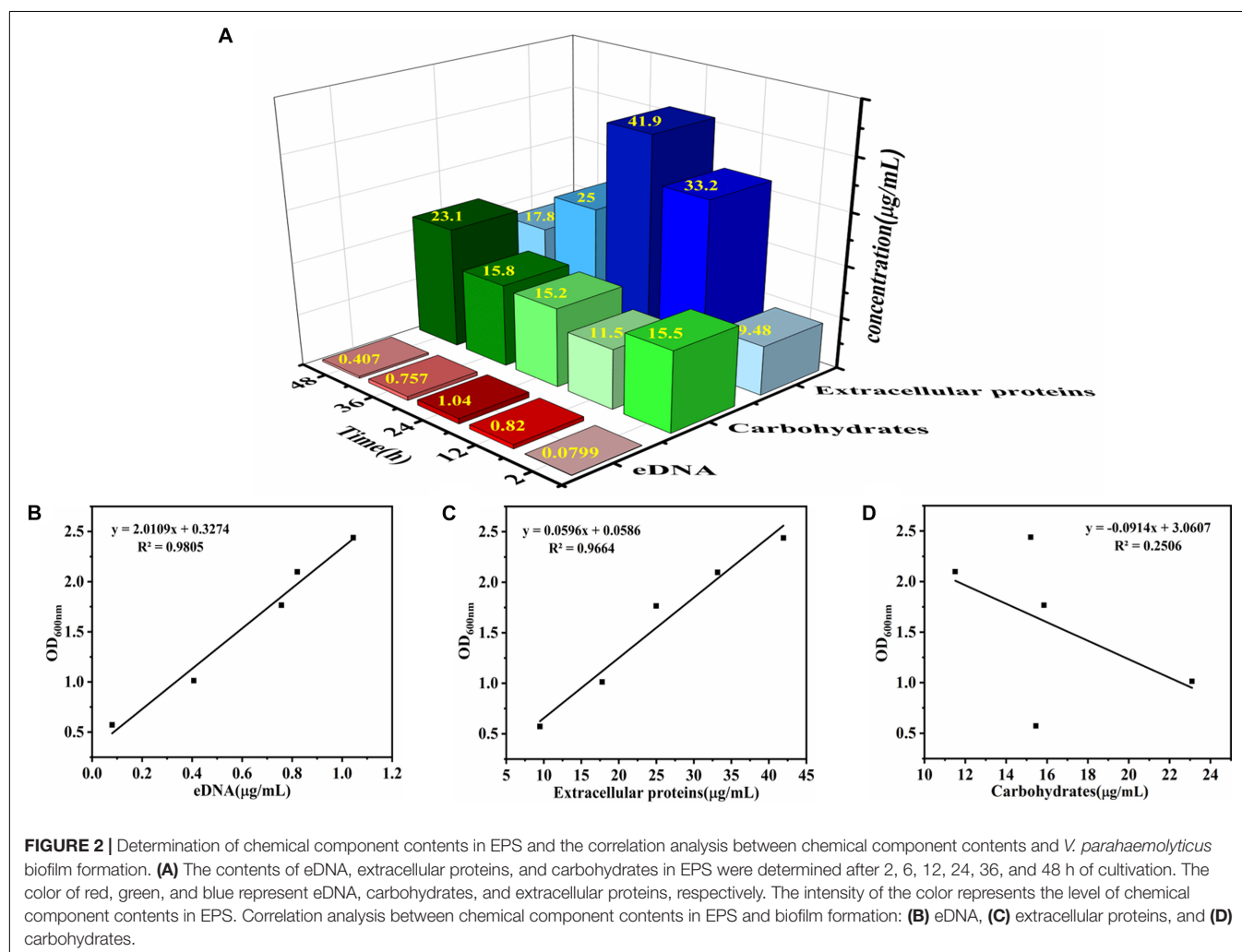
FIGURE 1 | The dynamic process of *V. parahaemolyticus* biofilm formation. **(A)** Biofilm biomass was measured by crystal violet binding at an OD₆₀₀ after static culture for different times (2, 6, 12, 24, 36, and 48 h). Error bars show standard deviations of three independent experiments. **(B)** Confocal laser scanning microscopic images of *V. parahaemolyticus* biofilm development process. The scale bar represents 100 μ m. **(C)** Scanning electron microscopic images of microstructure during the development of *V. parahaemolyticus* biofilm. The scale bar represents 5 μ m. I–VI represent 2, 6, 12, 24, 36, and 48 h, respectively. Pictures are representative of three independent experiments with at least three replicates each.

TABLE 1 | Quantification of the biofilm structure of *V. parahaemolyticus* after 2, 6, 12, 24, 36, and 48 h of incubation.

Structural parameters	Time points (h)					
	2	6	12	24	36	48
Biovolume $\times 10^5$ (μm^3)	3.39 ± 0.80	4.38 ± 0.46	6.57 ± 0.26	9.36 ± 0.85	5.24 ± 0.68	3.73 ± 0.38
Mean thickness (μm)	1.55 ± 0.37	2.47 ± 0.34	5.32 ± 0.37	8.44 ± 0.75	4.10 ± 0.27	3.59 ± 0.50
Biofilm roughness	1.49 ± 0.09	1.21 ± 0.10	0.96 ± 0.06	0.89 ± 0.12	1.26 ± 0.10	1.27 ± 0.09
Porosity	0.92 ± 0.01	0.86 ± 0.01	0.82 ± 0.01	0.77 ± 0.01	0.87 ± 0.01	0.92 ± 0.02

TABLE 2 | Quantification of the length of biofilm cells of *V. parahaemolyticus* after 2, 6, 12, 24, 36, and 48 h of incubation.

Cell length (μm)	Time points (h)					
	2	6	12	24	36	48
Mean length	2.05 ± 0.62	2.64 ± 2.14	2.36 ± 4.27	Not measurable	2.01 ± 0.76	1.59 ± 0.45
Maximum length	4.48	15.50	34.23	Not measurable	6.81	2.77



of cells and subsequent biofilm development. However, the 24-h-incubated biofilms with dense 3D structures were more resistant to individual DNase I and proteinase K treatment. However, great damage of biofilm treated by the combination of DNase

I and proteinase K was obtained during all stages compared to individual enzyme treatment. Therefore, the combination of DNase I and proteinase K could effectively remove the mature biofilms, resulting in a reduction of 62.86% of the biomass.

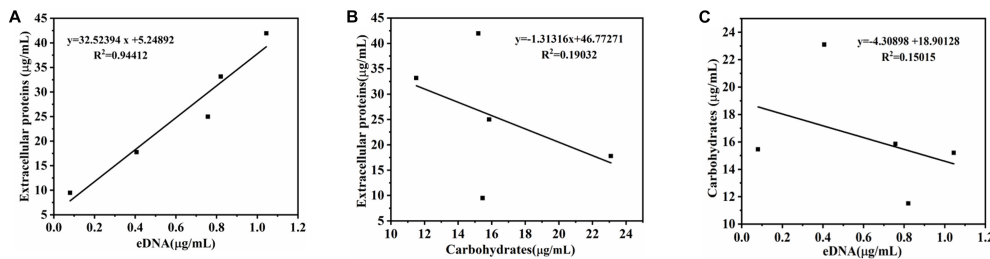


FIGURE 3 | Correlation analysis between eDNA, extracellular proteins, and carbohydrates of EPS in biofilm development of *V. parahaemolyticus*. **(A)** eDNA and extracellular proteins, **(B)** eDNA and carbohydrates, and **(C)** carbohydrates and extracellular proteins.

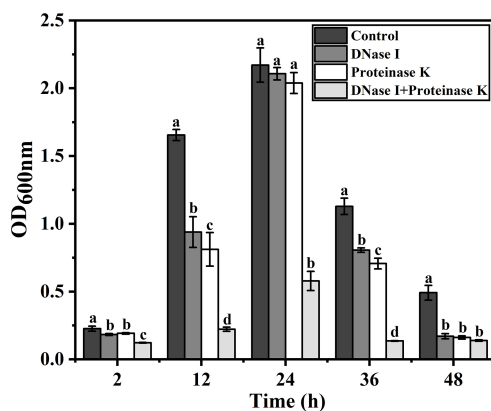


FIGURE 4 | Effect of eDNA and extracellular proteins on biofilm formation of *V. parahaemolyticus*. To confirm whether the eDNA and extracellular proteins serve as structural components in biofilms of *V. parahaemolyticus*, DNase I, proteinase K, and their combination were added to the biofilms incubated at different times (2, 12, 24, 36, and 48 h). Error bars show standard deviations of three independent experiments, and the different letters represent significant differences among treatments ($P < 0.05$).

Effects of eDNA and Extracellular Proteins on Architectures of the *V. parahaemolyticus* Biofilms

Confocal laser scanning microscopy was employed to verify the effects of eDNA and extracellular proteins on the architectures of *V. parahaemolyticus* biofilms in combination with ISA-2 software. The morphology differences of treated and untreated biofilms in development (12 h), maturation (24 h), and dispersion stage (48 h) are shown in **Figures 5, 6**. The biofilms in development stage (12 h) were corroded and showed irregular black holes after individual DNase I or proteinase K treatment. More sparse and decreased biofilms were observed after DNase I–proteinase K treatment. Likewise, the 48-h-incubated biofilms almost disappeared after DNase I, proteinase K, and DNase I–proteinase K treatment. However, there were no significant differences in the morphology of mature biofilms treated by individual enzyme compared to control samples. However, the DNase I–proteinase K-treated biofilms presented the markedly reduced amount and unevenly dispersed structures. Quantitative analysis revealed that the biovolume of biofilms

was $6.4 \times 10^5 \mu\text{m}^3$ in control samples (**Figure 6A**). After treatment of DNase I, proteinase K, and DNase I–proteinase K, the biovolume of 12-h-incubated biofilms was highly decreased to 4.6×10^5 , 4.3×10^5 , and $3.6 \times 10^5 \mu\text{m}^3$, respectively. However, the individual DNase I or proteinase K lost the ability to destroy the mature biofilms (24 h), although these DNase I–proteinase K could still greatly decrease the biomass of mature biofilms. When the biofilms entered the dispersion stage, the changes in the structural parameters were similar to those of 12-h-incubated samples under different enzyme treatment. Furthermore, the biofilm thickness of 12-h-incubated biofilms treated with different enzymes exhibited a great ($P < 0.05$) decrease ranging from 5.0 to $2.1 \mu\text{m}$ (**Figure 6B**). Such similar changes also occurred in 48-h-incubated biofilms. However, only the mature biofilms (24 h) treated by DNase I–proteinase K showed a reduction of $6\text{-}\mu\text{m}$ thickness and disappearance of multilayer structures. In **Figure 6C**, the biofilm roughness values of 12-h-incubated biofilms markedly ($P < 0.05$) increased from 0.96 to 1.58 after different enzyme treatment. When the biofilms entered the maturation stage, the mature biofilms presented intensively distributed architectures, which effectively prevented the actions of the individual DNase I or proteinase K. Nonetheless, the mature biofilms treated with DNase I–proteinase K showed a higher biofilm roughness ($1.18 > 0.77$) than the control samples. For the 48-h-incubated samples, the changes in their roughness were similar to those of 12-h-incubated samples. In addition, the porosity significantly ($P < 0.05$) increased in both 12- and 48 h-incubated biofilms treated by different enzymes (**Figure 6D**). For mature biofilms (24 h), their porosity did not present significant change after individual enzyme treatment. However, the porosity obviously increased from $0.72 \mu\text{m}$ in control samples to $0.90 \mu\text{m}$ in DNase I–proteinase K-treated samples. All the results suggested that eDNA and extracellular proteins were the key structural components of biofilm maintaining the mechanical stability of the mature *V. parahaemolyticus* biofilms.

Raman Analysis of Enzyme-Treated Mature Biofilms of *Vibrio parahaemolyticus*

Raman spectrum was used to monitor the chemical structure changes of eDNA and extracellular proteins in mature biofilms

TABLE 3 | Clearance of biofilm by different enzymes (%).

Enzyme treatment (30 min)	Time points (h)				
	2	12	24	36	48
DNase I	21.49 ^j ± 1.82	46.35 ^f ± 1.37	6.87 ^l ± 0.23	27.46 ^g ± 0.80	66.85 ^c ± 1.99
Proteinase K	18.11 ⁱ ± 0.54	50.98 ^e ± 2.38	6.04 ^k ± 0.21	37.41 ^h ± 0.43	65.64 ^{cd} ± 3.34
DNase I + proteinase K	46.70 ^f ± 3.82	88.69 ^a ± 2.38	62.86 ^d ± 2.6	87.78 ^a ± 0.52	71.57 ^b ± 2.78

The different letters represent significant differences among treatments (*P* < 0.05).

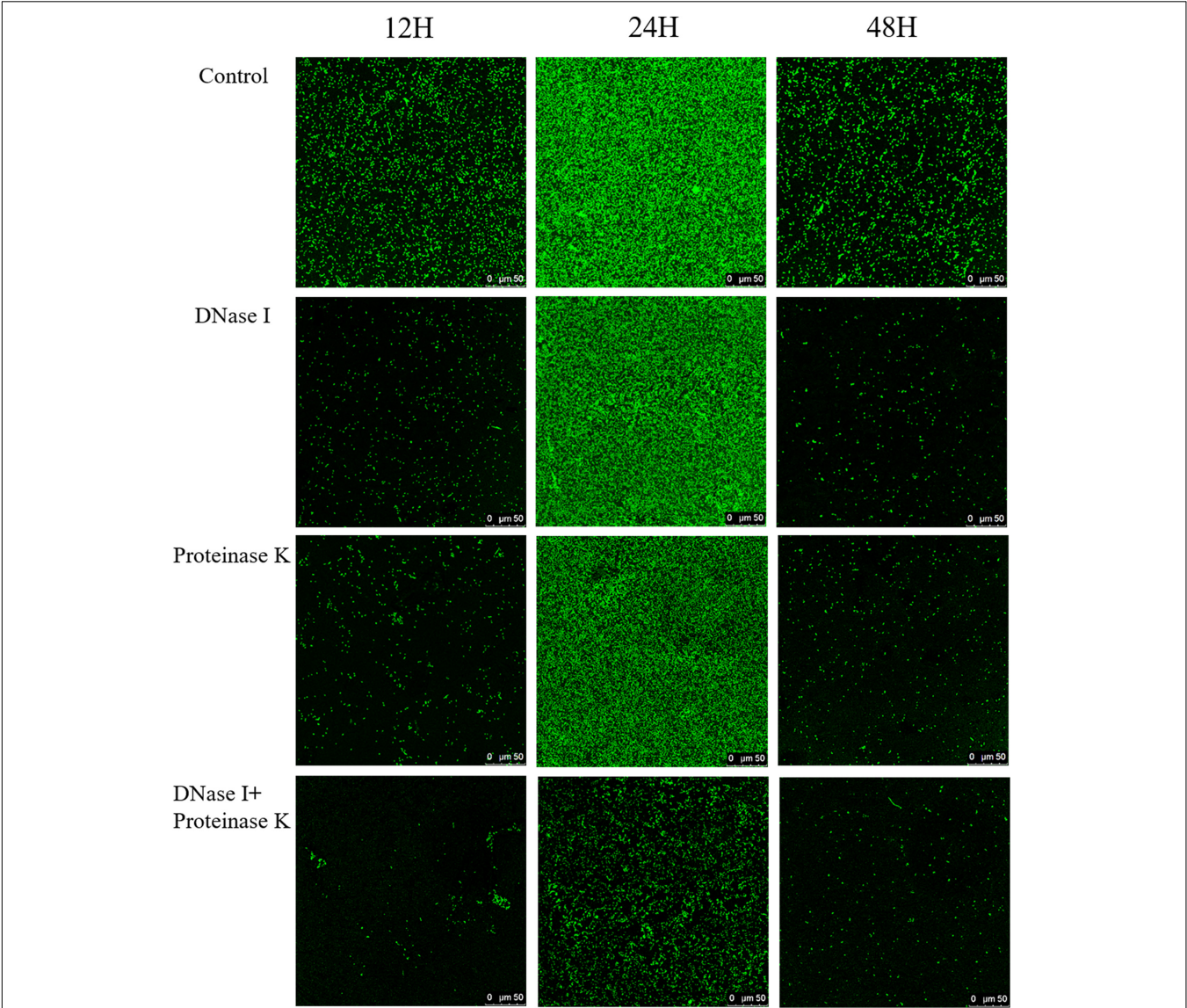
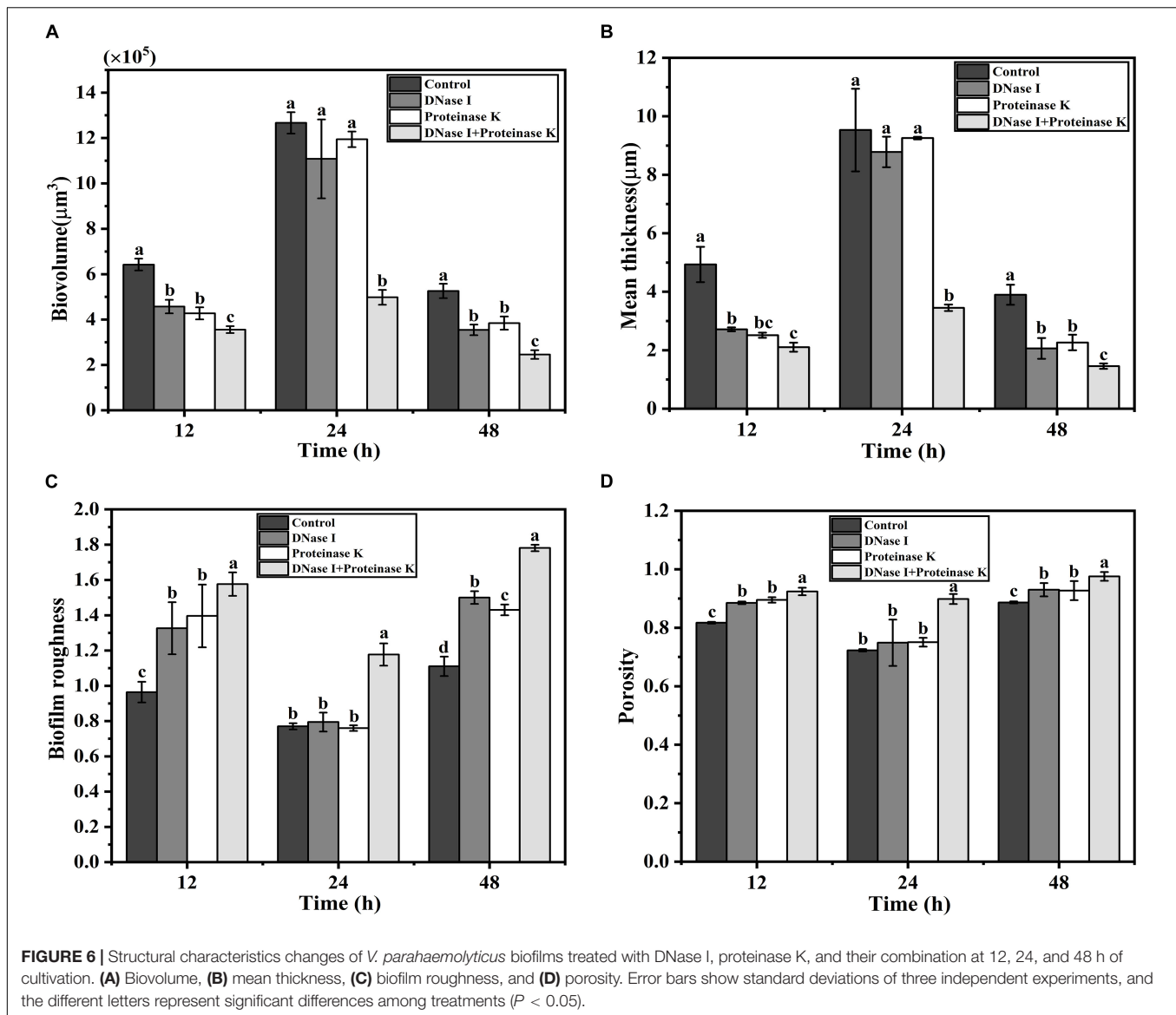


FIGURE 5 | Representative CLSM images of *V. parahaemolyticus* biofilms treated with DNase I, proteinase K, and their combination at 12, 24, and 48 h of cultivation. The scale bar represents 50 μm. Pictures are representative of at least three individual scans from three independent experiments.

treated by different enzymes. The representative Raman spectra of eDNA and extracellular proteins are shown in **Figure 7**, and the tentative peak assignments are summarized in **Table 4**. The typical bands of 561 to 582 cm⁻¹ could be assigned to glycosidic ring deformation vibration (COC) in carbohydrates.

In this region, the band intensity of the EPS were dramatically weakened after DNase I–proteinase K treatment. Similar change trends were also observed in the region of 780–788 cm⁻¹ (O–P–O stretching; cytosine, uracil) corresponding to DNA. Amide III (1200–1300 cm⁻¹, associated with C–N stretching and N–H



bending) bands were the indicator of the secondary structure of proteins. No significant change in the peak intensity of proteins was observed after individual DNase I or proteinase K treatment, but the intensity was obviously decreased after DNase I–proteinase K treatment, indicating that the enzymes induced the changes of secondary structure of proteins.

DISCUSSION

Vibrio parahaemolyticus has been considered as the main human pathogen in marine bacteria because of the increasing number of outbreaks and infections and the ability to form biofilms easily on various surfaces (Martinez-Urtaza et al., 2013; Mizan et al., 2016). Biofilm formation is a serious problem in food industries where the biofilms can be a persistent source of contamination (Van Houdt and Michiels, 2010). Biofilm development is a complex

physiological process guided by a series of physical, chemical, and biological factors, and the importance of EPS are well established for biofilm formation (Flemming et al., 2016; Dragos and Kovacs, 2017; Koo et al., 2017). Although EPS provide structural support to maintain the biofilm stability of *V. parahaemolyticus*, their respective functional role is still unclear (Han et al., 2017; Tan et al., 2018).

The production of high amount of EPS and the formation of densely distributed architectures were the predominant characteristics of the mature biofilms (Gupta et al., 2015; Zhang et al., 2015). After 24 h incubation, the biofilms with 3D structures and multilayers formed (Figure 1B). Moreover, a large amount of EPS secreted by *V. parahaemolyticus* was observed (Figure 1C). All these results indicated that the biofilm formation of *V. parahaemolyticus* reached maturation stage after 24-h incubation. Tan et al. (2018) reported that the biofilm formation of *V. parahaemolyticus* VPS36 entered the maturation stage after

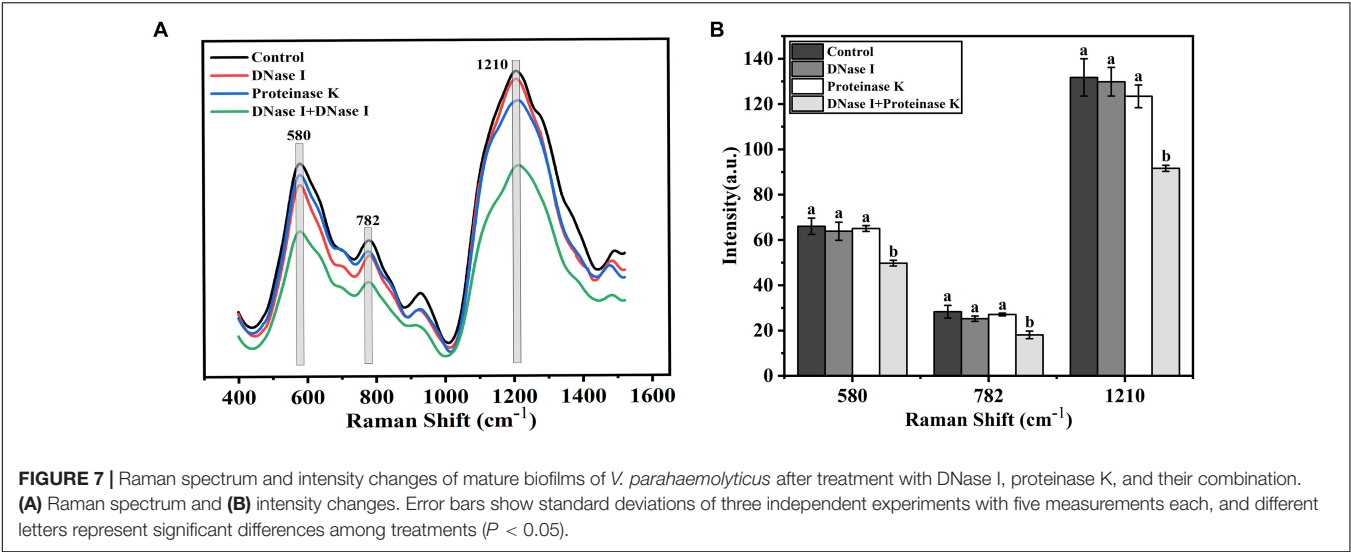


TABLE 4 | Peak assignment for Raman spectra of EPS in biofilms.

Peak position (cm ⁻¹)	Assignment	Macromolecular assignment	References
561–582	C-O-C glycosidic ring def; COO- wag; C-C skeletal	Carbohydrates	Guicheteau et al., 2008; Ileva et al., 2008; Han et al., 2017
780–788	O-P-O str; cytosine (C), uracil (U)	Nucleic acids	Ileva et al., 2009; Samek et al., 2010; Liu et al., 2014; Ramirez-Mora et al., 2019
1200–1300	Amide III	Proteins	Nottingham, 2007; Samek et al., 2014

def, deformation vibration; str, stretching.

48-h incubation, in which the mature cycle was twice the fold of that of *V. parahaemolyticus* ATCC17802. Such significant difference was collectively contributed by the following factors including the bacterial species, the type of attachment surfaces, and the environmental conditions (pH, temperature, nutritional conditions) (Whitehead and Verran, 2015). Among these factors, the bacterial species appears to act a pivotal role in biofilm formation owing to the heterogeneity of *Vibrio* strains (Song et al., 2016; Odeyemi and Ahmad, 2017; Mougín et al., 2019).

Once a mature biofilm community is established, the resistance to the harsh environments will be strengthened due to the functions of EPS (Nilsson et al., 2011). It is now widely accepted that three chemical components of the EPS, namely, eDNA, proteins, and exopolysaccharides, are assigned to specific structural roles in biofilm formation (Dragos and Kovacs, 2017). The quantitative analysis of the EPS from *V. parahaemolyticus* showed that the extracellular proteins and carbohydrates were the main components of EPS of the mature biofilm, followed by eDNA (Figure 2). Furthermore, the amount of eDNA and extracellular proteins was highly correlated with the biofilm formation of *V. parahaemolyticus*, but the carbohydrate content showed no correlation (Figure 2). Meanwhile, a significant correlation ($r_p = 0.972$, $P < 0.01$) was observed between eDNA and extracellular proteins (Figure 3). All these facts suggested that the eDNA and extracellular proteins acted a leading role in biofilm formation. Such results were consistent with previous

studies. For example, eDNA and DNABII proteins were central to the overall architecture and structural integrity of the non-typable *Haemophilus influenzae* biofilms (Goodman et al., 2011; Jursicek et al., 2017). Additionally, eDNA acted as an electrostatic net to interconnect cells surrounded by positively charged matrix proteins in the *Staphylococcus aureus* biofilms (Dengler et al., 2015). Likewise, Huseby et al. (2010) found that eDNA-mediated cross-linking of β toxin facilitated the formation of the skeletal framework during the biofilm development of *Staphylococcus*. However, in this study, the amount of carbohydrates did not seem to have an effect on biofilm formation, despite its high content. Similar results were obtained by Ding et al. (2019), who reported that the polysaccharide content showed no correlation ($r_p = 0.61$, $P > 0.05$) to biofilm growth. In addition, the group demonstrated that proteins rather than polysaccharides in the EPS from strain XL-2 played the dominant role in biofilm formation. In *Helicobacter pylori*, eDNA may not be the main component of biofilm matrix, but studies have shown that eDNA played an important role in biofilm formation by “bridging” OMV–OMV (outer membrane vesicles) and OMV–cell interactions (Grande et al., 2011, 2015). Hence, we speculated that the above phenomenon was due to that the components of EPS exhibited different roles in the biofilm formed by different bacteria.

Extracellular DNA has been reported to possess a significant effect on the initial attachment and stability of biofilm structure in Gram-positive and Gram-negative bacteria (Das et al., 2013;

Okshevsy et al., 2015). In this study, the DNase I treatment induced different degrees of damage to the biofilm (**Figure 4**). In particular, the addition of DNase I significantly decreased the amount of eDNA at early stage (2 and 12 h) leading to an obvious collapse of biofilms (**Figure 4**), which indicated that eDNA was crucial for initial attachment and development of biofilms. Previously, Godeke et al. (2011) applied DNase I to investigate the functions of eDNA in the biofilm formation; their results suggested that eDNA enhanced the initial surface attachment of bacterial cells and was the key structural component in all stages of *Shewanella oneidensis* biofilm formation. Meanwhile, Harmsen et al. (2010) found that eDNA played an essential role in the attachment and development of the *Listeria monocytogenes* biofilms. In addition, Das et al. (2010, 2011) revealed that eDNA contributed to the bacterial adhesion and aggregation mainly by the attractive Lifshitz–van der Waals and acid–base interactions.

Extracellular proteins, the main component of EPS, were proved to be an indispensable functional component for biofilm formation of *V. parahaemolyticus*. It was reported that extracellular proteins were structural elements of biofilm and exerted important functions during biofilm formation (Karunakaran and Biggs, 2011). Additionally, the present results were also supported by both Kumar Shukla and Rao (2013) and Ding et al. (2019), finding that the biofilm hydrolyzed with proteinase K showed a significant decrease in biomass. However, individual protease K treatment did not induce the dispersion of mature biofilm. Similar results were also observed for DNase I treatment (**Figure 4**). Notably, DNase I–protease K treatment induced the dispersion of 62.86% biofilm compared to control samples (**Table 3**). Therefore, the eDNA and extracellular proteins collectively played a critical role in the development and structure integrity of the *V. parahaemolyticus* biofilm. Moreover, Lappann et al. (2010) found that the crude chromosomal DNA could readily promote the biofilm formation and structure of *Neisseria meningitidis*, whereas pure DNA or DNase I-treated or proteinase K-treated crude DNA lost the improvement ability. The above phenomenon suggested that there should be a coaction of DNA and proteinaceous constituents, which promoted the biofilm formation and mechanical stability.

Structural parameters analysis showed that the density of biofilm cells decreased and the porosity of biofilm increased after DNase I–protease K treatment, indicating that the biomass of biofilm was decreased and the structure stability was destroyed (**Figures 5, 6**). The results of Raman spectrum also supported above facts. Compared with individual enzyme treatment, the DNase I–protease K treatment destroyed the loop configuration of eDNA and the secondary structure of proteins, which caused the collapse of EPS leading to the dispersion of biofilm (**Figure 7**). A similar finding was reported by Jung et al. (2014), who observed that the destruction of DNA ring structure and conformational changes of proteins decreased DNA and proteins when the biofilms were treated with antibiotics. In addition, Chen et al. (2020) revealed the degradation of DNA (guanine, cytosine, and uracil) and proteins (amide III phenylalanine), or altering the conformation of functional groups destroyed the chemical composition of EPS under photodynamic inactivation treatment. Previously, Das et al. (2011) proposed that when the loop

configuration of the eDNA in *Streptococcus* was changed into a more trainlike configuration, no specific adsorption sites were available for cross-linking with other bacteria on the cell surface, which led to the decrease of aggregation. Moreover, Liu et al. (2008) and Das et al. (2011) also found that the loop configuration of the eDNA played a vital role in biofilm formation and aggregation. In addition, the key role of protein secondary structures in promoting adhesion, aggregation, and biofilm formation has been widely reported (Wang et al., 2018; Ding et al., 2019). Although this study has clarified that eDNA and extracellular proteins collectively contributed to the mature biofilm formation of *V. parahaemolyticus*, the interactions between these two components are needed to be further investigated. Swinger and Rice (2004) reported that IHF (DNABII proteins) binds DNA, depending on significant sequence specificity. Additionally, Kavanaugh et al. (2019) suggested that extracellular proteins facilitated *S. aureus* biofilm formation by linking individual bacterial cells together through non-covalent cross-links with eDNA.

CONCLUSION

The EPS, mainly composed of eDNA, extracellular proteins, exopolysaccharides, and so on, directly mediate the adhesion of microorganisms to surfaces to develop the complex 3D structure of biofilms. In this study, the amount of eDNA and extracellular proteins was positively correlated with the biofilm formation of *V. parahaemolyticus*, but the carbohydrates showed no correlation. The destruction of the eDNA or extracellular proteins greatly decreased the attachment and stability of the formed biofilms in early stage, but did not produce obvious destruction on mature biofilms. However, the concurrent destruction of the eDNA and extracellular proteins induced the dispersion of the mature biofilms after DNase I–protease K treatment. Further analysis showed that the collapse of biofilms was mainly attributed to the damage of the loop configuration of eDNA and the secondary structure of proteins caused by the enzymes. Therefore, the illumination of the role of chemical components in EPS may provide a further understanding of biofilm formation mechanisms of *V. parahaemolyticus* and also give novel insight to establish environmentally friendly cleaning methods to eliminate the biofilms in food industry.

DATA AVAILABILITY STATEMENT

All datasets generated for this study are included in this manuscript.

AUTHOR CONTRIBUTIONS

YZ, JW, YP, and HL conceived and supervised the study. WL and HQ designed the experiments. WL performed the experiments, analyzed the data, and wrote the manuscript. JW, LT, ZZ, and YZ revised the manuscript.

FUNDING

This research was supported by the National Natural Science Foundation of China (31972188 and 31671779), National

Key R&D Program of China (2018YFC1602205), Shanghai Agriculture Applied Technology Development Program (T20170404), and Innovation Program of Shanghai Municipal Education Commission (2017-01-07-00-10-E00056).

REFERENCES

- Beyenal, H., Donovan, C., Lewandowski, Z., and Harkin, G. (2004a). Three-dimensional biofilm structure quantification. *J. Microbiol. Methods* 59, 395–413. doi: 10.1016/j.mimet.2004.08.003
- Beyenal, H., Lewandowski, Z., and Harkin, G. (2004b). Quantifying biofilm structure: facts and fiction. *Biofouling* 20, 1–23. doi: 10.1080/0892701042000191628
- Brown, H. L., Hanman, K., Reuter, M., Betts, R. P., and van Vliet, A. H. (2015). *Campylobacter jejuni* biofilms contain extracellular DNA and are sensitive to DNase I treatment. *Front. Microbiol.* 6:699. doi: 10.3389/fmicb.2015.00699
- Chen, B., Huang, J., Li, H., Zeng, Q.-H., Wang, J. J., Liu, H., et al. (2020). Eradication of planktonic *Vibrio parahaemolyticus* and its sessile biofilm by curcumin-mediated photodynamic inactivation. *Food Control* 113:107181. doi: 10.1016/j.foodcont.2020.107181
- Chen, Y. S., Dai, J. L., Morris, J. G., and Johnson, J. A. (2010). Genetic analysis of the capsule polysaccharide (K antigen) and exopolysaccharide genes in pandemic *Vibrio parahaemolyticus* O3:K6. *BMC Microbiol.* 10:274. doi: 10.1186/1471-2180-10-274
- Chimileski, S., Dolas, K., Naor, A., Gophna, U., and Papke, R. T. (2014). Extracellular DNA metabolism in *Haloflex volcarm*. *Front. Microbiol.* 5:57. doi: 10.3389/fmicb.2014.00057
- Colvin, K. M., Gordon, V. D., Murakami, K., Borlee, B. R., Wozniak, D. J., Wong, G. C., et al. (2011). The pel polysaccharide can serve a structural and protective role in the biofilm matrix of *Pseudomonas aeruginosa*. *PLoS Pathog.* 7:e1001264. doi: 10.1371/journal.ppat.1001264
- Costa, E. M., Silva, S., Tavará, F. K., and Pintado, M. M. (2013). Study of the effects of chitosan upon *Streptococcus mutans* adherence and biofilm formation. *Anaerobe* 20, 27–31. doi: 10.1016/j.anaerobe.2013.02.002
- Costerton, J. W., Stewart, P. S., and Greenberg, E. P. (1999). Bacterial biofilms: a common cause of persistent infections. *Science* 284, 1318–1322. doi: 10.1126/science.284.5418.1318
- Crofts, A. A., Giovanetti, S. M., Rubin, E. J., Poly, F. M., Gutierrez, R. L., Talaat, K. R., et al. (2018). Enterotoxigenic *E. coli* virulence gene regulation in human infections. *Proc. Natl. Acad. Sci. U.S.A.* 115, E8968–E8976. doi: 10.1073/pnas.1808982115
- Cugini, C., Shanmugam, M., Landge, N., and Ramasubbu, N. (2019). The role of exopolysaccharides in oral biofilms. *J. Dent. Res.* 98, 739–745. doi: 10.1177/0022034519845001
- da Rosa, J. V., da Conceicao, N. V., da Conceicao, R. D. D., and Timm, C. D. (2018). Biofilm formation by *Vibrio parahaemolyticus* on different surfaces and its resistance to sodium hypochlorite. *Cienc. Rural* 48:e20180612. doi: 10.1590/0103-8478cr20180612
- Das, T., Krom, B. P., van der Mei, H. C., Busscher, H. J., and Sharma, P. K. (2011). DNA-mediated bacterial aggregation is dictated by acid-base interactions. *Soft Matter* 7, 2927–2935. doi: 10.1039/c0sm01142h
- Das, T., Sehar, S., and Manefield, M. (2013). The roles of extracellular DNA in the structural integrity of extracellular polymeric substance and bacterial biofilm development. *Environ. Microbiol. Rep.* 5, 778–786. doi: 10.1111/1758-2229.12085
- Das, T., Sharma, P. K., Busscher, H. J., van der Mei, H. C., and Krom, B. P. (2010). Role of extracellular DNA in initial bacterial adhesion and surface aggregation. *Appl. Environ. Microbiol.* 76, 3405–3408. doi: 10.1128/AEM.03119-09
- DeFrancesco, A. S., Masloboeva, N., Syed, A. K., DeLoughery, A., Bradshaw, N., Li, G. W., et al. (2017). Genome-wide screen for genes involved in eDNA release during biofilm formation by *Staphylococcus aureus*. *Proc. Natl. Acad. Sci. U.S.A.* 114, E5969–E5978. doi: 10.1073/pnas.1704544114
- Dengler, V., Foulston, L., DeFrancesco, A. S., and Losick, R. (2015). An electrostatic net model for the role of extracellular DNA in biofilm formation by *Staphylococcus aureus*. *J. Bacteriol.* 197, 3779–3787. doi: 10.1128/jb.00726-15
- Ding, X. S., Zhao, B., An, Q., Tian, M., and Guo, J. S. (2019). Role of extracellular polymeric substances in biofilm formation by *Pseudomonas stutzeri* strain XL-2. *Appl. Microbiol. Biotechnol.* 103, 9169–9180. doi: 10.1007/s00253-019-10188-4
- Dragos, A., and Kovacs, A. T. (2017). The peculiar functions of the bacterial extracellular matrix. *Trends Microbiol.* 25, 257–266. doi: 10.1016/j.tim.2016.12.010
- Elexson, N., Afsah-Hejri, L., Rukayadi, Y., Soopna, P., Lee, H. Y., Tuan Zainazor, T. C., et al. (2014). Effect of detergents as antibacterial agents on biofilm of antibiotics-resistant *Vibrio parahaemolyticus* isolates. *Food Control* 35, 378–385. doi: 10.1016/j.foodcont.2013.07.020
- Flemming, H. C., and Wingender, J. (2010). The biofilm matrix. *Nat. Rev. Microbiol.* 8, 623–633. doi: 10.1038/nrmicro2415
- Flemming, H. C., Wingender, J., Szewzyk, U., Steinberg, P., Rice, S. A., and Kjelleberg, S. (2016). Biofilms: an emergent form of bacterial life. *Nat. Rev. Microbiol.* 14, 563–575. doi: 10.1038/nrmicro.2016.94
- Godeke, J., Paul, K., Lassak, J., and Thormann, K. M. (2011). Phage-induced lysis enhances biofilm formation in *Shewanella oneidensis* MR-1. *ISME J.* 5, 613–626. doi: 10.1038/ismej.2010.153
- Goodman, S. D., Obergfell, K. P., Jurcisek, J. A., Novotny, L. A., Downey, J. S., Ayala, E. A., et al. (2011). Biofilms can be dispersed by focusing the immune system on a common family of bacterial nucleoid-associated proteins. *Mucosal Immunol.* 4, 625–637. doi: 10.1038/mi.2011.27
- Grande, R., Di Giulio, M., Bessa, L. J., Di Campli, E., Baffoni, M., Guarnieri, S., et al. (2011). Extracellular DNA in *Helicobacter pylori* biofilm: a backstairs rumour. *J. Appl. Microbiol.* 110, 490–498. doi: 10.1111/j.1365-2672.2010.04911.x
- Grande, R., Di Marcantonio, M. C., Robuffo, I., Pompilio, A., Celia, C., Di Marzio, L., et al. (2015). *Helicobacter pylori* ATCC 43629/NCTC 11639 outer membrane vesicles (OMVs) from biofilm and planktonic phase associated with extracellular DNA (eDNA). *Front. Microbiol.* 6:1369. doi: 10.3389/fmicb.2015.01369
- Guicheteau, J., Argue, L., Emge, D., Hyre, A., Jacobson, M., and Christesen, S. (2008). *Bacillus spore* classification via surface-enhanced Raman spectroscopy and principal component analysis. *Appl. Spectrosc.* 62, 267–272. doi: 10.1366/000370208783759623
- Gupta, P., Sarkar, S., Das, B., Bhattacharjee, S., and Tribedi, P. (2015). Biofilm, pathogenesis and prevention—a journey to break the wall: a review. *Arch. Microbiol.* 198, 1–15. doi: 10.1007/s00203-015-1148-6
- Guvener, Z. T., and McCarter, L. L. (2003). Multiple regulators control capsular polysaccharide production in *Vibrio parahaemolyticus*. *J. Bacteriol.* 185, 5431–5441. doi: 10.1128/jb.185.18.5431-5441.2003
- Han, N., Mizan, M. F. R., Jahid, I. K., and Ha, S. D. (2016). Biofilm formation by *Vibrio parahaemolyticus* on food and food contact surfaces increases with rise in temperature. *Food Control* 70, 161–166. doi: 10.1016/j.foodcont.2016.05.054
- Han, Q., Song, X., Zhang, Z., Fu, J., Wang, X., Malakar, P. K., et al. (2017). Removal of foodborne pathogen biofilms by acidic electrolyzed water. *Front. Microbiol.* 8:988. doi: 10.3389/fmicb.2017.00988
- Harmsen, M., Lappann, M., Knochel, S., and Molin, S. (2010). Role of extracellular DNA during biofilm formation by *Listeria monocytogenes*. *Appl. Environ. Microbiol.* 76, 2271–2279. doi: 10.1128/AEM.02361-09
- Heydorn, A., Nielsen, A. T., Hentzer, M., Sternberg, C., Givskov, M., Ersboll, B. K., et al. (2000). Quantification of biofilm structures by the novel computer program COMSTAT. *Microbiology* 146, 2395–2407. doi: 10.1099/00221287-146-10-2395
- Hobley, L., Harkins, C., MacPhee, C. E., and Stanley-Wall, N. R. (2015). Giving structure to the biofilm matrix: an overview of individual strategies and

- emerging common themes. *FEMS Microbiol. Rev.* 39, 649–669. doi: 10.1093/femsre/fuv015
- Huseby, M. J., Kruse, A. C., Digre, J., Kohler, P. L., Vocke, J. A., Mann, E. E., et al. (2010). Beta toxin catalyzes formation of nucleoprotein matrix in *Staphylococcal* biofilms. *Proc. Natl. Acad. Sci. U.S.A.* 107, 14407–14412. doi: 10.1073/pnas.0911032107
- Ibanez de Aldecoa, A. L., Zafra, O., and Gonzalez-Pastor, J. E. (2017). Mechanisms and regulation of extracellular DNA release and its biological roles in microbial communities. *Front. Microbiol.* 8:1390. doi: 10.3389/fmicb.2017.01390
- Ivleva, N. P., Wagner, M., Horn, H., Niessner, R., and Haisch, C. (2008). *In situ* surface-enhanced raman scattering analysis of biofilm. *Anal. Chem.* 80, 8538–8544. doi: 10.1021/ac801426m
- Ivleva, N. P., Wagner, M., Horn, H., Niessner, R., and Haisch, C. (2009). Towards a nondestructive chemical characterization of biofilm matrix by Raman microscopy. *Anal. Bioanal. Chem.* 393, 197–206. doi: 10.1007/s00216-008-2470-5
- Jin, H. P., Lee, B., Jo, Y., and Sang, H. C. (2016). Role of extracellular matrix protein CAbA in resistance of *Vibrio vulnificus* biofilms to decontamination strategies. *Int. J. Food Microbiol.* 236, 123–129. doi: 10.1016/j.ijfoodmicro.2016.07.032
- Jung, G. B., Nam, S. W., Choi, S., Lee, G.-J., and Park, H.-K. (2014). Evaluation of antibiotic effects on *Pseudomonas aeruginosa* biofilm using Raman spectroscopy and multivariate analysis. *Biomed. Opt. Express* 5, 3238–3251. doi: 10.1364/boe.5.003238
- Jung, Y. L., Lee, M. A., and Lee, K. H. (2019). Role of flagellin-homologous proteins in biofilm formation by pathogenic *Vibrio* species. *Mol. Biol. Physiol.* 10:e01793-19. doi: 10.1128/mBio.01793-19
- Jurcisek, J. A., Brockman, K. L., Novotny, L. A., Goodman, S. D., and Bakaletz, L. O. (2017). *Nontypeable Haemophilus influenzae* releases DNA and DNABII proteins via a T4SS-like complex and ComE of the type IV pilus machinery. *Proc. Natl. Acad. Sci. U.S.A.* 114, E6632–E6641. doi: 10.1073/pnas.1705508114
- Karunakaran, E., and Biggs, C. A. (2011). Mechanisms of *Bacillus cereus* biofilm formation: an investigation of the physicochemical characteristics of cell surfaces and extracellular proteins. *Appl. Microbiol. Biotechnol.* 89, 1161–1175. doi: 10.1007/s00253-010-2919-2
- Kavanaugh, J. S., Flack, C. E., Lister, J., Ricker, E. B., Ibberson, C. B., Jenul, C., et al. (2019). Identification of extracellular DNA-binding proteins in the biofilm matrix. *mBio* 10:e01137-19. doi: 10.1128/mBio.01137-19
- Kim, H. S., and Park, H. D. (2013). Ginger extract inhibits biofilm formation by *Pseudomonas aeruginosa* PA14. *PLoS One* 8:e76106. doi: 10.1371/journal.pone.0076106
- Koo, H., Allan, R. N., Howlin, R. P., Stoodley, P., and Hall-Stoodley, L. (2017). Targeting microbial biofilms: current and prospective therapeutic strategies. *Nat. Rev. Microbiol.* 15, 740–755. doi: 10.1038/nrmicro.2017.99
- Kumar Shukla, S., and Rao, T. S. (2013). Dispersal of Bap-mediated *Staphylococcus aureus* biofilm by proteinase K. *J. Antibiot.* 66, 55–60. doi: 10.1038/ja.2012.98
- Lappann, M., Claus, H., van Alen, T., Harmsen, M., Elias, J., Molin, S., et al. (2010). A dual role of extracellular DNA during biofilm formation of *Neisseria meningitidis*. *Mol. Microbiol.* 75, 1355–1371. doi: 10.1111/j.1365-2958.2010.07054.x
- Liao, S., Klein, M. I., Heim, K. P., Fan, Y., Bitoun, J. P., Ahn, S. J., et al. (2014). *Streptococcus mutans* extracellular DNA is upregulated during growth in biofilms, actively released via membrane vesicles, and influenced by components of the protein secretion machinery. *J. Bacteriol.* 196, 2355–2366. doi: 10.1128/JB.01493-14
- Liu, H., Xu, Q., Huo, L., Wei, X., and Ling, J. (2014). Chemical composition of *Enterococcus faecalis* in biofilm cells initiated from different physiologic states. *Folia Microbiol.* 59, 447–453. doi: 10.1007/s12223-014-0319-1
- Liu, H. H., Yang, Y. R., Shen, X. C., Zhang, Z. L., Shen, P., and Xie, Z. X. (2008). Role of DNA in bacterial aggregation. *Curr. Microbiol.* 57, 139–144. doi: 10.1007/s00284-008-9166-0
- Martinez-Urtaza, J., Baker-Austin, C., Jones, J. L., Newton, A. E., Gonzalez-Aviles, G. D., and DePaola, A. (2013). Spread of Pacific Northwest *Vibrio parahaemolyticus* Strain. *N. Engl. J. Med.* 369, 1573–1574. doi: 10.1056/NEJMc1305535
- Mizan, M. F., Jahid, I. K., Kim, M., Lee, K. H., Kim, T. J., and Ha, S. D. (2016). Variability in biofilm formation correlates with hydrophobicity and quorum sensing among *Vibrio parahaemolyticus* isolates from food contact surfaces and the distribution of the genes involved in biofilm formation. *Biofouling* 32, 497–509. doi: 10.1080/08927014.2016.1149571
- Mougin, J., Copin, S., Bojolly, D., Raguene, V., Robert-Pillot, A., Quilici, M.-L., et al. (2019). Adhesion to stainless steel surfaces and detection of viable but non cultivable cells of *Vibrio parahaemolyticus* and *Vibrio cholerae* isolated from shrimps in seafood processing environments: Stayin' alive? *Food Control* 102, 122–130. doi: 10.1016/j.foodcont.2019.03.024
- Nilsson, R. E., Ross, T., and Bowman, J. P. (2011). Variability in biofilm production by *Listeria monocytogenes* correlated to strain origin and growth conditions. *Int. J. Food. Microbiol.* 150, 14–24. doi: 10.1016/j.ijfoodmicro.2011.07.012
- Nottingham, I. (2007). Raman Spectroscopy cell-based Biosensors. *Sensors* 7, 1343–1358. doi: 10.3390/s7081343
- Odeyemi, O. A., and Ahmad, A. (2017). Population dynamics, antibiotics resistance and biofilm formation of *Aeromonas* and *Vibrio* species isolated from aquatic sources in Northern Malaysia. *Microb. Pathog.* 103, 178–185. doi: 10.1016/j.micpath.2017.01.007
- Okshevsy, M., and Meyer, R. L. (2013). The role of extracellular DNA in the establishment, maintenance and perpetuation of bacterial biofilms. *Crit. Rev. Microbiol.* 41, 341–352. doi: 10.3109/1040841X.2013.841639
- Okshevsy, M., Regina, V. R., and Meyer, R. L. (2015). Extracellular DNA as a target for biofilm control. *Curr. Opin. Biotechnol.* 33, 73–80. doi: 10.1016/j.copbio.2014.12.002
- Ophir, T., and Gutnick, D. L. (1994). A role for exopolysaccharides in the protection of microorganisms from desiccation. *Appl. Environ. Microbiol.* 60, 740–745. doi: 10.1128/aem.60.2.740-745.1994
- Ramirez-Mora, T., Dávila-Pérez, C., Torres-Méndez, F., and Valle-Bourrouet, G. (2019). Raman Spectroscopic Characterization of Endodontic Biofilm Matrices. *J. Spectrosc.* 2019:1307397. doi: 10.1155/2019/1307397
- Rasz, S. M., Froelich, B. A., Vieira, C. R., Blackwood, A. D., and Noble, R. T. (2016). *Vibrio parahaemolyticus* and *Vibrio vulnificus* in South America: water, seafood and human infections. *J. Appl. Microbiol.* 121, 1201–1222. doi: 10.1111/jam.13246
- Rose, S. J., Babrak, L. M., and Bermudez, L. E. (2015). *Mycobacterium avium* possesses extracellular DNA that contributes to biofilm formation, structural integrity, and tolerance to antibiotics. *PLoS One* 10:e0128772. doi: 10.1371/journal.pone.0128772
- Samek, O., Al-Marashi, J. F. M., and Telle, H. H. (2010). The potential of Raman spectroscopy for the identification of biofilm formation by *Staphylococcus epidermidis*. *Laser Phys. Lett.* 7, 378–383. doi: 10.1002/lapl.200910154
- Samek, O., Mlynarikova, K., Bernatova, S., Jezek, J., Krzyzanek, V., Siler, M., et al. (2014). *Candida parapsilosis* biofilm identification by Raman spectroscopy. *Int. J. Mol. Sci.* 15, 23924–23935. doi: 10.3390/ijms151223924
- Song, X., Ma, Y., Fu, J., Zhao, A., Guo, Z., Malakar, P. K., et al. (2016). Effect of temperature on pathogenic and non-pathogenic *Vibrio parahaemolyticus* biofilm formation. *Food Control* 73, 485–491. doi: 10.1016/j.foodcont.2016.08.041
- Swinger, K. K., and Rice, P. A. (2004). IHf and HU: flexible architects of bent DNA. *Curr. Opin. Struct. Biol.* 14, 28–35. doi: 10.1016/j.sbi.2003.12.003
- Tan, L., Zhao, F., Han, Q., Zhao, A., Malakar, P. K., Liu, H., et al. (2018). High correlation between structure development and chemical variation during biofilm formation by *Vibrio parahaemolyticus*. *Front. Microbiol.* 9:1881. doi: 10.3389/fmicb.2018.01881
- Urmersbach, S., Aho, T., Alter, T., Hassan, S. S., Autio, R., and Huehn, S. (2015). Changes in global gene expression of *Vibrio parahaemolyticus* induced by cold- and heat-stress. *BMC Microbiol.* 15:13. doi: 10.1186/s12866-015-0565-7
- Van Houdt, R., and Michiels, C. W. (2010). Biofilm formation and the food industry, a focus on the bacterial outer surface. *J. Appl. Microbiol.* 109, 1117–1131. doi: 10.1111/j.1365-2672.2010.04756.x
- Wang, L., Ling, Y., Jiang, H. W., Qiu, Y. F., Qiu, J. F., Chen, H. P., et al. (2013). AphA is required for biofilm formation, motility, and virulence in pandemic *Vibrio parahaemolyticus*. *Int. J. Food Microbiol.* 160, 245–251. doi: 10.1016/j.ijfoodmicro.2012.11.004
- Wang, X., An, Q., Zhao, B., Guo, J. S., Huang, Y. S., and Tian, M. (2018). Auto-aggregation properties of a novel aerobic denitrifier *Enterobacter* sp. strain FL. *Appl. Microbiol. Biotechnol.* 102, 2019–2030. doi: 10.1007/s00253-017-8720-8

- Whitchurch, C. B., Tolker-Nielsen, T., Ragas, P. C., and Mattick, J. S. (2002). Extracellular DNA required for bacterial biofilm formation. *Science* 295, 1487–1487. doi: 10.1126/science.295.5559.1487
- Whitehead, K. A., and Verran, J. (2015). Formation, architecture and functionality of microbial biofilms in the food industry. *Curr. Opin. Food Sci.* 2, 84–91. doi: 10.1016/j.cofs.2015.02.003
- Zhang, Y., Wang, F., Zhu, X., Zeng, J., Zhao, Q., and Jiang, X. (2015). Extracellular polymeric substances govern the development of biofilm and mass transfer of polycyclic aromatic hydrocarbons for improved biodegradation. *Bioresour. Technol.* 193, 274–280. doi: 10.1016/j.biortech.2015.06.110

Conflict of Interest: The authors declare that the research was conducted in the absence of any commercial or financial relationships that could be construed as a potential conflict of interest.

Copyright © 2020 Li, Wang, Qian, Tan, Zhang, Liu, Pan and Zhao. This is an open-access article distributed under the terms of the Creative Commons Attribution License (CC BY). The use, distribution or reproduction in other forums is permitted, provided the original author(s) and the copyright owner(s) are credited and that the original publication in this journal is cited, in accordance with accepted academic practice. No use, distribution or reproduction is permitted which does not comply with these terms.



Formation and Control of the Viable but Non-culturable State of Foodborne Pathogen *Escherichia coli* O157:H7

Yanmei Li^{1†}, Teng-Yi Huang^{2†}, Congxiu Ye³, Ling Chen⁴, Yi Liang⁵, Kan Wang^{6*} and Junyan Liu^{7*}

OPEN ACCESS

Edited by:

Xihong Zhao,
Wuhan Institute of Technology, China

Reviewed by:

Hengyi Xu,
Nanchang University, China
Wensen Jiang,
Cedars Sinai Medical Center,
United States
Yuting Tian,
Fujian Agriculture and Forestry
University, China

*Correspondence:

Junyan Liu
jliu81@uthsc.edu
Kan Wang
120384746@qq.com

[†] These authors have contributed
equally to this work

Specialty section:

This article was submitted to
Food Microbiology,
a section of the journal
Frontiers in Microbiology

Received: 23 March 2020

Accepted: 12 May 2020

Published: 16 June 2020

Citation:

Li Y, Huang T-Y, Ye C, Chen L,
Liang Y, Wang K and Liu J (2020)
Formation and Control of the Viable
but Non-culturable State
of Foodborne Pathogen *Escherichia*
coli O157:H7.
Front. Microbiol. 11:1202.
doi: 10.3389/fmicb.2020.01202

¹ Department of Haematology, Guangzhou Women and Children's Medical Center, Guangzhou Medical University, Guangzhou, China, ² Department of Laboratory Medicine, The Second Affiliated Hospital of Shantou University Medical College, Shantou, China, ³ Department of Dermato-Venereology, Third Affiliated Hospital of Sun Yat-sen University, Guangzhou, China, ⁴ School of Food Science and Engineering, Guangdong Province Key Laboratory for Green Processing of Natural Products and Product Safety, South China University of Technology, Guangzhou, China, ⁵ Guangdong Zhongqing Font Biochemical Science and Technology Co. Ltd., Maoming, China, ⁶ Research Center for Translational Medicine, The Second Affiliated Hospital, Medical College of Shantou University, Shantou, China, ⁷ Department of Civil and Environmental Engineering, A. James Clark School of Engineering, University of Maryland, College Park, MD, United States

As a common foodborne pathogen, *Escherichia coli* O157:H7 produces toxins causing serious diseases. However, traditional methods failed in detecting *E. coli* O157:H7 cells in the viable but non-culturable (VBNC) state, which poses a threat to food safety. This study aimed at investigating the formation, control, and detection of the VBNC state of *E. coli* O157:H7. Three factors including medium, salt, and acid concentrations were selected as a single variation. Orthogonal experiments were designed with three factors and four levels, and 16 experimental schemes were used. The formation of the VBNC state was examined by agar plate counting and LIVE/DEAD® BacLight™ bacterial viability kit with fluorescence microscopy. According to the effects of environmental conditions on the formation of the VBNC state of *E. coli* O157:H7, the inhibition on VBNC state formation was investigated. In addition, *E. coli* in the VBNC state in food samples (crystal cake) was detected by propidium monoazide–polymerase chain reaction (PMA-PCR) assays. Acetic acid concentration showed the most impact on VBNC formation of *E. coli* O157:H7, followed by medium and salt concentration. The addition of 1.0% acetic acid could directly kill *E. coli* O157:H7 and eliminate its VBNC formation. In crystal cake, 25, 50, or 100% medium with 1.0% acetic acid could inhibit VBNC state formation and kill *E. coli* O157:H7 within 3 days. The VBNC cell number was reduced by adding 1.0% acetic acid. PMA-PCR assay could be used to detect *E. coli* VBNC cells in crystal cake with detection limit at 10⁴ CFU/ml. The understanding on the inducing and inhibitory conditions for the VBNC state of *E. coli* O157:H7 in a typical food system, as well as the development of an efficient VBNC cell detection method might aid in the control of VBNC *E. coli* O157:H7 cells in the food industry.

Keywords: *E. coli* O157:H7, VBNC, food system, control, detection

HIGHLIGHTS

- The induction of the VBNC state of *Escherichia coli* by nutritional conditions, acetic acid concentration, and salt concentration was investigated.
- In crystal cake, the VBNC state of *E. coli* could be inhibited by adding 1.0% acetic acid in volume fraction at 4 or -20°C .
- Propidium monoazide–polymerase chain reaction (PMA-PCR) assays could be applied in detection of the VBNC state of *E. coli*.

INTRODUCTION

Escherichia coli is one of the major bacterial contaminants associated with foodborne infections worldwide (Zhao et al., 2010b; Sayad et al., 2016; Bao et al., 2017a,b; Xie et al., 2017a; Liu et al., 2018a,b; Renuka et al., 2018; Xu et al., 2020). Since food safety accident caused by *E. coli* was first reported in the United States in 1982, various reports have been posted in China, the United Kingdom, Japan, Australia, and other countries. In recent years, *E. coli* has gradually developed into a health and safety issue of worldwide concern (Xu et al., 2007, 2008a,b, 2011b, 2016a,b; You et al., 2012; Lin et al., 2016; Miao et al., 2016, 2017a,b, 2018; Zhao et al., 2018a,b). The high incidence rate of *E. coli* in food products underlies the urgent need of appropriate strategies for early detection (Zhao et al., 2010b,c, 2011, 2014, 2018; Wang et al., 2011; Xu et al., 2011c, 2012b; Lin et al., 2017; Miao et al., 2017c; Liu et al., 2019; Miao et al., 2019). *E. coli* O157:H7, capable of producing Shiga toxin or Shiga-like toxin, can cause hemorrhagic colitis and hemolytic uremic syndrome in human beings (Neil et al., 2012). Shiga toxin causes various diseases including bloody diarrhea and severe hemolytic uremic syndrome, leading to kidney failure. *E. coli* O157:H7 is a typical foodborne pathogen, colonizing in food systems and drinking water (Ercumen et al., 2017; Bourelly et al., 2018; Zeinhom et al., 2018).

The standard detection method for foodborne pathogens is agar plate counting (Xu et al., 2008a,b, 2009; 2010; 2011a; 2012a; 2016c; 2017a; 2017b; 2018; Zhong et al., 2013; Zhang et al., 2015; Bao et al., 2017c; Xie et al., 2017b; Jia et al., 2018; Wen et al., 2020). However, this method fails in detecting viable but non-culturable (VBNC) state cells that were first reported in 1982 (Xu et al., 1982). Up to now, 85 types of microorganisms have been found to enter the VBNC state, including 18 non-pathogenic bacteria and 67 pathogenic bacteria (Ramamurthy et al., 2014). Studies have shown that *E. coli* has the ability to enter the VBNC state (Yaron and Matthews, 2002; Zhang et al., 2015; Liu et al., 2017b; Afari et al., 2019). VBNC cells differ from normal cells in both physiology and morphology. However, VBNC cells acquire high ATP concentrations (Lindback et al., 2010) and metabolic activity based on the expression of certain genes (Yaron and Matthews, 2002).

Bacteria in the VBNC state fail to form colonies in routine detection agar plates under certain environmental stresses. However, these cells have food spoilage and pathogenic capacity (Liu et al., 2017b). Factors including adverse nutrition levels,

temperatures, and osmotic pressures, which are frequently encountered during food processing and storage environments, have been reported to induce bacteria entering the VBNC state. With the failure in detection by routine method and the capability in causing food safety problems, the VBNC state of *E. coli* O157:H7 is a major concern in the food industry (Liu et al., 2017b).

Crystal cake is a traditional Chinese snack that has the characteristics of rich nutrition. Its rich nutrients and sufficient water make it a natural medium for various pathogenic bacteria and spoilage bacteria, including *E. coli*. In this study, crystal cake was applied as a representative food system to study the formation, control, and detection of the VBNC state of *E. coli* O157:H7 under food processing and storage conditions.

MATERIALS AND METHODS

Cultivation of *E. coli* O157:H7

Escherichia coli O157:H7 ATCC25922 was stored at -80°C in Luria-Bertani (LB) broth containing 20% (v/v) glycerol. It was streaked on LB agar plate and grown at 37°C for 24 h. Then, a single colony was inoculated into 2 ml of LB broth and incubated at 37°C for 12 h using a shaker incubator set at 150 r/min. The bacteria suspension was diluted 1:100 in fresh medium and cultured for 4 h to the log phase upon further experiments.

Induction of the VBNC State

According to the optimal culture conditions of *E. coli* O157:H7, and the principle of reverse adjustment, conditions that are unfavorable to bacterial growth were selected as candidate factors to induce the VBNC state. Three factors including nutritional state, salt concentration, and acidity were taken as a single variable. To investigate possible VBNC induction conditions, three factors and four levels of orthogonal experiments were designed, and 16 protocols (Table 1) were applied. Log phase cells were centrifuged for 10 min at 5000 r/min and the pellet was washed once with $1 \times$ phosphate buffer solution and then resuspended in the induced solution. The initial concentration of the bacterial solution was diluted to approximately 10^7 CFU/ml. To avoid the effects of repeated freezing and thawing, the bacterial suspension under each condition was mixed and divided into multiple 1.5-ml centrifuge tubes, followed by induction in refrigerators at 4 and -20°C , respectively.

Determination of Culturable Cell Number During Storage

The culturable cell number in each of the VBNC inducing bacterial culture was determined every 3 days by a plate counting method. Briefly, the culture of *E. coli* O157:H7 was serially diluted in 0.9% NaCl, spread on LB agar plates, and incubated at 37°C for 24 h. When the culturable number is 1 CFU/ml, the cells were considered non-culturable and possibly enter the VBNC state (Piao et al., 2019).

Determination of Viable Cell Number

To determine if the non-culturable cells are in the VBNC state after exposure to the respective treatment conditions, the

TABLE 1 | The experimental methods of orthogonal array design of VBNC induction of *E. coli* O157:H7.

Protocol number	LB medium concentration (%)	NaCl concentration (m/v) (%)	Acetic acid concentration (v/v) (%)
1	0	0.9	0
2	25	0.9	0.3
3	50	0.9	0.7
4	100	0.9	1
5	25	5	0
6	0	5	0.3
7	100	5	0.7
8	50	5	1
9	50	10	0
10	100	10	0.3
11	0	10	0.7
12	25	10	1
13	100	15	0
14	50	15	0.3
15	25	15	0.7
16	0	15	1

TABLE 2 | Inhibition assay of acidity on the formation of VBNC state of *E. coli* O157:H7.

Protocol number	LB medium concentration (%)	NaCl concentration (m/v) (%)	Acetic acid concentration (v/v) (%)
1	100	10	0.7
2			1
3	100	15	0.7
4			1
5	50	15	0.7
6			1

LIVE/DEAD® BacLight™ bacterial viability kit (Thermo Fisher Scientific, China) was used. Five hundred microliters of the non-culturable bacterial cell sample was centrifuged at 5000 r/min for 15 min, washed with saline twice, and resuspended in saline. Subsequently, 1.5 µl of SYTO 9 dye and 1.5 µl of propidium iodide were added to the sample, followed by mixing and 30 min incubation in the dark. After incubation, 5-µl cells were captured between a slide and a coverslip and used for fluorescence microscopy. The appearance of green cells indicates the existence of VBNC cells.

Inhibition of VBNC State by Acidity and Nutritional Conditions

According to the VBNC state induction process, appropriate conditions were selected to inhibit the formation of the VBNC state. The configured medium was resuspended, and the initial concentration of *E. coli* O157:H7 was adjusted to 10⁷ CFU/ml. The bacterial solution with a volume of 30 ml was stored at 4 and −20°C, respectively. The number of cultivable bacteria was measured by plate counting every 3 days (Tables 2, 3).

TABLE 3 | Inhibition assay of nutritional status on the formation of VBNC state of *E. coli* O157:H7.

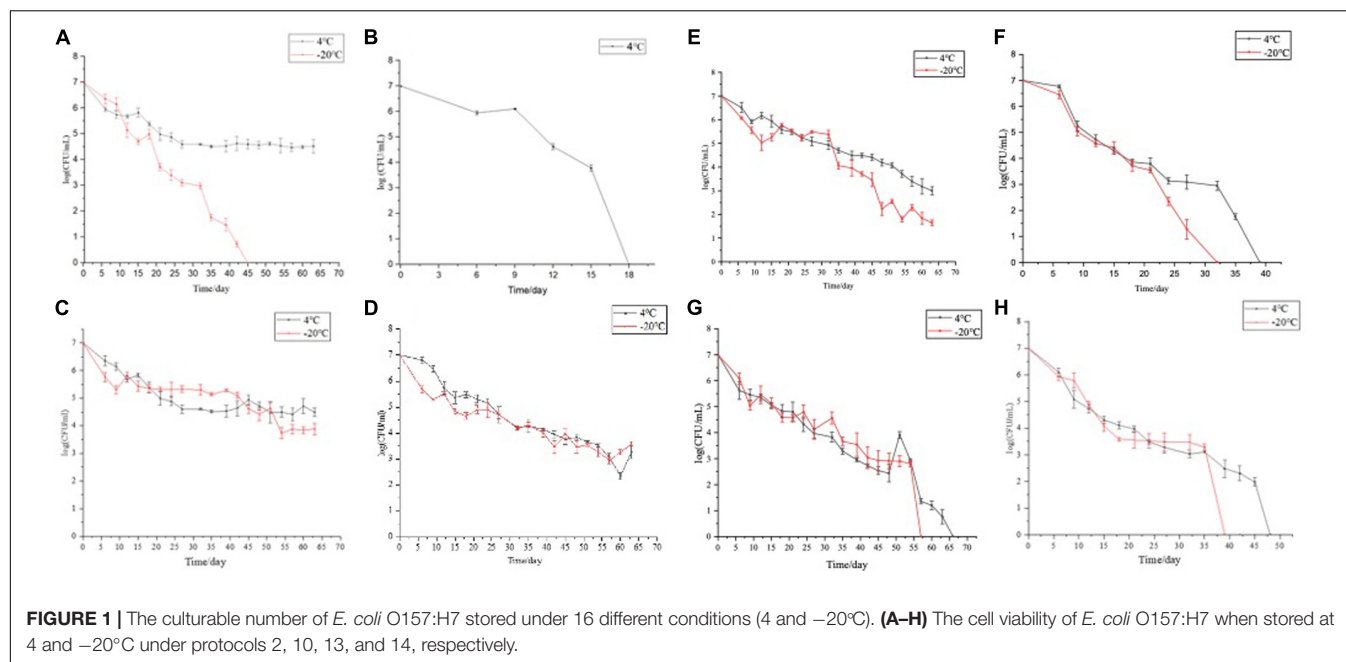
Protocol number	LB medium concentration (%)	NaCl concentration (m/v) (%)	Acetic acid concentration (v/v) (%)
1	0	10	0.3
2	25		
3	0	15	0
4	25		
5	0	15	0.3
6	25		

Elimination of the VBNC State in Crystal Cake

According to the National Food Safety standards (GB4789.3-2016) in China, 25 g of crystal cake was added to 225 ml of saline, and the concentration of this medium was determined to be 100, 25, and 50% of the food sample culture medium and is configured by dilution and used after autoclaving. Subsequently, *E. coli* O157:H7 was cultured to the logarithmic phase and centrifuged at 4°C, the supernatant was discarded, and the suspension was resuspended three times with physiological saline. The bacterial cells were resuspended using the sterilized food sample medium, and the concentrations of *E. coli* O157:H7 were adjusted to 10⁷ CFU/ml, respectively, and a sterile acetic acid solution was added to fix the volume fraction of acetic acid to 1.0%. The induction solution was stored at 4°C, and the culturable number and activity were detected by a plate method combined with a LIVE/DEAD® BacLight™ bacterial viability kit.

PMA-PCR Assays

Twenty-five grams of crystal cake was mixed with 225 ml of physiological saline and sterilized, and *E. coli* in the VBNC state was added. Bacterial suspensions with initial concentrations of 10⁶, 10⁵, 10⁴, 10³, 10², and 10 CFU/ml were obtained. Five hundred microliters of the bacteria suspension was added to a 1.5-ml centrifuge tube, and the PMA working solution was added to a final concentration of 5 µg/ml (to distinguish between the VBNC state and dead cells). After mixing, the samples were kept at room temperature for 10 min in the dark. Subsequently, the centrifuge tube was placed on ice, and 15 cm away from a 650 W halogen lamp for 5 min to complete the binding of PMA and DNA. The PMA-DNA was centrifuged at 10,000 r/min for 5 min, and the supernatant was discarded. DNA was then extracted using a bacterial group DNA extraction kit (Dongsheng Biotech, Guangzhou). The extracted DNA was detected by PCR. PCR assay was performed in a 25-µl volume and with 0.6 µM primers (*rfbE*-F: TTGGCATCGTGTGGACAGGGTAGGACCGCAGAGGAAAG A; *rfbE*-R: TGGGACAGGTGTGCTACGGTTTCCACGCC AACCAAGATC). The thermal profile for PCR mixtures was 94°C for 5 min, followed by 30 cycles of 94°C for 30 s, 52°C for 60 s, and 72°C for 90 s and a final extension cycle at 72°C for 7 min. The amplified products (5 µl/well) were analyzed by gel electrophoresis in 2% agarose gels and stained with ethidium



bromide for 10 min. A negative control was included using sterile water instead of culture or DNA template.

RESULTS AND DISCUSSION

Formation of the VBNC State

To induce the formation of the VBNC state, 16 induction solutions were applied (Table 1). In induction solution 1, when stored at 4°C , the culturable cell number of *E. coli* O157:H7 was reduced to 5×10^4 CFU/ml in 66 days. When stored at -20°C , the culturable cell number of *E. coli* O157:H7 dropped to 0 in 3 days (Figure 1A). In induction solution 2, the number of culturable cells reduced to 0 after 18 days of storage at 4°C , and the number of culturable cells reduced to 0 within 3 days of storage at -20°C (Figure 1B). In induction solution 10, the number of culturable cells reduced to 0 after storing at 4 and -20°C for 39 and 33 days, respectively (Figure 1F). In induction solution 13, the culturable cell number reduced to 0 in 48 and 39 days of storage at 4 and -20°C , respectively (Figure 1G). In induction solution 14, the culturable cell number reduced to 0 in 57 and 66 days when stored at 4 and -20°C , respectively (Figure 1H). In induction solution 5, 7, and 9, although with a downtrend within 66 days, the number of culturable cells did not decrease to 0 (Figures 1C–E). In addition, in induction solutions 3, 4, 6, 8, 11, 12, 15, and 16, the number of culturable cells of *E. coli* O157:H7 reduced to 0 in 3 days.

For the induction solutions that were capable of inducing the culturable cell number of *E. coli* O157:H7 to 0 (Table 4), the existence of viable cells was determined. When the *E. coli* O157:H7 culture in induction solution 2 was stored at 4°C for 18 days, the cells were all dead, indicating that *E. coli* O157:H7 did not enter the VBNC state (Figure 2). The fluorescence results of *E. coli* O157:H7 in induction solutions 1, 10, 13, and 14 showed

that both dead and viable cells were detected, indicating that *E. coli* O157:H7 entered the VBNC state under these conditions.

Factors Affecting the Survival of *E. coli* O157:H7 Cells

In the 16 induction solutions, factors including salt, acetic acid, and medium concentrations were applied and analyzed on the effect on the survival of *E. coli* O157:H7 cells. First, the effect of salt and acid concentrations on the survival of *E. coli* O157:H7 cells was investigated. In induction solutions 3, 8, 9, and 14, the medium concentration is 50%. In induction solutions 3 (acid: 0.7%, salt: 0.9%) and 8 (acid: 1%, salt: 5%), the culturable cell number of *E. coli* O157:H7 reduced to 0 in 3 days. However, in induction solutions 9 (acid: 0, salt: 10%) and 14 (acid: 0.3%, salt: 15%), *E. coli* O157:H7 cells survived for more than 57 days. Especially in induction solution 9, the *E. coli* O157:H7 cells

TABLE 4 | The time of culturable number of *E. coli* O157:H7 decreased to 0 stored at different methods.

Protocol number	4°C	−20°C	Protocol number	4°C	−20°C
1	+	45 days	9	+	+
2	18 days	/	10	39 days	33 days
3	/	/	11	/	/
4	/	/	12	/	/
5	+	+	13	48 days	39 days
6	/	/	14	57 days	66 days
7	+	+	15	/	/
8	/	/	16	/	/

“+” stands for *E. coli* is culturable and “/” stands for the number of cultivable *E. coli* in 3 days has dropped to 0.

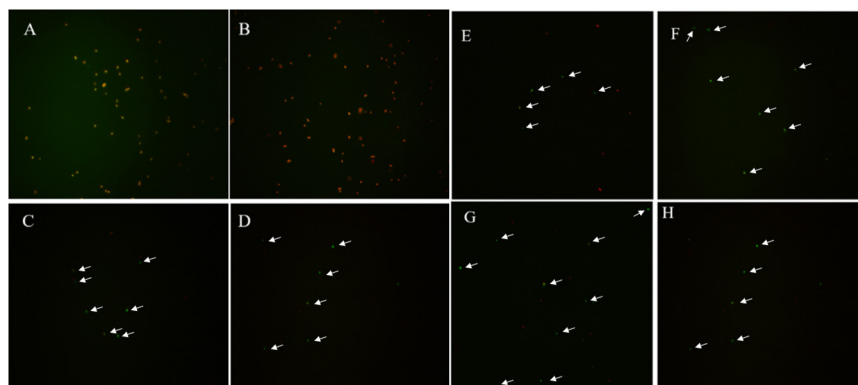


FIGURE 2 | The viability of un-culturable *E. coli* O157:H7 stored at different conditions with fluorescence. (A–H) *E. coli* O157:H7 inoculated in the medium configured according to the method 2, 10, 13, 14, and stored at 4 or -20°C , respectively.

survived for more than 66 days. In induction solutions 4, 10, and 13, the medium concentration is 100%. In induction solution 4 (acid: 1%, salt: 0.9%), *E. coli* O157:H7 all died in 3 days and did not enter the VBNC state. In induction solutions 10 (acid: 0.3%, salt: 10%) and 13 (acid: 0, salt: 15%), *E. coli* O157:H7 cells were able to survive for 33–48 days. These results suggest that the effect of acetic acid concentration on the survival of *E. coli* O157:H7 is stronger than that of salt concentration.

Second, the effect of acid and medium conditions on the survival of *E. coli* O157:H7 cells under a certain salt concentration were investigated. In induction solutions 1, 2, 3, and 4, the salt concentration is 0.9%. In induction solutions 1 (medium: 0, acid: 0) and 2 (medium: 25%, acid: 0.3%), *E. coli* O157:H7 cells survived for more than 66 and 18 days at 4°C , respectively. However, in induction solutions 3 (medium: 50%, acid: 0.7%) and 4 (medium: 100%, acid: 1%), the *E. coli* O157:H7 cells all died in 3 days. It showed the effect of acid on the survival of *E. coli* O157:H7 is stronger than that of nutrients. In addition, when the acid concentration is 1% in induction solutions 4, 8, 12, and 16, *E. coli* O157:H7 cells died in 3 days regardless of the medium and salt concentrations. Especially in induction solution 4 (medium: 100%, acid: 0.9%) with the premium centration of medium and acid, *E. coli* O157:H7 cells still died in 3 days, indicating that acidity has the most significant effect on the survival of *E. coli* O157:H7 cells.

Third, under the same acetic acid concentration, the effects of salt and medium concentrations on the survival of *E. coli* O157:H7 were investigated. In induction solutions 6, 10, and 14, the acetic acid concentration is 0.3%. In induction solution 6 (medium: 0, salt: 5%), *E. coli* O157:H7 cells died within 3 days. However, in induction solutions 10 (medium: 100%, salt: 10%) and 14 (medium: 50%, salt: 15%), although the salt concentration increased, *E. coli* O157:H7 cells were able to survive from 33 to 66 days due to the high medium concentration. It indicated that the increase in the medium concentration eliminated the adverse effect of the increase in salt concentration. Among the factors on the survival of *E. coli* O157:H7, the effect of the medium concentration might be greater than that of the salt concentration.

When the environment changes, porin is crucial for the survival of *E. coli*. The major external protein omp (ompF, ompC) of *E. coli* is regulated by *envZ* (osmotic pressure sensor protein) and *ompR*. Studies have showed that wild-type, *ompF*, and *ompC* mutant strain of *E. coli* can enter the VBNC state under environmental pressure (pH, osmotic pressure, and starvation stress conditions), but in the *envZ* mutant strain, they cannot enter the VBNC state. This shows that the *envZ* mutant strains cannot sense changes in the external environment. When the strains are exposed to adverse conditions, they cannot enter the VBNC state (Pienaar et al., 2016). The expression of (p) ppGpp (guanosine pentaphosphate or guanosine tetraphosphate) synthetic genes *relA* and *spoT* are identified to upregulate in the VBNC state of *E. coli* O157:H7 (Magnusson et al., 2005; Mishra et al., 2012). Compared with normal strains, mutants that failed to synthesize (p) ppGpp lost culturability more quickly, and their ability to enter the VBNC state was significantly reduced. When (p) ppGpp was overexpressed, the number of VBNC cells was significantly increased (Boaretti et al., 2003). When bacteria suffered from amino acid starvation, the expression of *RelA* or *SpoT* increased. (p) ppGpp synthesis increased and degradation decreased. In addition, exopolyphosphatase (PPX) was degraded by (p) ppGpp of polyphosphates (Ayrapetyan et al., 2018).

Effects of Acidity and Nutrition on Formation of the VBNC State

Among the factors affecting the survival of *E. coli* O157:H7, acetic acid concentration plays a major role, followed by medium and salt concentrations. Considering the actual situation in the food system and in the process of food processing, exploring the concentration of acetic acid and culture medium to control the normal state of *E. coli* O157:H7 and VBNC is meaningful.

When the acetic acid concentration is 1%, the *E. coli* O157:H7 cells died within 3 days in induction solutions 3 (medium: 100%, salt: 10%), 4 (medium: 100%, salt: 15%), and 6 (medium: 50%, salt: 15%). When the acetic acid concentration is 0.7%, *E. coli* O157:H7 could survive in induction solutions 1 (medium: 100%, salt: 10%) and 3 (medium: 100%, salt: 15%). In induction solution

TABLE 5 | Inhibition of acidity on the formation of VBNC state of *E. coli* O157:H7.

Protocol number	Culturable		Viable	
	4°C	−20°C	4°C	−20°C
1	+	+	ND	ND
2	/	/	—	—
3	+	+	ND	ND
4	/	/	—	—
5	/	/	—	—
6	/	/	—	—

“+” stands for *E. coli* is culturable, “/” stands for *E. coli* is not culturable, “—” stands for *E. coli* is not active, and “ND” stands for *E. coli* activity not detected.

TABLE 6 | Inhibition of nutritional status on the formation of VBNC state of *E. coli* O157:H7.

Protocol number	Culturable		Viable	
	4°C	−20°C	4°C	−20°C
1	/	/	—	—
2	+	+	ND	ND
3	+	+	ND	ND
4	+	+	ND	ND
5	/	/	—	—
6	+	+	ND	ND

“+” stands for *E. coli* is culturable, “/” stands for *E. coli* is not culturable, “—” stands for *E. coli* is not active, and “ND” stands for *E. coli* activity not detected.

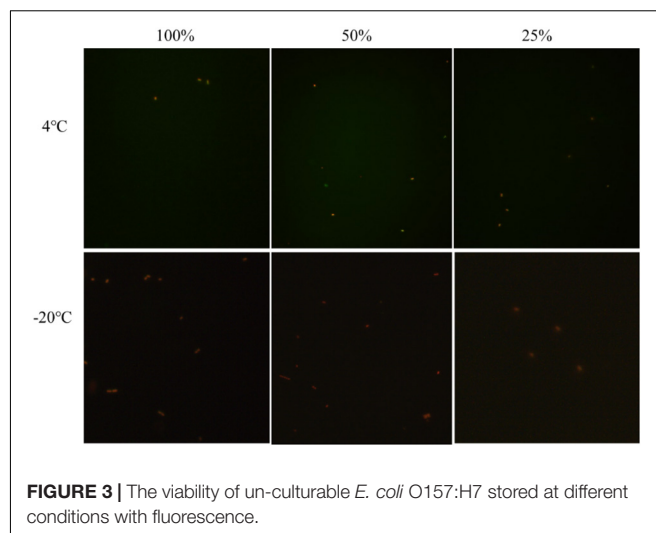
5 (medium: 50%, salt: 15%), *E. coli* O157:H7 cells died within 3 days. When the medium concentration is higher than 50%, treatment with 1.0% acetic acid directly killed *E. coli* O157:H7 without entering the VBNC state (Table 5).

When the medium concentration is 25%, *E. coli* O157:H7 cells survived more than 3 days in induction solutions 2 (salt: 10%, acid: 0.3%), 4 (salt: 15%, acid: 0), and 6 (salt: 15%, acid: 0.3). When the medium concentration is 0, in induction solutions 1 (salt: 10%, acid: 0.3%) and 5 (salt: 15%, acid: 0.3%), the number of culturable and viable cells was both 0 in 3 days. In induction solution 3 (salt: 15%, acid: 0), *E. coli* O157:H7 cells were able to survive for more than 3 days. Under weak acid and high salt conditions, the formation of the VBNC state of *E. coli* O157:H7 was controlled by changing the nutritional condition (Table 6).

In induction solutions 2, 3, 4, and 6, the culturable cell number of *E. coli* O157:H7 did not decrease to 0 in 3 days. However, the culturable cell numbers of *E. coli* O157:H7 reduced to 0 after storing at 4 and −20°C for 3 days in induction solutions 1 and 5, and the cells were not viable. Thus, changing the acid concentration with cold storage might be efficient to control the formation of the VBNC state of *E. coli* O157:H7.

Elimination of the VBNC State in Crystal Cake

In the crystal cake food system with 100, 50, and 25% nutrient concentrations and 1.0% acetic acid, the culturable cell numbers of *E. coli* O157:H7 were 0 after storing at 4 and −20°C for 3 days. The results of fluorescence microscopy showed that all the *E. coli*

**FIGURE 3 |** The viability of un-culturable *E. coli* O157:H7 stored at different conditions with fluorescence.

O157:H7 cells died, suggesting *E. coli* O157:H7 was not capable of entering into the VBNC state under these conditions (Figure 3). In the food system, without affecting the flavor and quality of the food, the normal and the VBNC state of *E. coli* O157:H7 was controlled and eliminated by adding 1% acetic acid.

The foodborne microorganisms in the VBNC state have food spoilage ability. Compared with normal state, VBNC state cells have reduced metabolic activity and increased resistance of the cell wall to external environmental stress, including high concentrations of antibiotics, heavy metal ions, high temperature, high salt, and higher acidity (Ayrapetyan and Oliver, 2016; Shekar et al., 2017; Schottroff et al., 2018). Due to the presence of resistance, *E. coli* O157:H7 in the VBNC state is more difficult to be completely eliminated. Under favorable conditions, *E. coli* O157:H7 in the VBNC state might be able to overcome this inactive state and become active again, thus being able to reproduce in the food system. During the processing of crystal cake, the surface of the processing equipment and the inside of the pipeline should be cleaned in time to ensure no residual nutrients, thereby inhibiting the survival of *E. coli* O157:H7. In addition, combined with a certain concentration of acetic acid treatment equipment surface (1.0% acetic acid), it ensures the elimination of *E. coli* O157:H7 and its VBNC state and avoid potential food safety risks.

Detection of the VBNC State of *E. coli* in Crystal Cake

The risk of food safety issues can be partially reduced by the efficient detection of the VBNC state of *E. coli* in food system. Propidium monoazide (PMA) is a photoreactive DNA-binding dye. Dead microorganisms lose their capability to keep their membranes intact, which leaves the “naked” DNA in the cytosol ready to react with PMA. DNA of living organisms are not exposed to the PMA, as they have a complete cell membrane. DNA extraction and PCR amplification of PMA-treated samples can effectively detect bacteria in the VBNC state. The detection limit was determined by detecting different concentrations of *E. coli* O157:H7 in the VBNC state. In this study, the detection

limit of the VBNC state *E. coli* O157 in the crystal cake food system using PMA–polymerase chain reaction (PMA-PCR) was 10^4 CFU/ml, which can effectively avoid the potential threat brought by VBNC state bacteria.

CONCLUSION

The effect of external environmental conditions on the formation of the VBNC state of *E. coli* O157:H7 was as follows: acidity > nutritional state > salt concentration. When the nutrient concentration is higher than 50%, *E. coli* O157:H7 was killed by adding 1.0% acetic acid. In the crystal cake system, when the nutrient concentration is 25, 50, and 100%, *E. coli* O157:H7 cells died in 3 days by adding 1.0% acetic acid with no VBNC cells identified. In the food system, the VBNC state formation of *E. coli* O157:H7 was inhibited by adding 1.0% acetic acid. In addition, PMA-PCR assays can be utilized in the detection of the VBNC state of *E. coli* in the food system.

REFERENCES

- Afari, G. K., Liu, H., and Hung, Y. (2019). The effect of produce washing using electrolyzed water on the induction of the viable but non-culturable (VBNC) state in *Listeria monocytogenes* and *Escherichia coli* O157:H7. *LWT Food Sci. Technol.* 110, 275–282. doi: 10.1016/j.lwt.2019.04.089
- Ayrappetyan, M., and Oliver, J. D. (2016). The viable but non-culturable state and its relevance in food safety. *Curr. Opin. Food Sci.* 8, 127–133. doi: 10.1016/j.cofs.2016.04.010
- Ayrappetyan, M., Williams, T., and Oliver, J. D. (2018). Relationship between the viable but nonculturable state and antibiotic persister cells. *J. Bacteriol.* 200:e0249–18.
- Bao, X., Jia, X., Chen, L., Peters, B. M., Lin, C., Chen, D., et al. (2017a). Effect of polymyxin resistance (pmr) on biofilm formation of *Cronobacter sakazakii*. *Microb. Pathogen.* 106, 16–19. doi: 10.1016/j.micpath.2016.12.012
- Bao, X., Yang, L., Chen, L., Li, B., Li, L., Li, Y., et al. (2017b). Analysis on pathogenic and virulent characteristics of the *Cronobacter sakazakii* strain BAA-894 by whole genome sequencing and its demonstration in basic biology science. *Microb. Pathogen.* 109, 280–286. doi: 10.1016/j.micpath.2017.05.030
- Bao, X., Yang, L., Chen, L., Li, B., Li, L., Li, Y., et al. (2017c). Virulent and pathogenic features on the *Cronobacter sakazakii* polymyxin resistant pmr mutant strain s-3. *Microb. Pathogen.* 110, 359–364. doi: 10.1016/j.micpath.2017.07.022
- Boaretti, M., Lleo, M. M., Bonato, B., Signoretto, C., and Canepari, P. (2003). Involvement of rpoS in the survival of *Escherichia coli* in the viable but non-culturable state. *Environ. Microbiol.* 5, 986–996. doi: 10.1046/j.1462-2920.2003.00497.x
- Bourelly, C., Chauvin, C., Jouy, E., Cazeau, G., Jarrige, N., Leblond, A., et al. (2018). Comparative epidemiology of *E. coli* resistance to third-generation cephalosporins in diseased food-producing animals. *Vet. Microbiol.* 223, 72–78. doi: 10.1016/j.vetmic.2018.07.025
- Ercumen, A., Pickering, A. J., Kwong, L. H., Arnold, B. F., Parvez, S. M., Alam, M., et al. (2017). Animal feces contribute to domestic fecal contamination: evidence from *E-coli* measured in water, hands, food, flies, and soil in Bangladesh. *Environ. Sci. Technol.* 51, 8725–8734. doi: 10.1021/acs.est.7b01710
- Jia, X., Hua, J., Liu, L., Xu, Z., and Li, Y. (2018). Phenotypic characterization of pathogenic *Cronobacter* spp. strains. *Microb. Pathogen.* 121, 232–237. doi: 10.1016/j.micpath.2018.05.033
- Lin, S., Li, L., Li, B., Zhao, X., Lin, C., Deng, Y., et al. (2016). Development and evaluation of quantitative detection of n-epsilon-carboxymethyl-lysine in *Staphylococcus aureus* biofilm by LC-MS method. *Basic Clin. Pharmacol.* 118, 33–33.
- Lin, S., Yang, L., Chen, G., Li, B., Chen, D., Li, L., et al. (2017). Pathogenic features and characteristics of food borne pathogens biofilm: biomass, viability and matrix. *Microb. Pathogen.* 111, 285–291. doi: 10.1016/j.micpath.2017.08.005
- Lindback, T., Rottenberg, M. E., Roche, S. M., and Rorvik, L. M. (2010). The ability to enter into an avirulent viable but non-culturable (VBNC) form is widespread among *Listeria monocytogenes* isolates from salmon, patients and environment. *Vet. Res.* 41:8.
- Liu, J., Li, L., Li, B., Peters, B. M., Deng, Y., Xu, Z., et al. (2017a). Study on spoilage capability and VBNC state formation and recovery of *Lactobacillus plantarum*. *Microb. Pathogen.* 110, 257–261. doi: 10.1016/j.micpath.2017.06.044
- Liu, J., Zhou, R., Li, L., Peters, B. M., Li, B., Lin, C., et al. (2017b). Viable but non-culturable state and toxin gene expression of enterohemorrhagic *Escherichia coli* O157 under cryopreservation. *Res. Microbiol.* 168, 188–193. doi: 10.1016/j.resmic.2016.11.002
- Liu, L., Lu, Z., Li, L., Li, B., Zhang, X., and Xu, Z. (2018a). Physical relation and mechanism of ultrasonic bactericidal activity on pathogenic *E. coli* with WPI. *Microb. Pathogen.* 117, 73–79. doi: 10.1016/j.micpath.2018.02.007
- Liu, L., Xu, R., Li, L., Li, B., Zhang, X., and Xu, Z. (2018b). Correlation and in vitro mechanism of bactericidal activity on *E. coli* with whey protein isolate during ultrasonic treatment. *Microb. Pathogen.* 115, 154–158. doi: 10.1016/j.micpath.2017.12.062
- Liu, L., Ye, C., Soteyome, T., Zhao, X., Xia, J., Xu, W., et al. (2019). Inhibitory effects of two types of food additives on biofilm formation by foodborne pathogens. *Microbiologyopen* 8:e00853.
- Magnusson, L. U., Farewell, A., and Nystrom, T. (2005). ppGpp: a global regulator in *Escherichia coli*. *Trends. Microbiol.* 13, 236–242. doi: 10.1016/j.tim.2005.03.008
- Miao, J., Chen, L., Wang, J., Wang, W., Chen, D., Li, L., et al. (2017a). Current methodologies on genotyping for nosocomial pathogen methicillin-resistant *Staphylococcus aureus* (MRSA). *Microb. Pathogen.* 107, 17–28. doi: 10.1016/j.micpath.2017.03.010
- Miao, J., Chen, L., Wang, J., Wang, W., Chen, D., Li, L., et al. (2017b). Evaluation and application of molecular genotyping on nosocomial pathogen-methicillin-resistant *Staphylococcus aureus* isolates in Guangzhou representative of Southern China. *Microb. Pathogen.* 107, 397–403. doi: 10.1016/j.micpath.2017.04.016
- Miao, J., Liang, Y., Chen, L., Wang, W., Wang, J., Li, B., et al. (2017c). Formation and development of *Staphylococcus* biofilm: with focus on food safety. *J. Food Saf.* 7:e012358.
- Miao, J., Lin, S., Soteyome, T., Peters, B. M., Li, Y., Chen, H., et al. (2019). Biofilm formation of *Staphylococcus aureus* under food heat processing conditions: first report on cml production within biofilm. *Sci. Rep.* 9:1331.
- Miao, J., Peters, B. M., Li, L., Li, B., Zhao, X., Xu, Z., et al. (2016). Evaluation of ERIC-PCR for fingerprinting methicillin-resistant *Staphylococcus aureus* strains. *Basic Clin. Pharmacol.* 118, 33–33.

DATA AVAILABILITY STATEMENT

All datasets presented in this study are included in the article/supplementary material.

AUTHOR CONTRIBUTIONS

JL and KW conceived the study and participated in its design and coordination. YML and T-YH performed the experimental work. CY and LC analyzed the data. YL and JL prepared and revised this manuscript. All authors reviewed and approved the final manuscript.

FUNDING

Fundamental Research Funds for the Central Universities (D2191310).

- Miao, J., Wang, W., Xu, W., Su, J., Li, L., Li, B., et al. (2018). The fingerprint mapping and genotyping systems application on methicillin-resistant *Staphylococcus aureus*. *Microb. Pathogen.* 125, 246–251. doi: 10.1016/j.micpath.2018.09.031
- Mishra, A., Taneja, N., and Sharma, M. (2012). Viability kinetics, induction, resuscitation and quantitative real-time polymerase chain reaction analyses of viable but nonculturable *Vibrio cholerae* O1 in freshwater microcosm. *J. Appl. Microbiol.* 112, 945–953. doi: 10.1111/j.1365-2672.2012.05255.x
- Neil, K. P., Biggerstaff, G., MacDonald, J. K., Trees, E., Medus, C., Musser, K. A., et al. (2012). A novel vehicle for transmission of *Escherichia coli* O157:H7 to humans: multistate outbreak of *E. coli* O157:H7 infections associated with consumption of ready-to-bake commercial prepackaged cookie dough—United States, 2009. *Clin. Infect. Dis.* 54, 511–518. doi: 10.1093/cid/cir831
- Piao, M., Li, Y., Wang, Y., Wang, F., Zhen, T., and Deng, Y. (2019). Induction of viable but putatively non-culturable *Lactobacillus acetotolerans* by thermosonication and its. *LWT Food Sci. Technol.* 109, 313–318. doi: 10.1016/j.lwt.2019.04.046
- Pienaar, J. A., Singh, A., and Barnard, T. G. (2016). The viable but non-culturable state in pathogenic *Escherichia coli*: a general review. *Sci. Direct.* 5:e00368.
- Ramamurthy, T., Ghosh, A., Pazhani, G. P., and Shinoda, S. (2014). Current perspectives on viable but non-culturable (VBNC) pathogenic bacteria. *Front. Public Health* 2:103. doi: 10.3389/fpubh.2014.00103
- Renuka, R. M., Achuth, J., Chandan, H. R., Venkataramana, M., and Kadirvelu, K. (2018). A fluorescent dual aptasensor for the rapid and sensitive onsite detection of *E. coli* O157:H7 and its validation in various food matrices. *New J. Chem.* 42, 10807–10817. doi: 10.1039/c8nj00997j
- Sayad, A. A., Ibrahim, F., Uddin, S. M., Pei, K. X., Mohktar, M. S., Madou, M., et al. (2016). A microfluidic lab-on-a-disc integrated loop mediated isothermal amplification for foodborne pathogen detection. *Sens. Actua. B Chem.* 227, 600–609. doi: 10.1016/j.snb.2015.10.116
- Schottroff, F., Froehling, A., Zunabovic, P. M., Krottenthaler, A., and Schlueter, O. (2018). Sublethal injury and viable but non-culturable (VBNC) state in microorganisms during preservation of food and biological materials by non-thermal processes. *Front. Microbiol.* 9:2773. doi: 10.3389/fpubh.2014.02773
- Shekar, A., Babu, L., Ramlal, S., Sripathy, M. H., and Batra, H. (2017). Selective and concurrent detection of viable *Salmonella* spp., *E. coli*, *Staphylococcus aureus*, *E. coli* O157:H7, and *Shigella* spp., in low moisture food products by PMA-mPCR assay with internal amplification control. *LWT Food Sci. Technol.* 86, 586–593. doi: 10.1016/j.lwt.2017.08.023
- Wang, L., Zhao, X., Chu, J., Li, Y., Li, Y., Li, C., et al. (2011). Application of an improved loop-mediated isothermal amplification detection of *Vibrio parahaemolyticus* from various seafood samples. *AFR J. Microbiol. Res.* 5, 5765–5771.
- Wen, S., Feng, D., Chen, D., Yang, L., and Xu, Z. (2020). Molecular epidemiology and evolution of *Haemophilus influenzae*. *Infect. Genet. Evol.* 80:104205. doi: 10.1016/j.meegid.2020.104205
- Xie, J., Peters, B. M., Li, B., Li, L., Yu, G., Xu, Z., et al. (2017a). Clinical features and antimicrobial resistance profiles of important *Enterobacteriaceae* pathogens in Guangzhou representative of Southern China, 2001–2015. *Microb. Pathogen.* 107, 206–211. doi: 10.1016/j.micpath.2017.03.038
- Xie, J., Yang, L., Peters, B. M., Chen, L., and Chen, D. (2017b). A 16-year retrospective surveillance aerport on the pathogenic features and antimicrobial susceptibility of *Pseudomonas aeruginosa* isolates from FAHJU in Guangzhou representative of Southern China. *Microb. Pathogen.* 110, 37–41. doi: 10.1016/j.micpath.2017.06.018
- Xu, H. S., Roberts, N., Singleton, F. L., Attwell, R. W., Grimes, D. J., and Colwel, R. R. (1982). Survival and viability of nonculturable *Escherichia coli* and *Vibrio cholerae* in the estuarine and marine environment. *Microb. Ecol.* 8, 313–323.
- Xu, Z., Gui, Z., Zhao, X., Zhang, Y., He, X., Li, W., et al. (2012a). Expression and purification of gp41-gp36 fusion protein and application in serological screening assay of HIV-1 and HIV-2. *AFR J. Microbiol. Res.* 6, 6295–6299.
- Xu, Z., Li, L., Chu, J., Peters, B. M., Harris, M. L., Li, B., et al. (2012b). Development and application of loop-mediated isothermal amplification assays on rapid detection of various types of staphylococci strains. *Food Res. Int.* 47, 166–173. doi: 10.1016/j.foodres.2011.04.042
- Xu, Z., Hou, Y., Peters, B. M., Chen, D., Li, B., Li, L., et al. (2016a). Chromogenic media for MRSA diagnostics. *Mol. Biol. Rep.* 43, 1205–1212. doi: 10.1007/s11033-016-4062-3
- Xu, Z., Hou, Y., Qin, D., Liu, X., Li, B., Li, L., et al. (2016b). Evaluation of current methodologies for rapid identification of methicillin-resistant *Staphylococcus aureus* strains. *Basic Clin. Pharmacol.* 118:33.
- Xu, Z., Liang, Y., Lin, S., Chen, D., Li, B., Li, L., et al. (2016c). Crystal violet and XTT assays on *Staphylococcus aureus* biofilm quantification. *Curr. Microbiol.* 73, 474–482. doi: 10.1007/s00284-016-1081-1
- Xu, Z., Li, L., Shirliff, M. E., Alam, M. J., Yamasaki, S., and Shi, L. (2009). Occurrence and characteristics of class 1 and 2 integrons in *Pseudomonas aeruginosa* isolates from patients in Southern China. *J. Clin. Microbiol.* 47, 230–234. doi: 10.1128/jcm.02027-08
- Xu, Z., Li, L., Shi, L., and Shirliff, M. E. (2011a). Class 1 integron in staphylococci. *Mol. Biol. Rep.* 38, 5261–5279. doi: 10.1007/s11033-011-0676-7
- Xu, Z., Li, L., Shirliff, M. E., Peters, B. M., Li, B., Peng, Y., et al. (2011b). Resistance class 1 integron in clinical methicillin-resistant *Staphylococcus aureus* strains in southern China, 2001–2006. *Clin. Microbiol. Infect.* 17, 714–718. doi: 10.1111/j.1469-0691.2010.03379.x
- Xu, Z., Li, L., Zhao, X., Chu, J., Li, B., Shi, L., et al. (2011c). Development and application of a novel multiplex polymerase chain reaction (PCR) assay for rapid detection of various types of staphylococci strains. *AFR J. Microbiol. Res.* 5, 1869–1873.
- Xu, Z., Li, L., Shirliff, M. E., Peters, B. M., Peng, Y., Alam, M. J., et al. (2010). First report of class 2 integron in clinical *Enterococcus faecalis* and class 1 integron in *Enterococcus faecium* in South China. *Diagn. Micro. Infect. Dis.* 68, 315–317. doi: 10.1016/j.diagmicrobio.2010.05.014
- Xu, Z., Luo, Y., Mao, Y., Peng, R., Chen, J., Soteyome, T., et al. (2020). Spoilage lactic acid bacteria in the brewing industry. *J. Microbiol. Biotech.* doi: 10.4014/jmb.1908.08069 [Epub ahead of print].
- Xu, Z., Li, L., Alam, M. J., Zhang, L., Yamasaki, S., and Shi, L. (2008a). First confirmation of integron-bearing methicillin-resistant *Staphylococcus aureus*. *Curr. Microbiol.* 57, 264–268. doi: 10.1007/s00284-008-9187-8
- Xu, Z., Shi, L., Alam, M. J., Li, L., and Yamasaki, S. (2008b). Integron-bearing methicillin-resistant coagulase-negative staphylococci in South China, 2001–2004. *FEMS Microbiol. Lett.* 278, 223–230. doi: 10.1111/j.1574-6968.2007.00994.x
- Xu, Z., Shi, L., Zhang, C., Zhang, L., Li, X., Cao, Y., et al. (2007). Nosocomial infection caused by class 1 integron-carrying *Staphylococcus aureus* in a hospital in South China. *Clin. Microbiol. Infect.* 13, 980–984. doi: 10.1111/j.1469-0691.2007.01782.x
- Xu, Z., Xie, J., Peters, B. M., Li, B., Li, L., Yu, G., et al. (2017a). Longitudinal surveillance on antibiogram of important Gram-positive pathogens in Southern China, 2001 to 2015. *Microb. Pathogen.* 103, 80–86. doi: 10.1016/j.micpath.2016.11.013
- Xu, Z., Xu, X., Qi, D., Yang, L., Li, B., Li, L., et al. (2017b). Effect of aminoglycosides on the pathogenic characteristics of microbiology. *Microb. Pathogen.* 113, 357–364. doi: 10.1016/j.micpath.2017.08.053
- Xu, Z., Xie, J., Yang, L., Chen, D., Peters, B. M., and Shirliff, M. E. (2018). Complete sequence of pCY-CTX, a plasmid carrying a phage-like region and an ISEcp1-Mediated Tn2 element from *Enterobacter cloacae*. *Microb. Drug Resist.* 24, 307–313. doi: 10.1089/mdr.2017.0146
- Yaron, S., and Matthews, K. R. (2002). A reverse transcriptase-polymerase chain reaction assay for detection of viable *Escherichia coli* O157:H7: investigation of species target genes. *J. Appl. Microbiol.* 92, 633–640. doi: 10.1046/j.1365-2672.2002.01563.x
- You, R., Gui, Z., Xu, Z., Shirliff, M. E., Yu, G., Zhao, X., et al. (2012). Methicillin-resistance *Staphylococcus aureus* detection by an improved rapid PCR assay. *Afr. J. Microbiol. Res.* 6, 7131–7133.
- Zeinhom, M. M. A., Wang, Y., Song, Y., Zhu, M., Lin, Y., and Du, D. (2018). A portable smart-phone device for rapid and sensitive detection of *E. coli* O157:H7 in Yoghurt and Egg. *Biosens. Bioelectron.* 99, 479–485. doi: 10.1016/j.bios.2017.08.002
- Zhang, S., Ye, C., Lin, H., Lv, L., and Yu, X. (2015). UV disinfection induces a vbnc state in *Escherichia coli* and *Pseudomonas aeruginosa*. *Environ. Sci. Technol.* 49, 1721–1728. doi: 10.1021/es505211e
- Zhao, X., Li, M., and Xu, Z. (2018a). Detection of foodborne pathogens by surface enhanced raman spectroscopy. *Front. Microbiol.* 9:1236. doi: 10.3389/fpubh.2014.001236

- Zhao, X., Yu, Z., and Xu, Z. (2018b). Study the features of 57 confirmed CRISPR Loci in 38 strains of *Staphylococcus aureus*. *Front. Microbiol.* 9:1591. doi: 10.3389/fpubh.2014.001591
- Zhao, X., Lin, C., Wang, J., and Oh, D. H. (2014). Advances in rapid detection methods for foodborne pathogens. *J. Microbiol. Biotechnol.* 24, 297–312.
- Zhao, X., Li, Y., Wang, L., You, L., Xu, Z., Li, L., et al. (2010a). Development and application of a loop-mediated isothermal amplification method on rapid detection *Escherichia coli* O157 strains from food samples. *Mol. Biol. Rep.* 37, 2183–2188. doi: 10.1007/s11033-009-9700-6
- Zhao, X., Wang, L., Chu, J., Li, Y., Li, Y., Xu, Z., et al. (2010b). Development and application of a rapid and simple loop-mediated isothermal amplification method for food-borne *Salmonella* detection. *Food Sci. Biotechnol.* 19, 1655–1659. doi: 10.1007/s10068-010-0234-4
- Zhao, X., Wang, L., Chu, J., Li, Y., Li, Y., Xu, Z., et al. (2010c). Rapid detection of vibrio parahaemolyticus strains and virulent factors by loop-mediated isothermal amplification assays. *Food Sci. Biotechnol.* 19, 1191–1197. doi: 10.1007/s10068-010-0170-3
- Zhao, X., Wang, L., Li, Y., Xu, Z., Li, L., He, X., et al. (2011). Development and application of a loop-mediated isothermal amplification method on rapid detection of *Pseudomonas aeruginosa* strains. *World J. Microb. Biot.* 27, 181–184. doi: 10.1007/s11274-010-0429-0
- Zhong, N., Gui, Z., Xu, L., Huang, J., Hu, K., Gao, Y., et al. (2013). Solvent-free enzymatic synthesis of 1, 3-diacylglycerols by direct esterification of glycerol with saturated fatty acids. *Lipids Health Dis.* 12:15.
- Conflict of Interest:** The author YL was employed by Guangdong Zhongqing Font Biochemical Science and Technology Co. Ltd.
- The remaining authors declare that the research was conducted in the absence of any commercial or financial relationships that could be construed as a potential conflict of interest.
- Copyright © 2020 Li, Huang, Ye, Chen, Liang, Wang and Liu. This is an open-access article distributed under the terms of the Creative Commons Attribution License (CC BY). The use, distribution or reproduction in other forums is permitted, provided the original author(s) and the copyright owner(s) are credited and that the original publication in this journal is cited, in accordance with accepted academic practice. No use, distribution or reproduction is permitted which does not comply with these terms.



The Characterization of Two-Component System PmrA/PmrB in *Cronobacter sakazakii*

Jingjing Hua¹, Xiangyin Jia², Liang Zhang^{1*} and Yanyan Li^{3*}

¹ National Engineering Laboratory for Cereal Fermentation Technology, Jiangnan University, Wuxi, China, ² State Key Laboratory of Food Science and Technology, Jiangnan University, Wuxi, China, ³ Key Laboratory of Structural Biology of Zhejiang Province, School of Life Sciences, Westlake University, Hangzhou, China

OPEN ACCESS

Edited by:

Yang Deng,
Qingdao Agricultural University, China

Reviewed by:

Zhongpeng Guo,
Institut National des Sciences
Appliquées de Toulouse (INSA),
France
Lianying Ma,
Guangdong Academy of Science,
China

*Correspondence:

Liang Zhang
zhangl@jiangnan.edu.cn
Yanyan Li
yanyanli1123@hotmail.com

Specialty section:

This article was submitted to
Food Microbiology,
a section of the journal
Frontiers in Microbiology

Received: 17 December 2019

Accepted: 16 April 2020

Published: 17 June 2020

Citation:

Hua J, Jia X, Zhang L and Li Y
(2020) The Characterization
of Two-Component System
PmrA/PmrB in *Cronobacter sakazakii*.
Front. Microbiol. 11:903.
doi: 10.3389/fmicb.2020.00903

Cronobacter sakazakii is an opportunistic Gram-negative pathogen that could cause meningitis and necrotizing enterocolitis. Several Gram-negative bacteria use the PmrA/PmrB system to sense and adapt to environmental change by resistance to cationic antimicrobial peptides of host immune systems. The PmrA/PmrB two-component system regulates several genes to modify LPS structure in the bacterial outer membrane. The role of PmrA/PmrB of *C. sakazakii* has been studied within the current study. The results suggest that PmrA/PmrB plays a crucial role in modifying LPS structure, cationic antimicrobial peptide susceptibility, cell membrane permeability and hydrophobicity, and invading macrophage.

Keywords: PmrA/PmrB two-component system, *Cronobacter sakazakii*, LPS, lipid A, polymyxin B

INTRODUCTION

Cronobacter sakazakii is a Gram-negative pathogen that can be isolated from contaminated infant formula. *C. sakazakii* infection may cause bacteremia, septicemia, necrotizing enterocolitis, and other serious diseases (Chenu and Cox, 2009). Invading the intestinal cells and surviving within macrophage are the main infective characteristics with *C. sakazakii* (Forsythe et al., 2014). The outer membrane protein OmpA and efflux operon gene cluster *cusA*, *cusB*, *cusC*, and *cusR* were previously characterized as the virulence markers that associated with neonatal infections (Jaradat et al., 2014). More regulatory systems and virulence factors need to be identified in *C. sakazakii*.

Lipopolysaccharide (LPS) is the main constituent of the outer leaflet of the outer membrane of Gram-negative bacteria (Raetz and Whitfield, 2002). Lipid A is the biologically active component of LPS, which can be recognized by the innate immune system through TLR4 (Wang et al., 2010). It triggers an inflammatory response with the production of a large number of cytokines and even leads to septic shock or death (Wang B. et al., 2015). In *C. sakazakii*, the backbone of the lipid A general structure is a hexa-acylated β -1', 6'-linked disaccharide of glucosamine, which has phosphate groups at the 1 and 4' positions, 3-hydroxymyristate (3-OH C14:0) at the 2 and 3' positions, and secondary fatty acid derivatives at the 2'b (C14:0) and 3'b (C12:0 or C14:0) positions (Li et al., 2016; Jia et al., 2018). Interestingly, the structure of lipid A can be modified with hydrophobic or hydrophilic groups to adapt to the change of environment. The phosphoethanolamine (pEtN) modification of lipid A was observed in *C. sakazakii* under low-pH conditions in 2016 (Liu et al., 2016). The modification contributes to the bacteria's resistance to antimicrobial

agents and, hence, to influence the ability of the host cell invasion. Currently, the lipid A modification in *C. sakazakii* has not been well characterized, and this might provide important information in terms of understanding the mechanism of bacterial infection and virulence.

Two-component regulatory systems (TCS) are quite important in regulating the virulence determinant of a lot of bacterial pathogens, which consist of sensor kinases and response regulators. The TCS PmrA/PmrB has been identified in a large amount of bacterial species, such as *Yersinia pestis* (Winfield et al., 2005), *Salmonella enterica* (Gunn, 2008), *Escherichia coli* (Hagiwara et al., 2004; Winfield and Groisman, 2004), *Klebsiella pneumonia* (Mitrophanov et al., 2008), *Citrobacter rodentium* (Viau et al., 2011), and *Pseudomonas aeruginosa* (McPhee et al., 2006). The TCS PmrA/PmrB of *Salmonella enterica* serovar Typhimurium encodes products with a sequence similarity to DNA binding response regulators and autophosphorylatable histidine kinases, respectively. It governs resistance to polymyxin B by controlling transcription of the 4-aminoarabinose biosynthetic genes (Wosten and Groisman, 1999). The TCS PmrA/PmrB of *Legionella pneumophila* triggered by acidity has a global effect on gene expression and is required for the intracellular proliferation of *Legionella pneumophila* within human macrophages and protozoa (Al-Khodori et al., 2009). The TCS PmrA/PmrB of *Escherichia coli*, also called the BasS–BasR system, is essential for iron-dependent induction of the *yfbE* operon, which is implicated in the modification of LPSs (Hagiwara et al., 2004). Briefly, PmrA/PmrB is located in the *pmrCAB* operon (Roland et al., 1993) and consists of a response regulator PmrA, a sensor kinase PmrB (Gunn, 2008; Chen and Groisman, 2013) and a pEtN transferase PmrC (Zhou et al., 2001; Lee et al., 2004; Murray et al., 2007). When bacteria lives at low pH, it is important to modify the pEtN of lipid A. The modification of pEtN increases bacteria resistance to cationic antimicrobial peptides (CAMPs) to maintain the bacterial infection in host cells. The effect of the *pmrA* gene in PmrA/PmrB on biofilm formation has been investigated (Bao et al., 2017). The *pmrA* gene may cause inhibition in biofilm formation. During biofilm formation, the *pmrA* gene may function at induction in biomass and inhibition in viability (Bao et al., 2017).

To investigate the role of PmrA/PmrB in *C. sakazakii*, we studied how pH affects *pmrA* on lipid A modification, cationic antimicrobial peptide susceptibility, cell membrane permeability and hydrophobicity, and invading macrophage. A *pmrA*-related mutant was generated under different pH conditions. The effect of environmental pH in lipid A modification is identified, and a *pmrA*-related mutant is generated. The *pmrA* mutant transcriptome is used to study all the gene regulations at the transcription level as compared to the wild type *C. sakazakii*.

MATERIALS AND METHODS

Bacterial Strains and Growth Condition

The related bacterial strains and plasmids in this research are listed in Table 1. *C. sakazakii* strains and other strains were

TABLE 1 | Bacterial strains and plasmids used in this study.

Strains and plasmids	Description	Source
<i>E. coli</i> JM109	<i>recA1 endA1 gyrA96 thi-1 hsdR17 supE44 relA1 Δ(lac-proAB)/F' [traD36 proAB + lac I^q lacZΔM15]</i>	Laboratory strain
BAA894	wild type <i>C. sakazakii</i> ATCC BAA894	Laboratory strain
BAA894 pKD46	BAA894 harboring pKD46	Laboratory strain
BAA894 Δ <i>pmrA</i>	BAA894 mutant with deletion of <i>pmrA</i>	This study
W3110/pWSK29- <i>pmrAB</i>	W3110 harboring pWSK29- <i>pmrAB</i>	This study
W3110/pWSK29- <i>pmrA</i>	W3110 harboring pWSK29- <i>pmrA</i>	This study
BAA894 Δ <i>pmrA</i> /pWSK29- <i>pmrA</i>	BAA894 mutant harboring pWSK29- <i>pmrA</i>	This study
BAA894/pWSK29- <i>pmrAB</i>	BAA894 harboring pWSK29- <i>pmrAB</i>	This study
Plasmids pWSK29	Low copy vector	Cai et al., 2013
pKD46	ParaByβ exo, Repts, AmpR	Datsenko and Wanner, 2000
pKD-Cre	ParaB cre, Repts, AmpR	Datsenko and Wanner, 2000
pBlueScript II SK+	Cloning vector, ColE1, <i>lacZ</i> , AmpR	Stratagene
pDTW202	loxPLE- <i>kan</i> -loxPRE, AmpR, KanR	Datsenko and Wanner, 2000

grown in Luria Bertani media (LB) (Zhang et al., 2018) at 37°C. If required, 30 μg/mL kanamycin or 100 μg/mL ampicillin was included in the medium. Strains containing the plasmid pKD46 that was temperature-sensitive were grown at 30°C, and plasmid pKD46 was cured when cells were grown at the high temperature 42°C.

Construction of *C. sakazakii* BAA894/pWSK29-*pmrA*/p*pmrB*

pmrA and *pmrB* (*ESA_RS16430/16435*) genes were amplified by PCR, taking the genome of *C. sakazakii* BAA894 (Kucerova et al., 2010) as a template. There was an *Xba*I site in the forward primer, and there was an *Xho*I site in the reverse primer. The PCR product was purified, digested with *Xba*I and *Xho*I, and ligated into the digested vector pWSK29. The pWSK29 expression vector that contains the T3/T7 *lacZ* operon on a replicon was induced by isopropyl-β-D-thiogalactopyranoside (IPTG). The constructed plasmid, designated pWSK29-*pmrAB*, was transformed into *C. sakazakii* BAA894, resulting in the strain *C. sakazakii*/pWSK29-*pmrA*.

Construction of *pmrA* Knockout Mutant

To knock out *pmrA* in *C. sakazakii*, the upstream and downstream fragments of the genes were amplified by PCR. *pmrA*-U-F/*pmrA*-U-R primers were used for amplifying the

upstream fragments of *pmrA*. *pmrA*-D-F/*pmrA* -D-R primers were used for obtaining the downstream fragments of *pmrA*. The kan-loxP-F and kan-loxP-R primers were used to amplify the DNA fragment loxP-kan-loxP, which contains the kanamycin resistance gene *kan* from pDTW202. The upstream PCR fragment was digested using *Pst*I and *Bam*HI, and the downstream PCR fragment was digested using *Xho*I and *Xba*I. PCR product of loxP-*kan*-loxP was digested using *Bam*HI and *Xba*I. The digested loxP-*kan*-loxP upstream and downstream fragments of *pmrA* were cloned into pBlueScript II SK, which was digested using *Pst*I and *Xho*I, constructing the plasmid pBS- *pmrA*, carrying the knockout fragment *pmrA* U-loxP-*kan*-loxP-*pmrA* D.

pmrA in the chromosomes of *C. sakazakii* BAA894 was removed by knockout fragment *pmrA* U-loxP-*kan*-loxP-*pmrA* D via Red recombination. First, the plasmid pKD46 was transformed into *C. sakazakii* BAA894; then, taking pBS-*pmrA* as the temple, the knockout fragment *pmrA* U-loxP-*kan*-loxP-*pmrA* D was amplified and transformed into the cells. With the expression of Red enzymes from pKD46, the DNA fragment loxP-*kan*-loxP was used to substitute the *pmrA* gene in the chromosome. Cells were cultured on LB plates with 30 µg/mL kanamycin to select the correct transformants, and the plasmid pKD46 was cured by culturing bacteria at 42°C. After which, the plasmid pKD-Cre was transformed into the bacterial cells, whose loxP recombinase Cre removed the *kan* gene previously inserted into the *C. sakazakii* chromosome. Then, the plasmid pKD-Cre was cured by growing bacteria at 42°C to obtain the *pmrA* deletion mutant strain *C. sakazakii*Δ*pmrA*. **Table 1** shows the plasmids and mutants mentioned in this research.

Isolation of Lipid A

Lipid A of *C. sakazakii* was isolated with the Bligh-Dyer method (Wang X. et al., 2015; Liu et al., 2016). Specifically, overnight culture was inoculated into 250-mL cultures, in which the initial OD₆₀₀ was 0.02, and then cells grew to an OD₆₀₀ of 1.0. All *C. sakazakii* cells were harvested by centrifugation at 4000 rpm for 30 min and then washed with ddH₂O twice. The cell pellet was first suspended with 76 mL of mixture containing chloroform/H₂O/methanol (1:0.8:2 v/v/v). The insoluble debris was then collected and washed with 60 mL mixture. The debris was heated and suspended with 12.5 mM sodium acetate (pH 4.5) by boiling water bath for 30 min. The suspension was mixed with methanol and chloroform and the mixture containing suspension/methanol/chloroform (27:30:30 v/v/v). The final mixture was centrifuged to remove its lower phase containing lipid A, which was used to extract lipid A with a rotary evaporator.

Mass Spectrum Analysis

All the mass spectra of *C. sakazakii* lipid A samples were obtained from a Waters SYNAPT mass spectrometer, which contains an electrospray ionization (ESI) source. ESI/MS in the negative ion mode was performed to detect lipid A samples, which were dissolved in chloroform (Raetz and Whitfield, 2002). The instrument was calibrated with sodium formate. ESI/MS was performed at −80 V, and its collisional activation of ions was

carried out at −8 V. MassLynx V4.1 software was used to acquire and analysis data.

MIC Assay of Cationic Antimicrobial Peptides

The minimum inhibitory concentrations (McPhee et al., 2006) of CAMPs susceptibility were determined by a twofold serial dilution method of polymyxin B (from 1000 to 0.095 µg/mL) and polymyxin E (colistin) (from 1000 to 0.45 µg/mL). Overnight culture was inoculated in a 96-well plate and grown at 37°C. The media for dilutions of polymyxin B and E was the used LB broth. By adding 100 µL per well in the 96-well plate, the overnight bacteria culture suspension was diluted 500 times with OD₆₀₀ = 0.5. If the culture was significantly cloudy, the growth was rated positive. For two different occasions, each test was performed three times (Wang Z. et al., 2015).

Membrane Permeability Assay

The outer membrane permeability (Wang et al., 2014) was detected by fluorescent probe 1-N-phenylanthranilic acid (NPN) access assay (Helander and Mattila-Sandholm, 2000). Briefly, *C. sakazakii* BAA894 was grown overnight in LB medium, and 1.5 mL cells were first harvested by centrifugation at 12,000 rpm for 3 min, then washed twice with potassium phosphate buffer (PBS, 50 mM, pH 7.4). The PBS buffer was used to adjust the OD₆₀₀ to 0.5. A fluorescence spectrophotometer (650–660, Hitachi, Japan) whose widths, excitation, and emission wavelengths were set as 5, 350, and 420 nm, respectively, was used to monitor the fluorescence of the mixture of 1.92 mL of cell suspension (OD₆₀₀ = 0.5) and 80 µL NPN (1 mM) (Wang et al., 2014).

Surface Hydrophobicity Assay

The surface hydrophobicity of cells was determined according to a surface hydrophobicity assay involving the method of Zavaglia et al. (2002) and (Wang et al., 2014). Briefly, the bacteria were collected from overnight culture and resuspended with PBS. After being washed twice by PBS (pH 7.4), the OD₆₀₀ of the culture was adjusted to 0.5. The mixture of 2 mL bacterial suspension and 800 µL xylene was incubated at room temperature for 3 h, which obtained the aqueous phase. The OD₆₀₀ of the aqueous phase was recorded as A, and the value of [(0.5 - A)/0.5] × 100 represents the surface hydrophobicity of the bacterial.

Macrophages Infection

RAW264.7 macrophage cells were seeded in 96-well plates and were grown in Phenol red-free DMEM with 10% fetal bovine serum at 37°C with 5% CO₂. The bacteria was grown in LB (pH 5.0) broth and added into the wells to adjust the macrophage:bacteria ratio of 1:100. After infection for 2 h, culture supernatant was removed and cells were washed with warm PBS four times to remove extracellular bacteria. Afterward, fresh, antibiotic-free media was added to wells. At a desired time point, intracellular bacteria were harvested by adding an equal volume of 0.5% Triton X-100 into wells and left at 37°C and 5% CO₂ for 5 min. To detach cells from wells, a pipette was used to scrape

out cells. Bacterial number was determined by serial dilution plating onto LB plates.

RNA Sequence

The RNA sequence of cells was conducted according to the manufacturer's protocol. Briefly, the cells were collected from the logarithmic phase at pH 5.0; DNA and rRNA were then removed from the total RNA with a kit (Dongsheng Biotech, Guangzhou, China). First, the mRNA was broken into short fragments; then cDNA was synthesized by taking the disrupted mRNA as template. Double-stranded cDNA was synthesized by a two-strand synthesis reaction system. The double-stranded cDNA was purified with QiaQuick PCR kit (QIAGEN, Hamburg, Germany). Next, cohesive ends were repaired. The base "A" was added to the 3' end of the cDNA, and products were ligated to the sequencing adapter; then suitable fragments were selected by agarose electrophoresis, and finally, PCR amplification was performed. In the quality control steps, an ABI StepOnePlus Real-Time PCR System and an Agilent 2100 Bioanalyzer were used for quantification and qualification of the sample library, which was prepared to be sequenced by Illumina HiSeqTM 2000.

RNA Extraction and Transcriptional Analysis Through RT-PCR

Ten DEGs relevant to phenotype were selected to verify the RNA-seq data by the quantitative mRNA transcripts with real-time polymerase chain reaction (qRT-PCR) using the ABI Step One RT-PCR System (Applied Biosystems, CA) according to the manufacturer's instructions. Total RNA samples were extracted using an RNA extraction kit (BioFlux, China). Then RNase-free DNase I was used to remove DNA contamination. Transcription of 500 ng RNA into cDNA was performed using a Revert Aid™ First Strand cDNA synthesis kit (Fermentas, Shanghai, China) with random hexamer primers. Primers for detection of various genes are listed in **Table 4**. 16S rRNA gene was used as an internal control for quantification of relative gene expression. Each qRT-PCR reaction was conducted in a final volume of 50 μ L. The thermal cycling profile was as follows: 94°C for 1 min, followed by 40 cycles of 94°C for 10 s, 55°C for 30 s, and 68°C for 15 s. Sterile water was used as negative control samples. The cycle threshold values (CT) were determined, and the $2^{-\Delta\Delta CT}$ method (Livak and Schmittgen, 2001) with 16S rRNA as the reference gene was used to calculate the relative fold differences. This experiment was repeated three times.

RESULTS AND DISCUSSION

Identification of the Genes Encoding PmrA/PmrB in *C. sakazakii*

The PmrA/PmrB two-component system involved in *S. typhimurium* was activated directly by the existing iron in the culture medium and indirectly through the PhoP/PhoQ and PmrA/PmrB signal systems at a low magnesium concentration or low pH (Wosten et al., 2000; Gibbons et al., 2005). Phosphoethanolamine (pEtN) is incorporated to lipid A

when bacteria are grown under low pH conditions in *S. typhimurium*. The pEtN modification of BAA894 lipid A can increase the resistance to CAMPs and reduce recognition and lethality by the host innate immune system (Liu et al., 2016). To identify *C. sakazakii* genes that are responsible for the PmrA/PmrB regulatory system, the amino acid sequence of the *S. typhimurium* PmrA, PmrB, PmrC protein was used as the query to perform a BLASTp search of the BAA894 genome.

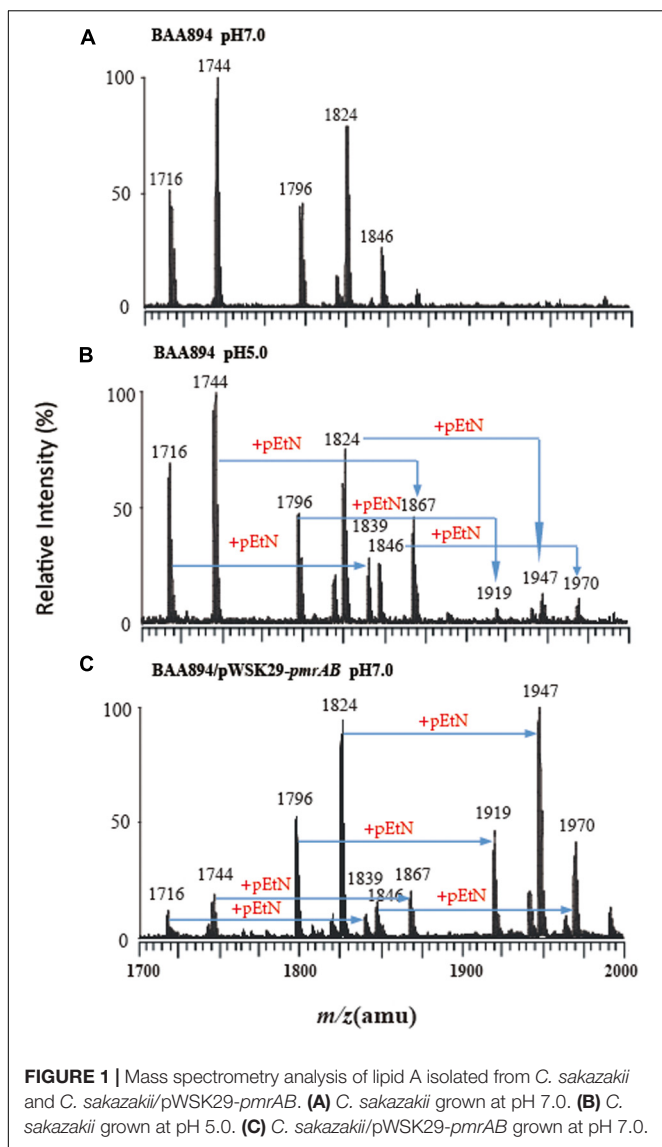
The *C. sakazakii* BAA894 *ESA_RS16430* showed 56.31% identity to *pmrA* in *S. typhimurium*, and *ESA_RS16435* exhibited 46.43% identity with *pmrB* in *S. typhimurium*. In the genomes of *S. typhimurium*, *eptA* (*pmrC*) locates in the same operon with *pmrA* and *pmrB* (Lee et al., 2004), and the gene expression is controlled by PmrA (Wosten and Groisman, 1999). In the genome of *C. sakazakii* BAA894 (Joseph et al., 2012), *ESA_RS16425* under the same operon with *pmrAB* showed 82.14% identity to *dacB* from *S. typhimurium*. Another gene of *ESA_RS09200*, which is outside of the operon, shows identity to *pmrC* in *C. sakazakii*. The functional relationship between *ESA_RS16425* and *pmrA/pmrB* is unknown. The gene organization of *C. sakazakii* is different with the *pmrCAB* operon identified in *S. typhimurium* and *E. coli*. The *pmrAB* overexpression and *pmrA* deletion strains were generated to study the function and regulation mechanism.

The Effect of PmrA/PmrB on Lipid A Structure Modification in *C. sakazakii*

To investigate the PmrA/PmrB effect on the lipid A structure in *C. sakazakii*, *pmrAB* were co-overexpressed and the *pmrA* mutant was generated in *C. sakazakii*. The lipid A was extracted from wild-type *C. sakazakii* BAA894 at pH 7.0 and pH 5.0, respectively (**Figures 1A,B**), and *pmrAB* overexpression strain *C. sakazakii/pWSK29-pmrAB* (**Figure 1C**) at pH 7.0 by the Bligh-Dyer method (Gunn et al., 2000; Bengoechea et al., 2003; Townsend et al., 2007; Wang X. et al., 2015). ESI/MS was used to analyze the extracted lipid A.

The lipid A from *C. sakazakii* BAA894 at pH 7.0 showed five major peaks at *m/z* 1716, 1744, 1796, 1824, and 1846 in the spectrum. The ions at *m/z* 1796 and 1824 are the $[M-H]^-$ ions of the two lipid A molecules, which are the backbone of the lipid A general structure (Li et al., 2016). The minor peaks at *m/z* 1716 and 1744 are the monophosphorylated form of lipid A (Helander and Mattila-Sandholm, 2000). The peak at *m/z* 1846 was generated from the sodium adduct of the ion at *m/z* 1824 (**Figure 1A**). The lipid A ions at pH 5.0 showed five additional peaks at *m/z* 1839, 1867, 1919, 1947, and 1970 (**Figure 1B**). All these ions with 123 amu higher *m/z* suggested the addition of a pEtN group into lipid A. The low pH condition upregulated the *pmrC* gene expression.

The lipid A isolated from *pmrAB* overexpression strain *C. sakazakii/pWSK29-pmrAB* at pH 7.0 also showed five additional peaks at *m/z* 1839, 1867, 1919, 1947, and 1970 with higher 123 amu compared to the wild-type grown at pH 7.0. In addition, the relative intensity of these peaks was also much higher than that of the wild-type grown at pH 5.0 (**Figure 1C**). The results suggest that the overexpression of *pmrAB* boosted the



pEtN modification in lipid A. The overexpression of *pmrAB* likely upregulated the *pmrC* gene transcription level and, hence, resulted in the modification of lipid A with the addition of the pEtN group. Compared to the wild-type grown at pH 7.0, the *pmrA* mutant did not show a significant difference in the lipid A profile, and there was no lipid A modification found as well.

PmrA/PmrB-Mediated Lipid A Modification Increases the Resistance to Cationic Antimicrobial Peptides

The PmrA/PmrB is the major regulator of LPS-modified genes in *S. typhimurium* and *E. coli*. The phosphate groups on the surface of the bacteria would be neutralized by the modification of pEtN on lipid A and, hence, become negatively charged and could interact with CAMPs, such as Polymyxin B and colistin (Anandan et al., 2016). To study whether *pmrAB*-mediated pEtN modification of lipid A in *C. sakazakii* BAA894 alters the bacterial

TABLE 2 | The minimal inhibitory concentrations of mutants derived from BAA894 cultured in pH 7.0 and pH 5.0.

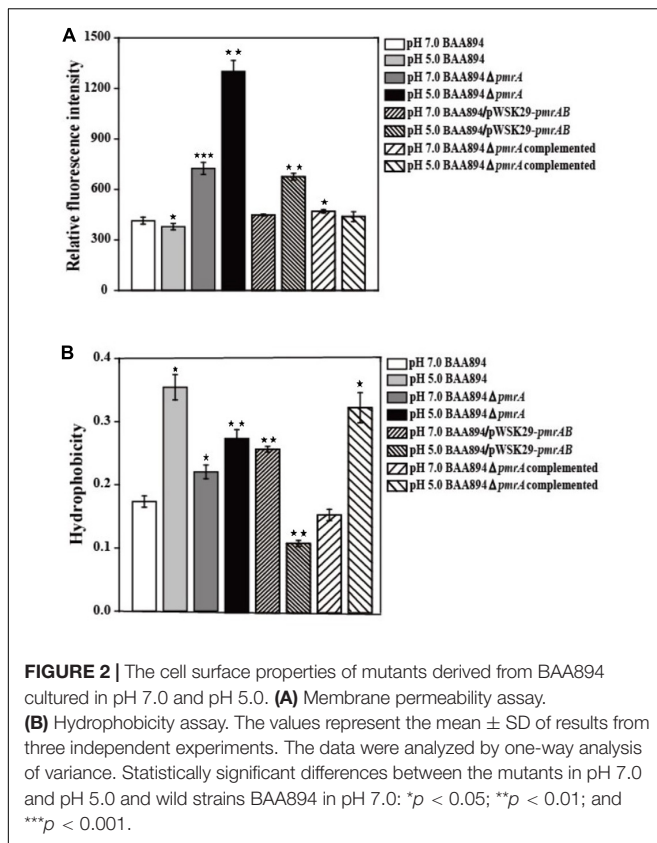
Strain	pH	Polymyxin B MIC ($\mu\text{g/mL}$)	Polymyxin E MIC ($\mu\text{g/mL}$)
<i>C. sakazakii</i>	pH 7.0	0.39 \pm 0.1	0.45 \pm 0.1
	pH 5.0	17.5 \pm 2.5	35 \pm 2.5
<i>C. sakazakii</i> Δ <i>pmrA</i>	pH 7.0	0.39 \pm 0.1	0.45 \pm 0.1
	pH 5.0	6.5 \pm 1.0	4.0 \pm 1.0
BAA894/pWSK29- <i>pmrAB</i>	pH7.0	0.39 \pm 0.1	0.45 \pm 0.1
	pH5.0	280 \pm 20	560 \pm 35
<i>C. sakazakii</i> Δ <i>pmrA</i> complemented	pH7.0	0.39 \pm 0.1	0.45 \pm 0.1
	pH5.0	17.5 \pm 2.5	35 \pm 2.5

The values represent the mean \pm SD of results from three independent experiments.

resistance to CAMPs (Liu et al., 2016), MIC of *C. sakazakii* wild-type strain, *pmrA* mutant strain, and *pmrAB* overexpressed strain grown at pH 7.0 and 5.0 to polymyxins B and colistin were investigated (Table 2). *C. sakazakii* BAA894 cells grown at pH 5.0 were highly resistant to CAMPs compared to the cells grown at pH 7.0; the MIC of polymyxin B increased from 0.39 to 17.5 $\mu\text{g/mL}$, and the MIC of polymyxin E increased from 0.45 to 35 $\mu\text{g/mL}$. When grown at pH 5.0, the MIC of polymyxin B and colistin of the *pmrA* mutant strain were 6.5 $\mu\text{g/mL}$ and 4 $\mu\text{g/mL}$, respectively. The result was still higher than that of the wild-type strain (Table 2). Compared to the BAA894 grown at pH 7.0, the MIC of *C. sakazakii* BAA894/pWSK29-*pmrAB* to polymyxin B and colistin grown at pH 5.0 were higher, which were increased to 280 and 560 $\mu\text{g/mL}$, respectively. Complementation of BAA894 Δ *pmrA* and pWSK29-*pmrA*, its MIC to polymyxin B and colistin returned to wild-type levels at pH 7.0 or 5.0. According to our study, pEtN modification of lipid A at acidic pH can improve bacteria resistance ability to CAMPs. On the minimal inhibitory concentrations table (Table 2), we found that *C. sakazakii* BAA894/pWSK29-*pmrAB* showed the highest resistance ability to CAMPs at pH 5.0, but remained at the same resistance level to CAMPs when compared with BAA894 at pH 7.0. The results suggested that the PmrA were related to the resistance to CAMPs, and PmrA/PmrB also influenced the resistance to CAMPs at acidic pH.

PmrA/PmrB-Mediated Lipid A Modification Changes the Cell Surface Properties of *C. sakazakii*

It has been shown previously that the OM permeability of Gram-negative bacteria is correlated with the structure of LPS (Bengoechea et al., 2003). Lipid A is the important hydrophobic component of LPS, which is the major component of the outer membrane; the structure changes of the lipid A might influence the cell membrane properties (Raetz and Whitfield, 2002; Bengoechea et al., 2003). Since our research suggested that the overexpression of *pmrAB* boosted the pEtN modification in lipid A, the OM permeability and hydrophobicity might be influenced through the change of structure of the LPS and outer membrane. The characteristics of the outer membrane, including



the permeability and hydrophobicity of mutants cells (Lehner et al., 2005) were evaluated (Figure 2).

When compared to the *C. sakazakii* BAA894 wild-type strain cultured at pH 7.0, the membrane permeability of BAA894 cultured at pH 5.0 slightly decreased. In comparison with the BAA894 wild-type strain, the membrane permeability of *pmrA* mutant strains cultured at pH 7.0 and pH 5.0 increased by twofold and threefold, respectively (Figure 2A). Compared with BAA894 grown at pH 5.0, the membrane permeability of BAA894/pWSK29-*pmrAB* cultured at pH 7.0 was slightly increased while the one that was cultured at pH 5.0 increased by 1.8-fold. Under the pH 7.0 or pH 5.0 condition, the *pmrA* overexpressed strain restored the membrane permeability to the wild-type levels. The PmrA/PmrB system-mediated lipid A modification changed the structure of the LPS and reduced outer membrane permeability. These results suggest that the *pmrA* and PmrA/PmrB system have an influence on membrane permeability.

The cell surface hydrophobicity of the *pmrA* mutant strain was essentially the same at pH 7.0 and pH 5.0. However, the cell surface hydrophobicity of the BAA894 wild-type strain and BAA894Δ*pmrA* complementation strain under pH 5.0 was twofold higher than at pH 7.0 (Figure 2B). Meanwhile, compared with the BAA894 wild-type strain, the cell surface hydrophobicity of BAA894/pWSK29-*pmrAB* cultured at pH 7.0 and pH 5.0 increased by 1.5- and 1.6-fold. These results suggest that modification of pEtN in lipid A might change the

characteristics of the outer membrane by increasing the surface hydrophobicity of cells.

PmrA/PmrB Inhibits the Ability to Invade and Survive in Macrophage

To invade microorganisms, macrophages utilize antimicrobial defense mechanisms (i.e., nutrient deprivation and oxidative burst) to eliminate harmful pathogens. The ability of bacteria to survive and replicate in immune cells provides them protection from the host immune response (Townsend et al., 2007). Some *C. sakazakii* can avoid the host immune response by exploiting immature dendritic cells and then persisting within human macrophages (Liu et al., 2016). The *pmrA* mutant strain grew faster than the BAA894 wild-type strain at pH 5.0, and more mutants were recovered from macrophage after infection for 6, 12, and 24 h. The intracellular numbers of the wild-type strain

TABLE 3 | List of the genes related to phenotype between BAA894 and *pmrA* mutant in pH 5.0.

gene ID	5.0WT RPKM	5.0 <i>pmrA</i> RPKM	Fold change	P value	Level
<i>pmrA</i>	90.13	0.00	0.00	$P < 0.01$	Down
<i>pmrB</i>	107.56	47.24	0.44	$P < 0.01$	Down
<i>phoP</i>	286.85	313.69	1.09	$P < 0.01$	Up
<i>phoQ</i>	175.54	134.05	0.76	$P < 0.01$	Down
<i>eptA</i>	158.65	184.59	1.16	$P < 0.01$	Up
<i>eptB</i>	425.35	334.12	0.79	$P < 0.01$	Down
<i>pagP</i>	145.53	132.29	0.91	$P < 0.01$	Down
<i>lpxA</i>	458.78	449.40	0.98	$P < 0.01$	Down
<i>cpxA</i>	224.27	141.26	0.63	$P < 0.01$	Down
<i>cpxR</i>	634.07	536.28	0.85	$P < 0.01$	Down
<i>marA</i>	29.74	22.07	0.74	$P < 0.01$	Down
<i>acrA</i>	382.12	377.03	0.99	$P < 0.01$	Down
<i>acrB</i>	228.82	210.03	0.92	$P < 0.01$	Down
<i>tolC</i>	315.09	316.41	1.00	$P < 0.01$	Up
<i>ramA</i>	87.80	74.79	0.85	$P < 0.01$	Down
<i>ompF</i>	7971.55	8755.51	1.10	$P < 0.01$	Up
<i>phoE</i>	58.84	80.38	1.37	$P < 0.01$	Up
<i>ompC</i>	11281.95	17012.45	1.51	$P < 0.01$	Up
<i>ESA_RS01970</i>	743.76	818.06	1.10	$P < 0.01$	Up
<i>ESA_RS03645</i>	61.54	131.54	2.14	$P < 0.01$	Up
<i>ESA_RS08640</i>	172.73	314.67	1.82	$P < 0.01$	Up
<i>ESA_RS19800</i>	50.24	138.89	2.77	$P < 0.01$	Up
<i>ESA_RS19805</i>	18.28	52.33	2.86	$P < 0.01$	Up
<i>ESA_RS11615</i>	23194.65	26474.44	1.14	$P < 0.01$	Up
<i>ompX</i>	3.08	3.63	1.18	$P < 0.01$	Up
<i>ESA_RS16175</i>	1.18	1.39	1.18	$P < 0.01$	Up
<i>ESA_RS17575</i>	12.88	14.19	1.10	$P < 0.01$	Up
<i>ESA_RS18760</i>	40.25	45.60	1.13	$P < 0.01$	Up
<i>ESA_RS18775</i>	27.72	35.70	1.29	$P < 0.01$	Up
<i>flhR</i>	69.80	100.78	1.44	$P < 0.01$	Up
<i>ESA_RS05890</i>	110.76	351.83	3.18	$P < 0.01$	Up
<i>flhS</i>	90.79	244.40	2.69	$P < 0.01$	Up
<i>flhU</i>	39.00	21.21	0.54	$P < 0.01$	Down
<i>ESA_RS05905</i>	649.94	307.50	0.47	$P < 0.01$	Down

TABLE 4 | Primers used in RT-PCR.

Primers	Nucleotide sequence (5' → 3')
RT-16SrDNA- F	CCTACGACCAAGGCTAC
RT-16SrDNA- R	GACTACGACGCACTTTATGAG
RT- <i>pmrB</i> - F	GCTCGGCGGATAATCTT
RT- <i>pmrB</i> - R	GATGTGGCTTCGTCGTGAG
RT- <i>phoP</i> - F	CTGGTCGTCGAGGATAACG
RT- <i>phoP</i> - R	TGTGAAACGGCTTGGTG
RT- <i>phoO</i> - F	GAGCGTCTGGAAGTGGTTAT
RT- <i>phoO</i> - R	GGTGAGCGTTGTGCGGT
RT- <i>eptA</i> - F	AACAGAACTATTCGCTTGCG
RT- <i>eptA</i> - R	GCAGGAGCCCTCTTTACAC
RT- <i>pagP</i> - F	ACCAGCGGAATCGGGAT
RT- <i>pagP</i> - R	GCCTGGGCTTCTGTGCTT
RT- <i>eptB</i> - F	GATACGCGGACCAAACTCT
RT- <i>eptB</i> - R	TCAACTCTGACGGCTAC
RT-ESA-RS01970- F	GAGCGACGAAGACAAACG
RT-ESA-RS01970- R	AGAGTGCCACAGGACCAC
RT-ESA-RS19805- F	ACCGTCTGTTGCAGGTC
RT-ESA-RS19805- R	TGCCGCCACATCAATACC
RT- <i>fljS</i> - F	TCAGGGTTTCAACTTCATTG
RT- <i>fljS</i> - R	CCTGGAAAGTGCGGTAAT
RT- <i>fljJ</i> - F	CGCCTGATCGACTTTGGT
RT- <i>fljJ</i> - R	ACGCTTAAAGATATGGCTG

increased 2.56-fold and 6.65-fold over T12 and T24, respectively, while those of the mutant strains were 4.15-fold and 10.4-fold over T12 and T24, respectively (Figure 3). However, the growth state of *C. sakazakii* BAA894/pWSK29-*pmrAB* in macrophage was worse than that of the BAA894 wild-type strain at pH 5.0. In addition, compared with BAA894 grown at pH 5.0, the intracellular numbers of the mutant decreased to 41% and 34% over T12 and T24, respectively (Figure 3). These results demonstrate that the *pmrA* mutant increased cell invasion and replication ability, which was restored to wild-type levels by complementation. All these suggested that the PmrA/PmrB two-component system in *C. sakazakii* BAA894 was important in regulating the system for host cell invasion and replication.

RNA-Sequencing of *C. sakazakii* *pmrA* Mutant

In our study, PmrA/PmrB shows influences on CAMPs, cell membrane permeability and hydrophobicity, and macrophage invasion. To verify the results, further analysis by RNA-sequencing were conducted (Table 3).

The gene expression levels related to phenotype were between the BAA894 and *pmrA* mutant at pH 5.0. RPKM is short for reads per kilobase transcriptome per million mapped reads; it is used to calculate the expression level of the gene. Fold change represents the ratio of *pmrA* mutant to wild-type gene RPKM; *p* value represents the significance level of the hypothesis test.

Similar transcriptional levels of some key genes relevant to phenotype were also observed by using RT-PCR analysis (Figure 4). This suggests that the transcriptomic analysis used in this study is reliable.

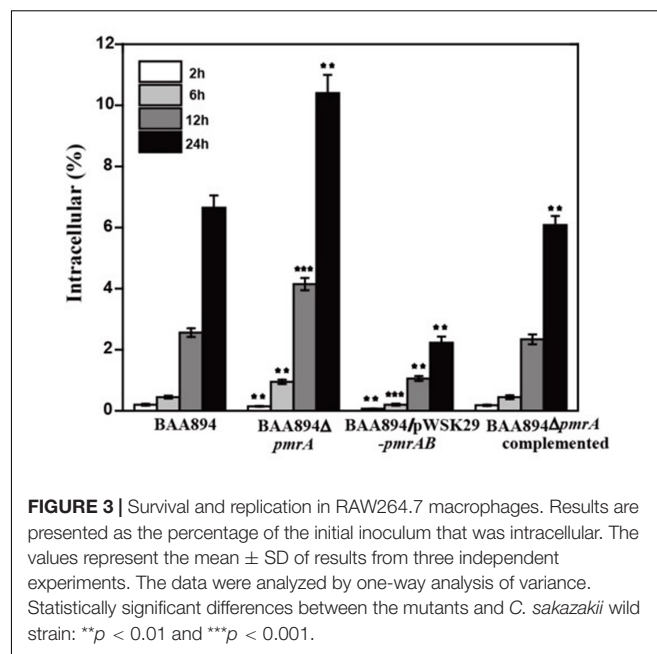


FIGURE 3 | Survival and replication in RAW264.7 macrophages. Results are presented as the percentage of the initial inoculum that was intracellular. The values represent the mean \pm SD of results from three independent experiments. The data were analyzed by one-way analysis of variance. Statistically significant differences between the mutants and *C. sakazakii* wild strain: ** $p < 0.01$ and *** $p < 0.001$.

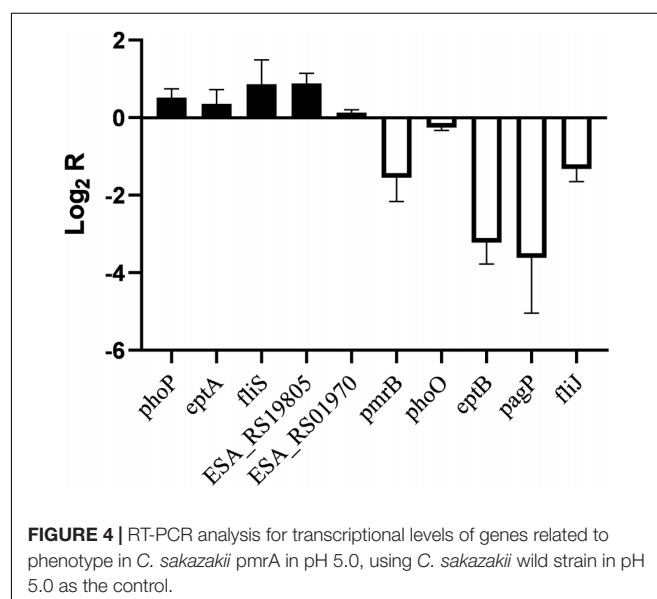


FIGURE 4 | RT-PCR analysis for transcriptional levels of genes related to phenotype in *C. sakazakii* *pmrA* in pH 5.0, using *C. sakazakii* wild strain in pH 5.0 as the control.

In *Salmonella enterica*, PmrB can sense environmental stimuli directly and can initiate a cascade to phosphorylate and activate PmrA. LPS modifications mediated by PmrA/PmrB and PhoP/PhoQ systems aid in survival in host cells and in the environment (Gunn, 2008). In the *pmrA* mutant, genes (*pmrB*, *phoQ*, *pagP*, and *eptB*) of PmrA/PmrB and PhoP/PhoQ were downregulated, which indicated that the *pmrA* mutant without a complete PmrAB regulon might weaken survival in host and non-host environments. In *C. sakazakii* and *E. coli*, PmrA/PmrB and PhoP/PhoQ changed the resistance to CAMPs by modifying fatty acid chains and phosphoric acid groups of lipid A (Townsend et al., 2007; Wang X. et al., 2015; Liu et al., 2016). In the *pmrA* mutant, some of the PmrAB-regulated genes were

downregulated while *eptA* and *phoP* were upregulated. Besides, genes (*lpxA*, *cpxA*, *cpxR*, *marA*, *acrA*, and *acrB*) involved in CAMPs resistance were downregulated in the *pmrA* mutant while *tolC* was upregulated. Most of the genes involved in CAMPs resistance were downregulated, which indicated that the *pmrA* mutant was weakly resistant to CAMPs.

Genes (*marA*, *ramA*, *ompF*, *phoE*, and *ompC*) are involved in regulating membrane permeability by changing the production of porin and the expression of bacterial envelope efflux pump systems (Bishop, 2005; Anne et al., 2008). In transcriptome data, genes (*ompF*, *phoE*, and *ompC*) were upregulated in *pmrA* mutant while *marA* and *ramA* were downregulated, suggesting the variation of membrane permeability.

Due to the difference in modification of LPS, cell hydrophobicity changed (Kim et al., 2010). Also, genes associated with hydrophobicity, such as *eptB*, *pagP*, were downregulated in *pmrA* mutant while *eptA* was upregulated, suggesting the variation of hydrophobicity.

Other influence factors for macrophage invasion include both virulence factors and bacterial motility (Delcour, 2009; Kim et al., 2010). Genes (*ESA_RS01970*, *ESA_RS03645*, *ESA_RS08640*, *ESA_RS19800*, and *ESA_RS1980*) involved in toxins were upregulated in *pmrA* mutant. Genes (*ompX*) involved in bacterial motility can promote bacterial adhesion and attachment to the host (Delcour, 2009). Fimbriae proteins (*ESA_RS12900*, *ESA_RS16175*, *ESA_RS17575*, *ESA_RS18760*, and *ESA_RS18775*) and flagellum proteins (*fliR*, *ESA_RS05890*, and *fliS*, except for *fliJ* and *ESA_RS059105*) were upregulated in the *C. sakazakii* *pmrA* mutant. Because of the impact of virulence and bacterial adhesion, the *pmrA* mutant increased the ability of cells to invade.

According to KEGG pathway enrichment analysis, “lysine biosynthesis,” “metabolic pathways,” “biosynthesis of secondary metabolites,” and “microbial metabolism in diverse environments” were significantly enriched. In the *pmrA* mutant, most differentially expressed genes (DEGs) in “microbial metabolism in diverse environments” were downregulated. DEGs (*ESA_RS15995*, *ESA_RS17800*, and *ESA_RS18990*) involved in the “pentose phosphate cycle” were also downregulated, which indicated that the *pmrA* mutant without a complete PmrAB regulon might weaken survival in diverse environments.

CONCLUSION

The PmrA/PmrB-regulated genes were identified and characterized in *C. sakazakii*. The pEtN is modified to lipid A in *C. sakazakii* when grown at a weak acid condition. The

enzyme encoded by *C. sakazakii* *eptA* could transfer pEtN to lipid A and was affected by acidic condition. More studies indicate that the *eptA* is not completely but partially regulated by PmrA/PmrB in *C. sakazakii* BAA894, and the PmrA/PmrB two-component system in *C. sakazakii* were involved in the lipid A structure modification.

Non-polar deletion was constructed in the *pmrAB* gene of the PmrA/PmrB, and the effect of this mutation on CAMPs resistance were measured. Negative-ion mass spectra revealed the presence of pEtN in lipid A isolated from the *pmrAB* overexpressed strain under the pH 7.0 condition. Meanwhile, we also tested mutant and wild-type strains for susceptibility to CAMPs and demonstrated the PmrA and PmrA/PmrB were related to the resistance of CAMPs. A defect of the *pmrA* gene and co-overexpression of *pmrAB* in *C. sakazakii* increased the outer membrane permeability and hydrophobicity at pH 5.0, which might improve the transmembrane capacity of antibiotics and then affect the outer membrane permeability and hydrophobicity.

Cronobacter sakazakii can utilize immature dendritic cells and remain in human macrophages, which indicates that *C. sakazakii* has certain immune evasion properties and can protect itself from host immune response and then reach and even penetrate the blood-brain barrier (Townsend et al., 2008; Emami et al., 2011; Wang X. et al., 2015). The BAA894 wild-type strain showed lower invasion ability than the *pmrA* mutant strain and higher invasion ability than BAA894/pWSK29-*pmrAB* under the pH 5.0 condition, suggesting that the PmrA/PmrB system is important in toxicity control in *C. sakazakii*. When *pmrA* was deleted, the bacteria showed a trend of increased toxicity and provided a survival advantage to bacteria in the host.

DATA AVAILABILITY STATEMENT

The dataset can be found in NCBI under the accession number GSE147019.

AUTHOR CONTRIBUTIONS

All authors listed have made a substantial, direct and intellectual contribution to the work, and approved it for publication.

FUNDING

This work was supported by Zhejiang Provincial Natural Science Foundation of China LR20C050001 to YL.

REFERENCES

- Al-Khodori, S., Kalachikov, S., Morozova, I., Price, C. T., and Abu Kwaik, Y. (2009). The PmrA/PmrB two-component system of *Legionella pneumophila* is a global regulator required for intracellular replication within macrophages and protozoa. *Infect Immun.* 77, 374–386. doi: 10.1128/IAI.01081-08
- Anandan, A., Evans, G. L., Condit-Jurkic, K., O'Mara, M. L., John, C. M., and Phillips, N. J. (2016). Structure of a lipid A phosphoethanolamine transferase suggests how conformational changes govern substrate binding. *PNAS* 114, 2218–2223. doi: 10.1073/pnas.1612927114
- Anne, D.-R., Bolla, J. M., James, C. E., Lavigne, J. P., Chevalier, J., Garnotel, E., et al. (2008). Membrane permeability and regulation of drug. *Curr. Drug Targets* 9, 750–759. doi: 10.2174/138945008785747824
- Bao, X., Jia, X., Chen, L., Peters, B. M., Lin, C.-W., Chen, D., et al. (2017). Effect of polymyxin resistance (*pmr*) on biofilm formation of *Cronobacter sakazakii*. *Microb. Pathog.* 106, 16–19. doi: 10.1016/j.micpath.2016.12.012

- Bengoechea, J. A., Brandenburg, K., Arraiza, M. D., Seydel, U., Skurnik, M., Moriyón, I., et al. (2003). Pathogenic *Yersinia enterocolitica* strains increase the outer membrane permeability in response to environmental stimuli by modulating lipopolysaccharide fluidity and lipid A structure. *Infect Immun.* 71, 2014–2021. doi: 10.1128/iai.71.4.2014-2021.2003
- Bishop, R. E. (2005). Fundamentals of endotoxin structure and function. *Contrib. Microbiol.* 12, 1–27. doi: 10.1159/000081687
- Cai, L., Li, Y., Tao, G., Guo, W., Zhang, C., and Wang, X. (2013). Identification of three genes encoding for the late acyltransferases of lipid A in *Cronobacter sakazakii*. *Mar. Drugs* 11, 377–386. doi: 10.3390/md11020377
- Chen, H. D., and Groisman, E. A. (2013). The biology of the PmrA/PmrB two-component system: the major regulator of lipopolysaccharide modifications. *Annu. Rev. Microbiol.* 67, 83–112. doi: 10.1146/annurev-micro-092412-155751
- Chenu, J. W., and Cox, J. M. (2009). *Cronobacter* ('*Enterobacter sakazakii*'): current status and future prospects. *Lett. Appl. Microbiol.* 49, 153–159. doi: 10.1111/j.1472-765X.2009.02651.x
- Datsenko, K. A., and Wanner, B. L. (2000). One-step inactivation of chromosomal genes in *Escherichia coli* K-12 using PCR products. *Proc. Nat. Acad. Sci. USA* 97, 6640–6645. doi: 10.1073/pnas.120163297
- Delcour, A. H. (2009). Outer membrane permeability and antibiotic resistance. *Biochim. Biophys. Acta* 1794, 808–816. doi: 10.1016/j.bbapap.2008.11.005
- Emami, C. N., Mittal, R., Wang, L., Ford, H. R., and Prasadara, N. V. (2011). Recruitment of dendritic cells is responsible for intestinal epithelial damage in the pathogenesis of necrotizing enterocolitis by *Cronobacter sakazakii*. *J. Immunol.* 186, 7067–7079. doi: 10.4049/jimmunol.1100108
- Forsythe, S. J., Dickins, B., and Jolley, K. A. (2014). *Cronobacter*, the emergent bacterial pathogen *Enterobacter sakazakii* comes of age; MLST and whole genome sequence analysis. *BMC Genomics* 15:1121. doi: 10.1186/1471-2164-15-1121
- Gibbons, H. S., Kalb, S. R., Cotter, R. J., and Raetz, C. R. (2005). Role of Mg²⁺ and pH in the modification of *Salmonella* lipid A after endocytosis by macrophage tumour cells. *Mol. Microbiol.* 55, 425–440. doi: 10.1111/j.1365-2958.2004.04409.x
- Gunn, J. S. (2008). The *Salmonella* PmrAB regulon: lipopolysaccharide modifications, antimicrobial peptide resistance and more. *Trends Microbiol.* 16, 284–290. doi: 10.1016/j.tim.2008.03.007
- Gunn, J. S., Ryan, S. S., Van Velkinburgh, J. C., Ernst, R. K., and Miller, S. I. (2000). Genetic and functional analysis of a PmrA-PmrB-regulated locus necessary for lipopolysaccharide modification, antimicrobial peptide resistance, and oral virulence of *Salmonella enterica* serovar typhimurium. *Infect Immun.* 68, 6139–6146. doi: 10.1128/iai.68.11.6139-6146.2000
- Hagiwara, D., Yamashino, T., and Mizuno, T. (2004). A Genome-wide view of the *Escherichia coli* BasS-BasR two-component system implicated in iron-responses. *Biosci. Biotechnol. Biochem.* 68, 1758–1767. doi: 10.1271/bbb.68.1758
- Helander, I. M., and Mattila-Sandholm, T. (2000). Fluorometric assessment of gram-negative bacterial permeabilization. *J. Appl. Microbiol.* 88:6. doi: 10.1046/j.1365-2672.2000.00971.x
- Jaradat, Z. W., Al Mousa, W., Elbetieha, A., Al Nabulsi, A., and Tall, B. D. (2014). *Cronobacter* spp. - opportunistic food-borne pathogens. A review of their virulence and environmental-adaptive traits. *J. Med. Microbiol.* 63, 1023–1037. doi: 10.1099/jmm.0.073742-0
- Jia, X., Hua, J., Liu, L., Xu, Z., and Li, Y. (2018). Phenotypic characterization of pathogenic *Cronobacter* spp. strains. *Microb. Pathog.* 121, 232–237. doi: 10.1016/j.micpath.2018.05.033
- Joseph, S., Desai, P., Ji, Y., Cummings, C. A., Shih, R., Degoricija, L., et al. (2012). Comparative analysis of genome sequences covering the seven *cronobacter* species. *PLoS One* 7:e49455. doi: 10.1371/journal.pone.0049455
- Kim, K., Kim, K. P., Choi, J., Lim, J. A., Lee, J., Hwang, S., et al. (2010). Outer membrane proteins A (OmpA) and X (OmpX) are essential for basolateral invasion of *Cronobacter sakazakii*. *Appl. Environ. Microbiol.* 76, 5188–5198. doi: 10.1128/AEM.02498-09
- Kucerova, E., Clifton, S. W., Xia, X. Q., Long, F., Porwollik, S., Fulton, L., et al. (2010). Genome sequence of *Cronobacter sakazakii* BAA-894 and comparative genomic hybridization analysis with other *Cronobacter* species. *PLoS One* 5:e9556. doi: 10.1371/journal.pone.0009556
- Lee, H., Hsu, F.-F., Turk, J., and Groisman, E. A. (2004). The PmrA-regulated pmrC gene mediates phosphoethanolamine modification of lipid A and polymyxin resistance in *Salmonella enterica*. *J. Bacteriol.* 186, 4124–4133. doi: 10.1128/JB.186.13.4124-4133.2004
- Lehner, A., Riedel, K., Eberl, L., Breeuwer, P., Diep, B., Stephan, R., et al. (2005). Biofilm formation, extracellular polysaccharide production, cell-to-cell signaling, in various *C.sakazakii* strains: aspects promoting environmental persistence. *Food Protoc.* 68:7. doi: 10.1002/9783527629237.ch1
- Li, Y., Yoon, S. H., Wang, X., Ernst, R. K., and Goodlett, D. R. (2016). Structural derivation of lipid A from *Cronobacter sakazakii* using tandem mass spectrometry. *Rapid Commun. Mass Spectr.* 30, 2265–2270. doi: 10.1002/rcm.7712
- Liu, L., Li, Y., Wang, X., and Guo, W. (2016). A phosphoethanolamine transferase specific for the 4'-phosphate residue of *Cronobacter sakazakii* lipid A. *J. Appl. Microbiol.* 121, 1444–1456. doi: 10.1111/jam.13280
- Livak, K. J., and Schmittgen, T. D. (2001). Analysis of relative gene expression data using real-time quantitative PCR and the 2- $\Delta\Delta$ CT method. *Methods* 25, 402–408. doi: 10.1006/meth.2001.1262
- McPhee, J. B., Bains, M., Winsor, G., Lewenza, S., Kwasnicka, A., Brazas, M. D., et al. (2006). Contribution of the PhoP-PhoQ and PmrA-PmrB two-component regulatory systems to Mg²⁺-induced gene regulation in *Pseudomonas aeruginosa*. *J. Bacteriol.* 188, 3995–4006. doi: 10.1128/JB.00053-06
- Mitrophanov, A. Y., Jewett, M. W., Hadley, T. J., and Groisman, E. A. (2008). Evolution and dynamics of regulatory architectures controlling polymyxin B resistance in enteric bacteria. *PLoS Genet.* 4:e1000233. doi: 10.1371/journal.pgen.1000233
- Murray, S. R., Ernst, R. K., Bermudes, D., Miller, S. I., and Low, K. B. (2007). pmrA(Con) confers pmrHFIJKL-dependent EGTA and polymyxin resistance on msbB *Salmonella* by decorating lipid A with phosphoethanolamine. *J. Bacteriol.* 189, 5161–5169. doi: 10.1128/JB.01969-06
- Raetz, C. R., and Whitfield, C. (2002). Lipopolysaccharide endotoxins. *Annu. Rev. Biochem.* 71, 635–700. doi: 10.1146/annurev.biochem.71.110601.135414
- Roland, K. L., Martin, L. E., Esther, C. R., and Spitznagel, J. K. (1993). Spontaneous pmrA mutants of *Salmonella typhimurium* LT2 define a new two-component regulatory system with a possible role in virulence. *J. Bacteriol.* 175, 4154–4164. doi: 10.1128/jb.175.13.4154-4164.1993
- Townsend, S., Hurrell, E., and Forsythe, S. (2008). Virulence studies of *Enterobacter sakazakii* isolates associated with a neonatal intensive care unit outbreak. *BMC Microbiol.* 8:64. doi: 10.1186/1471-2180-8-64
- Townsend, S. M., Hurrell, E., Gonzalez-Gomez, I., Lowe, J., Frye, J. G., Forsythe, S., et al. (2007). *Enterobacter sakazakii* invades brain capillary endothelial cells, persists in human macrophages influencing cytokine secretion and induces severe brain pathology in the neonatal rat. *Microbiology* 153, 3538–3547. doi: 10.1099/mic.0.2007/009316-0
- Viau, C., Le Sage, V., Ting, D. K., Gross, J., and Le Moual, H. (2011). Absence of PmrAB-mediated phosphoethanolamine modifications of *Citrobacter rodentium* lipopolysaccharide affects outer membrane integrity. *J. Bacteriol.* 193, 2168–2176. doi: 10.1128/JB.01449-10
- Wang, B., Han, Y., Li, Y., Li, Y., and Wang, X. (2015). Immuno-stimulatory activity of *Escherichia coli* mutants producing Kdo2-monophosphoryl-lipid A or Kdo2-pentaacyl-monophosphoryl-lipid A. *PLoS One* 10:e0144714. doi: 10.1371/journal.pone.0144714
- Wang, X., Quinn, P. J., and Yan, A. (2015). Kdo2-lipid A: structural diversity and impact on immunopharmacology. *Biol. Rev. Camb. Philos. Soc.* 90, 408–427. doi: 10.1111/brv.12114
- Wang, Z., Wang, J., Ren, G., Li, Y., and Wang, X. (2015). Influence of core oligosaccharide of lipopolysaccharide to outer membrane behavior of *Escherichia coli*. *Mar. Drugs* 13, 3325–3339. doi: 10.3390/md13063325
- Wang, J., Ma, W., Wang, Z., Li, Y., and Wang, X. (2014). Construction and characterization of an *Escherichia coli* mutant producing Kdo2-lipid A. *Mar. Drugs* 12, 1495–1511. doi: 10.3390/md12031495
- Wang, L., Wang, Q., and Reeves, P. R. (2010). *Endotoxins: Structure, Function and Recognition*. Berlin: Springer.
- Winfield, M. D., and Groisman, E. A. (2004). Phenotypic differences between *Salmonella* and *Escherichia coli* resulting from the disparate regulation of homologous genes. *Proc. Natl. Acad. Sci. U.S.A.* 101, 17162–17167. doi: 10.1073/pnas.0406038101

- Winfield, M. D., Latifi, T., and Groisman, E. A. (2005). Transcriptional regulation of the 4-amino-4-deoxy-L-arabinose biosynthetic genes in *Yersinia pestis*. *J. Biol. Chem.* 280, 14765–14772. doi: 10.1074/jbc.M413900200
- Wosten, M., and Groisman, E. (1999). Molecular characterization of the PmrA regulon. *J. Biol. Chem.* 274:38. doi: 10.1074/jbc.274.38.27185
- Wosten, M., Kox, L., Chamnongpol, S., Soncini, F., and Groisman, E. (2000). A signal transduction system that responds to extracellular iron. *Cell* 103, 113–125. doi: 10.1016/s0092-8674(00)00092-1
- Zavaglia, G. A., Kociubinski, G., Pérez, P., Disalvo, E., and De Antoni, G. (2002). Effect of bile on the lipid composition and surface properties of bifidobacteria. *J. Appl. Microbiol.* 93, 794–799. doi: 10.1046/j.1365-2672.2002.01747.x
- Zhang, H., Li, Y., Wang, C., and Wang, X. (2018). Understanding the high L-valine production in *Corynebacterium glutamicum* VWB-1 using transcriptomics and proteomics. *Sci. Rep.* 8:3632. doi: 10.1038/s41598-018-21926-5
- Zhou, Z., Ribeiro, A. A., Lin, S., Cotter, R. J., Miller, S. I., Raetz, C. R., et al. (2001). Lipid A modifications in polymyxin-resistant *Salmonella typhimurium*: PMRA-dependent 4-amino-4-deoxy-L-arabinose, and phosphoethanolamine incorporation. *J. Biol. Chem.* 276, 43111–43121. doi: 10.1074/jbc.M106960200
- Conflict of Interest:** The authors declare that the research was conducted in the absence of any commercial or financial relationships that could be construed as a potential conflict of interest.

Copyright © 2020 Hua, Jia, Zhang and Li. This is an open-access article distributed under the terms of the Creative Commons Attribution License (CC BY). The use, distribution or reproduction in other forums is permitted, provided the original author(s) and the copyright owner(s) are credited and that the original publication in this journal is cited, in accordance with accepted academic practice. No use, distribution or reproduction is permitted which does not comply with these terms.



Isolation of Antibacterial, Nitrosylmyoglobin Forming Lactic Acid Bacteria and Their Potential Use in Meat Processing

Yinglian Zhu* and Qingli Yang

College of Food Science and Engineering, Qingdao Agricultural University, Qingdao, China

OPEN ACCESS

Edited by:

Xihong Zhao,
Wuhan Institute of Technology, China

Reviewed by:

Shumin Yi,
Bohai University, China
Qilong Shi,
Shandong University of Technology,
China

*Correspondence:

Yinglian Zhu
cjs52002@163.com

Specialty section:

This article was submitted to
Food Microbiology,
a section of the journal
Frontiers in Microbiology

Received: 17 April 2020

Accepted: 25 May 2020

Published: 19 June 2020

Citation:

Zhu Y and Yang Q (2020) Isolation
of Antibacterial, Nitrosylmyoglobin
Forming Lactic Acid Bacteria
and Their Potential Use in Meat
Processing.
Front. Microbiol. 11:1315.
doi: 10.3389/fmicb.2020.01315

The use of nitrite as a colorant and preservative in meat processing is associated with health risks. This study aimed to isolate nitrite-substituting lactic acid bacteria for use as natural biological colorants and preservatives. Among the 106 strains isolated from fermented foods, two strains with excellent ability to convert myoglobin and metmyoglobin (Met-Mb) to red nitrosylmyoglobin (Mb-NO) were selected. The superior ability to form Mb-NO was confirmed through UV-visible spectrophotometry, Fourier transform infrared spectrometry, electron spin resonance analysis, nitric oxide synthase activity assay, and Met-Mb reductase activity assay. The potent antibacterial activity was confirmed through biofilm and cytomembrane breakage of the indicator bacteria. Though performing 16S rDNA sequencing, they were identified as two different strains of *Lactobacillus plantarum*. Based on their favorable characteristics, their applications in the meat industry were further evaluated. This study identified a novel dual-function natural biological colorant and preservative to substitute nitrite in meat products. The application of the two strains would decrease the hazardous of nitrite to health.

Keywords: lactic acid bacteria, nitrosylmyoglobin, antibacterial activity, meat, nitrite, colorant

INTRODUCTION

Color is a very important sensory property for meat processing since it affects the freshness and quality of meat and meat products (Ramanathan et al., 2011; Biswas et al., 2012). The most common approach to retain color and freshness of meat products is to add food additives like nitrite to the meat products. Addition of nitrite can cure the red color of meat products and extend their shelf life. Unfortunately, the use of nitrite as a food additive can lead to the formation of strong carcinogens, resulting in the development of esophageal and stomach cancers on long-term consumption (Rosato et al., 2019). Consequently, the demand for nitrite-free meat products has increased, and the effort to develop nitrite substitutes for the curing of meat products has intensified.

Lactic acid bacteria (LAB) are a group of gram positive, non-spore forming, micro-aerophilic cocci and rods, which produce lactic acid (Domingos-Lopes et al., 2017). Since previous studies (Arihara et al., 1993) have reported the ability of *Lactobacillus fermentum* JCM1173 to convert brown metmyoglobin (Met-Mb) to bright red myoglobin derivatives, numerous researchers have demonstrated the chromogenic ability of LAB in meat products such as fresh meat, dry meat, etc. (Luo et al., 2013; Chen et al., 2016; Deraz and Khalil, 2018). The characteristic pink color of nitrite-free sausages can be achieved by using 10^8 CFU/g of *L. fermentum* AS1.1880 as starting culture in

meat batters (Zhang et al., 2007). Studies have also reported the beneficial effect of *Lactobacillus salivarius* on the color stability of fresh pork (Luo et al., 2013). The nitrite reductase activity of the strains promotes nitroization of myoglobin and intensifies the formation of nitrosylmyoglobin (Mb-NO), which provides a typical pink color to meat products (Chen et al., 2016). Furthermore, the role of Nitric Oxide (NO) was studied while substituting nitrite with three lactic acid bacterial strains. The results showed that both nitrate reductase and nitric oxide synthase (NOS) participated in the formation of Mb-NO (Gou et al., 2019). All the aforementioned studies have demonstrated the great potential of LAB to form a characteristic pink color and maintain the color stability of meat products.

Additionally, LAB are considered as generally regarded as safe (GRAS) strains for human consumption (Liu et al., 2011). They are not only beneficial for the balance of the intestinal flora, but they also inhibit the growth of undesired microorganisms. Previous studies have shown that LAB inhibits the growth of spoilage organisms (Angmo et al., 2016) and fungal pathogens (Gerez et al., 2010). Thus, the addition of LAB strains could prolong the shelf-life of meat products. Moreover, the addition of LAB could result in large differences in organoleptic, biochemical, and flavor characteristics of food products, owing to their physiological features like substrate utilization, metabolic capabilities, and probiotic properties (Bao et al., 2012). Therefore, the selected LAB strains can function as ideal alternatives for nitrite, owing to their ability to intensify color and inhibit the growth of spoilage organisms. However, previously reported LAB didn't have simultaneous antibacterial and Mb-NO-synthesizing functions, and NOS and Met-Mb reductase activity were low.

The objective of this study was to isolate bacterial strains with simultaneous Mb-NO-synthesizing and antibacterial functions for use as biological colorants and preservatives, thereby allowing for the substitution of nitrite, either partly or wholly, in meat products. The physiological characteristics of the isolates support their potential for use in the meat industry, like dynamic growth, acid production ability, and tolerance to chemical additives like NaCl and NaNO₂, were assessed.

MATERIALS AND METHODS

Strains

Escherichia coli (*E. coli*) (CGMCC 1.8723) and *Staphylococcus aureus* (*S. aureus*) (CGMCC 1.8721) were provided by the China General Microbiological Culture Collection Center (Beijing, China) and preserved in the Microbial Fermentation Engineering Laboratory, Qingdao Agricultural University (Qingdao, Shandong, China). Luria-Bertani (LB) medium was used for activation and culturing of the indicator bacteria.

Isolation of LAB Strains From Fermented Products

The isolation of LAB was performed in accordance with a previously reported protocol (Luo et al., 2013). Sausage samples (25 g) were cut into pieces and added to 225 mL of sterile saline solution (0.85%). The mixture was homogenized for 90 s

to obtain a 1:10 sample homogenate with a BagMixer (400CC, Interscience, Saint Nom, France).

For yogurt, 25 mL of yogurt sample was added to 225 mL of sterile saline solution (0.85%) containing glass beads, and the mixture was shaken thoroughly to obtain a 1:10 sample homogenate. The samples continued to be diluted to 10-fold series. Subsequently, 0.1 mL of this dilution was spread on an MRS agar plate containing 2% CaCO₃ and incubated at 37°C for 48 h. The gram positive colonies, identified by the presence of a clear dissolved calcium circle surrounding the colony on the agar plate, were picked as candidate LAB strains.

Chromogenic Effect in Met-Mb-Containing Medium

Met-Mb solution (20 mg/mL) was heated at 50°C for half an hour to inhibit any residual Met-Mb reductase activity. Following filtration on a microporous membrane, Met-Mb was added to MRS medium to attain a final myoglobin concentration of 2 mg/mL. The selected strains were inoculated, and immediately covered with a layer of paraffin oil to prevent oxidation during incubation. Subsequently, the strains were incubated anaerobically at 37°C until the medium turned red. The strains were not inoculated in the control group.

Antibacterial Activity

The strains were further screened for their antibacterial activity. The selected strains were cultivated at 37°C for 24 h, and centrifuged at 10,000 × *g* for 10 min, at 4°C. The supernatant pH was adjusted with NaOH (1 mol/L) to 6.0 to eliminate the interference of organic acids, and then was used to test for antibacterial activity against *E. coli* and *S. aureus* through agar well diffusion method in LB agar plate with the diameter of Oxford cup 6 cm (Gerez et al., 2010).

Physiological and Biochemical Reactions

The selected strains were studied for certain physiological and biochemical reactions consisting of amino acid decarboxylase activity (including lysine, ornithine, and arginine), glucose aerogenesis, lipoxidase activity, and their ability to produce lactic acid and H₂S (Luo et al., 2013).

Chromogenic Effect in Meat Products

Fresh lean pork was purchased from the local supermarket and minced. The control contained 3% sodium chloride, 2% glucose, and 0.01% nitrite. The inoculated groups (nitrite-free) contained 3% sodium chloride, 2% glucose, and the appropriate volume of inoculum (about 8 log CFU/g of batters). Each sample was enclosed in plastic intestines with 100 g of batters and cured at 4°C for 24 h, then fermented at 37°C for 4 h in 85% humidity. The sausages were baked in a smoke house at 85°C for 1.5 h until the internal temperature reached 74°C. Subsequently, they were smoked at 85°C for 3.5 h using wood chip, and cooled below 10°C for storage. The chromatic value of the meat samples was evaluated using the CIELAB system (CromaMeter CR-400, Conica Minolta, Japan), and the average

value of lightness (L^*), redness (a^*), and yellowness (b^*), was recorded (Cullere et al., 2018).

Effect of Mb-NO Formation

The selected strains were cultured at 37°C anaerobically until the inoculum turned red. Subsequently, the inoculum was centrifuged at $10,000 \times g$ for 10 min, at 4°C. The Mb-NO formed was detected by measuring the absorption of the supernatant using a UV-Vis spectrophotometer (UV-6000PC, Shanghai Metash Instruments Co., Ltd., China) at wavelengths ranging from 400 to 700 nm, at 1 nm intervals, in accordance with a previously reported protocol (Møller et al., 2003). The presence of Mb-NO in the supernatant was further determined by the electron spin resonance (ESR) analysis method described previously (Gøtterup et al., 2007), with minor alternations. Each sample (0.2 mL) was transferred to an ESR tube and analyzed on a Bruker ESC 106 spectrometer (JES-TE2X, JEOL Ltd., Tokyo) using the following conditions: microwave power, 4 mW; modulation frequency and width, 100 kHz and 1.0 mT; temperature, 77 K; measurement time, 8 min.

Extraction of NO-Mb from meat products was performed in accordance with a previously reported protocol (Gao et al., 2014), with slight modifications. The fermented samples (10 g) were minced and homogenized in 90 mL phosphate buffer (pH 6.0, 20 mM) for 1.5 min with a high-speed beating BagMixer (400CC, Interscience, Saint Nom, France). Following incubation in a dark room at 4°C for 1 h, the homogenates were centrifuged at $6000 \times g$ for 10 min. The extracted, cured pigment was filtered on a nitrocellulose membrane. The Mb-NO analysis was performed using a UV-Vis spectrophotometer (UV-6000PC, Shanghai Metash Instruments Co., Ltd., China) at wavelengths ranging from 350 to 700 nm, at 1 nm increments. The Fourier transform infrared (FTIR) spectra of the extracted pigment was analyzed from 550 to 3750 cm^{-1} on a FTIR Spectrometer (Nexus 470, Nicolet Instrument Corp, United States).

NOS Activity and Met-Mb Reductase Activity

Enzyme extraction was performed following cultivation of the strains at 37°C for 24 h. After centrifugation at $10,000 \times g$ for 10 min, at 4°C, the cell pellets were washed thrice using 2.0 mM phosphate buffer solution (PBS, pH 7.0) and the supernatant was stored as later use. The washed cell pellets were re-suspended in 4 mL of 2.0 mM PBS (pH 7.0), and subjected to ultrasonic disruption at 4°C for 10 min, with 800 W power and 50% amplitude. Following disruption, the cell supernatant was mixed with the previously stored supernatant and used as enzyme extracts to detect the enzyme activity of the cells.

NOS activity was measured according to the method described by Luo et al. (2013). The NOS assay reaction system (1 mL) comprised of 50 mM PBS (pH 7.0), 1.0 mM CaCl_2 , 10 μM Flavin Adenine Dinucleotide (FAD), 10 μM Flavin Mononucleotide (FMN), 0.1 mM Nicotinamide Adenine Dinucleotide Phosphate (NADPH), and 0.5 mL of enzyme extracts. The reaction was initiated by the addition of L-arginine (1.0 mM). NADPH was oxidized during the conversion of L-arginine to L-citrulline, and

its consumption was assessed by the decrease in absorbance at 340 nm. NOS activity was determined as the NADPH consumption per min per ml of enzyme extract.

Met-Mb reductase activity was measured according to the method described by Luo et al. (2013). The assay mixture contained 0.1 mL of 5.0 mM EDTA, 0.1 mL of 50 mM PBS (pH 7.0), 0.1 mL of 3.0 mM $\text{K}_4\text{Fe}(\text{CN})_6$, 0.1 mL of ultrapure water, 0.2 mL of 0.75 mM Met-Mb in 2.0 mM PBS (pH 7.0), 0.3 mL of enzyme extract, and 0.1 mL of 2.0 mM NADH. The reaction was initiated by the addition of NADH at 25°C, and the absorbance at 580 nm was measured every 12 s for 5 min, until no change in absorbance was observed. The difference in the absorbance at 580 nm for Met-Mb and Oxy-myoglobin (MbO_2) reached the maximum, and the molar extinction coefficient was 1.2×10^4 L/molcm. Met-Mb reductase activity was defined as the change in absorbance per min per ml of enzyme extract.

Antibacterial Characteristics of the Selected Strains

Dynamic growth of indicator bacteria: After culturing *E. coli* and *S. aureus* at 37°C for 24 h and centrifugation at $10,000 \times g$ for 10 min at 4°C, the cells were collected and suspended in LB broth to obtain a bacterial concentration of 10^5 CFU/mL. Subsequently, 5 mL of the bacterial suspension was mixed with an equal volume of the fermentation supernatant of the selected strains and incubated at 37°C. Dynamic growth of the indicator bacteria was assessed every 2 h by plotting the absorbance curve at 600 nm according to the method of Lv et al. (2018), using a UV spectrophotometer (TU-1810, Purkinje, China). The LB broth which provided the substitute for the fermentation supernatant of the selected strains, was used as the control.

Fluorescence spectrum analysis: After being centrifuged at $10,000 \times g$ for 10 min, at 4°C, and washed thrice using PBS (pH 7.0), the above treated indicator bacterial cells were harvested. Then the indicator bacterial cells were stained by addition of 20 μL fluorescein diacetate (FDA), 60 μL propidium iodide (PI), and 920 μL sterile saline solution (0.85%), and placed in the dark for 12 h at 4°C (Yu et al., 2017). A fluorescent spectrum scan was conducted using a fluorescence spectrophotometer (F-4600, HITACHI, Japan), at an excitation wavelength of 450 nm.

Fluorescence microscope analysis: The stained indicator bacterial cells were centrifuged at $10,000 \times g$ for 10 min at 4°C and washed three times with PBS (pH 7.0), and then re-suspended in 1 mL PBS (pH 7.0). The re-suspended cells were detected using a fluorescence microscope.

16S rDNA Sequence Analysis

The selected strains were identified by 16S rDNA sequence analysis. The template DNA of each strain was extracted in accordance with a previously reported protocol (Minas et al., 2011). The PCR mix (50 μL) included template DNA (1 μL), forward primer (2 μL), reverse primer (2 μL), dNTPs (4 μL), Taq DNA polymerase (1 μL), PCR buffer (with Mg^{2+}) (5 μL), and ddH₂O (35 μL). The 16S rDNA was amplified by PCR using the following universal primers: forward primer 8F (5'-AGAGTTTGATCCTGGCTCAG-3'), and reverse

primer 1492R (5'-TACGGCTACCTTGTACGACTT-3'). The PCR amplification program comprised of pre-denaturation at 94°C for 5 min, and 30 cycles of denaturation at 94°C for 30 s, annealing at 55°C for 30 s, and extension at 72°C for 1.5 min, followed by further extension at 72°C for 10 min with a PCR instrument (PCT-1148, BIO-RAD, United States). The PCR products were separated by agarose gel electrophoresis (1%, w/v) at 80 V for 30 min, and the gels were scanned using a gel documentation system, and analyzed using the DNA Bio Imaging Systems Software. The 16S rDNA sequencing was performed at Sangon Biotechnology Co., Ltd. (Shanghai, China). The sequences were acquired using the BioEdit software, and submitted to the National Center for Biotechnology Information (NCBI), and their accession numbers were MH357373 and MH357374, respectively. Thereafter, the sequences were compared with the sequences in the GenBank database using the Basic Local Alignment Search Tool (BLAST) program¹.

Physiological Characteristics of the Isolates for Meat Processing Use

Following cultivation of the selected strains at 37°C for 24 h, 1 mL of the inoculum was added to 100 mL of MRS broth and incubated at 37°C. Dynamic growth of each strain was assessed by measuring the absorbance at 600 nm, every 2 h using a UV spectrophotometer (TU-1810, Purkinje, China), as described by Polak-Berecka et al. (2013), with minor modifications. The tolerance of the selected strains to sodium chloride was examined by inoculating the strains in MRS broth containing 0 (control), 2, 4, 6, 8, 10, and 12% (w/v) NaCl, respectively, and incubating at 37°C for 24 h. The tolerance of the selected strains to sodium nitrite was detected by inoculating the strains in MRS broth containing 0 (control), 20, 40, 60, 80, 100, and 120 mg/mL sodium nitrite, respectively, and incubating at 37°C for 24 h. The cell density of each strain following cultivation was assessed by measuring the absorbance at 600 nm, using a UV spectrophotometer (TU-1810, Purkinje, China). The acid production ability of the selected strains was examined by inoculating the strains in MRS broth, and incubating at 37°C. The pH of the broth was measured using a pH meter (ORP-013M, Kelilong Electron Co., Ltd., China) at 0, 2, 4, 6, 8, 10, and 12 h, respectively.

Statistical Analysis

Statistical analysis was carried out with SPSS Version 18.0 and the data was analyzed with multiple comparisons with Duncan method. Probability level of 0.05 was accepted as a significance limit.

RESULTS

Isolation of LAB Strains

One hundred and six Gram positive strains were selected in terms of colony morphology, size, presence of a calcium

dissolved circle, and Gram staining. Among them, 12 strains with chromogenic effect were picked and inoculated in Met-Mb-containing medium. The antibacterial activity of the 12 strains is listed in **Table 1**. **Table 1** shows that strains e, 2, and 33 had the best antibacterial activity against *S. aureus*, while strains b, d, e, 2, 32, and 33 had the best antibacterial activity against *E. coli*. Consequently, the six strains b, d, e, 2, 32, and 33 with the value (D2/D1 and D3/D1) over 2.0 were selected for further study.

The physiological and biochemical characteristics of the six strains are listed in **Table 2**. The results showed that all six strains produced lactic acid, did not show any H₂S producing capability, lipoxidase activity, and lysine, ornithine, arginine decarboxylase activity. However, strain b and strain 33 had glucose aerogenesis capability, which might have negative effect on the texture of meat products. Consequently, the four strains d, e, 2, and 32 were chosen for further chromogenic activity study.

Chromogenic Activity in Meat Products

In **Figure 1A**, the *L** value of the inoculated groups d and e was 51.82 and 52.75, respectively, which showed no significant difference in comparison with the control ($P > 0.05$). The *a** value was 15.07 for group d, which was no significant difference with the control ($P > 0.05$), but higher than other inoculated groups ($P < 0.05$). The *a** value of group e was 16.13 and was higher than both the control and other inoculated groups ($P < 0.05$). The *b** value of the groups d and e was lower than other inoculated groups ($P < 0.05$), and had no significant difference in comparison with the control ($P > 0.05$). The results indicated that the strains d and e had excellent chromogenic activity in meat products, as compared to the control and other strains. **Figure 1B** shows the absorbance peaks of the two inoculated groups d and e, and the control, which were at 421, 548, and 579 nm, respectively. These values almost matched the typical absorbance peaks of Mb-NO (Gao et al., 2014). In the

TABLE 1 | Antibacterial activity of the two selected strains.

Strains	<i>E. coli</i> (D2/D1)	<i>S. aureus</i> (D3/D1)
Strain a	1.81 ± 0.12 ^a	1.64 ± 0.05 ^a
Strain b	1.94 ± 0.22 ^{abcde}	1.88 ± 0.21 ^{abc}
Strain c	1.75 ± 0.06 ^a	1.86 ± 0.11 ^{ab}
Strain d	2.22 ± 0.07 ^e	1.88 ± 0.08 ^{abc}
Strain e	2.18 ± 0.11 ^{de}	2.21 ± 0.15 ^d
Strain 2	2.14 ± 0.10 ^{bcdde}	2.11 ± 0.09 ^{bcd}
Strain 3	1.85 ± 0.09 ^{ab}	1.71 ± 0.10 ^a
Strain 8	1.88 ± 0.21 ^{abc}	1.73 ± 0.28 ^a
Strain 18	1.73 ± 0.33 ^a	1.85 ± 0.15 ^{ab}
Strain 32	2.03 ± 0.08 ^{abcde}	1.90 ± 0.08 ^{abc}
Strain 33	2.16 ± 0.10 ^{cde}	2.15 ± 0.02 ^{cd}
Strain 44	1.93 ± 0.22 ^{abcd}	1.65 ± 0.19 ^a

Values are represented as means ± SD from triplicate experiments. different lowercase superscript in the same column indicates that the antibacterial effect is significantly different ($P < 0.05$); D2 denotes the diameter of the zone of inhibition against *E. coli*; D3 denotes the diameter of the zone of inhibition against *S. aureus*; D1 denotes the diameter of Oxford cup; The ratio of diameter (D2/D1 and D3/D1) is used to indicate antibacterial activity.

¹ <http://blast.ncbi.nlm.nih.gov>

TABLE 2 | Physiological and biochemical characteristics of the six strains.

Strain	Lactic acid production	H ₂ S production	Lysine decarboxylase activity	Ornithine decarboxylase activity	Arginine decarboxylase activity	Glucose aerogenesis	Lipoxidase activity
Strain b	+	—	—	—	—	+	—
Strain d	+	—	—	—	—	—	—
Strain e	+	—	—	—	—	—	—
Strain 2	+	—	—	—	—	—	—
Strain 32	+	—	—	—	—	—	—
Strain 33	+	—	—	—	—	+	—

The sign “+” denotes a positive reaction, and “—” denotes a negative reaction.

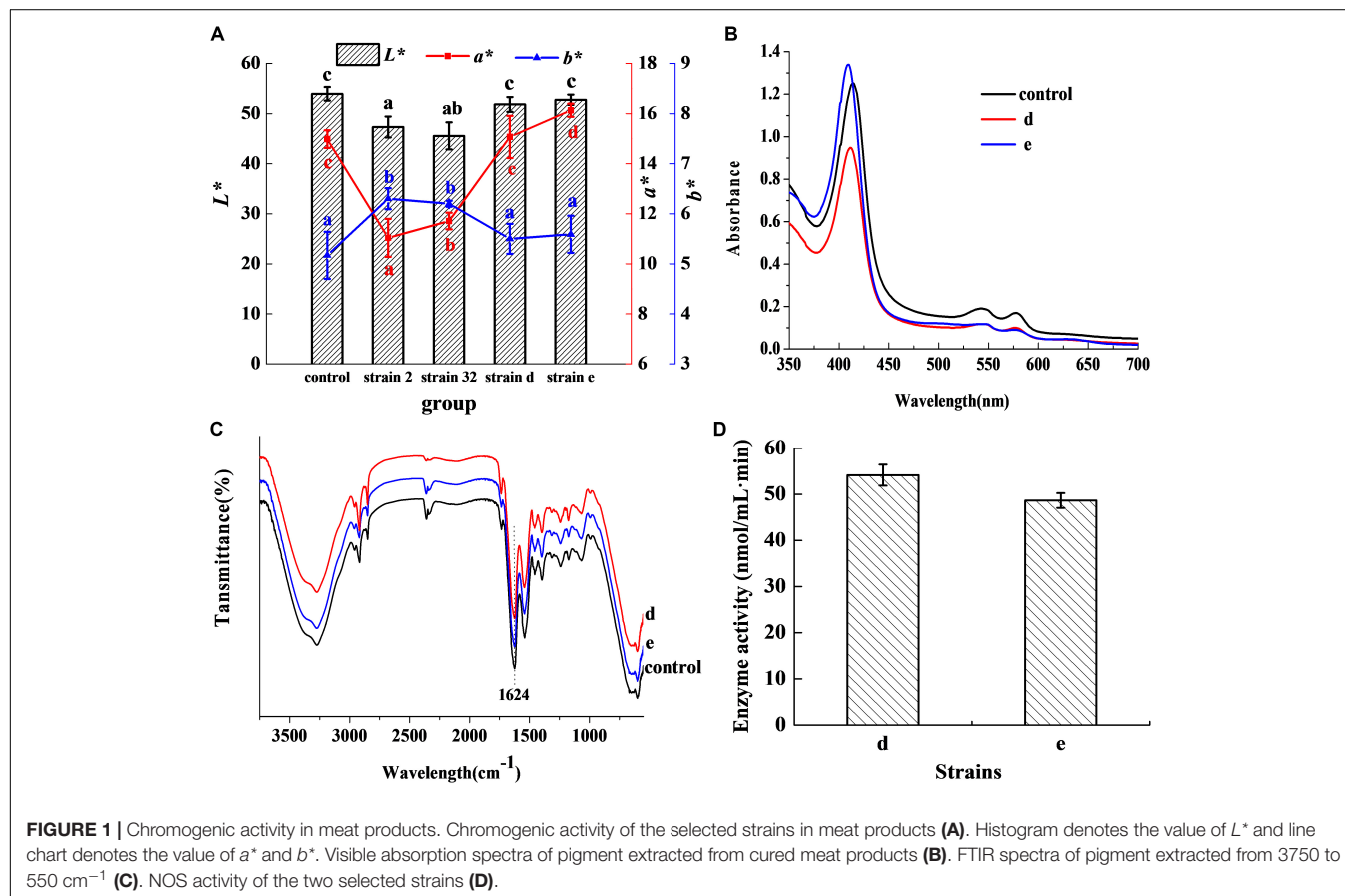


FIGURE 1 | Chromogenic activity in meat products. Chromogenic activity of the selected strains in meat products (A). Histogram denotes the value of L^* and line chart denotes the value of a^* and b^* . Visible absorption spectra of pigment extracted from cured meat products (B). FTIR spectra of pigment extracted from 3750 to 550 cm^{-1} (C). NOS activity of the two selected strains (D).

FTIR of extracted pigment, the bands at 1624 cm^{-1} of the three groups (Figure 1C) coincided with the stretching frequency of Fe-NO (Maxwell and Caughey, 1976), which further confirmed that Mb-NO was present in the control and the two inoculated groups, d and e. Figure 1D indicated that both the selected strains d and e had NOS activity.

Mb-NO Formation Effect

Figure 2A revealed that the control group had two absorbance peaks at approximate wavelengths of 505 and 635 nm, which are the typical absorbance peaks of Met-Mb (Li et al., 2016). However, both experimental samples had two new absorbance peaks at approximate wavelengths of 545 and 579 nm, which were consistent with the typical absorbance peaks of Mb-NO (Gao

et al., 2014). Figure 2B shows that both the selected strains d and e possessed Met-Mb reductase activity. Met-Mb reductase activity was calculated as the Met-Mb reduced during the initial linear phase when the absorbance values at 580 nm increased in a short time. The presence of Mb-NO was further verified by ESR as seen in Figure 2C. Significant ESR signals of the g factors (around 2.0) were observed in groups with NaNO_2 addition, strains d and e inoculation, while no signal of the g factors (around 2.0) was detected in the control group lacking any additives.

Antibacterial Ability

Figure 3 shows that the fermentation products of the selected strains, d and e, had the ability to significantly inhibit the dynamic growth of the two pathogenic bacteria, *S. aureus* and *E. coli*,

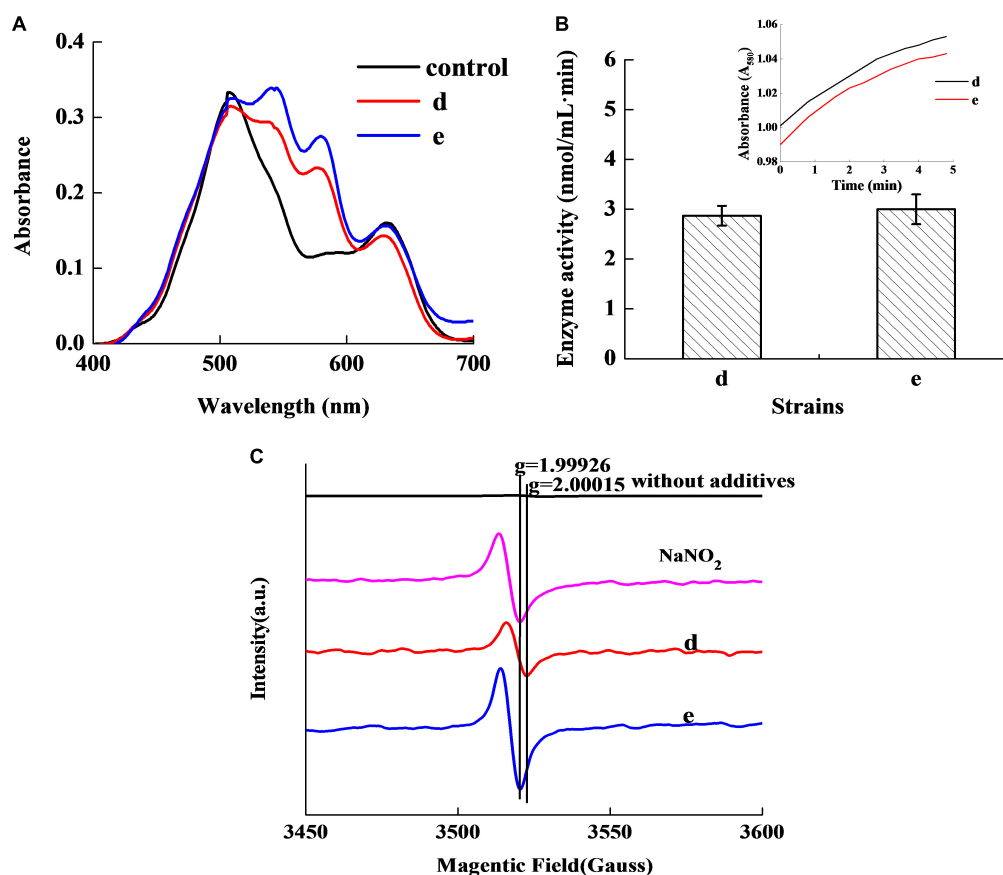


FIGURE 2 | Chromogenic activity of the two selected stains in Met-Mb-containing medium. Visible absorption spectra of pigment extracted from Met-Mb-containing MRS inoculum (A). Met-Mb reductase activity of the two selected strains (B). ESR spectra of pigment extracted from Met-Mb-containing MRS inoculum (C).

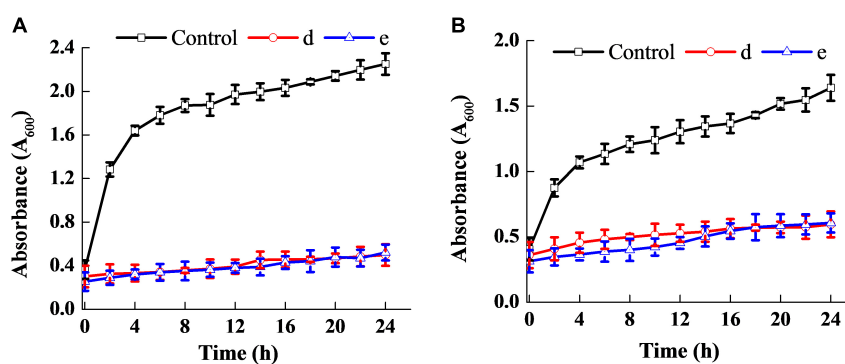


FIGURE 3 | Antibacterial ability of the two selected strains. Effect on the dynamic growth of *S. aureus* (A). Effect on the dynamic growth of *E. coli* (B).

with negligible change in the total counts of the two bacteria. **Figure 4** shows the fluorescence microscopic spectrum of the two indicator bacteria dyed with FDA and PI. Yellow-green fluorescence was observed in the control and red fluorescence mostly appeared in the two experimental samples. Fluorescence scan spectrum revealed that the untreated indicator bacteria had only one peak at 518 nm, which was the absorbance peak of FDA (**Figure 5**). However, a new absorbance peak appeared at

597 nm following treatment of the bacteria with the fermentation products of strains d and e.

Results of 16s rDNA

The 1468 and 1470 bp 16s rDNA fragments of strains d and e obtained during agarose gel electrophoresis are shown in **Figure 6**. BLAST analysis of the base sequence of 16s rDNA revealed that the two strains d and e were

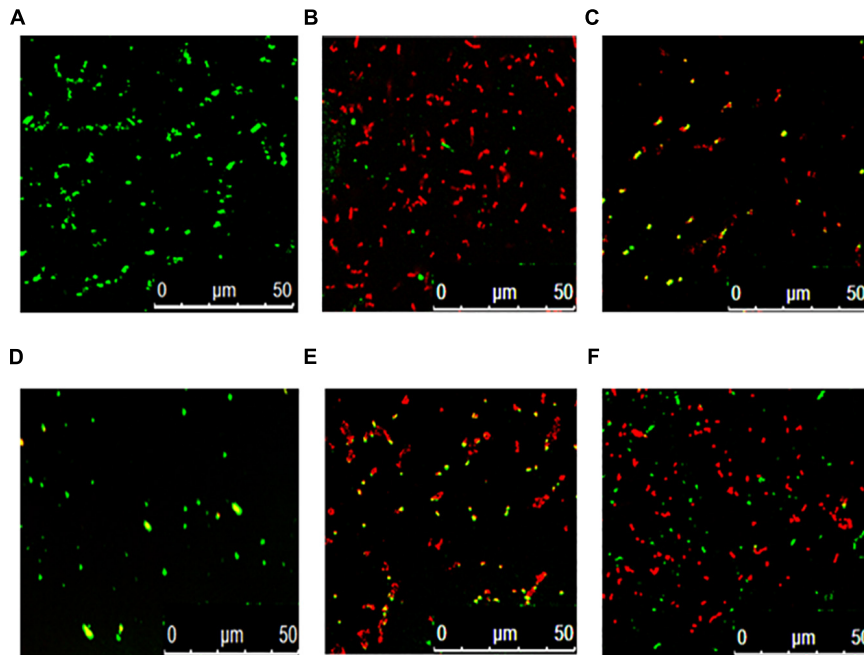


FIGURE 4 | Fluorescence microscopic spectrum of the two indicator bacteria dyed with FDA and PI: *E. coli* as control (A), *E. coli* treated with fermentation supernatant of strain d (B), *E. coli* treated with the fermentation supernatant of strain e (C), *S. aureus* as control (D), *S. aureus* treated with the fermentation supernatant of strain d (E), *S. aureus* treated with the fermentation supernatant of strain e (F).

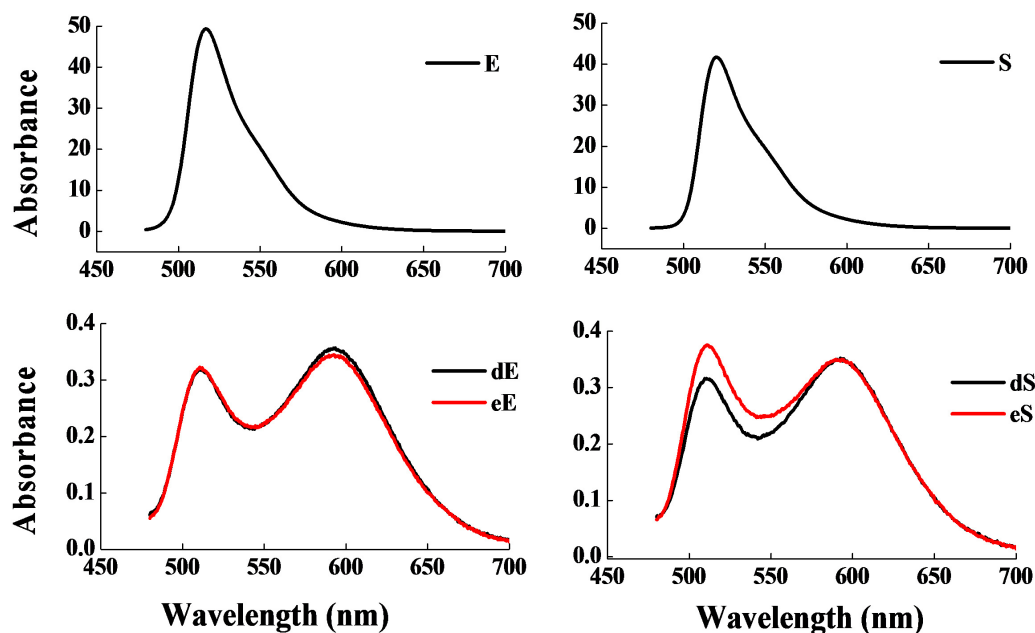
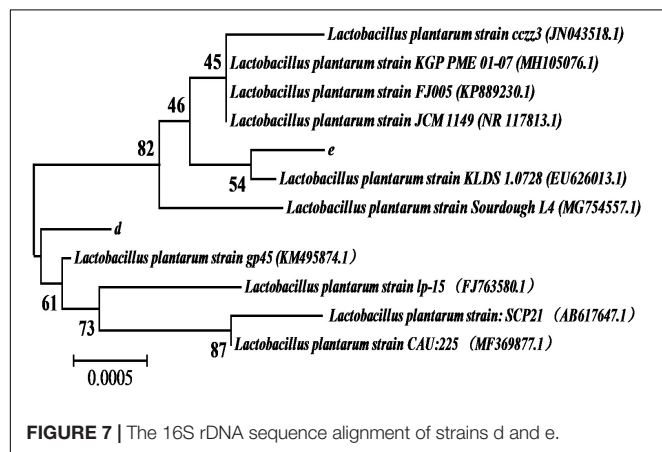
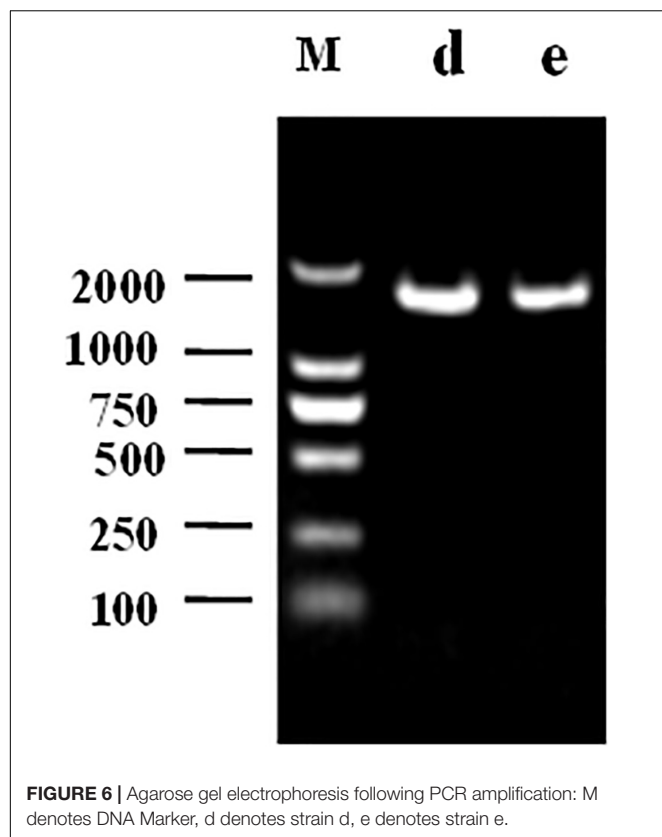


FIGURE 5 | Fluorescence scan spectrum of the two indicator bacteria dyed with FDA and PI: *E. coli* as control (E), *E. coli* treated with the fermentation supernatant of strains d (dE), *E. coli* treated with the fermentation supernatant of strain e (eE), *S. aureus* as control (S), *S. aureus* treated with the fermentation supernatant of strain d (dS), *S. aureus* treated with the fermentation supernatant of strain e (eS).

homogenous to *L. plantarum* (Figure 7), and the similarity was 99%. The sequences have been deposited in the GenBank database with the accession numbers MH357373 and MH357374,

respectively. The strains have been stored in the Microbial Fermentation Engineering Laboratory, Qingdao Agricultural University, China, and China General Microbiological Culture



Collection Center, and the strain numbers are CGMCC 17078 and CGMCC16130, respectively.

Physiological Characteristics of the Isolates for Meat Processing Use

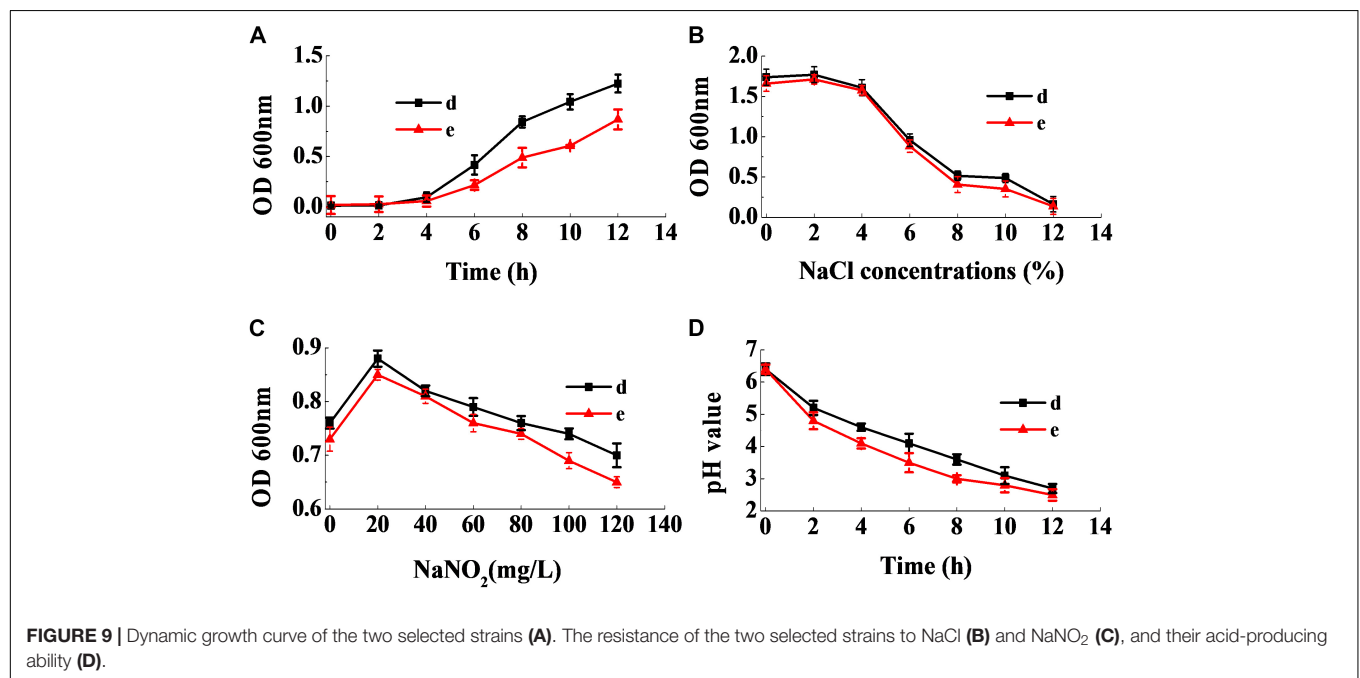
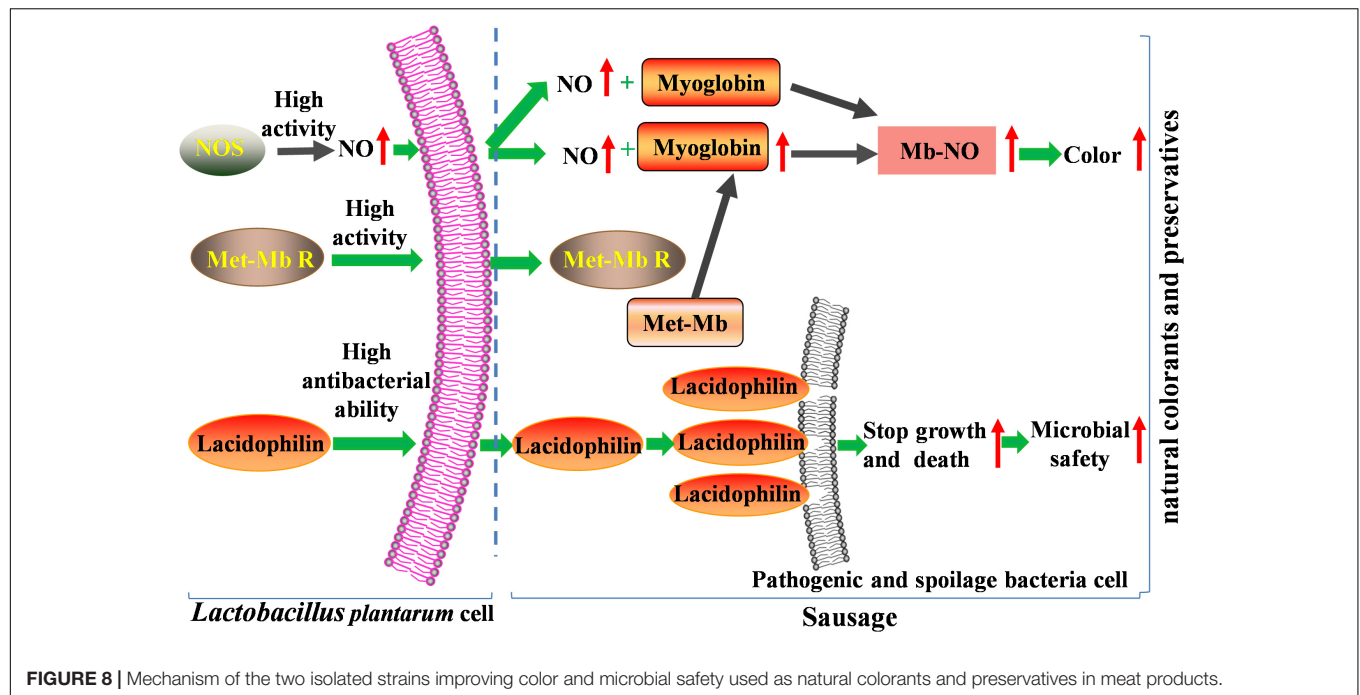
Figure 9A shows that the lag phase of the two strains were short, and the logarithmic phase of both strains began at the fourth hour, owing to their fast growth rate. **Figure 9B** reveals that a sodium chloride concentration less than 4% had no effect on the growth of the two strains, and that they were able to grow relatively well at a sodium chloride concentration of 10%. **Figure 9C** revealed that the strains had good sodium

nitrite tolerance. On addition of 120 mg/mL of sodium nitrite, the absorbance values of the inoculum reached above 0.6. Furthermore, as seen in **Figure 9D**, the two strains rapidly reduced the pH of the fermentation broth. Therefore, the physiological characteristics of the isolates illustrated that they had good potential for use in the meat industry.

DISCUSSION

As demonstrated, the typical absorbance peaks of oxymyoglobin (MbO) were at 544 and 582 nm, while those of Mb-NO were at 548 and 579 nm, respectively (Millar et al., 1996). The typical peaks of Mb-NO were detected in the experimental samples as well as the control (**Figure 1B**), which indicates that the two strains in meat products produce chromogenic effects similar to that of nitrite. Additionally, previous research has reported that the stretching frequency of Fe-NO in FTIR was in the range of 1600–1700 cm^{-1} (Maxwell and Caughey, 1976). Hence, the bands at 1624 cm^{-1} (**Figure 1C**) correspond to the stretching frequency of Fe-NO, which further confirms that the two strains form Mb-NO in a nitrite-free manner. Mb-NO is an important pigment responsible for the attractive pink color of meat products, and it forms a stable color on heating (Kim et al., 2019). Mb-NO in the control sample was generated through the interaction between myoglobin and NO, which was produced from nitrite (Gao et al., 2014). Therefore, the two strains inoculated in meat products generated NO during the fermentation process, which was further confirmed by presence of NOS (**Figure 1D**). So the NOS pathway is the major source of NO in the two strains, which forms Mb-NO instead of depending on nitrite, and the NOS function was also proposed in strains *Lactobacillus salivarius* (Luo et al., 2013) and coagulase-negative staphylococci (Huang et al., 2019). But the NOS activity of the two strains (54.15 and 48.65 nmol/mLmin) was significantly higher than that previously reported (34.14 nmol/mLmin) (Luo et al., 2013), which constitutes a novel finding herein, showing that the two strains had robust Mb-NO-synthesizing and nitrite-substituting potential.

The absorption bands of the experimental samples (**Figure 2A**) indicated that the two strains can revert Met-Mb, which also confirmed by Met-Mb reductase activity of the strains (**Figure 2B**). The presence of Met-Mb might cause the meat to appear brown. The Met-Mb reductase was the controlling factor in retarding the accumulation of Met-Mb (Chiou et al., 2001) and played key role in the color stability of meat products (Djimisa et al., 2017). As shown in **Figure 2C**, the ESR signals of the g factors (around 2.0) in the experimental samples and the control were all detected, which showed paramagnetic characteristics of typical penta-coordinate Mb-NO (Götterup et al., 2007). Thus, ESR result indicates the existence of Mb-NO as one of the Met-Mb reduction products. The Met-Mb reductase activity of strains d (2.87 nmol/mLmin) and e (3.01 nmol/mLmin) was higher than that reported previously (0.21 nmol/mLmin), indicating that the two strains can regulate color stability in meat products than previously reported strains by the reduction of Met-Mb greatly.



FDA emitted yellow-green fluorescence under a blue laser when it was bound to living cells (Xiao et al., 2011). However, PI was a cell-membrane impermeable fluorescent dye which exclusively combined with DNA in cells that were dead or had broken membranes and emitted red fluorescence (Boyd et al., 2008). Fluorescence microscopic analysis illustrated that the fermentation products of strains d and e destroyed the biofilm and cytomembrane of indicator bacteria, resulting in most cell death (Figures 4B,C,E,F). For fluorescence spectrum,

compared with the control, the new absorbance peaks were typical absorbance peaks of PI (Figure 5), which also indicated the destruction of biofilm and cytomembrane of the indicator bacteria by the fermentation products of strains d and e. Peaks at 518 nm had a blue-shift, which attributed to the fewer amount of the treated bacteria compared to the control. The stronger antibacterial ability of the two strains attributed to the Lacidophilin production during fermentation (Liu et al., 2017), which damage the protective effect of biofilm and cytomembrane

of the indicator bacteria. Several of the *L. plantarum* strains have been used as probiotics (Geeta and Yadav, 2017). Hence, they had potential to replace nitrite as preservative in meat products. This is an innovative result for natural biological colorants that has not confirmed by other studies.

Therefore, in the present study, high activity of NOS and Met-Mb reductase of the two strains promote accumulation of nitric oxide and myoglobin, which result in the Nb-NO production and color formation increase significantly. Moreover, high antibacterial ability of lacidophilin induces most pathogenic and spoilage bacteria to death through cell-membrane destruction, which enhances microbial safety of meat products. So the two isolated strains with superior dual functions have great potential to substitute nitrite (Figure 8).

The physiological, biochemical and phenotypic characteristics are the basis for identifying LAB, and also the prerequisite for exploring its potential value (Guley et al., 2015; Vasiee et al., 2018). The amino acid decarboxylase activity has been described in many microorganisms. However, lysine, ornithine and arginine decarboxylase, leads to the production of cadaverine, putrescine, and spermine, respectively, which increases the toxicity and risk of fermented foods, especially meat products (Espinosa-Pesqueira et al., 2018). Additionally, lipid antioxidant enzyme results in the oxidation and acidification of high-fat food products (Mukumbo et al., 2020) and glucose aerogenesis affects the texture of sausages. Moreover, the absence of H₂S affects the flavor and leads to the spoilage of fermented foods (Luo et al., 2013). Hence, only strains d, e, 2, and 32 were feasible for application in food products, since they didn't possess the characteristics of amino acid decarboxylase, lipid antioxidant enzyme, glucose aerogenesis, and H₂S production (Table 2). The strains d and e were further selected as candidate strains owing to their strong color formation effect.

The two strains d and e exhibited a rapid growth rate, which enabled them to become dominant strains and inhibit the growth of other bacteria effectively (Figure 9A). Lucke and Hechelmann reported that, if the initial concentration of sodium chloride in fermented sausages were about 3%, the resultant concentration could go up to more than 3% at the end of the ripening stage (Lucke and Hechelmann, 1987). Our findings show that the tolerance of the two strains to sodium chloride was much stronger than *L. curvatus* and *Pediococcus acidilactici*, the ubiquitous starting cultures used in fermented sausages. In addition, although certain nitrite-replacers have been identified for application in fermented sausages, the addition of sodium nitrite was essential, since no alternative could substitute nitrite completely. Therefore, the starting cultures were required to grow normally in the presence of at least 100 mg/mL of sodium nitrite (Özcelik et al., 2016). Figure 9C shows that the strains grew well in the presence of 120 mg/mL of sodium nitrite. Moreover, the two strains had the ability to rapidly reduce the pH of the fermentation broth (Figure 9D), which is an essential characteristic of starting cultures. Additionally, low pH stimulates the release of actin-derived peptides, which provides unique flavors to the sausages (Berardo et al., 2017). Our results illustrate that the two strains have superior industrial potential for use as starting cultures in meat products than previous reported strains.

CONCLUSION

In conclusion, the two LAB strains having both chromogenic and antibacterial activity were screened, and identified as *L. plantarum* using 16S rDNA sequence analysis. They had a higher ability to convert myoglobin and Met-Mb to red Mb-NO than previously reported strains owing to high NOS and Met-Mb reductase activity. Importantly, they had great antibacterial activity through destruction of the biofilm and cytomembrane of indicator bacteria, which has not been confirmed for natural biological colorants by other studies. Besides, the two strains possessed all the good characteristics required for use in meat products, like high growth rate, rapid acid production ability, and strong tolerance to sodium chloride and nitrite. Consequently, the two strains have great potential for application as partial or whole nitrite replacers in meat products, owing to their high potential for synthesizing Mb-NO and their antibacterial activity, and the superior dual function for natural biological colorants has not been confirmed by other studies.

DATA AVAILABILITY STATEMENT

The datasets presented in this study can be found in online repositories. The names of the repository/repositories and accession number(s) can be found in the article/Supplementary Material.

AUTHOR CONTRIBUTIONS

YZ was designed the study and drafted the original draft. QY was responsible for the method, data acquisition, curation, and analysis. Both authors contributed to the article and approved the submitted version.

FUNDING

This research was financially supported by the National Natural Science Foundation of China (No. 31501512), Shandong Province Key Research and Development Plan-Special Plan for Medical Food (2019YYSP023), and the regulation mechanism of quality deterioration of fresh produce through water activity and microorganism (No. 2016YFD0400105).

ACKNOWLEDGMENTS

We would like to thank Editage (www.editage.cn) for English language editing.

SUPPLEMENTARY MATERIAL

The Supplementary Material for this article can be found online at: <https://www.frontiersin.org/articles/10.3389/fmicb.2020.01315/full#supplementary-material>

REFERENCES

- Angmo, K., Kumari, A., and Bhalla, T. C. (2016). Antagonistic activities of lactic acid bacteria from fermented foods and beverage of Ladakh against *Yersinia enterocolitica* in refrigerated meat. *Food Biosci.* 13, 26–31. doi: 10.1016/j.fbio.2015.12.004
- Arihara, K., Kushida, H., Kondo, Y., Itoh, M., Luchansky, J. B., and Cassens, R. G. (1993). Conversion of metmyoglobin to bright red myoglobin derivatives by *Chromobacterium violaceum*, *Kurthia* sp., and *Lactobacillus fermentum* JCM1173. *J. Food Sci.* 58, 38–42. doi: 10.1111/j.1365-2621.1993.tb03205.x
- Bao, Q., Liu, W., Yu, J., Wang, W., Qing, M., Chen, X., et al. (2012). Isolation and identification of cultivable lactic acid bacteria in traditional yak milk products of Gansu Province in China. *J. Gen. Appl. Microbiol.* 58, 95–105. doi: 10.2323/jgam.58.95
- Berardo, A., Devreese, B., Maere, H. D., Stavropoulou, D. A., Royen, G. V., Leroy, F., et al. (2017). Actin proteolysis during ripening of dry fermented sausages at different pH values. *Food Chem.* 221, 1322–1332. doi: 10.1016/j.foodchem.2016.11.023
- Biswas, A. K., Chatli, M. K., and Sahoo, J. (2012). Antioxidant potential of curry (*Murraya koenigii* L.) and mint (*Mentha spicata*) leaf extracts and their effect on colour and oxidative stability of raw ground pork meat during refrigeration storage. *Food Chem.* 133, 467–472. doi: 10.1016/j.foodchem.2012.01.073
- Boyd, V., Cholewa, O. M., and Papas, K. K. (2008). Limitations in the use of fluorescein diacetate/propidium iodide (FDA/PI) and cell permeable nucleic acid stains for viability measurements of isolated islets of Langerhans. *Curr. Trends Biotechnol. Pharm.* 2, 66–84.
- Chen, X., Li, J., Zhou, T., Li, J., Yang, J., Chen, W., et al. (2016). Two efficient nitrite-reducing *Lactobacillus* strains isolated from traditional fermented pork (Nanx Wudl) as competitive starter cultures for Chinese fermented dry sausage. *Meat Sci.* 121, 302–309. doi: 10.1016/j.meatsci.2016.06.007
- Chiou, T. K., Pong, C. Y., Nieh, F. P., and Jiang, S. T. (2001). Effect of metmyoglobin reductase on the color stability of blue fin tuna during refrigerated storage. *Fish. Sci.* 67, 694–702. doi: 10.1046/j.1444-2906.2001.00308.x
- Cullere, M., Zotte, A. D., Tasoniero, G., Giaccone, V., Szendrői, Z., Szin, M., et al. (2018). Effect of diet and packaging system on the microbial status, pH, color and sensory traits of rabbit meat evaluated during chilled storage. *Meat Sci.* 141, 36–43. doi: 10.1016/j.meatsci.2018.03.014
- Deraz, S. F., and Khalil, A. A. (2018). A model system for conversion of metmyoglobin to bright red myoglobin derivatives in organic sausages using potential probiotic lactic acid bacteria. *S. Asian J. Life Sci.* 6, 22–35. doi: 10.17582/journal.sajls/2018/6.1.22.35
- Djimsa, B. A., Abraham, A., Mafi, G. G., VanOverbeke, D. L., and Ramanathan, R. (2017). Effects of Metmyoglobin reducing activity and thermal stability of NADH-dependent reductase and lactate dehydrogenase on premature browning in ground beef. *J. Food Sci.* 82, 304–313. doi: 10.1111/1750-3841.13606
- Domingos-Lopes, M. F. P., Stanton, C., Ross, P. R., Dapkevicius, M. L. E., and Silva, C. C. G. (2017). Genetic diversity, safety and technological characterization of lactic acid bacteria isolated from artisanal Pico cheese. *Food Microbiol.* 63, 178–190. doi: 10.1016/j.fm.2016.11.014
- Espinosa-Pesqueira, D., Roig-Sagués, A., and Hernández-Herrero, M. (2018). Screening Method to Evaluate Amino Acid-Decarboxylase Activity of Bacteria Present in Spanish artisanal ripened cheeses. *Foods* 7:182. doi: 10.3390/foods7110182
- Gao, Y., Li, D., and Liu, X. (2014). Bacteriocin-producing *Lactobacillus sakei* C2 as starter culture in fermented sausages. *Food Control* 35, 1–6. doi: 10.1016/j.foodcont.2013.06.055
- Geeta, P., and Yadav, A. S. (2017). Antioxidant and antimicrobial profile of chicken sausages prepared after fermentation of minced chicken meat with *Lactobacillus plantarum* and with additional dextrose and starch. *LWT-Food Sci. Technol.* 77, 249–258. doi: 10.1016/j.lwt.2016.11.050
- Gerez, C. L., Carbajo, M. S., Rollán, G., Leal, G. T., and Valdez, G. F. D. (2010). Inhibition of citrus fungal pathogens by using lactic acid bacteria. *J. Food Sci.* 75, M354–M359. doi: 10.1111/j.1750-3841.2010.01671.x
- Götterup, J., Olsen, K., Knöchel, S., Tjener, K., Stahnke, L. H., and Möller, J. K. (2007). Relationship between nitrate/nitrite reductase activities in meat associated staphylococci and nitrosylmyoglobin formation in a cured meat model system. *Int. J. Food Microbiol.* 120, 303–310. doi: 10.1016/j.ijfoodmicro.2007.08.034
- Gou, M., Liu, X., and Qu, H. (2019). The role of nitric oxide in the mechanism of lactic acid bacteria substituting for nitrite. *CyTA-J. Food* 17, 593–602. doi: 10.1080/19476337.2019.1621949
- Guley, Z., Uysal, H. R., and Kilic, S. (2015). Lactic acid bacteria flora of Konya Kufllu cheese: a traditional cheese from Konya province in Turkey. *J. Microbiol. Biotech. Food Sci.* 4, 238–242. doi: 10.15414/jmbfs.2014-15.4.3.238-242
- Huang, P., Xu, B., Shao, X., Chen, C., Wang, W., and Li, P. (2019). Theoretical basis of nitrosomyoglobin formation in a dry sausage model by coagulase-negative staphylococci: behavior and expression of nitric oxide synthase. *Meat Sci.* 2019:108022. doi: 10.1016/j.meatsci.2019.108022
- Kim, T. K., Hwang, K. E., Lee, M. A., Paik, H. D., Kim, Y. B., and Choi, Y. S. (2019). Quality characteristics of pork loin cured with green nitrite source and some organic acids. *Meat Sci.* 152, 141–145. doi: 10.1016/j.meatsci.2019.02.015
- Li, P., Luo, H., Kong, B., Liu, Q., and Chen, C. (2016). Formation of red myoglobin derivatives and inhibition of spoilage bacteria in raw meat batters by lactic acid bacteria and *Staphylococcus xylosum*. *LWT-Food Sci. Technol.* 68, 251–257. doi: 10.1016/j.lwt.2015.12.035
- Liu, G., Ren, G., Zhao, L., Cheng, L., Wang, C., and Sun, B. (2017). Antibacterial activity and mechanism of bifidocin A against *Listeria monocytogenes*. *Food Control* 73, 854–861. doi: 10.1016/j.foodcont.2016.09.036
- Liu, S. N., Han, Y., and Zhou, Z. J. (2011). Lactic acid bacteria in traditional fermented Chinese foods. *Food. Res. Int.* 44, 643–651. doi: 10.1016/j.foodres.2010.12.034
- Lucke, F. K., and Hechelmann, H. (1987). Starter cultures for dry sausages and raw ham composition and effect. *Fleischwirtschaft* 67, 307–314.
- Luo, Z., Gasasira, V., Huang, Y., Liu, D., Yang, X., Jiang, S., et al. (2013). Effect of *Lactobacillus salivarius* H strain isolated from Chinese dry-cured ham on the color stability of fresh pork. *Food Sci. Hum. Wellness* 2, 139–145. doi: 10.1016/j.fshw.2013.11.001
- Lv, X., Ma, H., Sun, M., Lin, Y., Bai, F., Li, J., et al. (2018). A novel bacteriocin DY4-2 produced by *Lactobacillus plantarum* from cutlassfish and its application as bio-preservative for the control of *Pseudomonas fluorescens* in fresh turbot (*Scophthalmus maximus*) fillets. *Food Control* 89, 22–31. doi: 10.1016/j.foodcont.2018.02.002
- Maxwell, J. C., and Caughey, W. S. (1976). An infrared study of nitric oxide bonding to heme B and hemoglobin A. Evidence for inositol hexaphosphate induced cleavage of proximal histidine to iron bonds. *Biochemistry* 15, 388–396. doi: 10.1021/bi00647a023
- Millar, S. J., Moss, B. W., and Stevenson, M. H. (1996). Some observations on the absorption spectra of various myoglobin derivatives found in meat. *Meat Sci.* 42, 277–288. doi: 10.1016/0309-1740(94)00045-x
- Minas, K., Mcewan, N. R., Newbold, C. J., and Scott, K. P. (2011). Optimization of a high-throughput CTAB-based protocol for the extraction of qPCR-grade DNA from rumen fluid, plant and bacterial pure cultures. *FEMS Microbiol. Lett.* 325, 162–169. doi: 10.1111/j.1574-6968.2011.02424.x
- Møller, J. K., Jensen, J. S., Skibsted, L. H., and Knöchel, S. (2003). Microbial formation of nitrite-cured pigment, nitrosylmyoglobin, from metmyoglobin in model systems and smoked fermented sausages by *Lactobacillus fermentum* strains and a commercial starter culture. *Eur. Food Res. Technol.* 216, 463–469. doi: 10.1007/s00217-003-0681-8
- Mukumbo, F. E., Descalzo, A. M., Collignan, A., Hoffman, L. C., Servent, A., Muchenje, V., et al. (2020). Effect of *Moringa oleifera* leaf powder on drying kinetics, physico-chemical properties, ferric reducing antioxidant power, α -tocopherol, β -carotene, and lipid oxidation of dry pork sausages during processing and storage. *J. Food Process Pres* 44:14300. doi: 10.1111/jfpp.14300
- Özcelik, S., Kuley, E., and Özogul, F. (2016). Formation of lactic, acetic, succinic, propionic, formic and butyric acid by lactic acid bacteria. *LWT-Food Sci. Technol.* 73, 536–542. doi: 10.1016/j.lwt.2016.06.066
- Polak-Berecka, M., Wasko, A., Szwajgier, D., and Choma, A. (2013). Bifidogenic and antioxidant activity of exopolysaccharides produced by *Lactobacillus rhamnosus* E/N cultivated on different carbon sources. *Pol. J. Microbiol.* 62, 181–188. doi: 10.33073/pjm-2013-023
- Ramanathan, R., Mancini, R. A., Joseph, P., Yin, S., Tatiyaborworntham, N., Petersson, K. H., et al. (2011). Effects of lactate on ground lamb colour stability and mitochondria-mediated metmyoglobin reduction. *Food Chem.* 126, 166–171. doi: 10.1016/j.foodchem.2010.10.093

- Rosato, V., Kawakita, D., Negri, E., Serraino, D., Garavello, W., Montella, M., et al. (2019). Processed meat and risk of selected digestive tract and laryngeal cancers. *Eur. J. Clin. Nutr.* 73, 141–149. doi: 10.1038/s41430-018-0153-7
- Vasice, A., Behbahani, B. A., Yazdi, F. T., Mortazavi, S. A., and Noorbakhsh, H. (2018). Diversity and probiotic potential of lactic acid bacteria isolated from horreh, a traditional Iranian fermented food. *Probiotics Antimicro.* 10, 258–268. doi: 10.1007/s12602-017-9282-x
- Xiao, X., Han, Z. Y., Chen, Y. X., Liang, X. Q., Li, H., and Qian, Y. C. (2011). Optimization of FDA-PI method using flow cytometry to measure metabolic activity of the cyanobacteria, *Microcystis aeruginosa*. *Phys. Chem. Earth* 36, 424–429. doi: 10.1016/j.pce.2010.03.028
- Yu, J., Zheng, J., Lin, J., Jin, L., Yu, R., Mak, S., et al. (2017). Indirubin-3-oxime prevents H₂O₂-induced neuronal apoptosis via concurrently inhibiting GSK3 β and the ERK pathway. *Cell Mol. Neurobiol.* 37, 655–664. doi: 10.1007/s10571-016-0402-z
- Zhang, X., Kong, B., and Xiong, Y. L. (2007). Production of cured meat color in nitrite-free Harbin red sausage by *Lactobacillus fermentum* fermentation. *Meat Sci.* 77, 593–598. doi: 10.1016/j.meatsci.2007.05.010

Conflict of Interest: The authors declare that the research was conducted in the absence of any commercial or financial relationships that could be construed as a potential conflict of interest.

Copyright © 2020 Zhu and Yang. This is an open-access article distributed under the terms of the Creative Commons Attribution License (CC BY). The use, distribution or reproduction in other forums is permitted, provided the original author(s) and the copyright owner(s) are credited and that the original publication in this journal is cited, in accordance with accepted academic practice. No use, distribution or reproduction is permitted which does not comply with these terms.



Reduction, Prevention, and Control of *Salmonella enterica* Viable but Non-culturable Cells in Flour Food

OPEN ACCESS

Edited by:

Xihong Zhao,
Wuhan Institute of Technology, China

Reviewed by:

Yuting Tian,
Fujian Agriculture and Forestry
University, China
Ying Mu,
University of Tennessee Health
Science Center (UTHSC),
United States
Wensen Jiang,
Cedars Sinai Medical Center,
United States

*Correspondence:

Xiangjun Gong
msxjgong@scut.edu.cn
Junyan Liu
jliu81@uthsc.edu

† These authors have contributed
equally to this work

Specialty section:

This article was submitted to
Food Microbiology,
a section of the journal
Frontiers in Microbiology

Received: 08 April 2020

Accepted: 15 July 2020

Published: 21 August 2020

Citation:

Li Y, Huang T, Bai C, Fu J,
Chen L, Liang Y, Wang K, Liu J,
Gong X and Liu J (2020) Reduction,
Prevention, and Control of *Salmonella*
enterica Viable but Non-culturable
Cells in Flour Food.
Front. Microbiol. 11:1859.
doi: 10.3389/fmicb.2020.01859

Yanmei Li^{1†}, Tengyi Huang², Caiying Bai³, Jie Fu¹, Ling Chen^{4,5}, Yi Liang⁶, Kan Wang⁷,
Jun Liu⁸, Xiangjun Gong^{8*} and Junyan Liu^{9*}

¹ Department of Haematology, Guangzhou Women and Children's Medical Center, Guangzhou Medical University, Guangzhou, China, ² Department of Laboratory Medicine, The Second Affiliated Hospital of Shantou University Medical College, Shantou, China, ³ Guangdong Women and Children Hospital, Guangzhou, China, ⁴ Guangdong Province Key Laboratory for Green Processing of Natural Products and Product Safety, School of Food Science and Engineering, South China University of Technology, Guangzhou, China, ⁵ Overseas Expertise Introduction Center for Discipline Innovation of Food Nutrition and Human Health (111 Center), Guangzhou, China, ⁶ Guangdong Zhongqing Font Biochemical Science and Technology Co., Ltd., Maoming, China, ⁷ Research Center of Translational Medicine, The Second Affiliated Hospital of Shantou University Medical College, Shantou, China, ⁸ School of Materials Science and Engineering, South China University of Technology, Guangzhou, China, ⁹ Department of Civil and Environmental Engineering, University of Maryland, College Park, MD, United States

The processing and storage conditions of flour food inevitably pose environmental stress, which promote bacteria to enter a viable but non-culturable (VBNC) state. The existence of VBNC cells causes false-negative detection in traditional culture-based detection methods, resulting in food quality and safety issues. This study aimed at investigating the influence factors including nutrition, acid, salt, and temperature for the entry into a VBNC state of *Salmonella enterica* and an efficient detection method. During induction with multi-stress conditions, nutrition starvation antagonizes with low-level acidity. Besides, high-level acidity was considered as an inhibitor for VBNC induction. Four inducers including nutrition starvation, salt stress, low-level acidity, and low temperature were concluded for a VBNC state. In addition, the keynote conditions for *S. enterica* entering a VBNC state included (i) nutrient-rich acidic environment, (ii) oligotrophic low-acidity environment, and (iii) oligotrophic refrigerated environment. Based on the keynote conditions, the environmental conditions of high acidity (1.0% v/v acetate) with low temperature (−20°C) could successfully eliminate the formation of *S. enterica* VBNC cells in flour food. In addition, combining with propidium monoazide pretreatment, PCR technology was applied to detect *S. enterica* VBNC cells. The sensitivity of the PMA-PCR technology was 10⁵ CFU/ml in an artificially simulated food system. The results derived from this study might aid in the detection and control of VBNC state *S. enterica* in flour food products.

Keywords: *Salmonella enterica*, propidium monoazide, viable but non-culturable, environmental stress conditions, food system

HIGHLIGHTS

- PMA-PCR technology was applied to detect *Salmonella enterica* viable but non-culturable (VBNC) cells with a sensitivity of 10^5 CFU/ml.
- The keynote conditions for *S. enterica* entering a VBNC state include nutrient-rich acidic environment, oligotrophic low-acidity environment, and oligotrophic refrigerated environment.
- A high acidity (1.0% v/v acetate) plus frozen temperature (-20°C) environmental condition could successfully inhibit the formation of *S. enterica* VBNC cells and eliminate it in flour food.

INTRODUCTION

In the food industry, flour food is frequently contaminated by foodborne bacteria including *Staphylococcus aureus*, *Salmonella enterica*, and *Escherichia coli* O157 (Kirk et al., 2015; Lin et al., 2017; Miao et al., 2017c; Zhao et al., 2018a,b; Liu et al., 2019; Sharma et al., 2019). Foodborne *S. enterica* is a typical zoonotic pathogen with multiple toxic effects including invasiveness, endotoxin, and enterotoxin (Eng et al., 2015; Bao et al., 2017b,c; Xie et al., 2017a; Jia et al., 2018; Wen et al., 2020). Recently, studies had reported that *S. enterica* can form viable but non-culturable (VBNC) cells under certain environmental stresses (e.g., low temperature, salt stress, nutrient starvation) (Roszak et al., 1984; Chmielewski and Frank, 1995; Gupte et al., 2003; Kusumoto et al., 2012; Zeng et al., 2013; Morishige et al., 2017; Highmore et al., 2018). In addition to the natural environment, the generation of an *S. enterica* VBNC state also occurred during chlorination of wastewater or food (Oliver et al., 2005; Highmore et al., 2018). In the food industrial environment, the common non-ionic detergents and sanitizers were found to induce an *S. enterica* VBNC state formation (Morishige et al., 2013; Purevdorj-Gage et al., 2018; Robben et al., 2018). Besides, oxidation stress induced by non-thermal sterilization technologies had been confirmed to have a positive relationship with generation of VBNC *S. typhimurium* cells (Liao et al., 2018). Moreover, storage and complex components of food inevitably cause multistress conditions including high acidity and salt, nutrient starvation, and low temperature (Xu et al., 2011b; Liu et al., 2018a,b). Therefore, *S. enterica* VBNC cells could exist in the food industry and processing plants, and even food production. As the detection of foodborne pathogens in foods was based on colony-counting method, bacterial VBNC cells cause false-negative results and remain in food (Bao et al., 2017a; Xie et al., 2017b; Xu et al., 2018). Although VBNC cells have low activity, some frozen food has a long shelf life so that VBNC cells have enough time to metabolize causing food spoilage, which poses a certain safety hazard to human health (Fakruddin et al., 2013; Zeng et al., 2013; Highmore et al., 2018).

Although *S. enterica* VBNC cells could be resuscitated by favorable conditions, the recovery of VBNC cells from different environmental stresses requires different methods, such as temperature upshift (Gupte et al., 2003; Zeng et al., 2013), catalase

(Zeng et al., 2013; Morishige et al., 2017), Tween 80 (Zeng et al., 2013), and nutrients (Roszak et al., 1984; Morishige et al., 2013). Therefore, the detection of *S. enterica* VBNC cells by resuscitation is infeasible. In recent years, combining propidium monoazide (PMA) treatment with nucleic acid amplification technologies has shown to be capable of rapidly detecting VBNC bacteria (Wang et al., 2011; Xu et al., 2011a,b, 2012a,b, 2016a,b; You et al., 2012; Liu et al., 2015, 2017; Jiang et al., 2016; Lin et al., 2016; Miao et al., 2016, 2017a,b, 2018; Ma et al., 2017; Wang et al., 2019).

In this study, the induction and control of VBNC state formation focused on specific environmental conditions were investigated (Zhang et al., 2013; Miao et al., 2017c; Xu et al., 2011a,c). Also, we applied the PMA-PCR method to detect the targeted gene *invA* of *S. enterica* VBNC cells in a food system (Xu et al., 2007, 2008a,b, 2009, 2010).

MATERIALS AND METHODS

Bacteria Strains and DNA Extraction

The bacterial strains (Table 1) were grown in tryptic soy broth (TSB, Huankai Microbial, China) cultures at 37°C at 200 rpm for 24 h until further use. Then 1.5–2 ml of culture was used in DNA extraction by a DNA extraction kit (Dongsheng Biotech, Guangzhou) following the manufacturer's instructions. Nano Drop 2000 (Thermo Fisher Scientific Inc., Waltham, MA, United States) was applied to measure the concentration of the extracted DNA for controlling the ratio value of $\text{OD}_{260}/\text{OD}_{280}$ from 1.8 to 2.0. All of the DNA samples were stored at -20°C until further use.

Induction of *S. enterica* VBNC Status

According to the food environmental condition, a total of three factors were selected as a single variable including nutrient, salt, and acid (Table 3). The designed orthogonal array was divided into 16 groups (Table 4), and the trend on the number of cultivable bacteria is used as an index to investigate the effect of external environmental pressure on the formation of *S. enterica* VBNC. The *S. enterica* VBNC status was induced by the 16 groups of conditions at low temperature (4° or -20°C). The overnight bacterial culture ($\sim 10^8$ CFU/ml) was washed three times and resuspended by sterile saline. Besides, aliquots of these bacterial suspensions were separated into 1.5 ml tubes (~ 20)

TABLE 1 | Bacteria used in the study.

Species	Source
<i>Escherichia coli</i> O157:H7 ATCC47853	ATCC
<i>Escherichia coli</i> O157:H7 ATCC25922	ATCC
<i>Salmonella enterica</i> ATCC14028	ATCC
<i>Salmonella enterica</i> ATCC29629	ATCC
<i>Pseudomonas aeruginosa</i> ATCC27853	ATCC
<i>Staphylococcus aureus</i> 10071	Laboratory strain
<i>Listeria monocytogenes</i> ATCC19115	ATCC
<i>L. monocytogenes</i> ATCC19116	ATCC
<i>Lactobacillus casei</i>	Laboratory strain

TABLE 2 | Primer sequences of the target genes.

Primer	Sequence (5'-3')	Length
<i>invA</i> -Ft	CACAAAGATGATAATGATGCCAATACTGGAAAGGGAAAGCC	41
<i>invA</i> -Bt	CCGTAGTAATAGTAGAAACACGACAGAGCGGAGGATAAA	39
<i>invA</i> -IF	TCATCGCACCGTCAAA	16
<i>invA</i> -IB	TGGCGGTATTTCGGTGGG	18

TABLE 3 | External environmental factors during induction of the VBNC state of *Salmonella*.

TSB (%)	NaCl (%)	Acetate (%)
0	0.9	0
25	10	0.3
50	20	0.7
100	30	1

to avoid the effect of repeated freeze-thaw. The viability of bacterial cells was characterized by the colony counting method, and the VBNC cells were determined by LIVE/DEAD BacLight® kit (Thermo Fisher Scientific, United States) with fluorescence microscope after the culturable colonies no longer form on an agar medium. The culturable and viable cell enumerations were performed every 3 days.

PMA-PCR

The *S. enterica*-specific gene *invA* was selected as the target gene, and corresponding primers were designed (Table 2). The selected conserved regions were determined to be highly specific by sequence comparison on the Blast website. Primer Premier 5 was used to design primers for the PCR amplification reaction. All primers were synthesized by Guangzhou Aiji Biotechnology Co., Ltd. The mentioned bacterial DNA extraction was employed as a template for PCR amplification. The PCR assay was performed in a 25 µl volume with 1.6 µl of detection primer (50 µM) and 0.8 µl of accelerated primer (50 µM). The thermal profile for PCR was 94°C for 5 min, followed by the condition for 30 cycles: denaturation of 94°C for 30 s, primer annealing at 55°C for 30 s, and extension at 72°C for 1 min and a final extension cycle at 72°C for 7 min. A negative control was performed using sterile water instead of culture or DNA template. Finally, the specificity and sensitivity of the designed primer was determined by electrophoresis.

PMA-PCR Detection on *S. enterica* VBNC Cells in a Food System

Twenty-five grams of crystal cake powder was added to 225 ml of sterile saline and autoclaved. The 1-ml overnight culture (~10⁸ CFU/ml) was diluted 10 fold by adding 9 ml of sterile flour solutions to prepare the artificially contaminated food samples with different concentrations (10⁷–10). Before the extraction of bacterial DNA, artificially contaminated samples were pretreated according to the following steps: (1) 1 ml of the flour solution was centrifuged for 10 min at 1,000 rpm to remove the macroparticles, then the supernatant was centrifuged again at 12,000 rpm for 10 min to collect precipitations. (2) The precipitations were

TABLE 4 | The experimental methods of orthogonal array design of VBNC induction of *Salmonella*.

Group	TSB (%)	NaCl (%)	Acetate (%)
1	0	0.9	0
2	25	0.9	0.3
3	50	0.9	0.7
4	100	0.9	1
5	25	10	0
6	0	10	0.3
7	100	10	0.7
8	50	10	1
9	50	20	0
10	100	20	0.3
11	0	20	0.7
12	25	20	1
13	100	30	0
14	50	30	0.3
15	25	30	0.7
16	0	30	1

resuspended in 500 µl of sterile saline and then mixed with 125 µl of ethyl acetate for 2 min to remove impurities such as oil and fat. After centrifugation at 12,000 rpm for 10 min, the precipitations were washed once with 500 µl of TE buffer and twice with 500 µl of sterile saline.

The range of *S. enterica* VBNC cell concentration was adjusted from 10 to 10⁶ cells/ml. Subsequently, the propidium monoazide (PMA) dye was added to the flour samples until its concentration reached 5 µg/ml. After incubation at room temperature for 10 min in the dark, the samples were exposed to a 650 W halogen lamp with a distance of 15 cm for 5 min, which inactivated unbinding PMA molecules rather than PMA–DNA molecules. All the dyeing process was performed in an ice bath to prevent DNA damage. Subsequently, the DNA extraction and PCR detection of PMA-treated cells were performed.

RESULTS

Induction of *S. enterica* VBNC State

The exponential-phase *S. enterica* cells were induced to a VBNC state by low-temperature storage (Figure 1). After 30 days of storage at 4° or –20°C, the culturable number dropped to 0. As fluorescent green cells could be captured by microscopy, *S. enterica* was considered to be successfully induced into a VBNC status (Figure 2), with live and dead cells that coexisted.

Effects of Environmental Conditions on *S. enterica* VBNC State

Culturable Number of *S. enterica* Cells

According to four external environmental factors (nutrient, salinity, acidity, and temperature), the orthogonal array was designed to induce *S. enterica* VBNC cells including 16 groups (Table 4). Non-culturable cells were found in eight groups (groups 3, 4, 6, 8, 11, 12, 15, and 16) after 3 days of induction.

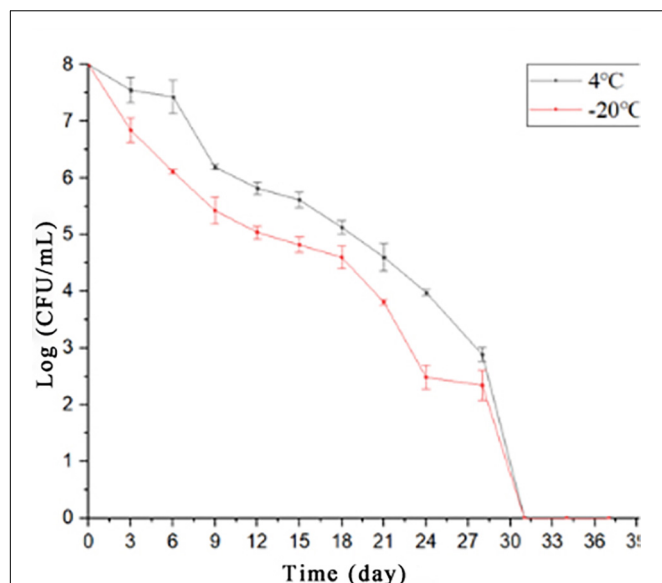


FIGURE 1 | The culturable cells of foodborne *Salmonella* under low nutrients at 4°C or -20°C.

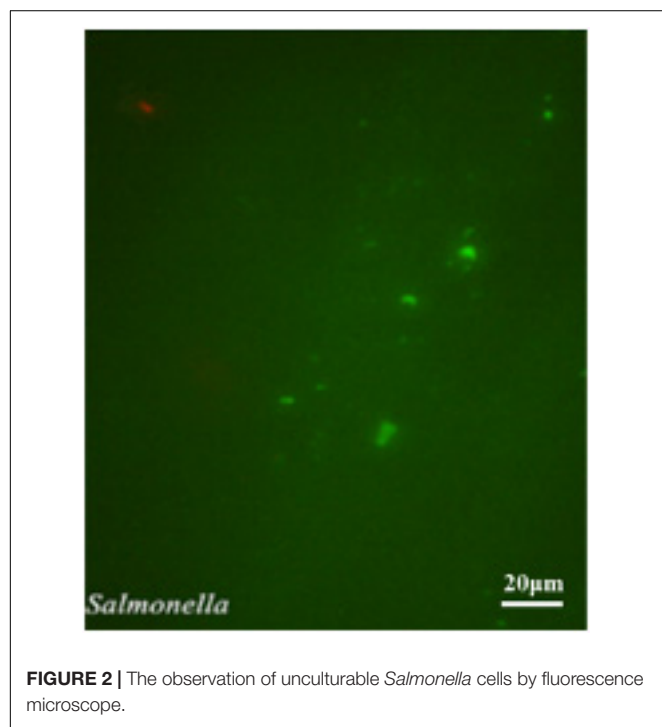


FIGURE 2 | The observation of unculturable *Salmonella* cells by fluorescence microscope.

Seven groups (groups 3, 4, 8, 11, 12, 15, and 16) had a high concentration ($\geq 0.7\%$ v/v) of acetate, indicating that the viability of *S. enterica* might be mainly inhibited by high acidity. When supplied with adequate nutrition, the *S. enterica* cells could survive under acidic stress from 0.7% v/v acetate within 30 days (group 7), suggesting that nutrition may be a stimulated bacterial stress response mechanism to resist acetate. The culturable number in the other groups (groups 1, 7, 9, 10,

13, and 14) showed a decreasing trend to reach 0 (**Figure 3**). The accurate time required for each protocol to reach a non-culturable cell state at 4°C and -20°C differed (**Table 5**). The cells grown in different concentrations of nutrients (groups 2, 5, 7, 9, 10, 13, and 14) could survive for more than 30 days. However, the result of group 4 showed that under a nutrient-rich condition (100%), high acidic stress (1% v/v acetate) still inactivated *S. enterica* cells within 3 days of storage, revealing that the effect of acidity on cell viability was stronger than nutrients. Interestingly, in protocols 2 and 5, the trend of culturable cell numbers had a significant difference, as the *S. enterica* remained at cell numbers higher than 10^4 CFU/ml at 4°C rather than at -20°C. This phenomenon demonstrated that freezing conditions (-20°C) might contribute to inhibit bacterial growth.

In summary, under higher than 0.7% v/v of acetate, the order of environmental conditions in affecting the survival of *S. enterica* was as follows: acidity > nutrients > salt. With the reduction in acidity, the supplemental stress promoted *S. enterica* to resist environmental stress.

Salmonella enterica VBNC State Formation

Although *S. enterica* were no longer culturable in eight groups (groups 1, 2, 5, 7, 9, 10, 13, and 14), the viable cells were still captured by fluorescence microscopy (**Figure 4**). These results demonstrated that VBNC cells were successfully induced by freezing conditions (-20°C) with long-term storage (~30 days). As none of viable *S. enterica* cells were observed from other groups (groups 3, 4, 6, 8, 11, 12, 15, and 16) in which bacteria lost culturability within a short-term storage (~3 days) (data not shown), the formation of a VBNC state might require *S. enterica* to suffer by long-term induction of sublethal environmental stress and low temperature.

Most non-viable cell groups contained more than 0.7% v/v acetate, indicating that high-level acidity environmental condition induced cell death rather than the formation of a VBNC state, although a previous study had reported that an *S. enterica* VBNC state could be induced by lactic acid or peracetic acid (Purevdorj-Gage et al., 2018). Interestingly, a VBNC state was induced under 0.7% v/v acetate by supplying sufficient nutrients (100%), suggesting that nutrients were essential for *S. enterica* entering a VBNC state in response to multistress conditions including inorganic salts and weak acid.

As described by Chen et al. (2019) more than 10 or 1% of *S. enterica* cells were induced into a VBNC state without nutrients at 4°C or -20°C, respectively. In our study, *S. enterica* entered into a VBNC state under starvation condition at 4°C or -20°C (groups 1, 2, 5, 7, 9, 10, 13, and 14). Other previous studies had described similar results and showed that temperature upshift and growth factors (catalase and Tween 20) were required for resuscitation (Gupte et al., 2003; Zeng et al., 2013). Moreover, groups 2 and 5 showed that a decreasing temperature could accelerate the reduction of culturable cells and the generation of VBNC cells, which revealed that the decrease in temperature was one of the essential inducers. Besides, consistent with previous report, our results showed that the generation of *S. enterica* VBNC cells could be induced by salt stress with different concentrations, indicating

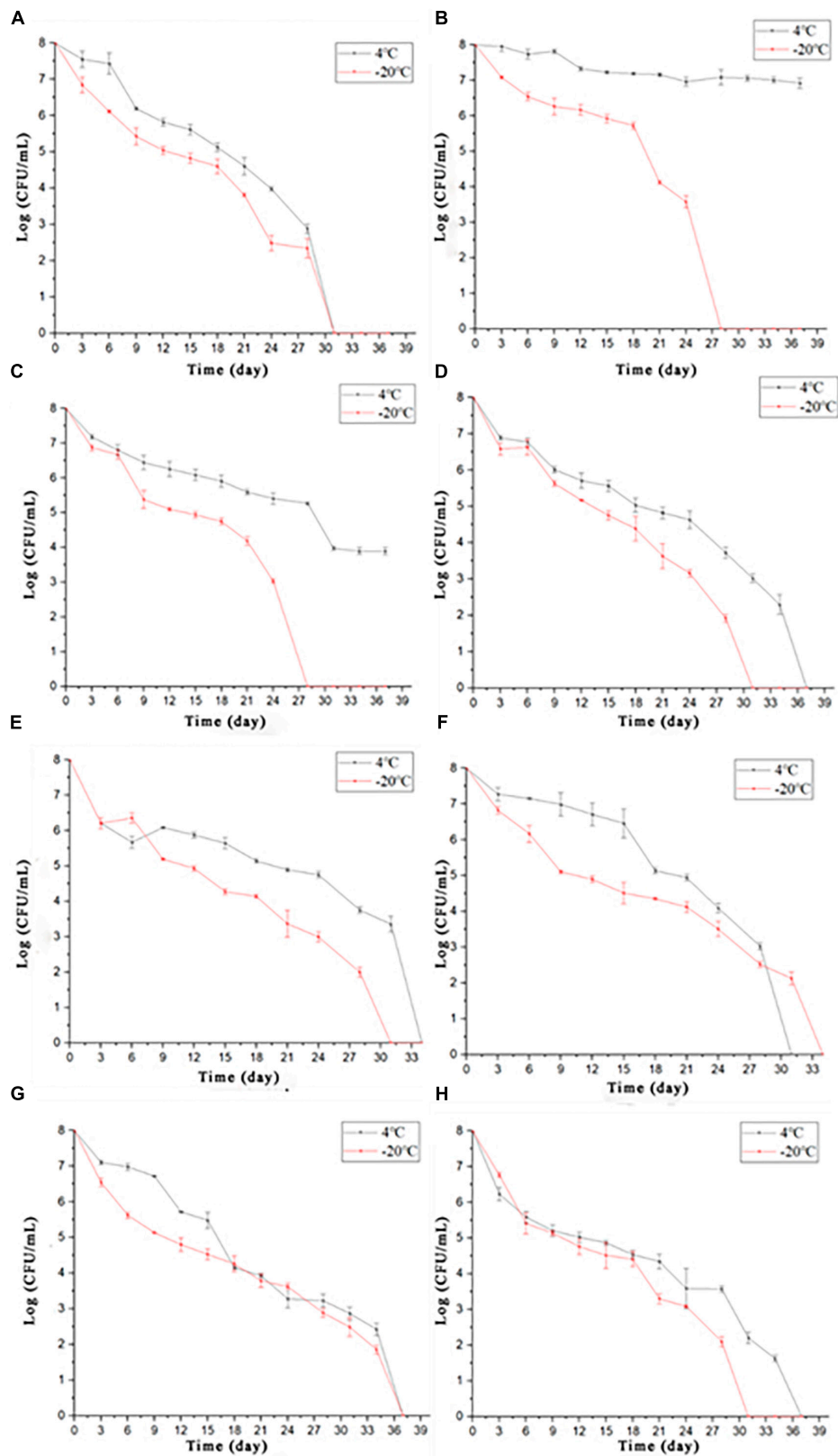


FIGURE 3 | The culturable number of *Salmonella* stored under 16 different conditions (A–H were the culturable number tendency of *Salmonella* under correspondent conditions according to methods 1, 2, 5, 7, 9, 10, 13, and 14 and stored at 4° or –20°C, respectively).

TABLE 5 | The time of culturable number of *Salmonella* decreased to 0 stored at different protocols.

Group	4°C	−20°C	Group	4°C	−20°C
1	31 d	31 d	9	34 d	31 d
2	+	28 d	10	31 d	34 d
3	/	/	11	/	/
4	/	/	12	/	/
5	+	28 d	13	37 d	37 d
6	/	/	14	37 d	31 d
7	37 d	31 d	15	/	/
8	/	/	16	/	/

“+” represents cultivable; “/” represents non-culturable within 3 days.

that salt stress was another inducer for a VBNC state formation (Asakura et al., 2002).

Together, four inducers including nutrition starvation, salt stress, low-level acidity, and low temperature were concluded for VBNC state induction. However, during

induction with multistress conditions, nutrition starvation antagonizes with low-level acidity. Besides, high-level acidity was considered as an inhibitor for VBNC induction. Therefore, the keynote environmental factors of VBNC state induction were concluded to be: (i) nutrient-rich acidic environment, (ii) oligotrophic low-acidity environment, and (iii) oligotrophic refrigerated environment.

Effects of Keynote Environmental Factors on *Salmonella* VBNC State Formation

Acidity

Acetate had been utilized as an antimicrobial chemical for many years in food production. As previously described by Liao et al. (2003) exposing *Salmonella* cells to 0.7 or 1.0% acetic acid for 7 min usually caused 90% cells with inactivation and 99% of culturable cells with injury. In agreement with a related study, cell viability was evaluated based on cultivability, neglecting the generation of *Salmonella* VBNC cells induced by acetate *in vitro* (Alvarez-Ordóñez et al., 2010). Encountering

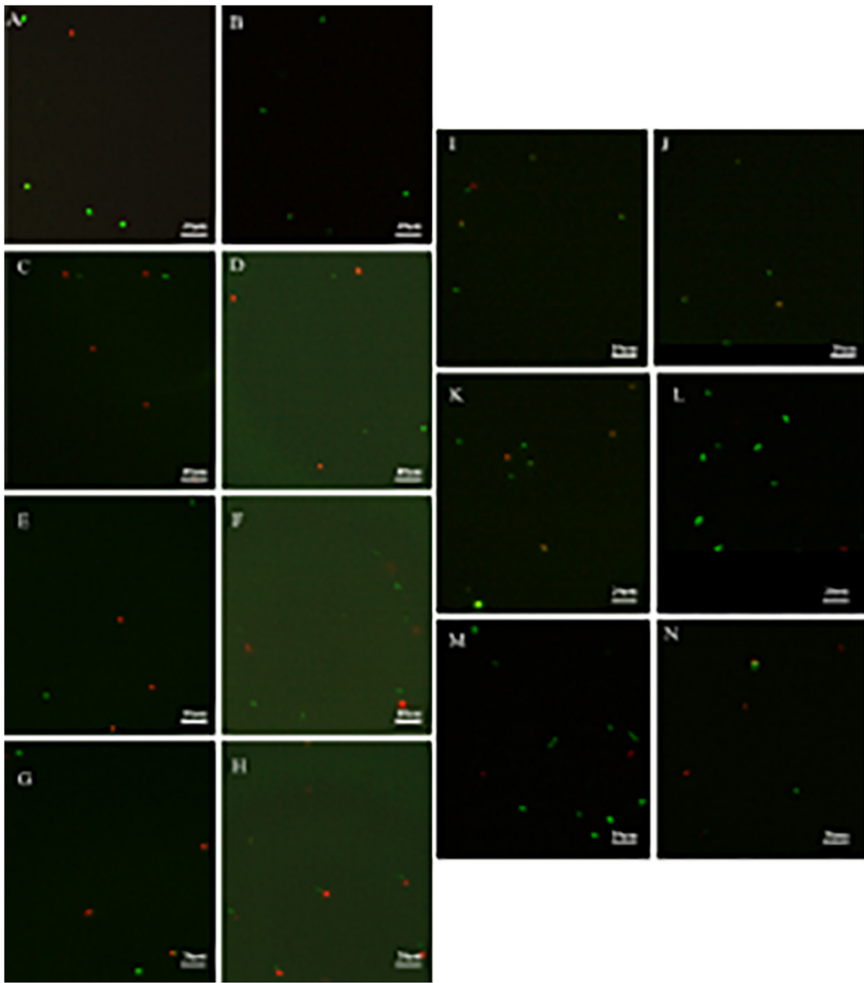


FIGURE 4 | The viability of non-culturable *Salmonella* stored at different conditions by fluorescent observation (A,B: group 1; C: group 2; D: group 5; E,F: group 7; G,H: group 9; I,J: group 10; K,L: group 13; M,N: group 14).

organic acid stress causing the acidification of the cytoplasm and the accumulation of intracellular anion, the available energy is required for *S. enterica* to efflux protons (H^+) by active transport maintaining intracellular pH homeostasis (Mani-López et al., 2012). Therefore, the effect of acidity (0.7 or 1.0% v/v) on the formation of an *S. enterica* VBNC state in flour food was investigated with different nutritional concentrations at low temperature (4° or −20°C).

Under oligotrophic conditions, *S. enterica* could not be cultured after 3 days of storage at low temperature (4° and −20°C) by adding 0.7 or 1.0% v/v acetic acid (Table 6). The bacterial activity test results showed that only dead cells were observed, indicating that *S. enterica* was unable to enter into a VBNC state. When supplied with sufficient nutrients ($\geq 50\%$), the culturable cells still existed under 0.7% v/v acetic acid after 3 days of storage, indicating that acid tolerance of *S. enterica* was improved by available nutrients, which might ultimately lead to generation of VBNC cells. However, when the concentration of acetate reached 1.0% v/v, no culturable cells could be found after 3 days of storage, whether provided with nutrients or not. As expected, the activity test results showed that all the bacterial cells were dead, indicating that the formation of a VBNC state of *S. enterica* could be controlled by adding 1.0% v/v acetate, even when supplied with rich nutrients. Interestingly, only group 7 had showed that all the bacteria were inviable with decreasing temperature under high-level acidity stress (1.0% v/v acetate). These results were consistent with those previously described by Alvarez-Ordóñez et al. (2010), who measured the organic acid tolerance of *S. typhimurium* at different growth temperatures and found that the reduction of low temperatures markedly decreased the acid resistance and increased the growth pH boundary of *S. typhimurium*. In summary, during the processing of flour foods, 1.0% v/v acetic acid could be used to clean the processing equipment, which can effectively eliminate the pollution of *S. enterica* and its VBNC cells.

Nutrients

Recently, Pu et al. (2019) proposed that protein aggresome is an important indicator of the *E. coli* VBNC state, which was promoted by nutrient starvation, but stress removal will facilitate the disaggregation of the proteins by the DnaK–ClpB cochaperone system (Pu et al., 2019). Although nutrients also play an important role in the formation of the *S. enterica* VBNC state, the reduction of nutrients may be a potential method to inhibit *S. enterica* VBNC cell formation. Under high salt and low acidity, *S. enterica* cells were still culturable with an oligotrophic condition after 3 days of storage (Table 7), which suggested that only an oligotrophic condition was incapable of inhibiting the formation of VBNC cells. Therefore, it is essential to combine oligotrophic condition with other environmental stress (e.g., high acidity) to prevent *S. enterica* from entering the state of VBNC.

Control and Reduction of *S. enterica* VBNC Cells in Flour Food

In order to confirm the inhibitory effect of the above keynote conditions on *Salmonella* VBNC formation in food samples, we selected crystal cake powders as a sole source of nutrients

TABLE 6 | Inhibition of acidity in the formation of VBNC state of *Salmonella*.

Group	TSB (%)	NaCl (%)	Acetate (%)	Cultivability		Viability	
				4°C	−20°C	4°C	−20°C
1	0	0.9	0.7	/	/	–	–
2			1.0	/	/	–	–
3	25	0.9	0.7	/	/	–	–
4			1.0	/	/	–	–
5	25	10	0.7	/	/	–	–
6			1.0	/	/	–	–
7	100	10	1.0	+	/	ND	–
8	50	20	0.7	+	+	ND	ND
9			1.0	/	/	–	–
10	100	20	0.7	+	+	ND	ND
11			1.0	/	/	–	–
12	100	30	0.7	+	+	ND	ND
13			1.0	/	/	–	–
14	50	30	0.7	+	+	ND	ND
15			1.0	/	/	–	–

“+” represents culturable; “/” represents non-culturable; “–” represents inactivation; “ND” represents non-detection.

TABLE 7 | Inhibition of nutritional status in the formation of VBNC state of *Salmonella*.

Group	TSB (%)	NaCl (%)	Acetate (%)	Cultivability		Viability	
				4°C	−20°C	4°C	−20°C
1	0	20	0	+	+	ND	ND
2	25			+	+	ND	ND
3	0	20	0.3	+	+	ND	ND
4	25			+	+	ND	ND
5	0	30	0	+	+	ND	ND
6	25			+	+	ND	ND
7	0	30	0.3	+	+	ND	ND
8	25			+	+	ND	ND

“+” represents culturable; “ND” represents non-detection.

instead of TSB to simulate the flour food environment. The keynote conditions used for investigation was high acidity (1.0% v/v acetate) combined with different concentrations (25, 50, and 100%) of nutrients. After 3 days of storage, the culturable number and viability of *S. enterica* in different conditions are shown in Figures 5, 6. Consistent with the results from non-food systems, only dead bacterial cells could be found in simulated food systems after 3 days of storage at −20°C, whether they were provided with nutrients or not (Figure 6). On the contrary, *Salmonella* could still survive after 3 days of storage at 4°C via a supplement of sufficient nutrients (100%) (Figure 6). Although the number of survival of *S. enterica* cells was significantly reduced, there is a possibility of culturable cells entering the VBNC state (Figure 5). Therefore, the best control conditions for the formation of VBNC status of *S. enterica* in flour food is to add 1.0% v/v acetic acid combined with storage at −20°C.

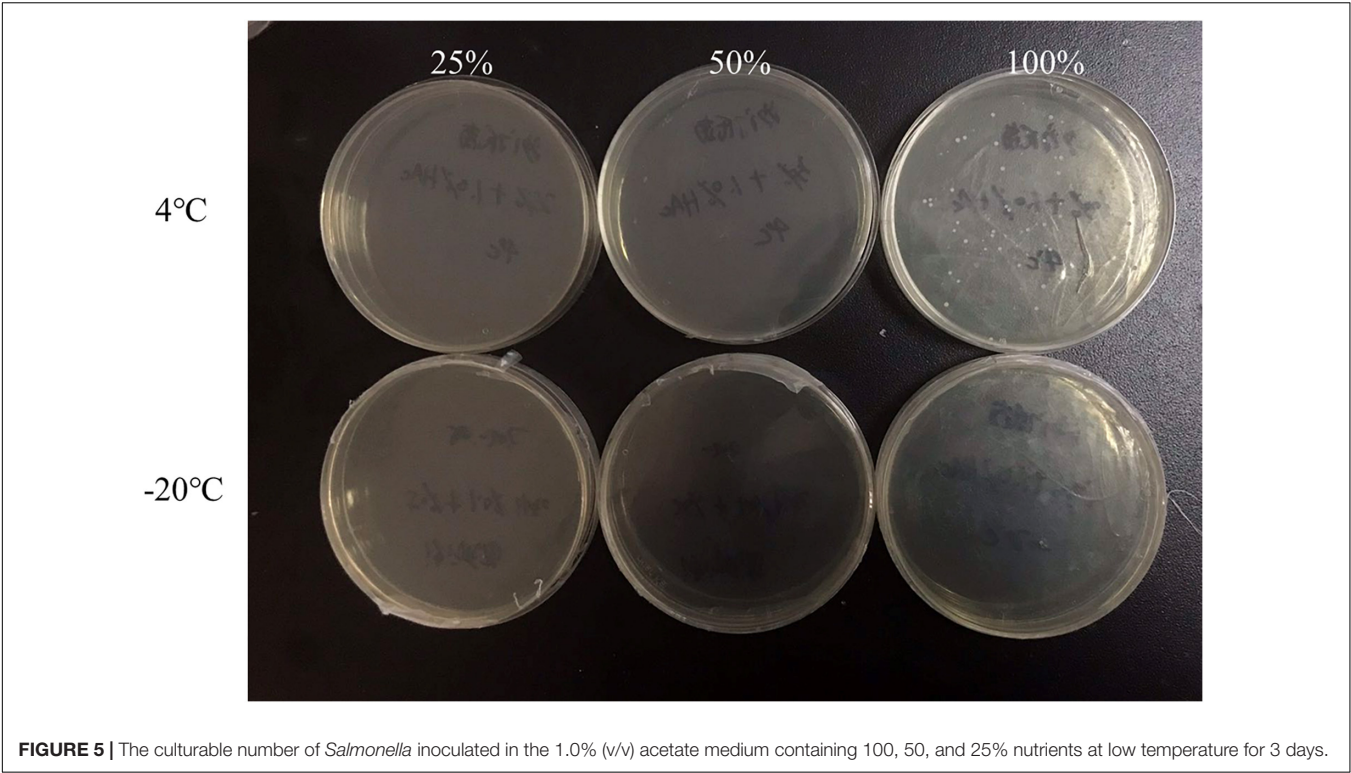


FIGURE 5 | The culturable number of *Salmonella* inoculated in the 1.0% (v/v) acetate medium containing 100, 50, and 25% nutrients at low temperature for 3 days.

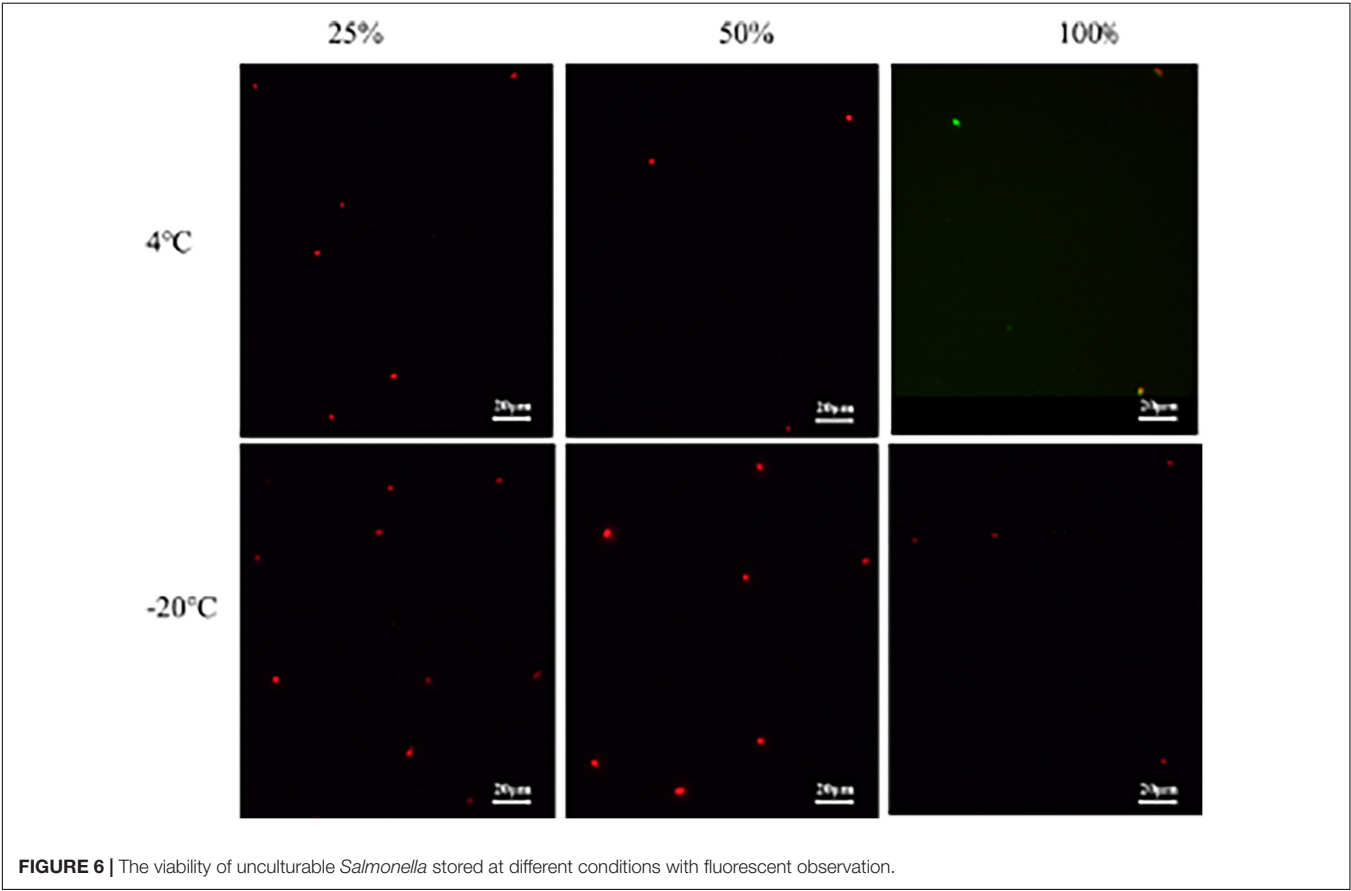


FIGURE 6 | The viability of unculturable *Salmonella* stored at different conditions with fluorescent observation.

Foodborne pathogenic and spoilage bacteria had been previously shown to enter into a VBNC state in a food system under a freezing environment. Therefore, the results of this study might provide a theoretical basis for the control and reduction of foodborne bacterial VBNC cells.

PMA-PCR Detection on VBNC Cells

In order to eliminate the interference of dead bacterial DNA, samples were subjected to PMA treatment before PCR amplification. The detection limit of *S. enterica* using the constructed PMA-PCR technology to detect the VBNC status in the crystal cake food system is 10^5 CFU/ml, which is consistent with the PMA-PCR results in the pure induction system (data not shown). Compared to the detection limit of PCR for culturable *S. enterica* in food systems, the detection limit of PMA-PCR has no significant changes, suggesting that the PCR method by the PMA dye is non-effective. Therefore, the PMA-PCR method can be better applied to detect viable bacteria (culturable and non-culturable) in a food sample, preventing false-negative detection of a culture-based method on VBNC cells.

CONCLUSION

In this study, the influence factors including nutrition, acid, salt, and temperature for the entry into a VBNC state of *S. enterica* and an efficient detection method were investigated. The order of environmental conditions in effecting the cultivability of *S. enterica* was as follows: acidity > nutrients > salt. Four inducers for the VBNC state including nutrition starvation, salt stress, low-level acidity, and low temperature were concluded. However, during induction with multistress conditions, nutrition starvation antagonizes with low-level acidity. Besides, high-level acidity was considered as an inhibitor for a VBNC state

formation. Therefore, the keynote conditions for *S. enterica* entering the VBNC state were concluded as (i) nutrient-rich acidic environment, (ii) oligotrophic low-acidity environment, and (iii) oligotrophic refrigerated environment. Thus, using an environment condition of high acidity (1.0% v/v acetate) with low temperature (-20°C), the formation of *S. enterica* VBNC state was eliminated in flour food. Combined with PMA pretreatment, the PCR technology could be applied to detect viable *S. enterica* cells (culturable and VBNC) removing the interference of dead cells. The detection limit of the PMA-PCR technology was 10^5 CFU/ml in an artificially simulated food system. In conclusion, this study identified specific environmental stresses to control, and applied a stable PMA-PCR method to detect, an *S. enterica* VBNC state, providing a theoretical basis for the control and reduction of foodborne bacterial VBNC cells.

DATA AVAILABILITY STATEMENT

All datasets presented in this study are included in the article/supplementary material.

AUTHOR CONTRIBUTIONS

JYL and KW conceived of the study and participated in its design and coordination. JF and TH performed the experimental work. CB and LC analyzed the data. YL and JL prepared and revised this manuscript. All authors reviewed and approved the final manuscript.

FUNDING

This work was supported by the 111 Project (B17018).

REFERENCES

- Alvarez-Ordóñez, A., Fernández, A., Bernardo, A., and López, M. (2010). Acid tolerance in *Salmonella* typhimurium induced by culturing in the presence of organic acids at different growth temperatures. *Food Microbiol.* 27, 44–49. doi: 10.1016/j.fm.2009.07.015
- Asakura, H., Makino, S., Takagi, T., Kuri, A., Kurazono, T., Watarai, M., et al. (2002). Passage in mice causes a change in the ability of *Salmonella enterica* serovar oranienburg to survive NaCl osmotic stress: resuscitation from the viable but non-culturable state. *FEMS Microbiol. Lett.* 212, 87–93. doi: 10.1111/j.1574-6968.2002.tb11249.x
- Bao, X., Jia, X., Chen, L., Peters, B. M., Lin, C., Chen, D., et al. (2017a). Effect of Polymyxin resistance (pmr) on biofilm formation of *Cronobacter sakazakii*. *Microb. Pathog.* 106, 16–19. doi: 10.1016/j.micpath.2016.12.012
- Bao, X., Yang, L., Chen, L., Li, B., Lin, L., Li, Y., et al. (2017b). Analysis on pathogenic and virulent characteristics of the *Cronobacter sakazakii* strain BAA-894 by whole genome sequencing and its demonstration in basic biology science. *Microb. Pathog.* 109, 280–286. doi: 10.1016/j.micpath.2017.05.030
- Bao, X., Yang, L., Chen, L., Li, B., Lin, L., Li, Y., et al. (2017c). Virulent and pathogenic features on the *Cronobacter sakazakii* polymyxin resistant pmr mutant strain s-3. *microbial pathogenesis. Microb. Pathog.* 110, 359–364. doi: 10.1016/j.micpath.2017.07.022
- Chen, H., Zhong, C., Zhang, T., Shu, M., Lin, L., Luo, Q., et al. (2019). Rapid and sensitive detection of viable but non-culturable *Salmonella* induced by low temperature from chicken using EMA-Rti-LAMP combined with BCAC. *Food Anal. Methods.* 13, 313–324. doi: 10.1007/s12161-019-01655-9
- Chmielewski, R. A., and Frank, J. F. (1995). Formation of viable but nonculturable *Salmonella* during starvation in chemically defined solutions. *Lett. Appl. Microbiol.* 20, 380–384. doi: 10.1111/j.1472-765x.1995.tb01326.x
- Eng, S.-K., Puspajajah, P., Ab Mutalib, N.-S., Ser, H.-L., Chan, K.-G., and Lee, L.-H. (2015). *Salmonella*: a review on pathogenesis, epidemiology and antibiotic resistance. *Front. Life Sci.* 8:284–293. doi: 10.1080/21553769.2015.1051243
- Fakruddin, M., Mannan, K. S., and Andrews, S. (2013). Viable but nonculturable bacteria: food safety and public health perspective. *ISRN Microbiol.* 2013:703813.
- Gupte, A. R., de Rezende, C. L. E., and Joseph, S. W. (2003). Induction and resuscitation of viable but nonculturable *Salmonella enterica* serovar typhimurium DT104. *Appl. Environ. Microbiol.* 69, 6669–6675. doi: 10.1128/aem.69.11.6669-6675.2003
- Highmore, C. J., Warner, J. C., Rothwell, S. D., Wilks, S. A., and Keevil, C. W. (2018). Viable-but-nonculturable listeria monocytogenes and *Salmonella enterica* serovar thompson induced by chlorine stress remain infectious. *mBio* 9:e00540-18.
- Jia, X., Hua, J., Liu, L., Xu, Z., and Li, Y. (2018). Phenotypic characterization of pathogenic *Cronobacter* spp. strains. *Microb. Pathog.* 121, 232–237. doi: 10.1016/j.micpath.2018.05.033
- Jiang, X., Dong, D., Bian, L., Zou, D., He, X., Ao, D., et al. (2016). Rapid detection of candida albicans by polymerase spiral reaction assay in clinical blood samples. *Front. Microbiol.* 7:916. doi: 10.3389/fmicb.2016.00916
- Kirk, M. D., Pires, S. M., Black, R. E., Caipo, M., Crump, J. A., Devleeschauwer, B., et al. (2015). World health organization estimates of the global and regional

- disease burden of 22 foodborne bacterial, protozoal, and viral diseases, 2010: a data synthesis. *PLoS Med.* 12:e1001921. doi: 10.1371/journal.pmed.1001921
- Kusumoto, A., Asakura, H., and Kawamoto, K. (2012). General stress sigma factor RpoS influences time required to enter the viable but non-culturable state in *Salmonella enterica*. *Microbiol. Immunol.* 56, 228–237. doi: 10.1111/j.1348-0421.2012.00428.x
- Liao, C., Shollenberger, L. M., and Phillips, J. G. (2003). Lethal and sublethal action of acetic acid on *Salmonella* in vitro and on cut surfaces of apple slices. *J. Food Sci.* 68, 2793–2798. doi: 10.1111/j.1365-2621.2003.tb05807.x
- Liao, H., Zhang, R., Zhong, K., Ma, Y., Nie, X., and Liu, Y. (2018). Induction of a viable but non-culturable state in *Salmonella typhimurium* is correlated with free radicals generated by thermosonication. *Int. J. Food Microbiol.* 286, 90–97. doi: 10.1016/j.ijfoodmicro.2018.07.017
- Lin, S., Li, L., Li, B., Zhao, X., Lin, C., Deng, Y., et al. (2016). Development and evaluation of quantitative detection of N-epsilon-carboxymethyl-lysine in *Staphylococcus aureus* biofilm by LC-MS method. *Basic Clin. Pharmacol. Toxicol.* 118, 33. doi: 10.1007/978-1-4614-3828-1_2
- Lin, S., Yang, L., Chen, G., Li, B., Chen, D., Lin, L., et al. (2017). Pathogenic features and characteristics of food borne pathogens biofilm: biomass, viability and matrix. *Microb. Pathog.* 111, 285–291. doi: 10.1016/j.micpath.2017.08.005
- Liu, J., Zhou, R., Li, L., Peters, B. M., Li, B., Lin, C., et al. (2017). Viable but non-culturable state and toxin gene expression of enterohemorrhagic *Escherichia coli* O157 under cryopreservation. *Res. Microbiol.* 168, 188–193. doi: 10.1016/j.resmic.2016.11.002
- Liu, L., Lu, Z., Li, L., Li, B., Zhang, X., Zhang, X., et al. (2018a). Physical relation and mechanism of ultrasonic bactericidal activity on pathogenic *E. coli* with WPI. *Microb. Pathog.* 117, 73–79. doi: 10.1016/j.micpath.2018.02.007
- Liu, L., Xu, R., Li, L., Li, B., Zhang, X., Zhang, X., et al. (2018b). Correlation and in vitro mechanism of bactericidal activity on *E. coli* with whey protein isolate during ultrasonic treatment. *Microb. Pathog.* 115, 154–158. doi: 10.1016/j.micpath.2017.12.062
- Liu, L., Ye, C., Soteyome, T., Zhao, X., Xia, J., Xu, W., et al. (2019). Inhibitory effects of two types of food additives on biofilm formation by foodborne pathogens. *MicrobiologyOpen* 8:e853. doi: 10.1002/mbio.3.853
- Liu, W., Dong, D., Yang, Z., Zou, D., Chen, Z., Yuan, J., et al. (2015). Polymerase spiral reaction (PSR): a novel isothermal nucleic acid amplification method. *Sci. Rep.* 5:12723. doi: 10.1038/srep12723
- Ma, Y., Deng, Y., Xu, Z., Liu, J., Dong, J., Yin, H., et al. (2017). Development of a propidium monoazide-polymerase chain reaction assay for detection of viable *Lactobacillus brevis* in beer. *Braz. J. Microbiol.* 48, 740–746. doi: 10.1016/j.bjm.2016.11.012
- Mani-López, E., García, H. S., and López-Malo, A. (2012). Organic acids as antimicrobials to control *Salmonella* in meat and poultry products. *Food Res. Int.* 45, 713–721. doi: 10.1016/j.foodres.2011.04.043
- Miao, J., Chen, L., Wang, J., Wang, W., Chen, D., Li, L., et al. (2017a). Current methodologies on genotyping for nosocomial pathogen methicillin-resistant *Staphylococcus aureus* (MRSA). *Microb. Pathog.* 107, 17–28. doi: 10.1016/j.micpath.2017.03.010
- Miao, J., Chen, L., Wang, J., Wang, W., Chen, D., Li, L., et al. (2017b). Evaluation and application of molecular genotyping on nosocomial pathogen-methicillin-resistant *Staphylococcus aureus* isolates in Guangzhou representative of Southern China. *Microb. Pathog.* 107, 397–403. doi: 10.1016/j.micpath.2017.04.016
- Miao, J., Liang, Y., Chen, L., Wang, W., Wang, J., Li, B., et al. (2017c). Formation and development of *Staphylococcus* biofilm: with focus on food safety. *J. Food Saf.* 37:e12358. doi: 10.1111/jfs.12358
- Miao, J., Peters, B. M., Li, L., Li, B., Zhao, X., Xu, Z., et al. (2016). Evaluation of ERIC-PCR for fingerprinting methicillin-resistant *Staphylococcus aureus* strains. *Basic Clin. Pharmacol. Toxicol.* 118:33.
- Miao, J., Wang, W., Xu, W., Su, J., Li, L., Li, B., et al. (2018). The fingerprint mapping and genotyping systems application on methicillin-resistant *Staphylococcus aureus*. *Microb. Pathog.* 125, 246–251. doi: 10.1016/j.micpath.2018.09.031
- Morishige, Y., Fujimori, K., and Amano, F. (2013). Differential resuscitative effect of pyruvate and its analogues on VBNC (viable but non-culturable) *Salmonella*. *Microbes Environ.* 28, 180–186. doi: 10.1264/jsm.2012174
- Morishige, Y., Koike, A., Tamura-Ueyama, A., and Amano, F. (2017). Induction of viable but nonculturable *Salmonella* in Exponentially grown cells by exposure to a low-humidity environment and their resuscitation by catalase. *J. Food Prot.* 80, 288–294. doi: 10.4315/0362-028x.jfp-16-183
- Oliver, J. D., Dagher, M., and Linden, K. (2005). Induction of *Escherichia coli* and *Salmonella typhimurium* into the viable but nonculturable state following chlorination of wastewater. *J. Water Health.* 3, 249–257. doi: 10.2166/wh.2005.040
- Pu, Y., Li, Y., Jin, X., Tian, T., Ma, Q., Zhao, Z., et al. (2019). Dependent dynamic protein aggregation regulates bacterial dormancy depth critical for antibiotic tolerance. *Mol. Cell.* 73:e4.
- Purevdorj-Gage, L., Nixon, B., Bodine, K., Xu, Q., and Doerrler, W. T. (2018). Differential effect of food sanitizers on formation of viable but nonculturable *Salmonella enterica* in poultry. *J. Food Protect.* 81, 386–393. doi: 10.4315/0362-028x.jfp-17-335
- Robben, C., Fister, S., Witte, A. K., Schoder, D., Rossmanith, P., and Mester, P. (2018). Induction of the viable but non-culturable state in bacterial pathogens by household cleaners and inorganic salts. *Sci. Rep.* 8:15132.
- Roszak, D. B., Grimes, D. J., and Colwell, R. R. (1984). Viable but nonrecoverable stage of *Salmonella enteritidis* in aquatic systems. *Can. J. Microbiol.* 30, 334–338. doi: 10.1139/m84-049
- Sharma, J., Kumar, D., Hussain, S., Pathak, A., Shukla, M., Prasanna Kumar, V., et al. (2019). Prevalence, antimicrobial resistance and virulence genes characterization of nontyphoidal *Salmonella* isolated from retail chicken meat shops in Northern India. *Food Control.* 102, 104–111. doi: 10.1016/j.foodcont.2019.01.021
- Wang, L., Zhao, X., Chu, J., Li, Y., Li, Y., Li, C., et al. (2011). Application of an improved loop-mediated isothermal amplification detection of *Vibrio parahaemolyticus* from various seafood samples. *Afr. J. Microbiol. Res.* 5, 5765–5771. doi: 10.5897/AJMR11.1237
- Wang, X., Xu, X., Hu, W., Zuo, K., Kan, Y., Yao, L., et al. (2019). Visual detection of porcine epidemic diarrhea virus using a novel reverse transcription polymerase spiral reaction method. *BMC Vet Res.* 15:116. doi: 10.1186/s12917-019-1851-7
- Wen, S., Feng, D., Chen, D., Yang, L., and Xu, Z. (2020). Molecular epidemiology and evolution of *Haemophilus influenzae*. *Infect. Genet. Evol.* 80:104205. doi: 10.1016/j.meegid.2020.104205
- Xie, J., Peters, B. M., Li, B., Lin, L., Yu, G., Xu, Z., et al. (2017a). Clinical features and antimicrobial resistance profiles of important *Enterobacteriaceae* pathogens in guangzhou representative of Southern China, 2001–2015. *Microb. Pathog.* 107, 206–211. doi: 10.1016/j.micpath.2017.03.038
- Xie, J., Yang, L., Peters, B. M., Chen, L., Chen, D., Li, B., et al. (2017b). A 16-year retrospective surveillance report on the pathogenic features and antimicrobial susceptibility of *Pseudomonas aeruginosa* isolated from Guangzhou representative of Southern China. *Microb. Pathog.* 110, 37–41. doi: 10.1016/j.micpath.2017.06.018
- Xu, Z., Gui, Z., Lin, L., Li, B., Su, J., Zhao, X., et al. (2012a). Expression and purification of gp41-gp36 Fusion protein and application in serological screening assay of HIV-1 and HIV-2. *Afr. J. Microbiol. Res.* 6, 6295–6299. doi: 10.5897/AJMR12.1075
- Xu, Z., Hou, Y., Peters, B. M., Chen, D., Li, B., and Li, L. (2016a). Chromogenic media for MRSA diagnostics. *Mol. Biol. Rep.* 43, 1205–1212. doi: 10.1007/s11033-016-4062-3
- Xu, Z., Hou, Y., Qin, D., Liu, X., Li, B., Li, L., et al. (2016b). Evaluation of current methodologies for rapid identification of methicillin-resistant staphylococcus aureus strains. *Basic Clin. Pharmacol. Toxicol.* 118:33.
- Xu, Z., Li, L., Alam, M. J., Zhang, L., Yamasaki, S., and Shi, L. (2008a). First confirmation of integron-bearing methicillin-resistant *Staphylococcus aureus*. *Curr. Microbiol.* 57, 264–268. doi: 10.1007/s00284-008-9187-8
- Xu, Z., Li, L., Shi, L., and Shirliff, M. E. (2011a). Class 1 integron in staphylococci. *Mol. Biol. Rep.* 38, 5261–5279. doi: 10.1007/s11033-011-0676-7
- Xu, Z., Li, L., Shirliff, M. E., Alam, M. J., Yamasaki, S., and Shi, L. (2009). Occurrence and characteristics of class 1 and 2 integrons in *Pseudomonas aeruginosa* isolates from patients in Southern China. *J. Clin. Microbiol.* 47, 230–234. doi: 10.1128/JCM.02027-08
- Xu, Z., Li, L., Shirliff, M. E., Peters, B. M., Peng, Y., Alam, M. J., et al. (2010). First report of class 2 integron in clinical *Enterococcus faecalis* and class 1 integron in *Enterococcus faecium* in South China. *Diagn. Microbiol. Infect. Dis.* 68, 315–317. doi: 10.1016/j.diagmicrobio.2010.05.014
- Xu, Z., Li, L., Zhao, X., Chu, J., Li, B., Shi, L., et al. (2011b). Development and application of a novel multiplex polymerase chain reaction (PCR) assay for

- rapid detection of various types of staphylococci strains. *Afr. J. Microbiol. Res.* 5, 1869–1873. doi: 10.5897/AJMR11.437
- Xu, Z., Liang, Y., Lin, S., Chen, D., Li, B., Lin, L., et al. (2016c). Crystal Violet and XTT Assays on *Staphylococcus aureus* Biofilm Quantification. *Curr. Microbiol.* 73, 474–482. doi: 10.1007/s00284-016-1081-1
- Xu, Z., Lin, L., Chu, J., Peters, B. M., Megan, M., Harris, L., et al. (2012b). Development and application of loop-mediated isothermal amplification assays on rapid detection of various types of staphylococci strains. *Food Res. Int.* 47, 166–173. doi: 10.1016/j.foodres.2011.04.042
- Xu, Z., Lin, L., Shirliff, M. E., Peters, B. M., Li, B., Peng, Y., et al. (2011c). Resistance class 1 integron in clinical methicillin-resistant *Staphylococcus aureus* strains in southern China, 2001–2006. *Clin. Microbiol. Infect.* 17, 714–718. doi: 10.1111/j.1469-0691.2010.03379.x
- Xu, Z., Shi, L., Alam, M. J., Li, L., and Yamasaki, S. (2008b). Integron-bearing methicillin-resistant coagulase-negative staphylococci in South China, 2001–2004. *FEMS Microbiol. Lett.* 278, 223–230. doi: 10.1111/j.1574-6968.2007.00994.x
- Xu, Z., Shi, L., Zhang, C., Zhang, L., Li, X., Cao, Y., et al. (2007). Nosocomial infection caused by class 1 integron-carrying *Staphylococcus aureus* in a hospital in South China. *Clin. Microbiol. Infect.* 13, 980–984. doi: 10.1111/j.1469-0691.2007.01782.x
- Xu, Z., Xie, J., Peters, B. M., Li, B., Li, L., Yu, G., et al. (2017a). Longitudinal surveillance on antibiogram of important gram-positive pathogens in Southern China, 2001 to 2015. *Microb. Pathog.* 103, 80–86. doi: 10.1016/j.micpath.2016.11.013
- Xu, Z., Xie, J., Yang, L., Chen, D., Peters, B. M., and Shirliff, M. E. (2018). Complete Sequence of pCY-CTX, a Plasmid Carrying a Phage-Like Region and ISEcp1-Mediated Tn2 Element from *Enterobacter cloacae*. *Microb. Drug Resist.* 24, 307–313. doi: 10.1089/mdr.2017.0146
- Xu, Z., Xu, X., Yang, L., Li, B., Lin, L., Li, X., et al. (2017b). Effect of aminoglycosides on the pathogenic characteristics of microbiology. *Microb. Pathog.* 113, 357–364. doi: 10.1016/j.micpath.2017.08.053
- You, R., Gui, Z., Xu, Z., Shirliff, M. E., Yu, G., Zhao, X., et al. (2012). Methicillin-resistance *Staphylococcus aureus* detection by an improved rapid PCR assay. *Afr. J. Microbiol. Res.* 6, 7131–7133. doi: 10.5897/AJMR12.708
- Zeng, B., Zhao, G., Cao, X., Yang, Z., Wang, C., and Hou, L. (2013). Formation and resuscitation of viable but Nonculturable *Salmonella typhi*. *BioMed Res. Int.* 2013, 1–7. doi: 10.1155/2013/907170
- Zhang, N., Gui, Z., Li, X., Huang, J., Hu, K., Gao, Y., et al. (2013). Solvent-free enzymatic synthesis of 1, 3-Diacylglycerols by direct esterification of glycerol with saturated fatty acids. *Lipids n Health nd Dis.* 12, 2–7. doi: 10.1186/1476-511X-12-65
- Zhao, X., Li, M., and Xu, Z. (2018a). Detection of foodborne pathogens by surface enhanced raman spectroscopy. *Front. Microbiol.* 9:1236. doi: 10.3389/fmicb.2018.01236
- Zhao, X., Yu, Z., and Xu, Z. (2018b). Study the features of 57 confirmed CRISPR Loci in 38 Strains of *Staphylococcus aureus*. *Front. Microbiol.* 9:1591. doi: 10.3389/fmicb.2018.01591

Conflict of Interest: YL was employed by the company Guangdong Zhongqing Font Biochemical Science and Technology Co. Ltd.

The remaining authors declare that the research was conducted in the absence of any commercial or financial relationships that could be construed as a potential conflict of interest.

Copyright © 2020 Li, Huang, Bai, Fu, Chen, Liang, Wang, Liu, Gong and Liu. This is an open-access article distributed under the terms of the Creative Commons Attribution License (CC BY). The use, distribution or reproduction in other forums is permitted, provided the original author(s) and the copyright owner(s) are credited and that the original publication in this journal is cited, in accordance with accepted academic practice. No use, distribution or reproduction is permitted which does not comply with these terms.



Flagellar Motility Is Critical for *Salmonella enterica* Serovar Typhimurium Biofilm Development

Feiying Wang, Le Deng*, Fangfang Huang, Zefeng Wang, Qiuju Lu and Chenran Xu

State Key Laboratory of Developmental Biology of Freshwater Fish, College of Life Science, Hunan Normal University, Changsha, China

OPEN ACCESS

Edited by:

Yang Deng,
Qingdao Agricultural University, China

Reviewed by:

Jose Antonio Ibarra,
National Polytechnic Institute, Mexico
Irfan Ahmad,
University of Health Sciences,
Pakistan
Andrea Battistoni,
University of Rome Tor Vergata, Italy

*Correspondence:

Le Deng
Dengle@hunnu.edu.cn

Specialty section:

This article was submitted to
Food Microbiology,
a section of the journal
Frontiers in Microbiology

Received: 19 September 2019

Accepted: 29 June 2020

Published: 09 September 2020

Citation:

Wang F, Deng L, Huang F,
Wang Z, Lu Q and Xu C (2020)
Flagellar Motility Is Critical
for *Salmonella enterica* Serovar
Typhimurium Biofilm Development.
Front. Microbiol. 11:1695.
doi: 10.3389/fmicb.2020.01695

The food-borne pathogen *Salmonella enterica* serovar Typhimurium (S. Typhimurium) causes self-limiting gastroenteritis in humans and is not easily eradicated because it often attaches to suitable surfaces to form biofilms that have high resistance to disinfectants and antimicrobials. To develop an alternative strategy for the treatment of biofilms, it is necessary to further explore the effects of flagellar motility on the development process of *Salmonella* biofilms. Here, we constructed flagella mutants ($\Delta flgE$ and $\Delta flhC$) to systematically study this process. By comparing them with wild-type strains, we found that these mutants lacking flagellar motility form fewer biofilms in the early stage, and the formed mature biofilms contain more cells and extracellular polymeric substances (EPS). In addition, fewer mutant cells adhered to glass plates compared with wild-type cells even after 6 h of incubation, suggesting that flagellar motility plays a significant role in preliminary cell-surface interactions. More importantly, the motility of wild-type strain was greatly decreased when they were treated with carbonyl cyanide m-chlorophenylhydrazone, which inhibited flagellar motility and reduced biofilm formation, as in the case of the $\Delta flgE$ mutant. Overall, these findings suggest that flagellar motility plays an important role in *Salmonella* biofilm initiation and maturation, which can help us to counteract the mechanisms involved in biofilm formation and to develop more rational control strategies.

Keywords: flagellum, biofilms, motility, S. Typhimurium, confocal laser scanning microscopy

INTRODUCTION

Contamination of fresh produce with food-borne pathogens is a potential threat to public health. *Salmonella enterica* serovar Typhimurium (S. Typhimurium) is a food-borne pathogen that causes high morbidity worldwide, including life-threatening infections in fetuses, newborns, and immunocompromised individuals (Achin et al., 2019). Its natural habitat is the gut of animals and humans, and infection occurs through fecal contamination of soil, water, plants and medical equipment, which spreads the bacteria to other hosts (Semenov et al., 2010; Jacobsen and Bech, 2012; MacKenzie et al., 2017). Once attached to one of these surfaces, the bacteria begin to form biofilms. Bacteria inside biofilms are more resistant to external antibiotics, disinfectants, and environmental stress, so they can be extremely difficult to eradicate, in contrast to planktonic bacteria (Pande et al., 2016). The biofilms cause food safety issues and can lead to enormous economic losses.

Biofilms are the preferred lifestyle for most microorganisms in nature (Stoodley et al., 2002). Biofilms begin to develop when bacteria adhere reversibly to a surface. The adhered cells then form microcolonies, which synthesize extracellular matrices to support mature three-dimensional biofilms. Bacteria within the biofilms can undergo controlled dissociation, resulting in biofilm dispersal (Watnick and Kolter, 2000; Koo et al., 2017). Biofilm formation is influenced by the structural composition (curli and other fimbriae, flagella, BapA et al.), the bacterial genome, environmental signals, and stress factors (Watnick and Kolter, 2000; Simm et al., 2014; MacKenzie et al., 2017). A variety of biofilms inhibitors have been developed that target these factors, including some that target the flagella. Previous research has shown that furanones reduce biofilm formation through interfering with *Salmonella* flagellar synthesis (Janssens et al., 2008). Moreover, zinc is required for flagellar expression, and the absence of flagella impairs the ability of *S. Typhimurium* to produce biofilms (Ammendola et al., 2016). However, in order to make more effective strategies for the treatment of biofilms targeting flagella, it is necessary to further clarify the effect of flagellar motility on the development process and composition of *Salmonella* biofilms.

Flagella, as main motility organs of bacteria, play important roles in the formation biofilm of several gram-negative bacteria (O'Toole et al., 2000; Haiko and Westerlund-Wikström, 2013). Some studies have proposed that flagella might act in biofilm formation both as providers of motility and as surface adhesins, however, in *Escherichia coli* and *Listeria monocytogenes* it is motility itself that is critical (O'Toole and Kolter, 1998; Pratt and Kolter, 1998; Lemon et al., 2007). In *S. Typhimurium*, previous studies performed with *motA* and *fliA* mutants have suggested that motility is necessary for biofilm development on the glass (Huber et al., 2002; Prouty and Gunn, 2003). Moreover, it has been described that *Salmonella* mutants with defective flagella (*flhC* or *flgE*) are unable to develop complete biofilms in the presence of bile (Crawford et al., 2010; Tsai et al., 2019). Previously, work regarding QseBC two-component system (TCS) function in *S. Typhimurium* revealed that QseBC functions as a global regulator of flagella, biofilm formation, and virulence (Merighi et al., 2009; Bearson et al., 2010; Ji et al., 2017). Recent studies have shown that the cyclic di-guanylate monophosphate (c-di-GMP) receptor YcgR and the phosphodiesterase YhjH can distinctively inhibit flagellar motility in *S. Typhimurium* (Le Guyon et al., 2015; Han and Yoon, 2019). Taken together, the role of flagellar motility in the development of *Salmonella* biofilm is very important. By observing the number and distribution of polysaccharides and cells, we can more intuitively judge the effect of flagellar motility on biofilm initiation and maturation. Therefore, this study aims to deepen the understanding of the effect of flagellar motility on biofilm development and to provide theoretical support for the development of biofilms inhibitors that interfere with flagella motility.

In many motile bacteria, the synthesis and assembly of flagella involve at least 50 genes that are divided into early, middle, and late genes, which are hierarchically and temporally synchronized (Aizawa, 1996). *flgE* is a middle gene that encodes the major component of the hook-basal body structure, which is necessary

for flagellar filament elongation (Bonifield et al., 2000). *fliC* is a late gene that encodes the major component of the flagellin structure, which is necessary for the formation of the helical filament (Chilcott and Hughes, 2000). Mutations in these two genes may impair flagellar motility, therefore, our primary approach involved deleting *flgE* and *fliC* and observing the effect on flagellar motility. Our results confirmed that a lack of flagellar motility affects bacterial contact with abiotic surfaces, and reduces cell colonization and early biofilm formation. Moreover, the mature biofilms formed by these flagella mutants had denser matrices and contained more aggregated cells.

EXPERIMENTAL

Bacterial Strains, Plasmids, and Growth Media, and Chemicals

S. Typhimurium CMCC 50115 is a *S. Typhimurium* LT2 derivative. All strains and plasmids used in this work are described in **Supplementary Table S1**. All strains were grown on Luria-Bertani (LB) broth agar plates or in LB broth liquid medium (Tryptone 10 g/L; Yeast Extract 5 g/L; NaCl 10 g/L) at 37°C. Chloramphenicol (Cm, 25 µg/mL), ampicillin (100 µg/mL), L – (+)– Arabinose (5 mmol/L) were added when required. SYTO® 9 (Invitrogen, S 34854); Alexa Fluor® 647 conjugate of Con A (Invitrogen, C 21421); Carbonyl cyanide m-chlorophenylhydrazine (CCCP, Sigma) acted as an inhibitor of proton-driven force of the flagella (Kosaka et al., 2019).

Rdara Morphotype and Pellicle Formation

After one colony of the bacteria from LB plates was transferred into a tube containing 3 mL of LB medium and incubated for 18 h at 37°C, the amount of inoculation was adjusted to optical density OD₆₀₀ = 1.0, and confirmed by plate counts of 10 fold dilutions of the bacteria. These bacterial cultures contained approximately 10⁸ CFU/mL. The *Salmonella* morphotype was judged visually on Congo red agar plates, 2 µL of bacterial suspension (OD₆₀₀ of 4.0) was plated onto LB agar plates without NaCl and complemented with Congo red (40 mg/L, Aladdin) and Coomassie brilliant blue G-250 (20 mg/L, Sangon). The inoculated plates were incubated at 28°C for 48 h and colonies were visualized macroscopically.

The method measures biofilm production on the air-liquid interface in a modified method as previously reported (Ramachandran et al., 2016). Briefly, overnight *Salmonella* strains were transferred into 3 mL of LB medium without NaCl (1:100 dilutions) for 5 days at 28°C without shaking. To observe the biofilms that form at the liquid-air interface, the culture was gently poured out and further stained with 1% crystal violet.

Biofilm Formation and Quantification Assay

Biofilm formation was observed as described previously with some modifications (Baugh et al., 2012). Experiments in 96-well polystyrene microtiter plates (Sangon) were performed. Overnight cultures were diluted to 10⁶ CFU/mL in LB medium

without NaCl. A total volume of 0.2 mL was added per well, followed by 24 h incubation at 28°C in static conditions. The total amount of biofilm biomass was quantified by crystal violet. After careful removal of the medium from wells, the biofilms were rinsed three times with deionized water. 1% crystal violet was used to stain biofilms for 15 min, and then the excess of stain was removed by gently washing with deionized water. Residual crystal violet was solubilized with 200 μ L of 33% glacial acetic acid per well and the OD₅₉₅ was measured using an ELISA reader (Thermo Scientific Labsystems 354). LB medium without NaCl was used as a negative control in all biofilm assays. All experiments were repeated three times at different time points.

Construction of Mutants and the Complemented Strains

The flagella-deficient strains were constructed by allelic replacement via homologous recombination (Datsenko and Wanner, 2000). Homologous regions and a chloramphenicol cassette with two FRT sites were PCR-amplified from pKD3, and the purified PCR product was digested with *DpnI* (Invitrogen) and electroporated into bacteria carrying pKD46. Antibiotic selection and the λ Red recombineering system led to homologous recombination between the fragments and the host strain genome, and the recombinants were selected for on agar plates containing chloramphenicol. The pCP20 plasmid was introduced to the recombinant strains to remove the DNA fragment containing the chloramphenicol resistance gene, resulting in a single FRT site within the targeted genomic segment. The markerless mutant strains were verified by genomic DNA PCR using primers that annealed to sequences flanking

the target gene and further confirmed by sequencing analysis (**Supplementary Table S2** and **Supplementary Figures S1, S2**).

To generate the Δ *flgE* complemented strain, the full-length *flgE* gene was PCR-amplified from *S. Typhimurium* wild-type strain CMCC50115 genomic DNA using the primers *flgE*-F3 and *flgE*-F4 (**Supplementary Table S2**). The PCR product was ligated into pBad/gIIIa, and the resulting plasmid was transformed into the Δ *flgE* strain by electroporation. The Δ *fliC* complemented strain was constructed by the same method.

Motility Assays

Swimming motility was performed as described previously (Duan et al., 2012). Briefly, 30 μ L cultured overnight of bacterial was re-inoculated into 3 mL of LB and incubated at 37°C with a shaker at 200 rpm until a density value of approximately 1.0 at OD₆₀₀. The culture samples were inoculated onto 0.4% tryptone agar plates as 1 μ L aliquots (Tryptone 1%, NaCl 0.5%, Agar 0.4%). The bacteria grew for 12 h at 37°C and the swimming diameter was measured. Photographs were taken by using the SONY Alpha 7 camera.

Transmission Electron Microscopy (TEM) Analysis

Flagellar morphology was visualized by TEM with negative staining. A single colony was picked and inoculated into fresh LB medium, and the OD₆₀₀ value of the bacteria was adjusted to about 0.5. The cells were washed once with deionized water and resuspended in sterile water. A sample of 5 μ L of the bacterial solution was added dropwise to a copper mesh having a carbon film and dried at room temperature. Using 1% phosphotungstic acid (pH 7.4) for negative staining 2 min, excess solution was blotted with filter paper and observed via electron microscopy (TecnaiG2 F20, FEI, America).

Western Blot Analysis

Flagellar expression using whole-cell lysates was detected by western blot analysis (Shao et al., 2018). Overnight cultures of the tested bacteria were transformed into the fresh LB medium and cultivated an optimal density value of 1.0 at OD₆₀₀. 2 mL cultures were centrifuged at 9000 \times g for 10 min at 4°C to pellet the bacteria. The bacterial cells from whole-cell lysates were loaded and separated by 12% SDS-PAGE, followed by transfer onto a PVDF membrane (GE Healthcare, Life Science). The blot was incubated with mouse polyclonal antiserum to H1 flagella (1: 2000 dilutions, TBC, China), followed by HRP-conjugated Goat anti-mouse IgG (1: 200 dilutions, Sangon, China) orderly. The signal was detected by Luminata Forte Western HRP Substrate (Millipore). Photographs were taken by using the Tanon 5500 imaging system.

Confocal Laser Scanning Microscopy (CLSM) Imaging of Biofilms

After being cultured overnight in LB medium in a shaking 37°C incubator, the cultures were taken to dilute to 10⁷ CFU/mL in 50 mL LB medium without NaCl in a 100 mL Conical flask. A sterile glass slide was gently added into the diluted culture and was taken to statically incubate at 28°C

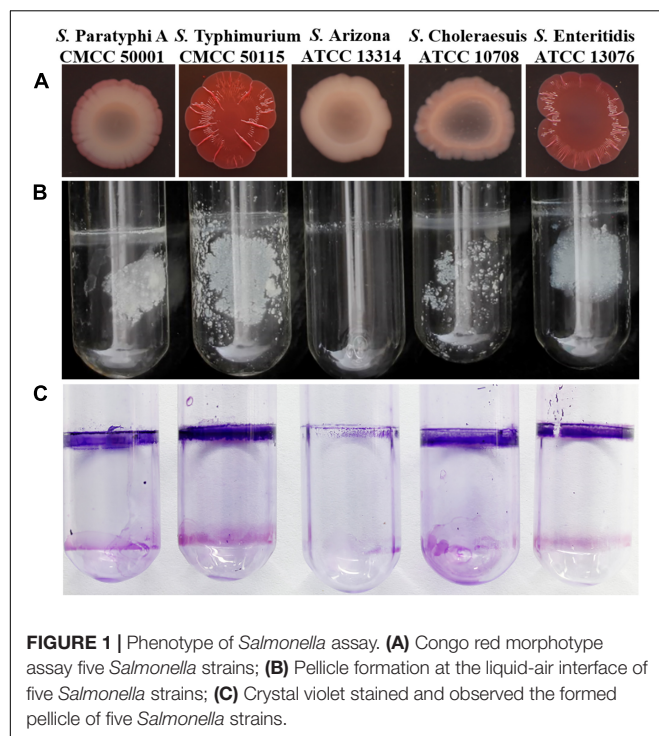
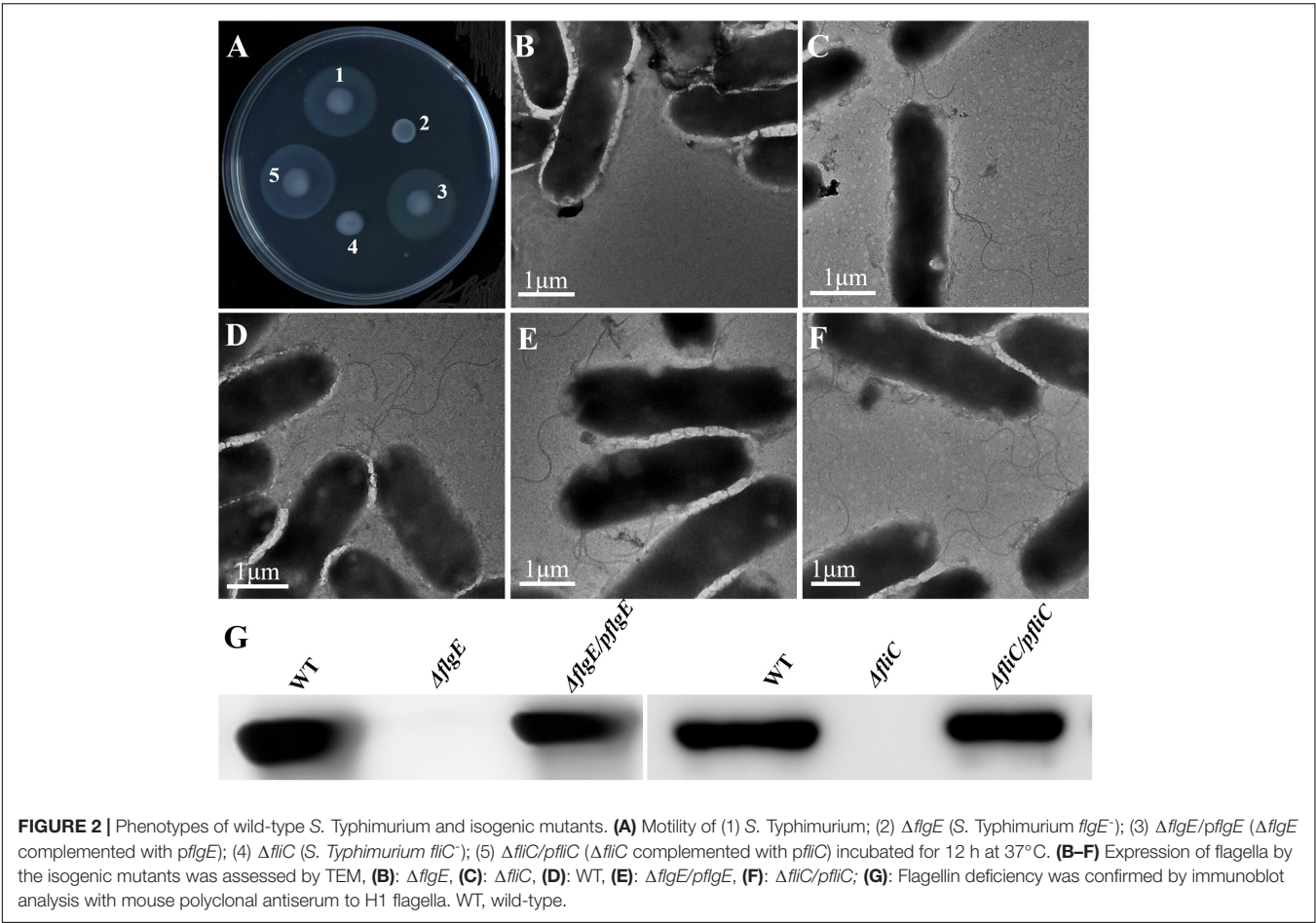


FIGURE 1 | Phenotype of *Salmonella* assay. **(A)** Congo red morphotype assay five *Salmonella* strains; **(B)** Pellicle formation at the liquid-air interface of five *Salmonella* strains; **(C)** Crystal violet stained and observed the formed pellicle of five *Salmonella* strains.

TABLE 1 | Collated biofilm assay results of *Salmonella* tested in this study.

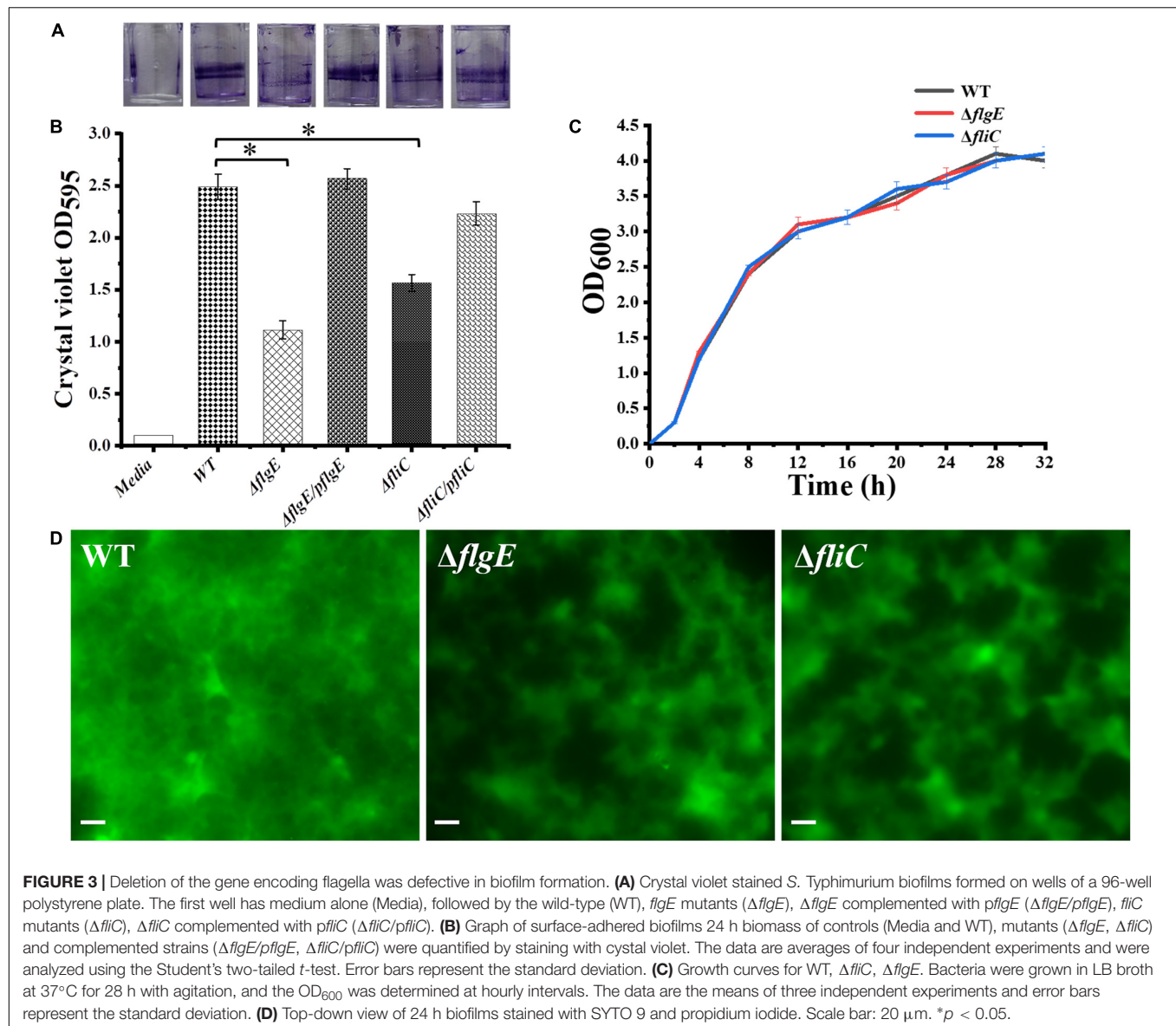
<i>Salmonella</i> Serotypes	Crystal Violet Assay (OD ₅₉₅)			Morphotype on Congo red ^b	Pellicle formation ^c
	LB	TSB	LB without salt		
<i>Salmonella</i> Typhimurium CMCC 50115	0.428 ± 0.131 ^a	0.945 ± 0.232	2.527 ± 0.612	rdar	+++
<i>Salmonella</i> Paratyphi A CMCC 50001	0.125 ± 0.056	0.545 ± 0.112	1.875 ± 0.423	bdar	+
<i>Salmonella</i> Enteritidis ATCC 13076	0.319 ± 0.081	0.613 ± 0.153	2.345 ± 0.103	rdar	+++
<i>Salmonella</i> Choleraesuis ATCC 10708	0.267 ± 0.061	0.322 ± 0.152	1.658 ± 0.064	bdar	++
<i>Salmonella</i> Arizona ATCC 13314	0.113 ± 0.03	0.214 ± 0.121	0.903 ± 0.032	saw	+

^aAverage OD (595 nm) ± standard error from two separate experiments. ^brdar: red, dry, and rough morphotype indicating curli and cellulose production; bdar: brown, dry, and rough morphotype indicating curli production but lack of cellulose synthesis; saw: smooth and white morphology. ^cpellicle formation: +++, strong pellicle; ++, moderate pellicle; +, weak pellicle.



(Supplementary Figure S4). After the culture time was terminated, the glass slide with biofilms was carefully taken out with tweezers and placed in a clean culture dish, and the residual culture medium on them was skimmed with deionized water. The glass slide was stained with 100 μ L of SYTO 9 (1 μ g/mL, green fluorescence, labeled bacterial cells) and Alexa Fluor 647 (50 μ g/mL, red fluorescence, labeled EPS) solution for 30 min, in the dark at room temperature. Confocal microscopy images were obtained on a Leica DMI8 microscope by using a 40 \times objective. The settings of the confocal microscope were as follows: the excitation/emission of Alexa Fluor 647 and SYTO 9

were 650/668 and 480/500 nm, respectively. Stack images were obtained by scanning the biofilms along the Z-axis at 0.5 μ m intervals. The confocal images were analyzed using COMSTAT software for simultaneous visualization and quantification of EPS and bacterial cells within intact biofilms (Heydorn et al., 2000). For each image stack, cell biomass ($\mu\text{m}^3/\mu\text{m}^2$) is defined as the percentage of area occupied by cells labeled by SYTO 9 (green fluorescence); EPS biomass ($\mu\text{m}^3/\mu\text{m}^2$) is defined as the percentage of area occupied by EPS labeled by concanavalin A-Alexa Fluor 647 (red fluorescence); Total biomass ($\mu\text{m}^3/\mu\text{m}^2$) is cell biomass plus EPS biomass.



Statistical Analysis

The statistical significance of numerical data was compared using variance analysis technology. Significant levels of *p* values were reported by the following symbols: **p* < 0.05, ***p* < 0.005, and ns, with no difference.

RESULTS

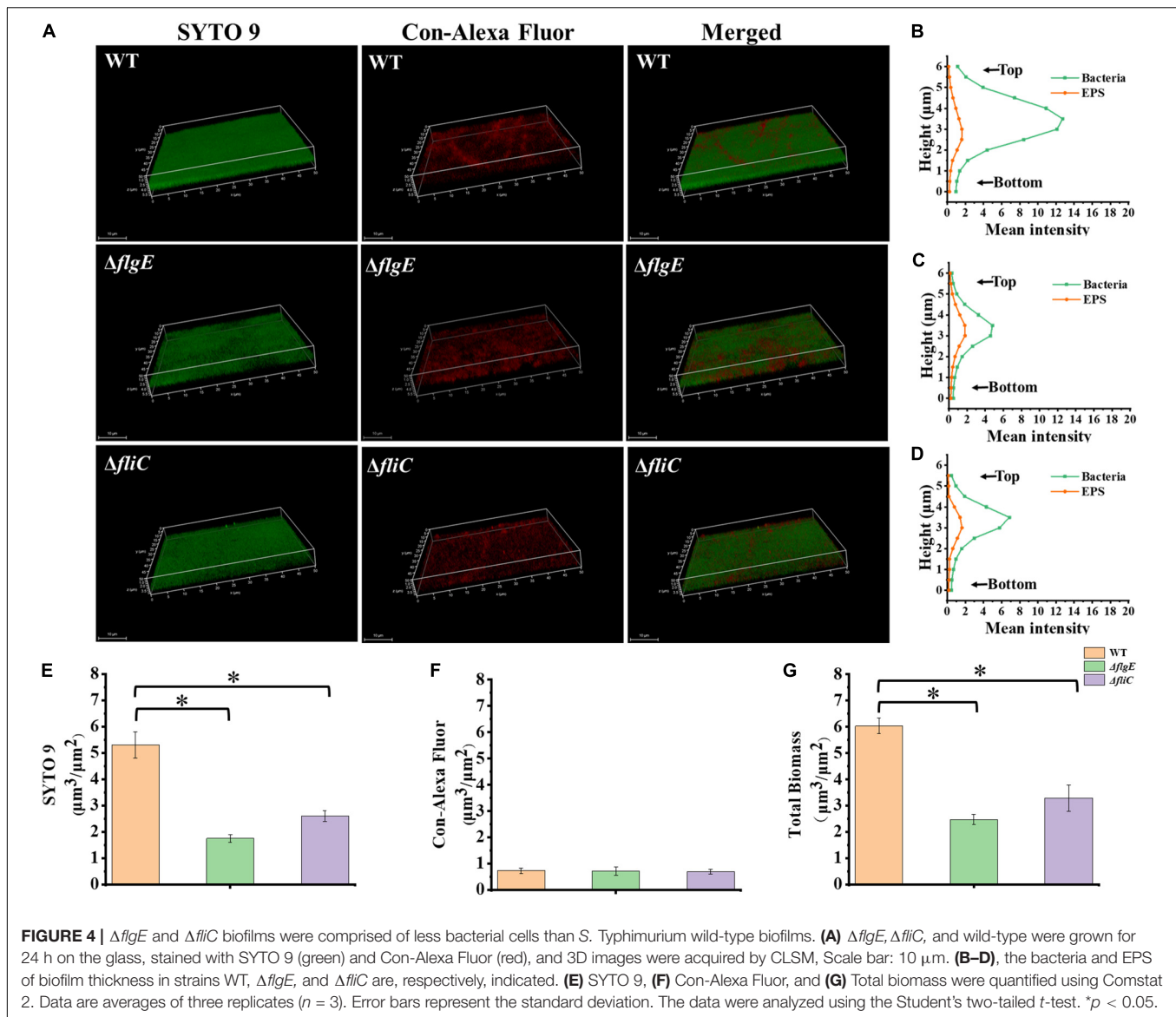
S. Typhimurium CMCC 50115 Biofilm Production

The best-studied *Salmonella* biofilm phenotype is the rdar morphotype (Römling et al., 1998). After culturing on media containing Congo red at 28°C for 2 days, both *S. Typhimurium* CMCC50115 and *S. Enteritidis* ATCC 13076 formed strong rdar morphotypes (Figure 1). In liquid culture, biofilms form a matrix

comprising curli and cellulose called pellicles, which appear as films of cell growth at the air-liquid interface (Solano et al., 2002). *S. Typhimurium* and *S. Enteritidis*, but not the other strains, formed obvious pellicles at the liquid-air interface (Figure 1). Since crystal violet staining showed that *S. Typhimurium* CMCC50115 formed more biofilms compared with the other strains (Table 1), we selected it for use as our wild-type control.

Construction and Characterization of Flagella Mutants

The wild-type strain was used to construct the $\Delta flgE$ and $\Delta fliC$ isogenic mutants via homologous recombination. The resulting $\Delta flgE$ and $\Delta fliC$ mutants exhibited impaired motility on 0.4% tryptone agar plates (Figure 2A). In the case of the $\Delta flgE$ strain, this may have been because of the loss of flagella. Confirming this, the flagellin protein was

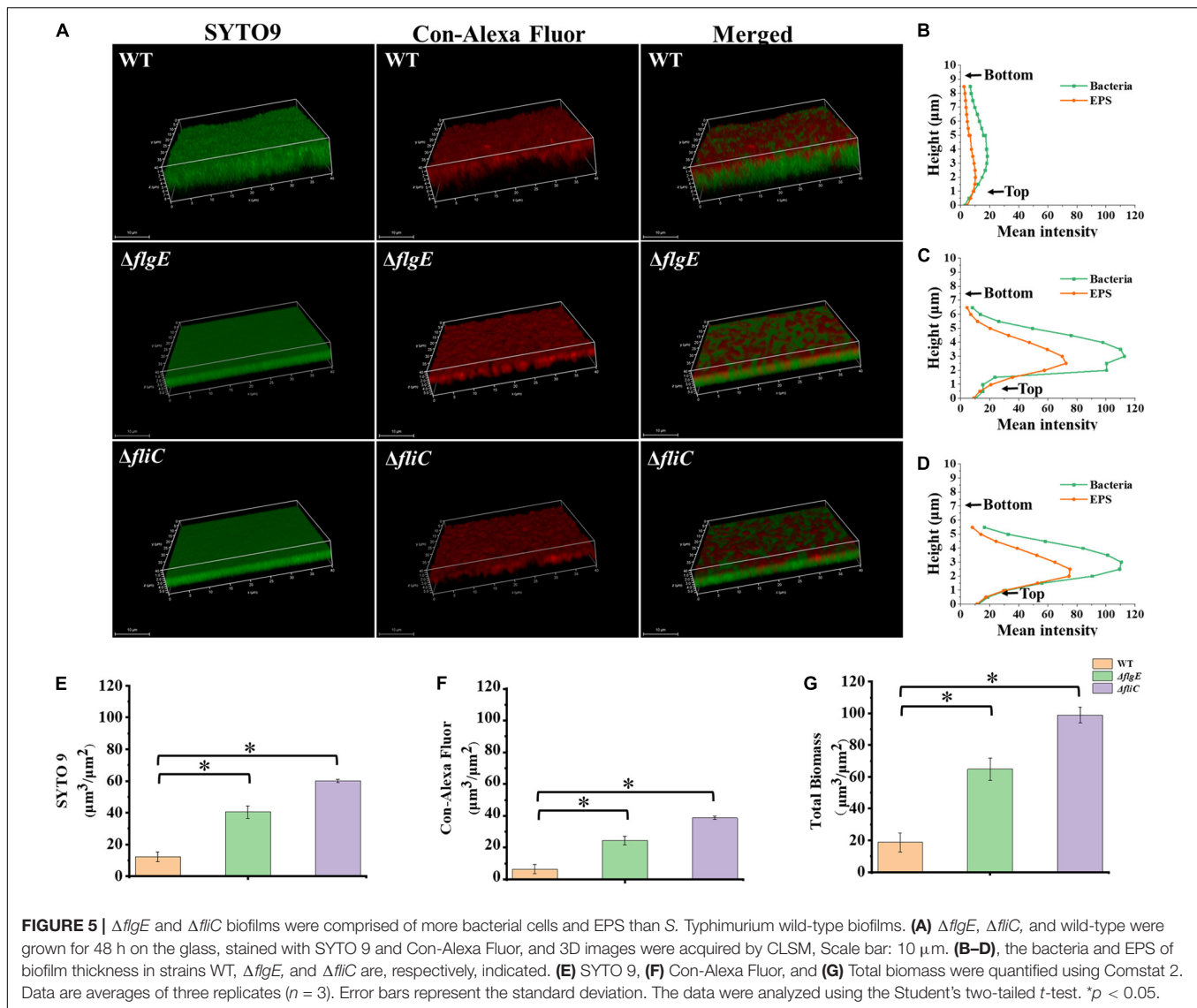


not detected by western blot analysis of whole-cell lysates (Figure 2G), and flagella were not observed by TEM in this mutant strain (Figures 2B,D). In contrast, flagellar protein expression (Figure 2G) and flagella production (Figure 2E) was restored in the complemented strain (*ΔflgE/pflgE*), which contained a recombinant plasmid expressing FlgE. In the *ΔfliC* strain, the impaired motility phenotype may be related to the absence of the FliC subunit, which plays a significant role in flagellar motility. As *S. Typhimurium* expresses two filament proteins, FliC (H1 flagellin) and FljB (H2 flagellin), the *ΔfliC* mutant could be flagellated under some circumstances. Corroborating this, flagellin protein was not detected by western blot analysis of whole-cell lysates (Figure 2G), but the *ΔfliC* strain had flagella (presumably composed of FljB), as observed by TEM (Figure 2C). In contrast, flagellar protein expression (Figure 2G) and flagella production (Figure 2F) was restored in the complemented strain (*ΔfliC/pfliC*), which contained a

recombinant plasmid expressing FliC. In addition, it was verified that the *fljB* sequence of the *ΔfliC* strain did not mutate (Supplementary Figure S7). Therefore, the *ΔfliC* strain lacking motility through FljB probably depends on some characteristics of the used strain. Taken together these data show that *flgE* and *fliC* are indispensable for flagellar motility.

Flagella Mutants Are Defective in the Early Stage of Biofilm Formation

The initial attachment of bacteria to a surface is a key step in their ability to form a biofilm. Compared with the wild-type strain, the two flagellar mutants were defective in the early stage of biofilm formation (Figure 3A). We measured biofilm formation by crystal violet staining and found that the two mutants formed fewer biofilms than the wild-type strain, with an average absorbance at 595 nm (OD_{595}) of 0.93 ± 0.13 and



1.61 ± 0.21 , respectively, compared with an OD_{595} of 2.47 ± 0.16 for the wild-type strain (Figures 3A,B). There was no difference in viability between the flagella mutants and the wild-type strain (Figure 3C). Importantly, biofilm formation was restored to wild-type levels when the mutants complemented (Figures 3A,B). Overall, these data demonstrate that flagella-mediated motility plays an important role in the early stage of biofilm formation.

Biofilm architecture can be assessed by staining with SYTO 9 and propidium iodide (Vermilyea et al., 2019). Fluorescence microscopy confirmed that biofilms formed by the $\Delta flgE$ and $\Delta fliC$ mutants comprised less biomass than those formed by the wild-type strain (Figures 3D, 4G). Biofilm composition was also evaluated by staining with SYTO 9 (which detects all bacteria) and concanavalin A-Alexa Fluor 647 (which detects EPS). There were significantly fewer bacteria in biofilms formed by the flagella mutants compared with those formed by the wild-type strain (Figure 4E). However, there was no significant difference in EPS content between the biofilms formed by the

mutant and wild-type strains (Figure 4F). In addition, there was no significant difference in biofilm thickness between the flagellar mutants and the wild-type strain (Figures 4A–D). Therefore, the reduced biofilm formation exhibited by the flagellar mutants could be due to reduced adhesion of planktonic cells at the initial stage compared with the wild-type strain.

Flagella Mutants Produce More Thick and Dense Biofilms

To explore the role of flagella on biofilm maturation, CLSM was used to directly observe biofilms that had been allowed to form for 48 h. The wild-type biofilms were twice as thick as the $\Delta flgE$ biofilms and had a looser inner structure than the mutant biofilms (Figures 5A–D). Additionally, the $\Delta flgE$ biofilms contained more cells and EPS than the wild-type biofilms (Figures 5E–G). The $\Delta fliC$ and $\Delta flgE$ biofilms exhibited similar phenotypes, and flagellar motility was impaired in both strains, suggesting that

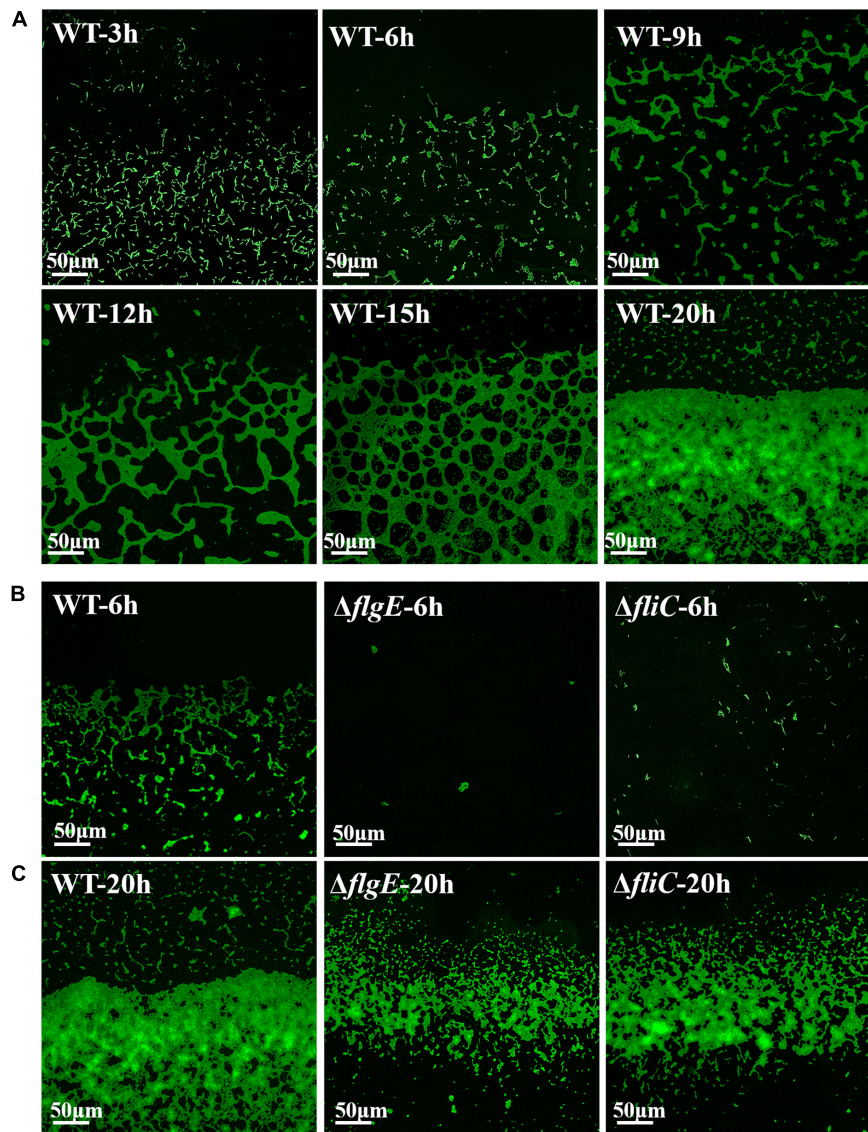


FIGURE 6 | Direct observation of biofilm formation on a sterile glass slide using a confocal fluorescence microscope. **(A)** Observed the adhesion of wild-type biofilms on the sterile glass slide over 20 h. **(B)** Shown are fluorescence micrographs of the wild-type strain, $\Delta flgE$, and $\Delta fliC$ after incubation for 6 h at 28°C. **(C)** The biofilms of the wild-type, $\Delta flgE$, and $\Delta fliC$ at 20 h were displayed. The micrographs were taken at 400 × magnification and the representative fields are shown and the experiments were repeated three times.

flagellar motility plays an important role in forming the structure of biofilms. Taken together, these findings indicate that the thick phenotype of biofilms formed by the flagella mutants is due to the accumulation of cells and EPS.

Flagella Mutants Exhibit Poor Adhesion, Which Inhibits the Initiation of Biofilm Formation

Next, we investigated the role of flagellar motility in the early steps in biofilm formation. To assess the initiation of biofilm formation by the flagella mutants and the wild-type strain, we directly visualized biofilm formation on sterile glass slides using

a confocal fluorescence microscope. **Figure 6A** shows a time-course of the development of wild-type biofilms on a sterile glass slide over 20 h at 28°C. Six hours after inoculation, the bacteria had aggregated into small clusters that gradually cross-linked together over the next 6–9 h. By 20 h, the clusters had developed into microcolonies comprising multiple layers of cells.

In contrast, 6 h after inoculation, the $\Delta flgE$ mutant had only formed a few scattered cell clusters (**Figure 6B**). By 20 h, the $\Delta flgE$ strain exhibited fewer colonies and a smaller total attachment area compared with the wild-type strain (**Figure 6C**). Further statistics on them continually supported the results (**Supplementary Figures S5, S6**). The $\Delta fliC$ mutants exhibited similar phenotypes. These observations are consistent with

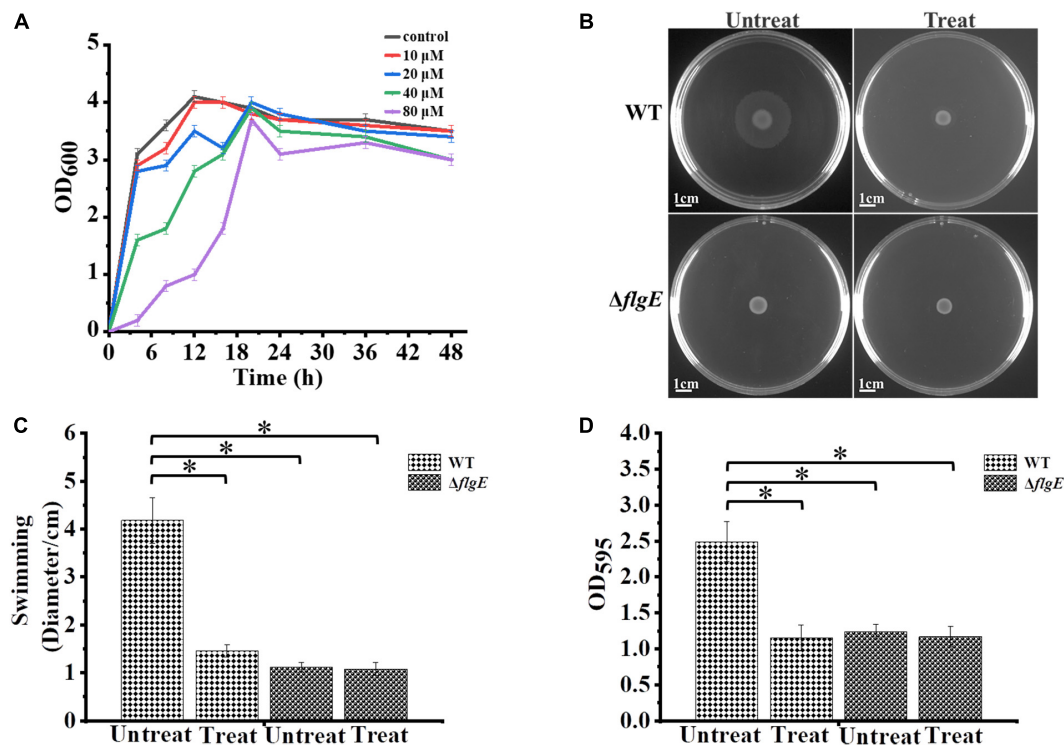


FIGURE 7 | Biofilm formation by *S. Typhimurium* after treatment with CCCP. **(A)** Analysis of the growth curve of wild-type strains treated with different concentrations of CCCP. **(B)** Swimming plates of different groups captured after incubation at 37°C for 12 h. Treat: add 1 μ L of 100 mM CCCP to a final concentration of 10 μ M CCCP per plate, Untreat: add 1 μ L DMSO according to the above treatment. **(C)** The quantitative analysis diameter of swimming. **(D)** The bacteria were cultured with or without 10 μ M protonophore CCCP, a quantitative analysis of the formation of biofilms cultured for 24 h by crystal violet staining. Data in **(B–D)** are representative of three independent experiments. Error bars represent the standard deviation. * $p < 0.05$.

our earlier results showing the importance of flagella-mediated motility in biofilm formation.

Effect of the Protonophore CCCP on Biofilm Formation

The motility of most bacterial flagella is driven by a proton gradient across the cytoplasmic membrane, so the protonophore CCCP was applied to explore the role of flagellar motility on biofilm formation (Kosaka et al., 2019). First, we treated the wild-type strain with CCCP to determine the optimal concentration for inhibiting cell spreading on semisolid agar. In the presence of 10 μ M of the protonophore CCCP on 0.4% tryptone agar plates, the growth of the wild-type strain was not affected (**Figure 7A**), but its motility was dramatically reduced (**Figures 7B,C**). Crystal violet staining revealed that the phenotype of the CCCP-treated wild-type strain was consistent with the phenotype of the Δ flgE strain (**Figure 7D**). These results clearly show that flagellar motility plays a key role in *S. Typhimurium* biofilm formation. Treatment with CCCP inhibited the motility of *S. Typhimurium* flagella and thereby reduced the formation of biofilms. Similar results were obtained when *Erwinia carotovora* subsp. *carotovora* was treated with CCCP, indicating that the role of flagellar motility in biofilm formation is relatively conserved (Hossain and Tsuyumu, 2006).

DISCUSSION

Salmonella is an important food-borne pathogen found all over the world. It has been implicated in the etiology of life-threatening diarrheal diseases, partially due to its ability to colonize and form biofilms on various equipment used in the food production industry (Waldner et al., 2012). Our findings show that the impaired flagellar motility mutant exhibits poor adhesion and smaller colonies in initial biofilms. However, the mutant has a denser and flatter inner structure in mature biofilms. In *E. coli*, flagellar motility is essential for overcoming electrostatic repulsion and tethering cells together during biofilm formation (Pratt and Kolter, 1998; Walker et al., 2004; Serra et al., 2013). Furthermore, high motility leads to vertical structures and low motility leads to flatter microcolonies in mature biofilm architecture (Wood et al., 2006). Our results also confirm that the flagellar motility and biofilm machinery of *S. Typhimurium* and *E. coli* are very similar.

Previous studies have shown that the behavior of a bacterial community at an air-liquid, surface-liquid, or cell-liquid interface changes in the absence of flagella (Römling and Rohde, 1999). Additionally, the flagellar filament (containing the FliC and FljB subunits), and specifically the FliC subunit, of serovar Typhimurium is necessary and specific for cholesterol binding during biofilm initiation (Crawford et al., 2010). Our results

show that flagellar motility is impaired in the $\Delta fliC$ strain, which exhibits a similar phenotype to the $\Delta flgE$ strain (which is aflagellate). Therefore, it was speculated that the FliC-type filament may play a key role in biofilm formation on abiotic surfaces. The $\Delta fliC$ also showed a somewhat intermediate biofilm phenotype between the WT and $\Delta flgE$, which may be the compensation effect of the *fljB* subunit. Detailed observation by confocal fluorescence microscopy revealed that the flagella mutants ($\Delta flgE$ and $\Delta fliC$) formed mature biofilms with increased content of aggregated cells and EPS compared with biofilms formed by the wild-type strain. It appears that motility and extracellular matrix production are mutually exclusive processes, as many motile bacteria only begin to produce matrix once they have made contact with a surface (Kolter and Greenberg, 2006). We speculate that this may also be true for *Salmonella*, although the specific mechanism regulating this switch requires further study.

Biofilm formation is a complex process that is affected by environmental conditions, gene expression profiles, and physiological shifts within the cell (Mireles et al., 2001). Modulating some of these factors could help prevent biofilm formation. Our results confirmed that flagella-mediated motility is very important in early biofilm formation by *S. Typhimurium*. Our observations regarding the early stages of biofilm development help clarify the mechanisms involved in biofilm resistance and hold promise for developing more effective control strategies for use in the food industry. For example, aptamers or zinc targeting flagella motility (Nielubowicz et al., 2010; Ning et al., 2015; Ammendola et al., 2016), anti-adhesive materials, and the combination of some anti-adhesion materials with antibiotics could be used to control biofilm formation. The results regarding the composition of mature biofilms help us make methods to clear them. Finally, the methods might be directed toward the degradation of the EPS and kill the bacteria in biofilms, which can achieve better therapeutic effects.

CONCLUSION

In summary, the formation of *Salmonella* biofilms is a threat to food safety and public health. Understanding the mechanisms underlying biofilm formation will help identify more effective means of treating and preventing the problems it causes. In this study, we constructed $\Delta flgE$ and $\Delta fliC$ mutants to further explore the development process of *Salmonella* biofilms. It has

been well proved by a series of experiments that impaired flagellar motility mutants exhibit poor adhesion and small colonies in initial biofilms, conversely, they have more dense and complex structures in their mature biofilms. In the near future, flagellar motility could be inhibited to help eliminate biofilms, but it is necessary to select the appropriate treatment time to achieve the desired therapeutic effect.

DATA AVAILABILITY STATEMENT

The raw data supporting the conclusions of this article will be made available by the authors, without undue reservation, to any qualified researcher.

AUTHOR CONTRIBUTIONS

FW designed, supervised the experiments, analyzed the results, revised the first draft, and prepared the last draft of the manuscript. LD performed part of the experiments, contributed significantly to analysis and manuscript preparation, and revised the last draft of the manuscript. FH performed part of the experiments, analyzed the data, and participated in the first draft of the manuscript. ZW and QL analyzed the data and helped perform the analysis with constructive discussions. CX collaborated in the design of the experiments and revised different versions of the manuscript. All authors contributed to the article and approved the submitted version.

FUNDING

This work was supported by the National Natural Science Foundation of China (31770109) and the Opening Fund of Key Laboratory of Chemical Biology and Traditional Chinese Medicine Research (Hunan Normal University), Ministry of Education (KLCBTCMR18-03).

SUPPLEMENTARY MATERIAL

The Supplementary Material for this article can be found online at: <https://www.frontiersin.org/articles/10.3389/fmicb.2020.01695/full#supplementary-material>

REFERENCES

- Achinas, S., Charalampogiannis, N., and Euverink, G.-J. (2019). A brief recap of microbial adhesion and biofilms. *Appl. Sci.* 9:2801. doi: 10.3390/app9142801
- Aizawa, S.-I. (1996). Flagellar assembly in *Salmonella typhimurium*. *Mol. Microbiol.* 19, 1–5. doi: 10.1046/j.1365-2958.1996.344874.x
- Ammendola, S., D'Amico, Y., Chirullo, B., Drumo, R., Civardelli, D., Pasquali, P., et al. (2016). Zinc is required to ensure the expression of flagella and the ability to form biofilms in *Salmonella enterica* sv Typhimurium. *Metallomics* 8, 1131–1140. doi: 10.1039/C6MT00108D
- Baugh, S., Ekanayaka, A. S., Piddock, L. J. V., and Webber, M. A. (2012). Loss of or inhibition of all multidrug resistance efflux pumps of *Salmonella enterica* serovar Typhimurium results in impaired ability to form a biofilm. *J. Antimicrob. Chemother.* 67, 2409–2417. doi: 10.1093/jac/dks228
- Bearson, B. L., Bearson, S. M. D., Lee, I. S., and Brunelle, B. W. (2010). The *Salmonella enterica* serovar Typhimurium QseB response regulator negatively regulates bacterial motility and swine colonization in the absence of the QseC sensor kinase. *Microb. Pathog.* 48, 214–219. doi: 10.1016/j.micpath.2010.03.005
- Bonifield, H. R., Yamaguchi, S., and Hughes, K. T. (2000). The flagellar hook protein, FlgE, of *Salmonella enterica* serovar typhimurium is posttranscriptionally regulated in response to the stage of flagellar assembly. *J. Bacteriol.* 182, 4044–4050. doi: 10.1128/jb.182.14.4044-4050.2000

- Chilcott, G. S., and Hughes, K. T. (2000). Coupling of flagellar gene expression to flagellar assembly in *Salmonella enterica* serovar typhimurium and *Escherichia coli*. *Microbiol. Mol. Biol. Rev.* 64, 694–708. doi: 10.1128/mmbr.64.4.694-708.2000
- Crawford, R. W., Reeve, K. E., and Gunn, J. S. (2010). Flagellated but not hyperfimbriated *Salmonella enterica* serovar typhimurium attaches to and forms biofilms on cholesterol-coated surfaces. *J. Bacteriol.* 192, 2981–2990. doi: 10.1128/jb.01620-09
- Datsenko, K. A., and Wanner, B. L. (2000). One-step inactivation of chromosomal genes in *Escherichia coli* K-12 using PCR products. *Proc. Natl. Acad. Sci. U.S.A.* 97, 6640–6645. doi: 10.1073/pnas.120163297
- Duan, Q., Zhou, M., Zhu, X., Bao, W., Wu, S., Ruan, X., et al. (2012). The flagella of F18ab *Escherichia coli* is a virulence factor that contributes to infection in a IPEC-J2 cell model in vitro. *Vet. Microbiol.* 160, 132–140. doi: 10.1016/j.vetmic.2012.05.015
- Haiko, J., and Westerlund-Wikström, B. (2013). The role of the bacterial flagellum in adhesion and virulence. *Biology* 2, 1242–1267. doi: 10.3390/biology2041242
- Han, D., and Yoon, J. W. (2019). Cyclic di-guanosine monophosphate signaling regulates bacterial life cycle and pathogenicity. *J. Prev. Vet. Med.* 43, 38–46. doi: 10.13041/jpvm.2019.43.1.38
- Heydorn, A., Nielsen, A. T., Hentzer, M., Sternberg, C., Givskov, M., Ersbøll, B. K., et al. (2000). Quantification of biofilm structures by the novel computer program comstat. *Microbiology* 146, 2395–2407. doi: 10.1099/00221287-146-10-2395
- Hossain, M. M., and Tsuyumu, S. (2006). Flagella-mediated motility is required for biofilm formation by *Erwinia carotovora* subsp. *carotovora*. *J. Gen. Plant Pathol.* 72, 34–39. doi: 10.1007/s10327-005-0246-8
- Huber, B., Riedel, K., Köthe, M., Givskov, M., Molin, S., and Eberl, L. (2002). Genetic analysis of functions involved in the late stages of biofilm development in *Burkholderia cepacia* H11. *Mol. Microbiol.* 46, 411–426. doi: 10.1046/j.1365-2958.2002.03182.x
- Jacobsen, C. S., and Bech, T. B. (2012). Soil survival of *Salmonella* and transfer to freshwater and fresh produce. *Food Res. Int.* 45, 557–566. doi: 10.1016/j.foodres.2011.07.026
- Janssens, J. C. A., Steenackers, H., Robijns, S., Gellens, E., Levin, J., Zhao, H., et al. (2008). Brominated furanones inhibit biofilm formation by *Salmonella enterica* serovar typhimurium. *Appl. Environ. Microbiol.* 74, 6639–6648. doi: 10.1128/AEM.01262-08
- Ji, Y., Li, W., Zhang, Y., Chen, L., Zhang, Y., Zheng, X., et al. (2017). QseB mediates biofilm formation and invasion in *Salmonella enterica* serovar Typhi. *Microb. Pathog.* 104, 6–11. doi: 10.1016/j.micpath.2017.01.010
- Kolter, R., and Greenberg, E. P. (2006). The superficial life of microbes. *Nature* 441, 300–302. doi: 10.1038/441300a
- Koo, H., Allan, R. N., Howlin, R. P., Stoodley, P., and Hall-Stoodley, L. (2017). Targeting microbial biofilms: current and prospective therapeutic strategies. *Nat. Rev. Microbiol.* 15, 740–755. doi: 10.1038/nrmicro.2017.99
- Kosaka, T., Goda, M., Inoue, M., Yakushi, T., and Yamada, M. (2019). Flagellum-mediated motility in *Pelotomaculum thermopropionicum* SI. *Biosci. Biotechnol. Biochem.* 83, 1362–1371. doi: 10.1080/09168451.2019.1597618
- Le Guyon, S., Simm, R., Rehn, M., and Römling, U. (2015). Dissecting the cyclic diguanylate monophosphate signalling network regulating motility in *Salmonella enterica* serovar Typhimurium. *Environ. Microbiol.* 17, 1310–1320. doi: 10.1111/1462-2920.12580
- Lemon, K. P., Higgins, D. E., and Kolter, R. (2007). Flagellar motility is critical for listeria monocytogenes biofilm formation. *J. Bacteriol.* 189, 4418–4424. doi: 10.1128/jb.01967-06
- MacKenzie, K. D., Palmer, M. B., Köster, W. L., and White, A. P. (2017). Examining the link between biofilm formation and the ability of pathogenic *Salmonella* strains to colonize multiple host species. *Front. Vet. Sci.* 4:138. doi: 10.3389/fvets.2017.00138
- Merighi, M., Septer, A. N., Carroll-Portillo, A., Bhatia, A., Porwollik, S., McClelland, M., et al. (2009). Genome-wide analysis of the PreA/PreB (QseB/QseC) regulon of *Salmonella enterica* serovar Typhimurium. *BMC Microbiol.* 9:42. doi: 10.1186/1471-2180-9-42
- Mireles, J. R., Toguchi, A., and Harshey, R. M. (2001). *Salmonella enterica* serovar typhimurium swarming mutants with altered biofilm-forming abilities: surfactin inhibits biofilm formation. *J. Bacteriol.* 183, 5848–5854. doi: 10.1128/JB.183.20.5848-5854.2001
- Nielubowicz, G. R., Smith, S. N., and Mobley, H. L. T. (2010). Zinc uptake contributes to motility and provides a competitive advantage to *Proteus mirabilis* during experimental urinary tract infection. *Infect. Immun.* 78, 2823–2833. doi: 10.1128/iai.01220-09
- Ning, Y., Cheng, L., Ling, M., Feng, X., Chen, L., Wu, M., et al. (2015). Efficient suppression of biofilm formation by a nucleic acid aptamer. *Pathog. Dis.* 73:ftv034. doi: 10.1093/femspd/ftv034
- O'Toole, G., Kaplan, H. B., and Kolter, R. (2000). Biofilm formation as microbial development. *Annu. Rev. Microbiol.* 54, 49–79. doi: 10.1146/annurev.micro.54.1.49
- O'Toole, G. A., and Kolter, R. (1998). Flagellar and twitching motility are necessary for *Pseudomonas aeruginosa* biofilm development. *Mol. Microbiol.* 30, 295–304. doi: 10.1046/j.1365-2958.1998.01061.x
- Pande, V. V., McWhorter, A. R., and Chousalkar, K. K. (2016). *Salmonella enterica* isolates from layer farm environments are able to form biofilm on eggshell surfaces. *Biofouling* 32, 699–710. doi: 10.1080/08927014.2016.1191068
- Pratt, L. A., and Kolter, R. (1998). Genetic analysis of *Escherichia coli* biofilm formation: roles of flagella, motility, chemotaxis and type I pili. *Mol. Microbiol.* 30, 285–293. doi: 10.1046/j.1365-2958.1998.01061.x
- Prouty, A. M., and Gunn, J. S. (2003). Comparative analysis of *Salmonella enterica* serovar typhimurium biofilm formation on gallstones and on glass. *Infect. Immun.* 71, 7154–7158. doi: 10.1128/iai.71.12.7154-7158.2003
- Ramachandran, G., Aheto, K., Shirliff, M. E., and Tennant, S. M. (2016). Poor biofilm-forming ability and long-term survival of invasive *Salmonella* Typhimurium ST313. *Pathog. Dis.* 74:ftw049. doi: 10.1093/femspd/ftw049
- Römling, U., Sierralta, W. D., Eriksson, K., and Normark, S. (1998). Multicellular and aggregative behaviour of *Salmonella* typhimurium strains is controlled by mutations in the agfD promoter. *Mol. Microbiol.* 28, 249–264. doi: 10.1046/j.1365-2958.1998.00791.x
- Römling, U., and Rohde, M. (1999). Flagella modulate the multicellular behavior of *Salmonella* typhimurium on the community level. *FEMS Microbiol. Lett.* 180, 91–102. doi: 10.1111/j.1574-6968.1999.tb08782.x
- Semenov, A. M., Kuprianov, A. A., and van Bruggen, A. H. C. (2010). Transfer of enteric pathogens to successive habitats as part of microbial cycles. *Microb. Ecol.* 60, 239–249. doi: 10.1007/s00248-010-9663-0
- Serra, D. O., Richter, A. M., Klauk, G., Mika, F., and Hengge, R. (2013). Microanatomy at cellular resolution and spatial order of physiological differentiation in a bacterial biofilm. *mBio* 4:e00103-13. doi: 10.1128/mBio.00103-13
- Shao, X., Zhang, X., Zhang, Y., Zhu, M., Yang, P., Yuan, J., et al. (2018). RpoN-dependent direct regulation of quorum sensing and the type VI secretion system in *Pseudomonas aeruginosa* PAO1. *J. Bacteriol.* 200:e00205-18. doi: 10.1128/jb.00205-18
- Simm, R., Ahmad, I., Rhen, M., Le Guyon, S., and Römling, U. (2014). Regulation of biofilm formation in *Salmonella enterica* serovar Typhimurium. *Future Microbiol.* 9, 1261–1282. doi: 10.2217/fmb.14.88
- Solano, C., García, B., Valle, J., Berasain, C., Ghigo, J.-M., Gamazo, C., et al. (2002). Genetic analysis of *Salmonella enteritidis* biofilm formation: critical role of cellulose. *Mol. Microbiol.* 43, 793–808. doi: 10.1046/j.1365-2958.2002.02802.x
- Stoodley, P., Sauer, K., Davies, D. G., and Costerton, J. W. (2002). Biofilms as complex differentiated communities. *Annu. Rev. Microbiol.* 56, 187–209. doi: 10.1146/annurev.micro.56.012302.160705
- Tsai, M.-H., Liang, Y.-H., Chen, C.-L., and Chiu, C.-H. (2019). Characterization of *Salmonella* resistance to bile during biofilm formation. *J. Microbiol. Immunol. Infect.* 53, 518–524. doi: 10.1016/j.jmii.2019.06.003
- Vermilyea, D. M., Ottenberg, G. K., and Davey, M. E. (2019). Citrullination mediated by PPAD constrains biofilm formation in *P. gingivalis* strain 381. *npj Biofilms Microb.* 5:7. doi: 10.1038/s41522-019-0081-x

- Waldner, L. L., MacKenzie, K. D., Köster, W., and White, A. P. (2012). From exit to entry: long-term survival and transmission of *Salmonella*. *Pathogens* 1, 128–155.
- Walker, S. L., Redman, J. A., and Elimelech, M. (2004). Role of cell surface lipopolysaccharides in *Escherichia coli* K12 adhesion and transport. *Langmuir* 20, 7736–7746. doi: 10.1021/la049511f
- Watnick, P., and Kolter, R. (2000). Biofilm, city of microbes. *J. Bacteriol.* 182, 2675–2679. doi: 10.1128/JB.182.10.2675-2679.2000
- Wood, T. K., González Barrios, A. F., Herzberg, M., and Lee, J. (2006). Motility influences biofilm architecture in *Escherichia coli*. *Appl. Microbiol. Biotechnol.* 72, 361–367. doi: 10.1007/s00253-005-0263-8

Conflict of Interest: The authors declare that the research was conducted in the absence of any commercial or financial relationships that could be construed as a potential conflict of interest.

Copyright © 2020 Wang, Deng, Huang, Wang, Lu and Xu. This is an open-access article distributed under the terms of the Creative Commons Attribution License (CC BY). The use, distribution or reproduction in other forums is permitted, provided the original author(s) and the copyright owner(s) are credited and that the original publication in this journal is cited, in accordance with accepted academic practice. No use, distribution or reproduction is permitted which does not comply with these terms.



Development and Application of a Simple “Easy To Operate” Propidium Monoazide-Crossing Priming Amplification on Detection of Viable and Viable But Non-culturable Cells of O157 *Escherichia coli*

OPEN ACCESS

Edited by:

Yang Deng,
Qingdao Agricultural University, China

Reviewed by:

Yuting Tian,
Fujian Agriculture and Forestry
University, China
Ying Mu,
University of Tennessee Health
Science Center (UTHSC),
United States
Wensen Jiang,
Cedars-Sinai Medical Center,
United States

*Correspondence:

Xin Fu
fuxin76@126.com
Junyan Liu
jliu81@uthsc.edu

Specialty section:

This article was submitted to
Food Microbiology,
a section of the journal
Frontiers in Microbiology

Received: 03 June 2020

Accepted: 24 August 2020

Published: 25 September 2020

Citation:

Zhou W, Wang K, Hong W, Bai C,
Chen L, Fu X, Huang T and Liu J
(2020) Development and Application
of a Simple “Easy To Operate”
Propidium Monoazide-Crossing
Priming Amplification on Detection
of Viable and Viable But
Non-culturable Cells of O157
Escherichia coli.
Front. Microbiol. 11:569105.
doi: 10.3389/fmicb.2020.569105

Wenqu Zhou¹, Kan Wang², Wei Hong¹, Caiying Bai³, Ling Chen^{4,5}, Xin Fu^{1*},
Tengyi Huang⁶ and Junyan Liu^{7*}

¹ GMU-GIBH Joint School of Life Sciences, Guangzhou Medical University, Guangzhou, China, ² Research Center for Translational Medicine, The Second Affiliated Hospital, Shantou University Medical College, Shantou, China,

³ Guangdong Women and Children Hospital, Guangzhou, China, ⁴ School of Food Science and Engineering, Guangdong Province Key Laboratory for Green Processing of Natural Products and Product Safety, South China University of Technology, Guangzhou, China, ⁵ Research Institute for Food Nutrition and Human Health, Guangzhou, China,

⁶ Department of Laboratory Medicine, The Second Affiliated Hospital of Shantou University Medical College, Shantou, China,

⁷ Department of Civil and Environmental Engineering, University of Maryland, College Park, MD, United States

O157 *Escherichia coli* is one of the most important foodborne pathogens causing disease even at low cellular numbers. Thus, the early and accurate detection of this pathogen is important. However, due to the formation of viable but non-culturable (VBNC) status, the golden standard culturing methodology fails to identify O157 *E. coli* once it enters VBNC status. Crossing priming amplification (CPA) is a novel, simple, easy-to-operate detection technology that amplifies DNA with high speed, efficiency, and specificity under isothermal conditions. The objective of this study was to firstly develop and apply a CPA assay with propidium monoazide (PMA) for the rapid detection of the foodborne *E. coli* O157:H7 in VBNC state. Five primers (2a/1s, 2a, 3a, 4s, and 5a) were specially designed for recognizing three targets, which were *rfbE*, *stx1*, and *stx2*, and evaluated for its effectiveness in detecting VBNC cell of *E. coli* O157:H7 with detection limits of pure VBNC culture at 10³, 10⁵, and 10⁵ colony-forming units (CFUs)/ml for *rfbE*, *stx1*, and *stx2*, respectively, whereas those of food samples (frozen pastry and steamed bread) were 10³, 10⁵, and 10⁵ CFUs/ml. The application of the PMA-CPA assay was successfully used on detecting *E. coli* O157:H7 in VBNC state from food samples. In conclusion, this is the first development of PMA-CPA assay on the detection of VBNC cell, which was found to be useful and a powerful tool for the rapid detection of *E. coli* O157:H7 in VBNC state. Undoubtedly, the PMA-CPA method can be of high value to the food industry owing to its various advantages such as speed, specificity, sensitivity, and cost-effectiveness.

Keywords: propidium monoazide-crossing priming amplification, viable but non-culturable state, *Escherichia coli* O157:H7, rapid detection, foodborne pathogens

HIGHLIGHTS

- This is the first development of a PMA-CPA method on VBNC detection.
- This detection assay has been successfully applied to three targets of *Escherichia coli* in VBNC state.
- This study proposes the necessity for viable cell detection instead of the conventional “golden standard” culturing methodology.

INTRODUCTION

In recent years, the outbreak of foodborne diseases caused by pathogens and its related virulence factors is a major threat for many countries, although much attention had been paid to food safety issues. Foodborne pathogens including enterohemorrhagic *Escherichia coli* (EHEC), *Staphylococcus aureus*, *Vibrio parahaemolyticus*, and *Pseudomonas aeruginosa* have posed great concern in the food industry and public health (Miao et al., 2016, 2019; Xie et al., 2017a; Xu et al., 2019), especially their acquisition of antimicrobial resistance (Xu et al., 2007, 2011a, 2017b; Yu et al., 2016; Xie et al., 2017b; Liu et al., 2018c,d), biofilm formation (Lin et al., 2016; Bao et al., 2017a; Miao et al., 2017b), and toxin production (Liu et al., 2016a). EHEC causes more than 63,000 illnesses, 2,100 hospitalizations, and 20 deaths each year in the United States (Jiang et al., 2016). *E. coli* O157:H7 is the main EHEC serotype that causes the majority of EHEC human infections. As one of the most commonly found foodborne pathogens, it can be transmitted by contaminated food such as cattle, milk, eggs and vegetables, rice cakes, and others (Ackers et al., 1998; Jacob et al., 2013; Marder et al., 2014). The methods are labor-intensive and time-consuming and cannot meet the requirement of rapid monitoring. Hence, developing a rapid, sensitive, and accurate method to detect *E. coli* O157:H7 in various foods with a complex matrix is crucial in preventing disastrous *E. coli* O157:H7 outbreaks and associated human infections.

In 1982, Xu et al. (1982) firstly reported “viable but non-culturable” (VBNC) state, which was considered to be a survival strategy of non-spore-forming bacteria in response to adverse conditions (Xu et al., 1982; Oliver, 2010). Bacteria can enter into VBNC state by the stimulation of adverse environmental conditions, such as low temperature, nutrient-limited conditions, high salt, low pH, and even ultraviolet-induced (Foster, 1999; Ramaiah et al., 2002; Cunningham et al., 2009; Deng et al., 2015; Liu et al., 2017a,b, 2018a,b; Guo et al., 2019). For now, 85 species of bacteria have been confirmed that can enter into VBNC state, including 18 non-pathogenic and 67 pathogenic species (Li et al., 2014). In recent years, many studies have determined that VBNC bacteria still can produce harmful substances (Deng et al., 2015; Liu et al., 2017a,b, 2018a,b). *Shigella dysenteriae* and *E. coli* O157 still retain Shiga toxin encoding gene (*stx*) and produce toxin in VBNC state (Rahman et al., 1996; Liu et al., 2017d). Moreover, bacteria in VBNC can resuscitate and grow again with suitable conditions (Pinto et al., 2015). Nowadays, the traditional culture method and a nucleic acid

detection method are widely used. However, the discovery of VBNC in recent years has brought difficulties to the detection method. The VBNC cell cannot grow on the plate medium due to low metabolic activity, which means that normal culture methods can lead to false-negative results of detection. Hence, rapid and accurate identification of VBNC bacteria is of utmost importance. Bacteria in the VBNC state remain metabolically and physiologically viable and continuing to express virulence genes (Liu et al., 2016b,c,d, 2017a,c, 2018a; Bao et al., 2017b; Xu et al., 2017a). Concerning conventional detection methods that are time-consuming and only suitable for experimental use, alternative rapid and cost-effective detection methods are desperately required to detect VBNC pathogens (Lin et al., 2016; Xu et al., 2016; Miao et al., 2017a; Zhao et al., 2018). As the ethidium bromide monoazide (EMA) or propidium monoazide (PMA) penetrates only into dead bacterial cells with compromised membrane integrity but not into live cells with intact cell membranes, EMA/PMA treatment to cultures with both viable and dead cells results in selective removal of DNA from dead cells. Therefore, scientists had utilized EMA/PMA combined with nucleic acid amplification techniques to complete the detection of VBNC cells. Recently, nucleic acid amplification methods combined with EMA/PMA have been widely used for the detection of pathogenic bacteria in the VBNC state, such as PMA-polymerase chain reaction (PCR) (Liu Y. et al., 2018; Zhong and Zhao, 2018).

Although numerous quick methods based on nucleic acids, such as PCR (Gehring and Tu, 2005; Xu et al., 2011b) and real-time PCR (O’Hanlon et al., 2004), have been developed and used for detecting *E. coli* O157:H7 in food, a quicker and less expensive technology is always most preferred. Isothermal amplification is a novel method for DNA amplification at a constant temperature, providing simple, fast, independent of sophisticated instruments and cost-effective techniques to detect biological targets, especially for less well-equipped laboratories, as well as for field detection. Isothermal technologies mainly include loop-mediated isothermal amplification, rolling circle amplification, single primer isothermal amplification, polymerase spiral reaction, strand displacement amplification, and recombinase polymerase amplification (Walker et al., 1992; Notomi et al., 2000; Haible et al., 2006; Zhao et al., 2009, 2010, 2011; Wang et al., 2011; Xu Z. et al., 2012; Xu et al., 2020; Liu et al., 2015; Yang et al., 2017). Cross priming amplification (CPA) is a novel isothermal method that relies on five primers (2a/1s, 2a, 3a, 4s, and 5a) to amplify the target nucleotide sequences (Xu G. et al., 2012). It does not require any special instrumentation and presents all the features, including rapidity, specificity, and sensitivity. Recently, CPA assays have been used for the detection of *E. coli* O157:H7, *Listeria monocytogenes*, *Enterobacter sakazakii*, *Salmonella enterica*, *Yersinia enterocolitica*, and other pathogens (Yulong et al., 2010; Wang et al., 2014, 2018; Zhang et al., 2015; Xu et al., 2020). Introducing the cross-priming principles, CPA is advantageous on reproducibility and stability with a similar level of sensitivity, specificity, and rapidity comparing with loop-mediated isothermal amplification, the most broadly applied isothermal methodologies. Therefore, CPA is a potentially

valuable tool for the rapid diagnosis of foodborne pathogens, as well as those in the VBNC state. However, there is no report of PMA-CPA assay for the detection of VBNC *E. coli* O157:H7.

This study aimed to develop a rapid PMA-CPA assay to detect *E. coli* O157:H7 in VBNC state targeting on *rfbE*, *stx1*, and *stx2* genes combining visual methods with the addition of calcein and applying this assay to detect the *E. coli* O157:H7 strains from food samples.

MATERIALS AND METHODS

Induction of Entry Into the Viable But Non-culturable State in Saline and Food Sample

Induction of VBNC cells and the establishment of PMA-CPA assays were performed on *E. coli* O157 ATCC43895. The bacterial strain was incubated in trypticase soy broth (Huankai Microbial, China) to reach the exponential phase [$\sim 10^9$ colony-forming units (CFUs)/ml]. To induce the entry of VBNC state, the culture was diluted to the final density of 10^8 CFU/ml with saline (pure culture system) and food homogenate (Cantonese rice cake, Guangzhou Restaurant, Guangzhou) (food system) and stored at -20°C .

Determination of the Culturable and Viable But Non-culturable State of *E. coli* O157

The conventional plate counting method was used to determine the cultivability of *E. coli* O157. The induction culture was serially diluted with 0.9% sodium chloride and inoculated on trypticase soy agar at 37°C for 24 h. When the number of colonies was <1 CFU/ml for 3 days, it was considered that the survived cells might have entered into the non-culturable state (Deng et al., 2015). Also, the final determination of the VBNC cell was evaluated by the LIVE/DEAD BacLight bacterial viability kit (Thermo Fisher Scientific, China) (Liu et al., 2017d). The stained induction culture was observed by fluorescence microscopy.

Design of Crossing Priming Amplification Primers

As mentioned before (Xu et al., 2020), the CPA primers were designed for specific O-antigen *rfbE* gene and Shiga toxin genes *stx1* and *stx2* of *E. coli* via Primer Premier 5. For each of the target

genes, a set of primers were designed, including five primers that recognized five distinct regions on corresponding sequences. Primers used in this study have been enumerated in Tables 1, 2. All primers were assessed for specificity before use in CPA assays by doing a Blast search with a sequence in GenBank¹.

Development of Propidium Monoazide-Crossing Priming Amplification Assay in Pure Bacterial Culture and Food Sample

For the pure bacterial culture, 500 μl of $10\text{--}10^6$ -CFU/ml VBNC culture was transformed into 1.5-ml centrifuge tubes. For the food sample culture, the $10\text{--}10^6$ -CFU/ml cultures were washed three times by saline to avoid the effect of substances in a food sample and placed in 1.5-ml centrifuge tubes. Then, PMA reagent was added to the final concentration of 5 $\mu\text{g}/\text{ml}$. Subsequently, the detection samples mixed with PMA were incubated in the dark at room temperature for 10 min before the tubes were placed horizontally on ice exposed to a halogen lamp (650 W) at a distance of 15 cm for 15 min to complete the combination of DNA and PMA (Chen et al., 2020). The mixed samples were centrifuged at 10,000 r/min for 5 min, and the precipitation under the tubes was processed by DNA extraction kit (Dongsheng Biotech, Guangzhou) followed the instruction of the manufacturer, which were prepared as DNA samples for PMA-CPA.

The CPA reaction was performed as mentioned before (Xu et al., 2020), using thermostatic equipment or water bath in 26 μl , which contained 20-mM Tris-HCl, 10-mM $(\text{NH}_4)_2\text{SO}_4$, 10-mM KCl, 8.0-mM MgSO_4 , 0.1% Tween 20, 0.7-M betaine (Sigma), 1.4-mM dNTP (each), 8-U Bst DNA polymerase (NEB, United States), a 1.0- μM primer of 2a/1s, a 0.5- μM (each) primer of 2a and 3a, 0.6- μM (each) primer of 4s and 5a, 1- μl mixture

¹<https://www.ncbi.nlm.nih.gov/tools/primer-blast/>

TABLE 2 | Primers sequence for detection.

Target gene	Primers	Sequence (5'-3')
<i>rfbE</i>	4s	AGGACCGCAGAGGAAAGA
	5a	TCCACGCCAACCAAGATC
	2a/1s	AGTACATTGGCATCGTGTGTCAGATAAACTCATCGAAACA
	2a	AGTACATTGGCATCGTGT
	3a	GGCATCGTGTGGACAGGGT
<i>stx1</i>	4s	AGTTGATGTCAGAGGGATAG
	5a	CGCTGTTGTACCTGGAAA
	2a/1s	ATCAGCAAAGCGATAAACTACGGCTTATTGTTGAA
	2a	ATCAGCAAAGCGATAAAA
	3a	CCTGTTAACAAATCCTGTAC
<i>stx2</i>	4s	GTTACGGGAAGGAATCAGG
	5a	AAATCAGCCACCCACAGC
	2a/1s	CGAACTGACGGTTTACGCATGGGACTTGCCGGTGT
	2a	CGAACTGACGGTTTACGC
	3a	TGGTCGTACGGACCTTTT

TABLE 1 | Reference strains and results of CPA assays.

Reference strains	No. of strains	PCR assays			CPA results		
		<i>rfbE</i>	<i>stx1</i>	<i>stx2</i>	<i>rfbE</i>	<i>stx1</i>	<i>stx2</i>
Gram-negative organisms							
<i>Escherichia coli</i> O157:H7 ATCC43895	1	+	+	+	+	+	+

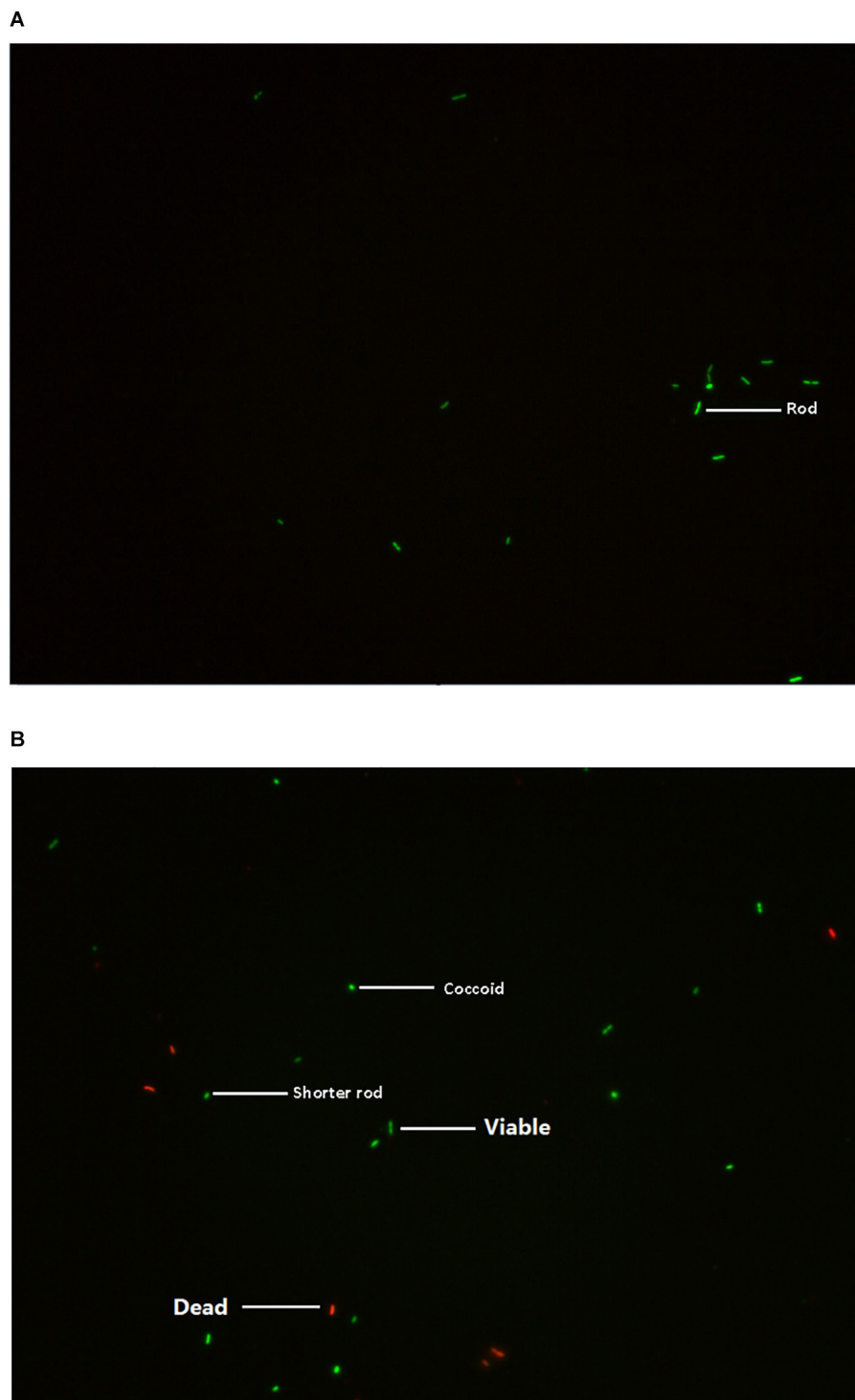


FIGURE 1 | Characterization of *E. coli* O157 in normal viable (A) and VBNC state (B) under fluorescence microscopy.

chromogenic agent (mixture with calcein and Mn^{2+}), and 1- μl template DNA, and the volume was made up to 26 μl with nuclease-free water. The mixed chromogenic agent consists of 0.13-mM calcein and 15.6-mM $\text{MnCl}_2 \cdot 4\text{H}_2\text{O}$.

The mixed reaction solution was incubated at 65°C for 60 min and heated at 80°C for 2 min to terminate it. PMA-CPA amplified products were visualized under visible light or the appearance of the laddering pattern on 1.5% agarose gel electrophoresis.

However, instead of the laddering pattern, apparent bright strip might present, which can also be regarded as positive results. This experiment was performed in triplicate to ensure reproducibility.

RESULTS

Observation of *E. coli* O157 in Viable But Non-culturable State With Fluorescence Microscopy

The *E. coli* O157 in normal viable and VBNC state was analyzed using the LIVE/DEAD® BacLight Bacterial Viability Kit. Under a fluorescence microscope, the VBNC cells showed green, whereas dead cells exhibited red (Figure 1). The results showed that the VBNC cell might change their morphological characterization from rod-shaped (normal state) to shorter rods or coccoid (VBNC state) (Liu et al., 2017c).

Propidium Monoazide-Crossing Priming Amplification Assay for Detection of Viable But Non-culturable Cells of *E. coli* O157 in Food Samples

Serial diluted DNA of VBNC cells evaluated the sensitivity of PMA-CPA. There was an obvious color change at the 10^3 – 10^6 CFU/ml DNA, and the ladder-like pattern was clearly observed under ultraviolet light. The detection limits of *E. coli* O157 VBNC were 10^3 , 10^5 , and 10^5 CFU/ml for *rfbE*, *stx1*, and *stx2* genes, respectively.

The PMA-CPA assays for the detection of *E. coli* O157 VBNC in food samples were successfully conducted. The detection limits of VBNC cells in the food system were 10^3 , 10^5 , and 10^5 CFU/ml for *rfbE*, *stx1*, and *stx2* genes, respectively, which were the same as the limits in pure VBNC cells (Figure 2).

DISCUSSION

Escherichia coli O157:H7 is currently a widespread foodborne pathogen throughout the world and has promoted a heightened interest and concern for the low-level detection of these foodborne pathogens (Pennington, 2010). There is a fast-increasing and urgent demand for high-performance techniques for monitoring bacteria in complex foods to reduce the risk of the associated food poisoning. In evaluating detection methodologies for ecologic and epidemiological purposes, a series of attributes should be considered and assessed, including specificity, sensitivity, simplicity, expense, and time. In this study, PMA-CPA assay targeting *rfbE*, *stx1*, and *stx2* successfully detected detection *E. coli* O157:H7 VBNC cell in pure culture and food samples. Notably, Shiga toxins 1 and 2 (Stx1 and Stx2) encoded by *stx1* and *stx2* can result in gastrointestinal symptoms, such as diarrhea and hemorrhagic colitis, and may also progress to a hemolytic uremic syndrome, a severe sequela of this infection (Saeedi et al., 2017). Considered to be an important health risk in the food testing, the detection of Shiga toxin, especially rapid and easy operating detection assay, may be of utmost significance and

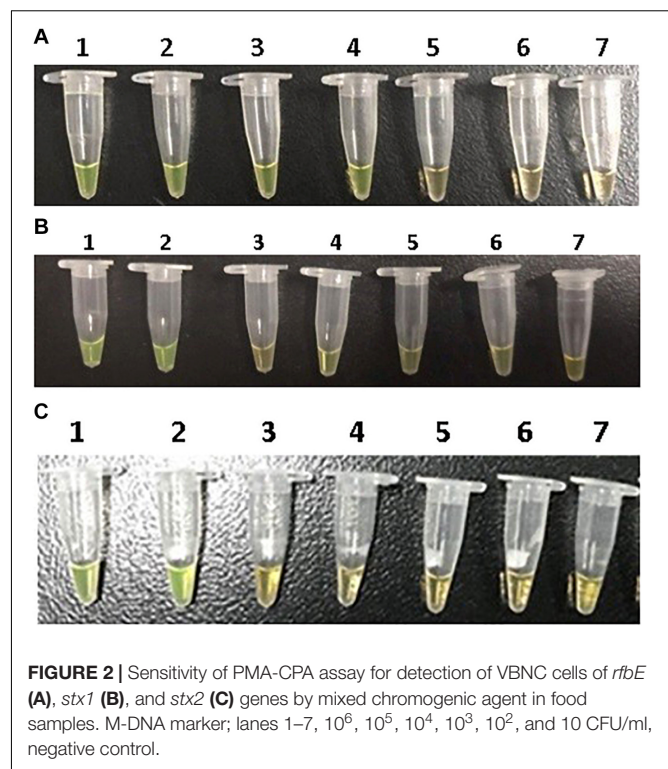


FIGURE 2 | Sensitivity of PMA-CPA assay for detection of VBNC cells of *rfbE* (A), *stx1* (B), and *stx2* (C) genes by mixed chromogenic agent in food samples. M-DNA marker; lanes 1–7, 10^6 , 10^5 , 10^4 , 10^3 , 10^2 , and 10 CFU/ml, negative control.

urgent necessity. Therefore, we established a PMA-CPA method for the detection of *E. coli* O157:H7 in VBNC cell, as well as its virulence factors. The detection limits of PMA-CPA assay showed consistency with that of CPA assay, no matter in pure bacterial culture or food samples, which had been performed previously (Xu et al., 2020). To the best of our knowledge, this is the first report of a PMA-CPA assay to detect *E. coli* O157:H7 in VBNC state from food samples.

CONCLUSION

In conclusion, the designed CPA primers targeted the *rfbE*, *stx1*, and *stx2* genes for the effective detection of *E. coli* O157:H7 VBNC cell. Therefore, being simple, rapid, sensitive, and specific, PMA-CPA assay can be a useful and powerful method in the field and also an alternative diagnostic tool for the detection of *E. coli* O157:H7 in VBNC cell and its related virulence factors in testing as part of an outbreak investigation.

DATA AVAILABILITY STATEMENT

All datasets presented in this study are included in the article/supplementary material.

AUTHOR CONTRIBUTIONS

All authors listed have made a substantial, direct and intellectual contribution to the work, and approved it for publication.

FUNDING

This work was supported by the National Natural Science Foundation of Guangdong (2017A030310419), Characteristic

Innovation Projects of Universities in Guangdong Province (2019KTSCX13), 2019 Laboratory Opening Project of Guangzhou Medical University (201910570001), and 111 Project (B17018).

REFERENCES

- Ackers, M. L., Mahon, B. E., Leahy, E., Goode, B., Damrow, T., Hayes, P. S., et al. (1998). An outbreak of *Escherichia coli* O157:H7 infections associated with leaf lettuce consumption. *J. Infect. Dis.* 177, 1588–1593.
- Bao, X., Jia, X., Chen, L., Peters, B. M., Lin, C., Chen, D., et al. (2017a). Effect of Polymyxin Resistance (pmr) on Biofilm Formation of *Cronobacter sakazakii*. *Microb. Pathogen.* 106, 16–19. doi: 10.1016/j.micpath.2016.12.012
- Bao, X., Yang, L., Chen, L., Li, B., Li, L., Li, Y., et al. (2017b). Analysis on pathogenic and virulent characteristics of the *Cronobacter sakazakii* strain BAA-894 by whole genome sequencing and its demonstration in basic biology science. *Microb. Pathogen.* 109, 280–286. doi: 10.1016/j.micpath.2017.05.030
- Chen, H., Zhong, C., Zhang, T., Shu, M., Lin, L., Luo, Q., et al. (2020). Rapid and Sensitive Detection of Viable but Non-culturable *Salmonella* Induced by Low Temperature from Chicken Using EMA-Rti-LAMP Combined with BCAC. *Food Anal. Methods* 13, 313–324. doi: 10.1007/s12161-019-01655-9
- Cunningham, E., O'Byrne, C., and Oliver, J. D. (2009). Effect of weak acids on *Listeria monocytogenes* survival: Evidence for a viable but nonculturable state in response to low pH. *Food Contr.* 20, 1141–1144. doi: 10.1016/j.foodcont.2009.03.005
- Deng, Y., Liu, J., Li, L., Fang, H., Tu, J., Li, B., et al. (2015). Reduction and restoration of culturability of beer-stressed and low-temperature-stressed *Lactobacillus acetotolerans* strain 2011-8. *Int. J. Food Microbiol.* 206, 96–101. doi: 10.1016/j.ijfoodmicro.2015.04.046
- Foster, J. W. (1999). When protons attack: microbial strategies of acid adaptation. *Curr. Opin. Microbiol.* 2, 170–174. doi: 10.1016/s1369-5274(99)80030-7
- Gehring, A. G., and Tu, S. I. (2005). Enzyme-linked immunomagnetic electrochemical detection of live *Escherichia coli* O157:H7 in apple juice. *J. Food Prot.* 68, 146–149. doi: 10.4315/0362-028x-68.1.146
- Guo, L., Ye, C., Cui, L., Wan, K., Chen, S., Zhang, S., et al. (2019). Population and single cell metabolic activity of UV-induced VBNC bacteria determined by CTC-FCM and D(2)O-labeled Raman spectroscopy. *Environ. Int.* 130:104883. doi: 10.1016/j.envint.2019.05.077
- Haible, D., Kober, S., and Jeske, H. (2006). Rolling circle amplification revolutionizes diagnosis and genomics of geminiviruses. *J. Virol. Methods* 135, 9–16. doi: 10.1016/j.jviromet.2006.01.017
- Jacob, M. E., Foster, D. M., Rogers, A. T., Balcomb, C. C., Shi, X., and Nagaraja, T. G. (2013). Evidence of non-O157 Shiga toxin-producing *Escherichia coli* in the feces of meat goats at a U.S. slaughter plant. *J. Food Prot.* 76, 1626–1629. doi: 10.4315/0362-028x:jfp-13-064
- Jiang, T., Song, Y., Wei, T., Li, H., Du, D., Zhu, M. J., et al. (2016). Sensitive detection of *Escherichia coli* O157:H7 using Pt-Au bimetal nanoparticles with peroxidase-like amplification. *Biosens Bioelectron* 77, 687–694. doi: 10.1016/j.bios.2015.10.017
- Li, L., Mendis, N., Trigui, H., Oliver, J. D., and Faucher, S. P. (2014). The importance of the viable but non-culturable state in human bacterial pathogens. *Front. Microbiol.* 5:258. doi: 10.3389/fmicb.2014.00258
- Lin, S., Li, L., Li, B., Zhao, X., Lin, C., Deng, Y., et al. (2016). Development and evaluation of quantitative detection of N-epsilon-carboxymethyl-lysine in *Staphylococcus aureus* biofilm by LC-MS method. *Basic Clin. Pharmacol.* 118:33. doi: 10.1007/978-1-4614-3828-1_2
- Liu, J., Chen, D., Peters, B. M., Li, L., Li, B., Xu, Z., et al. (2016a). Staphylococcal chromosomal cassettes mec (SCCmec): A mobile genetic element in methicillin-resistant *Staphylococcus aureus*. *Microb. Pathogen.* 101, 56–67. doi: 10.1016/j.micpath.2016.10.028
- Liu, J., Deng, Y., Peters, B. M., Li, L., Li, B., Chen, L., et al. (2016b). Transcriptomic analysis on the formation of the viable putative non-culturable state of beer-spoilage *Lactobacillus acetotolerans*. *Sci. Rep.* 6:36753.
- Liu, J., Ji, L., Peters, B. M., Li, L., Li, B., Duan, J., et al. (2016c). Whole genome sequence of two *Bacillus cereus* strains isolated from soy sauce residues. *Basic Clin. Pharmacol.* 118:34.
- Liu, J., Li, L., Peters, B. M., Li, B., Deng, Y., Xu, Z., et al. (2016d). Draft genome sequence and annotation of *Lactobacillus acetotolerans* BM-LA14527, a beer-spoilage bacteria. *FEMS Microbiol. Lett.* 363:fnw201. doi: 10.1093/femsle/fnw201
- Liu, J., Deng, Y., Li, L., Li, B., Li, Y., Zhou, S., et al. (2018a). Discovery and control of culturable and viable but non-culturable cells of a distinctive *Lactobacillus harbinensis* strain from spoiled beer. *Sci. Rep.* 8:11446.
- Liu, J., Deng, Y., Soteyome, T., Li, Y., Su, J., Li, L., et al. (2018b). Induction and recovery of the viable but nonculturable state of hop-resistance *Lactobacillus brevis*. *Front. Microbiol.* 9:2076. doi: 10.3389/fmicb.2018.02076
- Liu, J., Xie, J., Yang, L., Chen, D., Peters, B. M., Xu, Z., et al. (2018c). Identification of the KPC plasmid pCT-KPC334: new insights on the evolution pathway of the epidemic plasmids harboring fosA3-blaKPC-2 genes. *Int. J. Antimicrob. Ag.* 52, 510–512. doi: 10.1016/j.ijantimicag.2018.04.013
- Liu, J., Yang, L., Chen, D., Peters, B. M., Li, L., Li, B., et al. (2018d). Complete sequence of pBM413, a novel multi-drug-resistance megaplasmid carrying qnrVC6 and blaIMP-45 from *Pseudomonas aeruginosa*. *Int. J. Antimicrob. Ag.* 51, 145–150. doi: 10.1016/j.ijantimicag.2017.09.008
- Liu, J., Li, L., Li, B., Peters, B. M., Deng, Y., Xu, Z., et al. (2017a). Study on spoilage capability and VBNC state formation and recovery of *Lactobacillus plantarum*. *Microb. Pathogen.* 110, 257–261. doi: 10.1016/j.micpath.2017.06.044
- Liu, J., Li, L., Li, B., Peters, B. M., Xu, Z., and Shirliff, M. E. (2017b). First study on the formation and resuscitation of viable but nonculturable state and beer spoilage capability of *Lactobacillus lindneri*. *Microb. Pathogen.* 107, 219–224. doi: 10.1016/j.micpath.2017.03.043
- Liu, J., Li, L., Peters, B. M., Li, B., Chen, D., Xu, Z., et al. (2017c). Complete genome sequence and bioinformatics analyses of *Bacillus thuringiensis* strain BM-BT15426. *Microb. Pathogen.* 108, 55–60. doi: 10.1016/j.micpath.2017.05.006
- Liu, J., Zhou, R., Li, L., Peters, B. M., Li, B., Lin, C. W., et al. (2017d). Viable but non-culturable state and toxin gene expression of enterohemorrhagic *Escherichia coli* O157 under cryopreservation. *Res. Microbiol.* 168, 188–193. doi: 10.1016/j.resmic.2016.11.002
- Liu, W., Dong, D., Yang, Z., Zou, D., Chen, Z., Yuan, J., et al. (2015). Polymerase Spiral Reaction (PSR): A novel isothermal nucleic acid amplification method. *Sci. Rep.* 5:12723.
- Liu, Y., Zhong, Q., Wang, J., and Lei, S. (2018). Enumeration of *Vibrio parahaemolyticus* in VBNC state by PMA-combined real-time quantitative PCR coupled with confirmation of respiratory activity. *Food Contr.* 91, 85–91. doi: 10.1016/j.foodcont.2018.03.037
- Marder, E. P., Garman, K. N., Ingram, L. A., and Dunn, J. R. (2014). Multistate outbreak of *Escherichia coli* O157:H7 associated with bagged salad. *Foodborne Pathog. Dis.* 11, 593–595. doi: 10.1089/fpd.2013.1726
- Miao, J., Chen, L., Wang, J., Wang, W., Chen, D., Li, L., et al. (2017a). Current methodologies on genotyping for nosocomial pathogen methicillin-resistant *Staphylococcus aureus* (MRSA). *Microb. Pathogen.* 107, 17–28. doi: 10.1016/j.micpath.2017.03.010
- Miao, J., Liang, Y., Chen, L., Wang, W., Wang, J., Li, B., et al. (2017b). Formation and development of *Staphylococcus* biofilm: With focus on food safety. *J. Food Safety* 7:e12358.
- Miao, J., Lin, S., Soteyome, T., Peters, B. M., Li, Y., Chen, H., et al. (2019). Biofilm Formation of *Staphylococcus aureus* under Food Heat Processing Conditions-First Report on CML Production within Biofilm. *Sci. Rep.* 9:1312.
- Miao, J., Peters, B. M., Li, L., Li, B., Zhao, X., Xu, Z., et al. (2016). "Evaluation of ERIC-PCR for Fingerprinting Methicillin-Resistant *Staphylococcus aureus* Strains," in *The 5th International Conference on Biotechnology and Bioengineering*, (Hyderabad: Scientific Federation).
- Notomi, T., Okayama, H., Masubuchi, H., Yonekawa, T., Watanabe, K., Amino, N., et al. (2000). Loop-mediated isothermal amplification of DNA. *Nucleic Acids Res.* 28:e63.

- O'Hanlon, K. A., Catarame, T. M., Duffy, G., Blair, I. S., and McDowell, D. A. (2004). RAPID detection and quantification of *E. coli* O157/O26/O111 in minced beef by real-time PCR. *J. Appl. Microbiol.* 96, 1013–1023. doi: 10.1111/j.1365-2672.2004.02224.x
- Oliver, J. D. (2010). Recent findings on the viable but nonculturable state in pathogenic bacteria. *FEMS Microbiol. Rev.* 34, 415–425. doi: 10.1111/j.1574-6976.2009.00200.x
- Pennington, H. (2010). *Escherichia coli* O157. *Lancet* 376, 1428–1435.
- Pinto, D., Santos, M. A., and Chambel, L. (2015). Thirty years of viable but nonculturable state research: unsolved molecular mechanisms. *Crit. Rev. Microbiol.* 41, 61–76. doi: 10.3109/1040841x.2013.794127
- Rahman, I., Shahamat, M., Chowdhury, M. A., and Colwell, R. R. (1996). Potential virulence of viable but nonculturable *Shigella dysenteriae* type 1. *Appl. Environ. Microbiol.* 62, 115–120. doi: 10.1128/aem.62.1.115-120.1996
- Ramaiah, N., Ravel, J., Straube, W. L., Hill, R. T., and Colwell, R. R. (2002). Entry of *Vibrio harveyi* and *Vibrio fischeri* into the viable but nonculturable state. *J. Appl. Microbiol.* 93, 108–116.
- Saeedi, P., Yazdanparast, M., Behzadi, E., Salmanian, A. H., Mousavi, S. L., Nazarian, S., et al. (2017). A review on strategies for decreasing *E. coli* O157:H7 risk in animals. *Microb. Pathog.* 103, 186–195. doi: 10.1016/j.micpath.2017.01.001
- Walker, G. T., Fraiser, M. S., Schram, J. L., Little, M. C., Nadeau, J. G., and Malinowski, D. P. (1992). Strand displacement amplification—an isothermal, in vitro DNA amplification technique. *Nucleic Acids Res.* 20, 1691–1696.
- Wang, L., Zhao, X., Chu, J., Li, Y., Li, Y., Li, C., et al. (2011). Application of an improved loop-mediated isothermal amplification detection of *Vibrio parahaemolyticus* from various seafood samples. *Afr. J. Microbiol. Res.* 5, 5765–5771.
- Wang, Y., Wang, Y., Ma, A., Li, D., and Ye, C. (2014). Rapid and sensitive detection of *Listeria monocytogenes* by cross-priming amplification of *lmo0733* gene. *FEMS Microbiol. Lett.* 361, 43–51. doi: 10.1111/1574-6968.12610
- Wang, Y. X., Zhang, A. Y., Yang, Y. Q., Lei, C. W., Cheng, G. Y., Zou, W. C., et al. (2018). Sensitive and rapid detection of *Salmonella enterica* serovar Indiana by cross-priming amplification. *J. Microbiol. Methods* 153, 24–30. doi: 10.1016/j.mimet.2018.08.003
- Xie, J., Peters, B. M., Li, B., Li, L., Yu, G., Xu, Z., et al. (2017a). Clinical features and antimicrobial resistance profiles of important *Enterobacteriaceae* pathogens in Guangzhou representative of Southern China, 2001–2015. *Microb. Pathogen.* 107, 206–211. doi: 10.1016/j.micpath.2017.03.038
- Xie, J., Yang, L., Peters, B. M., Chen, L., Chen, D., Li, B., et al. (2017b). A 16-year retrospective surveillance report on the pathogenic features and antimicrobial susceptibility of *Pseudomonas aeruginosa* isolated from Guangzhou representative of Southern China. *Microb. Pathogen.* 110, 37–41. doi: 10.1016/j.micpath.2017.06.018
- Xu, G., Hu, L., Zhong, H., Wang, H., Yusa, S., Weiss, T. C., et al. (2012). Cross priming amplification: mechanism and optimization for isothermal DNA amplification. *Sci. Rep.* 2:246.
- Xu, H. S., Roberts, N., Singleton, F. L., Attwell, R. W., Grimes, D. J., and Colwell, R. R. (1982). Survival and viability of nonculturable *Escherichia coli* and *Vibrio cholerae* in the estuarine and marine environment. *Microb. Ecol.* 8, 313–323. doi: 10.1007/bf02010671
- Xu, Z., Hou, Y., Qin, D., Liu, X., Li, B., Li, L., et al. (2016). “Evaluation of current methodologies for rapid identification of methicillin-resistant staphylococcus aureus strains,” in *The 5th International Conference on Biotechnology and Bioengineering*, (China: South China University of Technology).
- Xu, Z., Li, L., Chu, J., Peters, B. M., Harris, M. L., Li, B., et al. (2012). Development and application of loop-mediated isothermal amplification assays on rapid detection of various types of staphylococci strains. *Food Res. Int.* 47, 166–173. doi: 10.1016/j.foodres.2011.04.042
- Xu, Z., Li, L., Shi, L., and Shirriff, M. E. (2011a). Class 1 integron in staphylococci. *Mol. Biol. Rep.* 38, 5261–5279. doi: 10.1007/s11033-011-0676-7
- Xu, Z., Li, L., Zhao, X., Chu, J., Li, B., Shi, L., et al. (2011b). Development and application of a novel multiplex polymerase chain reaction (PCR) assay for rapid detection of various types of staphylococci strains. *Afr. J. Microbiol. Res.* 5, 1869–1873.
- Xu, Z., Luo, Y., Soteyome, T., Lin, C.-W., Xu, X., Mao, Y., et al. (2020). Rapid Detection of Food-Borne *Escherichia coli* O157:H7 with Visual Inspection by Crossing Priming Amplification (CPA). *Food Analy. Methods* 13, 474–481. doi: 10.1007/s12161-019-01651-z
- Xu, Z., Shi, L., Zhang, C., Zhang, L., Li, X., Cao, Y., et al. (2007). Nosocomial infection caused by class 1 integron-carrying *Staphylococcus aureus* in a hospital in South China. *Clin. Microbiol. Infect.* 13, 980–984. doi: 10.1111/j.1469-0691.2007.01782.x
- Xu, Z., Xie, J., Liu, J., Ji, L., Soteyome, T., Peters, B. M., et al. (2017a). Whole-genome resequencing of *Bacillus cereus* and expression of genes functioning in sodium chloride stress. *Microb. Pathogen.* 104, 248–253. doi: 10.1016/j.micpath.2017.01.040
- Xu, Z., Xie, J., Peters, B. M., Li, B., Li, L., Yu, G., et al. (2017b). Longitudinal Surveillance on Antibigram of Important Gram-positive Pathogens in Southern China, 2001 to 2015. *Microb. Pathogen.* 103, 80–86. doi: 10.1016/j.micpath.2016.11.013
- Xu, Z., Xie, J., Soteyome, T., Peters, B. M., Shirriff, M. E., Liu, J., et al. (2019). Polymicrobial interaction and biofilms between *Staphylococcus aureus* and *Pseudomonas aeruginosa*: an underestimated concern in food safety. *Curr. Opin. Food Sci.* 26, 57–64. doi: 10.1016/j.cofs.2019.03.006
- Yang, Y., Yang, Q., Ma, X., Zhang, Y., Zhang, X., and Zhang, W. (2017). A novel developed method based on single primer isothermal amplification for rapid detection of *Alicyclobacillus acidoterrestris* in apple juice. *Food Control.* 75, 187–195. doi: 10.1016/j.foodcont.2016.12.005
- Yu, G., Wen, W., Peters, B. M., Liu, J., Ye, C., Che, Y., et al. (2016). First report of novel genetic array *aacA4-bla(IMP-25)-oxa30-catB3* and identification of novel metallo-beta-lactamase gene *bla(IMP25)*: A Retrospective Study of antibiotic resistance surveillance on *Pseudomonas aeruginosa* in Guangzhou of South China, 2003–2007. *Microb. Pathogen.* 95, 62–67. doi: 10.1016/j.micpath.2016.02.021
- Yulong, Z., Xia, Z., Hongwei, Z., Wei, L., Wenjie, Z., and Xitai, H. (2010). Rapid and sensitive detection of *Enterobacter sakazakii* by cross-priming amplification combined with immuno-blotting analysis. *Mol. Cell Probes.* 24, 396–400. doi: 10.1016/j.mcp.2010.09.001
- Zhang, H., Feng, S., Zhao, Y., Wang, S., and Lu, X. (2015). Detection of *Yersinia enterocolitica* in milk powders by cross-priming amplification combined with immunoblotting analysis. *Int. J. Food Microbiol.* 214, 77–82. doi: 10.1016/j.ijfoodmicro.2015.07.030
- Zhao, X., Li, M., and Xu, Z. (2018). Detection of Foodborne Pathogens by Surface Enhanced Raman Spectroscopy. *Front. Microbiol.* 9:1236. doi: 10.3389/fmicb.2018.01236
- Zhao, X., Li, W., Li, Y., Xu, Z., Li, L., He, X., et al. (2011). Development and application of a loop-mediated isothermal amplification method on rapid detection of *Pseudomonas aeruginosa* strains. *World J. Microb. Biot.* 27, 181–184. doi: 10.1007/s11274-010-0429-0
- Zhao, X., Li, Y., Chu, J., Wang, L., Shirriff, M. E., He, X., et al. (2010). Rapid detection of *Vibrio parahaemolyticus* strains and virulent factors by loop-mediated isothermal amplification assays. *Food Sci. Biotechnol.* 19, 1191–1197. doi: 10.1007/s10068-010-0170-3
- Zhao, X., Wang, L., Chu, J., Li, Y., Li, Y., Xu, Z., et al. (2009). Development and application of a rapid and simple loop-mediated isothermal amplification method for food-borne *Salmonella* detection. *Food Sci. Biotechnol.* 19, 1655–1659. doi: 10.1007/s10068-010-0234-4
- Zhong, J., and Zhao, X. (2018). Detection of viable but non-culturable *Escherichia coli* O157:H7 by PCR in combination with propidium monoazide. *Biotech* 8:28.

Conflict of Interest: The authors declare that the research was conducted in the absence of any commercial or financial relationships that could be construed as a potential conflict of interest.

Copyright © 2020 Zhou, Wang, Hong, Bai, Chen, Fu, Huang and Liu. This is an open-access article distributed under the terms of the Creative Commons Attribution License (CC BY). The use, distribution or reproduction in other forums is permitted, provided the original author(s) and the copyright owner(s) are credited and that the original publication in this journal is cited, in accordance with accepted academic practice. No use, distribution or reproduction is permitted which does not comply with these terms.



Effect of Environmental Conditions on the Formation of the Viable but Nonculturable State of *Pediococcus acidilactici* BM-PA17927 and Its Control and Detection in Food System

Yanmei Li^{1†}, Teng-Yi Huang^{2†}, Yuzhu Mao³, Yanni Chen³, Fan Shi³, Ruixin Peng³, Jinxuan Chen³, Caiying Bai⁴, Ling Chen^{3,5}, Kan Wang^{6*} and Junyan Liu^{7*}

OPEN ACCESS

Edited by:

Xihong Zhao,
Wuhan Institute of Technology, China

Reviewed by:

Wensen Jiang,
Cedars Sinai Medical Center,
United States
Siyuan Liu,
University of Saskatchewan, Canada

*Correspondence:

Junyan Liu
jliu81@uthsc.edu
Kan Wang
120384746@qq.com

[†]These authors have contributed
equally to this work

Specialty section:

This article was submitted to
Food Microbiology,
a section of the journal
Frontiers in Microbiology

Received: 24 July 2020

Accepted: 25 August 2020

Published: 29 September 2020

Citation:

Li Y, Huang T-Y, Mao Y, Chen Y, Shi F,
Peng R, Chen J, Bai C, Chen L,
Wang K and Liu J (2020)
Effect of Environmental Conditions on
the Formation of the Viable but
Nonculturable State of *Pediococcus*
acidilactici BM-PA17927 and Its
Control and Detection in Food System.
Front. Microbiol. 11:586777.
doi: 10.3389/fmicb.2020.586777

¹Department of Haematology, Guangzhou Women and Children's Medical Center, Guangzhou Medical University, Guangzhou, China, ²Department of Laboratory Medicine, The Second Affiliated Hospital of Shantou University Medical College, Shantou, China, ³School of Food Science and Engineering, Guangdong Province Key Laboratory for Green Processing of Natural Products and Product Safety, South China University of Technology, Guangzhou, China, ⁴Guangdong Women and Children Hospital, Guangzhou, China, ⁵Research Institute for Food Nutrition and Human Health, Guangzhou, China, ⁶Research Center for Translational Medicine, The Second Affiliated Hospital, Medical College of Shantou University, Shantou, China, ⁷Department of Civil and Environmental Engineering, University of Maryland, College Park, MD, United States

Objective: This study aimed to investigate the effect of environmental conditions including nutrient content, acetic acid concentration, salt concentration, and temperature on the formation of viable but nonculturable (VBNC) state of *Pediococcus acidilactici*, as well as its control and detection in food system.

Methods: Representing various environmental conditions in different food systems, 16 induction groups were designed for the formation of VBNC state of *P. acidilactici*. Traditional plate counting was applied to measure the culturable cell numbers, and Live/Dead Bacterial Viability Kit combined with fluorescent microscopy was used to identify viable cells numbers. The inhibition of bacterial growth and VBNC state formation by adjusting the environmental conditions were investigated, and the clearance effect of VBNC cells in crystal cake system was studied. In addition, a propidium monoazide-polymerase chain reaction (PMA-PCR) assay was applied to detect the VBNC *P. acidilactici* cells in crystal cake food system.

Results: Among the environmental conditions included in this study, acetic acid concentration had the greatest effect on the formation of VBNC state of *P. acidilactici*, followed by nutritional conditions and salt concentration. Reducing nutrients in the environment and treating with 1.0% acetic acid can inhibit *P. acidilactici* from entering the VBNC state. In the crystal cake system, the growth of *P. acidilactici* and the formation of VBNC state can be inhibited by adding 1.0% acetic acid and storing at -20°C . In crystal cake system, the PMA-PCR assay can be used to detect VBNC *P. acidilactici* cells at a concentration higher than 10^4 cells/ml.

Conclusion: The VBNC state of *P. acidilactici* can be influenced by the changing of environmental conditions, and PMA-PCR assay can be applied in food system for the detection of VBNC *P. acidilactici* cells.

Keywords: *Pediococcus acidilactici*, viable but nonculturable state, environmental conditions, food system, propidium monoazide-polymerase chain reaction

HIGHLIGHTS

1. Acetic acid concentration had the greatest effect on the formation of VBNC state of *P. acidilactici*, followed by nutritional conditions and salt concentration.
2. Reducing nutrients and treating with 1.0% acetic acid are able to inhibit *P. acidilactici* from entering into the VBNC state.
3. In the crystal cake food system, the growth of *P. acidilactici* and the formation of VBNC state can be inhibited by adding 1.0% acetic acid and storing at -20°C .
4. In the crystal cake food system, the PMA-PCR assay can be used to detect VBNC *P. acidilactici* cells at a concentration higher than 104 cells/ml.

INTRODUCTION

Under stress conditions, various species of bacteria can enter a physiologically viable but nonculturable (VBNC) state. Bacteria entering into the VBNC state are a survival strategy to cope with adverse conditions. However, food-borne spoilage and pathogenic bacteria pose a threat to food safety and even public health after entering the VBNC state (Bao et al., 2017a,b; Wen et al., 2020). The presence of VBNC state bacteria can lead to false negative results from the traditional plate counting detection. In addition, VBNC cells retain viability and can cause fatal infections even when completely uncultivable. Bacteria can recover from the VBNC state to an active metabolic state, bringing certain safety risks to human health and food safety (Du et al., 2007; Xu et al., 2011a; Lin et al., 2017; Miao et al., 2017a; Xie et al., 2017a; Hu et al., 2019).

Lactic acid bacteria are widely distributed and are usually found in food products, including meat, milk, and vegetables. When lactic acid bacteria are subjected to external environmental pressures during the production and application process, they are capable of activating a variety of stress reactions and may enter into the VBNC state (Xu et al., 2012a, 2017a; Xie et al., 2017b; Jia et al., 2018; Liu et al., 2018c, 2019). Studies had shown that a variety of lactic acid bacteria are able to enter into the VBNC state, including *Lactobacillus plantarum* (Liu et al., 2017a; Olszewska and Bialobrzeski, 2019), *Lactobacillus acetate* (Piao et al., 2019), *Lactobacillus lindenbergii* (Liu et al., 2017b), *Bifidobacteria*, etc. However, few studies on the VBNC of *Pediococcus* had been reported. *Pediococcus acidilactici* is a homofermentative bacterium that can grow in a wide range of pH, temperature, and osmotic pressure (Klaenhammer, 1993; Xu et al., 2007; Miao et al., 2017b,c). They are commonly found in fermented vegetables,

fermented dairy products, and meat (Barros et al., 2001; Bao et al., 2017c; Xu et al., 2017b).

Lactic acid bacteria contaminated food is mainly caused by incomplete sterilization after fermentation. It is also possible that lactic acid bacteria enter into the VBNC state under environmental pressure and causes false negative detection during shipment. During food storage, transportation, and marketing, bacteria in VBNC state resume activity, causing food spoilage (Lin et al., 2016; Miao et al., 2016; Xu et al., 2016a,b,c). Therefore, the detection of VBNC state bacteria is of great significance. The methods commonly used for the detection of VBNC state bacteria are currently based on micro-optic, immunological, and molecular detection techniques (You et al., 2012; Zhong et al., 2013). Propidium monoazide-polymerase chain reaction (PMA-PCR) is a method for detecting bacteria in VBNC state based on conventional PCR technology developed in recent years (Xu et al., 2008a, 2018; Miao et al., 2018; Zhao et al., 2018a,b). This method overcomes the defect that conventional PCR technology cannot distinguish free DNA released from living bacteria and dead bacteria, and can effectively avoid false positive test results (Xu et al., 2008b; Liu et al., 2018a).

This study aimed to investigate the effect of environmental conditions, including nutrient content, acetic acid concentration, and salt concentration on the formation of VBNC state of *P. acidilactici*, as well as its control and detection in food system.

MATERIALS AND METHODS

Bacterial Strains and Culture Conditions

Pediococcus acidilactici BM-PA17927 was stored at -80°C in MRS broth containing 20% (v/v) glycerol. It was streaked on MRS agar plate for 48 h at 37°C . Subsequently, a single colony was inoculated into a culture tube containing 2 ml of MRS broth and cultured at 37°C for 24 h. *P. acidilactici* was grown overnight in MRS broth at 37°C for 12 h. The bacterial suspension was diluted 1:100 in fresh MRS medium. Subsequently, the cultivation continued to the log phase.

Induction of Entry Into VBNC State

According to the optimal culture conditions of *P. acidilactici*, and in accordance with the principle of reverse adjustment, conditions which are unfavorable to bacterial growth were selected as candidate factors for inducing VBNC state. Three factors, including nutrition, salt concentration, and acid, were taken as a single variable. Three factors and four levels of orthogonal experiments were designed to reach 16 experimental groups (Table 1). The 16 experimental groups were stored at

TABLE 1 | The experimental methods of orthogonal array design of VBNC induction of *P. acidilactici*.

Group	MRS medium concentration (%)	NaCl concentration (m/v) (%)	Acetic acid concentration (v/v) (%)
1	0	0.9	0
2	25	0.9	0.1
3	50	0.9	1
4	100	0.9	2
5	25	5	0
6	0	5	0.1
7	100	5	1
8	50	5	2
9	50	10	0
10	100	10	0.1
11	0	10	1
12	25	10	2
13	100	15	0
14	50	15	0.1
15	25	15	1
16	0	15	2

4 and -20°C , respectively. The change trend of the culturable cell number of bacteria was used as an observation index to investigate the influence of environmental pressure on the formation of VBNC state of *P. acidilactici*. *P. acidilactici* cultured to logarithmic phase was inoculated into the induction culture, and the concentration of *P. acidilactici* in the induction culture was guaranteed to be approximately 1×10^8 cells/ml.

Culturability and Viability Assays

The induction culture was removed from the refrigerator and placed at room temperature. When the induction culture completely melted, it was serially diluted in 0.9% NaCl, spread on MRS agar plates, and incubated at 37°C for 24 h. When the culturable cell number of *P. acidilactici* bacteria in the induction culture is 1 cells/ml, it is considered that the cells may enter into the VBNC state (Deng et al., 2015). In order to determine whether *P. acidilactici* cells in the induction culture enter into the VBNC state, the LIVE/DEAD® BacLight™ Bacterial Viability Kit (Thermo Fisher Scientific, China) was used. The fluorescent probes SYTO 9 and PI were used with fluorescence microscope to distinguish intact from membrane-permeabilized cells. For these assays, 500 μl sample was obtained and centrifuged at 5,000 rpm for 15 min. Subsequently, the cells of *P. acidilactici* were washed twice with physiological saline (PBS). The supernatant was removed, and the pellet was resuspended in 500 μl of PBS. The cell suspensions were incubated with 1.5 μl of a dye mixture containing SYTO 9 and PI for 30 min at room temperature in the dark. Five microliter of cells incubated with the dye mixture was trapped between a slide and a square coverslip. The slide was placed under a fluorescent microscope for further observation. Live cells were observed under red excitation light with a wavelength of A480 nm/450 nm, and dead cells were observed under blue excitation light with a carrier length of A490 nm/635 nm. The results were then superimposed using Image J software. Under fluorescence microscope, the viable cells showed green, whereas dead cells exhibited red.

Inhibition of VBNC State Formation

According to the key environmental conditions for the formation of *P. acidilactici* VBNC state, the effect of acid (0.7 and 1.0%) and nutrition (0 and 25%) on the formation of *P. acidilactici* VBNC state were studied (Tables 2 and 3).

In order to investigate the inhibition of acid and nutrition change on the VBNC state formation of *P. acidilactici* in food system, the logarithmic phase cells were inoculated into a crystal cake food system with nutrient concentrations of 100, 50, and 25% and a volume fraction of 1.0% acetic acid. At the same time, the initial concentration of *P. acidilactici* in the food system was guaranteed to be 10^8 cells/ml and stored at 4 and -20°C , respectively. After 3 days of culture, the formation of VBNC state of *P. acidilactici* was observed using plate counting method and fluorescence microscopy.

Detection of VBNC State in Food Systems by PMA-PCR Assay

According to the National Food Safety standards (GB4789.3–2016) in China, 25 g of ground crystal cake was added to 225 ml of PBS and sterilized. Subsequently, *P. acidilactici* VBNC cells were inoculated into PBS. The initial concentrations of *P. acidilactici* were adjusted to be 10^6 , 10^5 , 10^4 , 10^3 , 10^2 , and 10 cells/ml. Five-hundred microliter of bacterial suspension and PMA (final concentration is 5 $\mu\text{g}/\text{ml}$, when PMA concentration is 5 $\mu\text{g}/\text{ml}$, it can effectively distinguish VBNC state bacteria and dead bacteria) were added to a 1.5 ml centrifuge tube, and they were thoroughly mixed and left at room temperature for 10 min. Subsequently, the centrifuge tube was placed on a crushed ice box, and light treatment was performed for 15 min at a distance of 15 cm from a 650 W halogen lamp to complete the binding of PMA and DNA. The PMA molecules remaining after the treatment are passivated. The PMA-treated bacteria suspension was centrifuged at 10,000 rpm/min for 5 min, and the supernatant was discarded. DNA was then extracted using a bacterial group DNA extraction kit (Dongsheng Biotech, Guangzhou, China). The extracted DNA was detected by PCR. PCR assay was performed in a

TABLE 2 | Inhibition assay of acid on the formation of VBNC state of *P. acidilactici*.

Group	MRS (%)	NaCl (%)	Acetic acid (%)
1	0	0.9	0.7
2			1.0
3	25	0.9	0.7
4			1.0
5	100	5	0.7
6			1.0

TABLE 3 | Inhibition assay of nutrition on the formation of VBNC state of *P. acidilactici*.

Group	MRS (%)	NaCl (%)	Acetic acid (%)
1	0	5	1
2	25		

25- μ l volume and with 0.6 μ M primers (*pheS*-F: CGCAGACAAGTCCAATGCAG; *pheS*-R: CACGTCGATAAA CCACCCCA). The thermal profile for PCR mixtures were 95°C for 5 min, followed by 35 cycles of 95°C for 30 s, 55°C for 30 s, and 72°C for 60 s and a final extension cycle at 72°C for 5 min. The amplified products (5 μ l/well) were analyzed by gel electrophoresis in 2% agarose gels and stained with ethidium bromide for 10 min. A negative control was performed using sterile water instead of culture or DNA template, and then visualized by UV transilluminator.

RESULTS AND DISCUSSION

Effect of Nutrient, Acid, and Salt on the Formation of VBNC State

Under the conditions corresponding to the experimental groups 3, 4, 6, 8, 11, 12, 15, and 16 (Table 1), the culturable cell numbers of *P. acidilactici* were reduced to zero (4 and -20°C) within 3 days (Figures 1A,B,D). Under the conditions corresponding to the experimental groups 5, 9, 10, 13, and 14, the culturable cell numbers of *P. acidilactici* were not able to reduce to zero within 45 days (Figures 1C,E-H). The culturable cell numbers were approximately 10^3 – 10^6 cells/ml and 10^7 cells/ml at 45 days when stored at 4 and -20°C , respectively. Under the experimental conditions corresponding to the experimental groups 1, 2, and 7, *P. acidilactici* could enter the VBNC state within 45 days (Table 4; Figure 2). In the conditions corresponding to experimental groups 1 and 7, the VBNC state was entered at 4°C for 31 and 37 days (chart). In 45 days, the culturable cell number of *P. acidilactici* did not decrease to zero when stored at -20°C . Under the

conditions corresponding to group 2 and under the conditions of 4 and -20°C , they entered the VBNC state at 34 and 44 days, respectively.

Under the conditions in which the acetic acid concentration is 2%, the medium concentration ranges from 0 to 100%, and the salt concentration ranges from 0.9 to 15%, the culturable and viable cell numbers of *P. acidilactici* reduced to zero within 3 days (experimental groups 4, 8, 12, and 16). In the induction culture with an acetic acid concentration of 1% (Figure 3), *P. acidilactici* lost culturability and viability within 3 days when nutrition is inadequate (medium concentration $\leq 50\%$; experimental groups 3, 11, and 15). However, when the culture medium concentration was 100% and *P. acidilactici* culture was stored at 4 and -20°C , it could survive for 37 and 45 days, respectively (experimental group 7). This shows that the concentration of nutrients has a certain effect on the survival of *P. acidilactici*, and sufficient nutrients can enhance the resistance of *P. acidilactici* to external acidic substances. When the acetic acid concentration was 0.1 and 0%, the culturable cell number of experimental group 6 reduced to zero in 3 days, the culturable cell number of experimental group 2 reduced to 0 in 34 and 44 days, and the culturable cell number of experimental group 1 reduced to 0 in 31 days at 4°C . *P. acidilactici* in the experimental groups 5, 9, 13, 10, and 14 could survive for more than 45 days. This shows that the acetic acid concentrations used in this study have the most significant effect on the survival of *P. acidilactici*.

In the experimental groups 5, 9, 10, 13 and 14, with the increase of the salt concentration, the *P. acidilactici* cells could survive for 45 days, and the culturable cell number of *P. acidilactici* was not significantly different. The salt concentration used in this experiment had no significant effect on the survival of

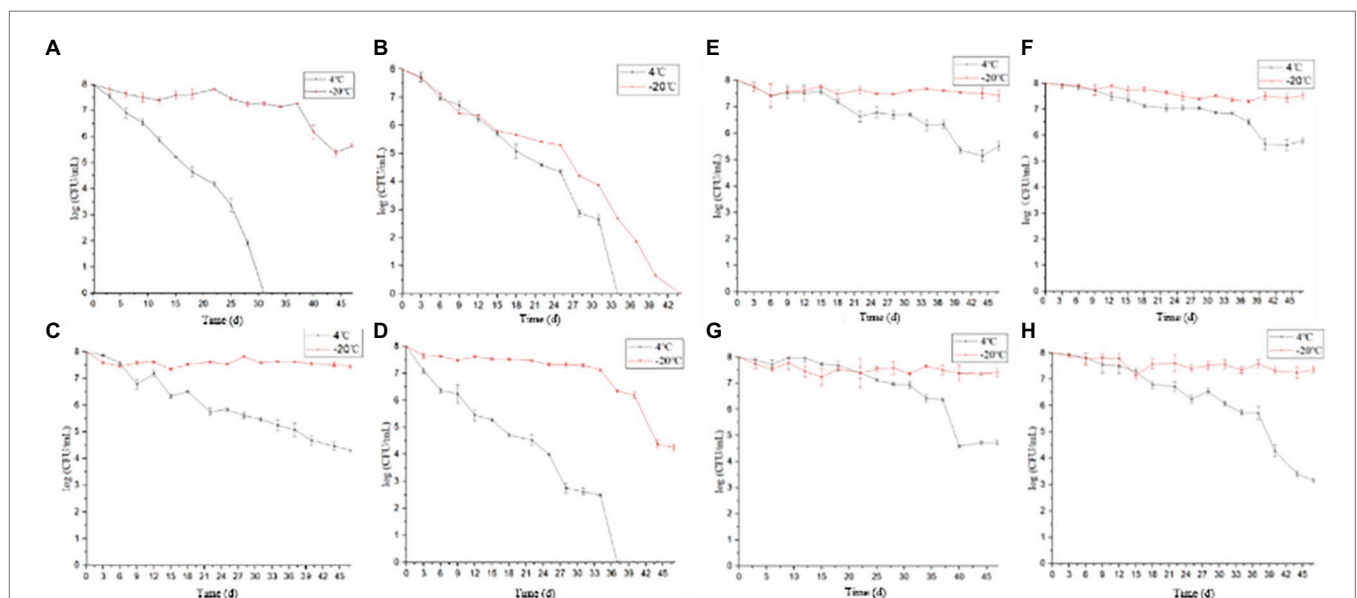
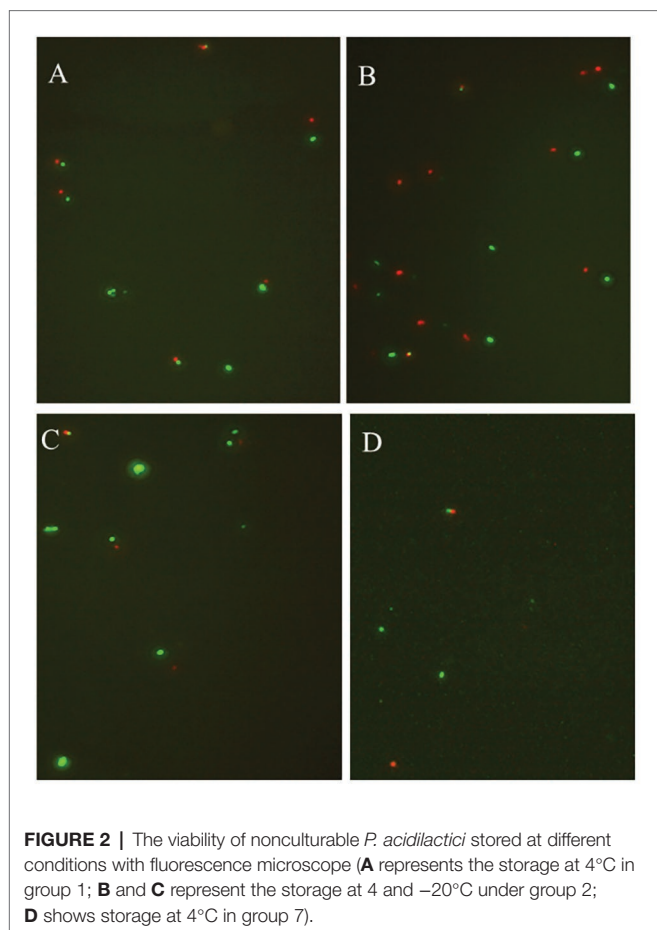


FIGURE 1 | The culturable cell number of *Pediococcus acidilactici* stored under 16 different conditions (4 and -20°C). (A–H) were the culturable cell number tendency of *P. acidilactici* inoculated in the medium configured according to the methods 1, 2, 5, 7, 9, 10, 13, and 14 and stored at 4 or -20°C , respectively).

TABLE 4 | The time of culturable cell number of *P. acidilactici* decreased to 0 stored at different methods.

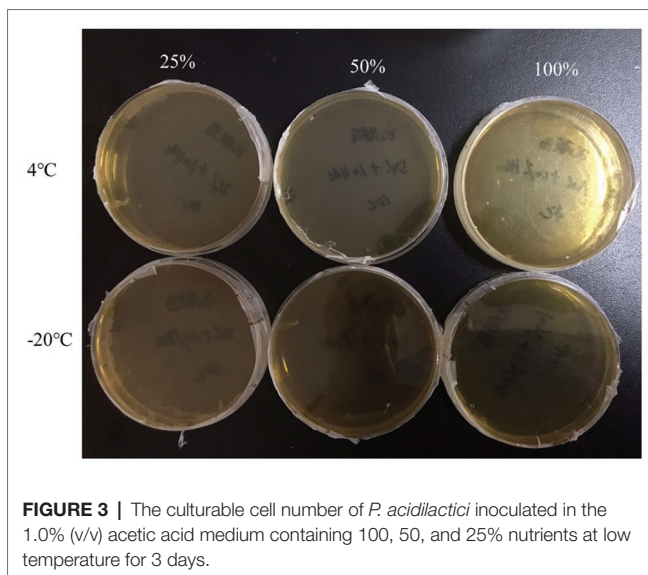
Group	4°C	−20°C	Group	4°C	−20°C
1	31 d	+	9	+	+
2	34 d	44 d	10	+	+
3	/	/	11	/	/
4	/	/	12	/	/
5	+	+	13	+	+
6	/	/	14	+	+
7	37 d	+	15	/	/
8	/	/	16	/	/

"+" stands for cell, which is culturable, and "/" stands for the number of cultivable cells in day 3 has dropped to 0.

**FIGURE 2** | The viability of nonculturable *P. acidilactici* stored at different conditions with fluorescence microscope (**A** represents the storage at 4°C in group 1; **B** and **C** represent the storage at 4 and −20°C under group 2; **D** shows storage at 4°C in group 7).

P. acidilactici. Therefore, among the environmental conditions discussed in this study, acid has the greatest impact on the survival of *P. acidilactici*, followed by nutrition, and salt concentration has the least effect on the survival of *P. acidilactici*.

Generally, a variety of environmental conditions can induce bacteria to enter the VBNC state, including the physiological cycle of bacteria (Oliver, 2010), temperature (Pawlowski et al., 2011; Liao et al., 2019), pH (Aurass et al., 2011), osmotic pressure (Aurass et al., 2011), nutritional content (Wong and Wang, 2004; Ramamurthy et al., 2014), high pressure carbon dioxide (Zhao et al., 2013), antibiotic stress (Pasquaroli et al., 2013),

**FIGURE 3** | The culturable cell number of *P. acidilactici* inoculated in the 1.0% (v/v) acetic acid medium containing 100, 50, and 25% nutrients at low temperature for 3 days.

water activity (Gruzdev et al., 2012), UV disinfection (Xu et al., 2009; Zhang et al., 2015; Liu et al., 2018b), and antibiotic (Lee and Bae, 2018) can induce bacteria to enter the VBNC state. This study used medium concentration (0, 25, 50, and 100%), sodium chloride concentration (0.9, 5, 10, and 15%), and acetic acid concentration (0, 0.1, 1, and 2%) as single factors to design an orthogonal experiment to explore the ability of environmental conditions to form *P. acidilactici* VBNC. Among the 16 induction cultures, only in three induction cultures successfully induced *P. acidilactici* entering into the VBNC state within 45 days. (1) The medium concentration is 0, the sodium chloride mass fraction is 0.9%, and the acetic acid volume fraction is 0. (2) The concentration of the medium is 25%, the mass fraction of sodium chloride is 0.9%, and the volume fraction of acetic acid is 0.1%. (3) Medium concentration is 100%, sodium chloride mass fraction is 5%, and acetic acid volume fraction is 1%. This shows that when the concentration of the medium is less than 25%, the concentration of sodium chloride is 0.9%, and the concentration of acetic acid is less than 0.1%, it is beneficial to the formation of VBNC state of *Escherichia coli*. That is, nutritional deficiencies and relatively low concentrations of sodium chloride and acetic acid are beneficial to VBNC state formation. Under this environmental pressure, *P. acidilactici* does not die directly, but enters the VBNC state. In addition, when the concentration of the culture medium is 100%, the concentration of sodium chloride is 5%, and the volume fraction of acetic acid is 1%, *P. acidilactici* can enter the VBNC state. This shows that under the condition of sufficient nutrition, *P. acidilactici* can resist higher sodium chloride concentration and acid (Xu et al., 2011b, 2012b).

Effect of Temperature on the Formation of VBNC State

In addition to the influence of the composition of the induction culture, temperature also affects the entry of *P. acidilactici* into VBNC (Table 4). Among the experimental

conditions discussed in this study, only the conditions corresponding to the three experimental groups can induce *P. acidilactici* to enter the VBNC state. In experimental groups 1 and 7, *P. acidilactici* entered into the VBNC state at 4°C in 31 and 37 days, respectively, but *P. acidilactici* was still active in 45 days at −20°C. In experimental group 2, *P. acidilactici* entered into VBNC state after 34 and 44 days, respectively. This shows that −20°C affected more on the survival of *P. acidilactici*.

Low temperature is the main factor that induces bacteria to enter the VBNC state. Food materials and finished products are mostly kept at low temperatures. During the low temperature storage process, the bacteria are easily affected by low temperature and enter the VBNC state. Food pass the test may contain VBNC state bacteria, which will become an invisible source of contamination and affect food safety (Xu et al., 2010, 2011c; Wang et al., 2011).

Effects of Acid and Nutrition on the Survival of *P. acidilactici*

Under the condition that the medium concentration is 0 (groups 1 and 2), by adding a certain amount of acetic acid (acetic acid volume fraction reaches 0.7 or 1.0%), the culturability of *P. acidilactici* was 0 after 3 days (Table 5). And bacterial activity test results showed that all bacteria died and could not enter into the VBNC state. When the nutrient concentration was 25 and 100%, and the acetic acid concentration was 7% (in groups 3 and 5), *P. acidilactici* was culturable at 3 days, but the culturable cell number was significantly reduced, indicating that *P. acidilactici* may enter into VBNC state. When the acetic acid concentration was 1.0%, *P. acidilactici* was culturable at 4 and −20°C for 3 days. When the nutrient concentration is 100%, *P. acidilactici* was culturable and had the potential to enter into the VBNC state (experimental group 6). However, when the nutrient concentration was 0 and 25%, *P. acidilactici* was not culturable and viable (experimental groups 2 and 4; Figure 4, Table 6). When the acetic acid concentration was 1.0% and the salt concentration was 5%, the nutrient content in the induction culture was reduced to 25% or less. After 3 days, the number of cultivable *P. acidilactici* and the bacterial activity were 0. During the processing of rice flour products, it is possible to control the formation of lactic acid bacteria VBNC state by minimizing the residual nutrients on the surface of the processing equipment and using acetic acid with a volume fraction of 1.0%.

Elimination of VBNC State in Rice Flour Products

Crystal cake is a traditional Chinese snack, which has the characteristics of rich nutrition. The rich nutrients and sufficient water in crystal cake make it a natural medium for the growth of various pathogenic and spoilage bacteria. In this study, crystal cake was applied as a representative food system to study the inhibition and detection of the VBNC state of *P. acidilactici* under food processing and storage conditions.

P. acidilactici was inoculated in food system with 25, 50, and 100% nutrient content and cultured at 4 and −20°C, respectively. After 3 days of culture, the culturability and activity of *P. acidilactici* were measured. Only when the nutrient content is 100% and stored at 4°C, *P. acidilactici* is not culturable and viable, but can survive in other experimental groups. Therefore, adding 1% acetic acid to rice flour products and storing them at −20°C can prevent *P. acidilactici* in rice flour products from entering the VBNC state and avoid potential threats caused by the presence of *P. acidilactici* in the VBNC state.

Detection of VBNC State of *P. acidilactici*

Propidium monoazide is a DNA intercalating molecule that can differentiate between live and dead or membrane-damaged bacteria. It can selectively penetrate the damaged cells and form a stable covalent high affinity bonds with DNA, following photo-activation exposure to strong visible light (Andreas et al., 2009). The DNA-PMA bond inhibits PCR amplification of the DNA strands of dead bacteria. It can be known from the results that when the concentration of *P. acidilactici* in the VBNC state in the crystal cake food system is higher than 10⁴ cells/ml,

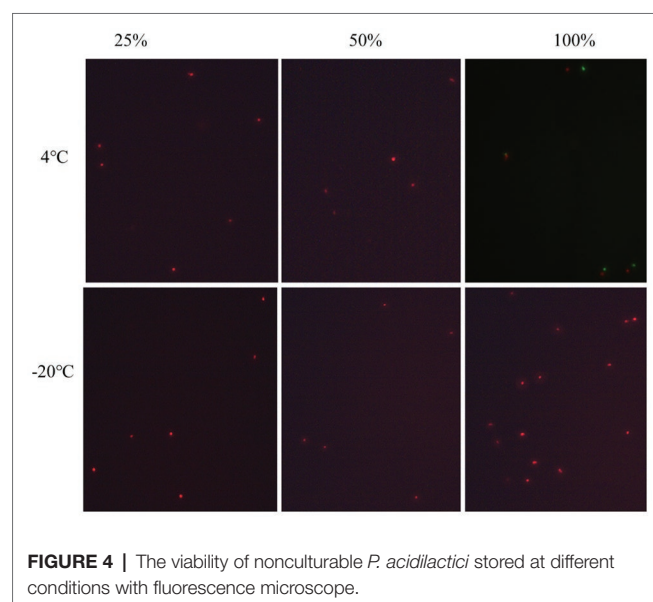


FIGURE 4 | The viability of nonculturable *P. acidilactici* stored at different conditions with fluorescence microscope.

TABLE 5 | Inhibition of acid on the formation of VBNC state of *P. acidilactici*.

Group	MRS (%)	NaCl (%)	Acetic acid (%)	Culturable		viable	
				4°C	−20°C	4°C	−20°C
1	0	0.9	0.7	/	/	/	/
2			1.0	/	/	/	/
3	25	0.9	0.7	+	+	ND	ND
4			1.0	/	/	—	—
5	100	5	0.7	+	+	ND	ND
6			1.0	+	+	ND	ND

“+” stands for cell, which is culturable, “/” for cell, which is nonculturable, “—” stands for cell, which is not active, and “ND” stands for cell activity not detection.

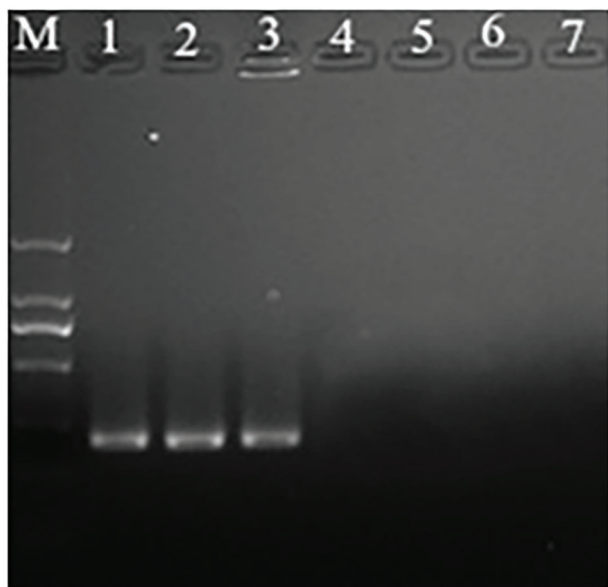


FIGURE 5 | The propidium monoazide-polymerase chain reaction (PMA-PCR) in detection of the viable but nonculturable (VBNC) state of *P. acidilactici* in crystal cake (Lane M, DNA marker; Lanes 1–6 represent crystal cake with *P. acidilactici* concentrations of 10^6 , 10^5 , 10^4 , 10^3 , 10^2 , and 10 cells/ml, respectively; Lane 7: negative control).

the *P. acidilactici* in the VBNC state can be successfully detected using the PMA-PCR technology (Figure 5).

CONCLUSION

Among the environmental conditions discussed in this study, acid had the greatest effect on the formation of VBNC state of *P. acidilactici*, followed by nutrition, and the effect of salt concentration on the survival of *P. acidilactici* was the least significant. In addition to the influence of the composition of the induction culture, 4°C is more favorable for *P. acidilactici* to enter into the VBNC state. By reducing the amount of nutrients in the environment and treating with 1.0% acetic

TABLE 6 | Inhibition of nutrition on the formation of VBNC state of *P. acidilactici*.

Group	MRS (%)	NaCl (%)	Acetic acid (v/v) (%)	Culturable		viable	
				4°C	−20°C	4°C	−20°C
1	0			/	/	-	-
2	25	5	1	/	/	-	-

"/" stands for cell, which is not culturable, and "-" for cell, which is not active.

acid, the formation of VBNC state can be suppressed. The addition of 1% acetic acid in rice flour products and storage at −20°C can inhibit *P. acidilactici* in rice flour products from entering into the VBNC state and avoid potential threats caused by the presence of *P. acidilactici* in the VBNC state. Also, PMA-PCR method can be applied to detect VBNC *P. acidilactici* cells with concentration higher than 10^4 cells/ml.

DATA AVAILABILITY STATEMENT

All datasets presented in this study are included in the article.

AUTHOR CONTRIBUTIONS

JL and KW conceived of the study and participated in its design and coordination. T-YH, YM, YC, FS, RP, and JC performed the experimental work. CB and LC analyzed the data. JL prepared and revised this manuscript. All authors reviewed and approved the final manuscript.

FUNDING

This work was supported by the National Key R&D Program of China (2016YFD0400203), YangFan Innovative and Entrepreneurial Research Team Project (2014YT02S029), the National Key Research and Development Program of China (2016YFD04012021), the Fundamental Research Funds for the Central Universities (D2191310), Collaborative grant with AEIC (KEO-2019-0624-001-1), and the 111 Project (B17018).

REFERENCES

- Andreas, N., Mazz, A., Masson, L. K., Camper, A. K., and Roland, B. (2009). Selective detection of live bacteria combining propidium monoazide sample treatment with microarray technology. *J. Microbiol. Methods* 76, 253–261. doi: 10.1016/j.mimet.2008.11.004
- Aurass, P., Prager, R., and Flieger, A. (2011). EHEC/EAEC O104:H4 strain linked with the 2011 German outbreak of haemolytic uremic syndrome enters into the viable but non-culturable state in response to various stresses and resuscitates upon stress relief. *Environ. Microbiol.* 13, 3139–3148. doi: 10.1111/j.1462-2920.2011.02604.x
- Bao, X. R., Jia, X. Y., Chen, L. Q., Peters, B. M., Lin, C. -W., Chen, D. Q., et al. (2017c). Effect of polymyxin resistance (pmr) on biofilm formation of *Cronobacter sakazakii*. *Microb. Pathog.* 106, 16–19. doi: 10.1016/j.micpath.2016.12.012
- Bao, X. R., Yang, L., Chen, L. Q., Li, B., Li, L., Li, Y. Y., et al. (2017a). Virulent and pathogenic features on the *Cronobacter sakazakii* polymyxin resistant pmr mutant strain s-3. *Microb. Pathog.* 110, 359–364. doi: 10.1016/j.micpath.2017.07.022
- Bao, X. R., Yang, L., Chen, L. Q., Li, B., Li, L., Li, Y. Y., et al. (2017b). Analysis on pathogenic and virulent characteristics of the *Cronobacter sakazakii* strain BAA-894 by whole genome sequencing and its demonstration in basic biology science. *Microb. Pathog.* 109, 280–286. doi: 10.1016/j.micpath.2017.05.030
- Barros, R. R., Carvalho, G. S., Peralta, J. M., Facklam, R. R., and Teixeira, L. M. (2001). Phenotypic and genotypic characterization of *Pediococcus* strains isolated from human clinical sources. *J. Clin. Microbiol.* 39, 1241–1246. doi: 10.1128/JCM.39.4.1241-1246.2001
- Deng, Y., Liu, J., Li, L., Fang, H., Tu, J., Li, B., et al. (2015). Reduction and restoration of culturability of beer-stressed and low-temperature-stressed

- Lactobacillus acetotolerans* strain 2011-8. *Int. J. Food Microbiol.* 206, 96–101. doi: 10.1016/j.jfoodmicro.2015.04.046
- Du, M., Chen, J., Zhang, X., Li, A., Li, Y., and Wang, Y. (2007). Retention of virulence in a viable but nonculturable *Edwardsiella tarda* isolate. *Appl. Environ. Microbiol.* 73, 1349–1354. doi: 10.1128/AEM.02243-06
- Gruzdev, N., Pinto, R., and Saldinger, S. (2012). Persistence of *Salmonella enterica* during dehydration and subsequent cold storage. *Food Microbiol.* 32, 415–422. doi: 10.1016/j.fm.2012.08.003
- Hu, B., Pan, Y., Li, Z., Yuan, W., and Deng, L. (2019). EmPis-1L, an effective antimicrobial peptide against the antibiotic-resistant VBNC state cells of pathogenic bacteria. *Probiotics Antimicro. Proteins* 11, 667–675. doi: 10.1007/s12602-018-9446-3
- Jia, X. Y., Hua, J. J., Liu, L., Xu, Z. B., and Li, Y. Y. (2018). Phenotypic characterization of pathogenic *Cronobacter* spp. strains. *Microb. Pathog.* 121, 232–237. doi: 10.1016/j.micpath.2018.05.033
- Klaenhammer, T. R. (1993). Genetics of bacteriocins produced by lactic acid bacteria. *FEMS Microbiol. Rev.* 12, 39–85. doi: 10.1111/j.1574-6976.1993.tb00012.x
- Lee, S., and Bae, S. (2018). Molecular viability testing of viable but non-culturable bacteria induced by antibiotic exposure. *Microb. Biotechnol.* 11, 1008–1016. doi: 10.1111/1751-7915.13039
- Liao, H., Xiao, W., Xu, L., Ma, Q., Wang, Y., Cai, Y., et al. (2019). Quorum-sensing systems trigger catalase expression to reverse the oxyR deletion-mediated VBNC state in *Salmonella typhimurium*. *Res. Microbiol.* 170, 65–73. doi: 10.1016/j.resmic.2018.10.004
- Lin, S. Q., Li, L., Li, B., Zhang, X. H., Lin, C. W., Deng, Y., et al. (2016). Development and evaluation of quantitative detection of N-epsilon-carboxymethyl-lysine in *Staphylococcus aureus* biofilm by LC-MS method. *Basic Clin. Pharmacol. Toxicol.* 118:33.
- Lin, S. Q., Yang, L., Chen, G., Li, B., Chen, D. Q., Li, L., et al. (2017). Pathogenic features and characteristics of food borne pathogens biofilm: biomass, viability and matrix. *Microb. Pathog.* 111, 285–291. doi: 10.1016/j.micpath.2017.08.005
- Liu, J., Deng, Y., Soteyome, T., Li, Y., Su, J., Li, L., et al. (2018c). Induction and recovery of the viable but Nonculturable state of hop-resistance *Lactobacillus brevis*. *Front. Microbiol.* 9:2076. doi: 10.3389/fmicb.2018.02076
- Liu, J., Li, L., Li, B., Peters, B. M., Deng, Y., Xu, Z., et al. (2017a). Study on spoilage capability and VBNC state formation and recovery of *Lactobacillus plantarum*. *Microb. Pathog.* 110, 257–261. doi: 10.1016/j.micpath.2017.06.044
- Liu, J. Y., Li, L., Li, B., Peters, B. M., Deng, Y., Xu, Z., et al. (2017b). First study on the formation and resuscitation of viable but nonculturable state and beer spoilage capability of *Lactobacillus lindneri*. *Microb. Pathog.* 107, 219–224. doi: 10.1016/j.micpath.2017.03.043
- Liu, L. Y., Lu, Z. R., Li, L., Li, B., Zhang, X., Zhang, X. M., et al. (2018a). Physical relation and mechanism of ultrasonic bactericidal activity on pathogenic *E. coli* with WPI. *Microb. Pathog.* 117, 73–79. doi: 10.1016/j.micpath.2018.02.007
- Liu, L. Y., Xu, R. R., Li, L., Li, B., Zhang, X., Zhang, X. M., et al. (2018b). Correlation and in vitro mechanism of bactericidal activity on *E. coli* with whey protein isolate during ultrasonic treatment. *Microb. Pathog.* 115, 154–158. doi: 10.1016/j.micpath.2017.12.062
- Liu, L., Ye, C., Soteyome, T., Zhao, X., and Harro, J. M. (2019). Inhibitory effects of two types of food additives on biofilm formation by foodborne pathogens. *Microbiologyopen* 8:e00853. doi: 10.1002/mbo3.853
- Miao, J., Chen, L. Q., Wang, J. W., Wang, W. X., Chen, D. Q., Li, L., et al. (2017a). Evaluation and application of molecular genotyping on nosocomial pathogen-methicillin-resistant *Staphylococcus aureus* isolates in Guangzhou representative of southern China. *Microb. Pathog.* 107, 397–403. doi: 10.1016/j.micpath.2017.04.016
- Miao, J., Chen, L. Q., Wang, J. W., Wang, W. X., Chen, D. Q., Li, L., et al. (2017c). Current methodologies on genotyping for nosocomial pathogen methicillin-resistant *Staphylococcus aureus* (MRSA). *Microb. Pathog.* 107, 17–28. doi: 10.1016/j.micpath.2017.03.010
- Miao, J., Liang, Y. R., Chen, L. Q., Wang, W. X., Wang, J. W., Li, B., et al. (2017b). Formation and development of *Staphylococcus* biofilm: with focus on food safety. *J. Food Saf.* 7:e12358. doi: 10.1111/jfs.12358
- Miao, J., Peters, B. M., Li, L., Li, B., Zhao, X. H., Xu, Z. B., et al. (2016). Evaluation of ERIC-PCR for fingerprinting methicillin-resistant *Staphylococcus aureus* strains. *Basic Clin. Pharmacol. Toxicol.* 118:33.
- Miao, J., Wang, W. X., Xu, W. Y., Su, J. Y., Li, L., Li, B., et al. (2018). The fingerprint mapping and genotyping systems application on methicillin-resistant *Staphylococcus aureus*. *Microb. Pathog.* 125, 246–251. doi: 10.1016/j.micpath.2018.09.031
- Oliver, J. D. (2010). Recent findings on the viable but nonculturable state in pathogenic bacteria. *FEMS Microbiol. Rev.* 34, 415–425. doi: 10.1111/j.1574-6976.2009.00200.x
- Olszewska, M. A., and Bialobrzewski, I. (2019). Mixed species biofilms of *Lactobacillus plantarum* and *Listeria innocua* show facilitated entrance to the VBNC state during chlorine-induced stress. *J. Food Saf.* 39:e12651. doi: 10.1111/jfs.12651
- Pasquaroli, S., Zandri, G., Vignaroli, C., Vuotto, C., Donelli, G., and Biavasco, F. (2013). Antibiotic pressure can induce the viable but non-culturable state in *Staphylococcus aureus* growing in biofilms. *J. Antimicrob. Chemother.* 68, 1812–1817. doi: 10.1093/jac/dkt086
- Pawlowski, D. R., Metzger, D. J., Raslawsky, A., Howlett, A., Siebert, G., Karalus, R. J., et al. (2011). Entry of *Yersinia pestis* into the viable but nonculturable state in a low-temperature tap water microcosm. *PLoS One* 6:e17585. doi: 10.1371/journal.pone.0017585
- Piao, M., Li, Y., Wang, Y., Wang, F., Zhen, T., and Deng, Y. (2019). Induction of viable but putatively non-culturable *Lactobacillus acetotolerans* by thermosonication and its characteristics. *LWT-Food Sci. Technol.* 109, 313–318. doi: 10.1016/j.lwt.2019.04.046
- Ramamurthy, T., Amit, G., Gururaj, P. P., and Sumio, S. (2014). Current perspectives on viable but non-culturable (VBNC) pathogenic bacteria. *Front. Public Health* 2:103. doi: 10.3389/fpubh.2014.00103
- Wang, L., Zhao, X. H., Chu, J., Li, Y., Li, Y. Y., Li, C. H., et al. (2011). Application of an improved loop-mediated isothermal amplification detection of *Vibrio parahaemolyticus* from various seafood samples. *Afr. J. Microbiol. Res.* 5, 5765–5771. doi: 10.5897/AJMR11.1237
- Wen, S. X., Feng, D. H., Chen, D. Q., Yang, L., and Xu, Z. B. (2020). Molecular epidemiology and evolution of *Haemophilus influenzae*. *Infect. Genet. Evol.* 80:104205. doi: 10.1016/j.meegid.2020.104205
- Wong, H. C., and Wang, P. (2004). Induction of viable but nonculturable state in *Vibrio parahaemolyticus* and its susceptibility to environmental stresses. *J. Appl. Microbiol.* 96, 359–366. doi: 10.1046/j.1365-2672.2004.02166.x
- Xie, J. H., Peters, B. M., Chen, L. Q., Chen, D. Q., Li, B., Li, L., et al. (2017a). A 16-year retrospective surveillance report on the pathogenic features and antimicrobial susceptibility of *Pseudomonas aeruginosa* isolated from Guangzhou representative of southern China. *Microb. Pathog.* 110, 37–41. doi: 10.1016/j.micpath.2017.06.018
- Xie, J. H., Peters, B. M., Li, B., Li, L., Yu, G. C., Xu, Z. B., et al. (2017b). Clinical features and antimicrobial resistance profiles of important Enterobacteriaceae pathogens in Guangzhou representative of southern China, 2001–2015. *Microb. Pathog.* 107, 206–211. doi: 10.1016/j.micpath.2017.03.038
- Xu, Z. B., Gui, Z. Y., Li, L., Li, B., Su, J. Y., Zhao, X. H., et al. (2012b). Expression and purification of gp41-gp36 fusion protein and application in serological screening assay of HIV-1 and HIV-2. *Afr. J. Microbiol. Res.* 6, 6295–6299. doi: 10.5897/AJMR12.1075
- Xu, Z. B., Hou, Y. C., Peters, B. M., Chen, D. Q., Li, B., and Li, L. (2016b). Chromogenic media for MRSA diagnostics. *Mol. Biol. Rep.* 43, 1205–1212. doi: 10.1007/s11033-016-4062-3
- Xu, Z. B., Hou, Y. C., Qin, D., Liu, X. C., Li, B., Li, L., et al. (2016a). Evaluation of current methodologies for rapid identification of methicillin-resistant *Staphylococcus aureus* strains. *Basic Clin. Pharmacol. Toxicol.* 118:33.
- Xu, Z. B., Li, L., Alam, M. J., Zhang, L. Y., Yamasaki, S., and Shi, L. (2008b). First confirmation of integron-bearing methicillin-resistant *Staphylococcus aureus*. *Curr. Microbiol.* 2008, 264–268. doi: 10.1007/s00284-008-9187-8
- Xu, Z. B., Li, L., Chu, J., Peters, B. M., Harris, M. L., Li, B., et al. (2012a). Development and application of loop-mediated isothermal amplification assays on rapid detection of various types of staphylococci strains. *Food Res. Int.* 47, 166–173. doi: 10.1016/j.foodres.2011.04.042
- Xu, Z. B., Li, L., Shi, L., and Shirliff, M. E. (2011c). Class 1 integron in staphylococci. *Mol. Biol. Rep.* 38, 5261–5279. doi: 10.1007/s11033-011-0676-7
- Xu, Z. B., Li, L., Shirliff, M. E., Peters, B. M., Li, B., Peng, Y., et al. (2011b). Resistance class 1 integron in clinical methicillin-resistant *Staphylococcus aureus* strains in southern China, 2001–2006. *Clin. Microbiol. Infect.* 17, 714–718. doi: 10.1111/j.1469-0691.2010.03379.x
- Xu, Z. B., Li, L., Shirliff, M. E., Alam, M. J., Yamasaki, S., and Shi, L. (2009). Occurrence and characteristics of class 1 and 2 integrons in *Pseudomonas*

- aeruginosa* isolates from patients in southern China. *J. Clin. Microbiol.* 47, 230–234. doi: 10.1128/JCM.02027-08
- Xu, Z. B., Li, L., Shirtliff, M. E., Peters, B. M., Peng, Y., Alam, M. J., et al. (2010). First report of class 2 integron in clinical enterococcus faecalis and class 1 integron in *Enterococcus faecium* in South China. *Diagn. Microbiol. Infect. Dis.* 68, 315–317. doi: 10.1016/j.diagmicrobio.2010.05.014
- Xu, Z. B., Li, L., Zhao, X. H., Chu, J., Li, B., Shi, L., et al. (2011a). Development and application of a novel multiplex polymerase chain reaction (PCR) assay for rapid detection of various types of staphylococci strains. *Afr. J. Microbiol. Res.* 2011, 1869–1873. doi: 10.5897/AJMR11.437
- Xu, Z. B., Liang, Y. R., Lin, S. Q., Chen, D. Q., Li, B., Li, L., et al. (2016c). Crystal violet and XTT assays on *Staphylococcus aureus* biofilm quantification. *Curr. Microbiol.* 73, 474–482. doi: 10.1007/s00284-016-1081-1
- Xu, Z. B., Shi, L., Alam, M. J., Li, L., and Yamasaki, S. (2008a). Integron-bearing methicillin-resistant coagulase-negative staphylococci in South China, 2001–2004. *FEMS Microbiol. Lett.* 278, 223–230. doi: 10.1111/j.1574-6968.2007.00994.x
- Xu, Z. B., Shi, L., Zhang, C., Zhang, L. Y., Li, X. H., Cao, Y. C., et al. (2007). Nosocomial infection caused by class 1 integron-carrying *Staphylococcus aureus* in a hospital in South China. *Clin. Microbiol. Infect.* 13, 980–984. doi: 10.1111/j.1469-0691.2007.01782.x
- Xu, Z. B., Xie, J. H., Peters, B. M., Li, B., Li, L., Yu, G. C., et al. (2017b). Longitudinal surveillance on antibiogram of important gram-positive pathogens in southern China, 2001 to 2015. *Microb. Pathog.* 103, 80–86. doi: 10.1016/j.micpath.2016.11.013
- Xu, Z. B., Xie, J. H., Yang, L., Chen, D. Q., Peters, B. M., and Shirtliff, M. E. (2018). Complete sequence of pCY-CTX, a plasmid carrying a phage-like region and ISEcp1-mediated Tn2 element from *Enterobacter cloacae*. *Microb. Drug Resist.* 24, 307–313. doi: 10.1089/mdr.2017.0146
- Xu, Z. B., Xu, X. Y., Yang, L., Li, B., Li, L., Li, X. X., et al. (2017a). Effect of aminoglycosides on the pathogenic characteristics of microbiology. *Microb. Pathog.* 113, 357–364. doi: 10.1016/j.micpath.2017.08.053
- You, R., Gui, Z. Y., Xu, Z. B., Shirtliff, M. E., Yu, G. C., Zhao, X. H., et al. (2012). Methicillin-resistance *Staphylococcus aureus* detection by an improved rapid PCR assay. *Afr. J. Microbiol. Res.* 6, 7131–7133.
- Zhang, S., Ye, C., Lin, H., Lv, L., and Yu, X. (2015). UV disinfection induces a Vbnc state in *Escherichia coli* and *Pseudomonas aeruginosa*. *Environ. Sci. Technol.* 49, 1721–1728. doi: 10.1021/es505211e
- Zhao, F., Bi, X., Hao, Y., and Liao, X. (2013). Induction of viable but nonculturable *Escherichia coli* O157: H7 by high pressure CO2 and its characteristics. *PLoS One* 8:e62388. doi: 10.1371/journal.pone.0062388
- Zhao, X. H., Li, M., and Xu, Z. B. (2018b). Detection of foodborne pathogens by surface enhanced Raman spectroscopy. *Front. Microbiol.* 9:1236. doi: 10.3389/fmicb.2018.01236
- Zhao, X. H., Yu, Z. X., and Xu, Z. B. (2018a). Study the features of 57 confirmed CRISPR loci in 38 strains of *Staphylococcus aureus*. *Front. Microbiol.* 9:1591. doi: 10.3389/fmicb.2018.01591
- Zhong, N. J., Gui, Z. Y., Liu, X., Huang, J. R., Hu, K., Gao, Y. Q., et al. (2013). Solvent-free enzymatic synthesis of 1, 3-Diacylglycerols by direct esterification of glycerol with saturated fatty acids. *Lipids Health Dis.* 12:65. doi: 10.1186/1476-511X-12-65

Conflict of Interest: The authors declare that the research was conducted in the absence of any commercial or financial relationships that could be construed as a potential conflict of interest.

Copyright © 2020 Li, Huang, Mao, Chen, Shi, Peng, Chen, Bai, Chen, Wang and Liu. This is an open-access article distributed under the terms of the Creative Commons Attribution License (CC BY). The use, distribution or reproduction in other forums is permitted, provided the original author(s) and the copyright owner(s) are credited and that the original publication in this journal is cited, in accordance with accepted academic practice. No use, distribution or reproduction is permitted which does not comply with these terms.



Distinct Roles for Bacterial and Fungal Communities During the Curing of Vanilla

Fei Xu^{1,2,3}, Yonggan Chen⁴, Yingying Cai¹, Fenglin Gu^{1,2,3*} and Kejing An⁵

¹Spice and Beverage Research Institute, Chinese Academy of Tropical Agricultural Sciences (CATAS), Wanning, China, ²National Center of Important Tropical Crops Engineering and Technology Research, Wanning, China, ³Hainan Provincial Engineering Research Center of Tropical Spice and Beverage Crops, Wanning, China, ⁴College of Fisheries and Life Science, Hainan Tropical Ocean University, Sanya, China, ⁵Sericulture and Agri-Food Research Institute Guangdong Academy of Agricultural Sciences/Key Laboratory of Functional Foods, Ministry of Agriculture/Guangdong Key Laboratory of Agricultural Products Processing, Guangzhou, China

OPEN ACCESS

Edited by:

Nguyen Thi Thanh Hanh,
Seoul National University,
South Korea

Reviewed by:

Gia Buu Tran,
Ho Chi Minh University of Industry,
Vietnam
Paola Mattarelli,
University of Bologna, Italy
Nguyen Quang Vinh,
Seoul National University,
South Korea

*Correspondence:

Fenglin Gu
xiaogu4117@163.com

Specialty section:

This article was submitted to
Food Microbiology,
a section of the journal
Frontiers in Microbiology

Received: 16 April 2020

Accepted: 31 August 2020

Published: 30 September 2020

Citation:

Xu F, Chen Y, Cai Y, Gu F and An K
(2020) Distinct Roles for Bacterial and
Fungal Communities During the
Curing of Vanilla.
Front. Microbiol. 11:552388.
doi: 10.3389/fmicb.2020.552388

Vanilla produces aroma after curing. There were a few reports about the possible involvement of microorganisms during the curing process. Bacterial and fungal community was analyzed to explore the distinct roles. Alpha diversity analysis indicated that the abundance and diversity of microorganisms did not increase regularly as the curing progressed. Weighted and unweighted principal coordinates analysis (PCoA) showed that the fungal community of blanching beans was significantly different from those of the vanilla beans of other stages, respectively. *Bacillus* and *Aspergillus* were the dominant genus during the curing process. Correlation analysis indicated that the bacterial and fungal structure was positively related to the vanillin formation, respectively. The study was conducive to reveal the formation of flavor components and the biosynthesis of vanillin. Furthermore, it proposed the possible curing methods of regulating the bacterial and fungal community to increase vanillin formation.

Keywords: vanilla, curing process, microbial community, bacterial and fungal, high-throughput sequencing

INTRODUCTION

Vanilla planifolia Andrews was native to Mexico and a typical tropical orchid crop known as the “king of food and spices” (Lubinsky et al., 2008). It is one of the most important and popular aromatic plants in food, beverages, and cosmetics (Kaur and Chakraborty, 2013). Fresh vanilla beans have almost no aroma, but produce unique aroma after curing. Early research has shown that conditioning vanilla beans were sweet, vanilla, floral, prune/raisin, spicy, woody, and smoky (Ranadive et al., 2011). Traditional curing processes typically involve four steps namely: blanching, sweating, drying, and conditioning. Fresh vanilla beans were blanched by heating or freezing to destroy the cell tissue structure. Then, the blanching vanilla beans were treated under conditions of high humidity and temperature. Sweating retains a sufficiently high moisture content for the enzyme-catalyzed reaction, while allowing sufficient moisture to escape from microbial spoilage. Then, the sweating vanilla beans were further dried by sun or air to inhibit mold growth. Lastly, the drying vanilla beans were stored in a closed box for few months, and formed the unique aroma of vanilla (Mariezcurrena et al., 2008; Sreedhar et al., 2009; Rao and Ravishankar, 2010).

It was generally believed that vanillin is mainly formed by the hydrolysis of glucovanillin by β -D-glucosidase. However, a very interesting phenomenon was that vanillin continued to accumulate as the activity of β -D-glucosidase gradually decreased during the curing process (Frenkel et al., 2011). Many researches supported that the microorganisms play an important role in the formation of vanillin. Generally, vanilla beans were blanched 3–5 min in hot water or air below 80°C, removing the microorganisms. But, lots of microorganisms were not removed from the vanilla beans (Lipkin 2013; Menon and Nayeem, 2013). In addition, no special sterilization step existed in the curing process. Vanilla beans were always in contact with the external environment. Therefore, microbial growth occurred on the vanilla beans, and the growth of the microorganisms inevitably produced abundant metabolites (Podstolski et al., 2002; Pak et al., 2004). Röling et al. (2001) found that thermophilic and thermotolerant bacilli mainly associated with *Bacillus*, which could be developed under sweating for more than a week. And, the authors also observed large differences in the number of microorganisms, species composition, and the enzymatic abilities of the isolated bacteria between different batches (Röling et al., 2001). General et al. (2009) showed that the diversity of yeast increased during the curing of vanilla. Gu et al. (2017) reported that the biosynthesis of vanillin by glucose, cresol, capsaicin, and vanillyl alcohol was widely distributed in the microbial metabolism. Chen et al. (2015) indicated that the *Bacillus* colonized on vanilla beans produced β -D-glucosidase, which mediated the hydrolysis of glucovanillin. These studies have shown that microorganisms may play an important role in the formation of the vanilla flavor.

Previous study proposed that microorganisms play an important role in the formation of vanilla flavor. In this study, the vanilla beans were cured by a hot air processing method. Based on the high-throughput sequencing method, the study analyzed the microorganisms that may involve in the curing of vanilla, and systematically studied the correlation between the microorganisms and vanilla flavor. In addition, it also partly explained the continued accumulation of vanillin at a low endogenous β -D-glucosidase activity.

MATERIALS AND METHODS

Determination of Vanillin

The extraction and determination of vanillin was carried out according to the method of Dong et al. (2014). Four grams of vacuum freeze-dried vanilla beans powder of different curing stages was thoroughly mixed with 100 ml of 70% ethanol water solution. The samples were microwaved for 20 min at 100 W. Then, the samples were filtered and made up to 100 ml after microwave extraction. Vanillin was quantified by an external standard method. HPLC conditions were as follows: Reversed phase C18 column (Zorbax, 4.6 mm \times 100 mm, 3.5 μ m, Agilent), injection volume: 5 μ l, flow rate: 1.0 ml/min, detection wavelength: 280 nm, column temperature: 26°C, mobile phase: 20% methanol, and 80% acidified water.

Microorganism Collection, DNA Extraction, and PCR Amplification

Vanilla beans were collected in Hainan, China, and cured by hot air processing (Gu et al., 2017). Fresh beans were blanched (70°C, 5 min), after that, they were immediately obtained as B1 samples. Then, they underwent daily sun exposure for about 6 h to be heated. The beans were packed in cotton blankets for oven sweating at 55°C for 6 h every day and cured for 6 days, they were obtained as S1 samples. Then, the beans were dried to reach a final moisture content of 30%, and they were obtained as D1 samples. Finally, the dry beans were conditioned in closed boxes at room temperature. At the 15th day of conditioning, they were acquired as F1 samples. And after conditioning (6 months), the cured beans were acquired as F2 samples. Two hundred grams (200 g) of vanilla beans at each stage were put into a bottle containing 400 ml of 0.9% NaCl salt solution. The bottle was shaken with a reciprocal shaker for 30 min. The microorganisms of each curing stage was washed from the vanilla beans, repeated three times, and mixed thoroughly. The mix was used for microbial collection. Bacteria and fungi were collected through a 0.45 μ m membrane filter before preservation with liquid nitrogen and stored at -80°C .

DNA was extracted using the FastDNA spin kit for soil (Q-BIOgene, Carlsbad, CA), following the manufacturer's instructions. The quality of the extracted DNA was examined by agarose gel electrophoresis, and the DNA was stored at -20°C until further analysis. Primer set: ITS1F (5'-CTTG GTCATTTAGAGGAAGTAA-3'; Gardes and Bruns, 1993) and ITS2R (5'-GCTGCGTTCTTCATCGATGC-3'; White et al., 1990) was selected to target the fungal region. 515F (5'-GTGCCAGCM GCCGCGG-3') and 907R (5'-CCGTCAATTCMTTTRAGTTT-3'; Xiong et al., 2012) was used to amplify target the bacterial 16S rRNA gene. Amplification reactions were conducted under the following conditions: 95°C for 2 min, followed by 25 cycles of denaturation at 95°C for 30 s, annealing at 55°C for 30 s, and extension at 72°C for 30 s, and a final extension at 72°C for 10 min. PCR products were purified using the AxyPrep DNA Gel Extraction Kit (Axygen Biosciences, Union City, CA, United States) following the manufacturer's instructions and quantified using the QuantiFluorTM-ST (Promega, United States).

Sequencing and Data Analysis

The DNA product was used to construct the Illumina Pair-End library and then amplicon library was paired-end sequenced (2 \times 250) on an Illumina MiSeq platform (Shanghai BIOZERON Co., Ltd). The obtained raw sequence data in the Fastq format were then demultiplexed and quality-filtered using the QIIME v1.9.0. Operational taxonomic units (OTUs) were clustered using the Usearch (V7.1) based on 97% similarity and chimeric sequences were identified and removed using Uchime (V4.2.40). The sequence was defined by the Ribosomal Database Project (RDP) Classifier against the SILVA database and UNITE database with a confidence threshold of 70% (Wang et al., 2007; Quast et al., 2013).

Statistical Analysis

Analysis of variance was determined using the SPSS 20. Differences between groups were tested using the one-way ANOVA

and Duncan's test. The difference was considered significant at $p < 0.05$. Alpha diversity of each sample was determined using the sample coverage, Chao 1 index, Shannon diversity index, and Simpson diversity index based on the Mothur version 1.30.1. Rarefaction analysis based on the Mothur version 1.30.1 was conducted to compare the richness of species in the samples with different amounts of sequencing data and, also indicated the sequencing depth of the samples (Schloss et al., 2009). Principal coordinates analysis (PCoA) was applied to study the difference of sample community composition. Analysis of similarity (ANOSIM) was conducted to identify the significant differences between the bacterial and fungal communities. To gain insight for the metabolic potential of glucovanillin, PICRUSt2 analysis was performed based on the 16S rRNA sequencing data (Langille et al., 2013). The gene family counts for each sample were derived from the KEGG ortholog (KO).

Sequence Accession Numbers

The bacterial and fungal raw sequences data are available in the NCBI Sequence Read Archive (SRA) database under the accession number PRJNA579849 and PRJNA579861, respectively.

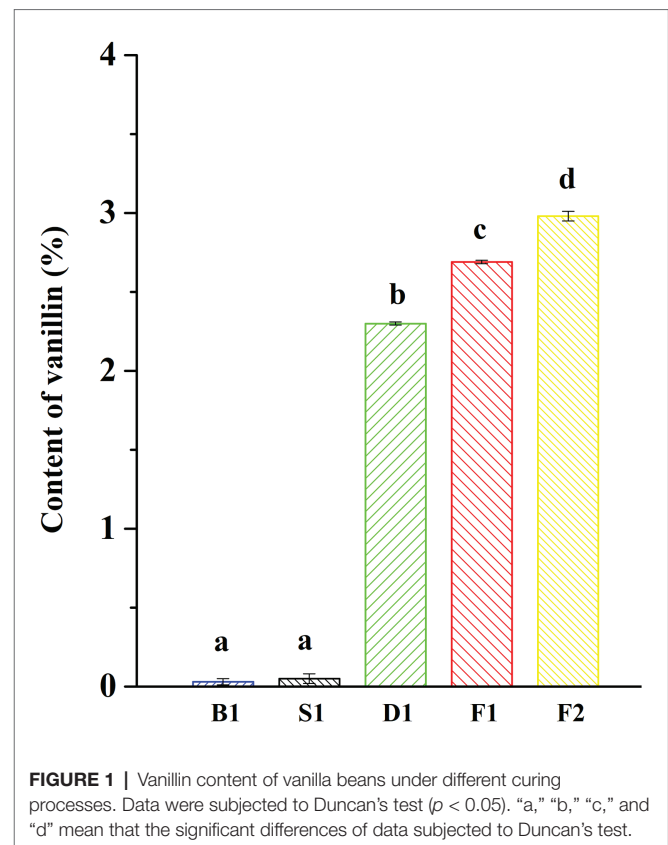
RESULTS

Vanillin Content

The characteristic aroma of natural vanilla was composed of a large number of aromatic compounds, including the main flavor, vanillin, and more than 200 other volatile compounds (Toth et al., 2011). One of the most important indicators for measuring the quality of vanilla beans was the content of vanillin. It could be seen from **Figure 1** that the vanillin content increased significantly during the progress of curing and the content of vanillin was significantly different between the different curing stages. The content of vanillin was the highest in the cured beans, reaching $2.98 \pm 0.03\%$, while the content of vanillin was only $0.03 \pm 0.02\%$ in the blanching beans. It was reported that the content of vanillin in *Vanilla tahitensis* Moore is not higher than 1.2–1.5%, which may be attributed to the difference of origins and curing methods (Ranadive et al., 2011).

α -Diversity

As can be seen from **Figures 2A,B**, the rarefaction curves all entered the smoothing zone in the five curing stages of vanilla, indicating that the sequencing depth can reflect the structural characteristics of the microorganisms under different curing processes. At the same time, it can be seen from **Table 1**, the coverage values of vanilla beans all reached above 0.99, which reflected that the sequencing results can represent the real situation of microorganisms in the vanilla beans of the different curing processes. The Chao1 index in **Table 1** indicated that the total number of species of the blanching beans was the highest for both bacteria and fungi. For bacteria, the total number of species showed a downward trend in the blanching, sweating, drying, and conditioning stages. However, the total number of species was on the rise for



fungi in the conditioning stages. It may be related to the ability of fungi colonized on vanilla beans to tolerate high concentrations of vanillin. Based on Shannon and Simpson indexes, it can be seen that the microbial diversity did not increase regularly (**Table 1**).

β -Diversity

According to the PCoA (**Figures 3A–D**), the first two principal components of bacteria can account for 66.71 and 93.70% based on the Unweighted and Weighted Unifrac distances. For fungi, the first two principal components accounted for 39.91 and 80.92%. According to the ANOSIM analysis, there was a significant difference of bacteria between the blanching beans and other curing stage beans based on the Weighted Unifrac distances, and there was a significant difference between the cured beans and other curing stage beans based on Unweighted Unifrac distances. For fungi, the blanching beans and other curing stage beans were significantly different based on the Unweighted/weighted Unifrac distances. Cured beans were significantly different from the other curing stage beans based on the Unweighted Unifrac distances (**Table 2**).

Bacterial Community Composition and Structure

Bacillus played a predominated role in the formation of the vanilla flavor under the curing processes (**Figure 4A**).

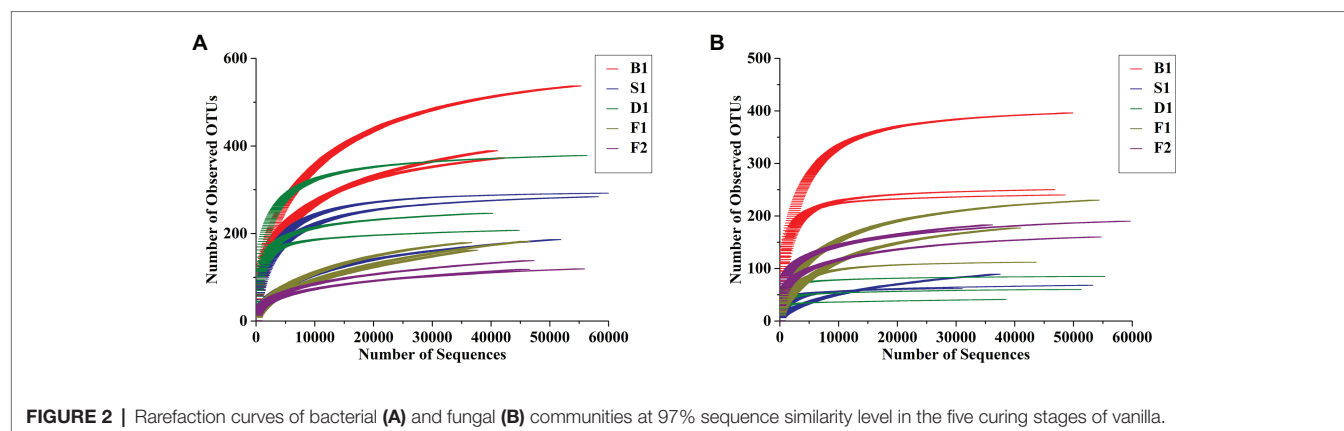


FIGURE 2 | Rarefaction curves of bacterial (A) and fungal (B) communities at 97% sequence similarity level in the five curing stages of vanilla.

TABLE 1 | Bacterial and fungal alpha-diversity indexes of five time-series curing of vanilla.

Microbial Community	Treatment	Coverage	Richness (Chao1)	Shannon	Simpson
Bacteria	B1	0.9985 ± 0.0004 ^b	477.6667 ± 83.2666 ^a	2.9600 ± 0.6780 ^{ab}	0.1807 ± 0.1145 ^{ab}
	S1	0.9995 ± 0.0004 ^a	275.3333 ± 46.7155 ^b	2.1600 ± 1.0916 ^{bc}	0.3525 ± 0.2940 ^a
	D1	0.9996 ± 0.0001 ^a	288.3333 ± 86.0717 ^b	3.9733 ± 0.1955 ^a	0.0387 ± 0.0059 ^b
	F1	0.9984 ± 0.0003 ^b	235.3333 ± 22.1435 ^{bc}	1.5067 ± 0.3213 ^c	0.3355 ± 0.0941 ^a
	F2	0.9993 ± 0.0002 ^a	158.0000 ± 22.6495 ^c	1.7533 ± 0.0586 ^c	0.2965 ± 0.0090 ^{ab}
Fungi	B1	0.9997 ± 0.0001 ^a	303.6667 ± 91.3583 ^a	3.3800 ± 0.2982 ^a	0.1294 ± 0.0498 ^c
	S1	0.9996 ± 0.0004 ^a	86.6667 ± 30.6649 ^c	1.4433 ± 0.8173 ^c	0.4452 ± 0.2360 ^a
	D1	0.9999 ± 0.0001 ^a	67.6667 ± 16.0728 ^c	2.3000 ± 0.3404 ^{bc}	0.1981 ± 0.0461 ^{bc}
	F1	0.9995 ± 0.0004 ^a	188.0000 ± 69.5414 ^b	1.5567 ± 0.2930 ^c	0.4011 ± 0.0890 ^{ab}
	F2	0.9995 ± 0.0003 ^a	194.6667 ± 18.5831 ^b	2.6800 ± 0.2858 ^{ab}	0.1820 ± 0.0247 ^{bc}

Values are presented as the mean ± standard deviation (n = 3). Means followed by the same letter for a given factor are not significantly different. p < 0.05.

Compared with the blanching beans ($0.0896 \pm 0.0512\%$), the relative abundance of *Bacillus* in the blanching stage was significantly increased to $72.0252 \pm 19.7724\%$. Sweating may contribute to activate the *Bacillus* strains. However, the relative abundance of *Bacillus* decreased to $3.2993 \pm 1.7674\%$ in the drying stage. The relative abundance of *Bacillus* increased to $87.5184 \pm 6.4880\%$ in the conditioning stage. It was speculated that there would be new *Bacillus* colonization due to the vanilla beans exposed to the external environment for nearly 1 month, or it may be attributed to the drying resistant *Bacillus* further proliferations at room temperature. The relative abundance of *Bacillus* decreased to $44.9957 \pm 2.1719\%$ in the cured beans. It was assumed that since the conditioning was carried out under a vacuum, some aerobic *Bacillus* were unable to adapt to the changed environment, or other species increased during this stage, resulting in a decrease in the number of *Bacillus*. In addition, compared with the other curing stages, the relative abundance of *Lactococcus* in the cured beans was much greater than other curing stages and the relative abundance was $41.6964 \pm 2.0479\%$. It was worth noting that *Streptococcus* and *Pseudomonas* also accounted for a certain proportion in the cured beans and the relative abundances were $3.3794 \pm 0.0876\%$ and $0.6907 \pm 0.0402\%$, respectively. This indicated that *Lactococcus*, *Streptococcus*, and *Pseudomonas* could also play an important role for the conditioning of vanilla beans. Previous study showed that *Pseudomona putida* IE27 were capable of converting

150 mM isoeugenol to 16.1 g/L vanillin (Yamada et al., 2007). Furthermore, some bacterial phylum are showed in Table 3.

Fungal Community Composition and Structure

As can be seen from Figure 4B, *Aspergillus* dominated under the whole curing stages, which indicated that *Aspergillus* played an important role in the flavor formation of vanilla beans. Early research showed that *Aspergillus niger* could deacetylate ferulic acid into vanillic acid, and then *Pycnoporus cinnabarinus* reduced vanillic acid to vanillin (Lesage-Meessen et al., 2002). It was reported that *A. niger* could effectively release ferulic acid and caffeic acid by two different feruloyl esterase (FAEA and FAEB) in apple pomace, coffee pulp, wheat straw, corn husk, and sugar beet pulp (Benoit et al., 2006).

Compared with other curing stages, the relative abundance of *Aspergillus* was only $0.3665 \pm 0.0912\%$ in the blanching beans, while the relative abundance of *Aspergillus* in other curing stages was higher than in the blanching beans, indicating that *Aspergillus* may be involved in the formation of vanilla flavor. The relative abundance of *Aspergillus* was the highest in the conditioning stage, reaching $91.0832 \pm 3.7684\%$. It may be attributed to the exposure of the vanilla beans to an external environment during the curing process, which made *Aspergillus* undergo further proliferation. The relative abundance of *Aspergillus* in sweating stage is $68.2543 \pm 30.7098\%$. It was speculated that heating

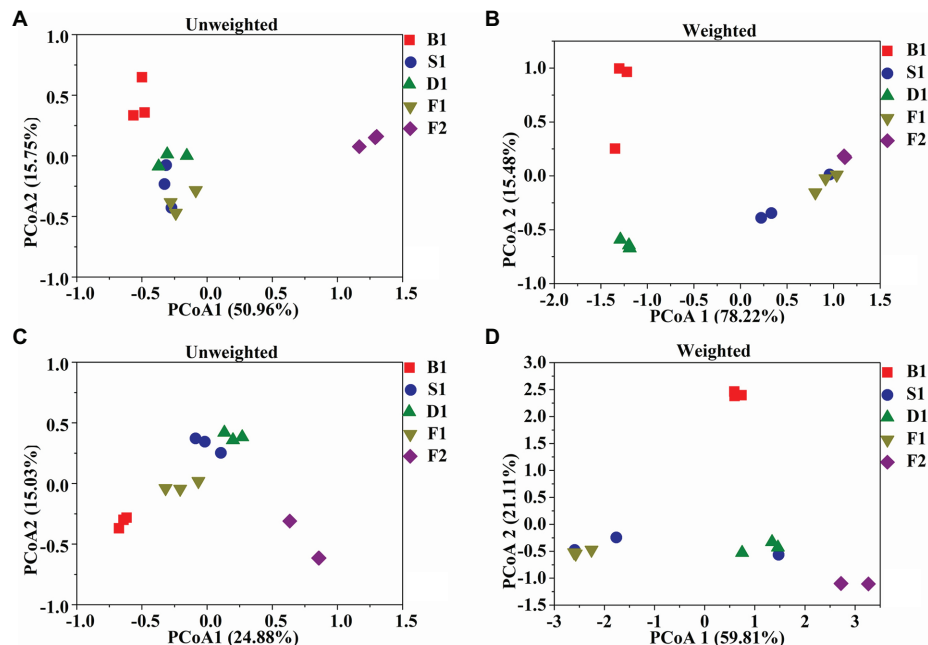


FIGURE 3 | Microbial community structures in the five curing stages of vanilla. UniFrac – unweighted principle coordinate the analysis of bacterial (A) and fungal (C) community structures, UniFrac – weighted principle coordinate the analysis of bacterial (B) and fungal (D) community structures.

TABLE 2 | Analysis of similarity (ANOSIM) analysis of the similarity of five curing stages of vanilla.

Groups	B1 vs. S1, D1, F1, and F2	B1 vs. S1, D1, F1, and F2	F2 vs. S1, D1, F1, and B1	F2 vs. S1, D1, F1, and B1	B1 vs. S1, D1, F1, and F2	B1 vs. S1, D1, F1, and F2	F2 vs. S1, D1, F1, and B1
Sample size	15	15	15	15	15	15	15
Number of groups	5	5	5	5	5	5	5
Test statistic (R)	0.148	0.756	0.958	0.211	0.560	0.486	0.296
p	0.167	0.005	0.005	0.070	0.001	0.010	0.097
Number of permutations	999	999	999	999	999	999	999
Kinds of microbe	Bacteria	Bacteria	Bacteria	Bacteria	Fungi	Fungi	Fungi
Unifrac distances	Unweighted	Weighted	Unweighted	Weighted	Unweighted	Weighted	Weighted

contributed to the activation or regeneration of *Aspergillus*. This was also supported by Röling et al. (2001), who found that the Indonesian vanilla beans were blanched (65–70°C, 2 min), resulting in significant reductions of the microbial diversity and regeneration of fungi. The abundances of *Tausonia*, *Nectria*, and *Mrakia* in the cured beans were much larger than that of other stages, which were $42.5048 \pm 1.8431\%$, $4.2314 \pm 2.9142\%$, and $3.5993 \pm 1.7638\%$, respectively. This indicated that these strains may play important roles in the conditioning stage. The dominant strains of the curing stages were different in vanilla beans. Furthermore, some fungal phylum are showed in Table 3.

Correlations Between Microbial Indicators and Vanillin

Bacterial richness, diversity, structure (Unweighted PCoA1), fungal richness, diversity, and structure (Unweighted PCoA1) were selected from the initial microbial indicators and vanillin content in the linear model, showing the best explanatory power

for correlations between the microbial indicators and vanillin formation. Importantly, based on the linear regression analyses between the vanillin content and selected microbial indicators, it was shown that the unweighted bacterial structure ($R^2 = 0.387$, $p = 0.013$), and unweighted fungal structure ($R^2 = 0.424$, $p = 0.009$) had significantly positive correlations with vanillin content. In contrast, the bacterial richness ($R^2 = 0.463$, $p = 0.005$) was negatively correlated with vanillin content (Figures 5A–F).

Prediction of β -Glucosidase Genes in the Microbial Community

To compare the functional characteristics of glucovanillin hydrolysis during the curing process, the PICRUST analyses was performed. Total β -glucosidase gene exceed 0.2% of the predicted genes (Figure 6). β -glucosidase gene K01188 nearly accounted 0 in all the samples. Specifically, K05349 ranged from $0.006 \pm 0.0047\%$ to $0.08 \pm 0.0129\%$ and K05350 ranged from $0.003 \pm 0.0005\%$ to $0.023 \pm 0.0031\%$.

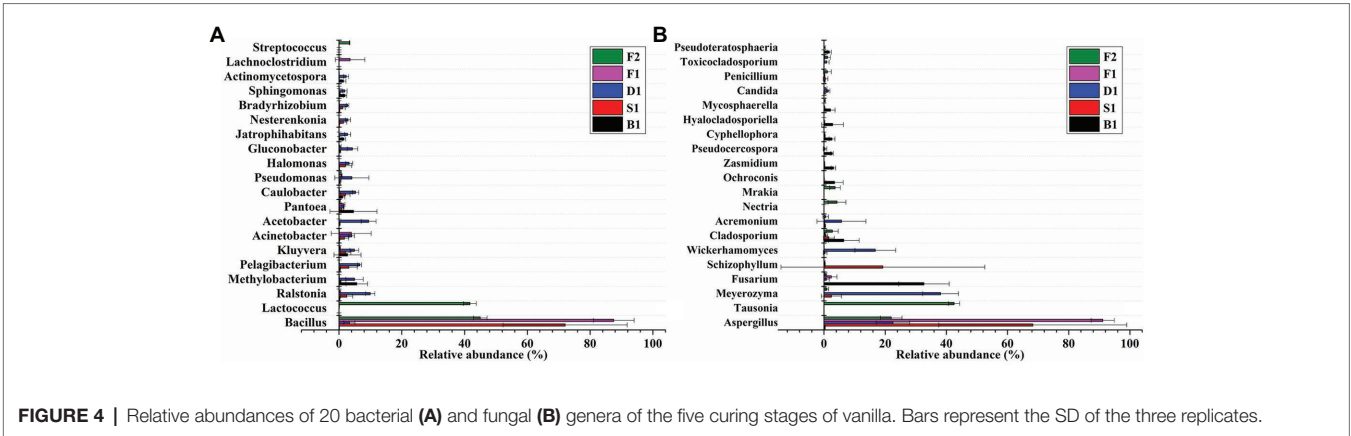


FIGURE 4 | Relative abundances of 20 bacterial (A) and fungal (B) genera of the five curing stages of vanilla. Bars represent the SD of the three replicates.

TABLE 3 | Relative abundances of bacterial and fungal phylum of the five curing stages of vanilla.

Samples	Bacterial phylum				Fungal phylum			
	Acidobacteria	Acidobacteria	Acidobacteria	Acidobacteria	Ascomycota	Basidiomycota	Chytridiomycota	Mucoromycota
B1	0.0312 ± 0.0283	0.0312 ± 0.0283	0.0312 ± 0.0283	0.0312 ± 0.0283	0.7673 ± 0.0351	0.0289 ± 0.0168	0.0001 ± 0.0001	0.0000 ± 0.0000
S1	0.0013 ± 0.0009	0.0013 ± 0.0009	0.0013 ± 0.0009	0.0013 ± 0.0009	0.7727 ± 0.3134	0.2116 ± 0.3224	0.0000 ± 0.0000	0.0008 ± 0.0014
D1	0.0084 ± 0.0087	0.0084 ± 0.0087	0.0084 ± 0.0087	0.0084 ± 0.0087	0.9360 ± 0.0196	0.0148 ± 0.0051	0.0000 ± 0.0000	0.0000 ± 0.0000
F1	0.0002 ± 0.0001	0.0002 ± 0.0001	0.0002 ± 0.0001	0.0002 ± 0.0001	0.9644 ± 0.0097	0.0138 ± 0.0054	0.0000 ± 0.0000	0.0000 ± 0.0000
F2	0.0000 ± 0.0000	0.0000 ± 0.0000	0.0000 ± 0.0000	0.0000 ± 0.0000	0.3869 ± 0.0933	0.5067 ± 0.0108	0.0000 ± 0.0000	0.0098 ± 0.0085

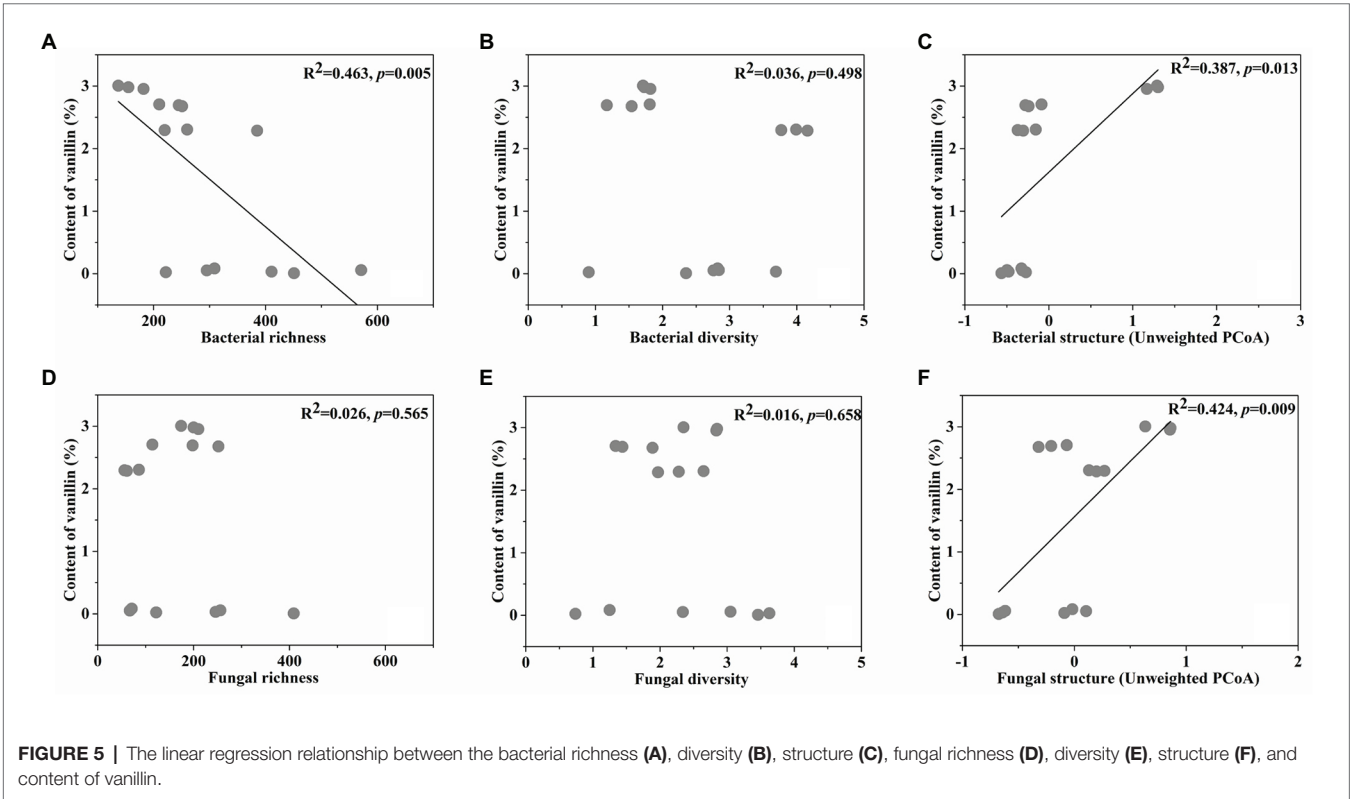
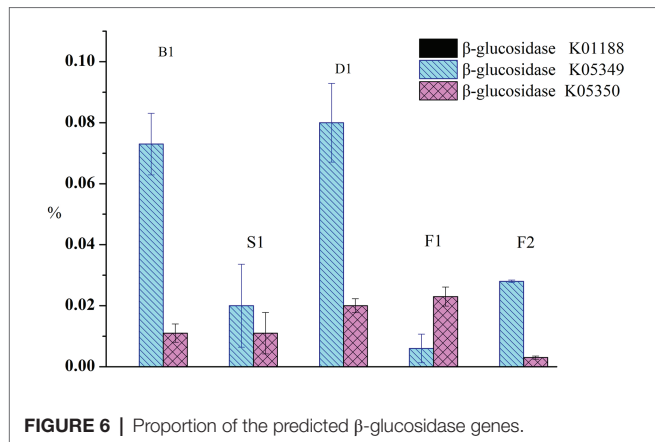


FIGURE 5 | The linear regression relationship between the bacterial richness (A), diversity (B), structure (C), fungal richness (D), diversity (E), structure (F), and content of vanillin.

DISCUSSION

The microorganism involved in the curing of vanilla beans was supported by many researches (Röling et al., 2001;

General et al., 2009; Chen et al., 2015). In this study, *Bacillus* and *Aspergillus* were found changed during the curing process. Conventional plating showed that the microbial communities mainly consisted of thermophilic and thermotolerant *Bacillus*



developing under the high temperatures and maintained for over a week after scalding (Röling et al., 2001). General et al. (2009) reported that the diversity of yeast with β -D-glucosidase in vanilla contributed to the vanilla flavor development. Differently, *Aspergillus* was found to dominate under the whole curing stages in this study, which indicated that *Aspergillus* could play an important role in the flavor formation of vanilla beans. Similarly, *Aspergillus* is also found to participate in the flavor formation in Shaoxing mechanized huangjiu and katsuobushi (Liu et al., 2019; Takenaka et al., 2020).

It was found that the structure of bacteria and fungi were closely related to the vanillin content in this study. Colonizing *Bacillus* isolates produced β -D-glucosidase, which mediated the glucovanillin hydrolysis and influenced the vanillin formation (Chen et al., 2015). Furthermore, it was reported that *Bacillus siamensis* XY18 and *Bacillus subtilis* XY20 isolated from vanilla beans could increase the vanillin content (Gu et al., 2015). Additionally, fungi and yeast could convert ferulic acid into vanillin (Taira et al., 2018). Khoyratty et al. (2015) isolated the fungal endophytes from green vanilla beans and leaves in seven different areas of Reunion Island, and the fungal endophyte species of beans were different with leaves. It may be related to the vanilla flavor formed in the beans, not leaves. And, β -glucosidase genes were predicted in the microbial community of the curing process. It indicated that the isolates producing β -D-glucosidase participated in vanillin formation.

Many studies illustrated that *Bacillus* promoted the formation of the characteristic flavor compounds during fermentation in Korean soy sauce, broccoli, and cocoa beans (Paramithiotis et al., 2010; Nam et al., 2012; de Melo Pereira et al., 2013). *Aspergillus* also played an important role in the formation of flavor during the fermentation of balsamic vinegar and liquor (Wang et al., 2016, 2018). Vanilla beans were usually blanched for 3–5 min in hot water or air, and the microorganism would be changed after blanching, for example, some strains with a low thermotolerance would be removed or inhibited (Röling et al., 2001; Frenkel et al., 2011). However, some heat-resistant microorganisms would survive. The cell structure was destroyed and many glycosides seeped out after blanching, it may be more likely to promote microbial growth (Mariezcurrana et al., 2008). In addition, the vanilla beans were always in contact with the

external environment during the curing process, and the microorganisms may be colonized again. The changed environment may influence the microbial structure, which may result in different flavor compounds. Ranadive et al. (2011) showed that the same variety of vanilla from different parts of the world could exhibit different flavors. It has been reported that although vanilla bean used the same curing procedure, the flavors were different in the vanilla beans from various areas of Reunion Island (Khoyratty et al., 2018). Therefore, vanilla beans cured by different methods would have the typical microorganisms during the curing process, which may induce a different flavor in vanilla beans (Zhang and Mueller, 2012; Takahashi et al., 2013).

The paper indicated that the microorganisms on vanilla beans underwent significant changes during the curing stages, especially *Bacillus* and *Aspergillus* which participated in the process. Vanilla beans under *Bacillus* – assisted vanilla curing and conventional curing produced more vanillin than those under the non-microorganism – assisted curing. Moreover, β -D-glucosidase-produced *Bacillus* isolates could be used to increase vanillin production without generating any unpleasant sensory attribute. This study provided another way to regulate the structure of microbiota used for increasing vanillin formation.

CONCLUSION

The microorganisms involved in the curing of vanilla beans have been analyzed, which was conducive to a further development of the curing methods. This study explored the changed colonizing microorganisms on vanilla beans during the curing process. In the future, separating the dominant strains and carrying out the auxiliary curing of vanilla were a prominent study in our lab. Furthermore, the definitive contribution microorganisms to flavor compounds are still unknown, and it is also necessary for future study.

DATA AVAILABILITY STATEMENT

All datasets presented in this study are included in the article/supplementary material.

AUTHOR CONTRIBUTIONS

YCh: software. FX, YCa, and YCh: formal analysis. FX and YCa: investigation. YCa and FX: writing – original draft preparation. FG: writing – review and editing. FG: supervision. FG and FX: project administration, and FG and FX: funding acquisition. All authors contributed to the article and approved the submitted version.

FUNDING

This research was funded by the National Natural Science Foundation of China, grant number: 31671848 and 31801499.

REFERENCES

- Benoit, I., Navarro, D., Marnet, N., Rakotomanomana, N., Lesage-Meessen, L., Sigoillot, J. C., et al. (2006). Feruloyl esterases as a tool for the release of phenolic compounds from agro-industrial by-products. *Carbohydr. Res.* 341, 1820–1827. doi: 10.1016/j.carres.2006.04.020
- Chen, Y. G., Gu, F. L., Li, J. H., He, S. Z., Xu, F., and Fang, Y. M. (2015). Involvement of colonizing *Bacillus* isolates in glucovanillin hydrolysis during the curing of *Vanilla planifolia* Andrews. *Appl. Environ. Microbiol.* 81, 4947–4954. doi: 10.1128/AEM.00458-15
- de Melo Pereira, G. V., Magalhães, K. T., de Almeida, E. G., da Silva Coelho, I., and Schwan, R. F. (2013). Spontaneous cocoa bean fermentation carried out in a novel-design stainless steel tank: influence on the dynamics of microbial populations and physical–chemical properties. *Int. J. Food Microbiol.* 161, 121–133. doi: 10.1016/j.jfoodmicro.2012.11.018
- Dong, Z. Z., Gu, F. L., Xu, F., and Wang, Q. H. (2014). Comparison of four kinds of extraction techniques and kinetics of microwave-assisted extraction of vanillin from *Vanilla planifolia* Andrews. *Food Chem.* 149, 54–61. doi: 10.1016/j.foodchem.2013.10.052
- Frenkel, C., Ranadive, A. S., Vázquez, J. T., and Havkin-Frenkel, D. (2011). “Curing of vanilla” in *Handbook of vanilla science and technology*. 2nd Edn. eds. D. Havkin-Frenkel and F. C. Belanger (Oxford: Wiley-Blackwell), 84–96.
- Gardes, M., and Bruns, T. D. (1993). ITS primers with enhanced specificity for basidiomycetes application to the identification of mycorrhizae and rusts. *Mol. Ecol.* 2, 113–118. doi: 10.1111/j.1365-294x.1993.tb00005.x
- General, T., Mamatha, V., Divya, V., and Appaiah, K. A. A. (2009). Diversity of yeast with β -glucosidase activity in vanilla (*Vanilla planifolia*) plant. *Curr. Sci.* 96, 1501–1505.
- Gu, F. L., Chen, Y. G., Fang, Y. M., Wu, G. P., and Tan, L. H. (2015). Contribution of *Bacillus* isolates to the flavor profiles of vanilla beans assessed through aroma analysis and chemometrics. *Molecules* 20, 18422–18436. doi: 10.3390/molecules201018422
- Gu, F. L., Chen, Y. G., Hong, Y. H., Fang, Y. M., and Tan, L. H. (2017). Comparative metabolomics in vanilla pod and vanilla bean revealing the biosynthesis of vanillin during the curing process of vanilla. *AMB Express* 7:116. doi: 10.1186/s13568-017-0413-2
- Kaur, B., and Chakraborty, D. (2013). Biotechnological and molecular approaches for vanillin production: a review. *Appl. Biochem. Biotechnol.* 169, 1353–1372. doi: 10.1007/s12010-012-0066-1
- Khoyraty, S., Dupont, J., Lacoste, S., Palama, T. L., Choi, Y. H., Kim, H. K., et al. (2015). Fungal endophytes of *Vanilla planifolia* across Réunion island: isolation, distribution and biotransformation. *BMC Plant Biol.* 15:142. doi: 10.1186/s12870-015-0522-5
- Khoyraty, S., Kodja, H., and Verpoorte, R. (2018). Vanilla flavor production methods: a review. *Ind. Crops Prod.* 125, 433–442. doi: 10.1016/j.indcrop.2018.09.028
- Langille, M. G., Zaneveld, J., Caporaso, J. G., McDonald, D., Knights, D., Reyes, J. A., et al. (2013). Predictive functional profiling of microbial communities using 16S rRNA marker gene sequences. *Nat. Biotechnol.* 31, 814–821. doi: 10.1038/nbt.2676
- Lesage-Meessen, L., Lomascolo, A., Bonnin, E., Thibault, J. F., Buleon, A., Roller, M., et al. (2002). A biotechnological process involving filamentous fungi to produce natural crystalline vanillin from maize bran. *Appl. Biochem. Biotechnol.* 102, 141–153. doi: 10.1385/abab:102-103:1-6:141
- Lipkin, W. I. (2013). The changing face of pathogen discovery and surveillance. *Nat. Rev. Microbiol.* 11, 133–141. doi: 10.1038/nrmicro2949
- Liu, S. P., Chen, Q. L., Zou, H. J., Yu, Y. J., Zhou, Z. L., Mao, J., et al. (2019). A metagenomic analysis of the relationship between microorganisms and flavor development in Shaoxing mechanized huangjiu fermentation mash. *Int. J. Food Microbiol.* 303, 9–18. doi: 10.1016/j.jfoodmicro.2019.05.001
- Lubinsky, P., Bory, S., Hernández Hernández, J., Kim, S. C., and Gómez-Pompa, A. (2008). Origins and dispersal of cultivated vanilla (*Vanilla planifolia* Jacks [Orchidaceae]). *Econ. Bot.* 62, 127–138. doi: 10.1007/s12231-008-9014-y
- Mariezcurrera, M. D., Zavaleta, H. A., Waliszewski, K. N., and Snchez, V. (2008). The effect of killing conditions on the structural changes in vanilla (*Vanilla planifolia*, Andrews) pods during the curing process. *Int. J. Food Sci. Technol.* 43, 1452–1457. doi: 10.1111/j.1365-2621.2007.01691.x
- Menon, S., and Nayeem, N. (2013). *Vanilla planifolia*: a review of a plant commonly used as flavouring agent. *Int. J. Pharm. Sci. Rev. Res.* 20, 225–228.
- Nam, Y. D., Lee, S. Y., and Lim, S. I. (2012). Microbial community analysis of Korean soybean pastes by next-generation sequencing. *Int. J. Food Microbiol.* 155, 36–42. doi: 10.1016/j.jfoodmicro.2012.01.013
- Pak, F. E., Gropper, S., Dai, W. D., Havkin-Frenkel, D., and Belanger, F. C. (2004). Characterization of a multifunctional methyltransferase from the orchid *Vanilla planifolia*. *Plant Cell Rep.* 22, 959–966. doi: 10.1007/s00299-004-0795-x
- Paramithiotis, S., Hondrodinou, O. L., and Drosinos, E. H. (2010). Development of the microbial community during spontaneous cauliflower fermentation. *Food Res. Int.* 43, 1098–1103. doi: 10.1016/j.foodres.2010.01.023
- Podstolski, A., Havkin-Frenkel, D., Malinowski, J., Blount, J. W., Kourteva, G., and Dixon, R. A. (2002). Unusual 4-hydroxybenzaldehyde synthase activity from tissue cultures of the vanilla orchid *Vanilla planifolia*. *Phytochemistry* 61, 611–620. doi: 10.1016/s0031-9422(02)00285-6
- Quast, C., Pruesse, E., Yilmaz, P., Gerken, J., Schweer, T., Yarza, P., et al. (2013). The SILVA ribosomal RNA gene database project: improved data processing and web-based tools. *Nucleic Acids Res.* 41, D590–D596. doi: 10.1093/nar/gks1219
- Ranadive, A. S., Havkinfrenkel, D., and Belanger, F. C. (2011). “Quality control of vanilla beans and extracts” in *Handbook of vanilla science and technology*. eds. D. Havkin-Frenkel and F. C. Belanger (Oxford: Wiley-Blackwell), 139–161.
- Rao, S. R., and Ravishankar, G. A. (2010). Vanilla flavour: production by conventional and biotechnological routes. *J. Sci. Food Agric.* 80, 289–304. doi: 10.1002/1097-0010(200002)80:3<289::AID-JSFA543>3.0.CO;2-2
- Röling, W. F. M., Kerler, J., Braster, M., Apriyanton, A., Stam, H., and van Verseveld, H. W. (2001). Microorganisms with a taste for vanilla: microbial ecology of traditional Indonesian vanilla curing. *Appl. Environ. Microbiol.* 67, 1995–2003. doi: 10.1128/AEM.67.5.1995-2003.2001
- Schloss, P. D., Westcott, S. L., Ryabin, T., Hall, J. R., Hartmann, M., Hollister, E. B., et al. (2009). Introducing mothur: open-source, platform-independent, community-supported software for describing and comparing microbial communities. *Appl. Environ. Microbiol.* 75, 7537–7541. doi: 10.1128/AEM.01541-09
- Sreedhar, R. V., Roohie, K., Maya, P., Venkatachalam, L., and Bhagyalakshmi, N. (2009). Biotic elicitors enhance flavour compounds during accelerated curing of vanilla beans. *Food Chem.* 112, 461–468. doi: 10.1016/j.foodchem.2008.05.108
- Taira, J., Toyoshima, R., Ameku, N., Iguchi, A., and Tamaki, Y. (2018). Vanillin production by biotransformation of phenolic compounds in fungus, *Aspergillus luchuensis*. *AMB Express* 8:40. doi: 10.1186/s13568-018-0569-4
- Takahashi, M., Inai, Y., Miyazawa, N., Kurobayashi, Y., and Fujita, A. (2013). Key odorants in cured Madagascar vanilla beans (*Vanilla planifolia*) of differing bean quality. *Biosci. Biotechnol. Biochem.* 77, 606–611. doi: 10.1271/bbb.120842
- Takenaka, S., Nakabayashi, R., Ogawa, C., Kimura, Y., Yokota, S., and Doi, M. (2020). Characterization of surface *Aspergillus* community involved in traditional fermentation and ripening of katsuobushi. *Int. J. Food Microbiol.* 327:108654. doi: 10.1016/j.jfoodmicro.2020.108654
- Toth, S., Lee, K. J., Havkin-Frenkel, D., Belanger, F. C., and Hartman, T. G. (2011). “Volatile compounds in vanilla” in *Handbook of vanilla science and technology*. eds. D. Havkin-Frenkel and F. C. Belanger (Oxford: Wiley-Blackwell), 183–219.
- Wang, X., Du, H., Zhang, Y., and Xu, Y. (2018). Environmental microbiota drives microbial succession and metabolic profiles during Chinese liquor fermentation. *Appl. Environ. Microbiol.* 84, e02369–e02317. doi: 10.1128/AEM.02369-17
- Wang, Q., Garrity, G. M., Tiedje, J. M., and Cole, J. R. (2007). Naïve Bayesian classifier for rapid assignment of rRNA sequences into the new bacterial taxonomy. *Appl. Environ. Microbiol.* 73, 5261–5267. doi: 10.1128/AEM.00062-07
- Wang, Z. M., Lu, Z. M., Shi, J. S., and Xu, Z. H. (2016). Exploring flavour-producing core microbiota in multispecies solid-state fermentation of traditional Chinese vinegar. *Sci. Rep.* 6:26818. doi: 10.1038/srep26818
- White, T. J., Bruns, T., Lee, S., and Taylor, J. W. (1990). “Amplification and direct sequencing of fungal ribosomal RNA genes for phylogenetics” in *PCR protocols: A guide to methods and applications*. eds. M. A. Innis, D. H. Gelfand, J. J. Sninsky and T. J. White (New York: Academic Press), 315–322.

- Xiong, J. B., Liu, Y. Q., Lin, X. G., Zhang, H. Y., Zeng, J., Hou, J. Z., et al. (2012). Geographic distance and pH drive bacterial distribution in alkaline lake sediments across Tibetan plateau. *Environ. Microbiol.* 14, 2457–2466. doi: 10.1111/j.1462-2920.2012.02799.x
- Yamada, M., Okada, Y., Yoshida, T., and Nagasawa, T. (2007). Biotransformation of isoeugenol to vanillin by *Pseudomonas putida* IE27 cells. *Appl. Microbiol. Biotechnol.* 73, 1025–1030. doi: 10.1007/s00253-006-0569-1
- Zhang, S., and Mueller, C. (2012). Comparative analysis of volatiles in traditionally cured Bourbon and Ugandan vanilla bean (*Vanilla planifolia*) extracts. *J. Agric. Food Chem.* 60, 10433–10444. doi: 10.1021/jf302615s

Conflict of Interest: The authors declare that the research was conducted in the absence of any commercial or financial relationships that could be construed as a potential conflict of interest.

Copyright © 2020 Xu, Chen, Cai, Gu and An. This is an open-access article distributed under the terms of the Creative Commons Attribution License (CC BY). The use, distribution or reproduction in other forums is permitted, provided the original author(s) and the copyright owner(s) are credited and that the original publication in this journal is cited, in accordance with accepted academic practice. No use, distribution or reproduction is permitted which does not comply with these terms.



Antibacterial Activity and Mechanism of Lacidophilin From *Lactobacillus pentosus* Against *Staphylococcus aureus* and *Escherichia coli*

Yinglian Zhu^{*†} and Shuang Zhang[†]

College of Food Science and Engineering, Qingdao Agricultural University, Qingdao, China

OPEN ACCESS

Edited by:

Zhenbo Xu,
University of Tennessee Health
Science Center (UTHSC),
United States

Reviewed by:

Sueli Fumie Yamada-Ogatta,
State University of Londrina, Brazil
Dennis Ken Bideshi,
California Baptist University,
United States

*Correspondence:

Yinglian Zhu
cjs52002@163.com

[†]These authors have contributed
equally to this work

Specialty section:

This article was submitted to
Food Microbiology,
a section of the journal
Frontiers in Microbiology

Received: 11 July 2020

Accepted: 30 September 2020

Published: 29 October 2020

Citation:

Zhu Y and Zhang S (2020)
Antibacterial Activity and Mechanism
of Lacidophilin From *Lactobacillus*
pentosus Against *Staphylococcus*
aureus and *Escherichia coli*.
Front. Microbiol. 11:582349.
doi: 10.3389/fmicb.2020.582349

The main purpose of this study was to explore the antibacterial activity and mechanism of lacidophilin from *Lactobacillus pentosus* against *Staphylococcus aureus* and *Escherichia coli*. The effects of temperature, enzyme, metal ions, and pH on the antibacterial activity of *L. pentosus* were evaluated. The result showed that lacidophilin had good thermal stability and could be decomposed by trypsin completely. The antibacterial ability was affected by high concentration of metal ions, and the best antibacterial ability was acquired under acidic conditions. The antibacterial mechanism of lacidophilin was explored through studying cytomembrane injury, phosphorus metabolism, protein changes, and oxidative stress response of the indicator bacteria. It was shown that lacidophilin destroyed the cytomembrane of the bacteria and increased the cytomembrane permeability, which resulted in the leak of proteins, nucleic acids, and electrolytes. In addition, it further restrained phosphorus metabolism, caused changes of some protein contents, and increased cytomembrane lipid peroxidation and cell oxidative damage. All these might inhibit the growth of bacteria and even cause their death. This study identified a natural biological preservative with strong antibacterial activity against both Gram-positive and Gram-negative foodborne pathogens. The high antibacterial activity against the two types of bacteria reflected its potential in food preservation used as a natural food preservative.

Keywords: *Lactobacillus pentosus*, lacidophilin, *Staphylococcus aureus*, *Escherichia coli*, antibacterial mechanism

INTRODUCTION

The food industry has made significant progress in food standards, food processing, and food testing, but health and safety concerns still persist. It was estimated that about one-third of food is wasted due to spoilage each year (Gills et al., 2015). Some physical and chemical methods have been adopted to extend the shelf life of foods, among which, the addition of chemical preservatives is the most effective way. However, long-term intake of chemical preservatives has adverse effects on human health (Yang et al., 2014). Therefore, more attention has been paid to natural preservatives for their safe and non-polluting character. Bacteriocins have been widely used in foods as natural preservatives because of their wide sources and diverse structures, which have high efficiency in killing various foodborne pathogens and spoilage bacteria (Lv et al., 2018).

Lacidophilin is a kind of bacteriocin produced by lactic acid bacteria (LAB), which has advantages than those from other biological resources because LAB is generally recognized as safe (GRAS) microorganisms (Sequeiros et al., 2015). However, most lacidophilin can only inhibit affinis strains of LAB, which limits their applications. Nisin, currently being used widely in food preservation, mainly inhibits most Gram-positive bacteria and spore bacteria and has no antibacterial effect on Gram-negative bacteria. Therefore, more researchers are exploring lacidophilin with wide range antibacterial spectrum. Bifidocin A, produced by *Bifidobacterium animalis* BB04, has been reported by Liu et al. (2017), and the antibacterial activity of bifidocin A against *Listeria* was mainly achieved by destroying the integrity of the cell membrane and increasing membrane permeability. A novel lacidophilin produced by *Lactobacillus plantarum* against *Pseudomonas fluorescens* has been reported by Lv et al. (2018), and it demonstrated wide antimicrobial spectrum against fish pathogens and spoilage bacteria. Previous studies have indicated that bacteriocins are generally antibacterial proteins or peptides (Lv et al., 2018; Vasilchenko et al., 2018). However, the number of bacteriocins is far less than the number of antimicrobial peptides developed (Vasilchenko et al., 2018). In view of the advantageous characteristics of lacidophilin, the development of lacidophilin with high antimicrobial activity against the two types of bacteria is urgent.

In recent years, probiotics have become a hot research topic, due to their safety, nutritional and health value, and antimicrobial function. *Lactobacillus pentosus* (*L. pentosus*) is a Gram-positive lactobacillus, which is widely used in the processing of fermented meat products (Liu et al., 2008; Zhu et al., 2019). The lacidophilin of LAB was considered to be critical for sausage processing because it enhanced the quality and safety of the sausages (Zhu et al., 2020). However, there are only a few studies that focused on the lacidophilin produced by *L. pentosus*. Pentocin 31-1 was identified as anti-*Listeria* lacidophilin produced by *L. pentosus* 31-1 (Liu et al., 2008). Motahari et al. (2016) optimized the fermentation conditions of lacidophilin by *L. pentosus* and revealed that low concentration of sodium chloride promoted the production of lacidophilin. The study by Hurtado et al. (2011) indicated that the appropriate concentration of sodium chloride could improve the bacteriostatic activity of *L. pentosus* B96 lacidophilin, compared with non-saline control and high-concentration sodium chloride group. However, few studies focused on the lacidophilin produced by *L. pentosus* against the two types of bacteria and explored its antibacterial mechanism.

Escherichia coli (*E. coli*) is one of the most common Gram-negative foodborne pathogens, which usually was used and is an indicator bacterium in test for fecal contamination of food. It can cause diarrhea, gastroenteritis, and a series of complications (Miri et al., 2017). *Staphylococcus aureus* (*S. aureus*) is a common Gram-positive foodborne pathogen that contaminates various foods, and staphylococcal foodborne diseases from food contamination pathogen, and is regarded as the second most common foodborne illnesses in the world (Di Pinto et al., 2005). The focus of this study is on the antimicrobial activity of *L. pentosus* lacidophilin against *S. aureus* and *E. coli* and further explore its antibacterial mechanism. The fermentation

supernatant of *L. pentosus* (lactic acid interference excluded) was used as the crude extract of lacidophilin. The effects of heat, enzyme, metal ions, and pH on the antibacterial effect of lacidophilin were measured to evaluate its antibacterial activity. In addition, the antibacterial mechanism of lacidophilin was further explored through studying cytomembrane injury, phosphorus metabolism, protein changes, and oxidative stress response of the indicator.

MATERIALS AND METHODS

Strains

Lactobacillus pentosus (strain no. 22226) and *L. plantarum* (strain no. 23941) were provided by China Center of Industrial Culture Collection (CICC). *E. coli* (strain no. 1.8723) and *S. aureus* (strain no. 1.8721) were provided by China General Microbiological Culture Collection Center (CGMCC).

Main Reagents

Fluorescein diacetate (FDA), propionyl iodide (PI), sodium dodecyl sulfate, acrylamide, and methylenebisacrylamide were provided by Suo Lai Bao Biotechnology Co., Ltd. Pepsin, papain, trypsin, and amylase were provided by Sinopharm Group Chemical Reagent Co., Ltd., Malondialdehyde (MDA), superoxide dismutase (SOD), peroxidase (POD), and catalase (CAT) reagent test kits were provided by Nanjing Jiancheng Biological Engineering Research Institute.

Cell-Free Supernatant Containing Lacidophilin Preparation

Lactobacillus pentosus was picked from MRS slope with an inoculation loop, transferred to 10 ml of MRS broth, and incubated at 37°C for 24 h. Then, 10 ml of the inoculum was transferred to 100 ml of MRS broth and incubated at 37°C for 72 h. Subsequently, the inoculum ($OD_{600} = 2.350$) was centrifuged at $8,000 \times g$ for 15 min at 4°C. The supernatant was collected, and pH was adjusted with NaOH (1 mol/L) to 5.5 to eliminate the interference of organic acids. Thus, the *L. pentosus* cell-free supernatant containing lacidophilin (*L. p.* supernatant) was obtained, which was used for subsequent antibacterial activity measurement.

Antibacterial Activity Measurement

The antibacterial activity of *L. pentosus* lacidophilin was carried out utilizing the agar diffusion method according to the previous report (Cai et al., 2019) with minor modifications: MRS medium (10 ml) containing 2% agar was used as the bottom plate. MRS medium (7 ml) containing 0.7% agar and 5% indicator bacteria cell suspension (OD_{600} , 0.6) was poured on the bottom plate as the upper plate. After the upper plate was completely solidified, three Oxford cups were placed on the plate. Then, 0.1 ml of the *L. p.* supernatant was injected into the Oxford cup, and the diameter of inhibition zone around the Oxford cup was measured to determine antibacterial activity after being incubated at 37°C for 24 h. The MRS broth (without *L. pentosus* inoculation) was

used as the negative control. In addition, the positive control was prepared through substituting *L. pentosus* with the *L. plantarum* strain capable of producing lacidophilin.

Total Protein Content of the *L. p.* Supernatant

The total protein content of the *L. p.* supernatant was detected with the Coomassie Brilliant Blue G-250 dye method according to the report by Cai et al. (2019). The *L. p.* supernatant (1 ml) was mixed with 5 ml of Coomassie Brilliant Blue G-250 dye and laid for 2 min. The total protein content of the *L. p.* supernatant was evaluated by measuring the OD value of the mixture at 595 nm. The standard curve of protein content was drawn as follows: the standard protein solution (0.0, 0.1, 0.2, 0.3, 0.4, and 0.5 ml) was added to 1 ml of volumetric flasks, respectively, and then the volume was made up to 1 ml with distilled water. Subsequently, 1 ml of the protein solution was mixed with 5 ml of Coomassie Brilliant Blue G-250, respectively, and placed for 2 min. Protein content was evaluated by measuring OD value at 595 nm.

Effects of Heat, Enzyme, and Metal Ions on Antibacterial Activity

The antibacterial activity was carried out according to the above chapter (section “Antibacterial Activity Measurement”). To determine the thermal stability of lacidophilin, the *L. p.* supernatant was treated at 65, 85, and 100°C in a water bath for 10 min, respectively, and then 0.1 ml of the supernatant was taken out for antibacterial activity measurement. The *L. p.* supernatant without heat treatment was used as the control. To evaluate the effect of enzymes, four enzymes (pepsin, papain, amylase, and trypsin) were added in the *L. p.* supernatant, respectively, to make the final concentration to be 1 mg/ml. After being reacted at 37°C for 2.5 h at appropriate pH, they were heated at 100°C in a water bath for 10 min to inactivate the enzymes (Lv et al., 2018), and then 0.1 ml of the supernatant was taken out for antibacterial activity measurement. The *L. p.* supernatant without enzyme treatment was used as the control. The effect of metal ions was carried out with different concentrations of NaCl, KCl, MgCl₂, and CaCl₂ solutions. Different volumes (1, 2, and 4 ml) of sterile metal ions solution (0.1 mol/L, with *L. p.* supernatant as solvent) were added to 4 ml of the *L. p.* supernatant to make the final metal ions concentrations be 0.02, 0.033, and 0.05 mol/L, which corresponded to 1, 2, and 4 ml, respectively. Then, 0.1 ml of the supernatant was taken out for antibacterial activity measurement. The *L. p.* supernatant without metal ions treatment was used as the control.

Effect of Lacidophilin on the Dynamic Growth of the Two Indicator Bacteria

The indicator bacteria were inoculated in 10 ml of LB broth, incubated at 37°C for 24 h, then transferred to 100 ml of LB broth, and incubated at 37°C for 12 h. After being centrifuged at 8,000 × *g* for 15 min at 4°C, the bacteria cell was resuspended in LB broth to adjust the absorbance value to 0.6 at 600 nm. Then, the bacterial suspension (100 ml) was mixed with an equal volume of *L. p.* supernatant and incubated at 37°C for 1.5, 3.5,

5.0, 7.0, 9.0, and 11.0 h, respectively. The absorbance at 600 nm (Yi et al., 2016) was recorded to measure the effect of lacidophilin on the dynamic growth of the two indicator bacteria.

Effect of Lacidophilin on Cell Membrane Integrity

Fluorescence Spectrum Analysis

The *L. p.* supernatant was prepared according to the above chapter (section “Cell-Free Supernatant Containing Lacidophilin Preparation”). Then, the indicator bacterial suspension (OD₆₀₀, 0.6) (4 ml) was mixed with an equal volume of *L. p.* supernatant and incubated at 37°C for 12 h. The inoculum (5 ml) was taken out and centrifuged at 8,000 × *g* for 15 min at 4°C. Then, the indicator bacteria cells were collected and washed with phosphate buffer solution (PBS, 0.1 mol/L, pH 7.0) three times. The bacterial cells were resuspended in 920 μl of 0.85% NaCl solution, and then 20 μl of FDA (5 mg/ml) and 60 μl of PI (1 mg/ml) were added. After staining at 4°C for 6 h in the dark (Liu et al., 2017), the fluorescence scan spectrum was measured using a fluorescence spectrophotometer at an excitation wavelength of 450 nm.

Fluorescence Microscope Observation

The staining steps of the indicator bacteria were consistent with fluorescence spectrum analysis. Then, the stained cells were centrifuged at 8,000 × *g* for 15 min at 4°C, and the cells were collected and washed with PBS (0.1 mol/L, pH 7.0) three times. Finally, the cells were resuspended in 1 ml of PBS (0.1 mol/L, pH 7.0) and observed under a fluorescence microscope.

Effect of Lacidophilin on Cell Membrane Permeability

Electrolyte leakage of the indicator bacteria was measured according to the method by Shen et al. (2015) with minor modification. The indicator bacteria were suspended in 50 ml of LB broth to make an OD₆₀₀ of 0.6. The bacterial suspension (50 ml) was mixed with an equal volume of *L. p.* supernatant and incubated at 37°C for 2.5 h. The conductivity of the mixture was measured at 0, 0.5, 1.0, 1.5, and 2.5 h, respectively, with a conductivity meter. Before measuring conductivity, 5 ml of the mixture was removed and filtered with 0.45 μm sterile filters to remove bacteria cells.

Leakage of the soluble nucleic acids was detected according to the method by Cai et al. (2019) with minor modification. The indicator bacterial suspension (20 ml, OD₆₀₀, 0.9) was mixed with an equal volume of *L. p.* supernatant and incubated at 37°C for 0, 1.5, 3, 5, and 7 h, respectively. Then, 5 ml of the inoculum was taken out and centrifuged at 10,000 × *g* for 10 min at 4°C, and the supernatant was collected, respectively. Subsequently, 4 ml of the supernatant was taken out to measure the OD value at 260 nm to determine the nucleic acid leakage.

Leakage of the soluble protein was detected with the Coomassie Brilliant Blue G-250 dye method according to the description of the previous chapter (Total Protein Content of the *L. p.* Supernatant). After leakage of the soluble nucleic acids being measured, the remaining supernatant (1 ml) was mixed with 5 ml of Coomassie Brilliant Blue G-250 dye and laid for

2 min. The soluble protein leakage was evaluated by measuring the OD value of the mixture at 595 nm. The standard curve of protein content was drawn as the description of the previous chapter (Total Protein Content of the *L. p.* Supernatant).

Effect of Lacidophilin on Phosphorus Metabolism

Phosphorus metabolism of the indicator bacteria was measured according to the previous method (Wang et al., 2020) with some modifications. The indicator bacteria were suspended in glucose solution (1 mg/ml) to make an OD₆₀₀ of 0.9. The bacterial suspension (7.5 ml) was mixed with an equal volume of *L. p.* supernatant, and then 1.5 ml phosphorus standard solution (50 µg/ml) was added. After being incubated at 37°C for 0, 0.5, 1.0, 1.5, and 2.5 h, the inoculum (2 ml) was taken out and centrifuged at 8,000 × g for 15 min at 4°C, and then the supernatant was collected. A 10% ascorbic acid solution (1 ml) was added in the collected supernatant and stood for 30 s; subsequently, 2 ml of 2.5% molybdate solution was added and reacted for 15 min. The OD value was measured at 700 nm to confirm the phosphorus concentration. The MRS medium (7.5 ml) was used to substitute the *L. p.* supernatant as the blank control to remove the interference of the medium. The standard curve of phosphorus content was drawn as follows: the phosphorus standard solution (0.0, 0.05, 0.1, 0.3, 0.5, 1.0, and 1.5 ml) was added to seven volumetric flasks (25 ml), and then the solution was made up to 25 ml with distilled water. Subsequently, the solution (2 ml) was taken out, mixed with 1 ml of 10% ascorbic acid solution, and stood for 30 s. Finally, 2 ml of 2.5% molybdate solution was added and reacted for 15 min.

Effect of Lacidophilin on Bacterial Protein

SDS-PAGE was carried out to measure the bacteria cell protein changes according to the method by Cai et al. (2019) with some modifications. The indicator bacterial suspension (4 ml, OD₆₀₀, 0.6) was mixed with an equal volume of *L. p.* supernatant and incubated at 37°C for 18 h. Then, 5 ml of the inoculum was taken out and centrifuged at 8,000 × g for 15 min at 4°C to collect the precipitate. After being washed three times with PBS (0.1 mol/L, pH 7.0), the bacteria cells were collected. The collected cells were resuspended in 500 µl of 0.85% NaCl, and then 20 µl of the suspension was taken out, mixed with 10 µl of protein loading buffer, boiled in a water bath for 5 min, and cooled to room temperature instantly. After being centrifuged at 3000 × g for 5 min, 15 µl of the supernatant was analyzed with SDS-PAGE gel electrophoresis using 5% concentrated gel and 12% separation gel. The gel was dyed with Coomassie Brilliant Blue R-250 for 30 min and decolorized overnight until the background became transparent.

Effect of Lacidophilin on Intracellular Enzyme (SOD, POD, and CAT) Activity and MDA Content

The SOD, POD, and CAT activities and MDA content were measured according to the previous method (Jia et al., 2014)

with some modifications. The indicator bacterial suspension (10 ml, OD₆₀₀, 0.9) was mixed with an equal volume of *L. p.* supernatant and incubated at 37°C for 5 h. Then, 5 ml of the inoculum was taken out and centrifuged at 8,000 × g for 15 min at 4°C to collect the precipitate. After being washed three times with PBS (0.1 mol/L, pH 7.0), the bacteria cells were collected. After being grinded with quartz sand and a mortar in an ice-bath for 5 min, the cells were removed into 10 ml of 0.85% NaCl solution, well mixed, and centrifuged at 8,000 × g for 15 min at 4°C. The collected supernatant was used to measure the activity of intracellular enzyme and the content of MDA. The measurements were conducted with SOD, POD, CAT, and MDA kits and read in a microplate reader.

Statistical Analysis

Statistical analysis was implemented using SPSS version 18.0, and the data were analyzed through multiple comparisons with the Duncan method. A probability level of 0.05 was regarded as a significance limit.

RESULTS

Antibacterial Activity of Lacidophilin

No antibacterial effect against *E. coli* and *S. aureus* was observed in the negative control (MRS medium alone) (Table 1), which eliminated the interference of the medium to the antibacterial effect. In addition, adjustment of pH to 5.5 with NaOH (1 mol/L) eliminated the interference of organic acids. The total protein content of the *L. p.* supernatant was 964 µg/ml measured with the Coomassie Brilliant Blue G-250 dye method. The diameters of inhibition zones around the Oxford cup against *E. coli* and *S. aureus* were 19.83 and 18.46, respectively (Table 1), which indicated that the lacidophilin from *L. pentosus* had high activity against the two strains. The cell density of the inoculum had no significant difference ($P > 0.05$) compared with the positive control, but the inhibition effect was higher ($P < 0.05$) than the positive control, which showed that lacidophilin had great potential as a food preservative in food preservation.

Effects of Heat, Enzyme, and Metal Ions on Antibacterial Activity

In Figure 1, heat treatment showed a certain negative effect on the antibacterial effect of lacidophilin, and the negative effect increased with heating temperature increased and time prolonged. However, after being treated at 65°C for 30 min, lacidophilin retained about 90% of the antibacterial activity against the two indicator bacteria. After being treated at 85 and 100°C for 30 min, lacidophilin retained about more than 80% of the antibacterial activity against the two bacteria. Figure 2 shows that different enzymes had different effects on the antibacterial effect of lacidophilin. Pepsin had no significant effect on the antibacterial activity ($P > 0.05$). However, the antibacterial effects of lacidophilin against the two bacteria were

TABLE 1 | Antibacterial activity of lacidophilin.

Groups	OD ₆₀₀ (37°C 72 h fermentation)	Inhibition zone diameter (against <i>E. coli</i>)	Inhibition zone diameter (against <i>S. aureus</i>)
Negative control	0.001 ± 0.001 ^b	0 ± 0 ^c	0 ± 0 ^c
Positive control	2.268 ± 0.189 ^a	16.593 ± 0.668 ^b	15.257 ± 0.386 ^b
The treated group	2.350 ± 0.063 ^a	19.830 ± 0.960 ^a	18.460 ± 0.685 ^a

Values are represented as mean ± SD from triplicate experiments. Different lowercase superscripts in the same column indicate that the antibacterial effect is significantly different ($P < 0.05$). The diameter of the inhibition zone around the Oxford cup is used to denote the antibacterial activity of lacidophilin.

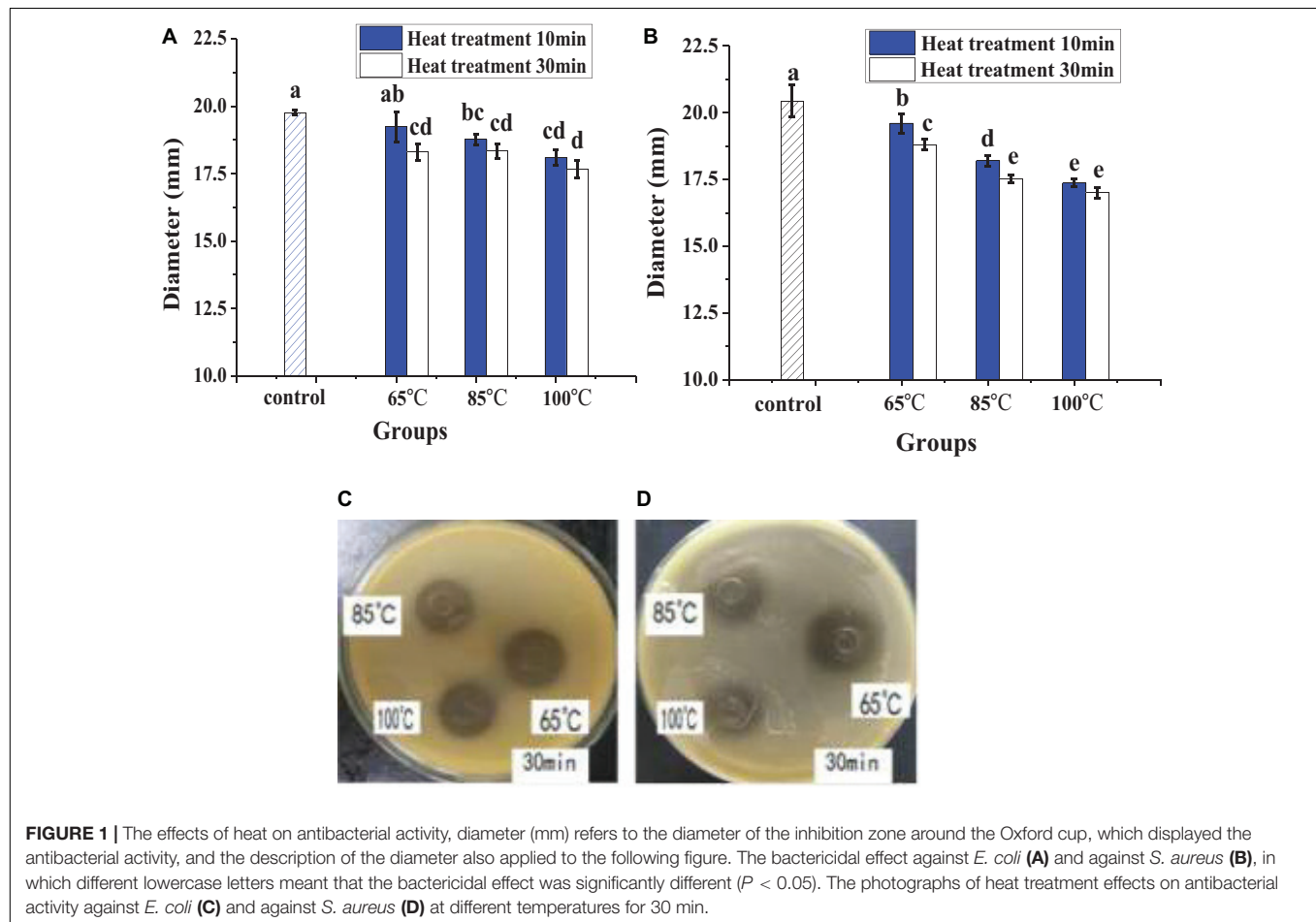


FIGURE 1 | The effects of heat on antibacterial activity, diameter (mm) refers to the diameter of the inhibition zone around the Oxford cup, which displayed the antibacterial activity, and the description of the diameter also applied to the following figure. The bactericidal effect against *E. coli* (A) and against *S. aureus* (B), in which different lowercase letters meant that the bactericidal effect was significantly different ($P < 0.05$). The photographs of heat treatment effects on antibacterial activity against *E. coli* (C) and against *S. aureus* (D) at different temperatures for 30 min.

both weakened after being treated with papain and amylase. After being treated with trypsin, lacidophilin lost its antibacterial effect, which indicated that lacidophilin could be degraded completely by trypsin. In addition, it could be seen from **Figure 3** that different types and different concentrations of metal ions had different effects on the antibacterial ability of lacidophilin. As the concentration of metal ions increased, the antibacterial effect against the two indicator bacteria gradually weakened.

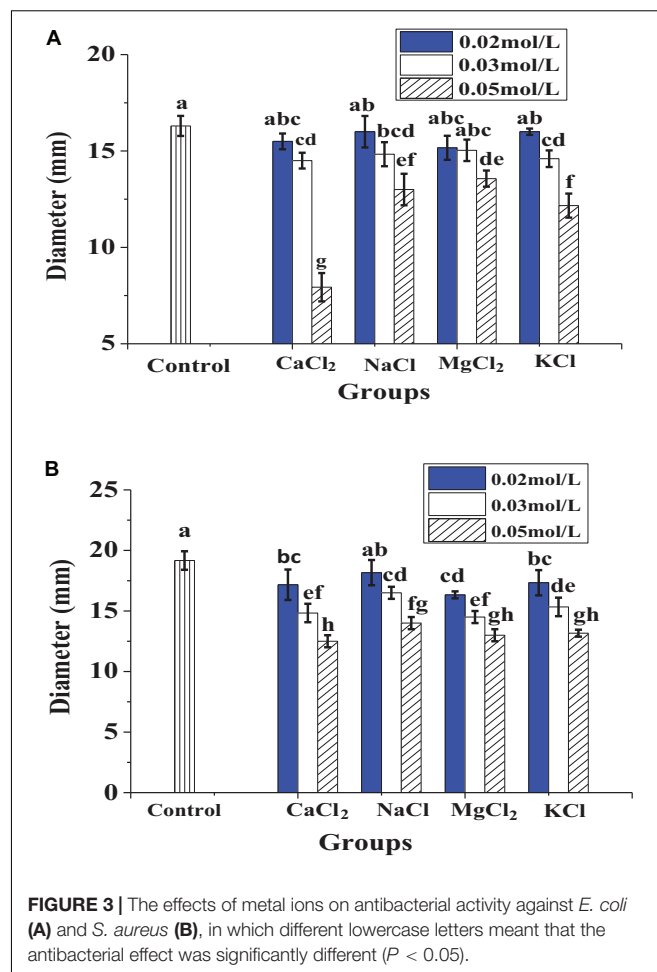
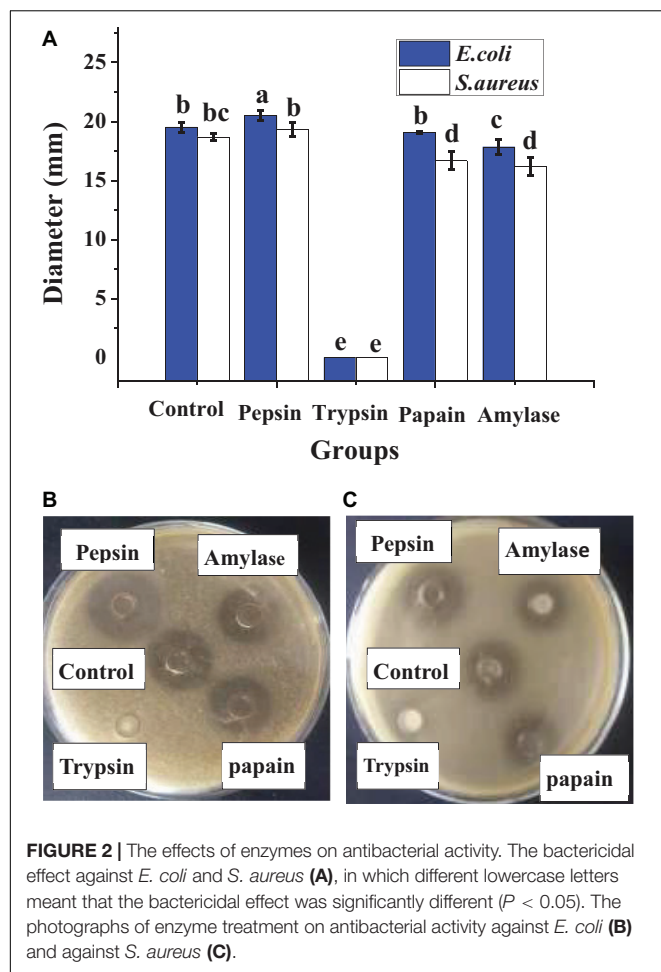
Dynamic Growth Curve of Two Indicator Bacteria

In **Figure 4**, the dynamic growth of the treated bacteria and the control was similar in the lagged period. After 1.5 h, the difference between treated bacteria and the control increased significantly.

The control had a high-speed growth trend, whereas the growth of the treated bacteria was significantly inhibited.

Effect of Lacidophilin on Cytoplasmic Integrity

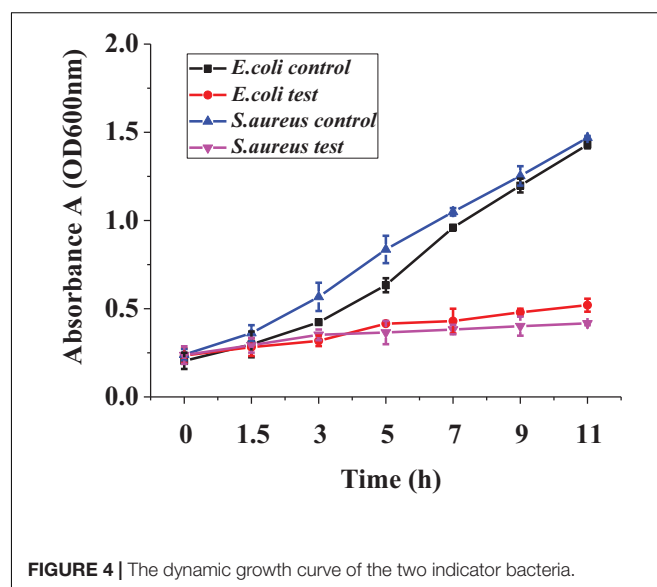
Figure 5A shows that the untreated *E. coli* and *S. aureus* emitted green fluorescence, whereas the treated *E. coli* and *S. aureus* both emitted red fluorescence, which illustrated that the cytoplasmic integrity of the indicator bacteria had been destroyed by lacidophilin. In the fluorescence spectrum of **Figure 5B**, the absorption peaks at about 520 nm were both observed in the untreated *E. coli* and *S. aureus*, which was corresponding to the absorbance peak of FDA, whereas the peaks of the treated *E. coli* and *S. aureus* were both moved to about 596 nm, which was



consistent with the absorbance peak of PI. The result of the fluorescence spectrum further indicated that the cytomembrane had been destroyed.

Effect of Lacidophilin on Cytomembrane Permeability

Figure 6A shows that the inoculum conductivity of the treated *E. coli* and *S. aureus* increased with the time prolonged, which indicated that the leakage of electrolyte increased, whereas the conductivity of the control did not change significantly. In Figure 6B, the inoculum absorbance of the treated *E. coli* and *S. aureus* at 260 nm was higher than that of the controls, indicating the leakage of nucleic acid from the treated strains. In addition, the absorbance differences between the treated strains and the controls increased significantly with time extension, which showed that the nucleic acid leakage was increasing gradually. In Figure 6C, *S. aureus* showed protein leakage after being treated for about 0.5 h; *E. coli* showed protein leakage after being treated for about 1.5 h. As time went on, protein leakage both kept increasing. In addition, as could be seen from Figure 6D, the phosphorus contents in the inoculum of the treated bacteria and the controls were all decreased with time



prolonged. However, the phosphorus contents in the inoculum of the two treated bacteria were both higher than those of the two controls throughout the processing, which indicated

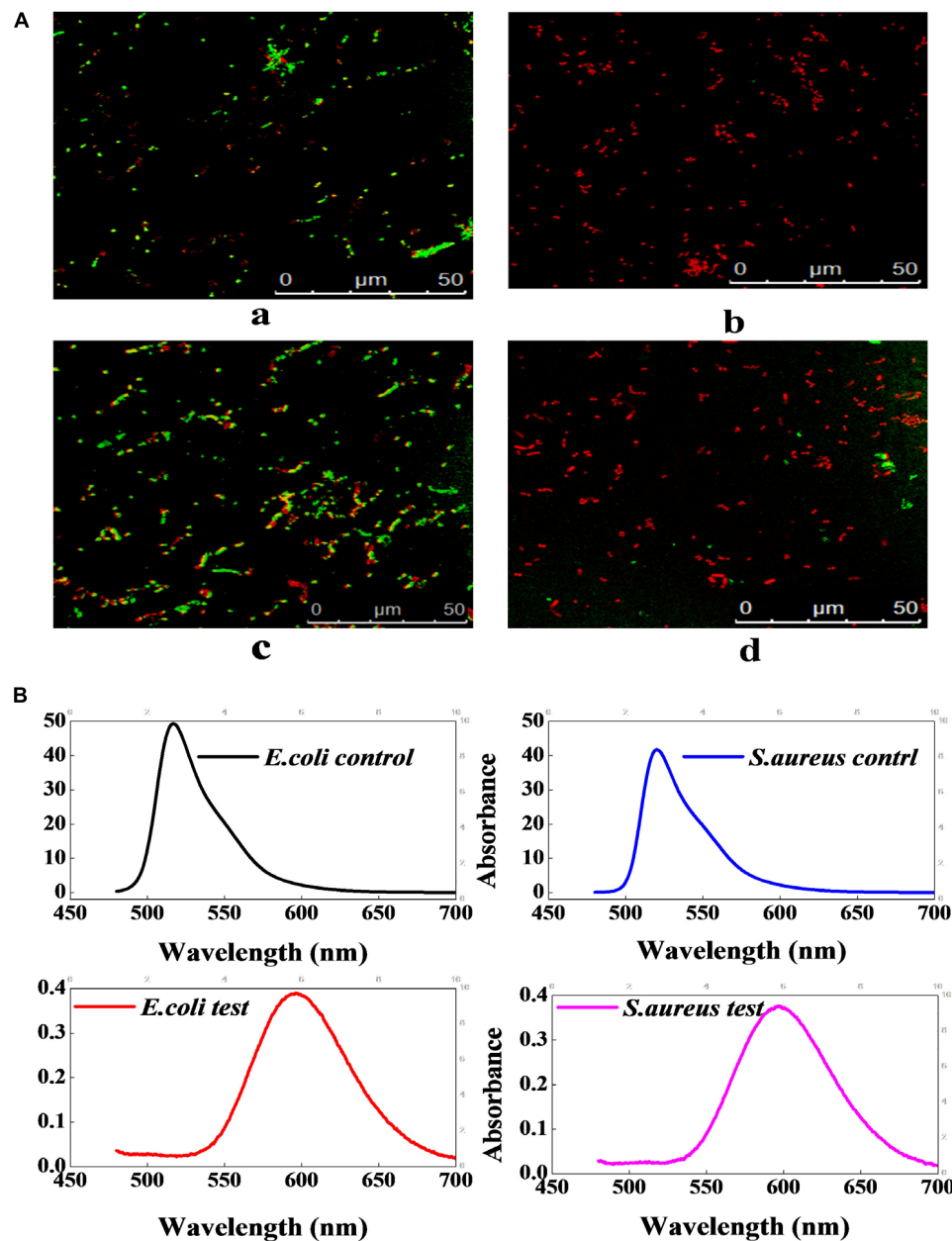


FIGURE 5 | The effect of lacidophilin on the cell membrane integrity of the two indicator bacteria. Fluorescence micrograph of *E. coli* and *S. aureus* with FDA/PI staining (A); the *S. aureus* used as control (a), the treated *S. aureus* (b), the *E. coli* used as control (c), the treated *E. coli* (d). Fluorescence spectrum of *E. coli* and *S. aureus* with FDA/PI staining (B); the excitation wavelength was 450 nm.

that lacidophilin inhibited the phosphorus metabolism of the indicator bacteria.

Effect of Lacidophilin on Bacterial Protein

Figure 7 shows that some typical bands of the treated *E. coli* in SDS-PAGE electropherogram obviously disappeared and faded, and some new protein bands also appeared. For the treated *S. aureus*, most of the typical bands disappeared and faded, and

an obvious new band appeared at about 70 kb. The above result illustrated that lacidophilin significantly affected the growth and the protein content of the indicator bacteria.

Effect of Lacidophilin on Intracellular Enzyme (SOD, POD, and CAT) Activity and MDA Content

For the two treated indicator bacteria, the contents of MDA in the cells were both higher than those of the controls, and the

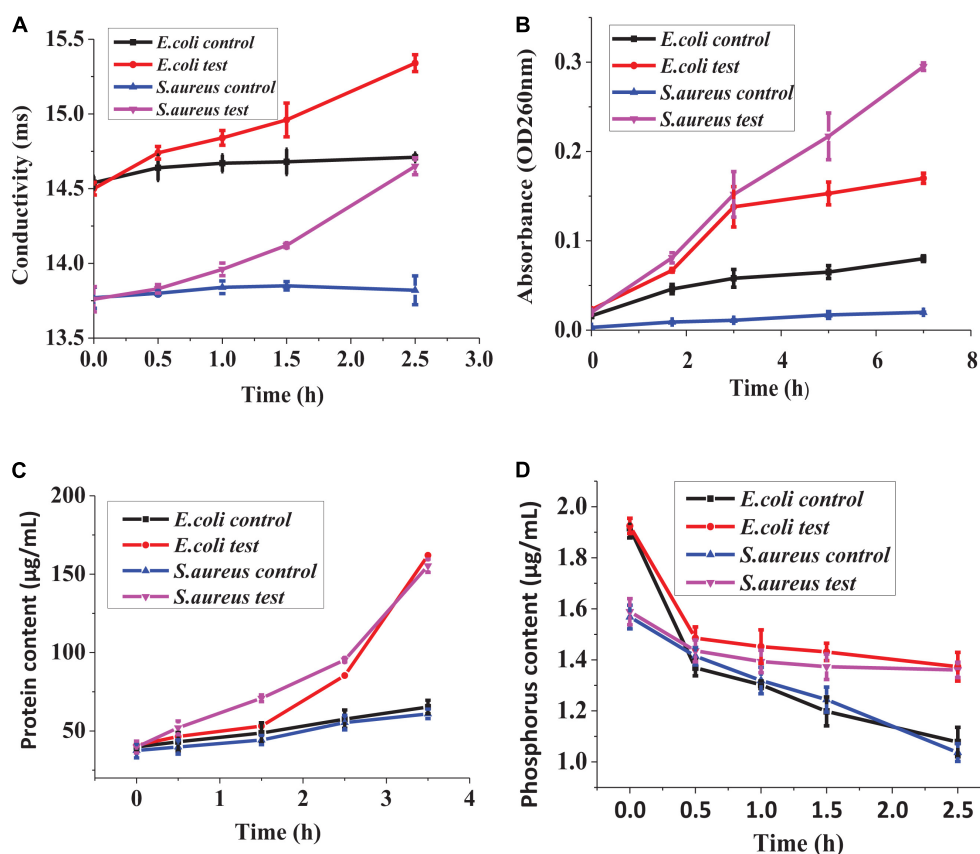


FIGURE 6 | Effect of lacidophilin on cell membrane permeability, leakage of electrolyte (A), leakage of nucleic acid (B), leakage of proteins (C), phosphorus metabolism (D).

activities of intracellular enzymes (SOD, CAT, and POD) also exceeded those of the controls significantly. The increase of MDA contents indicated that the damage to the cell increased. The increase of the activity of SOD, CAT, and POD inferred that the lipid peroxidation of the cytomembrane increased.

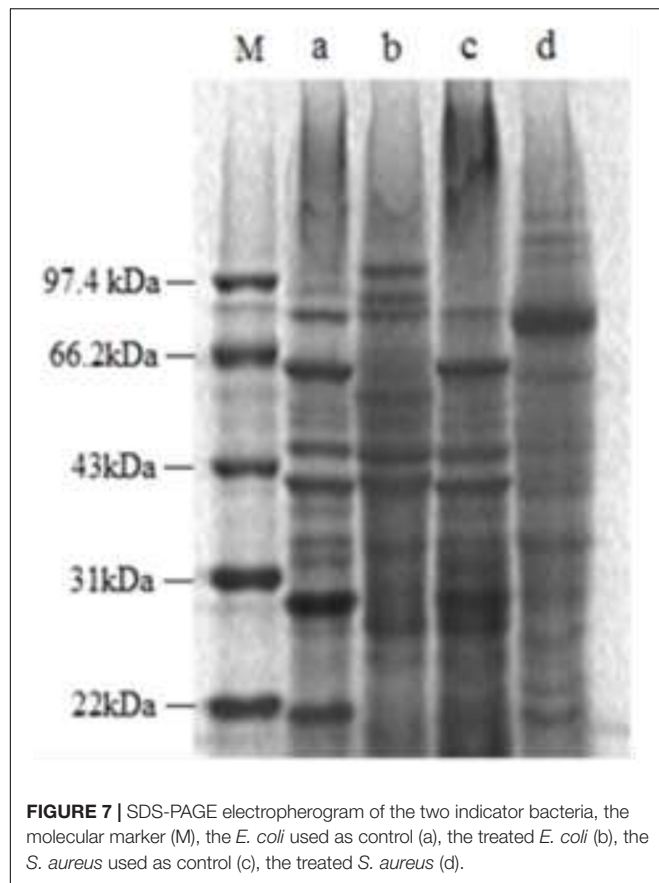
DISCUSSION

The negative control (MRS medium) had no antibacterial activity, whereas the antibacterial activity of lacidophilin and the positive control had no significant difference ($P > 0.05$), which indicated a potential application of lacidophilin as a food preservative. The heat treatment indicated that lacidophilin had relatively high thermal stability, as 90% of the bactericidal activity was retained with heat treatment at 65°C for 30 min. Thus, it could be used as a preservative in pasteurized food (Thirumurugan et al., 2016). This was similar to the previous report about the thermal stability of KF1 bacteriocin (Zahid, 2015). The result of trypsin treatment indicated that lacidophilin might be a protein or peptide that could be completely hydrolyzed by trypsin (Lv et al., 2018). The amylase treatment illustrated that the protein or peptide might contain some glycosidic bonds, as amylase

mainly hydrolyzes glycosidic bonds. Certain concentration of metal ions weakened the antibacterial activity of lacidophilin (Figure 3). Previous research also indicated that divalent cations were antagonists of the bacteriocin (Vloten, 2015). Thus, it was speculated that certain concentration of metal ions might reduce the antibacterial activity of lacidophilin by changing its spatial conformation, which was associated with antimicrobial activity.

The growth curves of the treated *S. aureus* and *E. coli* lagged significantly behind the controls (Figure 4), which illustrated that the bacteriocin inhibited the dynamic growth of two indicator bacteria greatly. Common lacidophilin, such as nisin, only has an antibacterial effect on Gram-positive bacteria and has no antibacterial effect on Gram-negative bacteria (Jeong and Ha, 2018), which might ascribe the amyloid formation between the lipopolysaccharide of Gram-negative bacteria cell wall and the antibacterial peptide (Wang et al., 2014). However, the lacidophilin in this study had high antibacterial activity against both Gram-positive and Gram-negative bacteria, which further illustrated its potential use as a food preservative.

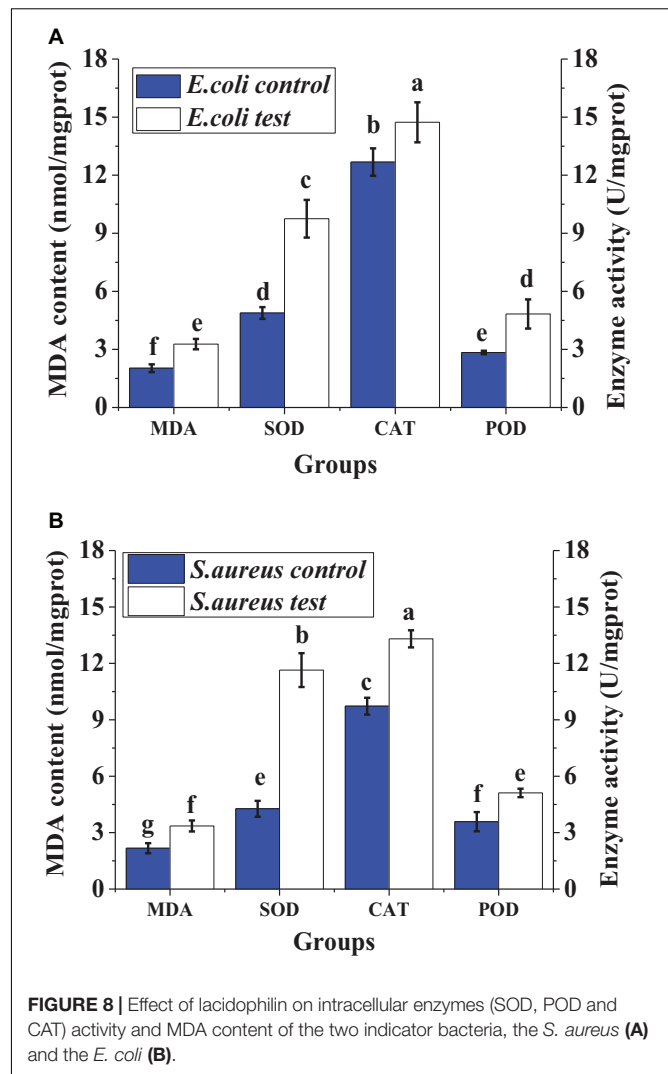
Propionyl iodide is a nucleic acid staining agent that cannot penetrate the entire cytomembrane, but can penetrate the damaged cytomembrane to stain the DNA. When PI crossed the destroyed cytomembrane and bound to DNA, the cell



emitted red fluorescence (Boyd et al., 2008). FDA could pass through the cytomembrane, and the living cells with FDA staining could emit yellow-green fluorescence (Boyd et al., 2008). Therefore, the result of **Figure 5** indicated that lacidophilin destroyed the cytomembrane of the bacteria and increased the cytomembrane permeability. Previous study had also suggested that the bacteriocins of bifidocin A produced from *B. animalis* played a bacteriostatic role by destroying the cytomembrane of *Listeria monocytogenes* (Liu et al., 2017).

Electrolyte, nucleic acid, and proteins are very important for the life of the indicator bacteria. The leakage of electrolyte, nucleic acid, and proteins further illustrated that the cytomembrane of the bacteria was damaged (Shen et al., 2015; Cai et al., 2019), resulting in the loss of the barrier function of the cytomembrane. The leakage might attribute to the formation of the selective pores in the bacteria cytomembrane (Liu et al., 2017), and the loss of the key cell contents affected the normal life of the cells, thereby inhibiting the growth of the bacteria.

Phosphorus is an important nutrient required for key biological reactions of cell life, and it is a crucial component of the cytomembrane (Razzaque, 2011). The metabolic capacity of the cells could be confirmed by detecting phosphorus consumption in the cultivation process (Tian and Wang, 2014). For the treated bacteria, the content of phosphorus in the inoculum decreased slower than the control, which indicated



that lacidophilin inhibited the phosphorus consumption of the indicator bacteria. Decrease of phosphorus consumption further illustrated that lacidophilin destroyed the metabolic capacity of the cell, inhibited the formation of the cytomembrane, and increased the permeability of the cytomembrane (Wang et al., 2020).

Proteins are critical parts of bacteria cells, and they are closely related to the metabolism of bacteria cells. Disappearance and fade of typical bands of the cell proteins in SDS-PAGE (**Figure 7**) indicate that lacidophilin had a significant effect on protein and the protein contents of the indicator bacteria. The SDS-PAGE result further suggested that the cytomembrane was destroyed and the growth of the bacteria was inhibited, resulting in the fade or disappearance of typical bands of cell proteins (Cai et al., 2019). In addition, the result also corroborates that lacidophilin damaged the cytomembrane of the indicator bacteria, leading to the leakage of major cell components, which seriously affected the synthesis of protein (Meng et al., 2016). The appearance of new protein bands might be that the bacteriocin changed the

metabolism of bacterial cells, resulting in the production of new proteins.

Malondialdehyde is the crucial lipid peroxidation product, which can be used to monitor the lipid peroxidation level of the cytomembrane (Jia et al., 2014). The increase of MDA content illustrated the increase of lipid peroxidation of the cytomembrane, resulting in the damage of the cytomembrane (Yun et al., 2013). The cellular enzymes including SOD, POD, and CAT can be used to detect the cell defense response against external stress (Yun et al., 2013). In order to protect itself from external injury, the activities of the enzymes including SOD, CAT, and POD in the cell were initiated, resulting in an increase of reactive oxygen removal and a reduction of oxidative damage (Jia et al., 2014). Therefore, the increase of the activities of SOD, CAT, and POD in the cell (**Figure 8**) illustrated that the cell was injured by lacidophilin. Thus, the result indicated that lacidophilin caused cytomembrane lipid peroxidation and cell oxidative damage simultaneously.

CONCLUSION

In this paper, the antibacterial activity of *L. pentosus* lacidophilin against *S. aureus* and *E. coli* was studied, and the antibacterial mechanism was further explored. The results showed that lacidophilin might be a polypeptide or protein, which had significant antibacterial activity against *S. aureus* and *E. coli*. Lacidophilin had strong thermal stability, so it might be used in pasteurization processing of foods. The antibacterial activity was decreased by metal ions; therefore, the influence of metal ions should be avoided during food processing using lacidophilin as preservative. Studies on antibacterial mechanism showed that lacidophilin mainly broke the integrity of the bacteria cytomembrane and increased the permeability of the

cytomembrane by melting the cytomembrane into holes, further leading to the leakage of electrolytes, nucleic acid, and proteins. In addition, it restrained phosphorus metabolism, inhibited the growth of the bacteria, and caused changes of some proteins. Moreover, lacidophilin injured the bacteria cell, which increased cytomembrane lipid peroxidation and cell oxidative damage, resulting in the increase of MDA content and activities of SOD, CAT, and POD in the cell. Consequently, lacidophilin has great potential for application as natural preservatives in foods, owing to their high antibacterial activity against both Gram-positive and Gram-negative foodborne pathogens and thermal stability.

DATA AVAILABILITY STATEMENT

The raw data supporting the conclusions of this article will be made available by the authors, without undue reservation.

AUTHOR CONTRIBUTIONS

YZ designed the study and drafted the original manuscript. SZ was responsible for the method, data acquisition, curation, and analysis. All authors contributed to the article and approved the submitted version.

FUNDING

The research was financially supported by the National Natural Science Foundation of China (No. 31501512), the Shandong Province Key Research and Development Plan—Special Plan for Medical Food (2019YYSP023), and the regulation mechanism of quality deterioration of fresh produce through water activity and microorganism (No. 2016YFD0400105).

REFERENCES

- Boyd, V., Cholewa, O. M., and Papas, K. K. (2008). Limitations in the use of fluorescein diacetate/propidium iodide (fda/pi) and cell permeable nucleic acid stains for viability measurements of isolated islets of langerhans. *Curr. Trends Biotechnol. Pharm.* 2, 66–84.
- Cai, R., Miao, M., Yue, T., Zhang, Y., Cui, L., Wang, Z., et al. (2019). Antibacterial activity and mechanism of cinnamic acid and chlorogenic acid against alicyclobacillus acidoterrestris vegetative cells in apple juice. *Int. J. Food Sci. Tech.* 54, 1697–1705. doi: 10.1111/ijfs.14051
- Di Pinto, A., Forte, V. T., Ciccarese, G., Conversano, M. C., and Tantillo, G. M. (2005). Comparison of reverse passive latex agglutination test and immunoblotting for detection of staphylococcal enterotoxin A and B. *J. Food Safety.* 24, 231–238. doi: 10.1111/j.1745-4565.2004.00533.x
- Gills, R., Sharma, J. P., and Bhardwaj, T. (2015). Achieving zero hunger through zero wastage: an overview of present scenario and future reflections. *Indian J. Agr. Sci.* 85, 1127–1133.
- Hurtado, A., Reguant, C., Bordons, A., and Rozès, N. (2011). Expression of lactobacillus pentosus b96 bacteriocin genes under saline stress. *Food Microbiol.* 28, 1339–1344. doi: 10.1016/j.fm.2011.06.004
- Jeong, J. H., and Ha, S. C. (2018). Crystal structure of nisi in a lipid-free form, the nisin immunity protein, from *Lactococcus lactis*. *Antimicrob. Agents Chemother.* 62:e1966-17. doi: 10.1128/AAC.01966-17
- Jia, W., Huang, X., and Li, C. (2014). A preliminary study of the algicidal mechanism of bioactive metabolites of *brevibacillus laterosporus* on oscillatoria in prawn ponds. *Sci. World J.* 2014:869149. doi: 10.1155/2014/869149
- Liu, G., Lv, Y., Li, P., Zhou, K., and Zhang, J. (2008). Pentocin 31-1, an anti-listeria bacteriocin produced by *lactobacillus pentosus* 31-1 isolated from xuan-wei ham, a traditional china fermented meat product. *Food Control* 19, 353–355. doi: 10.1016/j.foodcont.2007.04.010
- Liu, G., Ren, G., Zhao, L., Cheng, L., Wang, C., and Sun, B. (2017). Antibacterial activity and mechanism of bifidocin A against *Listeria monocytogenes*. *Food Control* 73, 854–861. doi: 10.1016/j.foodcont.2016.09.036
- Lv, X., Ma, H., Sun, M., Lin, Y., Bai, F., Li, J., et al. (2018). A novel bacteriocin dy4-2 produced by *lactobacillus plantarum* from cutlassfish and its application as bio-preservative for the control of *Pseudomonas fluorescens* in fresh turbot (*scophthalmus maximus*) filets. *Food Control* 89, 22–31. doi: 10.1016/j.foodcont.2018.02.002
- Meng, X., Li, D., Zhou, D., Wang, D., Liu, Q., and Fan, S. (2016). Chemical composition, antibacterial activity and related mechanism of the essential oil from the leaves of *Juniperus rigida* Sieb. et Zucc against *Klebsiella pneumoniae*. *J. Ethnopharmacol.* 194, 698–705. doi: 10.1016/j.jep.2016.10.050
- Miri, S. T., Dashti, A., Mostaan, S., Kazemi, F., and Bouzari, S. (2017). Identification of different *Escherichia coli* pathotypes in north and north-west provinces of Iran. *J. Microbiol.* 9, 33–37.

- Motahari, P., Mirdamadi, S., and Rad, M. K. (2016). A sequential statistical approach towards an optimized production of bacteriocin by *Lactobacillus pentosus* tshs: a sequential statistical optimization. *J. Food Process Pres.* 40, 1238–1246. doi: 10.1111/jfpp.12708
- Razzaque, S. M. (2011). Phosphate toxicity: new insights into an old problem. *Clin. Sci.* 120, 91–97. doi: 10.1042/CS20100377
- Sequeiros, C., Garcés, Marisa, E., Vallejo, M., Marguet, E. R., and Olivera, N. L. (2015). Potential aquaculture probiont *Lactococcus lactis* w34 produces nisin Z and inhibits the fish pathogen *Lactococcus garvieae*. *Arch. Microbiol.* 197, 449–458. doi: 10.1007/s00203-014-1076-x
- Shen, S., Zhang, T., Yuan, Y., Lin, S., Xu, J., and Ye, H. (2015). Effects of cinnamaldehyde on *Escherichia coli* and *Staphylococcus aureus* membrane. *Food Control* 47, 196–202. doi: 10.1016/j.foodcont.2014.07.003
- Thirumurugan, A., Ramachandran, S., and Sivamani, S. (2016). Bacteriocin produced from *Lactobacillus plantarum* atm11: kinetic and thermodynamic studies. *Int. J. Food Eng.* 12, 501–505. doi: 10.1515/ijfe-2015-0376
- Tian, L., and Wang, Z. (2014). Study on antibacterial activity of radix isatidis extracts and preliminary investigation of their antibacterial mechanism. *LNEE* 251, 1681–1688. doi: 10.1007/978-3-642-37925-3_180
- Vasilchenko, A. S., Vasilchenko, A. V., Valyshev, A. V., and Rogozhin, E. A. (2018). A novel high-molecular-mass bacteriocin produced by *Enterococcus faecium*: biochemical features and mode of action. *Probiotics Antimicro. Proteins*. 10, 427–434. doi: 10.1007/s12602-018-9392-0
- Vloten, A. M. V. (2015). The role of authenticity in improving subjective well-being for narcissistic adolescents: a randomized experiment. *Int. J. Food Microbiol.* 46, 207–217. doi: 10.1016/S0168-1605(98)00205-0
- Wang, J., Li, Y., Wang, X., Chen, W., Sun, H., and Wang, J. (2014). Lipopolysaccharide induces amyloid formation of antimicrobial peptide HAL-2. *Biochim. Biophys. Acta* 1838, 2910–2918. doi: 10.1016/j.bbame.2014.07.028
- Wang, N., Liu, X., Li, J., Zhang, Q., and Wenjun, W. (2020). Antibacterial mechanism of the synergistic combination between streptomycin and alcohol extracts from the *Chimonanthus salicifolius* S. Y. Hu. Leaves. *J. Ethnopharmacol.* 250:112467. doi: 10.1016/j.jep.2019.112467
- Yang, S. C., Lin, C. H., Sung, C. T., and Fang, J. Y. (2014). Corrigendum: antibacterial activities of bacteriocins: application in foods and pharmaceuticals. *Front. Microbiol.* 5:241. doi: 10.3389/fmicb.2014.00683
- Yi, L., Dang, Y., Wu, J., Zhang, L., Liu, X., Liu, B., et al. (2016). Purification and characterization of a novel bacteriocin produced by *Lactobacillus crustorum* mn047 isolated from koumiss from Xinjiang, China. *J. Dairy Sci.* 99, 7002–7015. doi: 10.3168/jds.2016-11166
- Yun, K., Xiangyang, X., Liang, Z., and Jaak, J. P. (2013). Cyanobactericidal effect of *Streptomyces* sp. hjc-d1 on *Microcystis aeruginosa*. *PLoS One* 8:e57654. doi: 10.1371/journal.pone.0057654
- Zahid, M. (2015). Antimicrobial activity of bacteriocins isolated from lactic acid bacteria against resistant pathogenic strains. *Int. J. Food Sci. Nutr.* 4, 326–331. doi: 10.11648/j.ijfns.20150403.20
- Zhu, Y., Guo, L., and Yang, Q. (2020). Partial replacement of nitrite with a novel probiotic *Lactobacillus plantarum* on nitrate, color, biogenic amines and gel properties of Chinese fermented sausages. *Food Res. Int.* 137:109351. doi: 10.1016/j.foodres.2020.109351
- Zhu, Y., Wang, P., Guo, L., Wang, J., Han, R., Sun, J., et al. (2019). Effects of partial replacement of sodium nitrite with *Lactobacillus pentosus* inoculation on quality of fermented sausages. *J. Food Process Pres.* 43:e13932. doi: 10.1111/jfpp.13932

Conflict of Interest: The authors declare that the research was conducted in the absence of any commercial or financial relationships that could be construed as a potential conflict of interest.

Copyright © 2020 Zhu and Zhang. This is an open-access article distributed under the terms of the Creative Commons Attribution License (CC BY). The use, distribution or reproduction in other forums is permitted, provided the original author(s) and the copyright owner(s) are credited and that the original publication in this journal is cited, in accordance with accepted academic practice. No use, distribution or reproduction is permitted which does not comply with these terms.



Study on the Viable but Non-culturable (VBNC) State Formation of *Staphylococcus aureus* and Its Control in Food System

Yanmei Li^{1†}, Teng-Yi Huang^{2†}, Yuzhu Mao³, Yanni Chen³, Fan Shi³, Ruixin Peng³, Jinxuan Chen³, Lei Yuan⁴, Caiying Bai⁵, Ling Chen^{3,6}, Kan Wang^{7*} and Junyan Liu^{8*}

¹ Department of Haematology, Guangzhou Women and Children's Medical Center, Guangzhou Medical University, Guangzhou, China, ² Department of Laboratory Medicine, The Second Affiliated Hospital of Shantou University Medical College, Shantou, China, ³ Guangdong Province Key Laboratory for Green Processing of Natural Products and Product Safety, School of Food Science and Engineering, South China University of Technology, Guangzhou, China, ⁴ College of Food Science and Engineering, Yangzhou University, Yangzhou, China, ⁵ Guangdong Women and Children Hospital, Guangzhou, China, ⁶ Research Institute for Food Nutrition and Human Health, Guangzhou, China, ⁷ Research Center for Translational Medicine, The Second Affiliated Hospital, Medical College of Shantou University, Shantou, China, ⁸ Department of Civil and Environmental Engineering, University of Maryland, College Park, MD, United States

OPEN ACCESS

Edited by:

Xihong Zhao,
Wuhan Institute of Technology, China

Reviewed by:

Wei Wu,
Qingdao Agricultural University, China
Siyuan Liu,
University of Saskatchewan, Canada

*Correspondence:

Junyan Liu
jliu81@uthsc.edu
Kan Wang
120384746@qq.com

[†] These authors have contributed
equally to this work

Specialty section:

This article was submitted to
Food Microbiology,
a section of the journal
Frontiers in Microbiology

Received: 28 August 2020

Accepted: 14 October 2020

Published: 26 November 2020

Citation:

Li Y, Huang T-Y, Mao Y, Chen Y,
Shi F, Peng R, Chen J, Yuan L, Bai C,
Chen L, Wang K and Liu J (2020)
Study on the Viable but
Non-culturable (VBNC) State
Formation of *Staphylococcus aureus*
and Its Control in Food System.
Front. Microbiol. 11:599739.
doi: 10.3389/fmicb.2020.599739

A Viable but non-culturable (VBNC) state is a bacterial survival strategy under reverse conditions. It poses a significant challenge for public health and food safety. In this study, the effect of external environmental conditions including acid, nutrition, and salt concentrations on the formation of *S. aureus* VBNC states at low temperatures were investigated. Different acidity and nutritional conditions were then applied to food products to control the VBNC state formation. Four different concentration levels of each factor (acid, nutrition, and salt) were selected in a total of 16 experimental groups. Nutrition showed the highest influence on the VBNC state formation *S. aureus*, followed by acid and salt. The addition of 1% acetic acid could directly kill *S. aureus* cells and inhibit the formation of the VBNC state with a nutrition concentration of 25, 50, and 100%. A propidium monoazide-polymerase chain reaction (PMA-PCR) assay was applied and considered as a rapid and sensitive method to detect *S. aureus* in VBNC state with the detection limit of 10⁴ CFU/mL.

Keywords: *Staphylococcus aureus*, VBNC state, induction, control, formation

HIGHLIGHTS

- The stress of nutrition, acid and salt could induce the VBNC state formation of *S. aureus* under low temperature.
- The effect of external environmental conditions on the state of VBNC formation of *S. aureus* was: nutrition > acid > salt concentrations.
- Addition of 1% acetic acid could directly kill the *S. aureus* and inhibit VBNC state formation with nutrition concentration of 25, 50, and 100%.
- The PMA-PCR assay is able to be applied on the detection of *S. aureus* VBNC cells with a detection limit at 10⁴ CFU/mL.

INTRODUCTION

Food-borne pathogens can cause diseases by contaminating food products and are the cause of serious concerns in public health and food safety. *Staphylococcus aureus* is widely distributed in the environment including air, water, and the surface of the skin, and has been found in raw meat, milk and dairy products, frozen products, and cooked foods (Xu et al., 2012a,b; Bao et al., 2017a,c). It is the source of major concern in the food industry due to its multi-drug resistance and virulence (Miao et al., 2017c; Jia et al., 2018). Foodborne outbreaks with vomiting cases caused by *S. aureus* have been frequently reported in recent years (Bennett et al., 2013). It can produce *Staphylococcus enterotoxins* (SEs) including SEA, SEB, SEC, SED, and SEE which can cause severe food poisoning incidents (Xu et al., 1982). Besides, Pantone-Valentine leukocidin (PVL) can also cause food poisoning with a high mortality rate (Kraushaar and Fetsch, 2014; Liu et al., 2019).

The “Viable but non-culturable” (VBNC) state, first reported by Xu et al. in 1982, is considered to be a survival strategy of non-spore-forming bacteria in response to adverse conditions (Xu et al., 1982; Oliver, 2010; Liu et al., 2018a,b). Environmental stresses including low temperature, nutrient-limited conditions, high salt, low pH, and even UV-induced conditions have been reported to induce the formation of a VBNC state (Foster, 1999; Ramaiah et al., 2002; Xu et al., 2008a,b; Cunningham et al., 2009; Wang et al., 2011; Guo et al., 2019). At present, 85 species of bacteria have been confirmed as capable of entering into a VBNC state, including 18 non-pathogenic and 67 pathogenic species (Li et al., 2014; Bao et al., 2017b; Miao et al., 2017a,b,c). VBNC cells are alive with low metabolic activity, and capable of producing biological toxins. *Shigella dysenteriae* type1 retained Shiga toxin encoding gene (*stx*) and produced toxin in the VBNC state (Rahman et al., 1996; Lin et al., 2016). VBNC *Escherichia coli* O157 cells had a higher expression of *rfaE* and relatively lower expression of *stx1* and *stx2* genes compared to normal cells (Liu et al., 2017b; Xu X. et al., 2017; Xu J. et al., 2017; Zhao et al., 2018a,b). Furthermore, VBNC cells can resuscitate when in suitable conditions (Pinto et al., 2015; Xu et al., 2016a,b,c; Miao et al., 2018). Therefore, VBNC pathogens pose a serious threat to food safety and human health.

The traditional detection method for foodborne microbes is culturing-based. However, in the VBNC state, bacteria remain metabolic activity but below detection levels, indicating the ability to cause false negative detection by culturing-based method (Xu M. E. et al., 2011; Xu L. et al., 2011; Xu Z. et al., 2011; Pinto et al., 2015; Miao et al., 2016). Thus, food safety incidents may occur if contaminated by the foodborne pathogen in the VBNC state (Xu et al., 2012a,b; Liu et al., 2017b) and traditional culturing-based methods cannot be trusted to detect VBNC cells. Furthermore, this method cannot identify living and dead cells which is a major limitation in nucleic acid diagnosis (Xu et al., 2010; Zhong et al., 2016; Lin et al., 2017). However, some reagents including photoreactive DNA-binding

dyes ethidium bromide monoazide (EMA) and propidium monoazide (PMA) can be used to amplify DNA in dead cells. Nucleic acid amplification methods have been combined with EMA/PMA and widely developed for the detection of pathogenic bacteria in a VBNC state, including PMA-PCR and PMA-LAMP (Li et al., 2017; Xie et al., 2017a,b; Liu et al., 2018; Zhong and Zhao, 2018).

This study aimed to investigate the effect of nutrition, acid, and salt concentrations on the viability and culturability of *S. aureus* at low temperature (4 and -20°C) to obtain a better understanding of the conditions of the formation of the VBNC state in food systems and to enable us to control it. A PMA-PCR assay was applied to detect the VBNC cells of *S. aureus*.

MATERIALS AND METHODS

Bacterial Strain and Culture Conditions

The strain used in this study was *S. aureus* ATCC25923, which was maintained as glycerol stock and stored at -80°C before use. The strain was streaked on tryptic soy agar (TSA) plate and incubated at 37°C for 24 h to recover. A single colony was then inoculated into 2 mL of TSB and incubated at 37°C with 150 rpm for 12 h prior to further experiments.

VBNC State Induction

The bacterial culture was inoculated into TSB with 1:100 dilution and was incubated until it reached the exponential phase according to the growth curve (data not shown). The exponential phase culture was centrifuged at $5,000 \times g$ for 10 min and the cells were washed with $1 \times$ phosphate buffer solution (PBS). The washed culture was resuspended in induction groups (Table 1) to a final concentration of approximately 10^7 CFU/mL. To avoid the effects of continuous freeze-thawing, the induction system was separated into multiple 1.5 mL centrifuge tubes.

TABLE 1 | The VBNC state induction groups.

Groups	TSB (%)	NaCl (%) (m/v)	Acetic acid (%) (v/v)
1	0	0.9	0
2	25	0.9	0.3
3	50	0.9	0.7
4	100	0.9	1
5	25	10	0
6	0	10	0.3
7	100	10	0.7
8	50	10	1
9	50	20	0
10	100	20	0.3
11	0	20	0.7
12	25	20	1
13	100	30	0
14	50	30	0.3
15	25	30	0.7
16	0	30	1

Subsequently, the tubes were placed at 4 and -20°C , respectively, to induce the VBNC state.

Determination of VBNC State

To determine the culturability of *S. aureus* cells, the plate counting method was applied to identify the culturable cell number. The induction culture was serially diluted with 0.9% NaCl and inoculated on TSA followed by incubation at 37°C for 24 h. When culturable, the cell number was < 1 CFU/mL for 3 days, and the cells were considered to be non-culturable (Deng et al., 2015). In addition, the LIVE/DEAD® BacLight™ bacterial viability kit (Thermo Fisher Scientific, China) combined with fluorescence microscopy was used to determine whether the non-culturable cells were in the VBNC state following the manufacturer's instructions.

Control of VBNC State

According to VBNC state induction results, suitable concentrations of nutrition, salt, and acid were selected to inhibit the formation of the VBNC state. The bacterial culture was washed and resuspended at the concentration of 5×10^7 CFU/mL with a total volume of 30 mL and stored at 4 and -20°C , respectively. The culturable cell number was measured by plate counting after 3 days (Tables 2, 3).

Control of VBNC State in Rice Product

Twenty-five grams of Cantonese rice cake (Guangzhou Restaurant, Guangzhou, China) was added to 225 mL of 0.9% NaCl and determined as a 100% food sample medium. Accordingly, 25 and 50% food sample medium were prepared with sterilization. 2 mL of *S. aureus* culture at exponential growth phase were centrifuged at 4°C and washed with 0.9% NaCl before resuspended with sterilized food sample medium to a final concentration of 5×10^7 CFU/mL as initial induction concentration. Simultaneously, the filtered acetic acid solution was added into the food induction

group at a final concentration of 1% (v/v). Then, the final induction group was stored at 4°C for 3 days and the culturability and viability were identified by plate counting method and LIVE/DEAD® BacLight™ bacterial viability kit, respectively.

PMA-PCR Assay

Twenty-five grams of Cantonese rice cake mixed with 225 mL saline was prepared as a diluting solution. The bacterial culture of *S. aureus* in the VBNC state was diluted to the final concentrations of 10^6 , 10^5 , 10^4 , 10^3 , 10^2 , and 10 cells/mL using the diluting solution, respectively. The PMA reagent was used at the concentration of 5 $\mu\text{g/mL}$. Subsequently, the detection samples mixed with PMA were incubated in the dark at room temperature for 10 min before the tubes were placed horizontally on ice exposed to a halogen lamp (650 W) at a distance of 15 cm for 15 min to complete the combination of DNA and PMA (Chen et al., 2020). The mixed samples were centrifuged at 10,000 rpm for 5 min. DNA from the precipitated cells was isolated using a DNA extraction kit (Dongsheng Biotech, Guangzhou) following the manufacturer's instruction.

The PCR assay was performed at a total volume of 25 μL . The reaction system consists of 12.5 μL 2 \times Taq PCR MasterMix (Dongsheng Biotech, Guangzhou), 3 μM each of forward and reverse primers (*femA*-F: AGGTATAGACTTCGATG TTTCAAATCGCGGTCCAGTG; *femA*-R: TTGTAGCTTCAGATATGGAAACCAA TCATTAC CAGCA), 2 μL of DNA template and added up to 25 μL with nuclease-free water. A mixture with 2 μL of nuclease-free water was used (instead of DNA) as a negative control. The protocol of PCR assay was as followed: 5 min denaturation at 95°C , 32 cycles of amplification at 95°C for 30 s, 52°C 30 s, 72°C for 35 s and final inactivation at 72°C for 5 min. The PCR products were detected by electrophoresis on 1.5% agarose gels and observed under UV light.

RESULTS AND DISCUSSION

Culturability of *S. aureus* During Induction

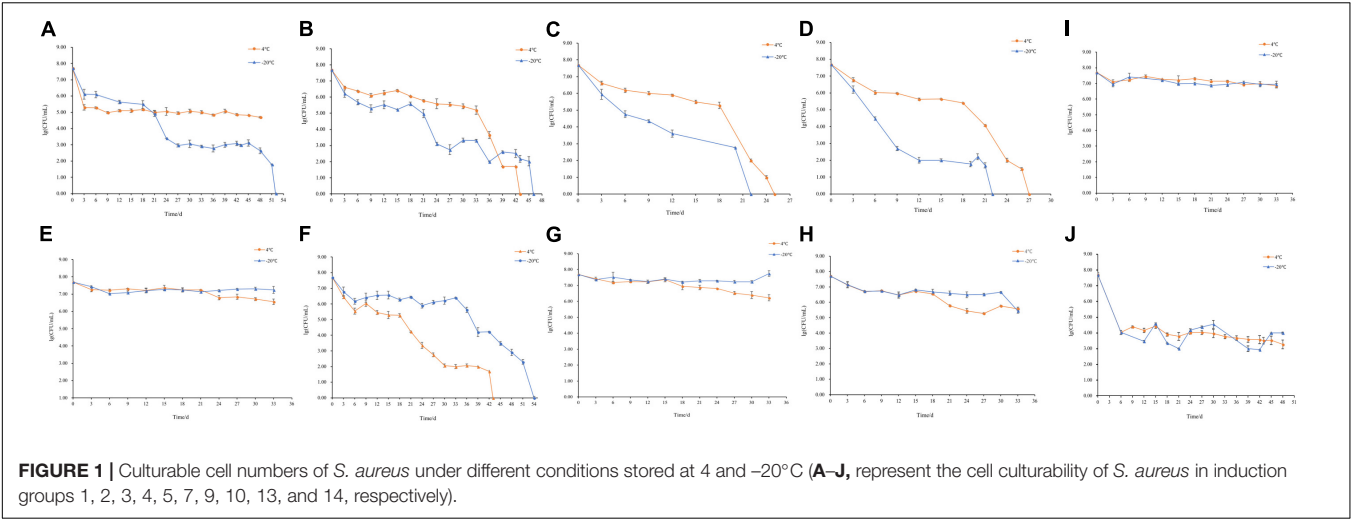
The changes of culturable cell numbers during VBNC state induction are shown in Figure 1. In induction group 1, for which stored at -20°C , the culturable cell number decreased to 0 in 52 days, while at 4°C the culturable cell number dropped in the first 3 days and remained unchanged (Figure 1A). In induction group 2, the culturable number declined to 0 in 43 days (-20°C) and 46 days (4°C), respectively (Figure 1B), which was similar to the result of induction groups 3 and 4 but with the longer induction time (Figures 1C,D). As for induction group 7, the culturable cell number reduced to 0 after stored at 4 and -20°C for 43 days and 54 days, respectively (Figure 1F). And in induction groups 5, 9, 10, 13, and 14, the culturable cell numbers remain the same which indicated the cells were unable to enter into the VBNC state (Figures 1E,G–J). The cells in induction groups 6, 8, 11, 12, 15, and 16 were non-culturable in 3 days. The

TABLE 2 | Inhibition assay of acidity on the VBNC state formation.

Group	TSB (%)	NaCl (%) (m/v)	Acetic acid (%) (v/v)
1	0.25	0.9	0.7
2			1
3	0.25	0.9	1.0
4			1
5	0.25	10	0.7
6			1

TABLE 3 | Inhibition assay of nutritional status on the VBNC state formation.

Group	TSB (%)	NaCl (%) (m/v)	Acetic acid (%) (v/v)
1	0	0.9	0.3
2			0.7
3			1
4	25	0.9	0.7
5			1.0



total times for *S. aureus* cells to become non-culturable are listed in **Table 4**.

Viability of *S. aureus* During Induction

The viability of *S. aureus* during the induction was observed by the fluorescence microscope after the treatment of the LIVE/DEAD® BacLight™ bacterial viability kit. In induction group 1 at −20°C, when the culturable cell number decreased to 0, viable cells still existed indicating that *S. aureus* can enter into VBNC state in saline at −20°C (**Figure 2**). The same results were obtained in induction group 2 at 4 and −20°C (**Figure 2**). As for induction groups 3, 4, and 7 at 4°C, a small percentage of cells entered into VBNC state (**Figure 2**). However, most cells were dead at −20°C (**Figure 2**).

In summary, under low temperature (4°C) and strong acidity with sufficient nutrition (medium concentration ≥ 50%), *S. aureus* could enter into VBNC state within a short time. Similar results were obtained under low salt and weak acidic environment with insufficient nutrition but with longer induction time, as well as the in conditions that were oligotrophic and acid-free. Briefly, under reverse conditions, including insufficient nutrition with weak acid and sufficient nutrition

with a strong acid, it was easier for *S. aureus* to enter into VBNC state at 4°C but more difficult to survive in freezing conditions (−20°C). These results showed that the key conditions for the VBNC state formation of *S. aureus* were adequate nutrition with strong acid at 4°C, insufficient nutrition with weak acid at 4°C, and oligotrophic system at −20°C.

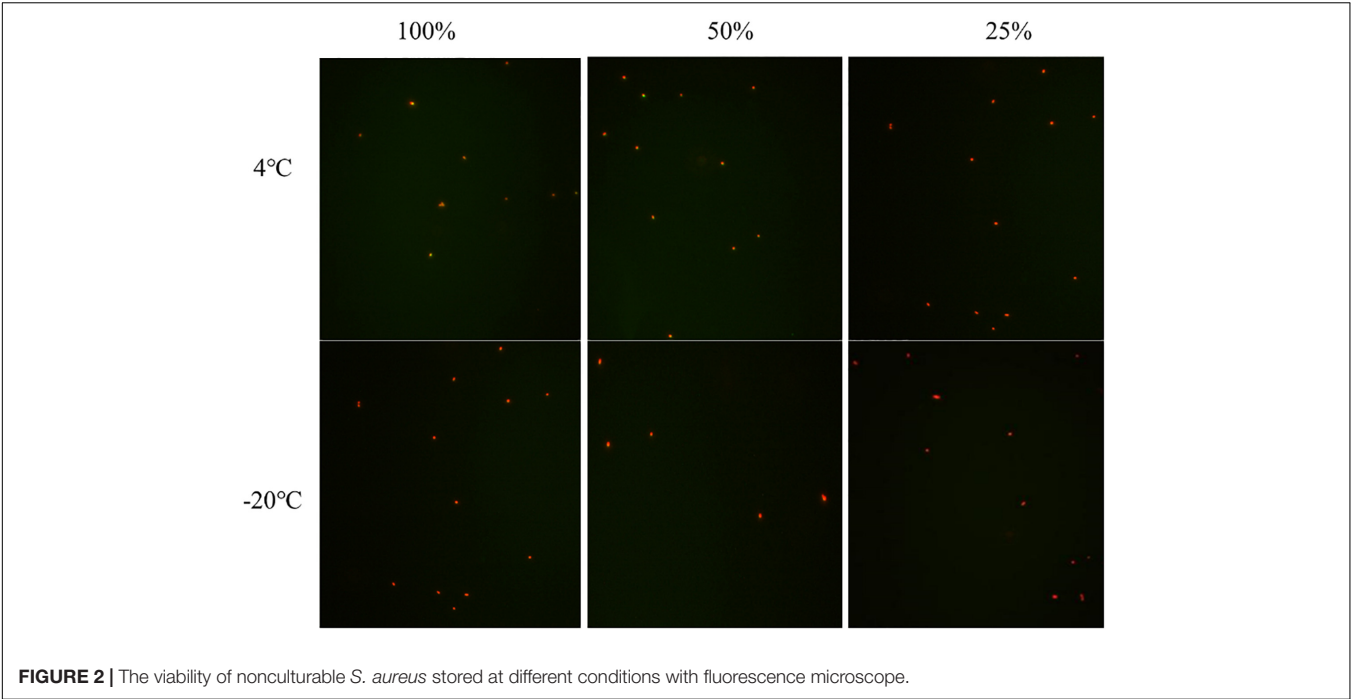
S. aureus was able to enter into VBNC state under strong acid with adequate nutrition but not under strong acid that lacked nutrition, indicating with the treatment of strong acid, nutrition plays an important role during the formation of VBNC state. By comparing induction groups 1 and 2, under weak acid, it took cells in group 2 a shorter time to enter into VBNC state, demonstrating that weak acid may have an active contribution to the formation of VBNC state. Due to the salt-tolerant property of *S. aureus*, salt concentration had no significant effect. Under insufficient nutrition (medium concentration ≤ 50%) with strong acid [concentration of acetic acid (v/v) ≥ 0.7%] and high salt concentration (≥10%) without nutrition, the cells died within 3 days. Therefore, nutrition had the strongest effect on the formation of the VBNC state, followed by the concentration of acetic acid and salt.

S. aureus cells with higher ATP concentration would enter into the VBNC state instead of dying. Similar phenomenon has been found in the VBNC *L. monocytogenes* (Lindbäck et al., 2010; Bai et al., 2019). ATP synthase was also found upregulated in VBNC *Vibrio parahaemolyticus* cells (Lai et al., 2009). The upregulation of genes or proteins related to ATP accumulation offset ATP consumption in VBNC bacteria might be due to the survival mechanism of VBNC *S. aureus* under the reverse condition and need to be confirmed by further study on the expression of ATP-related genes or proteins in VBNC *S. aureus* cells (Bai et al., 2019). In the VBNC *S. aureus* cells, the mutational inactivation of catalase (KatA) or superoxide dismutase (SodA) encoded by *katA* and *sodA* gene was present. The changes on the expression of genes rendered cell

TABLE 4 | Duration for culturable cell number decreased to 0.

Group	4°C	−20°C	Group	4°C	−20°C
1	+	52 days	9	+	+
2	46 days	43 days	10	+	+
3	25 days	22 days	11	/	/
4	27 days	22 days	12	/	/
5	+	+	13	+	+
6	/	/	14	+	+
7	43 days	54 days	15	/	/
8	/	/	16	/	/

“+” stands for *S. aureus* is culturable and “/” stands for the number of culturable *S. aureus* in 3 d dropped to 0.



hypersensitive to seawater with a high concentration of salt at 4°C (Masmoudi et al., 2010).

Control of VBNC State

Under weak acid with insufficient nutrition (medium concentration ≤ 25%) conditions, *S. aureus* was capable of entering into VBNC state and acid concentration influenced the survival of *S. aureus* cells. Thus, a further experiment on the inhibitory effect of 0.3, 0.7, and 1.0% acetic acid on the control of VBNC state was performed.

In saline with 0.3, 0.7, and 1.0% acetic acid (induction groups 1, 2, and 3), *S. aureus* lost culturability and viability in 3 days, while low salt concentration with nutrition (medium concentration ≤ 25%) and 0.7%, 1.0% acetic acid (induction group 4 and 5), *S. aureus* remained culturability when stored at 4°C for 3 days. Among all, only the cells in induction group 5 stored at −20°C were non-culturable, indicating that eliminating VBNC state formation only by acetic acid treatment is not sufficient. *S. aureus* died at low nutrition, high salt, and strong acidity, indicating salt concentration can restrain the formation of the VBNC state. However, given the low salt concentration in the food processing and storage of rice product, only acid treatment is less effective in eliminating *S. aureus* and its VBNC state (Table 5).

Since *S. aureus* could enter into VBNC state with strong acid treatment, the elimination of VBNC state by different nutrition conditions with strong acid were studied. Under low temperature (4 and −20°C), all cells were dead within 3 days in groups with no nutrition and strong acid (induction groups 1, 3, and 5). *S. aureus* may enter into VBNC under the treatment of some nutrition and low salt with strong acid. These results indicated that in low salt and strong acid environment, the VBNC state of

S. aureus cannot be eliminated by only reducing nutrients. Thus, the control of VBNC state formation can be achieved by changing nutrition concentration in combination with other treatments. One way of eliminating the VBNC state of *S. aureus*, which

TABLE 5 | Inhibition of acidity on the formation of VBNC state of *S. aureus*.

Group	Culturability		Viability	
	4°C	−20°C	4°C	−20°C
1	/	/	−	−
2	/	/	−	−
3	/	/	−	−
4	+	+	ND	ND
5	+	+	ND	ND

" + " stands for culturable, "/" for unculturable, "−" for inactive and "ND" for activity is not detected.

TABLE 6 | Inhibition of nutritional status on the VBNC state formation.

Group	Culturability		Viability	
	4°C	−20°C	4°C	−20°C
1	−	−	−	−
2	+	+	ND	ND
3	−	−	−	−
4	+	−	ND	0
5	−	−	−	−
6	+	+	ND	ND

" + " stands for culturable, "/" for unculturable, "−" for inactive and "ND" for activity is not detected.

could be applicable in food processing or used when cleaning equipment, would be to provide a condition of no nutrition with acid (Table 6).

Recently, several studies have reported on the formation of *Staphylococcus* biofilm on different surfaces during food processing, including polystyrene, polypropylene, stainless steel, and glass (Sattar et al., 2001; DeVita et al., 2007; Simon and Sanjeev, 2007). VBNC state induced in *S. aureus* biofilm under the antibiotic pressure has also been confirmed by RT-PCR (Pasquaroli et al., 2013, 2014). *S. aureus*, as well as its VBNC state formation, is emerging as a major concern of food product contamination and poses a threat to human health.

Control of VBNC State in Rice Product

The culturable cell numbers under low temperature stress are shown in Figure 3. In food systems with 100, 50, and 25% nutrients and 1.0% acetic acid, the cells lost their culturability in 3 days. Observation under a fluorescence microscope (Figure 4) confirmed that all cells were dead, which is different from the results in the induction in TSB due to complex food matrix with unfavorable factors. Thus, 1% of acetic acid can be applied in the control of normal and VBNC state *S. aureus* cells in rice products.

Foodborne pathogens and spoilage bacteria in the VBNC state can produce toxins and cause food spoilage. This is emerging as a leading concern for the food industry (Xu et al., 2009; Liu et al., 2017a). Over the past few decades, it has been confirmed that

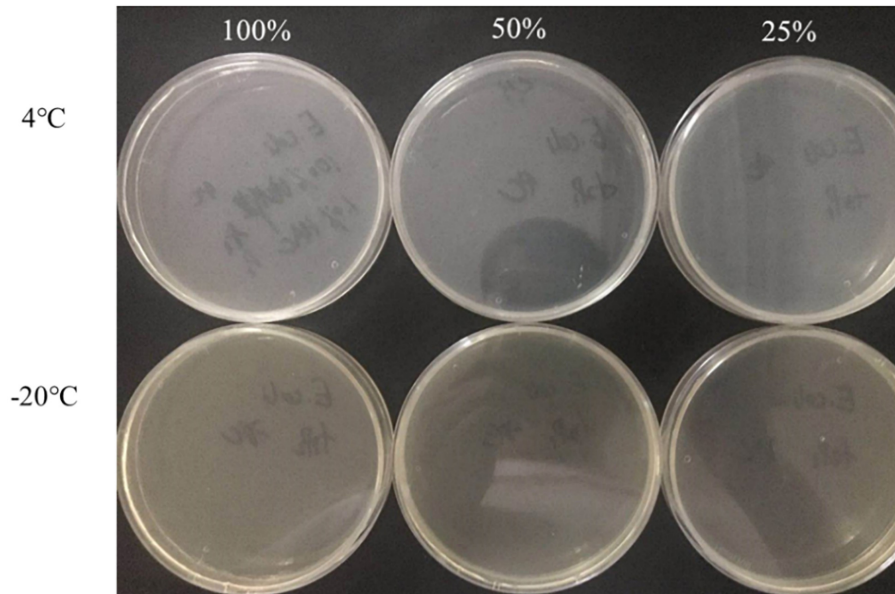


FIGURE 3 | The culturable cell number of *S. aureus* inoculated in the 1.0% (v/v) acetic acid containing 100, 50, 25% nutrients at low temperature for 3 days.

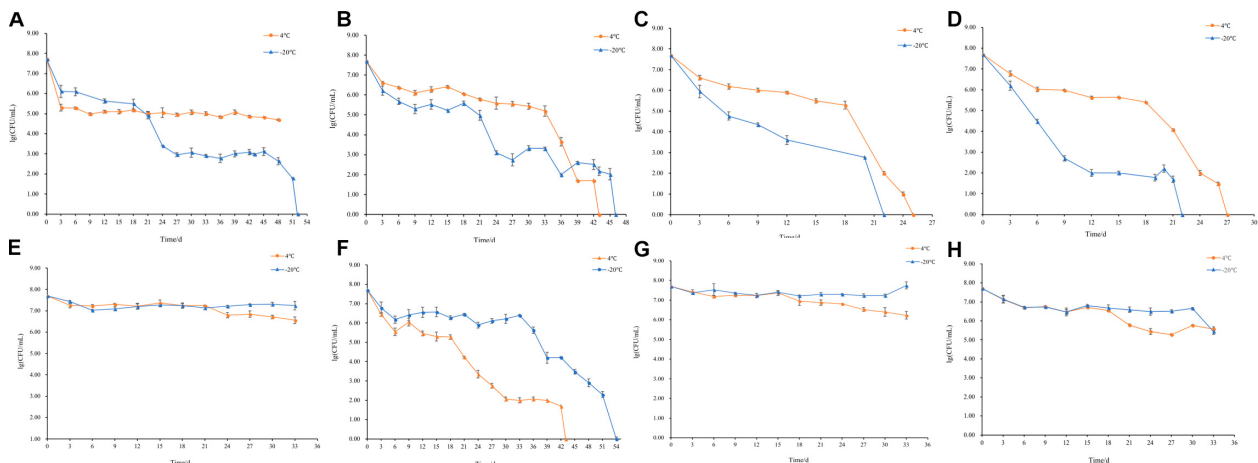


FIGURE 4 | The viability of non-culturable *S. aureus* stored at different conditions (A) group 1 (−20°C); (B,C) group 2 (4°C, −20°C); (D,E) group 3 (4°C, −20°C); (F,G) group 4 (4°C, 20°C); (H) group 7 (4°C).

VBNC cells are capable of recovering, with restored metabolic activity. However, resuscitation conditions vary among species and strains. VBNC *E. coli* O157:H7 and *Vibrio vulnificus* cells can recover with the treatment of fresh TSB and a temperature upshift (Dinu and Bach, 2013; Zhao et al., 2013; Zhong et al., 2013; Rao et al., 2014; Xu et al., 2018). Moreover, the VBNC state pathogens recover or maintain virulence after resuscitation (Cappelier et al., 2007; You et al., 2012; Zeng et al., 2013). Several foodborne outbreaks were due to the resuscitation of VBNC cells (Xu et al., 2007; Zhao et al., 2017; Wen et al., 2020). Therefore, the control of the VBNC state formation in food products is of importance.

Application of PMA-PCR on VBNC Cell Detection in Rice Product

The detection limit of PMA-PCR for detection of the VBNC state *S. aureus* in rice products was 10^4 CFU/mL. Compared with the conventional culturing-based method, which uses the LIVE/DEAD® BacLight™ fluorescence staining method to detect VBNC cells, the PMA-PCR assay can detect specific concentrations of VBNC cells with high rapidity and sensitivity (Yoon et al., 2019).

CONCLUSION

This study investigated the impact of three elements including nutrition, acid and salt concentrations in food systems on the VBNC state formation of *S. aureus*. Nutrition showed the highest influence on the VBNC state formation *S. aureus*, followed by acid and salt. The addition of 1% acetic acid could directly kill *S. aureus* cells and

inhibit the formation of VBNC states with a nutrition concentration of 25, 50, and 100%. Propidium monoazide-polymerase chain reaction (PMA-PCR) assay was applied and considered to be a rapid and sensitive method for detecting *S. aureus* in the VBNC state, with the detection limit of 10^4 CFU/mL.

DATA AVAILABILITY STATEMENT

The original contributions presented in the study are included in the article/supplementary material, further inquiries can be directed to the corresponding authors.

AUTHOR CONTRIBUTIONS

JL and KW conceived of the study and participated in its design and coordination. T-YH, YM, YC, FS, RP, and JC performed the experimental work. CB, LY, and LC analyzed the data. JL prepared and revised this manuscript. All authors reviewed and approved the final manuscript.

FUNDING

This study was funded by the National Key Research and Development Program of China (2016YFD04012021), the Science and Technology Planning Project of Guangdong Province (2017A050501007), the Fundamental Research Funds for the Central Universities (2017ZD092), and the 111 Project (B17018).

REFERENCES

- Bai, H., Zhao, F., Li, M., Qin, L., Yu, H., Lu, L., et al. (2019). Citric acid can force *Staphylococcus aureus* into viable but nonculturable state and its characteristics. *Int. J. Food Microbiol.* 305:108254. doi: 10.1016/j.ijfoodmicro.2019.108254
- Bao, X., Jia, X., Chen, L., Peters, B. M., Lin, C., Chen, D., et al. (2017a). Effect of polymyxin resistance (*pmr*) on biofilm formation of *Cronobacter sakazakii*. *Microb. Pathog.* 106, 16–19. doi: 10.1016/j.micpath.2016.12.012
- Bao, X., Yang, L., Chen, L., Li, B., Li, L., Li, Y., et al. (2017b). Analysis on pathogenic and virulent characteristics of the *Cronobacter sakazakii* strain BAA-894 by whole genome sequencing and its demonstration in basic biology science. *Microb. Pathog.* 109, 280–286. doi: 10.1016/j.micpath.2017.05.030
- Bao, X., Yang, L., Chen, L., Li, B., Li, L., Li, Y., et al. (2017c). Virulent and pathogenic features on the *Cronobacter sakazakii* polymyxin resistant *pmr* mutant strain s-3. *Microb. Pathog.* 110, 359–364. doi: 10.1016/j.micpath.2017.07.022
- Bennett, S. D., Walsh, K. A., and Gould, L. H. (2013). Foodborne disease outbreaks caused by bacillus cereus, clostridium perfringens, and staphylococcus aureus—united states, 1998–2008. *Clin. Infect. Dis.* 57, 425–433. doi: 10.1093/cid/cit244
- Cappelier, J. M., Besnard, V., Roche, S. M., Velge, P., and Federighi, M. (2007). Avirulent viable but non culturable cells of listeria monocytogenes need the presence of an embryo to be recovered in egg yolk and regain virulence after recovery. *Vet. Res.* 38, 573–583. doi: 10.1051/vetres:2007017
- Chen, H., Zhong, C., Zhang, T., Shu, M., Lin, L., Luo, Q., et al. (2020). Rapid and sensitive detection of viable but non-culturable *Salmonella* induced by low temperature from chicken using EMA-Rti-LAMP combined with BCAC. *Food Anal. Methods* 13, 313–324. doi: 10.1007/s12161-019-01655-9
- Cunningham, E., O'Byrne, C., and Oliver, J. D. (2009). Effect of weak acids on listeria monocytogenes survival: evidence for a viable but nonculturable state in response to low pH. *Food Control* 20, 1141–1144. doi: 10.1016/j.foodcont.2009.03.005
- Deng, Y., Liu, J., Li, L., Fang, H., Tu, J., Li, B., et al. (2015). Reduction and restoration of culturability of beer-stressed and low-temperature-stressed *Lactobacillus acetotolerans* strain 2011-8. *Int. J. Food Microbiol.* 206, 96–101. doi: 10.1016/j.ijfoodmicro.2015.04.046
- DeVita, M. D., Wadhwa, R. K., Theis, M. L., and Ingham, S. C. (2007). Assessing the potential of *Streptococcus pyogenes* and *Staphylococcus aureus* transfer to foods and customers via a survey of hands, hand-contact surfaces and food-contact surfaces at foodservice facilities. *J. Foodservice* 18, 76–79. doi: 10.1111/j.1745-4506.2007.00049.x
- Dinu, L.-D., and Bach, S. (2013). Detection of viable but non-culturable *Escherichia coli* O157:H7 from vegetable samples using quantitative PCR with propidium monoazide and immunological assays. *Food Control* 31, 268–273. doi: 10.1016/j.foodcont.2012.10.020
- Foster, J. W. (1999). When protons attack: microbial strategies of acid adaptation. *Curr. Opin. Microbiol.* 2, 170–174. doi: 10.1016/s1369-5274(99)80030-7
- Guo, L., Ye, C., Cui, L., Wan, K., Chen, S., Zhang, S., et al. (2019). Population and single cell metabolic activity of UV-induced VBNC bacteria determined by CTC-FCM and D(2)O-labeled raman spectroscopy. *Environ. Int.* 130:104883. doi: 10.1016/j.envint.2019.05.077

- Jia, X., Hua, J., Liu, L., Xu, Z., and Li, Y. (2018). Phenotypic characterization of pathogenic *Cronobacter* spp. strains. *Microb. Pathog.* 121, 232–237. doi: 10.1016/j.micpath.2018.05.033
- Kraushaar, B., and Fetsch, A. (2014). First description of PVL-positive methicillin-resistant *Staphylococcus aureus* (MRSA) in wild boar meat. *Int. J. Food Microbiol.* 186, 68–73. doi: 10.1016/j.jfoodmicro.2014.06.018
- Lai, C. J., Chen, S. Y., Lin, I. H., Chang, C. H., and Wong, H. C. (2009). Change of protein profiles in the induction of the viable but nonculturable state of *Vibrio parahaemolyticus*. *Int. J. Food Microbiol.* 135, 118–124. doi: 10.1016/j.jfoodmicro.2009.08.023
- Li, L., Mendis, N., Trigui, H., Oliver, J. D., and Faucher, S. P. (2014). The importance of the viable but non-culturable state in human bacterial pathogens. *Front. Microbiol.* 5:258. doi: 10.3389/fmicb.2014.00258
- Li, Y., Yang, L., Fu, J., Yan, M., Chen, D., and Zhang, L. (2017). The novel loop-mediated isothermal amplification based confirmation methodology on the bacteria in viable but non-culturable (VBNC) state. *Microb. Pathog.* 111, 280–284. doi: 10.1016/j.micpath.2017.09.007
- Lin, S., Li, L., Li, B., Zhao, X., Lin, C., Deng, Y., et al. (2016). Development and evaluation of quantitative detection of N-epsilon-carboxymethyl-lysine in *Staphylococcus aureus* biofilm by LC-MS method. *Basic Clin. Pharmacol. Toxicol.* 118:33.
- Lin, S., Yang, L., Chen, G., Li, B., Chen, D., Li, L., et al. (2017). Pathogenic features and characteristics of food borne pathogens biofilm: biomass, viability and matrix. *Microb. Pathog.* 111, 285–291. doi: 10.1016/j.micpath.2017.08.005
- Lindbäck, T., Rottenberg, M. E., Roche, S. M., and Rørvik, L. M. (2010). The ability to enter into an avirulent viable but non-culturable (VBNC) form is widespread among *Listeria monocytogenes* isolates from salmon, patients and environment. *Vet. Res.* 41:8. doi: 10.1051/vetres/2009056
- Liu, J., Li, L., Li, B., Peters, B. M., Deng, Y., Xu, Z., et al. (2017a). First study on the formation and resuscitation of viable but nonculturable state and beer spoilage capability of *Lactobacillus lindneri*. *Microb. Pathog.* 107, 219–224. doi: 10.1016/j.micpath.2017.03.043
- Liu, J., Zhou, R., Li, L., Peters, B. M., Li, B., Lin, C. W., et al. (2017b). Viable but non-culturable state and toxin gene expression of enterohemorrhagic *Escherichia coli* O157 under cryopreservation. *Res. Microbiol.* 168, 188–193. doi: 10.1016/j.resmic.2016.11.002
- Liu, L., Lu, Z., Li, L., Li, B., Zhang, X., Zhang, X., et al. (2018a). Physical relation and mechanism of ultrasonic bactericidal activity on pathogenic *E. coli* with WPI. *Microb. Pathog.* 117, 73–79. doi: 10.1016/j.micpath.2018.02.007
- Liu, L., Xu, R., Li, L., Li, B., Zhang, X., Zhang, X., et al. (2018b). Correlation and in vitro mechanism of bactericidal activity on *E. coli* with whey protein isolate during ultrasonic treatment. *Microb. Pathog.* 115, 154–158. doi: 10.1016/j.micpath.2017.12.062
- Liu, L., Ye, C., Soteyome, T., Zhao, X., Xia, J., Xu, W., et al. (2019). Inhibitory effects of two types of food additives on biofilm formation by foodborne pathogens. *Microbiol. Open* 8:e853. doi: 10.1002/mbo3.853
- Liu, Y., Zhong, Q., Wang, J., and Lei, S. (2018). Enumeration of *Vibrio parahaemolyticus* in VBNC state by PMA-combined real-time quantitative PCR coupled with confirmation of respiratory activity. *Food Control* 91, 85–91. doi: 10.1016/j.foodcont.2018.03.037
- Masmoudi, S., Denis, M., and Maalej, S. (2010). Inactivation of the gene *katA* or *sodA* affects the transient entry into the viable but non-culturable response of *Staphylococcus aureus* in natural seawater at low temperature. *Mar. Pollut. Bull.* 60, 2209–2214. doi: 10.1016/j.marpolbul.2010.08.017
- Miao, J., Chen, L., Wang, J., Wang, W., Chen, D., Li, L., et al. (2017a). Current methodologies on genotyping for nosocomial pathogen methicillin-resistant *Staphylococcus aureus* (MRSA). *Microb. Pathog.* 107, 17–28. doi: 10.1016/j.micpath.2017.03.010
- Miao, J., Chen, L., Wang, J., Wang, W., Chen, D., Li, L., et al. (2017b). Evaluation and application of molecular genotyping on nosocomial pathogen-methicillin-resistant *Staphylococcus aureus* isolates in guangzhou representative of southern china. *Microb. Pathog.* 107, 397–403. doi: 10.1016/j.micpath.2017.04.016
- Miao, J., Liang, Y., Chen, L., Wang, W., Wang, J., Li, B., et al. (2017c). Formation and development of *Staphylococcus aureus* biofilm: with focus on food safety. *J. Food Safety* 37:e12358. doi: 10.1111/jfs.12358
- Miao, J., Peters, B. M., Li, L., Li, B., Zhao, X., Xu, Z., et al. (2016). Evaluation of ERIC-PCR for fingerprinting methicillin-resistant *Staphylococcus aureus* strains. *Basic Clin. Pharmacol. Toxicol.* 118:33.
- Miao, J., Wang, W., Xu, W., Su, J., Li, L., Li, B., et al. (2018). The fingerprint mapping and genotyping systems application on methicillin-resistant *Staphylococcus aureus*. *Microb. Pathog.* 125, 246–251. doi: 10.1016/j.micpath.2018.09.031
- Oliver, J. D. (2010). Recent findings on the viable but nonculturable state in pathogenic bacteria. *FEMS Microbiol. Rev.* 34, 415–425. doi: 10.1111/j.1574-6976.2009.00200.x
- Pasquaroli, S., Citterio, B., Cesare, A. D., Amiri, M., Manti, A., Vuotto, C., et al. (2014). Role of daptomycin in the induction and persistence of the viable but non-culturable state of *Staphylococcus aureus* biofilms. *Pathogens* 3, 759–768. doi: 10.3390/pathogens3030759
- Pasquaroli, S., Zandri, G., Vignaroli, C., Vuotto, C., Donelli, G., and Biavasco, F. (2013). Antibiotic pressure can induce the viable but non-culturable state in *Staphylococcus aureus* growing in biofilms. *J. Antimicrob. Chemother.* 68, 1812–1817. doi: 10.1093/jac/dkt086
- Pinto, D., Santos, M. A., and Chambel, L. (2015). Thirty years of viable but nonculturable state research: unsolved molecular mechanisms. *Crit. Rev. Microbiol.* 41, 61–76. doi: 10.3109/1040841x.2013.794127
- Rahman, I., Shahamat, M., Chowdhury, M. A., and Colwell, R. R. (1996). Potential virulence of viable but nonculturable *Shigella dysenteriae* type 1. *Appl. Environ. Microbiol.* 62, 115–120.
- Ramaiah, N., Ravel, J., Straube, W. L., Hill, R. T., and Colwell, R. R. (2002). Entry of *Vibrio harveyi* and *Vibrio fischeri* into the viable but nonculturable state. *J. Appl. Microbiol.* 93, 108–116. doi: 10.1046/j.1365-2672.2002.01666.x
- Rao, N. V., Shashidhar, R., and Bandekar, J. R. (2014). Induction, resuscitation and quantitative real-time polymerase chain reaction analyses of viable but nonculturable *Vibrio vulnificus* in artificial sea water. *World J. Microbiol. Biotechnol.* 30, 2205–2212. doi: 10.1007/s11274-014-1640-1
- Sattar, S. A., Springthorpe, S., Mani, S., Gallant, M., Nair, R. C., Scott, E., et al. (2001). Transfer of bacteria from fabrics to hands and other fabrics: development and application of a quantitative method using *Staphylococcus aureus* as a model. *J. Appl. Microbiol.* 90, 962–970. doi: 10.1046/j.1365-2672.2001.01347.x
- Simon, S. S., and Sanjeev, S. (2007). Prevalence of enterotoxigenic *Staphylococcus aureus* in fishery products and fish processing factory workers. *Food Control* 18, 1565–1568. doi: 10.1016/j.foodcont.2006.12.007
- Wang, L., Zhao, X., Chu, J., Li, Y., Li, Y., Li, C., et al. (2011). Application of an improved loop-mediated isothermal amplification detection of *Vibrio parahaemolyticus* from various seafood samples. *Afr. J. Microbiol. Res.* 5, 5765–5771. doi: 10.5897/AJMR11.1237
- Wen, S., Feng, D., Chen, D., Yang, L., and Xu, Z. (2020). Molecular epidemiology and evolution of *Haemophilus influenzae*. *Infect. Genet. Evol.* 80:104205. doi: 10.1016/j.meegid.2020.104205
- Xie, J., Peters, B. M., Li, B., Li, L., Yu, G., Xu, Z., et al. (2017a). Clinical features and antimicrobial resistance profiles of important *Enterobacteriaceae* pathogens in guangzhou representative of southern china, 2001–2015. *Microb. Pathog.* 107, 206–211. doi: 10.1016/j.micpath.2017.03.038
- Xie, J., Yang, L., Peters, B. M., Chen, L., Chen, D., Li, B., et al. (2017b). A 16-year retrospective surveillance report on the pathogenic features and antimicrobial susceptibility of *Pseudomonas aeruginosa* isolated from guangzhou representative of southern china. *Microb. Pathog.* 110, 37–41. doi: 10.1016/j.micpath.2017.06.018
- Xu, H. S., Roberts, N., Singleton, F. L., Attwell, R. W., Grimes, D. J., and Colwell, R. R. (1982). Survival and viability of nonculturable *Escherichia coli* and *Vibrio cholerae* in the estuarine and marine environment. *Microb. Ecol.* 8, 313–323. doi: 10.1007/bf02010671
- Xu, Z., Hou, Y., Peters, B. M., Chen, D., Li, B., and Li, L. (2016a). Chromogenic media for MRSA diagnostics. *Mol. Biol. Rep.* 43, 1205–1212. doi: 10.1007/s11033-016-4062-3
- Xu, Z., Hou, Y., Qin, D., Liu, X., Li, B., Li, L., et al. (2016b). Evaluation of current methodologies for rapid identification of methicillin-resistant *Staphylococcus aureus* strains. *Basic Clin. Pharmacol. Toxicol.* 118:33.
- Xu, Z., Liang, Y., Lin, S., Chen, D., Li, B., Li, L., et al. (2016c). Crystal violet and XTT assays on *Staphylococcus aureus* biofilm quantification. *Curr. Microbiol.* 73, 474–482. doi: 10.1007/s00284-016-1081-1
- Xu, Z., Gui, Z., Li, B., Li, L., Su, J., Zhao, X., et al. (2012a). Expression and purification of gp41-gp36 Fusion protein and application in serological

- screening assay of HIV-1 and HIV-2. *Afr. J. Microbiol. Res.* 6, 6295–6299. doi: 10.5897/AJMR12.1075
- Xu, Z., Li, L., Chu, J., Peters, B. M., Harris, M. L., Li, B., et al. (2012b). Development and application of loop-mediated isothermal amplification assays on rapid detection of various types of staphylococci strains. *Food Res. Int.* 47, 166–173.
- Xu, Z., Li, L., Mark, E., Shirliff, M. E., Peters, B. M., Peng, Y., et al. (2010). First report of class 2 integron in clinical *Enterococcus faecalis* and class 1 integron in *Enterococcus faecium* in south china. *Diag. Microbiol. Infect. Dis.* 68, 315–317. doi: 10.1016/j.diagmicrobio.2010.05.014
- Xu, L., Li, Z., Shirliff, M. E., Peters, B. M., Li, B., Peng, Y., et al. (2011). Resistance class 1 integron in clinical methicillin-resistant *Staphylococcus aureus* strains in southern china, 2001–2006. *Clin. Microbiol. Infect.* 17, 714–718. doi: 10.1111/j.1469-0691.2010.03379.x
- Xu, M. E., Li, L., Shi, L., and Shirliff, Z. (2011). Class 1 integron in staphylococci. *Mol. Biol. Rep.* 38, 5261–5279. doi: 10.1007/s11033-011-0676-7
- Xu, Z., Li, L., Zhao, X., Chu, J., Li, B., Shi, L., et al. (2011). Development and application of a novel multiplex polymerase chain reaction (PCR) assay for rapid detection of various types of staphylococci strains. *Afr. J. Microbiol. Res.* 5, 1869–1873. doi: 10.1186/1471-2105-12-291
- Xu, Z., Li, L., Shirliff, M. E., Alam, M. J., Yamasaki, S., and Shi, L. (2009). Occurrence and characteristics of class 1 and 2 integrons in *Pseudomonas aeruginosa* isolates from patients in southern china. *J. Clin. Microbiol.* 47, 230–234. doi: 10.1128/JCM.02027-08
- Xu, Z., Li, L., Li, L., Zhang, L., Yamasaki, S., and Shi, L. (2008a). First confirmation of integron-bearing methicillin-resistant *Staphylococcus aureus*. *Curr. Microbiol.* 57, 264–268. doi: 10.1007/s00284-008-9187-8
- Xu, Z., Shi, L., Alam, M. J., Li, L., and Yamasaki, S. (2008b). Integron-bearing methicillin-resistant coagulase-negative staphylococci in south china, 2001–2004. *FEMS Microbiol. Lett.* 278, 223–230. doi: 10.1111/j.1574-6968.2007.00994.x
- Xu, Z., Shi, L., Zhang, C., Zhang, L., Li, X., Cao, Y., et al. (2007). Nosocomial infection caused by class 1 integron-carrying *Staphylococcus aureus* in a hospital in south china. *Clin. Microbiol. Infect.* 13, 980–984. doi: 10.1111/j.1469-0691.2007.01782.x
- Xu, Z., Xie, J., Yang, L., Chen, D., Peters, B. M., and Shirliff, M. E. (2018). Complete Sequence of pCY-CTX, a plasmid carrying a phage-like region and ISEcp1-Mediated Tn2 element from *Enterobacter cloacae*. *Microb. Drug. Resist.* 24, 307–313. doi: 10.1089/mdr.2017.0146
- Xu, X., Xu, Z., Yang, L., Li, B., Li, L., Li, X., et al. (2017). Effect of aminoglycosides on the pathogenic characteristics of microbiology. *Microb. Pathog.* 113, 357–364. doi: 10.1016/j.micpath.2017.08.053
- Xu, J., Xie, Z., Peters, B. M., Li, B., Li, L., Yu, G., et al. (2017). Longitudinal surveillance on antibiogram of important gram-positive pathogens in southern china, 2001 to 2015. *Microb. Pathog.* 103, 80–86. doi: 10.1016/j.micpath.2016.11.013
- Yoon, J. H., Moon, S. K., Choi, C., Ryu, B. Y., and Lee, S. Y. (2019). Detection of viable but nonculturable vibrio parahaemolyticus induced by prolonged cold-starvation using propidium monoazide real-time polymerase chain reaction. *Lett. Appl. Microbiol.* 68, 537–545. doi: 10.1111/lam.13157
- You, R., Gui, Z., Xu, Z., Shirliff, M. E., Yu, G., Zhao, X., et al. (2012). Methicillin-resistance *Staphylococcus aureus* detection by an improved rapid PCR assay. *Afr. J. Microbiol. Res.* 6, 7131–7133. doi: 10.5897/AJMR12.708
- Zeng, B., Zhao, G., Cao, X., Yang, Z., Wang, C., and Hou, L. (2013). Formation and resuscitation of viable but nonculturable *Salmonella typhi*. *Biomed. Res. Int.* 2013:907170. doi: 10.1155/2013/907170
- Zhao, F., Bi, X., Hao, Y., and Liao, X. (2013). Induction of viable but nonculturable *Escherichia coli* O157:H7 by high pressure CO₂ and its characteristics. *PLoS One* 8:e62388. doi: 10.1371/journal.pone.0062388
- Zhao, X., Gui, Z., and Xu, Z. (2018a). Detection of foodborne pathogens by surface enhanced raman spectroscopy. *Front. Microbiol.* 9:1236. doi: 10.3389/fmicb.2018.01236
- Zhao, X., Yu, Z., and Xu, Z. (2018b). Study the features of 57 confirmed CRISPR loci in 38 strains of *Staphylococcus aureus*. *Front. Microbiol.* 9:1591. doi: 10.3389/fmicb.2018.01591
- Zhao, X., Zhong, J., Wei, C., Lin, C. W., and Ding, T. (2017). Current perspectives on viable but non-culturable state in foodborne pathogens. *Front. Microbiol.* 8:580. doi: 10.3389/fmicb.2017.00580
- Zhong, J., and Zhao, X. (2018). Detection of viable but non-culturable *Escherichia coli* O157:H7 by PCR in combination with propidium monoazide. *3 Biotech* 8:28. doi: 10.1007/s13205-017-1052-7
- Zhong, N., Gui, Z., Liu, X., Huang, J., Hu, K., Gao, X., et al. (2013). Solvent-free enzymatic synthesis of 1, 3-Diacylglycerols by direct esterification of glycerol with saturated fatty acids. *Lipids Health Dis.* 12, 2–7. doi: 10.1186/1476-511X-12-65
- Zhong, Q., Tian, J., Wang, B., and Wang, L. (2016). PMA based real-time fluorescent LAMP for detection of *Vibrio parahaemolyticus* in viable but nonculturable state. *Food Control* 63, 230–238. doi: 10.1016/j.foodcont.2015.11.043

Conflict of Interest: The authors declare that the research was conducted in the absence of any commercial or financial relationships that could be construed as a potential conflict of interest.

Copyright © 2020 Li, Huang, Mao, Chen, Shi, Peng, Chen, Yuan, Bai, Chen, Wang and Liu. This is an open-access article distributed under the terms of the Creative Commons Attribution License (CC BY). The use, distribution or reproduction in other forums is permitted, provided the original author(s) and the copyright owner(s) are credited and that the original publication in this journal is cited, in accordance with accepted academic practice. No use, distribution or reproduction is permitted which does not comply with these terms.



Inactivation Efficacy of 405 nm LED Against *Cronobacter sakazakii* Biofilm

Yixiao Huang¹, Quanwei Pei¹, Ruisha Deng¹, Xiaoying Zheng¹, Jialu Guo¹, Du Guo¹, Yanpeng Yang¹, Sen Liang² and Chao Shi^{1*}

¹ College of Food Science and Engineering, Northwest A&F University, Yangling, China, ² Beijing Advanced Innovation Center for Food Nutrition and Human Health, Beijing Technology and Business University, Beijing, China

OPEN ACCESS

Edited by:

Viduranga Y. Waisundara,
Australian College of Business and
Technology—Kandy Campus,
Sri Lanka

Reviewed by:

Huhu Wang,
Nanjing Agricultural University, China
Yong Zhao,
Shanghai Ocean University, China

*Correspondence:

Chao Shi
meilixinong@nwsuaf.edu.cn

Specialty section:

This article was submitted to
Food Microbiology,
a section of the journal
Frontiers in Microbiology

Received: 25 September 2020

Accepted: 06 November 2020

Published: 27 November 2020

Citation:

Huang Y, Pei Q, Deng R, Zheng X,
Guo J, Guo D, Yang Y, Liang S and
Shi C (2020) Inactivation Efficacy of
405 nm LED Against *Cronobacter*
sakazakii Biofilm.
Front. Microbiol. 11:610077.
doi: 10.3389/fmicb.2020.610077

The objectives of this study were to evaluate the inactivation efficacy of a 405-nm light-emitting diode (LED) against *Cronobacter sakazakii* biofilm formed on stainless steel and to determine the sensitivity change of illuminated biofilm to food industrial disinfectants. The results showed that LED illumination significantly reduced the population of viable biofilm cells, showing reduction of 2.0 log (25°C), 2.5 log (10°C), and 2.0 log (4°C) between the non-illuminated and LED-illuminated groups at 4 h. Images of confocal laser scanning microscopy and scanning electron microscopy revealed the architectural damage to the biofilm caused by LED illumination, which involved destruction of the stereoscopic conformation of the biofilm. Moreover, the loss of biofilm components (mainly polysaccharide and protein) was revealed by attenuated total reflection Fourier-transformed infrared spectroscopy, and the downregulation of genes involved in *C. sakazakii* biofilm formation was confirmed by real time quantitative PCR analysis, with greatest difference observed in *fliD*. In addition, the sensitivity of illuminated-biofilm cells to disinfectant treatment was found to significantly increased, showing the greatest sensitivity change with 1.5 log reduction between non-LED and LED treatment biofilms in the CHX-treated group. These results indicated that 405 nm LED illumination was effective at inactivating *C. sakazakii* biofilm adhering to stainless steel. Therefore, the present study suggests the potential of 405 nm LED technology in controlling *C. sakazakii* biofilms in food processing and storage, minimizing the risk of contamination.

Keywords: *Cronobacter sakazakii*, LED, biofilm, ATR-FTIR, disinfectant

INTRODUCTION

Cronobacter sakazakii is a rod-shaped, non-spore-forming, peritrichous, facultative anaerobic Gram-negative foodborne pathogen, belonging to the *Enterobacteriaceae* family (Stephan et al., 2014). *C. sakazakii* is occasionally detected in meat, vegetables, cereals and dairy (Beuchat et al., 2009). In particular, powdered infant formula has been linked with many *C. sakazakii* infections, according to an epidemiological report (Yan et al., 2012). *C. sakazakii* contamination more frequently causes infection in infants or adults with lowered immunity, suffering from bacteremia, meningitis, necrotizing enterocolitis or other diseases, and a lethality rate of more than 50% has been reported (Ye et al., 2014). Furthermore, surviving patients may suffer further acute neurological complications such as quadriplegia, brain abscesses, neural-development delay, and hydrocephalus.

Biofilms are defined as matrix-enclosed bacterial populations that are adherent to each other and to interfaces or surfaces, including adherent populations within the pore spaces of porous media, as well as microbial aggregates and flocs (Park et al., 2012). Prior studies have shown that biofilms have complex structures that are surrounded by extracellular polymeric substances (EPS), which enhance the resistance of pathogens to external stress (Ling et al., 2020) and even conventional antibiotics (Davies, 2003). *C. sakazakii* can form biofilms on multiple contact surfaces such as stainless steel, glass, and Teflon (Reich et al., 2010). Furthermore, *C. sakazakii* biofilm formed on the food contact surface can provide a physical defense to protect them from stronger external stress such as high voltage and many antibiotics (Kuo et al., 2013). *C. sakazakii* biofilms have become the main source of contamination for food, either directly or indirectly, and therefore pose a serious threat to consumers' health (Bayoumi et al., 2012).

Conventional antibiofilm methods mainly include disinfectants, exogenous detergents (da Silva and De Martinis, 2013), near-infrared radiant heating and ultraviolet (UV) light (Ha and Kang, 2014). The anti-biofilm effect of natural antibiotics has also been reported (Tong et al., 2018). However, the disadvantages of disinfectants and exogenous detergents cannot be ignored since they can induce resistance in pathogens to conventional treatments, which increases the difficulty of eliminating biofilm (Simões et al., 2010). Infrared radiant heating and UV light irradiation may cause the loss of sensitive nutrients from the food and have limitations because of the high capital costs for installation (Harouna et al., 2015). Natural antibiotics are also limited in their use because of their complex extraction process and high cost (Moloney, 2016). Therefore, new methods for eliminating biofilm that are safe, residue-free and efficient, and could be applied to a variety of processing environments, are needed.

A light-emitting diode (LED) is a semiconductor device that can emit monochromatic light in a narrow range of the spectrum. It has many merits such as low-energy, high stability, long service life, availability in various shapes, and small volume (Quishida et al., 2016). LEDs have advanced in response to the growing need for non-thermal, physical methods for food processing, and storage (Krames and Grandjean, 2017). Some molecules, known as photosensitizers, in bacteria will absorb light when exposed to an LED and produce reactive oxygen species (ROS) that in turn react with DNA, proteins, lipids, and other components to produce cytotoxic effects (Luksiene, 2010). In the field of food safety, LEDs were first studied *in vitro* for their effects against several planktonic foodborne pathogens, including *Escherichia coli*, *Salmonella*, *Listeria*, and *Staphylococcus aureus* (Ghate et al., 2013; Kumar et al., 2016). In recent years, LED light within the range of 400–520 nm has been demonstrated to have inactivation efficacy against *Streptococcus mutans*, *L. monocytogenes*, and *Pseudomonas aeruginosa* on the surface of food and packaging materials (McKenzie et al., 2013; Ghate et al., 2019). However, there have been no studies about the inactivation efficacy of LEDs against *C. sakazakii* biofilms or how they exert photodynamic inactivation.

The current study was carried out to evaluate the inactivation efficacy of a 405 nm LED against *C. sakazakii* biofilm. After LED treatment, the population of viable cells in the biofilm was determined and structural damage to the biofilm was examined using confocal laser scanning microscopy (CLSM) and scanning electron microscopy (SEM). Then, attenuated total reflection Fourier-transformed infrared spectroscopy (ATR-FTIR) combined with real time quantitative PCR (RT-qPCR) analysis were performed to further confirm the 405 nm LED inactivation of *C. sakazakii* biofilm. In addition, the change in sensitivity of LED-illuminated biofilm cells to disinfectants such as chlorhexidine (CHX) and cetylpyridinium chloride (CTPC) was determined. A stainless steel sheet was chosen as the contact surface since it is a common material in food processing, storage and consumption. Three common storage and processing temperatures (25, 10, and 4°C) were selected as illumination temperatures. The inactivation efficacy of 405 nm LED illumination against biofilms was evaluated at room temperature (25°C) to simulate commonly encountered conditions. Cooler temperatures (4 and 10°C) were used to simulate retail storage and processing conditions, respectively.

MATERIALS AND METHODS

Creation of a Biofilm Removal Device With a 405 nm LED

The LED illumination system was prepared according to the previous method reported by Ghate et al. (2013). LED intensity was 26 ± 2 mW/cm², as measured by a 405 nm radiometer (UHC405, UVATA Ltd., Hong Kong). An acrylonitrile butadiene styrene (ABS) housing was used to surround the LED system, preventing incoming light. LEDs were attached by a heat sink and cooling fan to avoid overheating. To avoid over-currents, the circuit was connected to a 5 Ω resistor. The distance between the stainless steel fixer and the LED light was set to 4.5 cm to ensure that the entire sheets could be illuminated. To measure changes in the sheet surface temperature during LED illumination in real time, a thermocouple sensor was used.

Cleaning of the 304 Stainless Steel Sheets

Stainless steel sheets (grade 304, size: 50 × 20 mm, No. 4 light cleaning face) were used in this study as the biofilm attachment surface for *C. sakazakii*. The procedure for cleaning the stainless steel sheets was conducted according to the method described previously (Yang et al., 2015). Briefly, the sheets were immersed in a test tube with ~20 mL of detergent solution and sonicated for 30 min. Then, the sheets were rinsed with sterile deionized water several times to dissipate any remaining material, and were transferred into 20 mL of 70% (v/v) ethanol and sonicated for another 15 min (Kim et al., 2019). After cleaning, the sheets were air-dried and sterilized in a high temperature autoclave for 15 min before use.

Strain Cultivation and Bacterial Suspension Preparation

C. sakazakii strain ATCC 29004 was purchased from the American Type Culture Collection (ATCC, Manassas, VA, USA)

and was preserved in tryptone soya broth (TSB, Land Bridge Technology, Beijing, China) containing 20% (v/v) glycerol at -80°C . For activation, the stock culture was inoculated onto trypticase soy agar (TSA, Land Bridge Technology, Beijing, China) and cultured at 37°C overnight. Then a single colony was inoculated into TSB and the culture was incubated at 37°C , with shaking at 180 rpm, for 8 h. After activation, the cells from the culture were obtained by centrifugation ($5000 \times g$, 4°C , 15 min). Precipitates were washed twice with phosphate-buffered saline (PBS, Land Bridge Technology, Beijing, China), and finally resuspended and adjusted to an $\text{OD}_{600\text{nm}} = 0.5$, with a cell concentration of 10^8 CFU/mL. Finally, the bacterial suspensions were diluted to a concentration of 10^7 CFU/mL prior to mature biofilm formation.

Mature Biofilm Formation

The assay protocol for mature biofilm formation was based on that reported by Kim et al. (2006). Briefly, 30 mL of diluted bacterial suspension, prepared as described above, were inoculated into each centrifuge tube along with a stainless steel sheet. The sheets were cultured for 24 h at 4°C to ensure the adherence of *C. sakazakii*. After the adhesion stage, each inoculated sheet was gently rinsed for 15 s using 400 mL of sterile water, followed by rinsing for 5 s using 200 mL of sterile water. Then each sheet was placed in 30 mL of TSB and cultured for 48 h at 25°C . The biofilm was further confirmed to be mature using SEM, and was used in the following study.

Population of Surviving Biofilm Cells After LED Illumination

Stainless steel sheets inoculated with mature biofilm were rinsed for 15 s using 400 mL of sterile water, then rinsed for 5 s using 200 mL of sterile water to remove loosely attached cells. For the LED-treated groups, the rinsed sheets in fixer were illuminated at 25, 10, and 4°C , respectively, while the rinsed sheets in fixer of the non-LED controls were placed in an incubator at 29.5, 15.5, and 12.5°C , protected from the light. At the specified times (0, 30, 60, 120, and 240 min), the sheets were transferred into 50 mL centrifuge tubes containing 3 g of glass beads (425–600 μm ; Sigma-Aldrich, St. Louis, MO, USA) and 30 mL PBS (Kim et al., 2019). After vortexing for 5 min, the detached bacterial suspension was serially diluted in PBS, then 0.1 mL was spread-plated onto TSA plates and incubated at 37°C for 24 h. Survival cell counts were expressed as $\log \text{CFU}/\text{cm}^2$.

Confocal Laser Scanning Microscopy (CLSM) Observations

CLSM observations were conducted as previously reported (Kang et al., 2018). After incubation, biofilms were illuminated at 25, 10, and 4°C for 2 h. Then sterile water was used to remove planktonic cells. SYTO 9 was used to stain the biofilm for 15 min at room temperature, protected from the light. After staining, the sheets were rinsed three times with sterile deionized water to remove excess stain. A Nikon A1 microscope (Nikon, Tokyo, Japan) was then used to obtain CLSM images using a $10\times$ objective lens. CLSM images of non-LED-treated biofilms were also obtained as a control to observe the damage caused by LED exposure.

Scanning Electron Microscopy (SEM) Observations

SEM imaging was performed to obtain a deeper understanding of the structure damage caused to *C. sakazakii* biofilm by exposure to the 405 nm LED, based on the method reported by Tong et al. (2018), with little modification. LED-illuminated and non-illuminated biofilms incubated at 25, 10, and 4°C for 2 h were fixed overnight with 2.5% glutaraldehyde at 4°C . The biofilms were then washed with sterile water and PBS, and soaked in 1% (v/v) osmic acid for 5 h, followed by gradient elution with 30, 50, 70, 80, 90, and 100% ethanol for 10 min. Finally, the dehydrated biofilms were sputter-coated with a thin layer of gold and examined under a S-4800 scanning electron microscope (Hitachi, Tokyo, Japan) at $4000\times$ magnification.

Effect of LED on Glycoconjugates in the Biofilm

The distribution of glycoconjugates within the biofilm matrix was analyzed according to a protocol described by Quilès et al. (2012). LED-illuminated and non-illuminated biofilms incubated at 25, 10, and 4°C for 2 h were stained with concanavalin A (Con-A) conjugated to fluorescein (excitation/emission: 494/518 nm, Invitrogen/Molecular Probes, Eugene, OR, USA) for 15 min at room temperature in the dark. Then, the plates were rinsed three times with sterile water to remove excess stain. Images of glycoconjugates were obtained with a Nikon A1 microscope (Nikon, Tokyo, Japan) using a $10\times$ objective lens.

Attenuated Total Reflection Fourier-Transformed Infrared Spectroscopy (ATR-FTIR)

Illuminated and non-illuminated biofilms incubated at 25, 10, and 4°C for 2 h were rinsed three times with 0.85% NaCl solution to remove loosely adhered thallus, and were then air-dried at room temperature for later use, according to a method described by Wang et al. (2018). The parameters of the ATR-FTIR spectrometer (NEXUS 670, Thermo Nicolet, USA) with 2 cm^{-1} resolution and 128 scans were set, and signals in the range of 2,000 to 800 cm^{-1} were captured. Sterile stainless steel was used to deduct the spectral background and OMNIC 8.2 software was used for data analysis.

Effect of the LED on the Transcription of Genes Involved in *C. sakazakii* Biofilm Formation

To describe transcription level changes of genes involved in *C. sakazakii* biofilm formation after exposure to LED, RT-qPCR analysis was used according to previous reports with minor modifications (Abdallah et al., 2015). After incubation, LED-illuminated and non-LED-treated biofilm cells incubated at 25°C for 2 h, were detached by vortexing for 5 min. Then the bacterial sediment was obtained by centrifugation at $4,500 \times g$ for 10 min (20°C) and washed twice with PBS. Total RNA extraction from the bacterial sediment was performed using the RNeasy Pure Bacteria Kit (Tiangeng, Beijing, China). RNA was reverse transcribed into cDNA using the PrimeScriptTM RT Master

TABLE 1 | RT-qPCR primer sequences.

Gene	Primer sequences (5'-3')
16SrRNA	F: AACCTTATCCTTTGTTGCCA R: CGGACTACGACGCACTTTATG
<i>bcsA</i>	F: AAGAAGAGTACGTGGACTGGGTGA R: CGCGAGGATAATCAGGTTGTAG
<i>bcsG</i>	F: GACGGGTATCTGAATTTCCAC R: GCCAGGTATCATGCCAGAACA
<i>flgJ</i>	F: TCAGGTGCCGATGAAGTTTG R: GCCCTTTCCAGGACGATGT
<i>motA</i>	F: CGTGCTTTGGACACCATTT R: TCTCGTTTCTTCCCTTTTCC
<i>motB</i>	F: TTCTGTTGCCTCCAGTTC R: CTCTTGTTGCTTGCTTCTTC
<i>luxR</i>	F: AGCCATATGGATAGCGACATAGAG R: GCCGGATCCCTATTGGGCGAAAG
<i>fliD</i>	F: ATCGAGATCGAGCGTTCCAC R: CGCCCTTATCAACTTTGACGTATT
<i>fliH</i>	F: GACTCTGCCGCAAATGGTG R: CCTTTTCTTCTGCGGACG

Mix (TaKaRa, Beijing, China), according to the manufacturer's instructions. Real-time PCR was conducted in a 25- μ L system using TB GreenTM Premix Ex TaqTM II (TaKaRa, Beijing, China). The IQ5 system (Bio-Rad Laboratories, Hercules, CA, USA) was used to run the samples. The PCR conditions were: 1 cycle at 95°C for 30 s, followed by 40 cycles consisting of 95°C for 5 s and 60°C for 30 s, and dissociation steps of 95°C for 15 s and 60°C for 30 s. Primer sequences and PCR parameters for detecting genes related to biofilm formation (*bcsA*, *bcsG*, *flgJ*, *motA*, *motB*, *luxR*, *fliD*, and *fliH*) are listed in Table 1. The 2^{- $\Delta\Delta$ CT} method was used to express changes at the transcript level caused by LED illumination (Livak and Schmittgen, 2001). For *C. sakazakii*, the levels of transcription of biofilm-forming genes in LED-illuminated cells were calculated and compared with the transcription levels in non-illuminated biofilm cells.

Changes in Sensitivity of LED-Illuminated *C. sakazakii* Biofilm Cells to Disinfectants

The changes in biofilm sensitivity to disinfectants were measured according to a previously reported method with minor modifications (Kang et al., 2018). At 2 and 4 h, illuminated and non-illuminated biofilms at 25, 10, and 4°C were carefully immersed in 50 mL centrifuge tubes containing a solution of CHX (30 mL, 100 ppm) and CTPC (30 mL, 100 ppm) for up to 15 min. They were then immediately transferred into 15 mL neutralization solution (Tween 80 30 g/L, saponin 30 g/L, sodium thiosulfate 5 g/L, L-histidine 1 g/L, lecithin 30 g/L, and TSB 9.5 g/L) to stop the activity of the disinfectant. After neutralization, each sample was transferred into a 50 mL centrifuge tube containing 3 g of glass beads (425–600 μ m; Sigma-Aldrich, St. Louis, MO, USA) and 30 mL PBS, then vortexed for 5 min as described above. The detached bacterial suspension was

serially diluted in PBS, then 0.1 mL of the diluted solutions was plated onto TSA plates and cultured at 37°C to determine the cell count. The difference between non-illuminated and 405-nm LED-illuminated *C. sakazakii* biofilm cell populations after disinfectants treatment was expressed as log reduction CFU/cm².

Statistical Analysis

Each treatment was replicated three times. Statistical analyses were performed using SPSS software (Version 18.0; SPSS, Inc., Chicago, IL, USA) and Tukey's test for average separation on an entirely randomized design with six sets of data. The data are presented as the mean \pm SD ($n = 3$), and differences between the means were tested by one-way ANOVA or a Student's *t*-test. Differences with *P*-values of < 0.05 were considered statistically significant.

RESULTS

Population of Viable Biofilm Cells After LED Illumination

The effect of 405-nm LED illumination on viable cells in the mature *C. sakazakii* biofilm was determined (Figure 1). The population of non-illuminated biofilm cells remained relatively stable during storage at 10 and 4°C, showing a 0.4 log (Figure 1B) and 0.2 log (Figure 1C) reduction after 4 h, but was significantly decreased at 25°C, showing a 1.5 log (Figure 1A) reduction. After LED treatment for 4 h, all of the test groups showed a significant reduction in the biofilm cell population compared with the controls, with 2.0 log, 2.5 log and 2.0 log reductions at 25°C (Figure 1A), 10°C (Figure 1B), and 4°C (Figure 1C), respectively.

Confocal Laser Scanning Microscopy (CLSM)

After LED illumination, damage to the conformational structure of the *C. sakazakii* biofilm was observed by CLSM (Figures 2A–F). For all of the biofilms in the non-illuminated groups, the whole field of vision showed green, indicating that the stereoscopic conformation of the biofilm was intact. However, after 2 h of illumination, the integrity and depth of the green fluorescence were significantly influenced by the more “porous” area, which indicated that the integrity of the biofilm stereoscopic conformation had been destroyed and the population of bacterial cells in the biofilm had decreased. This destruction was temperature-independent, revealing more “porous” areas and architectural damage at a set temperature of 25°C (Figures 2A,D) than at 10°C (Figures 2B,E) or 4°C (Figures 2C,F).

Scanning Electron Microscopy (SEM) Imaging

To confirm the effects of LED on *C. sakazakii* biofilm in greater detail, images of inoculated sheets were taken under a scanning electron microscope (Figures 2G–L). The typical structure of mature biofilm was observed in the control groups, characterized by a complex three-dimensional structure formed by many cell colonies integrated by a network of

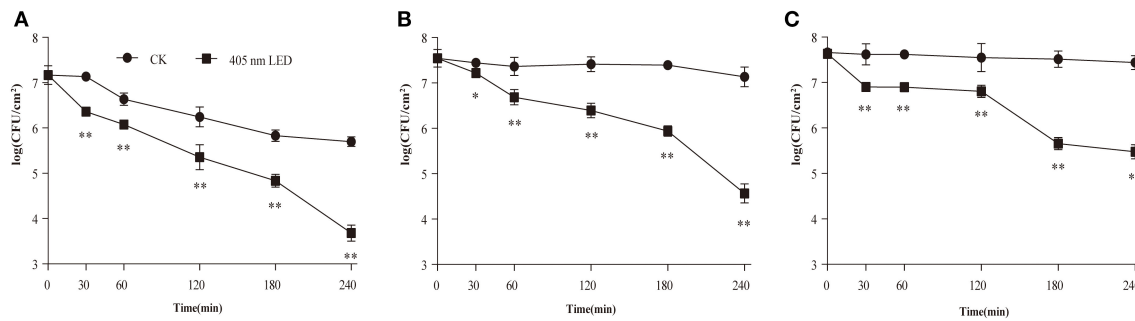


FIGURE 1 | Inhibition of *C. sakazakii* biofilm cells on stainless steel by 405 nm LED illumination at 25°C (A), 10°C (B), and 4°C (C). The errors bars indicate the standard error of the mean. *P < 0.05; **P < 0.01 vs. the control.

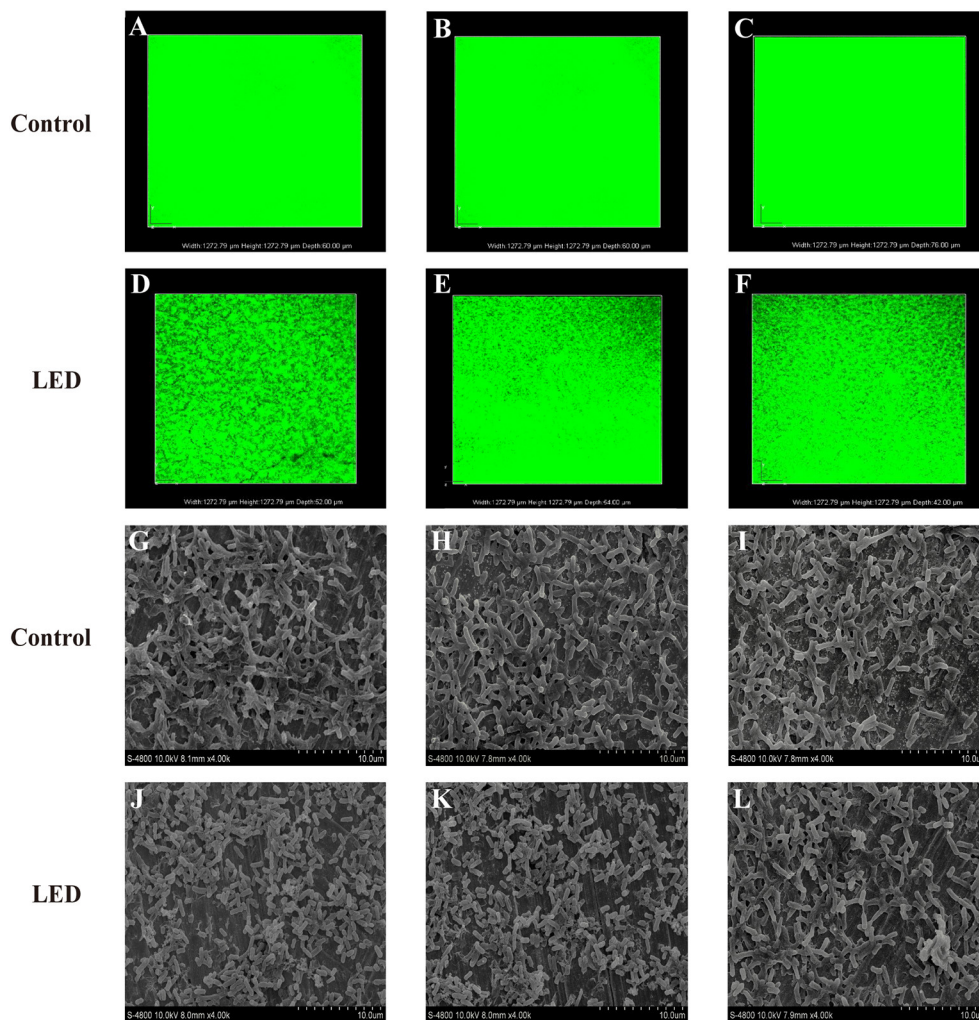


FIGURE 2 | Confocal laser scanning microscopic images of *C. sakazakii* biofilms on stainless steel with or without 405 nm LED treatment for 2 h at 25°C (A,D), 10°C (B,E), and 4°C (C,F). Scanning electron microscopic images of *C. sakazakii* biofilms on stainless steel with or without 405 nm LED treatment for 2 h at 25°C (G,J), 10°C (H,K), and 4°C (I,L).

extracellular matrix. By contrast, in the LED-treated groups, significant removal of the network of extracellular matrix and destruction of the dense three-dimensional structure

were observed, resulting in biofilms of reduced thickness and separate cells without aggregation. Moreover, when the illumination temperature increased from 4°C (Figures 2I,L) and

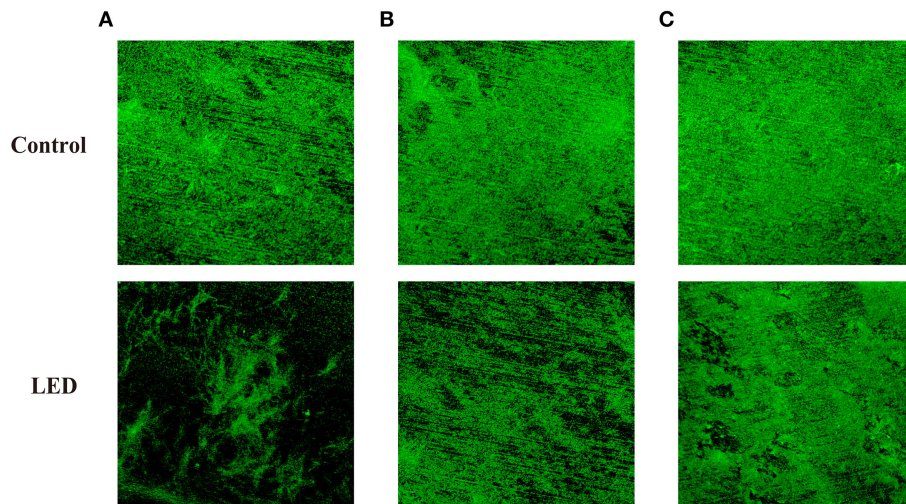


FIGURE 3 | Glycoconjugates in the EPS of *C. sakazakii* biofilms formed on stainless steel after non-LED treatment and LED treatment for 2 h at 25°C (A), 10°C (B), and 4°C (C).

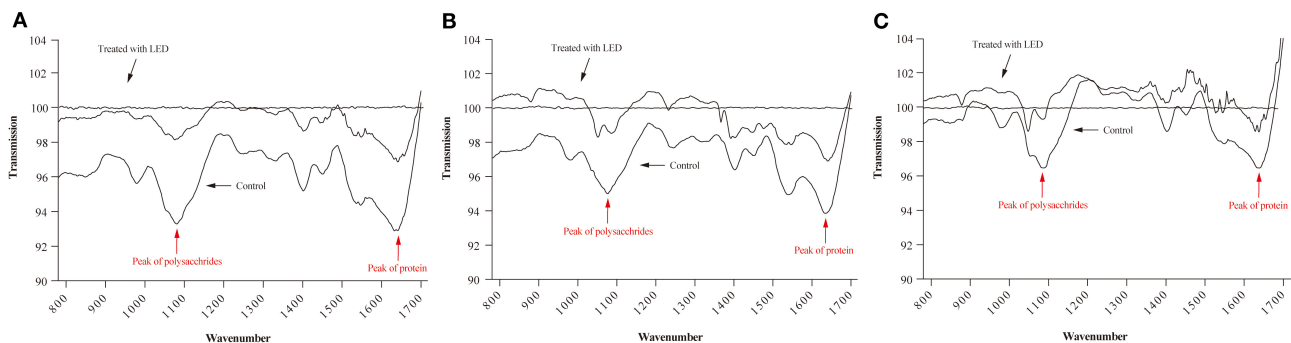


FIGURE 4 | ATR-FTIR spectra of *C. sakazakii* biofilms formed on stainless steel after non-LED treatment and LED treatment for 2 h at 25°C (A), 10°C (B), and 4°C (C).

10°C (Figures 2H,K) to 25°C (Figures 2G,J), the network of extracellular matrix and the three-dimensional structure of the biofilm gradually disappeared.

Effect of LED Illumination on the Glycoconjugates in the Biofilm

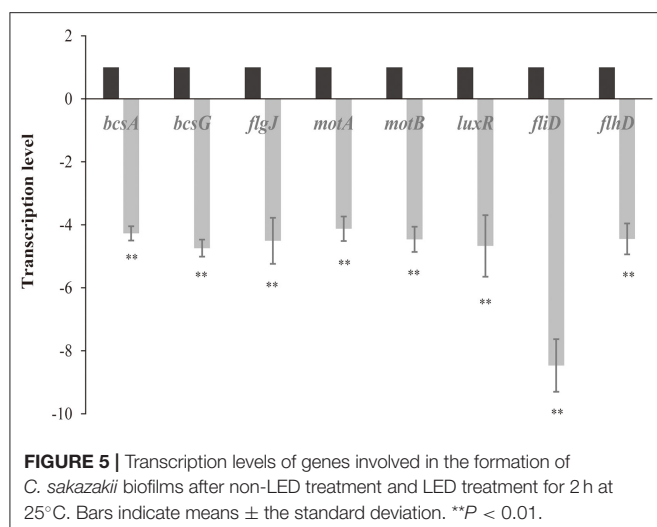
ConA-fluorescein was used to determine the effects of LED illumination on the glycoconjugates in the EPS of *C. sakazakii* biofilm (Figure 3). Changes to the concentration and thickness of glycoconjugates in the biofilm were evident under the microscope. In contrast to the control biofilm that appeared well established in structure and contained glycoconjugates of the correct thickness, the LED-treated biofilm appeared damaged in structure with a lower concentration of glycoconjugates that were thinner, which supported the findings of CLSM and SEM. The damage to glycoconjugates caused by LED illumination was influenced by temperature, which was also in accordance with the CLSM and SEM observations, with a greater eliminating effect at 25°C (Figure 3A) than at 10°C (Figure 3B) and 4°C (Figure 3C).

Effect of LED Illumination on Biofilm Composition

The ATR-FTIR spectra of LED-illuminated biofilms and non-illuminated biofilms were determined directly on stainless steel sheets at 25, 10, and 4°C (Figure 4). According to the functional groups associated with major bands in the ATR-FTIR spectra the spectral peaks at 1,084 and 1,056 cm^{-1} were assigned to polysaccharides and the peak at 1,647 cm^{-1} related to a specific protein peak. After LED illumination, the spectral peaks at 1,084, 1,056, and 1,647 cm^{-1} increased, which indicated the removal of polysaccharides and protein after LED illumination at 25, 10, and 4°C. These results showed that LED illumination caused significant removal of representative components of the biofilm, with the greatest eliminating effect observed at 25°C (Figure 4A), followed by 10°C (Figure 4B) and 4°C (Figure 4C).

Effect of LED Illumination on the Transcription Level of Genes Involved in *C. sakazakii* Biofilm Formation

The levels of transcription of genes related to *C. sakazakii* biofilm formation (*bcsA*, *bcsG*, *flgJ*, *motA*, *motB*, *luxR*, *fliD*, and *flhD*)



under non-LED treatment and LED-illuminated treatment are shown in **Figure 5**. In the LED-illuminated groups, a significant reduction in the transcript level of all eight genes related to biofilm formation was observed ($P < 0.01$), with the greatest difference observed for the *fliD* gene.

Sensitivity Changes of LED-Illuminated *C. sakazakii* Biofilm Cells to Disinfectants

The effect of LED illumination on the sensitivity of *C. sakazakii* biofilm cells to disinfectants (CTPC and CHX) at 25, 10, and 4°C was determined (**Figure 6**). In the CHX-treated groups, after LED illumination for 2 h, reductions of 1.0 log, 0.7 log and 0.5 log between the LED-illuminated and non-illuminated groups at 25°C (**Figure 6A**), 10°C (**Figure 6C**), and 4°C (**Figure 6E**) were determined, respectively. After LED illumination for 4 h, reductions of 1.5 log (**Figure 6A**), 1.3 log (**Figure 6C**), and 1.1 log (**Figure 6E**) were observed, respectively. The results indicated that LED illumination significantly increase the sensitivity of *C. sakazakii* biofilm cells to CHX treatment, and stronger sensitivity changes were observed at 25°C.

The observations in groups treated with CTPC were a little different, showing reductions of 0.3 log, 0.4 log and 0.3 log between LED-illuminated and non-illuminated cells after 2 h, at 25°C (**Figure 6B**), 10°C (**Figure 6D**), and 4°C (**Figure 6F**), respectively. After LED illumination for 4 h, reductions of 0.9 log (**Figure 6B**), 0.1 log (**Figure 6D**), and 0.4 log (**Figure 6F**) were determined, respectively. The differences between the reductions in cell numbers between non-LED and LED treatment groups indicated that biofilm cells showed stronger sensitivity to CTPC after LED illumination, in which greater sensitivity changes were observed at 25°C.

DISCUSSION

C. sakazakii shows good tolerance to a variety of external stresses (Ling et al., 2020) and conventional antibiotics (Davies, 2003) as a result of its strong biofilm-forming ability, which

reduces the effects of traditional decontamination methods. *C. sakazakii* has therefore become a major source of infant formula contamination (Bayoumi et al., 2012). On infection, *C. sakazakii* can cause bacteremia, meningitis, necrotic enteritis and other serious diseases in infants or adults with low immunity, and is therefore a cause of widespread concern (Abdesselam and Pagotto, 2014). A safe and effective new method for the removal of *C. sakazakii* biofilm would therefore be of great value. Studies have shown that LED illumination has an inactivation effect on a variety of pathogens in food (McKenzie et al., 2013; Ghate et al., 2019). In this study, we evaluated the inactivation effect of 405 nm LED illumination on the biofilm of *C. sakazakii* and compared the sensitivity of LED-illuminated and non-illuminated biofilm cells to disinfectant treatment.

Before determining the population of surviving biofilm cells after 405 nm LED illumination, the face temperature changes of the stainless steel sheets were monitored and recorded at 2-min intervals for 120 min during illumination (data not shown). For the three set temperatures (25, 10, and 4°C), the temperatures were maintained at 29.5, 15.5, and 12.5°C after 120 min. To compensate for this heating effect and to ascertain whether the anti-biofilm effect was only a result of photodynamic inactivation, non-illuminated control experiments were adjusted to 29.5, 15.5, and 12.5°C.

The population of surviving *C. sakazakii* biofilm cells after LED illumination was first determined in this study. The results showed that LED illumination was able to significantly reduce the population of surviving biofilm cells at 25, 10, and 4°C (**Figure 1**). Besides, previous reports have confirmed the mechanism of LED inactivation against planktonic pathogens. Ghate et al. (2013) and Kumar et al. (2016) provided evidence of the inactivation effect of LED illumination against planktonic *E. coli*, *Salmonella*, *Listeria*, and *S. aureus* based on the reduction in the cell population and reported that LED inactivation is a direct consequence of DNA and cell membrane function loss caused by ROS generated by LED light. Our study thus indicated that, although biofilm could protect a certain number of cells from external hazards, 405 nm LED illumination might still exert its inactivation efficacy against surviving *C. sakazakii* cells via the generation of ROS.

Interestingly, we found that the total reduction of viable biofilm cells between the LED-illuminated groups after 4 h and the controls at 0 h was dependent on temperature, with a 3.5-log (**Figure 1A**), 2.9-log (**Figure 1B**) and 2.2-log (**Figure 1C**) reduction after LED treatment at 25, 10, and 4°C, respectively. This may be because the effect of temperature on the reduction of biofilm cells, especially at 25°C, showed a 1.5-log (**Figure 1A**) reduction for non-illuminated biofilm cells after 4 h, enhancing the inactivation efficacy of 405 nm LED illumination against biofilm cells significantly. However, previous study has reported the opposite phenomenon, which showed that low temperatures could induce the increase the proportion of unsaturated fatty acids in bacteria (Luksiene, 2003). Unsaturated fatty acids are susceptible to ROS generated by cells, thus enhance the inactivation efficacy of LED and resulting in more cell death (Beales, 2004). Hence, the effects of temperature on the efficacy of LED illumination against *C. sakazakii* biofilm should be further confirmed in future studies.

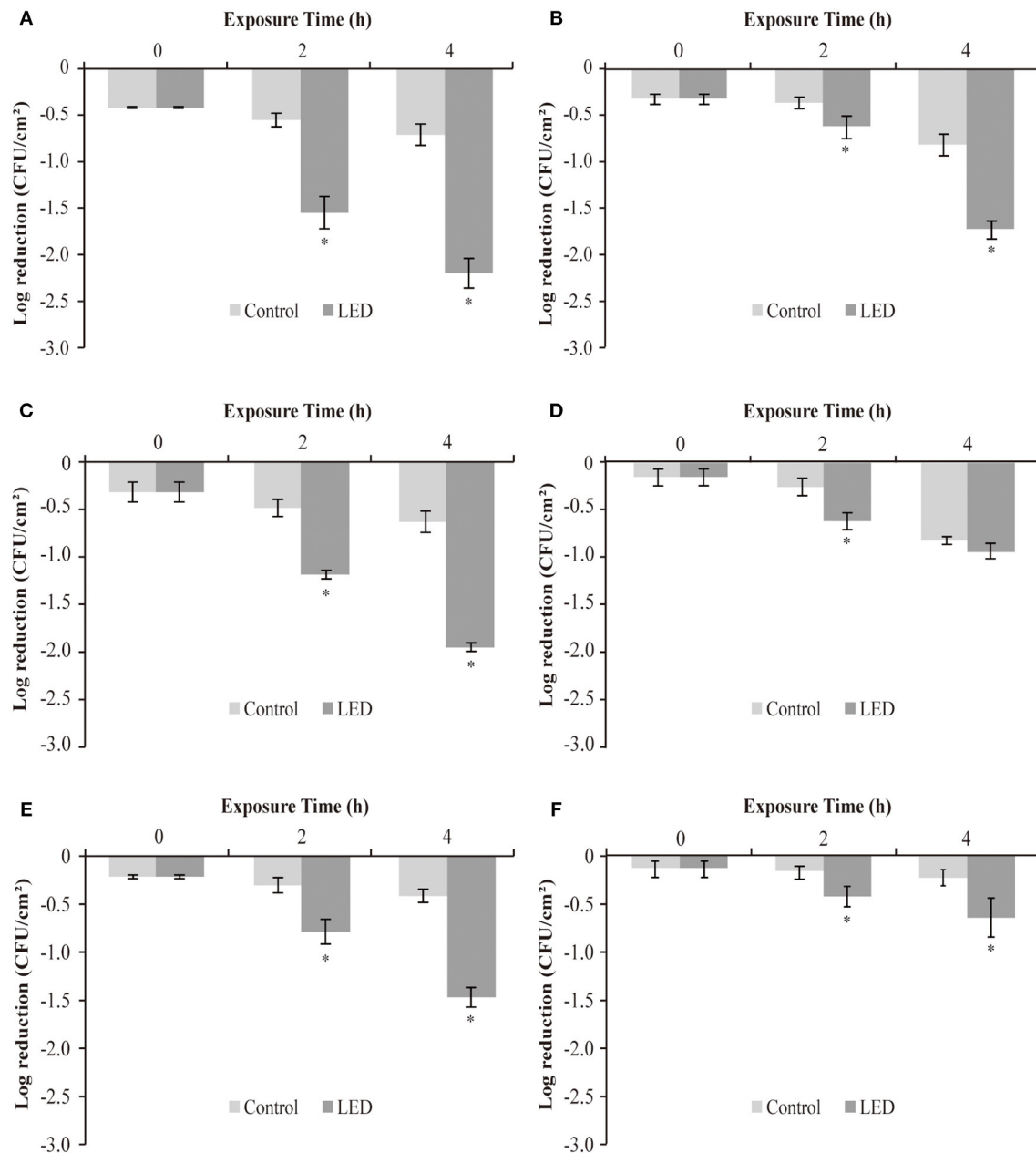


FIGURE 6 | Log reduction between non-illuminated and 405-nm LED-illuminated *C. sakazakii* biofilm cells on stainless steel at 25°C (A,B), 10°C (C,D), and 4°C (E,F), also treated with 100 ppm CHX (A,C,E) and CTPC (B,D,F) for 15 s. The errors bars indicate the standard error of the mean. The asterisk (*) indicates that the difference between non-illuminated control and illuminated biofilm cells population is significant ($P < 0.05$).

An intact biofilm matrix is essential for biofilm to protect pathogen cells from death (Wang et al., 2018). In the current study, the integrity of the biofilm stereoscopic conformation of LED treatment groups was damaged compared with the control groups by observation of CLSM images (Figures 2A–F), and greater damage was observed at 25°C which was consistent with the results of cells population determination (Figures 2A,D). Similarly, Loo et al. (2016) observed that the integrity and thickness of the *S. aureus* biofilm was significantly reduced after

the treatment with 50 µg/mL of silver nanoparticles, as evidenced by CLSM images. Wang et al. (2018) presented the CLSM images of *P. fluorescens* biofilm with a reduced biofilm matrix and killed cells, when treated with 200 mg/L sodium hypochlorite and 40 mg/L acidic electrolyzed water.

As the complement of CLSM, SEM images showed that 405 nm LED illumination caused significant destruction of the biofilm architecture (Figures 2G–L), especially at 25°C (Figures 2G,J), by destroying the complex three-dimensional

structure formed by cell colonies integrated by the network of extracellular matrix. Previous reports also showed the similar destructions to biofilms caused by other antibiofilm strategies, which lead to the detachment of cells. Mamone et al. (2016) found that 5,10,15,20-tetrakis[4-(3-N,N-dimethylammoniumpropoxy)phenyl]porphyrin-mediated photodynamic inactivation could lead to the detachment of parts of the *S. aureus* biofilm and disruption of its architecture, as evidenced by SEM images. Di Poto et al. (2009) also provided SEM images and reported that photodynamic treatment combined with vancomycin caused a significant reduction in the matrix and the size of cell aggregates in *S. aureus* biofilm. Our study provided clear evidence of the reduction of *C. sakazakii* biofilm matrix as well as the destruction of architectural features of biofilm caused by LED illumination, thus making the structure of the entire biofilm less stable and the cells more detached. The current results indicate that the damaged biofilm structure might be caused by reduced cells population which confirmed above or the reduction of biofilm matrix.

To further evaluate the loss of biofilm matrix, ATR-FTIR and glycoconjugates observation were conducted in the current study. **Figure 4** confirmed the removal of polysaccharide and protein by LED treatment, which were two representative components of the biofilm (Misba et al., 2017), and this effect was greatest at 25°C (**Figure 4A**). In similar studies, the removal of EPS compounds (mainly proteins and polysaccharides) from biofilms has been demonstrated by other types of treatment. Lee et al. (2017) reported that the combination of Cu (II) with norspermidine caused significant degradation of EPS (44 and 63% degradation of proteins and polysaccharides, respectively), by calculating the respective bioareas of proteins and polysaccharides using MetaMorph software. Misba et al. (2017) also reported that phenothiazinium dyes could decrease the EPS contents of *Enterococcus faecalis* and *Klebsiella pneumoniae* biofilms based on a Congo red binding assay.

The results of glycoconjugates observation confirmed that LED illumination could significantly reduce the concentration of glycoconjugates (**Figure 3**), especially at 25°C (**Figure 3A**). Paramanantham et al. (2018) reported a 54.93% reduction in the exopolysaccharide content of biofilm after treatment with an amino-functionalized mesoporous silica-rose Bengal nanoconjugate using a Congo red binding assay. The mechanism of action of LED illumination against several intracellular substances has been reported and is thought to involve ROS generated by cells in response to LED light that may react with DNA, proteins, lipids, and other components to produce cytotoxic effects (Luksiene, 2010). Combined the results of CLSM and SEM images, we hypothesize that accumulated ROS generated by LED illumination might also play an important role in the removal of protein and polysaccharide in *C. sakazakii* biofilm, resulting in the detached cells and damaged structure.

The RT-qPCR results showed that LED illumination significantly reduced the transcription level of genes related to *C. sakazakii* biofilm (**Figure 5**). Flagellum mediated motility has been reported to play an important role in initiation of biofilm formation through increasing the likelihood of bacterial interacts with the contacting surfaces as well as providing physical frames

in biofilm matrix (Jung et al., 2019). The *motA*, *motB*, *fliD*, *flhD*, and *flgJ* genes observed in this study have been showed to be responsible for the synthesis process of flagellum that are involved in bacterial biofilm formation. FlhD is a specific activator of flagellin synthesis (Prüß et al., 2001) and FlgJ is a two-domain flagellar protein, with one domain involved in rod assembly and the other playing an enzymatic role as a muramidase (Li et al., 2012). FliD protein is an important protein for the *in vivo* colonization and the formation of functional flagella (Ratthawongjirakul et al., 2016). *motA*, *motB* genes are responsible for the synthesis of flagellin complexes which is important for the motility of bacteria (Kojima and Blair, 2004). Our results indicated that LED could regulate functions of *motA*, *motB*, *fliD*, *flhD*, and *flgJ*, controlling the synthesis of flagellum, thus influencing the bacterial motility and biofilm structure.

Quorum sensing is a cell-cell communication which bacteria use to utilize diverse signal recognition systems and subsequent regulatory mechanisms to achieve timely expression of EPS components during the specific stages of biofilm formation or under specific conditions (Waters et al., 2008). For the *luxR* determined in current study, previous study has reported that it encodes the LuxR-type regulators which is responsible for the regulation of quorum sensing protein synthesis then influence the establishment of biofilm (Hou et al., 2018). The results in current study indicated that LED illumination could control the synthesis of quorum sensing protein which are important for the timely expression of EPS, thereby affecting the biofilm-forming ability of *C. sakazakii* cells. Cellulose is a major component of biofilm matrix and may also act as an adhesion factor (El Hag et al., 2017). *bcsA* and *bcsG* genes are necessary to produce cellulose, and are involved in cell-cell aggregation and biofilm formation (Hu et al., 2015; Anderson et al., 2020). Our study suggested that LED may control the synthesis of cellulose and adhesion ability of *C. sakazakii* cells by regulating the function of *bcsA* and *bcsG*, thus influencing the biofilm forming process.

Some biofilm cells possess a degree of resistance to disinfectants, which increases the difficulty of using disinfectants to eliminate biofilms (Simões et al., 2009). What's worse, the overuse of disinfectants may induce stronger resistance in pathogens and leave harmful residues to environment (Li et al., 2014). Therefore, in current study, we studied how 405 nm LED illumination would influence the resistance of biofilm cells to disinfectant treatment. Two food disinfectants (CTPC and CHX) were selected to determine the effect of LED treatment on the sensitivity of biofilm cells. CHX is a protein synthesis inhibitor (Barros et al., 2015) and CTPC is a quaternary ammonium salt that functions as a disinfectant. Both exert their antibacterial activity by denaturing proteins and enzymes, destroying cell membrane integrity and causing the leakage of cell contents (Imai et al., 2017). **Figure 6** showed that the sensitivity of *C. sakazakii* biofilm cells to CTPC and CHX increased after exposure to the LED. Regarding biofilm resistance, Harper et al. (2019) provided evidence that the extracellular polymer substances generated by biofilms confer resistance to antimicrobial agents through electrostatic and steric interactions that hinder molecular diffusion. Our study

further established that LED illumination may cause damage to the biofilm by denaturing the composition and architectural features of biofilm, reducing the resistance of the biofilm to disinfectants and allowing disinfectant molecules access into cells. In addition, the change in resistance was influenced by both the illumination temperature and the type of disinfectant. The results of current study indicated that 405 nm LED could be used in food industry to eliminate biofilms as the complement of disinfectants to reduce the dosage of disinfectants used and enhance the antibiofilm effect of disinfectants.

CONCLUSION

In conclusion, 405-nm LED illumination was effective at inactivating mature *C. sakazakii* biofilm. Significant reduction of the population of viable biofilm cells was observed after LED illumination. Clear evidence of the structural damage caused by LED was provided by the images of CLSM, SEM and glycoconjugates, which showed the significant destruction of the architectural feature of LED-treated biofilms. Results of ATR-FTIR and RT-qPCR analysis revealed that LED could remove the biofilm compositions (mainly polysaccharide and protein) and influence genes function related to biofilm formation. In addition, the sensitivity of biofilm cells to disinfectants treatment was also observed to increase, enhancing the antibacterial effect of disinfectants against biofilm. Our findings suggested that 405-nm LED illumination has the potential to be administered directly as a new antibacterial method to inactivate *C. sakazakii* biofilm in various food processing applications, such as milk powder processing, packaging tank processing and the cleaning of household brewing utensils. In the future, studies are expected to evaluate

LED inactivation efficacy against biofilms formed by multiple pathogens that attach to various contact surfaces, such as glass, silicone, and Teflon. The combined inactivation efficacy of LED illumination with photosensitizers should also be studied.

DATA AVAILABILITY STATEMENT

The raw data supporting the conclusions of this article will be made available by the authors, without undue reservation.

AUTHOR CONTRIBUTIONS

YH, QP, and CS conceived and designed the experiments. YH, RD, XZ, and JG performed the experiments. YH, QP, and DG analyzed the data. YY and SL contributed reagents/materials/analysis tools. YH and CS wrote the manuscript. All authors contributed to the article and approved the submitted version.

FUNDING

This work was supported by National Natural Science Foundation of China (31801659), General Financial Grant from the China Postdoctoral Science Foundation (No. 2017M623256), and the class General Financial Grant from the Shaanxi Postdoctoral Science Foundation (2018BSHEDZZ150).

SUPPLEMENTARY MATERIAL

The Supplementary Material for this article can be found online at: <https://www.frontiersin.org/articles/10.3389/fmicb.2020.610077/full#supplementary-material>

REFERENCES

- Abdallah, M., Khelissa, O., Ibrahim, A., Benoliel, C., Heliot, L., Dhulster, P., et al. (2015). Impact of growth temperature and surface type on the resistance of *Pseudomonas aeruginosa* and *Staphylococcus aureus* biofilms to disinfectants. *Int. J. Food Microbiol.* 214, 38–47. doi: 10.1016/j.ijfoodmicro.2015.07.022
- Abdesselam, K., and Pagotto, F. (2014). Bacteria: *Cronobacter* (*Enterobacter*) *sakazakii* and other *Cronobacter* spp. *Encycl. Food Safety* 1, 424–432. doi: 10.1016/B978-0-12-378612-8.00097-4
- Anderson, A. C., Burnett, A. J. N., Hiscock, L., Maly, K. E., and Weadge, J. T. (2020). The *Escherichia coli* cellulose synthase subunit G (BcsG) is a Zn²⁺-dependent phosphoethanolamine transferase. *J. Biol. Chem.* 295, 6225–6235. doi: 10.1074/jbc.RA119.011668
- Barros, J., Grenho, L., Fernandes, M. H., Manuel, C. M., Melo, L. F., Nunes, O. C., et al. (2015). Anti-sessile bacterial and cytocompatibility properties of CHX-loaded nanohydroxyapatite. *Colloid. Surf. B* 130, 305–314. doi: 10.1016/j.colsurfb.2015.04.034
- Bayoumi, M. A., Kamal, R. M., Abd El Aal, S. F., and Awad, E. I. (2012). Assessment of a regulatory sanitization process in Egyptian dairy plants in regard to the adherence of some food-borne pathogens and their biofilms. *Int. J. Food Microbiol.* 158, 225–231. doi: 10.1016/j.ijfoodmicro.2012.07.021
- Beales, N. (2004). Adaptation of microorganisms to cold temperatures, weak acid preservatives, low pH, and osmotic stress: a review. *Compr. Rev. Food Sci. F* 3, 1–20. doi: 10.1111/j.1541-4337.2004.tb00057.x
- Beuchat, L. R., Kim, H., Gurtler, J. B., Lin, L. C., Ryu, J. H., and Richards, G. M. (2009). *Cronobacter sakazakii* in foods and factors affecting its survival, growth, and inactivation. *Int. J. Food Microbiol.* 136, 204–213. doi: 10.1016/j.ijfoodmicro.2009.02.029
- da Silva, E. P., and De Martinis, E. C. P. (2013). Current knowledge and perspectives on biofilm formation: the case of *Listeria monocytogenes*. *Appl. Microbiol. Biotechnol.* 97, 957–968. doi: 10.1007/s00253-012-4611-1
- Davies, D. (2003). Understanding biofilm resistance to antibacterial agents. *Nat. Rev. Drug Discov.* 2, 114–122. doi: 10.1038/nrd1008
- Di Poto, A., Sbarra, M. S., Provenza, G., Visai, L., and Speziale, P. (2009). The effect of photodynamic treatment combined with antibiotic action or host defence mechanisms on *Staphylococcus aureus* biofilms. *Biomaterials* 30, 3158–3166. doi: 10.1016/j.biomaterials.2009.02.038
- El Hag, M., Feng, Z., Su, Y., Wang, X., Yassin, A., Chen, S., et al. (2017). Contribution of the *csgA* and *bcsA* genes to *Salmonella enterica* serovar Pullorum biofilm formation and virulence. *Avian Pathol.* 46, 541–547. doi: 10.1080/03079457.2017.1324198
- Ghate, V., Zelinger, E., Shoyhet, H., and Hayouka, Z. (2019). Inactivation of *Listeria monocytogenes* on paperboard, a food packaging material, using 410 nm light emitting diodes. *Food Control* 96, 281–290. doi: 10.1016/j.foodcont.2018.09.026
- Ghate, V. S., Ng, K. S., Zhou, W., Yang, H., Khoo, G. H., Yoon, W. B., et al. (2013). Antibacterial effect of light emitting diodes of visible wavelengths on selected foodborne pathogens at different illumination temperatures. *Int. J. Food Microbiol.* 166, 399–406. doi: 10.1016/j.ijfoodmicro.2013.07.018
- Ha, J. W., and Kang, D. H. (2014). Synergistic bactericidal effect of simultaneous near-infrared radiant heating and UV radiation against *Cronobacter sakazakii* in powdered infant formula. *Appl. Environ. Microbiol.* 80, 1858–1863. doi: 10.1128/AEM.03825-13

- Harouna, S., Carramiñana, J. J., Navarro, F., Pérez, M. D., Calvo, M., and Sánchez, L. (2015). Antibacterial activity of bovine milk lactoferrin on the emerging foodborne pathogen *Cronobacter sakazakii*: effect of media and heat treatment. *Food Control* 47, 520–525. doi: 10.1016/j.foodcont.2014.07.061
- Harper, R. A., Carpenter, G. H., Proctor, G. B., Harvey, R. D., Gambogi, R. J., Geonnotti, A. R., et al. (2019). Diminishing biofilm resistance to antimicrobial nanomaterials through electrolyte screening of electrostatic interactions. *Colloid. Surf. B* 173, 392–399. doi: 10.1016/j.colsurfb.2018.09.018
- Hou, H., Wang, Y., Zhang, G., Zhu, Y., Xu, L., and Hao, H., et al. (2018). Effects of sulfide flavors on AHL-Mediated quorum sensing and biofilm formation of *Hafnia alvei*. *J. Food Sci.* 83, 2550–2559. doi: 10.1111/1750-3841.14345
- Hu, L., Grim, C. J., Franco, A. A., Jarvis, K. G., Sathyamoorthy, V., Kothary, M. H., et al. (2015). Analysis of the cellulose synthase operon genes, *bcsA*, *bcsB*, and *bcsC* in *Cronobacter* species: prevalence among species and their roles in biofilm formation and cell-cell aggregation. *Food Microbiol.* 52, 97–105. doi: 10.1016/j.fm.2015.07.007
- Imai, H., Kita, F., Ikesugi, S., Abe, M., Sogabe, S., Nishimura-Danjobara, Y., et al. (2017). Cetylpyridinium chloride at sublethal levels increases the susceptibility of rat thymic lymphocytes to oxidative stress. *Chemosphere* 170, 118–123. doi: 10.1016/j.chemosphere.2016.12.023
- Jung, Y. C., Lee, M. A., and Lee, K. H. (2019). Role of flagellin-homologous proteins in biofilm formation by pathogenic *Vibrio* species. *mBio* 10, e01793–e01719. doi: 10.1128/mBio.01793-19
- Kang, J., Liu, L., Liu, M., Wu, X., and Li, J. (2018). Antibacterial activity of gallic acid against *Shigella flexneri* and its effect on biofilm formation by repressing *mdoH* gene expression. *Food Control* 94, 147–154. doi: 10.1016/j.foodcont.2018.07.011
- Kim, H., Ryu, J. H., and Beuchat, L. R. (2006). Attachment of and biofilm formation by *Enterobacter sakazakii* on stainless steel and enteral feeding tubes. *Appl. Environ. Microbiol.* 72:5846. doi: 10.1128/AEM.00654-06
- Kim, Y., Kim, H., Beuchat, L. R., and Ryu, J. H. (2019). Inhibition of *Listeria monocytogenes* using biofilms of non-pathogenic soil bacteria (*Streptomyces* spp.) on stainless steel under desiccated condition. *Food Microbiol.* 79, 61–65. doi: 10.1016/j.fm.2018.11.007
- Kojima, S., and Blair, D. F. (2004). Solubilization and purification of the MotA/MotB complex of *Escherichia coli*. *Biochemistry* 43:26. doi: 10.1021/bi035405l
- Krames, M., and Grandjean, N. (2017). Light-emitting diode technology and applications: introduction. *Photonics Res.* 5, 6–7. doi: 10.1364/PRJ.5.00LED1
- Kumar, A., Ghate, V., Kim, M. J., Zhou, W., Khoo, G. H., and Yuk, H. G. (2016). Antibacterial efficacy of 405, 460, and 520 nm light emitting diodes on *Lactobacillus plantarum*, *Staphylococcus aureus* and *Vibrio parahaemolyticus*. *J. Appl. Microbiol.* 120, 49–56. doi: 10.1111/jam.12975
- Kuo, L. S., Wang, B. J., He, Y. S., and Weng, Y. M. (2013). The effects of ultraviolet light irradiation and drying treatments on the survival of *Cronobacter* spp. (*Enterobacter sakazakii*) on the surfaces of stainless steel, Teflon and glass. *Food Control* 30, 106–110. doi: 10.1016/j.foodcont.2012.06.015
- Lee, H.-J., Seo, J., Kim, M. S., and Lee, C. (2017). Inactivation of biofilms on RO membranes by copper ion in combination with norspermidine. *Desalination*, 424, 95–101. doi: 10.1016/j.desal.2017.09.034
- Li, R., Kuda, T., and Yano, T. (2014). Effect of food residues on efficiency of surfactant disinfectants against food related pathogens adhered on polystyrene and ceramic surfaces. *LWT Food Sci. Technol.* 57, 200–206. doi: 10.1016/j.lwt.2013.11.018
- Li, X., Xu, J., Xie, Y., Qiu, Y., Fu, S., Yuan, X., et al. (2012). Vaccination with recombinant flagellar proteins *FlgJ* and *FliN* induce protection against *Brucella abortus* 544 infection in BALB/c mice. *Vet. Microbiol.* 161, 137–144. doi: 10.1016/j.vetmic.2012.07.016
- Ling, N., Forsythe, S., Wu, Q., Ding, Y., Zhang, J., and Zeng, H. (2020). Insights into *Cronobacter sakazakii* biofilm formation and control strategies in the food industry. *Engineering*, 6, 393–405. doi: 10.1016/j.eng.2020.02.007
- Livak, K. J., and Schmittgen, T. D. (2001). Analysis of relative gene expression data using real-time quantitative PCR and the $2^{-\Delta\Delta CT}$ method. *Methods* 25, 402–408. doi: 10.1006/meth.2001.1262
- Loo, C. Y., Rohanizadeh, R., Young, P. M., Traini, D., Cavaliere, R., Whitchurch, C. B., et al. (2016). Combination of silver nanoparticles and curcumin nanoparticles for enhanced anti-biofilm activities. *J. Agric. Food Chem.* 64, 2513–2522. doi: 10.1021/acs.jafc.5b04559
- Luksiene, Z. (2003). Photodynamic therapy: mechanism of action and ways to improve the efficiency of treatment. *Medicina* 39, 1137–1150. doi: 10.1590/S0100-40422002000500016
- Luksiene, Z. (2010). Photosensitization and food safety. *Chem. Technol.* 4, 62–65. doi: 10.1081/E-EBAF-120045486
- Mamone, L., Ferreyra, D. D., Gándara, L., Di Venosa, G., Vallecorsa, P., Sáenz, D., et al. (2016). Photodynamic inactivation of planktonic and biofilm growing bacteria mediated by a meso-substituted porphyrin bearing four basic amino groups. *J. Photochem. Photobiol. B* 161, 222–229. doi: 10.1016/j.jphotobiol.2016.05.026
- McKenzie, K., Maclean, M., Timoshkin, I. V., Endarko, E., MacGregor, S. J., and Anderson, J. G. (2013). Photoinactivation of bacteria attached to glass and acrylic surfaces by 405 nm light: potential application for biofilm decontamination. *Photochem. Photobiol.* 89, 927–935. doi: 10.1111/php.12077
- Misba, L., Zaidi, S., and Khan, A. U. (2017). A comparison of antibacterial and antibiofilm efficacy of phenothiazinium dyes between Gram positive and Gram negative bacterial biofilm. *Photodiagn. Photodyn.* 18, 24–33. doi: 10.1016/j.pdpdt.2017.01.177
- Moloney, M. G. (2016). Natural products as a source for novel antibiotics. *Trends Pharmacol. Sci.* 37, 689–701. doi: 10.1016/j.tips.2016.05.001
- Paramanathan, P., Antony, A. P., Sruthil Lal, S. B., Sharan, A., Syed, A., Ahmed, M., et al. (2018). Antimicrobial photodynamic inactivation of fungal biofilm using amino functionalized mesoporous silica-rose bengal nanoconjugate against *Candida albicans*. *Sci. Afr.* 1:e00007. doi: 10.1016/j.sciaf.2018.e00007
- Park, J. H., Lee, J. H., Cho, M. H., Herzberg, M., and Lee, J. (2012). Acceleration of protease effect on *Staphylococcus aureus* biofilm dispersal. *FEMS Microbiol. Lett.* 335, 31–38. doi: 10.1111/j.1574-6968.2012.02635.x
- Prüß, B. M., Liu, X., Hendrickson, W., and Matsumura, P. (2001). *FlhD/FlhC*-regulated promoters analyzed by gene array and *lacZ* gene fusions. *FEMS Microbiol. Lett.* 197, 91–97. doi: 10.1016/S0378-1097(01)00092-1
- Quilès, F., Polyakov, P., Humbert, F., and Francius, G. J. B. (2012). Production of extracellular glycogen by *Pseudomonas fluorescens*: spectroscopic evidence and conformational analysis by biomolecular recognition. *Biomacromolecules* 13:2118. doi: 10.1021/bm300497c
- Quishida, C. C. C., De Oliveira Mima, E. G., Jorge, J. H., Vergani, C. E., Bagnato, V. S., and Pavarina, A. C. (2016). Photodynamic inactivation of a multispecies biofilm using curcumin and LED light. *Lasers Med. Sci.* 31, 997–1009. doi: 10.1007/s10103-016-1942-7
- Rathawongjirakul, P., Thongkerd, V., and Chaicumpa, W. (2016). The impacts of a *flhD* mutation on the biofilm formation of *Helicobacter pylori*. *Asian Pac. J. Trop. Bio.* 6, 1008–1014. doi: 10.1016/j.apjtb.2016.10.005
- Reich, F., König, R., von Wiese, W., and Klein, G. (2010). Prevalence of *Cronobacter* spp. in a powdered infant formula processing environment. *Int. J. Food Microbiol.* 140, 214–217. doi: 10.1016/j.ijfoodmicro.2010.03.031
- Simões, M., Bennett, R. N., and Rosa, E. A. S. (2009). Understanding antimicrobial activities of phytochemicals against multidrug resistant bacteria and biofilms. *Nat. Prod. Rep.* 26, 746–757. doi: 10.1039/b821648g
- Simões, M., Simões, L. C., and Vieira, M. J. (2010). A review of current and emergent biofilm control strategies. *LWT Food Sci. Technol.* 43, 573–583. doi: 10.1016/j.lwt.2009.12.008
- Stephan, R., Grim, C. J., Gopinath, G. R., Mammel, M. K., Sathyamoorthy, V., Trach, L. H., et al. (2014). Re-examination of the taxonomic status of *Enterobacter helveticus*, *Enterobacter pulveris* and *Enterobacter turicensis* as members of the genus *Cronobacter* and their reclassification in the genera *Franconibacter* gen. nov. and *Siccibacter* gen. nov. as *Franconibacter helveticus* comb. nov., *Franconibacter pulveris* comb. nov., and *Siccibacter turicensis* comb. nov., respectively. *Int. J. Food Microbiol.* 64, 3402–3410. doi: 10.1099/ijfs.0.059832-0
- Tong, L., Jiao, R., Zhang, X., Ou, D., Wang, Y., Zhang, J., et al. (2018). Inhibitory effects of chitosan on *Cronobacter malonaticus* cells and biofilm formation. *LWT-Food Sci. Technol.* 97, 302–307. doi: 10.1016/j.lwt.2018.07.008
- Wang, H., Cai, L., Li, Y., Xu, X., and Zhou, G. (2018). Biofilm formation by meat-borne *Pseudomonas fluorescens* on stainless steel and its resistance to disinfectants. *Food Control* 91, 397–403. doi: 10.1016/j.foodcont.2018.04.035
- Waters, C. M., Lu, W., Rabinowitz, J. D., and Bassler, B. L. (2008). Quorum sensing controls biofilm formation in *Vibrio cholerae* through modulation of cyclic di-GMP levels and repression of *vpsT*. *J. Bacteriol.* 190, 2527–2536. doi: 10.1128/JB.01756-07

- Yan, Q. Q., Condell, O., Power, K., Butler, F., Tall, B. D., and Fanning, S. (2012). *Cronobacter* species (formerly known as *Enterobacter sakazakii*) in powdered infant formula: a review of our current understanding of the biology of this bacterium. *J. Appl. Microbiol.* 113, 1–15. doi: 10.1111/j.1365-2672.2012.05281.x
- Yang, Y., Kumar, A., Zheng, Q., and Yuk, H. G. (2015). Preacclimation alters *Salmonella Enteritidis* surface properties and its initial attachment to food contact surfaces. *Colloid. Surf. B.* 128, 577–585. doi: 10.1016/j.colsurfb.2015.03.011
- Ye, Y., Li, H., Wu, Q., Zhang, J., and Lu, Y. (2014). The *Cronobacter* spp. in milk and dairy products: detection and typing. *Int. J. Dairy Technol.* 67, 167–175. doi: 10.1111/1471-0307.12111

Conflict of Interest: The authors declare that the research was conducted in the absence of any commercial or financial relationships that could be construed as a potential conflict of interest.

Copyright © 2020 Huang, Pei, Deng, Zheng, Guo, Guo, Yang, Liang and Shi. This is an open-access article distributed under the terms of the Creative Commons Attribution License (CC BY). The use, distribution or reproduction in other forums is permitted, provided the original author(s) and the copyright owner(s) are credited and that the original publication in this journal is cited, in accordance with accepted academic practice. No use, distribution or reproduction is permitted which does not comply with these terms.



First Report on the Rapid Detection and Identification of Methicillin-Resistant *Staphylococcus aureus* (MRSA) in Viable but Non-culturable (VBNC) Under Food Storage Conditions

OPEN ACCESS

Edited by:

Zhenbo Xu,
University of Tennessee Health
Science Center (UTHSC),
United States

Reviewed by:

Wensen Jiang,
Cedars Sinai Medical Center,
United States
Yuting Tian,
Fujian Agriculture and Forestry
University, China
Hao Jianxiong,
Hebei University of Science
and Technology, China

*Correspondence:

Yimin Zou
2314022@zju.edu.cn
Tengyi Huang
h-hty@hotmail.com

[†]These authors have contributed
equally to this work

Specialty section:

This article was submitted to
Food Microbiology,
a section of the journal
Frontiers in Microbiology

Received: 10 October 2020

Accepted: 23 November 2020

Published: 07 January 2021

Citation:

Ou A, Wang K, Mao Y, Yuan L,
Ye Y, Chen L, Zou Y and Huang T
(2021) First Report on the Rapid
Detection and Identification
of Methicillin-Resistant
Staphylococcus aureus (MRSA)
in Viable but Non-culturable (VBNC)
Under Food Storage Conditions.
Front. Microbiol. 11:615875.
doi: 10.3389/fmicb.2020.615875

Aifen Ou^{1†}, Kan Wang^{2†}, Yanxiong Mao³, Lei Yuan⁴, Yanrui Ye⁵, Ling Chen⁶, Yimin Zou^{1*}
and Tengyi Huang^{7*}

¹ Department of Food, Guangzhou City Polytechnic, Guangzhou, China, ² Center for Translational Medicine, The Second Affiliated Hospital of Shantou University Medical College, Shantou, China, ³ Key Laboratory of Respiratory Disease of Zhejiang Province, Department of Respiratory and Critical Care Medicine, Second Affiliated Hospital of Zhejiang University School of Medicine, Hangzhou, China, ⁴ College of Food Science and Engineering, Yangzhou University, Yangzhou, China, ⁵ School of Biological Science and Engineering, South China University of Technology, Guangzhou, China, ⁶ School of Food Science and Engineering, Guangdong Province Key Laboratory for Green Processing of Natural Products and Product Safety, South China University of Technology, Guangzhou, China, ⁷ Department of Laboratory Medicine, The Second Affiliated Hospital of Shantou University Medical College, Shantou, China

Formation of viable but non-culturable (VBNC) status in methicillin-resistant *Staphylococcus aureus* (MRSA) has never been reported, and it poses a significant concern for food safety. Thus, this study aimed to firstly develop a rapid, cost-effective, and efficient testing method to detect and differentiate MRSA strains in the VBNC state and further apply this in real food samples. Two targets were selected for detection of MRSA and toxin, and rapid isothermal amplification detection assays were developed based on cross-priming amplification methodology. VBNC formation was performed for MRSA strain in both pure culture and in artificially contaminated samples, then propidium monoazide (PMA) treatment was further conducted. Development, optimization, and evaluation of PMA-crossing priming amplification (CPA) were further performed on detection of MRSA in the VBNC state. Finally, application of PMA-CPA was further applied for detection on MRSA in the VBNC state in contaminated food samples. As concluded in this study, formation of the VBNC state in MRSA strains has been verified, then two PMA-CPA assays have been developed and applied to detect MRSA in the VBNC state from pure culture and food samples.

Keywords: VBNC (viable but non-culturable), MRSA – methicillin-resistant *Staphylococcus aureus*, food storage, *mecA*, *femA*

INTRODUCTION

Food safety has been found to be a leading concern for public health worldwide, and food pathogens remain the major factor as a causative for foodborne diseases (Deng et al., 2015a). A few microorganisms are top food pathogens, among which methicillin-resistant *Staphylococcus aureus* (MRSA) is an important one (Monteiro et al., 1997; Corrente et al., 2007). Since the first

report in 1961, MRSA has become one of the leading human pathogens (Salisbury et al., 1997; Xu et al., 2010a; Wang et al., 2012). Firstly considered to be a major nosocomial pathogen, MRSA has been found to be an important foodborne pathogen in recent years. Aside from its biofilm formation capability and thus known to be a typical biofilm former, MRSA could also produce different types of toxins and is responsible for various human diseases (Kadariya et al., 2014; Miao et al., 2017a,b). In recent years, a number of foodborne outbreaks were reported to be caused by MRSA (Voss et al., 2005; Xu et al., 2017, 2019).

Prior to consumption, the most effective way to prevent food contamination by MRSA is accurate and rapid detection (Fang et al., 2009; Zhao et al., 2010b,c; Xu et al., 2020a). Currently, the gold standard for identification of MRSA is culturing and colony-forming unit (CFU) counting (Felten et al., 2002; Deng et al., 2015b). Routine detection will provide results on the random selected food samples as an indicator for the microorganisms inside such samples. However, such methodologies are based on the culturing, and microorganisms are capable of formation of the viable but non-culturable (VBNC) state. When entering the VBNC state, microorganisms are no longer culturable and thus yield false-negative results by culturing (Xu et al., 2011b; Liu et al., 2018a,b,d). Not limited within food safety, culturing is also the routine detection method for clinical strains (Wang et al., 2014, 2018; Xie et al., 2017a,b). Therefore, formation of the VBNC state is an important issue for both food safety and clinicians.

Concerning the VBNC formation and identification, rapid detection of the VBNC state of MRSA is of urgent necessity and importance, along with the formation of the VBNC state (Liu et al., 2016c, 2017a,b,c). In this study, formation of the VBNC state has been performed on MRSA strains, then development and evaluation of an isothermal nucleic acid amplification-based propidium monoazide (PMA) detection assay have been conducted on MRSA.

MATERIALS AND METHODS

Bacterial Strains and Culturing

A total of five MRSA strains and 18 non-MRSA strains, including *Escherichia coli*, *Salmonella*, *Listeria monocytogenes*, *Vibrio parahaemolyticus*, and *Pseudomonas aeruginosa*, are included in this study. All strains had been previously identified by PCR and sequencing on the staphylococci species-specific target *femA*, methicillin-resistant gene *mecA*.

Study Design

Two targets were selected to differentiate MRSA and non-MRSA strains, and one more target was based on an important toxin factor. In detail, the protocol was designed to (i) distinguish between *S. aureus* and coagulase-negative staphylococci or non-*S. aureus* strains based on amplification of the *S. aureus*-specific *femA* gene and (ii) distinguish methicillin-resistant *Staphylococcus* and methicillin-susceptible *Staphylococcus* based on amplification of the *mecA* gene. The sequences are as follows: *femA*: 4s-TCAAA TCGCGGTCCAGTG; 5a-AACCAATCATTACCAGCA; 2a/1s-T

ACCTGTAATCT CGCCAT AACATCGTTGTCTATACCT; 2a-TACCTGTAATCTCGCCAT; 3a-GGTAAATATGGATCGATA TG. *mecA*: 4s-GCGATAATGGTGAAGTAG; 5a-GATCAATGT TACCGTAGTT; 2a/1s-TTACGATCCTGAATGTTT ATGACT GAA CGTCCGATA; 2a-TTACGATCCTGAATGTTT; 3a-TCTT TAACGCCTAAACTA.

Strains Processing and Template DNA Preparation

Development and evaluation of CPA assay were performed on a total of five MRSA strains and 18 non-MRSA strains, of which *S. aureus* strains are isolated from raw milk and pork. All strains used in this study had been preliminarily identified. Crude DNA from MRSA and other bacteria strains used as template for amplification was prepared from overnight trypticase soy broth (TSB, Huankai Microbial, Guangzhou, China) culture, and DNA was extracted using a DNA Extraction Kit (Dongsheng Biotech, Guangzhou, China) according to the manufacturer's instructions. The concentration and quality of the extracted DNA were measured using a Nano Drop 2000 (Thermo Fisher Scientific Inc., Waltham, MA, United States) at 260 and 280 nm. The processed DNA was stored at -20°C until further use.

Development, Optimization, and Evaluation of CPA Assays

CPA reaction was carried out in a total of 26- μl reaction mixture containing 20 mM Tris-HCl, 10 mM $(\text{NH}_4)_2\text{SO}_4$, 10 mM KCl, 8 mM MgSO_4 , 0.1% Tween 20, 0.7 M betaine (Sigma, United States), 1.4 mM of dNTP mix, 8 U of Bst DNA polymerase large fragment (NEB, United States), 1.0 μM primer of 2a/1s, 0.5 μM (each) primer of 2a and 3a, 0.6 μM (each) primer of 4s and 5a, 1 μl DNA template, and 1 μl mixed chromogenic agent, and the total reaction mixture was made up to 26 μl with nuclease-free water (Xu G. et al., 2012; Zhang et al., 2015). The mixed chromogenic agent consists of 0.13 mM calcein and 15.6 mM $\text{MnCl}_2 \cdot 4\text{H}_2\text{O}$. CPA reaction system was carried out at 63°C for 1 h and then heated at 80°C for 2 min to stop the amplification reaction. The negative control was performed by the 1 μl nuclease-free water instead of DNA template. PCR reaction was performed in a total 25 μl reaction system with five primers (4s, 5a, 2a, 1s, 2a, and 3a). The protocol of PCR was 95°C for 5 min, followed by 32 cycles of amplification at 95°C for 30 s, 52°C for 30 s, 72°C for 35 s, and final amplification at 72°C for 5 min. The specificity of primers was evaluated by amplification of the genomic DNA extracted from five MRSA strains isolated from raw milk and pork and 18 non-target bacteria, including *E. coli*, *Salmonella*, *L. monocytogenes*, *V. parahaemolyticus*, and *P. aeruginosa*. To study the sensitivity reaction on the DNA solution, 10-fold serial dilutions of total genomic DNA were subjected to CPA in triplicate. The products were detected by 1.5% agarose gel electrophoresis. The CPA assays for *femA* and *mecA* were established using MRSA 10071. The amplified products were detected by 1.5% agarose gel electrophoresis, and the bands were observed under UV light. In addition, 1 μl mixture chromogenic agent (MgCl_2 and calcein) were added

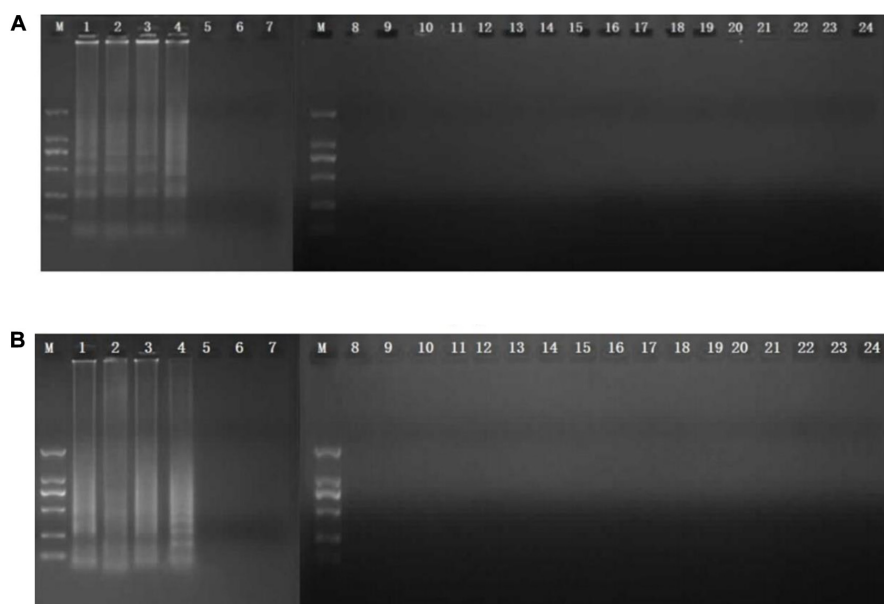


FIGURE 1 | Specificity of CPA detection for different strains by 1.5% agarose gel electrophoresis and mixed chromogenic agent. For *femA* (A) and *mecA* (B) genes, lanes/tubes 1–5, *Staphylococcus aureus* 971311004, 0313113664, 0314030668, and 10071; lanes/tubes 5–24; non-MRSA strains, negative control.

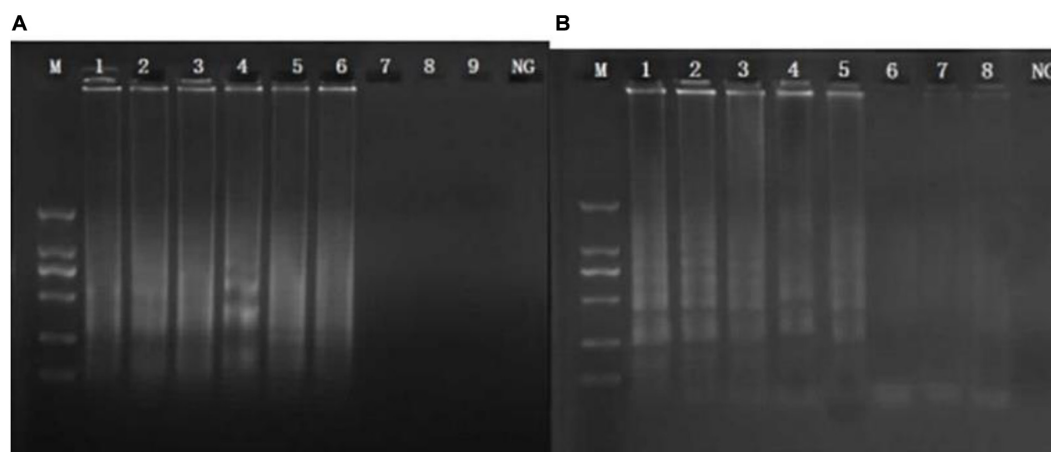


FIGURE 2 | Sensitivity of the CPA assay in genomic DNA by 1.5% agarose gel electrophoresis. Sensitivity from 10,071 of *femA* (A) and *mecA* (B) genes. M, DNA marker; lanes 1–8, 3.0 ng/μl, 300 pg/μl, 30 pg/μl, 3 pg/μl, 300 fg/μl, 30 fg/μl, 3 fg/μl, and 300 ag/μl; NG, negative control.

into the reaction system, wherein the dye color simultaneously changed from original to green in the positive sample or water retained the original orange color. The CPA assay was evaluated for its specificity using five MRSA strains and non-MRSA strains as control. Of these strains, only MRSA strains were amplified. No cross-reaction was found with all the related non-MRSA microorganism strains, indicating the high specificity of the designed primers (Figures 1, 2).

Artificial Contamination of Food Samples

In this study, Cantonese pastry has been selected to be the food sample for artificial contamination and further detection. Rice

and flour products are the major food type in China, which takes up the largest consumption market. Cantonese pastry is one of the most common for rice and flour products in China and thus was selected. For artificial contamination, 25 g of frozen Cantonese pastry (Guangzhou Restaurant, Guangzhou, China) was added to 225 ml of 0.9% NaCl, which was sterilized as food samples and contaminated by MRSA strains. The strains were incubated overnight ($\sim 10^8$ CFU/ml) in TSB (Huankai Microbial, Guangzhou, China), which were mixed with the food samples to the final concentration of $10\sim 10^8$ CFU/ml. The contaminated food samples were subjected to complex preprocessing, then extracted with a rapid DNA processing, as described previously.

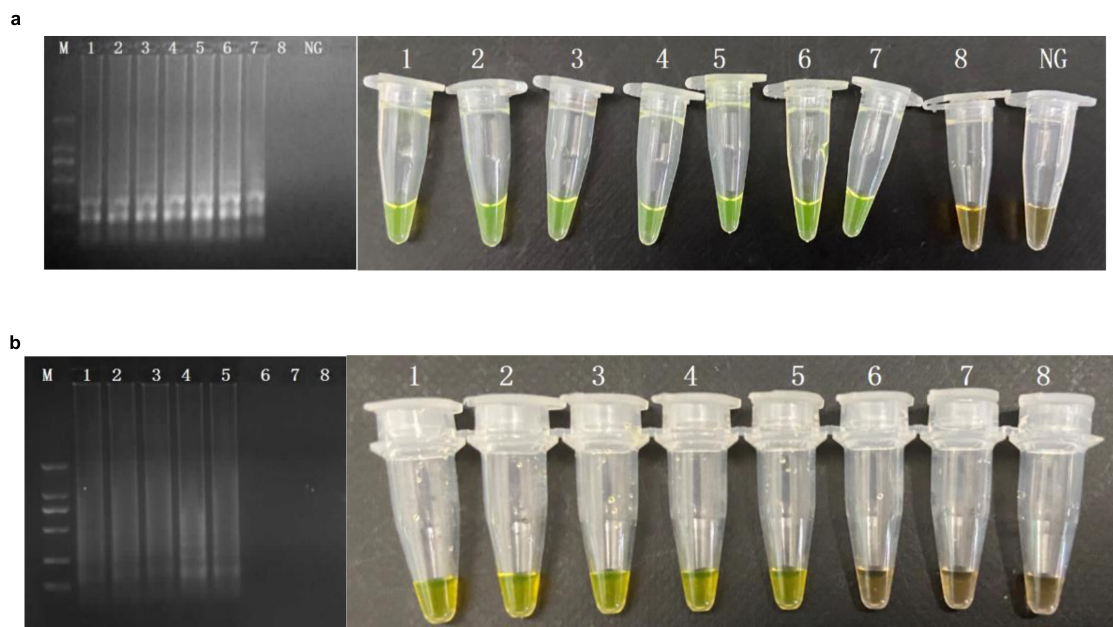


FIGURE 3 | Sensitivity of the CPA by 1.5% agarose gel electrophoresis in food samples of *femA* (a), *mecA* (b). M, DNA marker; lanes 1–8, 10^7 CFU/ml, 10^6 CFU/ml, 10^5 CFU/ml, 10^4 CFU/ml, 10^3 CFU/ml, 10^2 CFU/ml, 10^1 CFU/ml, 1 CFU/ml; NG, negative control.

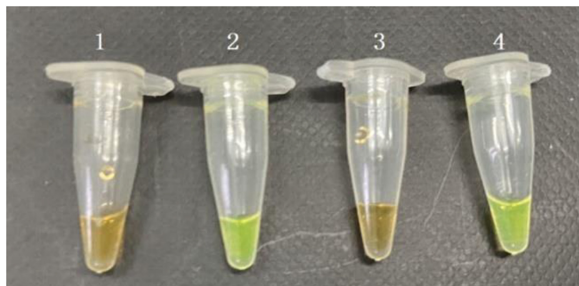


FIGURE 4 | Detection of the viable but non-culturable (VBNC) state of *S. aureus* in pure cultures and food samples by PMA-CPA assays. 1, dead cells in pure cultures; 2, VBNC cells in pure cultures; 3, dead cells in food samples; 4, VBNC cells in food samples.

Formation of Viable but Non-culturable State and Application of PMA-CPA

The developed CPA assays were utilized to detect the VBNC cells. The experimental strains were cultured to the exponential growth period. To induce the VBNC state of MRSA, the culture was diluted to the final concentration at 10^8 CFU/ml with food homogenate (Cantonese pastry, steamed bread, rice flour; Guangzhou Restaurant, Guangzhou, China). Then, they were stored at -20°C to induce the VBNC state for further use of PMA-CPA. The trend of the number of culturable bacteria was used to make sure that the cells enter into culturable state. And culturable and viable cell enumerations were preformed every 3 days by traditional culture method. The LIVE/DEAD BacLight™ kit (Thermo Fisher Scientific, United States) was performed under fluorescence microscope after the culturable

colonies no longer form on agar medium. After confirmation of the VBNC state, PMA-CPA has been applied for detection.

RESULTS

Development of CPA Assays

The analytical sensitivity of the CPA assay for MRSA was measured using 10-fold serial dilutions of MRSA. After CPA reaction, it revealed that the DNA detection limit of CPA were 30 fg/ μl for *femA*, 300 fg/ μl for *mecA* (Figures 1, 2). These results indicated that the analytical sensitivity and specificity of CPA are distinctly higher than those of conventional PCR.

Application of the CPA Assays in Artificially Contaminated Food

Sensitivity values of CPA and PCR assays for MRSA in food samples (rice, frozen pastry, and steamed bread) were 10^2 CFU/ml and 10^4 CFU/ml (Figure 3).

Formation of Viable but Non-culturable and Evaluation of PMA-CPA Assay and in Food Samples

The VBNC status of MRSA has been studied according to a previous procedure. After confirmation of the VBNC status, the VBNC cell was added to pure culture and food samples. The PMA agent was used at the concentration of 5 $\mu\text{g}/\text{ml}$. Subsequently, the detection samples mixed with PMA were incubated in the dark at room temperature for 10 min before the tubes were placed horizontally on ice exposed to a halogen lamp (650 W) at a distance of 15 cm for 15 min to complete the combination

of DNA and PMA. The mixed samples were centrifuged at 10,000 rpm for 5 min, and the precipitation under the tubes was processed by the rapid DNA processing methodology, which were prepared as DNA samples for PMA-CPA (Figure 4). The results showed that the VBNC cells in pure culture and food samples both can be detected by PMA-CPA assays.

DISCUSSION

Methicillin-resistant *Staphylococcus aureus* is considered one of the leading causes of food poisoning worldwide (Weese et al., 2010). A rapid and accurate detection method is required to detect MRSA as a result of its prevalence in various food samples (Crago et al., 2012). In this study, new approaches were evaluated for accurate detection of MRSA from food samples (Xu et al., 2009, 2020b, Xu Z. et al., 2012). CPA assays were developed utilizing a visual method. As a novel nucleic acid amplification method, CPA assays are both successfully performed to detect MRSA if there is co-occurrence of *S. aureus*-specific *femA* and methicillin-resistance marker *mecA* (Tacconelli et al., 2009; Miao et al., 2019). Since the invention of CPA technology, it has been employed for the detection of various bacteria. However, CPA is not suitable for the detection of multiple genes (*femA*, *mecA*) in the same system due to products that would differ in size (Xu et al., 2008, 2010b, 2011a; Yu et al., 2016; Liu et al., 2017d). Therefore, we established two CPA assays targeting *mecA* and *femA* to replace a single or multiple PCR assay.

Current methods available for detection of MRSA, including routine standard procedures (colony morphology, Gram staining, and testing of catalase, hyaluronidase, and coagulase), the Vitek 2 automated system, the API-Staph kit, immunological assays, mass spectrometry, and PCR (regular PCR as well as quantitative PCR), are time-consuming and required highly trained personnel (Graveland et al., 2011; Zhao et al., 2011; Liu et al., 2016a,b). This stricture can be overcome as the results from CPA methods require only a conventional heating block or

a water bath, and the result can be judged through observing color change by adding SYBR Green I, calcein, or hydroxy naphthol blue (HNB) into the reaction tube (Liu et al., 2019). Furthermore, the CPA reaction can be accomplished in 40 min through designing accelerated primer (date was not shown), which is much shorter than the reaction times of PCR (Yulong et al., 2010; Zhao et al., 2010a). Overall, the detection of MRSA by CPA has resolved the major limitation of time consumption or complex procedure by culture-based methods and costly PCR molecular techniques (Liu et al., 2018c).

Taking specificity and sensitivity into consideration, CPA assays were developed as sensitive and rapid MRSA detection systems, and the experimental data indicated the utility of the established system in point-of care testing (Moellering, 2012; Xu et al., 2020a). The high specificity of CPA was evidenced by the successful detection of all MRSA, but not of non-target pathogens.

DATA AVAILABILITY STATEMENT

The raw data supporting the conclusions of this article will be made available by the authors, without undue reservation.

AUTHOR CONTRIBUTIONS

AO and KW conceived the study and participated in its design and coordination. YM, LY, LC, and YY performed the experimental work and collected the data. YZ and TH analyzed the data and wrote the manuscript. All authors read and approved the final manuscript.

FUNDING

This study was supported by the National Key Research and Development Program of China (No. 2016YFD04012021).

REFERENCES

- Corrente, M., Normanno, G., Martella, V., Bellacicco, A. L., Quaglia, N. C., Dambrosio, A., et al. (2007). Comparison of methods for the detection of methicillin resistance in *Staphylococcus aureus* isolates from food products. *Lett. Appl. Microbiol.* 45, 535–539. doi: 10.1111/j.1472-765X.2007.02226.x
- Crago, B., Ferrato, C., Drews, S. J., Svenson, L. W., Tyrrell, G., and Louie, M. (2012). Prevalence of *Staphylococcus aureus* and methicillin-resistant *S. aureus* (MRSA) in food samples associated with foodborne illness in Alberta, Canada from 2007 to 2010. *Food Microbiol.* 32, 202–205. doi: 10.1016/j.fm.2012.04.012
- Deng, Y., Liu, J., Li, L., Fang, H., and Xu, Z. (2015a). Reduction and restoration of culturability of beer-stressed and low-temperature-stressed *Lactobacillus acetotolerans* strain 2011-8. *Int. J. Food Microbiol.* 206, 96–101. doi: 10.1016/j.jfoodmicro.2015.04.046
- Deng, Y., Liu, J., Peters, B. M., Chen, L., Miao, J., et al. (2015b). Antimicrobial resistance investigation on *Staphylococcus* strains in a local hospital in Guangzhou, China, 2001–2010. *Microb. Drug Resist.* 21, 102–104. doi: 10.1089/mdr.2014.0117
- Fang, R., Li, X., Hu, L., You, Q., Li, J., Wu, J., et al. (2009). Cross-priming amplification for rapid detection of *Mycobacterium tuberculosis* in sputum specimens. *J. Clin. Microbiol.* 47, 845–847.
- Felten, A., Grandry, B., Lagrange, P. H., and Casin, I. (2002). Evaluation of three techniques for detection of low-level methicillin-resistant *Staphylococcus aureus* (MRSA): a disk diffusion method with cefoxitin and moxalactam, the Vitek 2 system, and the MRSA-screen latex agglutination test. *J. Clin. Microbiol.* 40, 2766–2771. doi: 10.1128/JCM.40.8.2766-2771.2002
- Graveland, H., Wagenaar, J. A., Bergs, K., Heesterbeek, H., and Heederik, D. (2011). Persistence of Livestock Associated MRSA CC398 in Humans Is Dependent on Intensity of Animal Contact. *PLoS One* 6:e16830. doi: 10.1371/journal.pone.0016830
- Kadariya, J., Smith, T. C., and Thapaliya, D. (2014). *Staphylococcus aureus* and *Staphylococcal* Food-Borne Disease: An Ongoing Challenge in Public Health. *Biomed Res. Int.* 2014:827965. doi: 10.1155/2014/827965
- Liu, J., Chen, D., Peters, B. M., Li, L., Li, B., Xu, Z., et al. (2016a). *Staphylococcal* chromosomal cassettes *mec* (*sccmec*): a mobile genetic element in methicillin-resistant *Staphylococcus aureus*. *Microb. Pathogenesis.* 101, 56–67. doi: 10.1016/j.micpath.2016.10.028
- Liu, J., Deng, Y., Peters, B. M., Li, L., Li, B., Chen, L., et al. (2016b). Transcriptomic analysis on the formation of the viable putative non-culturable state of beer-spoilage *Lactobacillus acetotolerans*. *Sci. Rep.* 6:36753. doi: 10.1038/srep36753
- Liu, J., Zhou, R., Li, L., Peters, B. M., Li, B., Lin, C. W., et al. (2016c). Viable but non-culturable state and toxin gene expression of enterohemorrhagic *Escherichia coli* O157 under cryopreservation. *Res. Microbiol.* 101, 56–57.

- Liu, J., Li, L., Li, B., Brian, M. P., Deng, Y., Xu, Z., et al. (2017a). Study on spoilage capability and VBNC state formation and recovery of *Lactobacillus plantarum*. *Microb. Pathogenesis*. 110, 257–261. doi: 10.1016/j.micpath.2017.06.044
- Liu, J., Li, L., Li, B., Brian, M. P., Deng, Y., Xu, Z., et al. (2017b). The viable but nonculturable state induction and genomic analyses of *Lactobacillus casei* bm-lc14617, a beer-spoilage bacterium. *Microbiologyopen* 6:e506. doi: 10.1002/mbo3.506
- Liu, J., Li, L., Li, B., Brian, M. P., Xu, Z., and Shirliff, M. E. (2017c). First study on the formation and resuscitation of viable but nonculturable state and beer spoilage capability of *Lactobacillus lindneri*. *Microb. Pathogenesis*. 107, 219–224. doi: 10.1016/j.micpath.2017.03.043
- Liu, J., Yang, L., Chen, D., Peters, B. M., Li, L., Li, B., et al. (2017d). Complete sequence of pbm413, a novel multi-drug-resistance megaplasmid carrying *qnrvc6* and *blaimp-45* from *Pseudomonas aeruginosa*. *Int. J. Antimicrob. Ag.* 51, 145–150. doi: 10.1016/j.ijantimicag.2017.09.008
- Liu, J., Deng, Y., Li, L., Li, B., Li, Y., Zhou, S., et al. (2018a). Discovery and control of culturable and viable but non-culturable cells of a distinctive *Lactobacillus harbinensis* strain from spoiled beer. *Sci. Rep.* 8:11446. doi: 10.1038/s41598-018-28949-y
- Liu, J., Deng, Y., Soteyome, T., Li, Y., Su, J., Li, L., et al. (2018b). Induction and recovery of the viable but nonculturable state of hop-resistance *Lactobacillus brevis*. *Front. Microbiol.* 9:2076. doi: 10.3389/fmicb.2018.02076
- Liu, J., Yang, L., Hou, Y., Soteyome, T., Zeng, B., Su, J., et al. (2018c). Transcriptomics study on *Staphylococcus aureus* biofilm under low concentration of ampicillin. *Front. Microbiol.* 9:2413. doi: 10.3389/fmicb.2018.02413
- Liu, J., Xie, J., Yang, L., Chen, D., Peters, B. M., Xu, Z., et al. (2018d). Identification of the kpc plasmid pcy-kpc334: new insights on the evolution pathway of the epidemic plasmids harboring *fosa3-blakpc-2* genes. *Int. J. Antimicrob. Ag.* 52, 510–512. doi: 10.1016/j.ijantimicag.2018.04.013
- Liu, L., Ye, C., Soteyome, T., Zhao, X., and Harro, J. M. (2019). Inhibitory effects of two types of food additives on biofilm formation by foodborne pathogens. *MicrobiologyOpen* 8:e00853. doi: 10.1002/mbo3.853
- Miao, J., Chen, L., Wang, J., Wang, W., Chen, D., Li, L., et al. (2017a). Current methodologies on genotyping for nosocomial pathogen methicillin-resistant *Staphylococcus aureus* (MRSA). *Microb. Pathogenesis*. 107, 17–28. doi: 10.1016/j.micpath.2017.03.010
- Miao, J., Liang, Y., Chen, L., Wang, W., Wang, J., Li, B., et al. (2017b). Formation and development of *Staphylococcus* biofilm: with focus on food safety. *J. Food Safety*. 7:e12358. doi: 10.1111/jfs.12358
- Miao, J., Lin, S., Soteyome, T., Peters, B. M., Li, Y., Chen, H., et al. (2019). Biofilm formation of *Staphylococcus aureus* under food heat processing conditions: first report on cml production within biofilm. *Sci. Rep.* 9:1312. doi: 10.1038/s41598-018-35558-2
- Moellering, R. C. (2012). MRSA: the first half century. *J. Antimicrob. Chemoth.* 67, 4–11. doi: 10.1093/jac/dkr437
- Monteiro, L., Bonnemaïson, D., Vekris, A., Petry, K. G., Bonnet, J., Vidal, R., et al. (1997). Complex polysaccharides as PCR inhibitors in feces: *Helicobacter pylori* model. *J. Clin. Microbiol.* 35, 995–998. doi: 10.1128/JCM.35.4.995-998.1997
- Salisbury, S. M., Sabatini, L. M., and Spiegel, C. A. (1997). Identification of methicillin-resistant *Staphylococci* by multiplex polymerase chain reaction assay. *Am. J. Clin. Pathol.* 107, 368–373. doi: 10.1093/ajcp/107.3.368
- Tacconelli, E., De Angelis, G., de Waure, C., Cataldo, M. A., La Torre, G., and Cauda, R. (2009). Rapid screening tests for methicillin-resistant *Staphylococcus aureus* at hospital admission: systematic review and meta-analysis. *Lancet Infect. Dis.* 9, 546–554. doi: 10.1016/S1473-3099(09)70150-1
- Voss, A., Loeffen, F., Bakker, J., Klaassen, C., and Wulf, M. (2005). Methicillin-resistant *Staphylococcus aureus* in pig farming. *Emerg. Infect. Dis.* 11, 1965–1966.
- Wang, L., Li, Y., Chu, J., Xu, Z., and Zhong, Q. (2012). Development and application of a simple loop-mediated isothermal amplification method on rapid detection of *Listeria monocytogenes* strains. *Mol. Biol. Rep.* 39, 445–449. doi: 10.1007/s11033-011-0757-7
- Wang, Y. X., Zhang, A. Y., Yang, Y. Q., Lei, C. W., Cheng, G. Y., Zou, W. C., et al. (2018). Sensitive and rapid detection of *Salmonella enterica* serovar Indiana by cross-primer amplification. *J. Microbiol. Methods* 153, 24–30. doi: 10.1016/j.mimet.2018.08.003
- Wang, Y., Wang, Y., Ma, A., Li, D., and Ye, C. (2014). Rapid and sensitive detection of *Listeria monocytogenes* by cross-primer amplification of lmo0733 gene. *FEMS Microbiol. Lett.* 361, 43–51. doi: 10.1111/1574-6968.12610
- Weese, J. S., Avery, B. P., and Reid-Smith, R. J. (2010). Detection and quantification of methicillin-resistant *Staphylococcus aureus* (MRSA) clones in retail meat products. *Lett. Appl. Microbiol.* 51, 338–342. doi: 10.1111/j.1472-765X.2010.02901.x
- Xie, J., Peters, B. M., Li, B., Li, L., Yu, G., Xu, Z., et al. (2017a). Clinical features and antimicrobial resistance profiles of important *Enterobacteriaceae* pathogens in Guangzhou representative of Southern China, 2001–2015. *Microb. Pathogenesis*. 107, 206–211. doi: 10.1016/j.micpath.2017.03.038
- Xie, J., Yang, L., Peters, B. M., Chen, L., Chen, D., Li, B., et al. (2017b). A 16-year retrospective surveillance report on the pathogenic features and antimicrobial susceptibility of *Pseudomonas aeruginosa* isolated from Guangzhou representative of Southern China. *Microb. Pathogenesis*. 110, 37–41. doi: 10.1016/j.micpath.2017.06.018
- Xu, G., Hu, L., Zhong, H., Wang, H., Yusa, S., Weiss, T. C., et al. (2012). Cross primer amplification: mechanism and optimization for isothermal DNA amplification. *Sci. Rep.* 2:246.
- Xu, Z., Li, L., Alam, M. J., Zhang, L., Yamasaki, S., and Shi, L. (2008). First confirmation of integron-bearing methicillin-resistant *Staphylococcus aureus*. *Curr. Microbiol.* 57, 264–268. doi: 10.1007/s00284-008-9187-8
- Xu, Z., Li, L., Chu, J., Peters, B. M., Harris, M. L., Li, B., et al. (2012). Development and application of loop-mediated isothermal amplification assays on rapid detection of various types of *Staphylococci* strains. *Food Res. Int.* 47, 166–173. doi: 10.1016/j.foodres.2011.04.042
- Xu, Z., Li, L., Shi, L., and Shirliff, M. E. (2011a). Class 1 integron in *Staphylococci*. *Mol. Biol. Rep.* 38, 5261–5279. doi: 10.1007/s11033-011-0676-7
- Xu, Z., Li, L., Shirliff, M. E., Peters, B. M., Li, B., Peng, Y., et al. (2011b). Resistance class 1 integron in clinical methicillin-resistant *Staphylococcus aureus* strains in southern China, 2001–2006. *Clin. Microbiol. Infect.* 17, 714–718. doi: 10.1111/j.1469-0691.1469-0691
- Xu, Z., Li, L., Shirliff, M. E., Peters, B. M., Yamasaki, S., and Shi, L. (2009). Occurrence and Characteristics of Class 1 and 2 Integrons in *Pseudomonas aeruginosa* Isolates from Patients in Southern China. *J. Clin. Microbiol.* 47, 230–234. doi: 10.1128/JCM.02027-08
- Xu, Z., Luo, Y., Mao, Y., Peng, R., Chen, J., Soteyome, T., et al. (2020a). Spoilage Lactic Acid Bacteria in the Brewing Industry. *J. Microbiol. Biotechnol.* 30, 955–961. doi: 10.4014/jmb.1908.08069
- Xu, Z., Luo, Y., Soteyome, T., Lin, C., Xu, X., Mao, Y., et al. (2020b). Rapid Detection of Food-Borne *Escherichia coli* O157:H7 with Visual Inspection by Crossing Priming Amplification (CPA). *Food Anal. Methods* 13, 474–481. doi: 10.1007/s12161-019-01651-z
- Xu, Z., Shi, L., Alam, M. J., Li, L., and Yamasaki, S. (2010a). Integron-bearing methicillin-resistant coagulase-negative *Staphylococci* in south china, 2001–2004. *FEMS Microbiol. Lett.* 278, 223–230. doi: 10.1111/j.1574-6968.2007.01782.x
- Xu, Z., Shi, L., Zhang, C., Zhang, L., and Yamasaki, S. (2010b). Nosocomial infection caused by class 1 integron-carrying *Staphylococcus aureus* in a hospital in south china. *Clin. Microbiol. Infect.* 13, 980–984. doi: 10.1111/j.1469-0691.2007.01782.x
- Xu, Z., Xie, J., Peters, B. M., Li, B., Li, L., Yu, G., et al. (2017). Longitudinal surveillance on antibiogram of important gram-positive pathogens in southern china, 2001 to 2015. *Microb. Pathogenesis*. 103, 80–86. doi: 10.1016/j.micpath.2016.11.013
- Xu, Z., Xie, J., Soteyome, T., Peters, B. M., Shirliff, M. E., Liu, J., et al. (2019). Polymicrobial interaction and biofilms between *Staphylococcus aureus* and *Pseudomonas aeruginosa*: an underestimated concern in food safety. *Curr. Opin. Food Sci.* 26, 57–64. doi: 10.1016/j.cofs.2019.03.006
- Yu, G., Wen, W., Peters, B. M., Liu, J., Ye, C., Che, Y., et al. (2016). First report of novel genetic array *aaca4-blaimp-25-oxa30-catb3* and identification of novel metallo- β -lactamase gene *blaimp25*: a retrospective study of antibiotic resistance surveillance on *Pseudomonas aeruginosa* in Guangzhou of south china, 2003–2007. *Microb. Pathogenesis*. 95, 62–67. doi: 10.1016/j.micpath.2016.02.021
- Yulong, Z., Xia, Z., Hongwei, Z., Wei, L., Wenjie, Z., and Xitai, H. (2010). Rapid and sensitive detection of *Enterobacter sakazakii* by cross-primer amplification combined with immuno-blotting analysis. *Mol. Cell Probes* 24, 396–400.

- Zhang, H., Feng, S., Zhao, Y., Wang, S., and Lu, X. (2015). Detection of *Yersinia enterocolitica* in milk powders by cross-priming amplification combined with immunoblotting analysis. *Int. J. Food Microbiol.* 214, 77–82.
- Zhao, X., Li, Y., Chu, J., Wang, L., Shirliff, M. E., He, X., et al. (2010a). Rapid detection of *Vibrio parahaemolyticus* strains and virulent factors by loop-mediated isothermal amplification assays. *Food Sci. Biotechnol.* 19, 1191–1197. doi: 10.1007/s10068-010-0170-3
- Zhao, X., Li, Y., Wang, L., You, L., Xu, Z., Li, L., et al. (2010b). Development and application of a loop-mediated isothermal amplification method on rapid detection *Escherichia coli* O157 strains from food samples. *Mol. Biol. Rep.* 37, 2183–2188. doi: 10.1007/s11033-009-9700-6
- Zhao, X., Wang, L., Chu, J., Li, Y., Li, Y., Xu, Z., et al. (2010c). Development and application of a rapid and simple loop-mediated isothermal amplification method for food-borne *salmonella* detection. *Food Sci. Biotechnol.* 19, 1655–1659. doi: 10.1007/s10068-010-0234-4
- Zhao, X., Wang, L., Li, Y., Xu, Z., Li, L., He, X., et al. (2011). Development and application of a loop-mediated isothermal amplification method on rapid detection of *pseudomonas aeruginosa* strains. *World J. Microbiol. Biot.* 27, 181–184. doi: 10.1007/s11274-010-0429-0
- Conflict of Interest:** The authors declare that the research was conducted in the absence of any commercial or financial relationships that could be construed as a potential conflict of interest.

Copyright © 2021 Ou, Wang, Mao, Yuan, Ye, Chen, Zou and Huang. This is an open-access article distributed under the terms of the Creative Commons Attribution License (CC BY). The use, distribution or reproduction in other forums is permitted, provided the original author(s) and the copyright owner(s) are credited and that the original publication in this journal is cited, in accordance with accepted academic practice. No use, distribution or reproduction is permitted which does not comply with these terms.



Inhibition of Biofilm Formation and Related Gene Expression of *Listeria monocytogenes* in Response to Four Natural Antimicrobial Compounds and Sodium Hypochlorite

Yunge Liu^{1,2}, Lina Wu^{1,2}, Jina Han^{1,2}, Pengcheng Dong^{1,2}, Xin Luo^{1,2,3}, Yimin Zhang^{1,2*} and Lixian Zhu^{1,2*}

¹Lab of Beef Processing and Quality Control, College of Food Science and Engineering, Shandong Agricultural University, Tai'an, China, ²National R&D Center for Beef Processing Technology, Tai'an, China, ³Jiangsu Synergetic Innovation Center of Meat Production and Processing Quality and Safety Control, Nanjing, China

OPEN ACCESS

Edited by:

Yang Deng,
Qingdao Agricultural University, China

Reviewed by:

Abhinav Upadhyay,
University of Connecticut, United States
Xiaodong Xia,
Northwest A & F University, China
Arumugam Veera Ravi,
Alagappa University, India

*Correspondence:

Yimin Zhang
ymzhang@sdaa.edu.cn
Lixian Zhu
zhlx@sdaa.edu.cn

Specialty section:

This article was submitted to
Food Microbiology,
a section of the journal
Frontiers in Microbiology

Received: 14 October 2020

Accepted: 18 December 2020

Published: 14 January 2021

Citation:

Liu Y, Wu L, Han J, Dong P, Luo X,
Zhang Y and Zhu L (2021) Inhibition
of Biofilm Formation and Related
Gene Expression of *Listeria*
monocytogenes in Response to Four
Natural Antimicrobial Compounds
and Sodium Hypochlorite.
Front. Microbiol. 11:617473.
doi: 10.3389/fmicb.2020.617473

The aim of this study was to assess the efficacy of four natural antimicrobial compounds (cinnamaldehyde, eugenol, resveratrol and thymoquinone) plus a control chemical disinfectant (sodium hypochlorite) in inhibiting biofilm formation by *Listeria monocytogenes* CMCC54004 (Lm 54004) at a minimum inhibitory concentration (MIC) and sub-MICs. Crystal violet staining assay and microscopic examination were employed to investigate anti-biofilm effects of the evaluated compounds, and a real-time PCR assay was used to investigate the expression of critical genes by Lm 54004 biofilm. The results showed that five antimicrobial compounds inhibited Lm 54004 biofilm formation in a dose dependent way. Specifically, cinnamaldehyde and resveratrol showed better anti-biofilm effects at $1/4 \times \text{MIC}$, while sodium hypochlorite exhibited the lowest inhibitory rates. A swimming assay confirmed that natural compounds at sub-MICs suppressed Lm 54004 motility to a low degree. Supporting these findings, expression analysis showed that all four natural compounds at $1/4 \times \text{MIC}$ significantly down-regulated quorum sensing genes (*agrA*, *agrC*, and *agrD*) rather than suppressing the motility- and flagella-associated genes (*degU*, *motB*, and *flaA*). This study revealed that sub-MICs of natural antimicrobial compounds reduced biofilm formation by suppressing the quorum sensing system rather than by inhibiting flagella formation.

Keywords: *Listeria monocytogenes*, anti-biofilm mechanism, gene expression, quorum sensing, microscopic examinations

INTRODUCTION

Listeria monocytogenes (*L. monocytogenes*) is a Gram-positive food-borne pathogen. It causes listeriosis with a high mortality rate (20–30%) among immunocompromised individuals (e.g., pregnant women, neonates, and the elderly; Gandra et al., 2019; Liu et al., 2020b). *L. monocytogenes* can survive for long periods under various harsh environmental conditions, such as high salt, low pH and

refrigerated temperatures (Oloketuyi and Khan, 2017). The biofilm formation of *L. monocytogenes* is the main cause for its persistence and stress resistance in food processing environments (García-Gonzalo and Pagán, 2015). Biofilms are microbial communities that adhere to abiotic or biotic surfaces, which are surrounded by extracellular polymeric substances (Shi and Zhu, 2009). Once established, microorganisms in biofilms can enhance their resistance to antimicrobial agents, and thus, are more difficult to eradicate compared with planktonic cells (Jolivet-Gougeon and Bonnaure-Mallet, 2014; Chen et al., 2019). Consequently, *L. monocytogenes* cells in biofilms often cause recurrent contamination in food products, which enhances the food safety risks and leads to potential human health threats.

The molecular mechanism of biofilm formation by *L. monocytogenes* has been widely explored but is still not completely elucidated. At the initial period of biofilm formation, the swimming ability of flagella has been reported to be critical for bacteria to stick on the surface (Lemon et al., 2007). The genes associated with flagellar synthesis and motility involved in *L. monocytogenes* attachment, include *flaA*, *fliP*, *fliG*, *flgE*, *motA*, *motB*, *mogR*, and *degU* (Williams et al., 2005; Chang et al., 2012). Moreover, the quorum sensing (QS) system of *L. monocytogenes* (*agr* system) plays a critical role in its biofilm formation (Rieu et al., 2007). The locus *agr* in *L. monocytogenes* is composed of four genes, including *agrB*, *agrD*, *agrC*, and *agrA* (Zetzmann et al., 2016). In addition, the virulence regulator PrfA and the stress response regulator SigB also play important roles in *L. monocytogenes* biofilm development (Lemon et al., 2010; van der Veen and Abee, 2010). For this reason, exploring the efficacy of biofilm inhibitors against *L. monocytogenes* based on regulating key genes related with biofilm formation is a crucial and urgent task for the food industry.

Currently, natural antimicrobials have received strong interest as alternative agents of chemical antimicrobial drugs to inhibit biofilm formation (Xiang et al., 2019). Several studies have proved that active ingredients in essential oils are effective anti-biofilm agents against a variety of bacteria. Among them, phenylpropenes and phenolic compounds are consistently reported to be capable of inhibiting biofilm formation of pathogens. For instance, cinnamaldehyde and eugenol (phenylpropenes) were effective against the attachment of *Pseudomonas aeruginosa* and *Escherichia coli* O157:H7 by down-regulating curli genes (*casA* and *casB*) and Shiga-like toxin gene *stx2* (Kim et al., 2015). Likewise, previous studies also demonstrated that phenolic compounds prevented biofilm formation by pathogens, e.g., resveratrol (trans - 3,5,4' - trihydroxystilbene) can disturb the expression of genes in the *agr* system related to QS and then inhibit biofilm formation of *Staphylococcus aureus* (Qin et al., 2014). It is worth mentioning that the *agr* operon of *L. monocytogenes* is homologous to the *S. aureus* system (Zetzmann et al., 2016), which means that the QS inhibitors (QSIs, such as resveratrol) which acts on the *agr* system in *S. aureus* is probably a promising anti-QS agent for *L. monocytogenes*. In addition, anti-neoplastic agent, the constituent of Black cumin (*Nigella sativa*) thymoquinone (2-isopropyl-5-methyl-1,4-benzoquinone) was found to have significant anti-biofilm ability against Gram-negative (*E. coli*

and *P. aeruginosa*) and Gram-positive bacteria (*Bacillus subtilis* and *S. aureus*; Goel and Mishra, 2018). A sub-inhibitory concentration of thymoquinone inhibited the production of AHL-regulated violacein pigment in *Chromobacterium violaceum*, meanwhile, RT-PCR assays also confirmed that thymoquinone down-regulated the transcription of the QS-relative gene *luxR* in *Cronobacter sakazakii* (Shi et al., 2017). Moreover, our previous study has investigated the effect of natural compounds on inhibiting the biofilm formation of wild *L. monocytogenes* (Lm 118) strain isolated from a beef processing plant (Liu et al., 2020a). However, the ability to form a biofilm was affected by the serotype and environmental conditions (Weiler et al., 2013), and the biofilm inhibition against a standard strain needs to be studied. Further, the inhibition mechanism of these compounds on *L. monocytogenes* should be more extensively elucidated.

This study is a continuation of our previous work (Liu et al., 2020a). Cinnamaldehyde, eugenol, resveratrol and thymoquinone were selected to compare the similarities and differences in the biofilm inhibition of *L. monocytogenes* CMCC54004 (Lm 54004), since they are different types of natural antibacterial compounds (phenylpropenes: cinnamaldehyde and eugenol; phenolic compound: resveratrol and benzoquinone compound: thymoquinone) which may help to elucidate the biofilm inhibitory mechanisms of this strain from different perspectives. Moreover, previous studies have identified numerous genes associated with *L. monocytogenes* biofilm formation at 37°C (Upadhyay et al., 2013; Miao et al., 2019), rather than the lower temperatures associated with ambient indoor room settings. In this study, in order to achieve the effective biofilm development, 25°C was used as the incubation temperature (Liu et al., 2020a). To determine the ability of natural antimicrobial compounds to prevent biofilm synthesis, sub-minimal inhibitory concentrations (concentrations that exhibited no significant inhibitory effect on the growth of planktonic bacteria) of the compounds were used. Firstly, the anti-biofilm activity of these four natural compounds and sodium hypochlorite (disinfectant frequently used in the food processing facilities) were evaluated against Lm 54004 on polystyrene surfaces. Polystyrene was chosen as it is one of the most utilized materials in the food industry. Secondly, scanning electron microscopy (SEM) and confocal laser scanning microscopy (CLSM) were used to evaluate the effects of antimicrobial compounds on the biofilm architecture and cellular viability of Lm 54004. Moreover, the effects of natural antimicrobial compounds on the expression of critical biofilm-associated genes (*agrA*, *agrC*, *agrD*, *prfA*, *sigB*, *relA*, *inlA*, *degU*, *motB*, and *flaA*) of Lm 54004 were measured by quantitative reverse transcription PCR (RT-qPCR).

MATERIALS AND METHODS

Bacterial Strains and Preparation of Inoculum

The bacterial strain *L. monocytogenes* CMCC 54004 (Lm 54004, serotype 1/2a) was purchased from the China National Center

for Medical Culture Collections (CMCC), source from Czech Institute of Epidemiology and Microbiology. The strain was stored at -80°C in the brain heart infusion (BHI; Beijing Land Bridge Technology, China) with 25% (v/v) glycerol. The strain was activated by transferring 0.2 ml of the frozen culture into 20 ml of BHI and incubating at 37°C for 18 h with two consecutive transfers.

Four natural antimicrobial compounds: cinnamaldehyde, eugenol, resveratrol, and thymoquinone were obtained from Macklin, China; Solarbio, China and Yuanyeshengwu, China respectively. The control compound, sodium hypochlorite (10% active chlorine), was obtained from Sinopharm Chemical Reagent, China. The purity of all the compounds was above 98%. The four natural compounds were diluted with 1% dimethyl sulfoxide (DMSO) in BHI, with 1% DMSO shown not to exhibit an adverse effect on the growth of *L. monocytogenes* (Fan et al., 2018).

Minimal Inhibitory Concentration Determination

Minimal inhibitory concentrations (MICs) of the above-mentioned four natural antimicrobial compounds and sodium hypochlorite were determined by the microdilution method, as described by the Clinical and Laboratory Standards Institute (CLSI) with some modification. Briefly, each of the compounds was diluted in a 96-well microtiter plate, final concentrations of cinnamaldehyde and eugenol ranging from 20 to 2,560 $\mu\text{g/ml}$, resveratrol and thymoquinone between 12.5 and 400 $\mu\text{g/ml}$ and sodium hypochlorite from 195 to 6,250 ppm. The final tested concentration of Lm 54004 was 5×10^5 CFU/ml. Broth only (microtiter wells containing uninoculated BHI medium) was used as negative control. The plate was incubated at 37°C for 24 h under static conditions. The MIC was defined as the lowest concentration of compounds that inhibited visible bacterial growth.

Sub-MICs Determination

Sub-MICs of the above-mentioned antimicrobial compounds against Lm 54004 were assessed using a growth curve analysis as previously described (Fan et al., 2018). The bacteria were grown overnight in BHI, and after that, the bacterial suspension was adjusted to a cell concentration of 5×10^5 CFU/ml. Then it was inoculated into BHI with or without compounds at $1/32 \times \text{MIC}$, $1/16 \times \text{MIC}$, $1/8 \times \text{MIC}$, $1/4 \times \text{MIC}$, $1/2 \times \text{MIC}$, MIC, $2 \times \text{MIC}$ and $4 \times \text{MIC}$. The cultures were incubated at 37°C for 24 h, and the assay optical density (OD) at 600 nm was determined at 1 h intervals.

Effects of Antimicrobial Compounds on Cell Motility

Swimming and swarming assays were conducted using a semisolid motility agar as previously described with some modifications (Li et al., 2018). Briefly, 3 μl of an overnight culture of Lm 54004 was inoculated at the center of swimming (10 g/L tryptone, 5 g/L NaCl and 0.3% agar) and swarming (25 g/L LB, 0.5 g/L glucose, 0.5% agar) plates containing different concentrations ($1/8 \times \text{MIC}$, $1/4 \times \text{MIC}$ and MIC) of four

natural antimicrobial compounds and sodium hypochlorite. BHI was set as the negative control. After incubation for 48 h at 25°C , the diameter (mm) of the motility zones was measured.

Effects of Antimicrobial Compounds on Biofilm Formation

Inhibition of biofilm formation by above mentioned antimicrobial compounds was studied using the crystal violet assay (Fan et al., 2018). Briefly, 100 μl BHI supplemented with different concentrations ($1/8 \times \text{MIC}$, $1/4 \times \text{MIC}$, $1/2 \times \text{MIC}$ and MIC) of antimicrobial compounds was added in 96-well microtiter plates. Subsequently, bacterial suspension of Lm 54004 (100 μl , 1×10^6 CFU/ml) was inoculated into wells. Bacterial cultures without the addition of antimicrobials were used as a positive control. Broth only (microtiter wells containing 200 μl of uninoculated BHI medium) was used as the negative control. After 72 h of incubation at 25°C , the wells were washed with sterile distilled water three times to remove the planktonic bacteria. Then, 200 μl of 0.25% (w/v) crystal violet was added to each well and stained for 30 min at room temperature. Next, the crystal violet solution was removed and 200 μl of 95% (v/v) ethanol was added to solubilize the stain, and absorbance was measured spectrophotometrically at 570 nm. The inhibitory rates were then calculated using the following formula: Inhibitory rate (%) = $[1 - \text{OD}_{570\text{nm}} (\text{Sample}) / \text{OD}_{570\text{nm}} (\text{positive control})] \times 100$. The whole experiment was replicated three times independently.

Effects of Antimicrobial Compounds on Biofilm Metabolic Activity

Bacterial viability was analyzed using the Cell Counting Kit-8 (CCK-8, 7Sea Biotech, Shanghai, China) as previously described (Yu et al., 2017). Biofilms were grown as stated above with BHI containing antimicrobial compounds ($1/8 \times \text{MIC}$, $1/4 \times \text{MIC}$, and MIC) in 96-well microtiter plates. The negative controls contained only BHI. After 72 h of incubation at 25°C , the supernatant was discarded and replaced with 100 μl sterile PBS and 10 μl CCK-8 dye solution. Then plates were incubated for 4 h at 25°C . The absorbance was then measured at 450 nm using the microplate reader (SpectraMax M5, Molecular Devices, United States). All experiments were repeated three times independently.

Analysis of Biofilms by Scanning Electron Microscopy and Confocal Laser-Scanning Microscopy

For the SEM analysis, individual polystyrene (PS) coupons (2 mm thick and 10 mm in diameter) were placed horizontal in 48-well polystyrene microtiter plates. Subsequently, 300 μl of BHI containing antimicrobial compounds ($1/8 \times \text{MIC}$, $1/4 \times \text{MIC}$ and MIC) was added into wells, respectively. The negative control contained only BHI was also visualized to determine the normal architecture of the biofilm. Next, a 300 μl bacterial suspension of Lm 54004 was inoculated into culture (final tested concentration of bacteria was 5×10^5 CFU/ml). The plates were incubated statically at 25°C for 72 h to

favor biofilm formation. After the incubation, the chips were gently washed with sterile PBS and immersed in 2.5% glutaraldehyde at 4°C for 24 h. After washing thrice with PBS, the cultures were then dehydrated in a gradient alcohol concentration (50, 70, 80, 90, and 100%) for 10 min at each concentration. After critical point drying with liquid carbon dioxide (CO₂), and gold coating, the samples were examined using a SU8020 scanning electron microscope (Hitachi, Tokyo, Japan).

For the CLSM analysis, Lm 54004 was inoculated into BHI with antimicrobial compounds (1/8 × MIC, 1/4 × MIC, and MIC) in cell culture dishes (35 mm × 10 mm, Sigma, United States). Biofilms not exposed to antimicrobial compounds (negative control) was also visualized to determine the normal architecture of the biofilm. The final concentration of bacteria was 5×10^5 CFU/ml. After 72 h of incubation at 25°C, the bacteria were gently washed with sterile PBS three times. Then the biofilms were stained with the LIVE/DEAD BacLight kit L-7012 (Molecular Probes, United States) for 30 min in the dark. The kit included Syto 9 which labels all bacteria with intact membranes, and propidium iodide which only penetrates and stains cells with damaged membranes. Biofilm samples were imaged under a confocal laser microscope (LSM 880, Zeiss, Germany) using a 63 × oil immersion objective lens with a 488-nm argon laser, and the emitted fluorescence was recorded within the range of 480–500 nm to collect Syto 9 emission fluorescence and 490–635 nm to collect propidium iodide-emitted fluorescence. Three-dimensional projections were reconstructed from z-stacks using the easy 3D function of the ZEN Blue Lite 2_3 software.

Quantitative Real-Time PCR

RT-qPCR was used to evaluate the effect of antimicrobial compounds on the expression of genes associated with biofilm formation. Firstly, Lm 54004 was inoculated into BHI with or without antimicrobial compounds (1/4 × MIC) in cell culture dishes, incubation at 25°C for 72 h. Cell culture dishes were washed with sterile PBS for three times. Total RNA of biofilms in cell culture dishes were extracted by using MiniBEAT Universal RNA Extraction Kit (Takara, China). Next, total RNA was reverse transcribed into cDNA by using Takara PrimeScript™ RT Reagent Kit (Takara, Beijing, China). SYBR® Premix Ex Taq™ (Takara, China) were applied in RT-PCR to quantify gene expression. The primers for evaluated genes (Table 1) were previously published (Upadhyay et al., 2013; Du et al., 2018) and synthesized by BioSune Co., Ltd. (Shanghai, China). 16S rRNA was selected as an internal standard. Quantification of mRNA was performed with a real-time PCR system (CFX96, Bio-Rad, United States) with CFX 96 (Bio-Rad, United States). The 2^{−ΔΔC_t} method was used to analyze the relative gene expression obtained according to the melting curve (Livak and Schmittgen, 2001).

Statistical Analyses

Triplicate independent experiments were conducted for each of the above assays. The MIXED procedure (Statistical Analysis System, SAS, version 9.0) was applied to analyze

the biofilm inhibitory rate while the fixed factors were concentration, compound type and their interaction, and the random factor was experiment replication. The Tukey Multiple Comparison Test was performed to determine the influence of concentration of each compound on motility ability and biofilm metabolic activity. The results of relative gene expressions were analyzed by a *t*-test using SPSS version 18.0 to compare the difference between the experimental groups and the control group. Differences were considered statistically different at *p* < 0.05.

RESULTS

Minimum Inhibitory Concentrations

All compounds inhibited the growth of Lm 54004, and the MICs for cinnamaldehyde, eugenol, resveratrol, thymoquinone, and sodium hypochlorite were 640 μg/ml, 1,280 μg/ml, 400 μg/ml, 50 μg/ml and 1560 ppm, respectively.

Growth Curves in Sub-MICs

Our results showed that the growth of planktonic bacteria was totally inhibited by compounds at MIC – 4 × MIC, while 1/32 × MIC – 1/4 × MIC of five compounds all exhibited no obvious impacts on the concentration of Lm 54004 at stationary phase (Figure 1). Thus, the concentration of 1/8 × MIC and 1/4 × MIC were chosen as the sub-MICs in this study for the following experiments. Specifically, as follows: Cinnamaldehyde (80 μg/ml and 160 μg/ml), eugenol (160 μg/ml and 320 μg/ml), resveratrol (50 μg/ml and 100 μg/ml), thymoquinone (6.25 μg/ml and 12.5 μg/ml) and sodium hypochlorite (195 and 390 ppm).

TABLE 1 | List of primers used in this study.

Gene name	Primer name	Primer sequence (5'-3')
16 s rRNA	16S-F	ACCGTCAAGGGACAAGCA
	16S-R	GGGAGGCAGCAGTAGGGA
<i>agrA</i>	<i>agrA</i> -F	GCAGCCGGACATGAATGG
	<i>agrA</i> -R	AACCACGCGGATCAAACCTTC
<i>agrC</i>	<i>agrC</i> -F	GGGGTCAATCGCAGGTTTTG
	<i>agrC</i> -R	CTTTAAGTTCGTTGGTTCGCGTA
<i>agrD</i>	<i>agrD</i> -F	AAATCAGTTGGTAAATTCCTTTCTAG
	<i>agrD</i> -R	AATGGACTTTTTGGTTCGTATACA
<i>relA</i>	<i>relA</i> -F	TGCGATGCCGAAGTCGAATA
	<i>relA</i> -R	GCAACCCCGTATTTCAGCGAT
<i>sigB</i>	<i>sigB</i> -F	TGGATTGCCGCTTACCAAGAA
	<i>sigB</i> -R	TCGGGCGATGGACTCTACTA
<i>prfA</i>	<i>prfA</i> -F	TGAGCAAGAATCTTACGCACATTTT
	<i>prfA</i> -R	GCTAGGCTGTATGAACTTGTTTTTG
<i>inlA</i>	<i>inlA</i> -F	ACTTGCGCAGTGGAGTATGGA
	<i>inlA</i> -R	CTGAAGCGTCGTAACCTTGGTC
<i>degU</i>	<i>degU</i> -F	ACGCATAGAGAGTGCAGGTATT
	<i>degU</i> -R	CCCAATCCGCGGTTACTT
<i>flaA</i>	<i>flaA</i> -F	GGCTGCTGAAATGTCCGAAA
	<i>flaA</i> -R	TGCCGTGTTTGGTTTGCTTG
<i>motB</i>	<i>motB</i> -F	AATCGCCAAAGAAATCGGCG
	<i>motB</i> -R	CGCCGGGGTTTACTTCACTA

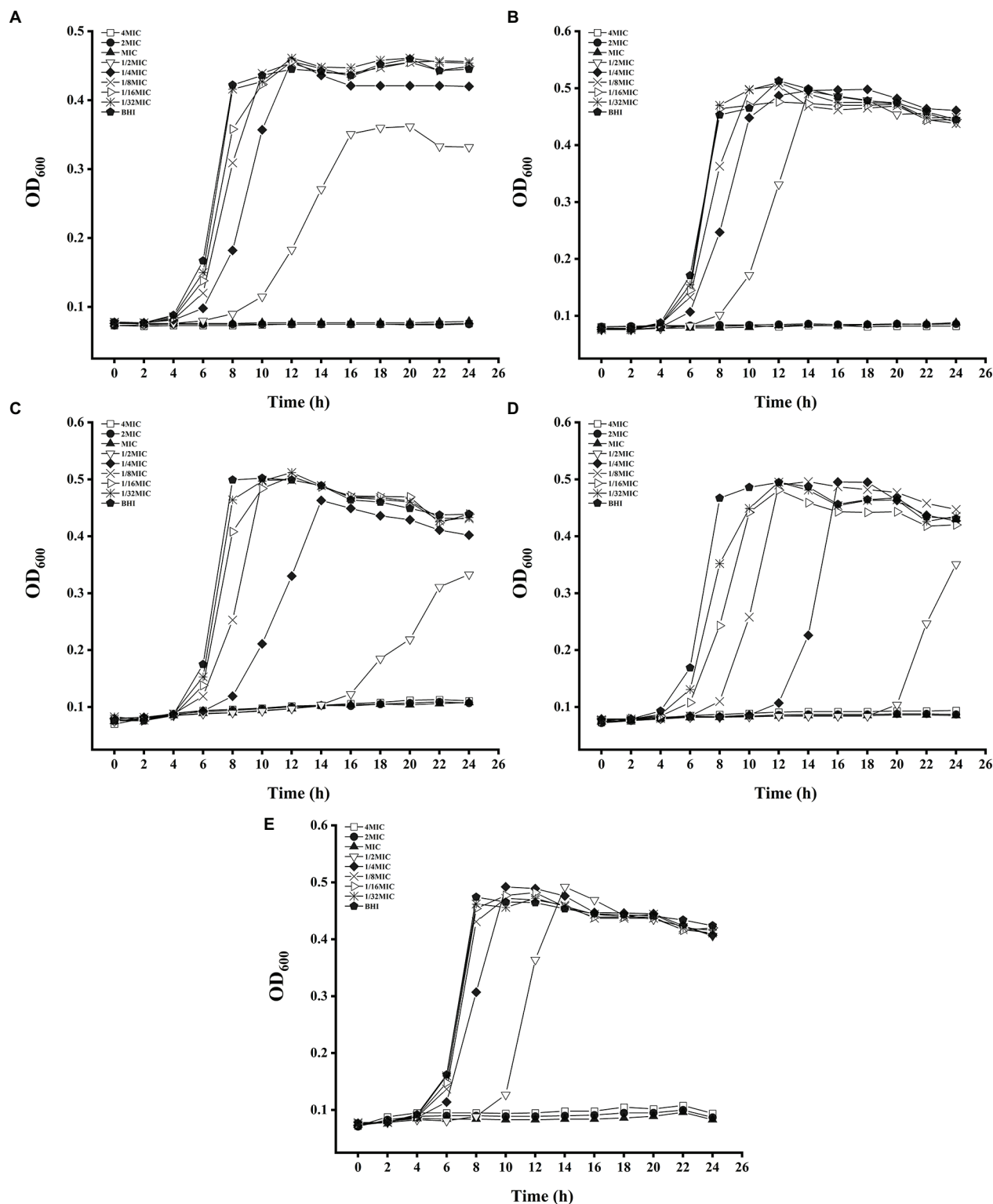


FIGURE 1 | Growth curves of *Listeria monocytogenes* CMCC 54004 incubated with five antimicrobials compounds for 24 h at 37°C. **(A):** cinnamaldehyde, **(B):** eugenol, **(C):** resveratrol, **(D):** thymoquinone, **(E):** sodium hypochlorite.

Cell Motility

Assays for swimming and swarming motility on semi-solid plates showed that Lm 54004 diffused on the agar, and after 48 h of incubation at 25°C, colony sizes were 3.34 mm and 5.47 mm, respectively (**Figure 2**, control). For swimming motility, at $1/8 \times \text{MIC}$ only eugenol significantly inhibited swimming motility of Lm 54004, while other compounds had no inhibitory effects on the colony diameters compared with the control group (**Figure 2A**). Treatment with $1/4 \times \text{MIC}$ of cinnamaldehyde, eugenol, thymoquinone and sodium hypochlorite all significantly reduced the swimming motility of Lm 54004, but resveratrol at $1/4 \times \text{MIC}$ had no inhibitory effects (**Figure 2A**). After treatment with MIC of all evaluated compounds, Lm 54004 showed a significantly low swimming motility ($p < 0.05$), with a colony size of below 3 mm (**Figure 2A**). For swarming motility, thymoquinone exerted no inhibitory effect at all test concentrations, resveratrol only inhibited it at MIC, cinnamaldehyde and eugenol significantly inhibited it at $1/4 \times \text{MIC}$ and $1/8 \times \text{MIC}$ (**Figure 2B**).

Biofilm Inhibitory Rate on the Polystyrene Surface

Results on the biofilm inhibitory rate of Lm 54004 treated by different antimicrobial compounds are shown in **Table 2**.

Four natural antimicrobial compounds all exerted strong biofilm inhibition, even at sub-MICs, where biofilm inhibitory rates on polystyrene microplate ranged from 37.6 to 53.8% at the presence of each compound at $1/8 \times \text{MIC}$, with a higher inhibitory rate of 46.4–68.0% evident as the concentration of compounds increased to $1/4 \times \text{MIC}$. Moreover, thymoquinone and eugenol showed a significantly lower biofilm inhibitory effect compared to cinnamaldehyde and resveratrol at $1/4 \times \text{MIC}$ s. The biofilm inhibitory effect of the common chemical disinfectant sodium hypochlorite was 34.5% ($1/4 \times \text{MIC}$) and 30.8% ($1/8 \times \text{MIC}$), which were significantly lower than the four natural antimicrobial compounds.

Biofilm Metabolic Activity

In this study, the Cell Counting Kit-8 (CCK-8) assay was used to reveal the metabolic status of the cells in biofilms (**Figure 3**). Our results of the CCK-8 assay confirmed that all evaluated antimicrobial compounds significantly inhibited metabolic activity of the biofilms formed by Lm 54004 ($p < 0.05$) at MIC (**Figure 3**). Sub-MICs ($1/4 \times \text{MIC}$ and $1/8 \times \text{MIC}$) of cinnamaldehyde, eugenol and resveratrol also showed significant impacts on reducing the Lm 54004 cell viability in the biofilms (**Figure 3**). However, the biofilm metabolic activity was

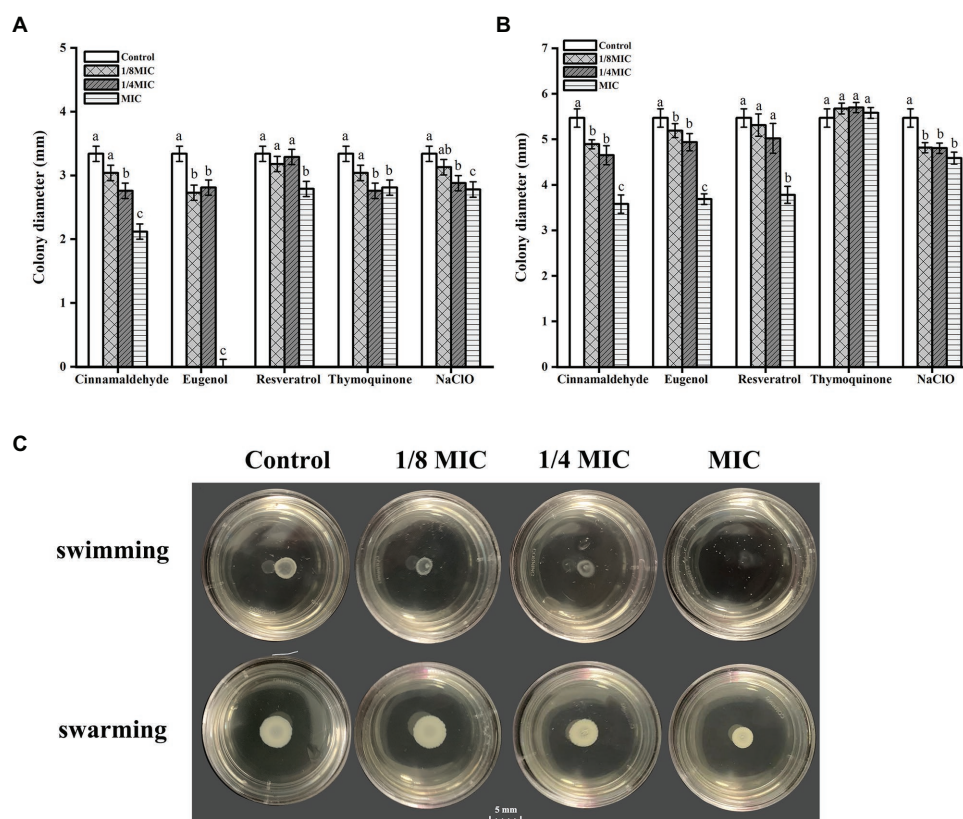


FIGURE 2 | Efficacy of five antimicrobials compounds in inhibiting motility ability of *Listeria monocytogenes* CMCC 54004 grown at 25°C. **(A):** swimming ability, **(B):** swarming ability, **(C):** representative plate images of swim and swarm rings of Eugenol (images of all compounds was shown in the attachment). a-c Indicate the same compound treatments at different concentrations with different letters are significantly different ($p < 0.05$). Mean values of three independent experiments and standard error are shown.

TABLE 2 | Biofilm inhibitory rate of *Listeria monocytogenes* CMCC 54004 on the polystyrene surface in different compounds and concentrations (25°C, 72 h).

Concentration	Biofilm inhibitory rate (%)					SE ^e
	Cinnamaldehyde	Eugenol	Resveratrol	Thymoquinone	Sodium hypochlorite	
1 × MIC	75.35 ^{ai}	74.57 ^{ai}	77.59 ^{ai}	71.41 ^{ai}	60.13 ^{bi}	2.94
1/4 × MIC	66.11 ^{aj}	51.09 ^{bj}	68.01 ^{aj}	46.66 ^{bj}	34.46 ^{ci}	
1/8 × MIC	40.88 ^{bck}	44.48 ^{bj}	53.76 ^{ak}	37.62 ^{bck}	30.83 ^{ci}	

^{a-c}Means with different letters in the same row indicate significant differences ($p < 0.05$).

^{i-k}Means with different letters in the same column indicate significant differences ($p < 0.05$).

^eSE = standard error.

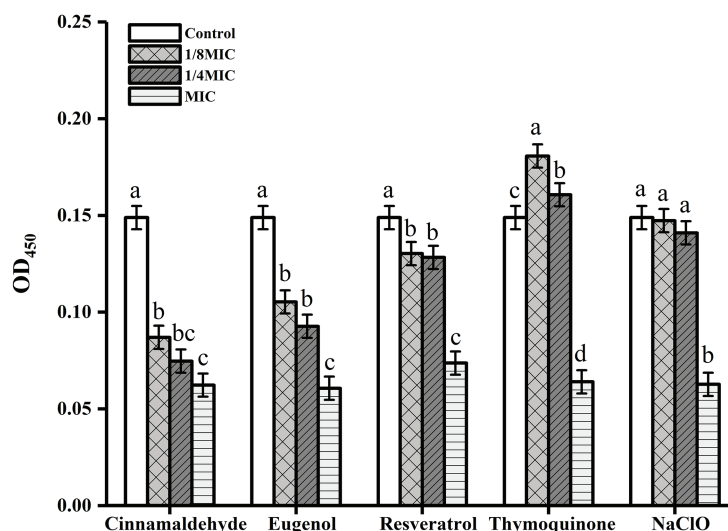


FIGURE 3 | Efficacy of five antimicrobials compounds in inhibiting biofilm metabolic activity of *Listeria monocytogenes* CMCC 54004 grown at 25°C. a-d Indicate the same compound treatments at different concentrations with different letters are significantly different ($p < 0.05$). Mean values of three independent experiments and standard error are shown.

significantly higher in thymoquinone sub-MICs (1/4 × MIC and 1/8 × MIC) treatment groups compared with that in the control group (Figure 3). Moreover, the control compound sodium hypochlorite at sub-MICs had no inhibitory effect on the cell viability.

SEM and CLSM Observation

The CLSM and SEM analysis showed that Lm 54004 biofilms revealed dose-related changes (Figure 4). The CLSM showed that all five antimicrobial compounds considerably reduced biofilm formation, with visible dose-dependent alterations and decreased cellular density in the three-dimensional structural organization of cells in the biofilm. Moreover, it is clear that the four natural antimicrobial compounds decreased the cellular density even at 1/4 × MIC (Figures 4A–D), but sodium hypochlorite had less inhibitory effect (Figure 4E). These changes were also in accord with the increasing numbers of dead bacteria (in red) seen by LIVE/DEAD staining. In the SEM images, the observation of cellular density was consistent with the CLSM results. The control cells in SEM images appeared intact, plump and typically rod-shaped with a smooth exterior,

however when exposed to antimicrobial compounds, the cell damage could be visualized directly, where cells distorted from their normal shape or even ruptured, and more extracellular matrix could be observed.

Effect of Antimicrobial Compounds on Expression of Genes Critical for Biofilm Formation

Quantitative reverse transcription PCR was used to analyze the transcriptional response of some genes related to biofilm and virulence in 1/4 × MIC antimicrobial-treated cells vs. untreated bacteria. The expression of the genes tested were compound dependent. As compared with the untreated control, four natural antimicrobial compounds substantially down-regulated the expression of quorum-sensing genes (*agrA*, *agrC*, and *agrD*) and starvation responses regulation gene *relA* (Figure 5A). Likewise, natural antimicrobial compounds also down-regulated the expression of *sigB* (global regulator of the stress response) except of the resveratrol (Figure 5A). As shown in Figure 5B, cinnamaldehyde and eugenol significantly down-regulated the transcription of *prfA* (the major regulator of

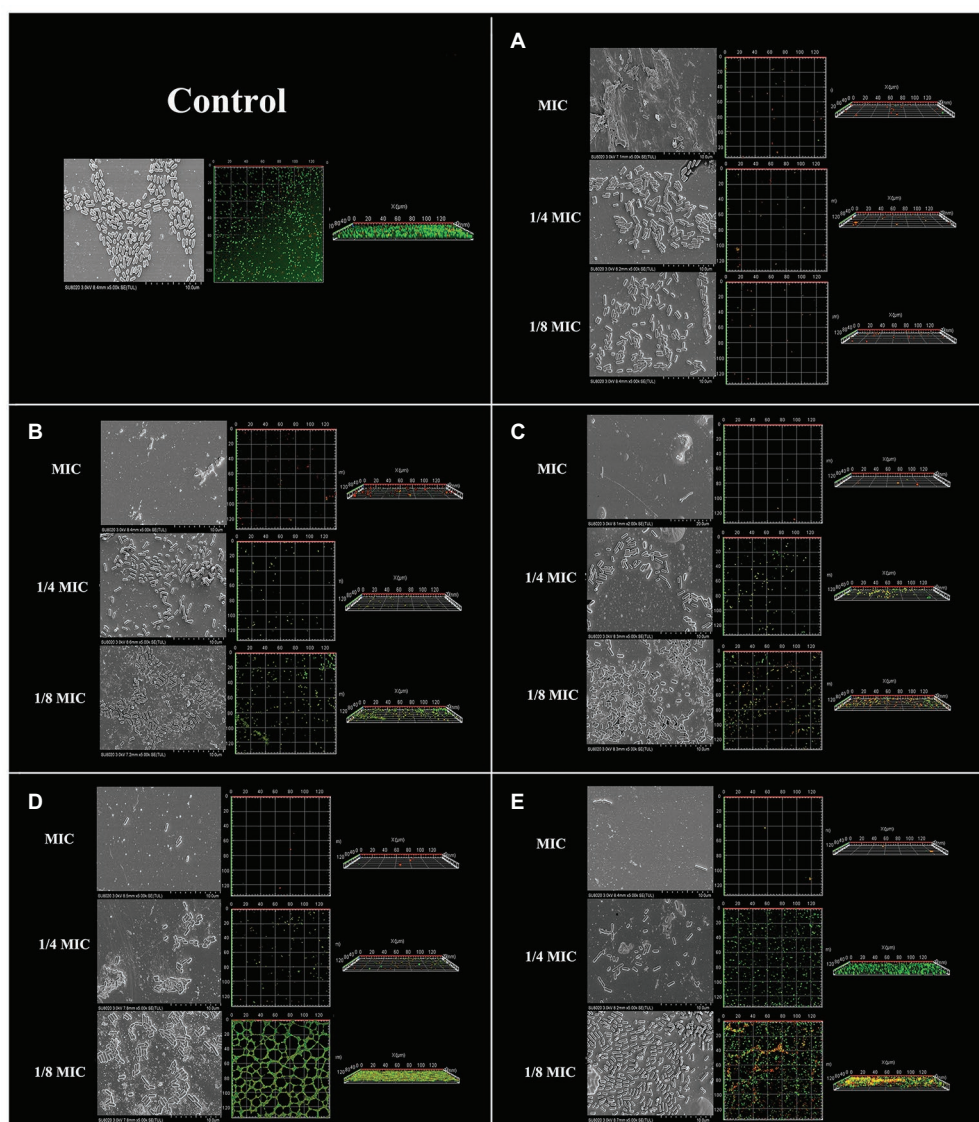


FIGURE 4 | Scanning electron microscopy (SEM) and confocal laser-scanning microscopy (CLSM) of *Listeria monocytogenes* CMCC 54004 biofilms formed in the presence of five antimicrobials compounds. (A): cinnamaldehyde, (B): eugenol, (C): resveratrol, (D): thymoquinone, (E): sodium hypochlorite.

L. monocytogenes virulence factors), while the gene was not obviously affected by resveratrol and thymoquinone. The virulence gene *inlA* (encodes internalin) was significantly suppressed ($p < 0.05$) by cinnamaldehyde, while not obviously affecting the expression of *inlA* ($p > 0.05$) when exposed to eugenol and thymoquinone, but resveratrol up-regulated the expression of *inlA*. Moreover, the expression of motility- and flagella-associated genes (*degU*, *flaA*, and *motB*) were all significantly up-regulated ($p < 0.05$) by resveratrol, and cinnamaldehyde induced the expression of *flaA* and *motB*, while eugenol exerted no effect on the expression of these genes and thymoquinone down-regulated the transcription of *degU*. Meanwhile, we found that the disinfectant sodium hypochlorite only down-regulated the expression of *agrA* and *agrD*, and no suppressive effect was found on other genes.

DISCUSSION

In the present study, we selected the common chemical disinfectant sodium hypochlorite as the control compound. Rodriguez-Melcon et al. (2019) reported that MIC or $1.5 \times$ MIC of sodium hypochlorite notably reduced the biovolume and cellular viability of *L. monocytogenes* biofilms. Similarly, our results showed that sodium hypochlorite at MIC exhibited a strong anti-biofilm activity against Lm 54004 (Table 2). However, compared to the natural antimicrobial compounds, sodium hypochlorite also showed significantly lower inhibitory effects on Lm 54004 biofilm both at MIC and $1/4 \times$ MIC. This finding is consistent with a previous report that the biofilm elimination effect of essential oils (cinnamon, marjoram, and thyme) was in most cases better compared to sodium hypochlorite

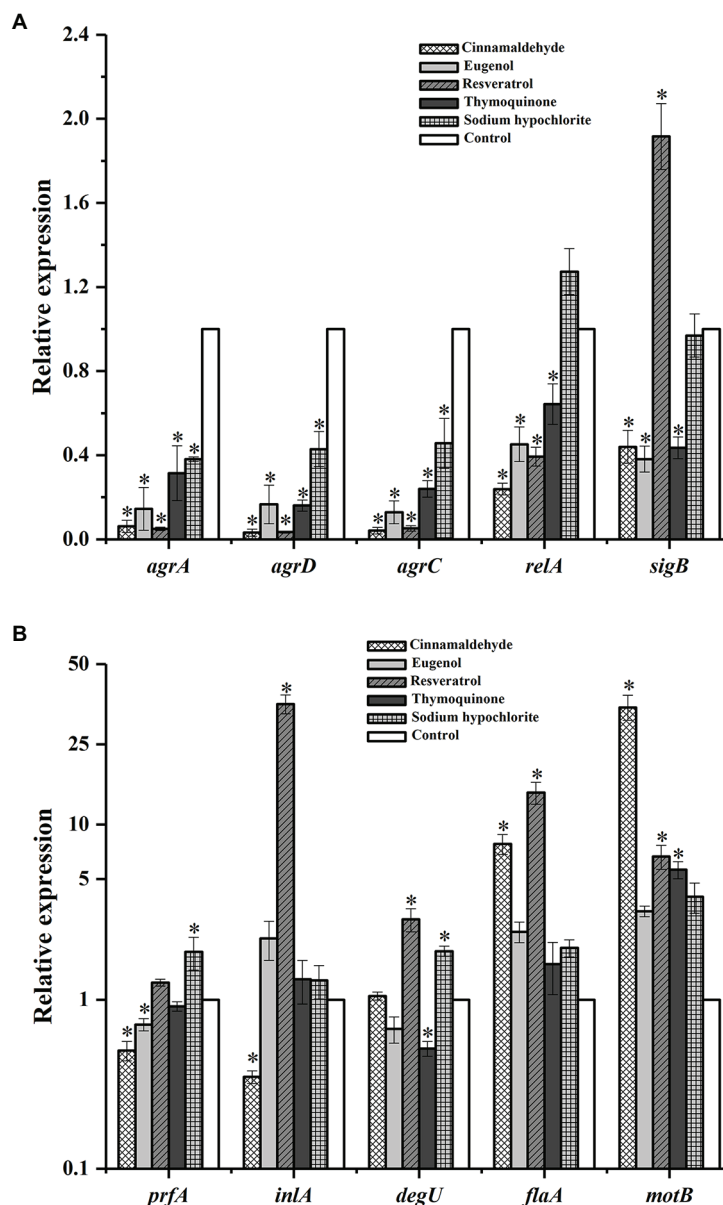


FIGURE 5 | Relative gene expression of *Listeria monocytogenes* CMCC 54004 in response to five antimicrobials compounds (at $1/4 \times \text{MIC}$). **(A):** relative expression of genes between 0 and 2.4, **(B):** relative expression of genes between 0.1 and 50. *Indicates $p < 0.05$ vs. the control group. Mean values of three independent experiments and SE are shown.

(Vidács et al., 2018). The corresponding results were also revealed by the RT-qPCR assays in this study (Figure 5), that sodium hypochlorite at $1/4 \times \text{MIC}$ had less suppressive effects on biofilm-related genes compared to the four natural antimicrobial compounds.

As mentioned above, biofilm inhibitory effects of the four natural antimicrobial compounds on Lm 54004 are different (Table 2). Miao et al. (2019) proved that thymoquinone effectively reduced biofilm biomass of *L. monocytogenes* ATCC19115 at sub-MICs. In the current study, we also found that thymoquinone

was an effective anti-biofilm agent compared to the sodium hypochlorite. However, thymoquinone showed a lower biofilm inhibition rate at sub-MICs compared to the phenylpropenes (cinnamaldehyde and eugenol) and the phenolic compound (resveratrol) against Lm 54004. In addition, the results were confirmed by the biofilm metabolic activity assay, that thymoquinone was the least compound to inhibit the biofilm metabolic activity of Lm 54004 at sub-MICs (Figure 3).

The gene *prfA* is a global regulator which positively regulates virulence genes (like *inlA*) in *L. monocytogenes* biofilms and

sigB is the global regulator of the stress response and is also closely related to virulence (Lemon et al., 2010; Vazquez-Armenta et al., 2020). Moreover, *relA* regulated the starvation responses in *L. monocytogenes*, which is an essential gene for cells survival in nutrient deficiency conditions (Kocot and Olszewska, 2017). Studies suggest that virulence genes are closely related to the biofilm development in *L. monocytogenes* (Vazquez-Armenta et al., 2020) and Sivaranjani et al. (2016) found that morin inhibited biofilm formation while interrupting the secretion of virulence determinant Listeriolysin O (LLO). In the present study, $1/4 \times \text{MIC}$ of all four natural compounds down-regulated the expression of *relA*. Cinnamaldehyde and eugenol were more effective in suppressing the *prfA* and *sigB*, and thymoquinone only down-regulated the transcription of *sigB* (Figure 5). These results are consistent with the biofilm inhibition assay, which indicates that the suppression of *prfA* and *sigB* was a critical reason for natural compounds to inhibit the formation of *L. monocytogenes* biofilm. However, resveratrol significantly induced the expression of *sigB*, and had no suppressive effects on *prfA*. Furthermore, resveratrol also up-regulated the virulence gene *inlA* while other natural compounds had no effects on this gene. These results suggest that resveratrol increased the stress responses of the *L. monocytogenes* cells to resist the external harsh environment. A similar result was found by Huang et al. (2020), such that the photodynamic inactivation treatment up-regulated the expression of *prfA* while it markedly reduced the adhesion ability of the biofilms of *L. monocytogenes*. Therefore, biofilm inhibition is a complex process, suggesting that the biofilm inhibitory pathway of various antimicrobial compounds differs. Further investigation is needed to explore the biofilm inhibitory pathway, based on the global regulators (*prfA* and *sigB*), of different antimicrobial compounds against *L. monocytogenes*.

Moreover, previous reports demonstrated that the motility ability of flagella was important in early biofilm formation (Bonsaglia et al., 2014). In this study, $1/4 \times \text{MIC}$ of cinnamaldehyde, eugenol and thymoquinone inhibited the swimming motility of Lm 54004 compared to the control (Figure 2A), although the colony diameters did not change much (within 0.6 mm), responding with inhibitory rates all below 18%. Additionally, resveratrol at $1/4 \times \text{MIC}$ had no inhibitory effects on the swimming and swarming motility of Lm 54004 cells. *degU* is the response regulator in *L. monocytogenes* which is involved in the flagellin expression and motility genes (Williams et al., 2005). The results of RT-qPCR showed that only thymoquinone was effective in down-regulating the expression of *degU*, while the other three natural compounds had no suppressive effects on this gene. *motB* is the gene that encodes for the motility protein involved in flagellar motor rotation, and *flaA* is a flagella-associated gene (Casey et al., 2014). The expression of these two motility-associated genes were both not suppressed or induced by the four natural compounds at $1/4 \times \text{MIC}$ compared to the control, but the biofilm formation was significantly reduced at this concentration when treated by these compounds. As showed in the previous studies, Upadhyay et al. (2013) and Miao et al. (2019) found that cinnamaldehyde, eugenol, and thymoquinone effectively

inhibited the motility of *L. monocytogenes* and significantly down-regulated the expression of *flaA*. The reason for these different findings as reported is probably due to the temperature (25°C) applied in the current study, and the bacterial strain (or serotype) we used was different to those in the studies of Upadhyay et al. (2013) and Miao et al. (2019). According to Bonsaglia et al. (2014), temperature is an important factor which may affect the formation of flagella in *L. monocytogenes*. The results confirmed that sub-MIC of natural antimicrobial compounds which reduced biofilm formation might not inhibit flagella formation.

It has been suggested that the QS system of *L. monocytogenes* plays a critical role in its biofilm formation (Rieu et al., 2007; Brackman and Coenye, 2015). QS is an intercellular communication system by which bacteria can coordinate their population density and control a variety of physiological processes (Solano et al., 2014). In *L. monocytogenes*, the QS is regulated by the Agr system for intraspecies communication (Skandamis and Nychas, 2012; Kocot and Olszewska, 2017). Previous study showed that mutations of *agrA* and *agrD* genes displayed significantly reduced biofilm formation of *L. monocytogenes* (Rieu et al., 2007; Riedel et al., 2009). In this study, the expression of three QS-associated genes (*agrA*, *agrC*, and *agrD*) were all significantly suppressed by four natural antimicrobial compounds at $1/4 \times \text{MIC}$ (Figure 5). The research of Du et al. (2018) reported similar results and found that low concentrations of epigallocatechin gallate inhibited biofilm formation by suppressing the QS system. Based on previous studies a number of different ways to inhibit the QS signaling molecules have been proposed, such as signal binding, degradation of the signaling molecules, competitive inhibition and genetic regulation systems (Sankar Ganesh and Ravishankar Rai, 2018). For example, Jakobsen et al. (2012) found that isothiocyanate produced from horseradish inhibited the expression of the *lasB*-gfp fusion, which compete with AHL signaling molecules (in Gram-negative bacteria) of regulator proteins. In this study, four natural compounds were all shown to block Agr QS systems of *L. monocytogenes*, probably by degrading signal receptors or secreting signal degrading enzymes and signal mimics, etc. Therefore, further research should be undertaken to investigate the direct mechanism of cinnamaldehyde, eugenol, resveratrol and thymoquinone on the QS system of *L. monocytogenes*. In summary, natural antimicrobial compounds at low concentrations were more likely to suppress the QS-associated genes to inhibit the biofilm formation of *L. monocytogenes*. For this reason, QS inhibition is a good point to study the anti-biofilm mechanism of natural antimicrobial compounds on *L. monocytogenes*.

CONCLUSION

This study showed that sub-MIC of cinnamaldehyde, eugenol, resveratrol, and thymoquinone were all efficient at inhibiting Lm 54004 biofilms, of which, cinnamaldehyde and resveratrol showed better anti-biofilm effects. Meanwhile, the transcriptional results showed that sub-MIC of natural antimicrobial compounds

reduced biofilm formation by suppressing the QS system rather than by inhibiting flagella formation. In addition, the biofilm inhibitory pathway of different antimicrobial compounds differs, which needs further exploration. The findings of present study suggest that low concentrations of natural compounds can serve as potential antimicrobials in controlling biofilm of *L. monocytogenes* in the food industry. The effective application of these compounds in industry could be achieved by using them in combination with chemical and physical disinfection methods commonly used in food processing, such as organic acids, sodium hypochlorite, or UV light, high temperature or high pressure.

DATA AVAILABILITY STATEMENT

The original contributions presented in the study are included in the article/**Supplementary Material**, further inquiries can be directed to the corresponding authors.

AUTHOR CONTRIBUTIONS

YL: conceptualization, investigation, formal analysis, data curation, and writing - original draft. LW: conceptualization, investigation, and resources. JH: conceptualization, resources, and methodology. PD: conceptualization, investigation, resources, and methodology. XL: conceptualization, writing - review and editing, and supervision. YZ: conceptualization, writing - reviewing and editing, and funding acquisition.

REFERENCES

- Bonsaglia, E. C. R., Silva, N. C. C., Fernandes Júnior, A., Araújo Júnior, J. P., Tsunemi, M. H., and Rall, V. L. M. (2014). Production of biofilm by *Listeria monocytogenes* in different materials and temperatures. *Food Control* 35, 386–391. doi: 10.1016/j.foodcont.2013.07.023
- Brackman, G., and Coenye, T. (2015). Quorum sensing inhibitors as anti-biofilm agents. *Curr. Pharm. Des.* 21, 5–11. doi: 10.2174/1381612820666140905114627
- Casey, A., Fox, E. M., Schmitz-Esser, S., Coffey, A., McAuliffe, O., and Jordan, K. (2014). Transcriptome analysis of *Listeria monocytogenes* exposed to biocide stress reveals a multi-system response involving cell wall synthesis, sugar uptake, and motility. *Front. Microbiol.* 5:68. doi: 10.3389/fmicb.2014.00068
- Chang, Y., Gu, W., Fischer, N., and McLandsborough, L. (2012). Identification of genes involved in *Listeria monocytogenes* biofilm formation by mariner-based transposon mutagenesis. *Appl. Microbiol. Biotechnol.* 93, 2051–2062. doi: 10.1007/s00253-011-3719-z
- Chen, L., Zhang, H., Liu, Q., Pang, X., Zhao, X., and Yang, H. (2019). Sanitising efficacy of lactic acid combined with low-concentration sodium hypochlorite on *Listeria innocua* in organic broccoli sprouts. *Int. J. Food Microbiol.* 295, 41–48. doi: 10.1016/j.ijfoodmicro.2019.02.014
- Du, W., Zhou, M., Liu, Z., Chen, Y., and Li, R. (2018). Inhibition effects of low concentrations of epigallocatechin gallate on the biofilm formation and hemolytic activity of *Listeria monocytogenes*. *Food Control* 85, 119–126. doi: 10.1016/j.foodcont.2017.09.011
- Fan, Q., Zhang, Y., Yang, H., Wu, Q., Shi, C., Zhang, C., et al. (2018). Effect of coenzyme Q0 on biofilm formation and attachment-invasion efficiency of *Listeria monocytogenes*. *Food Control* 90, 274–281. doi: 10.1016/j.foodcont.2018.02.047
- LZ: conceptualization, supervision, funding acquisition, and methodology. All authors contributed to the article and approved the submitted version.
- ## FUNDING
- This study was supported by the earmarked fund for China Agriculture Research System (beef) (CARS-37), funds from Shandong Province Agricultural Innovation Team (SDAIT-09-09), and a special intergovernmental project for international cooperation in Science, Technology and Innovation (2019YFE0103800).
- ## ACKNOWLEDGMENTS
- Thanks to Dr. David Hopkins (NSW DPI) for providing feedback on the paper.
- ## SUPPLEMENTARY MATERIAL
- The Supplementary Material for this article can be found online at: <https://www.frontiersin.org/articles/10.3389/fmicb.2020.617473/full#supplementary-material>
- Supplementary Figure 1** | Plate images of five antimicrobials compounds in inhibiting motility ability of *Listeria monocytogenes* CMCC 54004 grown at 25°C. (A): cinnamaldehyde, (B): eugenol, (C): resveratrol, (D): thymoquinone, (E): sodium hypochlorite.
- Gandra, T. K. V., Volcan, D., Kroning, I. S., Marini, N., de Oliveira, A. C., Bastos, C. P., et al. (2019). Expression levels of the agr locus and *prfA* gene during biofilm formation by *Listeria monocytogenes* on stainless steel and polystyrene during 8 to 48h of incubation 10 to 37 degrees C. *Int. J. Food Microbiol.* 300, 1–7. doi: 10.1016/j.ijfoodmicro.2019.03.021
- García-Gonzalo, D., and Pagán, R. (2015). Influence of environmental factors on bacterial biofilm formation in the food industry: a review. *Postdoc J.* 3, 3–13. doi: 10.14304/SURYA.JPR.V3N6.2
- Goel, S., and Mishra, P. (2018). Thymoquinone inhibits biofilm formation and has selective antibacterial activity due to ROS generation. *Appl. Microbiol. Biotechnol.* 102, 1955–1967. doi: 10.1007/s00253-018-8736-8
- Huang, J., Chen, B., Li, H., Zeng, Q.-H., Wang, J. J., Liu, H., et al. (2020). Enhanced antibacterial and antibiofilm functions of the curcumin-mediated photodynamic inactivation against *Listeria monocytogenes*. *Food Control* 108:106886. doi: 10.1016/j.foodcont.2019.106886
- Jakobsen, T. H., Bragason, S. K., Phipps, R. K., Christensen, L. D., van Gennip, M., Alhede, M., et al. (2012). Food as a source for quorum sensing inhibitors: iberin from horseradish revealed as a quorum sensing inhibitor of *Pseudomonas aeruginosa*. *Appl. Environ. Microbiol.* 78, 2410–2421. doi: 10.1128/AEM.05992-11
- Jolivet-Gougeon, A., and Bonnaure-Mallet, M. (2014). Biofilms as a mechanism of bacterial resistance. *Drug Discov. Today Technol.* 11, 49–56. doi: 10.1016/j.ddtec.2014.02.003
- Kim, Y. G., Lee, J. H., Kim, S. I., Baek, K. H., and Lee, J. (2015). Cinnamon bark oil and its components inhibit biofilm formation and toxin production. *Int. J. Food Microbiol.* 195, 30–39. doi: 10.1016/j.ijfoodmicro.2014.11.028
- Kocot, A. M., and Olszewska, M. A. (2017). Biofilm formation and microscopic analysis of biofilms formed by *Listeria monocytogenes* in a food processing context. *LWT-Food Sci. Technol.* 84, 47–57. doi: 10.1016/j.lwt.2017.05.042

- Lemon, K. P., Freitag, N. E., and Kolter, R. (2010). The virulence regulator PrfA promotes biofilm formation by *Listeria monocytogenes*. *J. Bacteriol.* 192, 3969–3976. doi: 10.1128/JB.00179-10
- Lemon, K. P., Higgins, D. E., and Kolter, R. (2007). Flagellar motility is critical for *Listeria monocytogenes* biofilm formation. *J. Bacteriol.* 189, 4418–4424. doi: 10.1128/JB.01967-06
- Li, T., Wang, D., Liu, N., Ma, Y., Ding, T., Mei, Y., et al. (2018). Inhibition of quorum sensing-controlled virulence factors and biofilm formation in *Pseudomonas fluorescens* by cinnamaldehyde. *Int. J. Food Microbiol.* 269, 98–106. doi: 10.1016/j.ijfoodmicro.2018.01.023
- Liu, Y., Dong, P., Zhu, L., Luo, X., and Zhang, Y. (2020a). Effect of four kinds of natural antimicrobial compounds on the biofilm formation ability of *Listeria monocytogenes* isolated from beef processing plants in China. *LWT-Food Sci. Technol.* 133:110020. doi: 10.1016/j.lwt.2020.110020
- Liu, Y., Sun, W., Sun, T., Gorris, L. G. M., Wang, X., Liu, B., et al. (2020b). The prevalence of *Listeria monocytogenes* in meat products in China: a systematic literature review and novel meta-analysis approach. *Int. J. Food Microbiol.* 312:108358. doi: 10.1016/j.ijfoodmicro.2019.108358
- Livak, K. J., and Schmittgen, T. D. (2001). Analysis of relative gene expression data using real-time quantitative PCR and the $2^{-\Delta\Delta C(T)}$ method. *Methods* 25, 402–408. doi: 10.1006/meth.2001.1262
- Miao, X., Liu, H., Zheng, Y., Guo, D., Shi, C., Xu, Y., et al. (2019). Inhibitory effect of Thymoquinone on *Listeria monocytogenes* ATCC 19115 biofilm formation and virulence attributes critical for human infection. *Front. Cell. Infect. Microbiol.* 9:304. doi: 10.3389/fcimb.2019.00304
- Oloketuyi, S. F., and Khan, F. (2017). Inhibition strategies of *Listeria monocytogenes* biofilms-current knowledge and future outlooks. *J. Basic Microbiol.* 57, 728–743. doi: 10.1002/jobm.201700071
- Qin, N., Tan, X., Jiao, Y., Liu, L., Zhao, W., Yang, S., et al. (2014). RNA-Seq-based transcriptome analysis of methicillin-resistant *Staphylococcus aureus* biofilm inhibition by ursolic acid and resveratrol. *Sci. Rep.* 4:5467. doi: 10.1038/srep05467
- Riedel, C. U., Monk, I. R., Casey, P. G., Waidmann, M. S., Gahan, C. G., and Hill, C. (2009). AgrD-dependent quorum sensing affects biofilm formation, invasion, virulence and global gene expression profiles in *Listeria monocytogenes*. *Mol. Microbiol.* 71, 1177–1189. doi: 10.1111/j.1365-2958.2008.06589.x
- Rieu, A., Weidmann, S., Garmyn, D., Piveteau, P., and Guzzo, J. (2007). Agr system of *Listeria monocytogenes* EGD-e: role in adherence and differential expression pattern. *Appl. Environ. Microbiol.* 73, 6125–6133. doi: 10.1128/AEM.00608-07
- Rodriguez-Melcon, C., Riesco-Pelaez, F., Garcia-Fernandez, C., Alonso-Calleja, C., and Capita, R. (2019). Susceptibility of *Listeria monocytogenes* planktonic cultures and biofilms to sodium hypochlorite and benzalkonium chloride. *Food Microbiol.* 82, 533–540. doi: 10.1016/j.fm.2019.03.020
- Sankar Ganesh, P., and Ravishankar Rai, V. (2018). “Alternative strategies to regulate quorum sensing and biofilm formation of pathogenic *Pseudomonas* by quorum sensing inhibitors of diverse origins” in *Biotechnological Applications of Quorum Sensing Inhibitors*. ed. V. Kalia (Singapore: Springer), 33–61.
- Shi, C., Yan, C., Sui, Y., Sun, Y., Guo, D., Chen, Y., et al. (2017). Thymoquinone inhibits virulence related traits of *Cronobacter sakazakii* ATCC 29544 and has anti-biofilm formation potential. *Front. Microbiol.* 8:2220. doi: 10.3389/fmicb.2017.02220
- Shi, X., and Zhu, X. (2009). Biofilm formation and food safety in food industries. *Trends Food Sci. Technol.* 20, 407–413. doi: 10.1016/j.tifs.2009.01.054
- Sivaranjani, M., Gowrishankar, S., Kamaladevi, A., Pandian, S. K., Balamurugan, K., and Ravi, A. V. (2016). Morin inhibits biofilm production and reduces the virulence of *Listeria monocytogenes* - an in vitro and in vivo approach. *Int. J. Food Microbiol.* 237, 73–82. doi: 10.1016/j.ijfoodmicro.2016.08.021
- Skandamis, P. N., and Nychas, G. J. (2012). Quorum sensing in the context of food microbiology. *Appl. Environ. Microbiol.* 78, 5473–5482. doi: 10.1128/AEM.00468-12
- Solano, C., Echeverez, M., and Lasa, I. (2014). Biofilm dispersion and quorum sensing. *Curr. Opin. Microbiol.* 18, 96–104. doi: 10.1016/j.mib.2014.02.008
- Upadhyay, A., Upadhyaya, I., Kollanoor-Johny, A., and Venkitanarayanan, K. (2013). Antibiofilm effect of plant derived antimicrobials on *Listeria monocytogenes*. *Food Microbiol.* 36, 79–89. doi: 10.1016/j.fm.2013.04.010
- van der Veen, S., and Abbe, T. (2010). Importance of SigB for *Listeria monocytogenes* static and continuous-flow biofilm formation and disinfectant resistance. *Appl. Environ. Microbiol.* 76, 7854–7860. doi: 10.1128/AEM.01519-10
- Vazquez-Armenta, F. J., Hernandez-Oñate, M. A., Martinez-Tellez, M. A., Lopez-Zavala, A. A., Gonzalez-Aguilar, G. A., Gutierrez-Pacheco, M. M., et al. (2020). Quercetin repressed the stress response factor (*sigB*) and virulence genes (*prfA*, *actA*, *inlA*, and *inlC*), lower the adhesion, and biofilm development of *L. monocytogenes*. *Food Microbiol.* 87:103377. doi: 10.1016/j.fm.2019.103377
- Vidács, A., Kerekes, E., Rajkó, R., Petkovits, T., Alharbi, N. S., Khaled, J. M., et al. (2018). Optimization of essential oil-based natural disinfectants against *Listeria monocytogenes* and *Escherichia coli* biofilms formed on polypropylene surfaces. *J. Mol. Liq.* 255, 257–262. doi: 10.1016/j.molliq.2018.01.179
- Weiler, C., Ifland, A., Naumann, A., Kleta, S., and Noll, M. (2013). Incorporation of *Listeria monocytogenes* strains in raw milk biofilms. *Int. J. Food Microbiol.* 161, 61–68. doi: 10.1016/j.ijfoodmicro.2012.11.027
- Williams, T., Joseph, B., Beier, D., Goebel, W., and Kuhn, M. (2005). Response regulator DegU of *Listeria monocytogenes* regulates the expression of flagella-specific genes. *FEMS Microbiol. Lett.* 252, 287–298. doi: 10.1016/j.femsle.2005.09.011
- Xiang, Q., Kang, C., Zhao, D., Niu, L., Liu, X., and Bai, Y. (2019). Influence of organic matters on the inactivation efficacy of plasma-activated water against *E. coli* O157:H7 and *S. aureus*. *Food Control* 99, 28–33. doi: 10.1016/j.foodcont.2018.12.019
- Yu, F., Dong, Y., Yu, H. H., Lin, P. T., Zhang, L., Sun, X., et al. (2017). Antibacterial activity and bonding ability of an orthodontic adhesive containing the antibacterial monomer 2-methacryloxyethyl hexadecyl methyl ammonium bromide. *Sci. Rep.* 7:41787. doi: 10.1038/srep41787
- Zetzmann, M., Sanchez-Kopper, A., Waidmann, M. S., Blombach, B., and Riedel, C. U. (2016). Identification of the agr peptide of *Listeria monocytogenes*. *Front. Microbiol.* 7:989. doi: 10.3389/fmicb.2016.00989

Conflict of Interest: The authors declare that the research was conducted in the absence of any commercial or financial relationships that could be construed as a potential conflict of interest.

Copyright © 2021 Liu, Wu, Han, Dong, Luo, Zhang and Zhu. This is an open-access article distributed under the terms of the Creative Commons Attribution License (CC BY). The use, distribution or reproduction in other forums is permitted, provided the original author(s) and the copyright owner(s) are credited and that the original publication in this journal is cited, in accordance with accepted academic practice. No use, distribution or reproduction is permitted which does not comply with these terms.



Direct Detection of Viable but Non-culturable (VBNC) *Salmonella* in Real Food System by a Rapid and Accurate PMA-CPA Technique

OPEN ACCESS

Edited by:

Yang Deng,

College of Food Science
and Engineering, Qingdao Agricultural
University, China

Reviewed by:

Wensen Jiang,

Cedars Sinai Medical Center,
United States

Yanmei Li,

University of Maryland, Baltimore,
United States

Yuting Tian,

School of Food Science, Fujian
Agriculture and Forestry University,
China

Ying Mu,

University of Tennessee Health
Science Center (UTHSC),
United States

*Correspondence:

Junyan Liu

jliu81@uthsc.edu

Lu Qian

qianlu@scut.edu.cn

[†] These authors have contributed
equally to this work

Specialty section:

This article was submitted to
Food Microbiology,
a section of the journal
Frontiers in Microbiology

Received: 28 November 2020

Accepted: 19 January 2021

Published: 18 February 2021

Citation:

Ou A, Wang K, Ye Y, Chen L,
Gong X, Qian L and Liu J (2021)
Direct Detection of Viable but
Non-culturable (VBNC) *Salmonella*
in Real Food System by a Rapid
and Accurate PMA-CPA Technique.
Front. Microbiol. 12:634555.
doi: 10.3389/fmicb.2021.634555

Aifen Ou^{1†}, Kan Wang^{2†}, Yanrui Ye³, Ling Chen⁴, Xiangjun Gong⁵, Lu Qian^{5*} and Junyan Liu^{6*}

¹ Department of Food, Guangzhou City Polytechnic, Guangzhou, China, ² Center for Translational Medicine, The Second Affiliated Hospital of Shantou University Medical College, Shantou, China, ³ School of Biological Science and Engineering, South China University of Technology, Guangzhou, China, ⁴ School of Food Science and Engineering, Guangdong Province Key Laboratory for Green Processing of Natural Products and Product Safety, South China University of Technology, Guangzhou, China, ⁵ School of Materials Science and Engineering, South China University of Technology, Guangzhou, China, ⁶ Department of Civil and Environmental Engineering, University of Maryland, College Park, College Park, MD, United States

Salmonella enterica is a typical foodborne pathogen with multiple toxic effects, including invasiveness, endotoxins, and enterotoxins. Viable but nonculturable (VBNC) is a type of dormant form preserving the vitality of microorganisms, but it cannot be cultured by traditional laboratory techniques. The aim of this study is to develop a propidium monoazide-crossing priming amplification (PMA-CPA) method that can successfully detect *S. enterica* rapidly with high sensitivity and can identify VBNC cells in food samples. Five primers (4s, 5a, 2a/1s, 2a, and 3a) were specially designed for recognizing the specific *invA* gene. The specificity of the CPA assay was tested by 20 different bacterial strains, including 2 standard *S. enterica* and 18 non-*S. enterica* bacteria strains covering Gram-negative and Gram-positive isolates. Except for the two standard *S. enterica* ATCC14028 and ATCC29629, all strains showed negative results. Moreover, PMA-CPA can detect the VBNC cells both in pure culture and three types of food samples with significant color change. In conclusion, the PMA-CPA assay was successfully applied on detecting *S. enterica* in VBNC state from food samples.

Keywords: *Salmonella enterica*, viable but non-culturable (VBNC), crossing priming amplification (CPA), propidium monoazide (PMA), rapid detection

INTRODUCTION

During food processing, food is frequently contaminated by foodborne bacteria, including *Staphylococcus aureus*, *Salmonella enterica*, and *Escherichia coli* O157 (Kirk et al., 2015; Miao et al., 2017a; Sharma et al., 2019). *S. enterica* is a typical foodborne pathogen with multiple toxic effects, including invasiveness, endotoxins, and enterotoxins (Eng et al., 2015). Various serotypes of *Salmonella* are implicated in foodborne infections and contaminate food products, including eggs, milk, poultry, meat, and vegetables. It is the main cause of human gastrointestinal and other related diseases (Bao et al., 2017a,b; Wen et al., 2020). Recently, studies confirmed that *S. enterica* is capable of entering into the viable but non-culturable state (VBNC) state under an adverse environment, which could include low-temperature, salt stress, and nutrient starvation (Roszak et al., 1984;

Chmielewski and Frank, 1995; Gupte et al., 2003; Zeng et al., 2013; Morishige et al., 2017; Highmore et al., 2018). VBNC cells cannot be detected by traditional culture-based methods (Xu et al., 2011a; Lin et al., 2017; Miao et al., 2017a; Xie et al., 2017a). Therefore, it is urgent to develop a rapid and sensitive assay to detect *S. enterica*, especially in the VBNC state.

The molecular biological method, classified into polymerase chain reaction (PCR) and isothermal amplification, is a new strategy to detect pathogens (Xu et al., 2012; Xu et al., 2012a; Liu et al., 2019). PCR and PCR-based assays have been well developed in the last few decades (You et al., 2012; Zhong et al., 2013; Xu et al., 2016c). However, these assays require complicated procedures that may increase the uncertainty in result determination (Tada et al., 1992; Zhong et al., 2013; Xu et al., 2017a; Xie et al., 2017b; Jia et al., 2018). Quantitative real-time PCR can achieve the result interpretation by digital curve without electrophoresis but with lower detection limits (Xu et al., 2007; Miao et al., 2017b,c). Isothermal amplification assays include loop-mediated isothermal amplification (LAMP), rolling circle amplification (RCA), and strand displacement amplification (SDA) (Fire and Xu, 1995; Zhao et al., 2009; Zhao et al., 2010a,b; Bao et al., 2017c; Xu et al., 2017b). Reverse transcription LAMP (RT-LAMP) or other isothermal amplification assays have been utilized to replace the PCR assay (Parida et al., 2005).

Cross Priming Amplification (CPA) is a novel isothermal method relying on five primers (2a/1s, 2a, 3a, 4s, and 5a) to amplify the target nucleotide sequences (Xu et al., 2012). It does not require any special instrumentation and presents high rapidity, specificity, and sensitivity. Recently, CPA assays have been used for the detection of *E. coli* O157:H7, *Listeria monocytogenes*, *Enterobacter sakazakii*, *Yersinia enterocolitica*, and other pathogens (Wang et al., 2014; Zhang et al., 2015; Wang et al., 2018; Xu et al., 2020). Therefore, CPA is a potentially valuable tool for the rapid detection of foodborne pathogens, and the combination of propidium monoazide (PMA) may achieve the detection of VBNC state (Xu et al., 2010; Wang et al., 2011; Xu et al., 2011c).

MATERIALS AND METHODS

Bacterial Strains

To standardize and evaluate the reaction system of CPA assay, non-*S. enterica* bacteria strains, including various species of Gram-negative and Gram-positive non-target strains, were used in this study (Table 1). Two standard *S. enterica* ATCC14028 and ATCC29629 were used as positive controls. All strains used in this study had been preliminarily identified in the Lab of Clinical Microbiology, Zhongshan Supervision Testing Institute of Quality and Metrology.

All bacteria were prepared for genomic DNA isolation after incubation in trypticase soy broth (TSB, Huankai Microbial, China) at 37°C at 200 rpm overnight. The genomic DNA was isolated by Bacterial DNA extraction Kit (Dongsheng Biotech, Guangzhou, China) according to the manufacturer's protocol. The concentration and quality of the DNA were measured using

Nano Drop 2000 (Thermo Fisher Scientific Inc., Waltham, MA, United States) at 260 and 280 nm. The isolated DNA was stored at −20°C for further use.

CPA Detection System Design

As a species specific gene in *Salmonella*, *invA* has been selected, and its specificity in *Salmonella* has been previously confirmed. The CPA primers were specifically designed for *invA* gene in *S. enterica* using Primer Premier 5, including five primers recognizing five distinct regions in the gene open reading frame sequence (Table 2). All primers were assessed for specificity by BLAST against the sequences in Genbank.

The PCR reaction was conducted to serve as a control in a total 25 µL volume with 12.5 µL 2× Taq PCR Master Mix (Dongsheng Biotech, Guangzhou, China), 3 µM each of forward and reverse primers, 2 µL of DNA template and the total volume was added up to 25 µL with nuclease-free water. The amplification procedure included a 5-min denaturation at 95°C, 32 cycles of amplification at 95°C for 30 s, 52°C 30 s, 72°C for 35 s, and final amplification at 72°C for 5 min. The PCR products were detected by electrophoresis on 1.5% agarose gels.

TABLE 1 | Reference strains and results of CPA assays.

Reference strain	PCR	CPA
<i>Salmonella enterica</i> ATCC29629	+	+
<i>Salmonella enterica</i> ATCC14028	+	+
<i>Listeria monocytogenes</i> ATCC19114	–	–
<i>Listeria monocytogenes</i> ATCC19116	–	–
<i>Listeria monocytogenes</i> ATCC19113	–	–
<i>Escherichia coli</i> O157:H7 ATCC43895	–	–
<i>Escherichia coli</i> O157:H7 E019	–	–
<i>Escherichia coli</i> O157:H7 E020	–	–
<i>Escherichia coli</i> O157:H7 E043	–	–
<i>Vibrio parahaemolyticus</i> ATCC27969	–	–
<i>Vibrio parahaemolyticus</i> ATCC17802	–	–
<i>Pseudomonas aeruginosa</i> ATCC27853	–	–
<i>Pseudomonas aeruginosa</i> C9	–	–
<i>Pseudomonas aeruginosa</i> C40	–	–
<i>Staphylococcus aureus</i> ATCC23235	–	–
<i>Staphylococcus aureus</i> 10085	–	–
<i>Staphylococcus aureus</i> 10071	–	–
<i>Lactobacillus casei</i>	–	–
<i>Lactobacillus acetotolerans</i> BM-LA14527	–	–
<i>Lactobacillus plantarum</i> BM-LP14723	–	–

TABLE 2 | Primers sequence for detection of CPA.

Target gene	Primers	Sequence (5'–3')
<i>invA</i>	4s	CTGAGCGATAACAGCATT
	5a	TGCGTTACCCAGAAATAC
	2a/1s	TGATGATAGGTCGTTGGATGCGTGGTAAATTATTCGG
	2a	TGATGATAGGTCGTTGGAT
	3a	GCCAAAGGAAGCGACTTC

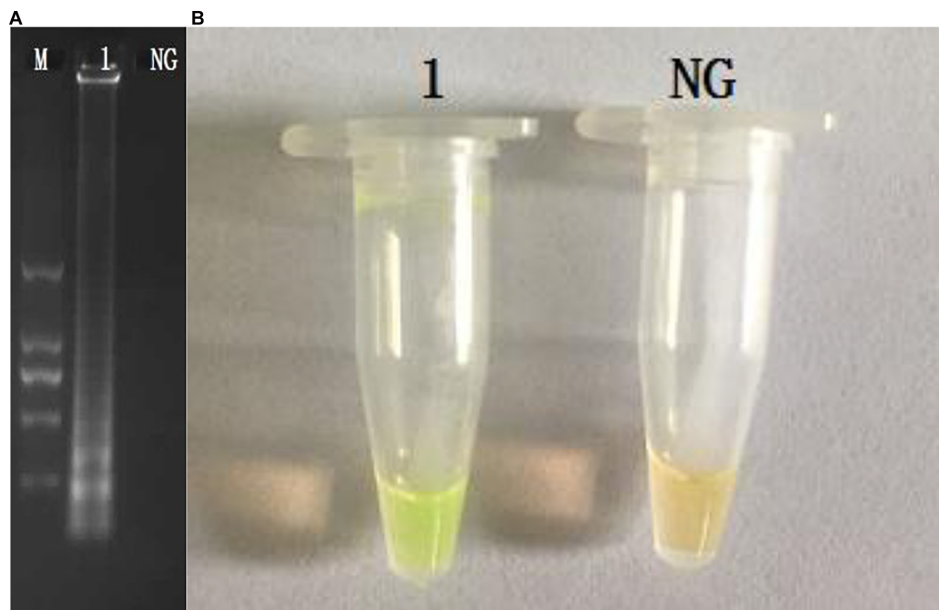


FIGURE 1 | Amplification products were visually detected both by 1.5% agarose gel electrophoresis under UV light **(A)** and observation at the color change by naked eye **(B)**. M, DNA marker; lane 1, positive control; lane NC, negative products **(A)**; tube 1, positive products; tube NC, negative control.

The CPA reaction system was performed using thermostatic equipment or a water bath in a 26 μ L system, containing 20 mM Tris-HCl, 10 mM $(\text{NH}_4)_2\text{SO}_4$, 10 mM KCl, 8.0 mM MgSO_4 , 0.1% Tween 20, 0.7 M betain (sigma), 1.4 mM dNTP (each), 8 U Bst DNA polymerase (NEB, United States), 1.0 μ M primer of 2a/1s, 0.5 μ M (each) primer of 2a and 3a, 0.6 μ M (each) primer of 4s and 5a, 1 μ L mixture chromogenic agent (mixture with calcein and Mn^{2+}), 1 μ L template DNA, and a volume of up to 26 μ L of nuclease-free water. The mixed chromogenic agent consists of 0.13 mM calcein and 15.6 mM $\text{MnCl}_2 \cdot 4\text{H}_2\text{O}$. And mixed reaction solution was incubated at 65°C for 60 min and heated at 80°C for 2 min to terminate the reaction. Nuclease-free water substituted target DNA was used as a negative control. Subsequently, the amplified products were analyzed by electrophoresis on 1.5% agarose gels and observed the color change by naked eyes.

CPA Detection System Optimization

The specificity of CPA was evaluated by amplifying the genomic DNA extracted from 2 standard *S. enterica* strains and 18 non-*S. enterica* strains.

To determine the sensitivity of the CPA assay, serial 10-fold dilutions of the genomic DNA of *S. enterica* ATCC14280 were prepared and used in the reaction. The sensitivity of the CPA method was compared with the PCR method. All the tests were performed in triplicate.

Application of CPA Assay in Food Products

The application of CPA assay in the detection of *S. enterica* was conducted in three rice products (Cantonese rice cake, steamed bread, and rice noodle purchased from Guangzhou Restaurant,

Guangzhou, China). Different concentrations (from 10^8 CFU/mL to 10 CFU/mL) of *S. enterica* ATCC14028 were applied to contaminate food samples. Subsequently, genomic DNA was extracted from the contaminated food samples and subjected to CPA and PCR methods in triplicate (Xu et al., 2020).

VBNC State Induction

The VBNC state of *S. enterica* was induced by oligotrophic medium (sterile saline) at a low temperature. The bacterial overnight culture ($\sim 10^8$ CFU/mL) was washed three times and resuspended by sterile saline and then stored at -20°C . The culturable cell number was measured by plate counting method, and viable cells were determined by LIVE/DEAD® BacLight kit™ (ThermoFisher scientific, United States) with a fluorescence microscope after the cells were no longer culturable. The culturable and viable cell enumerations were performed every three days.

PMA-CPA Detection System

The PMA-CPA were developed to detect the VBNC cells of *S. enterica* with the observation of color change. The PMA-CPA was further applied in the detection of VBNC cells in contaminated rice food products (Cantonese rice cake, steamed bread, and rice noodle from Guangzhou Restaurant, Guangzhou, China).

RESULTS

Development of CPA Assay

The CPA assays for the detection of *invA* gene were set up using *S. enterica* ATCC14028. The products were analyzed by 1.5%

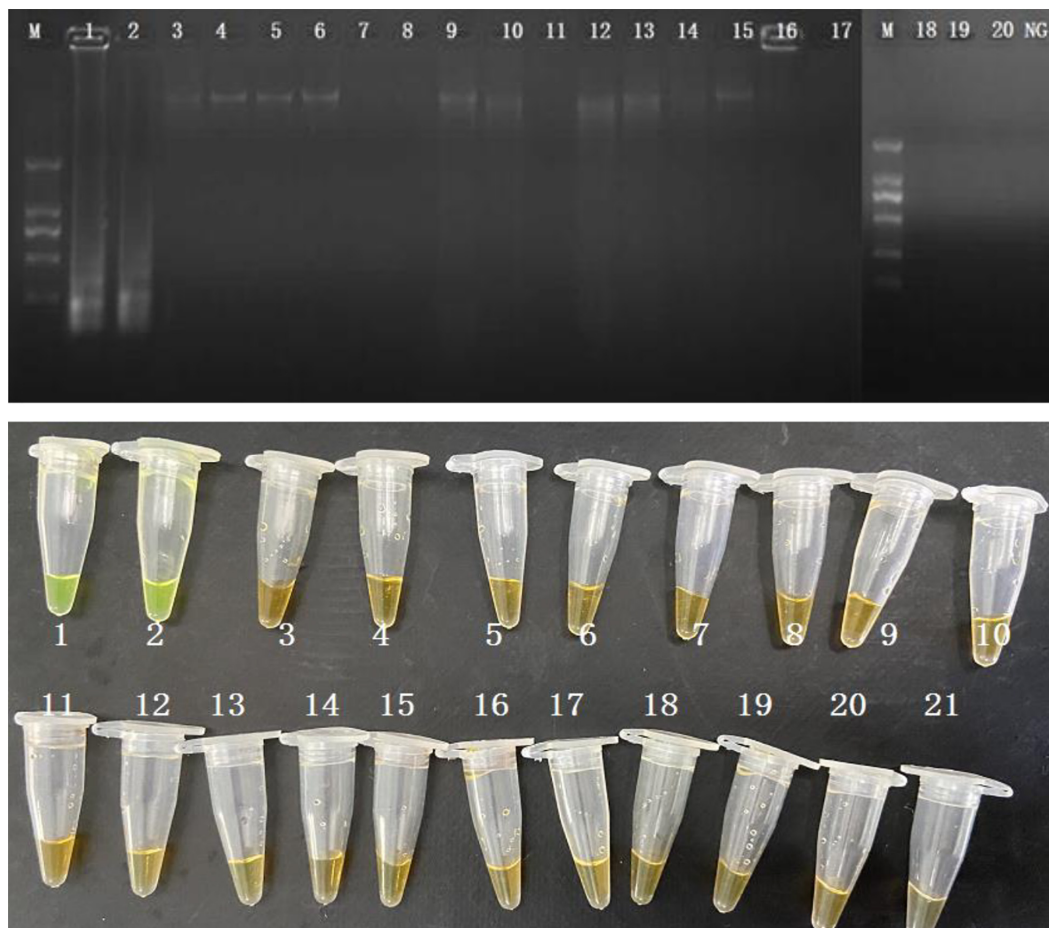


FIGURE 2 | Specificity of CPA assay for detection *S. enterica* strains with *invA* genes by 1.5% agarose gel electrophoresis and observation at the color change by naked eye; M-DNA marker; lane 1–2, *S. enterica* ATCC 29629 and ATCC 14028; lane 2–20, non-*S. enterica* strains. NG/21, negative control.



FIGURE 3 | Sensitivity of the CPA assay in food samples of *S. enterica* with *invA* genes by 1.5% agarose gel electrophoresis (A) and agent mixture (B); M-DNA marker; lane 1–8, 10^7 CFU/mL, 10^6 CFU/mL, 10^5 CFU/mL, 10^4 CFU/mL, 10^3 CFU/mL, 10^2 CFU/mL, 10 CFU/mL negative control.

agarose gel electrophoresis, and the bands were observed under UV light (**Figure 1A**). The results of electrophoresis revealed that the amplicons of CPA are of various sizes, showing as a ladder pattern on agarose gel instead of a single band. The fluorescent dye (MgCl₂ and calcein) changes the reaction system from orange to green in the reaction system (**Figure 1B**).

The evaluation of the specificity of CPA assay was performed in 2 *S. enterica* strains and 18 non-*S. enterica* reference strains. Results were recorded by 1.5% agarose gel electrophoresis and color change. Ladder pattern bands and orange to yellow color changes were only observed in the 2 *S. enterica* strains (**Figure 2**). It indicated that only the target *S. enterica* strains were

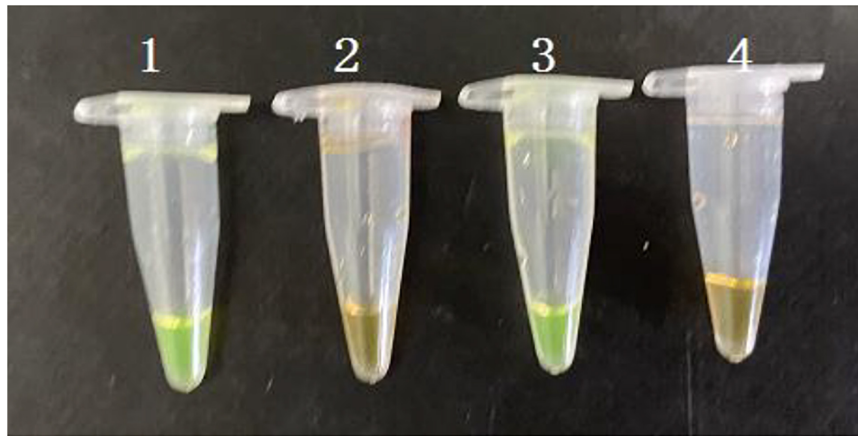


FIGURE 4 | Detection of VBNC state of *S. enterica* in pure cultures and food samples by PMA-CPA assay with observation at the color change by naked eye. 1 – VBNC cells in pure cultures; 2 – dead cells in pure cultures; 3 – VBNC cells in food samples; 4 – dead cells in food samples.

detected with positive results, showing the high specificity of the CPA assay.

Detection of *S. enterica* in Food Products

The CPA assays were applied in the detection of *S. enterica* in three food samples (Cantonese rice cake, steamed bread, and rice noodle). The homogenized rice products (9 mL) were inoculated with 1 mL 10-fold serial dilution of pure *S. enterica* culture. The concentration of artificial contamination food samples ranging from 10^8 CFU/mL to 10 CFU/mL with 10-fold series dilutions was applied. All three food samples were included for the application. As expected, the LOD shows an insignificant difference among food samples, and the results are identical. Only the samples with a concentration higher than 10^3 CFU/mL were able to be detected (Figure 3). Thus, the detection limit of the CPA assay was 10^3 CFU/mL.

Detection of VBNC Cells by PMA-CPA Assay

The PMA-CPA assay was established using VBNC cells of *S. enterica*. The PMA dye was added to either pure culture or flour samples with a final concentration of 5 μ g/mL. After incubation at room temperature for 10 min in dark, the samples were exposed to a 650 W halogen lamp with a distance of 15 cm for 5 min, which inactivates unbinding PMA molecules rather than PMA-DNA molecules. All the dying process was performed in an ice bath to prevent DNA damage. Results showed that PMA-CPA can detect the VBNC cells both in pure culture and food samples with significant color change from orange to yellow (Figure 4). The samples with dead cells remain orange in both pure culture and food samples.

DISCUSSION

Salmonella enterica is a common foodborne pathogen that may cause severe illness. The generation of *S. enterica*

VBNC state occurs during the chlorination of wastewater or food (Oliver et al., 2005; Zeng et al., 2013). Non-ionic detergents and sanitizers can also induce *S. enterica* into VBNC state (Morishige et al., 2013; Purevdorj-Gage et al., 2018; Robben et al., 2018). Furthermore, a multi-stress environment in complex components of food and storage conditions may induce the VBNC state formation of foodborne pathogens (Lin et al., 2016; Miao et al., 2016; Xu et al., 2016a,b).

Various molecular techniques have been developed to identify microbes. PCR is a mature method to detect foodborne microbes, but it has low sensitivity and complex variable temperature programs (Kim et al., 1999). RT-PCR has been used to detect microbes compared with the method in ISO 21872-1:2007. RT-PCR achieved higher sensitivity but with long pre-enrichment and 24 h of complicate procedure. Although RT-PCR is able to show results via a digital curve, the sensitivity of this method is limited and the procedure is complicated (Xu et al., 2008a; Miao et al., 2018; Xu et al., 2018; Zhao et al., 2018a,b). RT-LAMP or other isothermal amplification has been used reported to replace RT-PCR to increase the detection limit (Xu et al., 2008b; Xu et al., 2009; Liu et al., 2018a,b; Lv et al., 2020). However, sophisticated equipment with these technologies has brought certain difficulties to rapid on-site testing (Xu et al., 2011b; Xu et al., 2012b). CPA technique is a new strategy to achieve rapid detection and can be performed under constant temperature using a simple water bath. Furthermore, with the improvement of fluorescence dye, results can be identified by the color change in the reaction tube by the naked eye. For VBNC and dead cells, they are both nonculturable. However, VBNC cells differ from dead cells in their intact cell membrane and thus could be differentiated via PMA, which is capable of differentiating viable and dead cells.

Therefore, the developed CPA method can successfully detect the *S. enterica* with high rapidity and sensitivity and can identify the VBNC cells in food samples when combining with PMA.

DATA AVAILABILITY STATEMENT

The raw data supporting the conclusions of this article will be made available by the authors, without undue reservation.

AUTHOR CONTRIBUTIONS

JL conceived of the study and participated in its design and coordination. AO and KW performed the experimental work and

collected the data. YY and XG organized the database. LC and LQ performed the statistical analysis. AO wrote the manuscripts. All authors contributed to manuscript revision, read, and approved the submitted manuscript.

FUNDING

This work was supported by the National Key Research and Development Program of China (2016YFD04012021).

REFERENCES

- Bao, X. R., Jia, X. Y., Chen, L. Q., Peters, B. M., Lin, C. W., Chen, D. Q., et al. (2017c). Effect of Polymyxin Resistance (pmr) on Biofilm Formation of *Cronobacter sakazakii*. *Microb. Pathog.* 106, 16–19.
- Bao, X. R., Yang, L., Chen, L. Q., Li, B., Li, L., Li, Y. Y., et al. (2017b). Analysis on pathogenic and virulent characteristics of the *Cronobacter sakazakii* strain BAA-894 by whole genome sequencing and its demonstration in basic biology science. *Microb. Pathog.* 109, 280–286.
- Bao, X. R., Yang, L., Chen, L. Q., Li, B., Li, L., Li, Y. Y., et al. (2017a). Virulent and pathogenic features on the *Cronobacter sakazakii* polymyxin resistant pmr mutant strain s-3. *Microb. Pathog.* 110, 359–364.
- Chmielewski, R. A., and Frank, J. F. (1995). Formation of viable but nonculturable *Salmonella* during starvation in chemically defined solutions. *Lett. Appl. Microbiol.* 20, 380–384.
- Eng, S.-K., Pusparajah, P., Ab Mutalib, N.-S., Ser, H.-L., Chan, K.-G., and Lee, L.-H. (2015). *Salmonella*: a review on pathogenesis, epidemiology and antibiotic resistance. *Front. Life Sci.* 8:284–293. doi: 10.1080/21553769.2015.1051243
- Fire, A., and Xu, S. Q. (1995). Rolling replication of short DNA circles. *Proc. Natl. Acad. Sci. U.S.A.* 92, 4641–4645.
- Gupte, A. R., de Rezende, C. L. E., and Joseph, S. W. (2003). Induction and resuscitation of viable but nonculturable *Salmonella enterica* serovar typhimurium DT104. *Appl. Environ. Microbiol.* 69, 6669–6675.
- Highmore, C. J., Warner, J. C., Rothwell, S. D., Wilks, S. A., and Keevil, C. W. (2018). Viable-but-nonculturable *Listeria monocytogenes* and *Salmonella enterica* serovar thompson induced by chlorine stress remain infectious. *mBio* 9:e540–18.
- Jia, X. Y., Hua, J. J., Liu, L., Xu, Z. B., and Li, Y. Y. (2018). Phenotypic characterization of pathogenic *Cronobacter* spp. strains. *Microb. Pathog.* 121, 232–237.
- Kim, Y. B., Okuda, J., Matsumoto, C., Takahashi, N., Hashimoto, S., and Nishibuchi, M. (1999). Identification of *Vibrio parahaemolyticus* strains at the species level by PCR targeted to the *toxR* gene. *J. Clin. Microbiol.* 37:1173.
- Kirk, M. D., Pires, S. M., Black, R. E., Caipo, M., Crump, J. A., Devleeschauwer, B., et al. (2015). World health organization estimates of the global and regional disease burden of 22 foodborne bacterial, protozoal, and viral diseases, 2010: a data synthesis. *PLoS Med.* 12:e1001921. doi: 10.1371/journal.pmed.1001921
- Kusumoto, A., Asakura, H., and Kawamoto, K. (2012). General stress sigma factor RpoS influences time required to enter the viable but non-culturable state in *Salmonella enterica*. *Microbiol. Immunol.* 56, 228–237.
- Lin, S. Q., Li, L., Li, B., Zhang, X. H., Lin, C. W., Deng, Y., et al. (2016). Development and evaluation of quantitative detection of N-epsilon-carboxymethyl-lysine in *Staphylococcus aureus* biofilm by LC-MS method. *Basic Clin. Pharmacol. Toxicol.* 118:33.
- Lin, S. Q., Yang, L., Chen, G., Li, B., Chen, D. Q., Li, L., et al. (2017). Pathogenic features and characteristics of food borne pathogens biofilm: Biomass, viability and matrix. *Microb. Pathog.* 111, 285–291.
- Liu, L., Ye, C., Soteyome, T., Zhao, X., and Harro, J. M. (2019). Inhibitory effects of two types of food additives on biofilm formation by foodborne pathogens. *MicrobiologyOpen* 8:e00853.
- Liu, L. Y., Lu, Z. R., Li, L., Li, B., Zhang, X., Zhang, X. M., et al. (2018a). Physical relation and mechanism of ultrasonic bactericidal activity on pathogenic *E. coli* with WPI. *Microb. Pathog.* 117, 73–79.
- Liu, L. Y., Xu, R. R., Li, L., Li, B., Zhang, X., Zhang, X. M., et al. (2018b). Correlation and *in vitro* mechanism of bactericidal activity on *E. coli* with whey protein isolate during ultrasonic treatment. *Microb. Pathog.* 115, 154–158.
- Lv, X., Wang, L., Zhang, J., Zeng, H., Chen, X., Shi, L., et al. (2020). Rapid and sensitive detection of VBNC *Escherichia coli* O157: H7 in beef by PMAXx and real-time LAMP. *Food Control* 115:107292.
- Miao, J., Chen, L. Q., Wang, J. W., Wang, W. X., Chen, D. Q., Li, L., et al. (2017a). Evaluation and application of molecular genotyping on nosocomial pathogen-methicillin-resistant *Staphylococcus aureus* isolates in Guangzhou representative of Southern China. *Microb. Pathog.* 107, 397–403.
- Miao, J., Chen, L. Q., Wang, J. W., Wang, W. X., Chen, D. Q., Li, L., et al. (2017c). Current methodologies on genotyping for nosocomial pathogen methicillin-resistant *Staphylococcus aureus* (MRSA). *Microb. Pathog.* 107, 17–28.
- Miao, J., Liang, Y., Chen, L., Wang, W., Wang, J., Li, B., et al. (2017a). Formation and development of *Staphylococcus* biofilm: with focus on food safety. *J. Food Safety* 37:e12358.
- Miao, J., Liang, Y. R., Chen, L. Q., Wang, W. X., Wang, J. W., Li, B., et al. (2017b). Formation and development of *Staphylococcus* biofilm: With focus on food safety. *J. Food Safety* 7:e12358.
- Miao, J., Peters, B. M., Li, L., Li, B., Zhao, X. H., Xu, Z. B., et al. (2016). Evaluation of ERIC-PCR for fingerprinting methicillin-resistant *Staphylococcus aureus* strains. *Basic Clin. Pharmacol. Toxicol.* 118:33.
- Miao, J., Wang, W. X., Xu, W. Y., Su, J. Y., Li, L., Li, B., et al. (2018). The fingerprint mapping and genotyping systems application on methicillin-resistant *Staphylococcus aureus*. *Microb. Pathog.* 125, 246–251.
- Morishige, Y., Fujimori, K., and Amano, F. (2013). Differential resuscitative effect of pyruvate and its analogues on VBNC (viable but non-culturable) *Salmonella*. *Microb. Environ.* 28, 180–186.
- Morishige, Y., Koike, A., Tamura-Ueyama, A., and Amano, F. (2017). Induction of viable but nonculturable *Salmonella* in exponentially grown cells by exposure to a low-humidity environment and their resuscitation by catalase. *J. Food Prot.* 80, 288–294.
- Oliver, J. D., Dagher, M., and Linden, K. (2005). Induction of *Escherichia coli* and *Salmonella typhimurium* into the viable but nonculturable state following chlorination of wastewater. *J. Water Health* 3, 249–257.
- Parida, M., Horioke, K., Ishida, H., Dash, P. K., Saxena, P., Jana, A. M., et al. (2005). Rapid detection and differentiation of dengue virus serotypes by a real-time reverse transcription-loop-mediated isothermal amplification assay. *J. Clin. Microbiol.* 43:2895.
- Purevdorj-Gage, L., Nixon, B., Bodine, K., Xu, Q., and Doerrler, W. T. (2018). Differential effect of food sanitizers on formation of viable but nonculturable *Salmonella enterica* in poultry. *J. Food Protect.* 81, 386–393.
- Robben, C., Fister, S., Witte, A. K., Schoder, D., Rossmanith, P., and Mester, P. (2018). Induction of the viable but non-culturable state in bacterial pathogens by household cleaners and inorganic salts. *Sci. Rep.* 8:15132.
- Roszak, D. B., Grimes, D. J., and Colwell, R. R. (1984). Viable but nonrecoverable stage of *Salmonella enteritidis* in aquatic systems. *Can. J. Microbiol.* 30, 334–338.
- Sharma, J., Kumar, D., Hussain, S., Pathak, A., Shukla, M., Prasanna Kumar, V., et al. (2019). Prevalence, antimicrobial resistance and virulence genes characterization of nontyphoidal *Salmonella* isolated from retail chicken meat shops in Northern India. *Food Control* 102, 104–111.
- Tada, J., Ohashi, T., Nishimura, N., Shirasaki, Y., Ozaki, H., Fukushima, S., et al. (1992). Detection of the thermostable direct hemolysin gene (*tdh*) and

- the thermostable direct hemolysin-related hemolysin gene (*trh*) of *Vibrio parahaemolyticus* by polymerase chain reaction. *Mol. Cell. Probes* 6, 477–487.
- Wang, L., Zhao, X. H., Chu, J., Li, Y., Li, Y. Y., Li, C. H., et al. (2011). Application of an improved loop-mediated isothermal amplification detection of *Vibrio parahaemolyticus* from various seafood samples. *African J. Microbiol. Res.* 5, 5765–5771.
- Wang, Y., Wang, Y., Ma, A., Li, D., and Ye, C. (2014). Rapid and sensitive detection of *Listeria monocytogenes* by cross-priming amplification of *lmo0733* gene. *FEMS Microbiol. Lett.* 361, 43–51.
- Wang, Y. X., Zhang, A. Y., Yang, Y. Q., Lei, C. W., Cheng, G. Y., Zou, W. C., et al. (2018). Sensitive and rapid detection of *Salmonella enterica* serovar Indiana by cross-priming amplification. *J. Microbiol. Methods* 153, 24–30.
- Wen, S. X., Feng, D. H., Chen, D. Q., Yang, L., and Xu, Z. B. (2020). Molecular epidemiology and evolution of *Haemophilus influenzae*. *Infect. Genet. Evol.* 80:104205.
- Xie, J., Yang, L., Peters, B. M., Chen, L., Chen, D., Li, B., et al. (2017a). A 16-year retrospective surveillance report on the pathogenic features and antimicrobial susceptibility of *Pseudomonas aeruginosa* isolated from Guangzhou representative of Southern China. *Microb. Pathog.* 110, 37–41.
- Xie, J. H., Peters, B. M., Li, B., Li, L., Yu, G. C., Xu, Z. B., et al. (2017b). Clinical features and antimicrobial resistance profiles of important *Enterobacteriaceae* pathogens in Guangzhou representative of Southern China, 2001–2015. *Microb. Pathog.* 107, 206–211.
- Xu, G., Hu, L., Zhong, H., Wang, H., Yusa, S.-I., Weiss, T. C., et al. (2012). Cross priming amplification: mechanism and optimization for isothermal DNA amplification. *Sci. Rep.* 2:246.
- Xu, Z., Luo, Y., Soteyome, T., Lin, C.-W., Xu, X., Mao, Y., et al. (2020). Rapid detection of food-borne *Escherichia coli* O157:H7 with visual inspection by crossing priming amplification (CPA). *Food Anal. Methods* 13, 474–481.
- Xu, Z. B., Gui, Z. Y., Li, L., Li, B., Su, J. Y., Zhao, X. H., et al. (2012b). Expression and purification of gp41-gp36 Fusion protein and application in serological screening assay of HIV-1 and HIV-2. *African J. Microbiol. Res.* 6, 6295–6299.
- Xu, Z. B., Hou, Y. C., Peters, B. M., Chen, D. Q., Li, B., and Li, L. (2016b). Chromogenic media for MRSA diagnostics. *Mol. Biol. Rep.* 43, 1205–1212.
- Xu, Z. B., Hou, Y. C., Qin, D., Liu, X. C., Li, B., Li, L., et al. (2016a). Evaluation of current methodologies for rapid identification of methicillin-resistant staphylococcus aureus strains. *Basic Clin. Pharmacol. Toxicol.* 118:33.
- Xu, Z. B., Li, L., Alam, M. J., Zhang, L. Y., Yamasaki, S., and Shi, L. (2008b). First confirmation of integron-bearing methicillin-resistant *Staphylococcus aureus*. *Curr. Microbiol.* 57, 264–268.
- Xu, Z. B., Li, L., Chu, J., Peters, B. M., Harris, M. L., Li, B., et al. (2012a). Development and application of loop-mediated isothermal amplification assays on rapid detection of various types of staphylococci strains. *Food Res. Int.* 47, 166–173.
- Xu, Z. B., Li, L., Shi, L., and Shirliff, M. E. (2011c). Class 1 integron in staphylococci. *Mol. Biol. Rep.* 38, 5261–5279.
- Xu, Z. B., Li, L., Shirliff, M. E., Peters, B. M., Li, B., Peng, Y., et al. (2011b). Resistance class 1 integron in clinical methicillin-resistant *Staphylococcus aureus* strains in southern China, 2001–2006. *Clin. Microbiol. Infect.* 17, 714–718.
- Xu, Z. B., Li, L., Shirliff, M. E., Alam, M. J., Yamasaki, S., and Shi, L. (2009). Occurrence and characteristics of class 1 and 2 integrons in *Pseudomonas aeruginosa* Isolates from patients in Southern China. *J. Clin. Microbiol.* 47, 230–234.
- Xu, Z. B., Li, L., Shirliff, M. E., Peters, B. M., Peng, Y., Alam, M. J., et al. (2010). First report of class 2 integron in clinical *Enterococcus faecalis* and class 1 integron in *Enterococcus faecium* in South China. *Diagn. Microbiol. Infect. Dis.* 68, 315–317.
- Xu, Z. B., Li, L., Zhao, X. H., Chu, J., Li, B., Shi, L., et al. (2011a). Development and application of a novel multiplex polymerase chain reaction (PCR) assay for rapid detection of various types of staphylococci strains. *African J. Microbiol. Res.* 5, 1869–1873.
- Xu, Z. B., Liang, Y. R., Lin, S. Q., Chen, D. Q., Li, B., Li, L., et al. (2016c). Crystal Violet and XTT assays on staphylococcus aureus biofilm quantification. *Curr. Microbiol.* 73, 474–482.
- Xu, Z. B., Shi, L., Alam, M. J., Li, L., and Yamasaki, S. (2008a). Integron-bearing methicillin-resistant coagulase-negative staphylococci in South China, 2001–2004. *FEMS Microbiol. Lett.* 278, 223–230.
- Xu, Z. B., Shi, L., Zhang, C., Zhang, L. Y., Li, X. H., Cao, Y. C., et al. (2007). Nosocomial infection caused by class 1 integron-carrying *Staphylococcus aureus* in a hospital in South China. *Clin. Microbiol. Infect.* 13, 980–984.
- Xu, Z. B., Xie, J. H., Peters, B. M., Li, B., Li, L., Yu, G. C., et al. (2017b). Longitudinal surveillance on antibiogram of important gram-positive pathogens in Southern China, 2001 to 2015. *Microb. Pathog.* 103, 80–86.
- Xu, Z. B., Xie, J. H., Yang, L., Chen, D. Q., Peters, B. M., and Shirliff, M. E. (2018). Complete sequence of pCY-CTX, a plasmid carrying a phage-like region and ISEcp1-mediated Tn2 element from *Enterobacter cloacae*. *Microb. Drug Resist.* 24, 307–313.
- Xu, Z. B., Xu, X. Y., Yang, L., Li, B., Li, L., Li, X. X., et al. (2017a). Effect of aminoglycosides on the pathogenic characteristics of microbiology. *Microb. Pathog.* 113, 357–364.
- You, R., Gui, Z. Y., Xu, Z. B., Shirliff, M. E., Yu, G. C., Zhao, X. H., et al. (2012). Methicillin-resistance staphylococcus aureus detection by an improved rapid PCR assay. *African J. Microbiol. Res.* 6, 7131–7133.
- Zeng, B., Zhao, G., Cao, X., Yang, Z., Wang, C., and Hou, L. (2013). Formation and resuscitation of viable but nonculturable *Salmonella typhi*. *BioMed. Res. Int.* 2013:907170.
- Zhang, H., Feng, S., Zhao, Y., Wang, S., and Lu, X. (2015). Detection of *Yersinia enterocolitica* in milk powders by cross-priming amplification combined with immunoblotting analysis. *Int. J. Food Microbiol.* 214, 77–82.
- Zhao, X., Li, Y., Wang, L., You, L., Xu*, Z., Li, L., et al. (2010a). Development and application of a loop-mediated isothermal amplification method on rapid detection *Escherichia coli* O157 strains from food samples. *Mol. Biol. Rep.* 37, 2183–2188. doi: 10.1007/s11033-009-9700-6
- Zhao, X., Li, Y., Chu, J., Wang, L., Shirliff, M. E., He, X., et al., (2010b). Rapid detection of *Vibrio parahaemolyticus* strains and virulent factors by loop-mediated isothermal amplification assays. *Food Sci. Biotechnol.* 19, 1191–1197. doi: 10.1007/s10068-010-0170-3
- Zhao, X., Wang, L., Chu, J., Li, Y., Li, L., Shirliff, M. E., He, X., et al., (2009). Development and application of a rapid and simple loop-mediated isothermal amplification method for food-borne *Salmonella* detection. *Food Sci. Biotechnol.* 19, 1655–1659. doi: 10.1007/s10068-010-0234-4
- Zhao, X. H., Li, M., and Xu, Z. B. (2018b). Detection of foodborne pathogens by surface enhanced raman spectroscopy. *Front. Microbiol.* 9:1236.
- Zhao, X. H., Yu, Z. X., and Xu, Z. B. (2018a). Study the features of 57 confirmed CRISPR Loci in 38 strains of staphylococcus aureus. *Front. Microbiol.* 9:1591. doi: 10.3389/fmicb.2018.01591
- Zhong, N. J., Gui, Z. Y., Liu, X., Huang, J. R., Hu, K., Gao, X. Q., et al. (2013). Solvent-free enzymatic synthesis of 1, 3-Diacylglycerols by direct esterification of glycerol with saturated fatty acids. *Lipids Health Dis.* 12:65.

Conflict of Interest: The authors declare that the research was conducted in the absence of any commercial or financial relationships that could be construed as a potential conflict of interest.

Copyright © 2021 Ou, Wang, Ye, Chen, Gong, Qian and Liu. This is an open-access article distributed under the terms of the Creative Commons Attribution License (CC BY). The use, distribution or reproduction in other forums is permitted, provided the original author(s) and the copyright owner(s) are credited and that the original publication in this journal is cited, in accordance with accepted academic practice. No use, distribution or reproduction is permitted which does not comply with these terms.



Pathogenic and Virulence Factor Detection on Viable but Non-culturable Methicillin-Resistant *Staphylococcus aureus*

Hua Jiang^{1†}, Kan Wang^{2†}, Muxia Yan¹, Qian Ye¹, Xiaojing Lin¹, Ling Chen³, Yanrui Ye⁴, Li Zhang¹, Junyan Liu^{5*} and Tengyi Huang^{6*}

OPEN ACCESS

Edited by:

Yang Deng,
Qingdao Agricultural University, China

Reviewed by:

Wensen Jiang,
Cedars Sinai Medical Center,
United States
Oana Dumitrescu,
Hospices Civils de Lyon, France
Yuting Tian,
Fujian Agriculture and Forestry
University, China

*Correspondence:

Junyan Liu
jliu81@uthsc.edu
Tengyi Huang
h-hty@hotmail.com

[†]These authors have contributed
equally to this work

Specialty section:

This article was submitted to
Food Microbiology,
a section of the journal
Frontiers in Microbiology

Received: 16 November 2020

Accepted: 04 January 2021

Published: 25 March 2021

Citation:

Jiang H, Wang K, Yan M, Ye Q,
Lin X, Chen L, Ye Y, Zhang L, Liu J
and Huang T (2021) Pathogenic and
Virulence Factor Detection on Viable
but Non-culturable
Methicillin-Resistant *Staphylococcus
aureus*. Front. Microbiol. 12:630053.
doi: 10.3389/fmicb.2021.630053

¹ Department of Haematology, Guangzhou Women and Children's Medical Center, Guangzhou Medical University, Guangzhou, China, ² Center for Translational Medicine, The Second Affiliated Hospital of Shantou University Medical College, Shantou, China, ³ School of Food Science and Engineering, Guangdong Province Key Laboratory for Green Processing of Natural Products and Product Safety, South China University of Technology, Guangzhou, China, ⁴ School of Biological Science and Engineering, South China University of Technology, Guangzhou, China, ⁵ Department of Civil and Environmental Engineering, University of Maryland, College Park, College Park, MD, United States, ⁶ Department of Laboratory Medicine, The Second Affiliated Hospital of Shantou University Medical College, Shantou, China

Food safety and foodborne infections and diseases have been a leading hotspot in public health, and methicillin-resistant *Staphylococcus aureus* (MRSA) has been recently documented to be an important foodborne pathogen, in addition to its recognition to be a leading clinical pathogen for some decades. Standard identification for MRSA has been commonly performed in both clinical settings and food routine detection; however, most of such so-called “standards,” “guidelines,” or “gold standards” are incapable of detecting viable but non-culturable (VBNC) cells. In this study, two major types of staphylococcal food poisoning (SFP), staphylococcal enterotoxins A (sea) and staphylococcal enterotoxins B (seb), as well as the panton-valentine leucocidin (pvl) genes, were selected to develop a cross-priming amplification (CPA) method. Limit of detection (LOD) of CPA for sea, seb, and pvl was 75, 107.5, and 85 ng/μl, indicating that the analytical sensitivity of CPA is significantly higher than that of conventional PCR. In addition, a rapid VBNC cells detection method, designated as PMA-CPA, was developed and further applied. PMA-CPA showed significant advantages when compared with PCR assays, in terms of rapidity, sensitivity, specificity, and accuracy. Compared with conventional VBNC confirmation methods, the PMA-CPA showed 100% accordance, which had demonstrated that the PMA-CPA assays were capable of detecting different toxins in MRSA in VBNC state. In conclusion, three CPA assays were developed on three important toxins for MRSA, and in combination with PMA, the PMA-CPA assay was capable of detecting virulent gene expression in MRSA in the VBNC state. Also, the above assays were further applied to real samples. As concluded, the PMA-CPA assay developed in this study was capable of detecting MRSA toxins in the VBNC state, representing first time the detection of toxins in the VBNC state.

Keywords: VBNC, MRSA, PMA-CPA, virulence detection, cross-priming amplification

INTRODUCTION

In the past few decades, public health has been a major issue for society. From various points of view, food safety and foodborne infections and diseases have been a leading area of concern. Among food safety problems, foodborne infections or diseases caused by food pathogens have made up the majority of the cases (Xu et al., 2021).

Staphylococcus aureus is an important foodborne pathogen that is responsible for a large variety of foodborne infections and diseases (Weese et al., 2010; Wang et al., 2012; Miao et al., 2017a,b, 2019). Capable of producing enterotoxins, it is also commonly found in food poisoning cases. Therefore, staphylococcal food poisoning (SFP) is a major concern in public health (Zhao et al., 2010a,b,c, 2011; Crago et al., 2012; Deng et al., 2015a,b; Yu et al., 2016). In addition, methicillin-resistant *S. aureus* (MRSA) is one of most widely distributed human and animal pathogens that produce a variety of toxins and cause a range of serious illnesses of the skin, soft tissue, bone, and bloodstream (Tacconelli et al., 2009). MRSA was previously limited as a clinical microorganism. However, in recent years, studies have reported that MRSA is strongly and closely associated with food safety. For example, the carriage of this pathogen by industrial staff and the prevalence of livestock-associated MRSA (LA-MRSA) have been clearly pointed out and well established as a foodborne pathogen (Liu et al., 2016a,b,c, 2017a,b,c,d, 2018a,b,c,d, 2019; Xie et al., 2017a,b). Apart from that, MRSA has seen an increase in numerous countries and emerged as an important pathogen, accounting for up to 40% of all *S. aureus* isolates in nosocomial infection, and has caused significant morbidity (Graveland et al., 2011). This is due to the effect of β -lactam resistance in *S. aureus*, which is mediated by the production of penicillin-binding protein 2a PBP2a or PBP2' encoded by the *mecA* gene (Moellering, 2012). The development of resistance to β -lactam antibiotics has been a cause of concern among the medical community.

Standard identification for MRSA has been commonly performed in both clinical settings and routine food detection. In 1982, viable but non-culturable (VBNC) was first proposed. A large proportion of studies have been done on foodborne microorganisms, as once having failed to allow detection of the bacterial cells, the food sample is likely to be mistakenly determined to be safe or qualified. In addition to foodborne pathogens, laboratory researchers in clinical settings commonly fail to detect or identify the pathogens responsible in apparently infected patients. Culturability-based methodology has been significantly challenged as the “gold standard” when it comes to microbiological identification. Therefore, rapid detection of MRSA is imperative for both MRSA-related foodborne outbreaks and clinical diagnosis. Current methodologies available for detection of MRSA include standard clinical testing (such as disk susceptibility tests or broth dilution) and molecular methods (such as polymerase chain reaction and real-time fluorescence PCR) (Salisbury et al., 1997; Felten et al., 2002; Corrente et al., 2007). The former usually takes 1–2 days to obtain results. At the same time, PCR is time-consuming and requires highly trained personnel. In addition, the sensitivity of PCR can be compromised by PCR inhibitors present in a biological

sample (Monteiro et al., 1997). Therefore, these methods are not appropriate for rapid screening. Recently, isothermal amplification methodologies have received much attention due to the omission of thermocyclers, simple protocols, and fast analysis, and they have an analytical performance that competes PCR. A recent innovation of isothermal nucleic acid amplification methodology, cross-priming amplification (CPA), was developed to detect the target DNA with exponential amplification (Xu et al., 2008, 2009, 2010a,b, 2011a,b, 2017, 2019; Xu Z. et al., 2012). Compared with PCR, this novel amplification assay can amplify the target nucleotide sequence isothermally in a short time, which is cost-effective and time-saving (Xu G. et al., 2012). This technique does not rely on sophisticated instruments or trained technicians but can be conducted in a water bath or heating block. In PCR methods, the progress of the reaction is usually verified by electrophoresis. Different from PCR, the CPA assay is able to produce massive amplicons with the obvious turbidity that can be observed by nucleic acid-specific fluorescent dye with or without UV illumination to improve detection efficiency (Wang et al., 2014; Xu et al., 2020a). So far, the CPA protocol has been successfully applied in the detection of virus and harmful microbes, such as *Escherichia coli* O157:H7, *Mycobacterium tuberculosis*, *Enterobacter sakazakii*, *Salmonella enterica*, and *Yersinia enterocolitica* (Fang et al., 2009; Yulong et al., 2010; Zhang et al., 2015; Wang et al., 2018; Xu et al., 2020a,b).

In this study, the VBNC state formation of MRSA has been studied in different real food samples. After confirmation of the VBNC formation, the expression of pathogenic, virulence factors was performed on three enterotoxins and *pvl*, based on the PMA-CPA methodologies.

MATERIALS AND METHODS

Strains and Targets

A total of 36 strains were included in this study, as shown in **Table 1**, including five MRSA strains, 13 MSSA strains, and 18 non-Staphylococci strains. All strains used in this study had been preliminarily identified, and all MRSA strains were identified at the species level using standard procedures as follows: first observation by colony morphology, Gram staining, and catalase test, followed by identification using the Vitek 2 automated system and the API-Staph commercial kit. Further determination of methicillin resistance was performed by susceptibility testing on oxacillin-screening agar, verified by latex agglutination for PBP2a and *mecA* detection by PCR as described previously. The MRSA and MSSA strains used in this study were previously detected by the toxins by PCR and further Sanger sequencing, which were found to carry different toxins. Thus, such strains are included in different detection assays in this study. Three pathogenic targets have been selected for primer design (**Table 2**). Staphylococcal enterotoxins A (*sea*) and staphylococcal enterotoxins B (*seb*) are the two most commonly detected enterotoxins in Staphylococci strains and are responsible for various foodborne cases. Another key toxin for Staphylococci is panton-valentine leukocidin (*pvl*), which is a cytotoxin produced by *Staphylococcus* and causes leukocyte destruction and tissue necrosis. *Pvl* is an important toxin for

TABLE 1 | Reference strains used and the results of CPA assays.

Reference strains	No. of strains	CPA/PCR assays				
		<i>mecA</i>	<i>femA</i>	<i>sea</i>	<i>seb</i>	<i>pvl</i>
<i>Staphylococcus aureus</i> (MRSA) 0314030635	1	+	+	–	–	–
<i>Staphylococcus aureus</i> (MRSA) 971311004	1	+	+	–	–	–
<i>Staphylococcus aureus</i> (MRSA) 0313113664	1	+	+	–	–	–
<i>Staphylococcus aureus</i> (MRSA) 0314030668	1	+	+	–	–	–
<i>Staphylococcus aureus</i> (MRSA) 10071	1	+	+	–	–	–
<i>Staphylococcus aureus</i> (MSSA) 132115, 0315022822, 0613120003, 0314020129	4	–	+	+	+	–
<i>Staphylococcus aureus</i> (MSSA) 0315011480	1	–	+	–	+	–
<i>Staphylococcus aureus</i> (MSSA) 130149	1	–	+	–	–	–
<i>Staphylococcus aureus</i> (MSSA) 132113, 0314030635, 971310004, 132112	4	–	+	–	–	–
<i>Staphylococcus aureus</i> (MSSA) 0315040330	1	–	+	–	–	+
<i>Staphylococcus aureus</i> (MSSA) 0713100037	1	–	+	–	–	+
<i>Staphylococcus aureus</i> (MSSA) 0314020556	1	–	+	–	–	+
<i>Staphylococcus aureus</i> (MSSA) 0315011480	1	–	+	–	–	+
<i>Escherichia coli</i> O157 ATCC43895	1	–	–	–	–	–
<i>Escherichia coli</i> O157 E019, E020, E043, E044	4	–	–	–	–	–
<i>Salmonella</i> ATCC29629, ATCC19585, ATCC14028, ATCC13076,	4	–	–	–	–	–
<i>Listeria monocytogenes</i> ATCC19118, ATCC19116, ATCC19114, ATCC19115, ATCC15313, ATCC19113	6	–	–	–	–	–
<i>Vibrio parahaemolyticus</i> ATCC27969, ATCC17802	2	–	–	–	–	–
<i>Lactobacillus casei</i>	1	–	–	–	–	–

MRSA, and it has been found in the recent decade that the community-associated MRSA (CA-MRSA), commonly carrying type IV or V SCCmec, is highly associated with these toxins. In addition, ST398 is well known to be a major type for livestock-associated MRSA (LA-MRSA), which has been reported to be primarily within CA-MRSA instead of hospital-associated MRSA (HA-MRSA), commonly carrying types I, II, and III SCCmec. Based on the correlation between toxins and CA-MRSA, the carriage of *pvl* is high in food-contaminated MRSA strains, as they are commonly CA-MRSA. The above three targets have been selected to be included in the following studies.

TABLE 2 | Primer sequence of CPA.

Target gene	Primers	Sequence (5'-3')
<i>femA</i>	4s	TCAATCGCGGTCCAGTG
	5a	AACCAATCATTACCAGCA
	2a/1s	TACCTGTAATCTCGCCAT AACATCGTTGTCTATACCT
	2a	TACCTGTAATCTCGCCAT
	3a	GGTAAATATGGATCGATATG
<i>mecA</i>	4s	GCGATAATGGTGAAGTAG
	5a	GATCAATGTTACCGTAGTT
	2a/1s	TTACGATCCTGAATGTTT ATGACTGAACGTCCGATA
	2a	TTACGATCCTGAATGTTT
	3a	TCTTTAACGCCTAAACTA
<i>sea</i>	4s	GCTTGTATGTATGGTGGT
	5a	CTGTAAATAACGTCTTGC
	2a/1s	GAAGATCCAACCTCTGAA GGCTAGACGGTAAACAAA
	2a	GAAGATCCAACCTCTGAA
	3a	TTCGTTTTAACCGTTTCC
<i>seb</i>	4s	ATTACTGTTCGGGTATTGT
	5a	TTCATAAGGCGAGTTGTT
	2a/1s	AATAGTGACGAGTTAGGT CTTTTGACGTACAAACTA
	2a	AATAGTGACGAGTTAGGT
	3a	CTAATTCTTGAGCAGTCACT
<i>pvl</i>	4s	GTTGGGATGTTGAAGCAC
	5a	TGGATAACACTGGCATT
	2a/1s	GTCCAGCATTTAAGTTGC GGACCATATGGCAGAGAT
	2a	GTCCAGCATTTAAGTTGC
	3a	CATTTCATTACCATAAG

Formation of the VBNC State

Culturing, incubation, and inoculation of MRSA and non-MRSA strains were performed using routine procedures. All strains were stored in -80°C and were streaked on TSB plates overnight at 37°C . Colonies were picked and then inoculated into fresh TSB medium to obtain different strains in log phase, ranging from 2 to 6 h. For genomic DNA extraction, bacterial cells after overnight culturing were used, and after centrifugation, DNA extraction was performed using the Dongsheng BioTech DNA extraction kit, according to their manufacturers' instructions. All extracted DNA samples were qualified and confirmed by both under 260/280 and electrophoresis. For VBNC formation, the procedure has been conducted as described previously. In brief, an initial concentration of bacterial cells at 10^8 CFU/ml was used, and the cells are kept at 4 and -20°C , respectively. CFU counting was performed first to obtain the growth curve, and 10 representative time points were selected. Then strains were grown strictly as described above, and for the selected time points, VBNC was confirmed. In addition, VBNC formation was also performed in the real food samples, such as Cantonese cake, as described previously. In brief, the same concentration of bacterial culture was inoculated into the food sample and was kept at 4 and -20°C , respectively. Similar time points

were selected as above, and VBNC cells were further confirmed. For VBNC confirmation, total cell numbers, culturable cell numbers, and viable cell numbers were determined as described previously. The LIVE/DEAD BacLight™ kit was used before performing subjecting to flow cytometry. CFU was counting for culturable cell numbers. After VBNC cells were obtained, introduction of PMA was performed as described previously. Further, DNA extraction was processed, and CPA was also performed for detection.

Development of CPA Assays

After primer design on three targets, primer was synthesized. CPA reaction was carried out as described previously. The reaction volume is first 25 μ l, and further 1 μ l mixed chromogenic agent (containing 0.13 mM calcein and 15.6 mM $\text{MnCl}_2 \cdot 4\text{H}_2\text{O}$) was added. For the reaction program, 63°C for 1 h then 80°C for 2 min was used.

Optimization of CPA Assays

To optimize the CPA assays, different reaction times ranging from 30 to 90 min were used. The reaction volume was used as above.

Limit of detection (LOD) was determined on the CPA assays, and 10-fold serial dilutions of total genomic DNA were used. All experiments were performed in triplicate.

The specificity study on the CPA assay consists of two parts. The first one is the specificity of primers. The CPA was performed with any one of the five primers (4s, 5a, 2a, 1s, 2a, and 3a) omitted to confirm that every single primer is strictly and specifically required for the reaction. Second, the specificity of the primers set was confirmed by including five MRSA strains with 31 non-MRSA strains.

Evaluation of CPA Assays

To evaluate the CPA reaction, PCR was also performed using all primers with the following program: 95°C for 3 min, 30 cycles of amplification at 95°C for 30 s, 55°C 30 s, 72°C for 1 min, and final amplification at 72°C for 7 min. Nuclease-free water was used as a negative control. All PCR products had been subjected to Sanger sequencing to confirm the highly conserved region used for CPA primers design.

Determination of Results

For all nucleic acid isothermal amplification assays, the determination of results shows significant advantages when compared with traditional methods like PCR. In this study, two ways were used as a basis of comparison for the determination of results. First, amplicons were detected by agarose gel electrophoresis, and the bands were observed under UV light. Second, color change was observed and determined by using a mixture of chromogenic agents (MgCl_2 and calcein), and the color green was an indicator of positive yielding.

Confirmation of VBNC Formation and Application of PMA-CPA

The VBNC formation in both pure culture and real samples was described as above. After the VBNC cells were

obtained, DNA extraction was performed, and PMA was introduced. Then the CPA assays on three target toxins were applied to determine the toxin expression in MRSA within VBNC state.

RESULTS

Establishment of CPA Assays

According to the results, the CPA assays for all three targets studied were able to yield expected bands, demonstrating that the CPA assays were successfully developed. According to the optimization of the CPA assays, the reaction temperature as 63°C was found to be the optimal temperature. The time duration of 60 min was found to be the optimal reaction time. Under such conditions, the reproducibility was found to be optimal.

Sensitivity of CPA Assays

The analytical sensitivity of the CPA assay for MRSA was measured using 10-fold serial dilutions of MRSA genomic DNA. The LOD of CPA for *sea*, *seb*, and *pvl* was 75, 107.5, and 85 ng/ μ l (Figure 1). Regular PCR was also performed, and expected bands were obtained as well. In a combination of the above results, it was indicated that the analytical sensitivity of CPA is significantly higher than that of conventional PCR.

Development of CPA Assays

Specificity of the CPA assays was also studied. For the specificity of primers, CPA was performed with any one of the five primers (4s, 5a, 2a/1s, 2a, and 3a) omitted. According to the results, every single primer is strictly and specifically required for the reaction. In addition, the specificity of the set of primers was confirmed by including five MRSA strains with 31 non-MRSA strains. As shown by the results (Table 1), all targets were strictly specific within the species and strains detected. It was indicated that the analytical specificity of CPA is significantly higher than that of conventional PCR.

Application of the CPA Assays in Artificially Contaminated Food

Limit of detection of CPA was also determined in real food samples, and the LOD was found to be approximately 10^4 CFU/ml for all three targets (data not shown). Compared with PCR, the sensitivity of CPA, as was demonstrated, is significantly higher than that of PCR. Furthermore, this result was obtained using real food samples, such as Cantonese cake, indicating the applicability of the developed assays.

Formation of VBNC and Application of PMA-CPA

Formation of VBNC was investigated using the previous procedure. After VBNC formation, the MRSA cells were detected using the PMA-CPA on the expression of *sea*, *seb*, and *pvl*. As PMA was concerned, the concentrate influenced the final results. The concentrate used in this study was 5 μ g/ml,

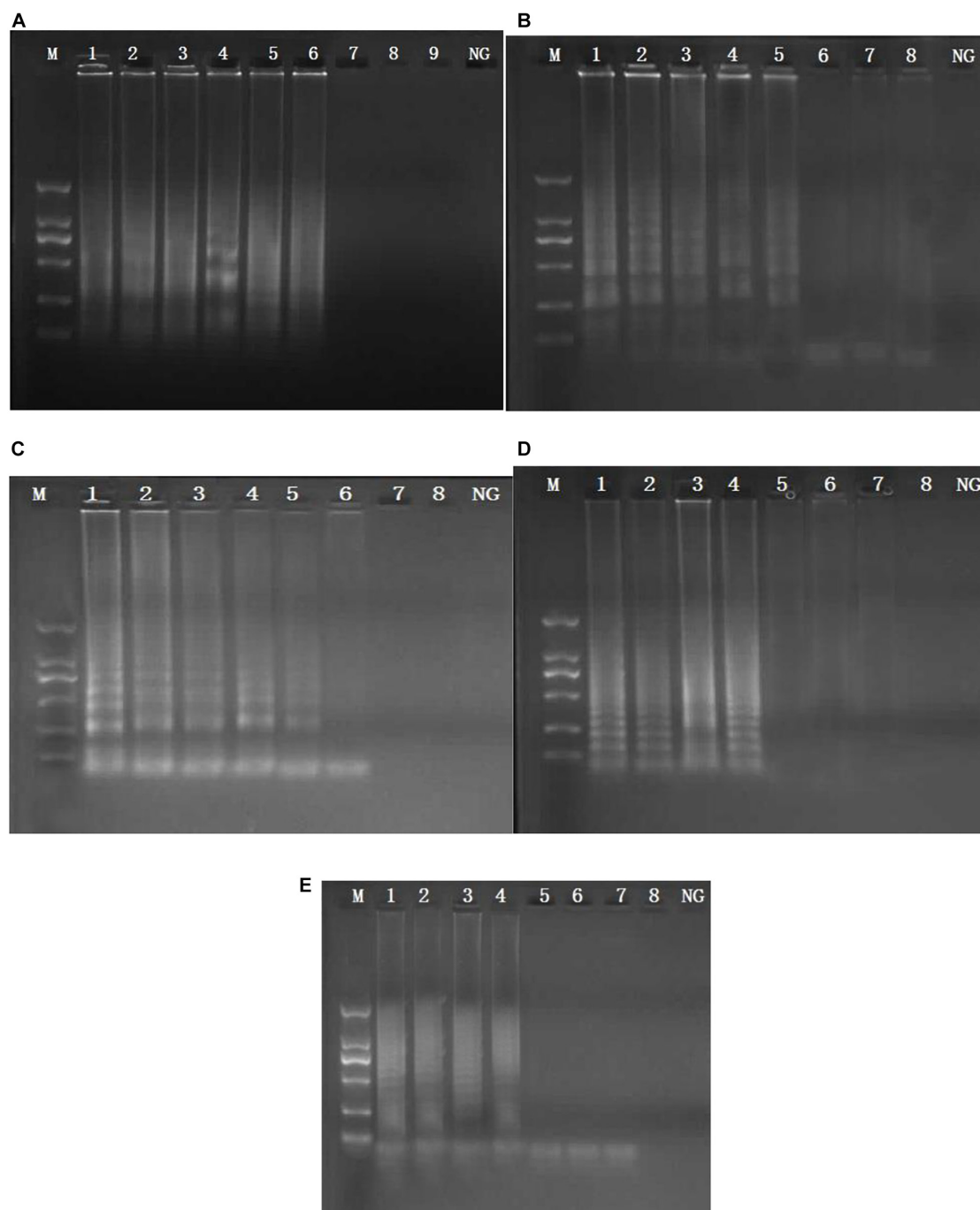


FIGURE 1 | Sensitivity of the CPA assay in genomic DNA by 1.5% agarose gel electrophoresis. Sensitivity from 10071 of *femA* (A) and *mecA* (B) genes. M, DNA marker; lanes 1–8, 3.0 ng/μl, 300 pg/μl, 30 pg/μl, 3 pg/μl, 300 fg/μl, 30 fg/μl, 3 fg/μl, 300 ag/μl NG—negative control. Sensitivity from 0214010085 of *sea* (C), DNA marker; lanes 1–8, 3.0 ng/μl, 300 pg/μl, 30 pg/μl, 3 pg/μl, 300 fg/μl, 30 fg/μl, 3 fg/μl, 300 ag/μl NG—negative control. Sensitivity from 0315011480 of *seb* (D): M, DNA marker; lanes 1–8, 4.3 ng/μl, 430 pg/μl, 43 pg/μl, 4.3 pg/μl, 430 fg/μl, 43 fg/μl, 4.3 fg/μl, 430 ag/μl NG—negative control. Sensitivity from 0214010085 of *pvl* (E): M, DNA marker; lanes 1–8, 3.4 ng/μl, 340 pg/μl, 34 pg/μl, 3.4 pg/μl, 340 fg/μl, 34 fg/μl, 3.4 fg/μl, 340 ag/μl NG—negative control.

as described previously. After the combination of PMA, the samples were first kept in the dark for 15 min and then under the halogen lamp for another 15 min, as described previously. Centrifugation was then performed and DNA was

extracted accordingly. PMA-CPA was further performed. In addition, the PMA-CPA was confirmed by using PCR and the VBNC confirmation. According to the results, PMA-CPA showed significant advantages when compared with PCR assays, in

terms of rapidity, sensitivity, specificity, and accuracy. Compared with conventional VBNC confirmation methods, the PMA-CPA showed 100% accordance, which demonstrated that the PMA-CPA assays were capable of detecting different toxins in MRSA in VBNC state.

DISCUSSION

Food safety and foodborne infections and diseases have been a leading hotspot in public health, and foodborne infections or diseases caused by food pathogens have made up the majority of the cases. MRSA has been recently documented to be an important foodborne pathogen, and its recognition as a leading clinical pathogen for some decades. Examples include the carriage of this pathogen in industrial staff and the prevalence of LA-MRSA, which has been clearly pointed out and established to be a foodborne pathogen. Recently, much attention has been paid to the potential role of different retail meat products from regions worldwide. Moreover, several foodborne acquired MRSA outbreaks have also been reported (Voss et al., 2005; Kadariya et al., 2014). Since food products contaminated with MRSA may not exhibit any spoilage appearance or bad smell, it is challenging for consumers to dispose of the contaminated foods prior to consumption. Apart from that, MRSA has exhibited an increasing trend in numerous countries and emerged as an important pathogen accounting for up to 40% of all *S. aureus* isolates in nosocomial infection and caused significant morbidity (Graveland et al., 2011). Capable of producing enterotoxins, it is also commonly found in food poisoning cases. SFP and PVL are both major concerns when it comes to the pathogenesis of MRSA. Consequently, in this study, two major types of SFP, *sea* and *seb*, as well as the *pvl* genes, were selected to be included to develop the related CPA detection assays.

Standard identification for MRSA has been commonly performed in both clinical settings and food routine detection. However, most of such so-called “standards” or “guidelines” or “gold standards” are based on the culturing of MRSA on different medium plates, including selective and non-selective plates. One major problem exists: whether the bacterial cells of MRSA are non-culturable, which, if so, will further lead to ineffective detection on such medium plates. VBNC was first proposed in 1982. A large proportion of the studies have been done on foodborne microorganisms, since once researchers have failed to detect these bacterial cells, the food sample is likely to be mistaken determined to be safe or qualified. In addition, it is very common, not only in foodborne pathogens, but in clinical settings for laboratory researchers to fail to detect or identify the responsible pathogens in apparent infection patients. Culturability-based methodology has been significantly challenged as the “gold standard” when it comes to microbiological identification. Therefore, rapid detection of MRSA is imperative for both MRSA-related foodborne outbreaks and clinical diagnosis. In this study combining the two concerns, a rapid VBNC cells detection method, designated PMA-CPA, was developed and further applied. The PMA-CPA, on the one hand, shows rapidity compared to all culturing methods or even

PCR. On the other hand, it shows accuracy when it comes to detection of VBNC cells.

Furthermore, this study is of great importance as the three PMA-CPA methodologies developed in this study are capable of detecting the toxins in the expression of MRSA in the VBNC state, not only within the bacteria themselves—which is distinctive from most currently available studies. The developed PMA-CPA assays were also further confirmed to be applicable with respect to detection of VBNC MRSA cells in real food samples. In addition, CPA has significant advantages when compared with regular PCR, in terms of rapidity, sensitivity, specificity, and simplicity in operation/requirement for equipment. In comparison, food samples are more complicated and contain more potential inhibitory substances than clinical samples. The CPA assays developed in this study, according to our previous experience, are definitely applicable in clinical samples, since they are able to be applied to food samples. In addition, in our experience, for clinical samples, non-culturable isolates are a major concern, as in many cases, conventional culturing methodologies are incapable of identifying the pathogen responsible for infection or diseases. The CPA assays developed in this study are capable of directly detecting those viable cells (even though they are non-culturable), which will significantly aid in the detection of MRSA in clinical samples, especially in the case of non-culturable cells.

CONCLUSION

Three CPA assays were developed on three important toxins for MRSA, and in combination with PMA, the PMA-CPA assays were capable of detecting the toxins from the expression of MRSA in the VBNC state. The above assays were further applied in real samples. We have concluded that the PMA-CPA assays developed in this study are capable of detecting MRSA toxins in the VBNC state, representing success for the first time in the detection of toxins in the VBNC state.

DATA AVAILABILITY STATEMENT

The raw data supporting the conclusions of this article will be made available by the authors, without undue reservation.

AUTHOR CONTRIBUTIONS

JL and KW conceived of the study and participated in its design and coordination. HJ, LC, MY, QY, XL, and YY performed the experimental work and collected the data. LZ and TH analyzed the data and wrote the manuscript. All authors read and approved the final manuscript.

FUNDING

Our work was supported by the National Key Research and Development Program of China (2016YFD04012021).

REFERENCES

- Corrente, M., Normanno, G., Martella, V., Bellacicco, A. L., Quaglia, N. C., Dambrosio, A., et al. (2007). Comparison of methods for the detection of methicillin resistance in *Staphylococcus aureus* isolates from food products. *Lett. Appl. Microbiol.* 45, 535–539. doi: 10.1111/j.1472-765X.2007.02226.x
- Crago, B., Ferrato, C., Drews, S. J., Svenson, L. W., Tyrrell, G., and Louie, M. (2012). Prevalence of *Staphylococcus aureus* and methicillin-resistant *S. aureus* (MRSA) in food samples associated with foodborne illness in Alberta, Canada from 2007 to 2010. *Food Microbiol.* 32, 202–205. doi: 10.1016/j.fm.2012.04.012
- Deng, Y., Liu, J., Li, L., Fang, H., and Xu, Z. (2015a). Reduction and restoration of culturability of beer-stressed and low-temperature-stressed *Lactobacillus acetotolerans* strain 2011-8. *Int. J. Food Microbiol.* 206, 96–101. doi: 10.1016/j.jifoodmicro.2015.04.046
- Deng, Y., Liu, J., Peters, B. M., Chen, L., Miao, J., et al. (2015b). Antimicrobial resistance investigation on staphylococcus strains in a local hospital in guangzhou, china, 2001–2010. *Microb. Drug Resist.* 21, 102–104. doi: 10.1089/mdr.2014.0117
- Fang, R., Li, X., Hu, L., You, Q., Li, J., Wu, J., et al. (2009). Cross-priming amplification for rapid detection of *Mycobacterium tuberculosis* in sputum specimens. *J. Clin. Microbiol.* 47, 845–847. doi: 10.1128/jcm.01528-08
- Felten, A., Grandry, B., Lagrange, P. H., and Casin, I. (2002). Evaluation of three techniques for detection of low-level methicillin-resistant *Staphylococcus aureus* (MRSA): a disk diffusion method with cefoxitin and moxalactam, the Vitek 2 system, and the MRSA-screen latex agglutination test. *J. Clin. Microbiol.* 40, 2766–2771. doi: 10.1128/JCM.40.8.2766-2771.2002
- Graveland, H., Wagenaar, J. A., Bergs, K., Heesterbeek, H., and Heederik, D. (2011). Persistence of livestock associated MRSA CC398 in humans is dependent on intensity of animal contact. *PLoS One* 6:e0016830. doi: 10.1371/journal.pone.0016830
- Kadariya, J., Smith, T. C., and Thapaliya, D. (2014). *Staphylococcus aureus* and Staphylococcal food-borne disease: an ongoing challenge in public health. *Biomed Res. Int.* 2014:827965. doi: 10.1155/2014/827965
- Liu, J., Chen, D., Peters, B. M., Li, L., Li, B., Xu, Z., et al. (2016a). Staphylococcal chromosomal cassettes *mec* (*scmcc*): a mobile genetic element in methicillin-resistant *Staphylococcus aureus*. *Microb. Pathog.* 101, 56–67. doi: 10.1016/j.micpath.2016.10.028
- Liu, J., Deng, Y., Li, L., Li, B., Li, Y., Zhou, S., et al. (2018a). Discovery and control of culturable and viable but non-culturable cells of a distinctive *Lactobacillus harbinensis* strain from spoiled beer. *Sci. Rep.* 8:11446. doi: 10.1038/s41598-018-28949-y
- Liu, J., Deng, Y., Peters, B. M., Li, L., Li, B., Chen, L., et al. (2016b). Transcriptomic analysis on the formation of the viable putative non-culturable state of beer-spoilage *Lactobacillus acetotolerans*. *Sci. Rep.* 6:36753. doi: 10.1038/srep36753
- Liu, J., Deng, Y., Soteyome, T., Li, Y., Su, J., Li, L., et al. (2018b). Induction and recovery of the viable but nonculturable state of hop-resistance *Lactobacillus brevis*. *Front. Microbiol.* 9:2076. doi: 10.3389/fmicb.2018.02076
- Liu, J., Li, L., Li, B., Brian, M. P., Deng, Y., Xu, Z., et al. (2017a). Study on spoilage capability and VBNC state formation and recovery of *Lactobacillus plantarum*. *Microb. Pathog.* 110, 257–261. doi: 10.1016/j.micpath.2017.06.044
- Liu, J., Li, L., Li, B., Brian, M. P., Deng, Y., Xu, Z., et al. (2017b). The viable but nonculturable state induction and genomic analyses of *Lactobacillus casei* bm-lc14617, a beer-spoilage bacterium. *Microbiologyopen* 2017:e506. doi: 10.1002/mbo3.506
- Liu, J., Li, L., Li, B., Brian, M. P., Xu, Z., and Shirliff, M. E. (2017c). First study on the formation and resuscitation of viable but nonculturable state and beer spoilage capability of *Lactobacillus lindneri*. *Microb. Pathogenesis*. 107, 219–224. doi: 10.1016/j.micpath.2017.03.043
- Liu, J., Xie, J., Yang, L., Chen, D., Peters, B. M., Xu, Z., et al. (2018d). Identification of the *kpc* plasmid *pcy-kpc334*: new insights on the evolution pathway of the epidemic plasmids harboring *fosa3-blakpc-2* genes. *Int. J. Antimicrob. Ag.* 52, 510–512. doi: 10.1016/j.ijantimicag.2018.04.013
- Liu, J., Yang, L., Chen, D., Peters, B. M., Li, L., Li, B., et al. (2017d). Complete sequence of *pbm413*, a novel multi-drug-resistance megaplasmid carrying *qnrvc6* and *blaimp-45* from *Pseudomonas aeruginosa*. *Int. J. Antimicrob. Agents* 51, 145–150. doi: 10.1016/j.ijantimicag.2017.09.008
- Liu, J., Yang, L., Hou, Y., Soteyome, T., Zeng, B., Su, J., et al. (2018c). Transcriptomics study on *Staphylococcus aureus* biofilm under low concentration of ampicillin. *Front. Microbiol.* 9:2413. doi: 10.3389/fmicb.2018.02413
- Liu, J., Zhou, R., Li, L., Peters, B. M., Li, B., Lin, C. W., et al. (2016c). Viable but non-culturable state and toxin gene expression of enterohemorrhagic *Escherichia coli* o157 under cryopreservation. *Res. Microbiol.* 101, 56–57.
- Liu, L., Ye, C., Soteyome, T., Zhao, X., and Harro, J. M. (2019). Inhibitory effects of two types of food additives on biofilm formation by foodborne pathogens. *MicrobiologyOpen* 8:e00853. doi: 10.1002/mbo3.853
- Miao, J., Chen, L., Wang, J., Wang, W., Chen, D., Li, L., et al. (2017a). Current methodologies on genotyping for nosocomial pathogen methicillin-resistant *Staphylococcus aureus* (MRSA). *Microb. Pathogenesis*. 107, 17–28. doi: 10.1016/j.micpath.2017.03.010
- Miao, J., Liang, Y., Chen, L., Wang, W., Wang, J., Li, B., et al. (2017b). Formation and development of *Staphylococcus biofilm*: with focus on food safety. *J. Food Saf.* 7:e12358. doi: 10.1111/jfs.12358
- Miao, J., Lin, S., Soteyome, T., Peters, B. M., Li, Y., Chen, H., et al. (2019). Biofilm formation of staphylococcus aureus under food heat processing conditions: first report on cml production within biofilm. *Sci. Rep.* 9:1312. doi: 10.1038/s41598-018-35558-2
- Moellering, R. C. (2012). MRSA: the first half century. *J. Antimicrob. Chemoth.* 67, 4–11. doi: 10.1093/jac/dkr437
- Monteiro, L., Bonnemaïson, D., Vekris, A., Petry, K. G., Bonnet, J., Vidal, R., et al. (1997). Complex polysaccharides as PCR inhibitors in feces: *Helicobacter pylori* model. *J. Clin. Microbiol.* 35, 995–998. doi: 10.1128/JCM.35.4.995-998.1997
- Salisbury, S. M., Sabatini, L. M., and Spiegel, C. A. (1997). Identification of methicillin-resistant staphylococci by multiplex polymerase chain reaction assay. *Am. J. Clin. Pathol.* 107, 368–373. doi: 10.1093/ajcp/107.3.368
- Tacconelli, E., De Angelis, G., de Waure, C., Cataldo, M. A., La Torre, G., and Cauda, R. (2009). Rapid screening tests for methicillin-resistant *Staphylococcus aureus* at hospital admission: systematic review and meta-analysis. *Lancet Infect. Dis.* 9, 546–554. doi: 10.1016/s1473-3099(09)70150-1
- Voss, A., Loeffen, F., Bakker, J., Klaassen, C., and Wulf, M. (2005). Methicillin-resistant *Staphylococcus aureus* in pig farming. *Emerg. Infect. Dis.* 11, 1965–1966.
- Wang, L., Li, Y., Chu, J., Xu, Z., and Zhong, Q. (2012). Development and application of a simple loop-mediated isothermal amplification method on rapid detection of *Listeria monocytogenes* strains. *Mol. Biol. Rep.* 39, 445–449. doi: 10.1007/s11033-011-0757-7
- Wang, Y., Wang, Y., Ma, A., Li, D., and Ye, C. (2014). Rapid and sensitive detection of *Listeria monocytogenes* by cross-priming amplification of *lmo733* gene. *FEMS Microbiol. Lett.* 361, 43–51. doi: 10.1111/1574-6968.12610
- Wang, Y. X., Zhang, A. Y., Yang, Y. Q., Lei, C. W., Cheng, G. Y., Zou, W. C., et al. (2018). Sensitive and rapid detection of *Salmonella enterica* serovar Indiana by cross-priming amplification. *J. Microbiol. Methods* 153, 24–30. doi: 10.1016/j.mimet.2018.08.003
- Weese, J. S., Avery, B. P., and Reid-Smith, R. J. (2010). Detection and quantification of methicillin-resistant *Staphylococcus aureus* (MRSA) clones in retail meat products. *Lett. Appl. Microbiol.* 51, 338–342. doi: 10.1111/j.1472-765X.2010.02901.x
- Xie, J., Peters, B. M., Li, B., Li, L., Yu, G., Xu, Z., et al. (2017a). Clinical features and antimicrobial resistance profiles of important *Enterobacteriaceae* pathogens in Guangzhou representative of Southern China, 2001–2015. *Microb. Pathog.* 107, 206–211. doi: 10.1016/j.micpath.2017.03.038
- Xie, J., Yang, L., Peters, B. M., Chen, L., Chen, D., Li, B., et al. (2017b). A 16-year retrospective surveillance report on the pathogenic features and antimicrobial susceptibility of *Pseudomonas aeruginosa* isolated from Guangzhou representative of Southern China. *Microb. Pathog.* 110, 37–41. doi: 10.1016/j.micpath.2017.06.018
- Xu, G., Hu, L., Zhong, H., Wang, H., Yusa, S., Weiss, T. C., et al. (2012). Cross priming amplification: mechanism and optimization for isothermal DNA amplification. *Sci. Rep.* 2:246.
- Xu, Z., Li, L., Alam, M. J., Zhang, L., Yamasaki, S., and Shi, L. (2008). First confirmation of integron-bearing methicillin-resistant staphylococcus aureus. *Curr. Microbiol.* 57, 264–268. doi: 10.1007/s00284-008-9187-8
- Xu, Z., Li, L., Chu, J., Peters, B. M., Harris, M. L., Li, B., et al. (2012). Development and application of loop-mediated isothermal amplification assays on rapid

- detection of various types of staphylococci strains. *Food Res. Int.* 47, 166–173. doi: 10.1016/j.foodres.2011.04.042
- Xu, Z., Li, L., Shi, L., and Shirliff, M. E. (2011a). Class 1 integron in staphylococci. *Mol. Biol. Rep.* 38, 5261–5279. doi: 10.1007/s11033-011-0676-7
- Xu, Z., Li, L., Shirliff, M. E., Peters, B. M., Alam, M. J., Yamasaki, S., et al. (2009). Occurrence and characteristics of class 1 and 2 integrons in *Pseudomonas aeruginosa* isolates from patients in Southern China. *J. Clin. Microbiol.* 47, 230–234. doi: 10.1128/JCM.02027-08
- Xu, Z., Li, L., Shirliff, M. E., Peters, B. M., Li, B., Peng, Y., et al. (2011b). Resistance class 1 integron in clinical methicillin-resistant *Staphylococcus aureus* strains in southern China, 2001–2006. *Clin. Microbiol. Infect.* 17, 714–718. doi: 10.1111/j.1469-0691.2011.02691.x
- Xu, Z., Lu, Z., Soteyome, T., Ye, Y., Huang, T., Liu, J., et al. (2021). Polymicrobial interaction between *Lactobacillus* and *Saccharomyces cerevisiae*: coexistence-relevant mechanisms. *Crit. Rev. Microbiol.* doi: 10.1080/1040841X.2021.1893265. [Epub ahead of print].
- Xu, Z., Luo, Y., Mao, Y., Peng, R., Chen, J., Soteyome, T., et al. (2020a). Spoilage lactic acid bacteria in the brewing industry. *J. Microbiol. Biotechnol.* 30, 955–961. doi: 10.4014/jmb.1908.08069
- Xu, Z., Luo, Y., Soteyome, T., Lin, C., Xu, X., Mao, Y., et al. (2020b). Rapid detection of food-borne *Escherichia coli* O157:H7 with visual inspection by crossing priming amplification (CPA). *Food Anal. Methods* 13, 474–481. doi: 10.1007/s12161-019-01651-z
- Xu, Z., Shi, L., Alam, M. J., Li, L., and Yamasaki, S. (2010a). Integron-bearing methicillin-resistant coagulase-negative staphylococci in south china, 2001–2004. *FEMS Microbiol. Lett.* 278, 223–230. doi: 10.1111/j.1574-6968.2007.01103.x
- Xu, Z., Shi, L., Zhang, C., Zhang, L., and Yamasaki, S. (2010b). Nosocomial infection caused by class 1 integron-carrying staphylococcus aureus in a hospital in south china. *Clin. Microbiol. Infect.* 13, 980–984. doi: 10.1111/j.1469-0691.2007.01782.x
- Xu, Z., Xie, J., Peters, B. M., Li, B., Li, L., Yu, G., et al. (2017). Longitudinal surveillance on antibiogram of important gram-positive pathogens in southern china, 2001 to 2015. *Microb. Pathog.* 103, 80–86. doi: 10.1016/j.micpath.2016.11.013
- Xu, Z., Xie, J., Soteyome, T., Peters, B. M., Shirliff, M. E., Liu, J., et al. (2019). Polymicrobial interaction and biofilms between staphylococcus aureus and *Pseudomonas aeruginosa*: an underestimated concern in food safety. *Curr. Opin. Food Sci.* 26, 57–64. doi: 10.1016/j.cofs.2019.03.006
- Yu, G., Wen, W., Peters, B. M., Liu, J., Ye, C., Che, Y., et al. (2016). First report of novel genetic array aaca4-blaimp-25-oxa30-catb3 and identification of novel metallo-(-lactamase gene blaimp25: a retrospective study of antibiotic resistance surveillance on pseudomonas aeruginosa in guangzhou of south china, 2003–2007. *Microb. Pathog.* 95, 62–67. doi: 10.1016/j.micpath.2016.02.021
- Yulong, Z., Xia, Z., Hongwei, Z., Wei, L., Wenjie, Z., and Xitai, H. (2010). Rapid and sensitive detection of *Enterobacter sakazakii* by cross-priming amplification combined with immuno-blotting analysis. *Mol. Cell. Probes* 24, 396–400. doi: 10.1016/j.mcp.2010.09.001
- Zhang, H., Feng, S., Zhao, Y., Wang, S., and Lu, X. (2015). Detection of *Yersinia enterocolitica* in milk powders by cross-priming amplification combined with immunoblotting analysis. *Int. J. Food Microbiol.* 214, 77–82. doi: 10.1016/j.jfoodmicro.2015.07.030
- Zhao, X., Li, Y., Chu, J., Wang, L., Shirliff, M. E., He, X., et al. (2010a). Rapid detection of *Vibrio parahaemolyticus* strains and virulent factors by loop-mediated isothermal amplification assays. *Food Sci. Biotechnol.* 19, 1191–1197. doi: 10.1007/s10068-010-0170-3
- Zhao, X., Li, Y., Wang, L., You, L., Xu, Z., Li, L., et al. (2010b). Development and application of a loop-mediated isothermal amplification method on rapid detection *Escherichia coli* O157 strains from food samples. *Mol. Biol. Rep.* 37, 2183–2188. doi: 10.1007/s11033-009-9700-6
- Zhao, X., Wang, L., Chu, J., Li, Y., Li, Y., Xu, Z., et al. (2010c). Development and application of a rapid and simple loop-mediated isothermal amplification method for food-borne *Salmonella* detection. *Food Sci. Biotechnol.* 19, 1655–1659. doi: 10.1007/s10068-010-0234-4
- Zhao, X., Wang, L., Li, Y., Xu, Z., Li, L., He, X., et al. (2011). Development and application of a loop-mediated isothermal amplification method on rapid detection of *Pseudomonas aeruginosa* strains. *World J. Microbiol. Biot.* 27, 181–184. doi: 10.1007/s11274-010-0429-0

Conflict of Interest: The authors declare that the research was conducted in the absence of any commercial or financial relationships that could be construed as a potential conflict of interest.

Copyright © 2021 Jiang, Wang, Yan, Ye, Lin, Chen, Ye, Zhang, Liu and Huang. This is an open-access article distributed under the terms of the Creative Commons Attribution License (CC BY). The use, distribution or reproduction in other forums is permitted, provided the original author(s) and the copyright owner(s) are credited and that the original publication in this journal is cited, in accordance with accepted academic practice. No use, distribution or reproduction is permitted which does not comply with these terms.



Pressure and Temperature Combined With Microbial Supernatant Effectively Inactivate *Bacillus subtilis* Spores

Jingyu Li, Yaxin Sun, Fang Chen, Xiaosong Hu and Li Dong*

College of Food Science and Nutritional Engineering, National Engineering Research Center for Fruit and Vegetable Processing, Key Laboratory of Fruits and Vegetables Processing, Ministry of Agriculture, Engineering Research Centre for Fruits and Vegetables Processing, Ministry of Education, China Agricultural University, Beijing, China

OPEN ACCESS

Edited by:

Zhenbo Xu,
University of Tennessee Health
Science Center (UTHSC),
United States

Reviewed by:

Fahmi Shaher,
Jiamusi University, China
Olajide Olaleye,
Chinese Academy of Sciences, China

*Correspondence:

Li Dong
li_dong127@163.com

Specialty section:

This article was submitted to
Food Microbiology,
a section of the journal
Frontiers in Microbiology

Received: 16 December 2020

Accepted: 22 March 2021

Published: 18 May 2021

Citation:

Li J, Sun Y, Chen F, Hu X and
Dong L (2021) Pressure and
Temperature Combined With
Microbial Supernatant Effectively
Inactivate *Bacillus subtilis* Spores.
Front. Microbiol. 12:642501.
doi: 10.3389/fmicb.2021.642501

Spores from the *Bacillus* species pose a challenge to the food industry because of their ubiquitous nature and extreme resistance. Accumulated evidence indicates that it is effective to induce spore germination homogenously before killing them. However, it is difficult to obtain and apply exogenous germination factors, which will affect food composition. Therefore, this study screened endogenous germinants from microorganisms by assessing the effect of *Escherichia coli*, *Bacillus subtilis*, *Saccharomyces cerevisiae*, *Lactiplantibacillus plantarum*, and *Streptococcus thermophilus* cultures (cell-free) on *B. subtilis* spore germination. The results showed that the supernatants from these five microorganisms induced spore germination instead of sediments. Moreover, the supernatants of *E. coli*, *B. subtilis*, and *S. cerevisiae* exhibited higher germination rates than *L. plantarum* and *S. thermophilus*, and the induction effects were concentration-dependent. Furthermore, plate counting confirmed that the microbial supernatants induced the lowest spore germination ratio on strains *B. subtilis* FB85 [germination receptors (GRs) mutant] but not strains *B. subtilis* PB705 (PrkC mutant). In addition, *B. subtilis* and *S. cerevisiae* supernatants, combined with pressure and temperature, were effective in spore inactivation. The findings suggested that microbial supernatants may include agents that induce spore germination and may be used for spore inactivation.

Keywords: spore germination, supernatants, germination receptor, pressure and temperature, spore inactivation

HIGHLIGHTS

- Supernatants, not sediments, from several bacteria could induce spore germination.
- Bacterial supernatants could induce spore germination through GRs and PrkC signaling pathways.
- Bacterial supernatants could be used to develop a germination agent, which could inactivate spore effectively combined with pressure and temperature.

INTRODUCTION

The *Bacillus* species is a major concern in the food industry as its spores can trigger food spoilage and even food poisoning (Kochan et al., 2018; Ortiz et al., 2019). Accumulated evidence indicates that microorganisms, especially spore-producing bacterium, contribute to more than 70% of food poisoning incidents (Ishaq et al., 2021). Therefore, it is urgent to search for efficient, simple, and rapid methods to control spores in food processing industries in particular, as their eradication from foodstuffs may be difficult. Previous studies showed that spores reduced resistance to various treatments and were relatively easily killed during germination (Drusano et al., 2009). Thus, spore germination has been found to be the key step to spore inactivation.

The germination pathways of most spores have been mainly divided into two types: nutrient and non-nutrient germinants (Setlow et al., 2017). In the former, various nutrient germinants, which commonly include sugars, amino acids, inorganic salts, purine nucleosides, or combinations of these molecules, pass through the outer layers of spores and interact with germinant receptors (GRs) located in the inner member of spores, such as GerA in response to L-alanine or L-valine and GerB and GerK in response to the combination of L-Asparagine, D-Glucose, D-Fructose, and potassium ions (K⁺; AGFK; Grela et al., 2018). In contrast, “non-nutrient” germinants, which may be chemical (Ca²⁺-dipicolinic acid, CaDPA), enzymic (lysozyme), or physical (pressure), induce spore germination in a receptor-independent process (Popham et al., 1999; Paidhungat et al., 2001, 2002; Perez-Valdespino et al., 2013). In addition, fragments of vegetative cell peptidoglycans (PGNs) induce spore germination by activating a protein kinase. PGNs can interact with the PASTA (penicillin binding-associated and serine/threonine kinase-associated) domain of PrkC kinase, and activated PrkC induces spore germination by delivering the signal to downstream proteins such as phosphorylating EF-G (Shah et al., 2008). However, most of these germinants are not used in food processing because it is difficult to gain substances such as peptidoglycans in large amounts. Therefore, it is of great significance to screen the germinants for inducing spore germination, and then sterilize them to effectively control food spoilage.

Previous studies showed that various bacteriocins derived from microorganisms could induce or inhibit the germination and outgrowth of different kinds of spores. For example, cell-free supernatants, derived from Gram-positive and Gram-negative species, could promote spore germination, mainly because of peptidoglycans (Shah et al., 2008). Moreover, various bacteriocins produced by bacteria, including *Lactiplantibacillus plantarum*, *Lactococcus lactis*, and *Streptococcus thermophilus*, have demonstrated a broad range of inhibitory activities against spores (Mathot et al., 2003). Bacteriocins including nisin could inhibit the outgrowth of the *Clostridium difficile* germinating spore (Nerandzic and Donskey, 2013; Le Lay et al., 2016). In addition, nisin A, produced by *L. lactis* was found to reduce spore viability by 40–50% (Le Lay et al., 2016; Chai et al., 2017). In addition, its combination with pressure or other chemicals could strengthen

the sensitization of spores (Modugno et al., 2019). Furthermore, bacteriocins have been developed as probiotic candidates owing to their antimicrobial potential.

Therefore, to identify more efficient germinants for spore germination that can be used to kill spores, this study comprehensively investigated the effects of cultural compounds derived from various bacteria. Utilizing the *Bacillus subtilis* spore as a model, *Escherichia coli*, *B. subtilis*, *Saccharomyces cerevisiae*, *L. plantarum*, and *S. thermophilus* were selected, and their cell-free supernatants and sediments were functionally analyzed. Furthermore, the pathway of *B. subtilis* spore germination was assessed using mutants. Finally, the effect of the supernatant on killing spores was analyzed by combining it with pressure and temperature. The results of this study can provide new ideas and methods for the inactivation of spores, which is of great significance to ensuring food safety.

MATERIALS AND METHODS

The Preparation of *Bacillus subtilis* Strains and Spore

All *B. subtilis* strains used in this study were derivatives from the strain 168 (China General Microbiological Culture Collection Center, CCGMC). The wild-type strain is the *B. subtilis* 168, and strains *B. subtilis* FB85 (GRs mutant) and PB705 (PrkC) were obtained from Peter Setlow, Department of Molecular, Microbial and Structural Biology, University of Connecticut Health Center, Farmington, CT 06030-3,305 United States. *Bacillus subtilis* spores of various strains were routinely prepared as follows.

A fresh single colony grown on a Luria Bertani (LB) plate was selected and diluted into a moderate LB broth medium at 37°C and 200 rpm until OD₆₀₀ = 0.5. Then, the vegetative cell of *B. subtilis* was obtained. The vegetative cell was inoculated into 2 L Difco Sporulation Medium (DSM) for a further 20–24 h at 37°C and 200 rpm. When >90% of cultures were deemed free spores *via* phase-contrast microscopy, the culture was centrifuged for 15 min at 8,000 g, and the supernatant was carefully removed. The spores were kept at 4°C overnight and cleaned with cold distilled water and a histodenz gradient several times through repeated centrifugation. Final spore suspensions were determined by phase-contrast microscopy and stored in 4 or –80°C.

Preparation of Supernatants and Sediments

Escherichia coli o157, *B. subtilis* 168, *S. cerevisiae* ATCC 9763, *S. thermophilus* CICC 6220, and *L. plantarum* CICC 20265 were used as the experimental materials. *Escherichia coli* and *B. subtilis* strains were cultured in LB broth medium at 37°C for 24 h. *Saccharomyces cerevisiae* was cultured in Yeast Extract Peptone Dextrose medium (YPD) at 30°C for 24 h. *Streptococcus thermophilus* and *L. plantarum* were cultured in de Man Rogosa and Sharp medium (MRS) at 37°C for 14 h. When the OD₆₀₀ of the full-concentration

broth was 3.0, the solution was collected and centrifuged. Then, the supernatants (F1) of various microorganisms were filtered with sterilized 0.22- μm millipore filters (Millipore, United States), and this was named the filterable supernatant (F2). The sediments were then cultivated on a plate for 12 h, resuspended with sterile water, and centrifuged, and the supernatant was named the sediment solution (F3). Then, the sediments were broken with an ultrasonic cell disruptor (at 400 Hz, 10 cycles, 10 s interval) and centrifuged, and the supernatant was named the ultrasonic sediment solution (F4; **Figure 1**). To avoid the detrimental effects of acidic substances produced in the cell culture process, the sediment and supernatant were concentrated by centrifugation and diluted with PBS at pH 7.0–8.0 for subsequent experiments. In addition, the different media were processed as a supernatant and detected in experiments to exclude the potential impact of nutrients from the culture medium (data not shown).

Induction Activity of the Supernatants

Cell-free filterable supernatants (F2) were prepared as described above (Materials and Methods Section “Preparation of Supernatants and Sediments”). When the OD_{600} value of bacterial suspensions was 3.0, the concentration of cell-free filterable supernatants was determined to be 1. Then, the concentration of the supernatant was diluted to 0.8, 0.6, 0.4, 0.2, 10^{-1} , 10^{-2} , and 10^{-3} times of the initial bacterial solution ($\text{OD}_{600} = 3.0$), respectively. Supernatants with different concentrations were diluted in sterile water. To completely clear the state of the spore, approximately 150 μl of the supernatants were added to each well that contained spores, and the assessment indexes were detected. In the control group, equal volumes of sterile water were added, and 10 mM AGFK or L-valine was added into the positive groups. When spores were cultivated at 37°C for 3 h, the levels of the dipicolinic acid (DPA) release and OD_{600} were Determined Every 5 min. After incubation, the count plates were performed and assessed.

DPA Detection

The spore germination experiment with nutrients was performed by using the DPA detection method described by Hindle and Hall (1999), with some adjustments. Spores with an initial OD_{600} value of 0.5 were used in the germination experiment at 37°C in 200 μK -HEPES buffer (25 mM, pH 7.4) containing TbCl_3 (50 μM). After adding the different germinants, the spore suspensions were cultured at 37°C . The Tb-DPA fluorescence was determined every 5 min for 100–180 min and expressed as relative fluorescence units (RFU) through a multi-well fluorescence plate reader TECAN Spark 10 M. The excitation and emission wavelengths were 270 and 545 nm, respectively. The DPA release ratio was calculated by using this formula: $\text{DPA \%} = (F_1 - F_0) / (F_2 - F_0)$ [F_0 , F_1 , and F_2 represent the fluorescence value of the control, treated, and positive ($121^\circ\text{C}/20$ min) groups, respectively].

OD_{600} Detection

The OD_{600} was measured by the TECAN Spark 10 M by using the measurement of absorbance. Then, 200 μl of spore suspension was transported in the transparent corning 96-well plate, and the value at 600 nm was collected. The fractional ratio of OD_{600} value represents the germination of spores, and the formula used is as follows: germination rate = $\text{OD}_t / \text{OD}_0$ (OD_0 , OD_t represent the absorbance value of initial time and measurement time groups, respectively). Moreover, the decrease in the ratio indicates spore germination, and the increase in the ratio signifies spore outgrowth. The detection was duplicated three times.

Cell Counting

The *B. subtilis* spore counts were performed through pour-plate enumeration three times. One milliliter of diluted spore suspension was inoculated into each plate and incubated aerobically at 37°C for 24 h. In each experiment, the spore counts of untreated samples represented the initial concentration,

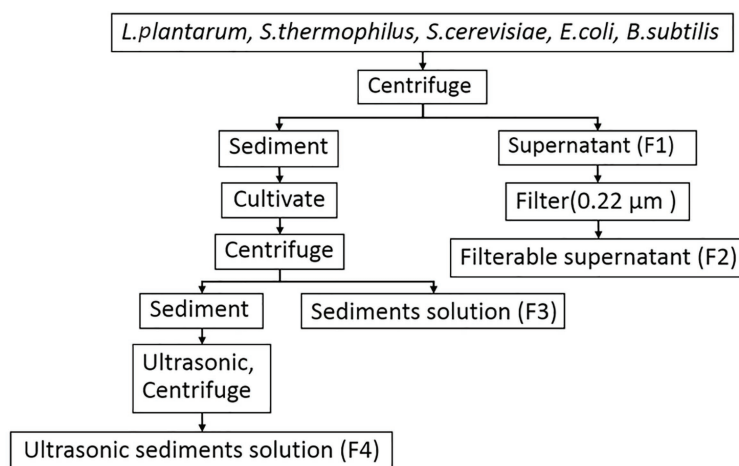


FIGURE 1 | The flow diagram for the treatment of the supernatant and sediment from microorganisms used in this study.

which was adjusted to approximately 10^8 spores/ml via a plate count. The logarithm of survivors [$\log_{10} (N_0/N_t)$] could indicate the number of reduced spores after different treatments. The spore counts before and after heating at 80°C for 20 min were marked as N_0 and N_t , respectively.

The Treatment With Pressure and Temperature

On the sterile operating table, the spore suspension was adjusted with sterile deionized water, AGFK, L-val, and supernatants from *B. subtilis* or *S. cerevisiae* to $\text{OD}_{600} = 0.5$. L-val, AGFK, and the untreated groups were used as the positive and negative control, respectively. Then, 2 ml of mixed samples were packed in sterilized nylon/polyethylene composite cooking bags (4 cm * 4 cm). These bags were treated with 90°C for 10 min and marked as heat shock treatment ($90^\circ\text{C}/10$ min). The pressure treatment conditions were 200 MPa with a holding time of 20 and 30 min at 80°C , which was followed with heat shock treatment. After treatment with pressure and temperature, spore suspension was performed with cell counting.

Statistical Analysis

Data are expressed as the mean value \pm SD of triplicates. Statistical analysis was determined by using the *t*-test, and differences with a value of $p < 0.05$ were considered statistically significant.

RESULTS

The Effect of Endogenous Materials Derived From Different Microorganisms on Spores

To screen spore germinants, we performed germination experiments using *B. subtilis* spores and five different cell-free supernatants. The supernatants, filtered supernatants, solid and liquid bacterial precipitation after ultrasonic crushing from *B. subtilis*, *E. coli*, *S. thermophilus*, *L. plantarum*, and *S. cerevisiae* were prepared and exposed to 10^8 CFU/ml spores of *B. subtilis* strain 168 at 37°C . Then, the levels of DPA release were determined, and the ratio of DPA release was calculated to determine their effect on spore germination. For comparison, *B. subtilis* spores were treated with L-val and AGFK. These results showed that exposure of 168 spores to L-val induced abundant DPA release during spore germination, with a 90% DPA release ratio. In the experiments with the treatment of supernatants, *S. thermophilus* and *L. plantarum* exhibited the same effect for DPA release of spores, which was better than the others, with a 30–40% ratio. The DPA release ratio of spores with *B. subtilis* and *E. coli* supernatants was 20–30%, although the supernatants from *S. cerevisiae* could induce a 10% DPA release ratio (Figure 2A). Interestingly, the filtered supernatants from five microorganisms showed the same induction effect on spore germination (Figure 2B), but the sediment solution and ultrasonic sediment

supernatant did not show any induction effect for the DPA release of spores (Figures 2C,D).

The optical density of the spore solution has been used as the assessment index for spore germination, and a decreasing OD_{600} indicates spore germination (Moir and Smith, 1990). Therefore, the absorbance at 600 nm every 10 min for 3 h was detected. Compared to the control, the OD_{600} of spore solution showed an increasing trend after an initial decrease with the treatment of supernatants (F1) and filtered supernatants (F2), but not the sediments solution (F3) and sediment supernatant (F4; Figures 3A–D). Furthermore, the decrease in OD_{600} was found in the first 40 min. These results suggested that the supernatants from *B. subtilis*, *E. coli*, *S. cerevisiae*, *S. thermophilus*, and *L. plantarum* may exhibit the benefits of inducing spore germination but not sediments.

The Effect of Microorganism Supernatants on Inducing Spore Germination

To explore the influence of bacterial supernatants on spore germination and outgrowth, we exposed 10^8 spores/ml of the *B. subtilis* 168 to L-val, AGFK, and five supernatants F2 at 37°C for 3 h and determined the level of germination by plate counting. Compared to the control, the *B. subtilis* 168 was treated using the same conditions but without the germinants. The exposure of spores to L-val could induce germination at a maximum rate of 2.0 log. Spores treated with the *B. subtilis*, *E. coli*, and *S. cerevisiae* supernatants displayed the same germination rate, close to 1.0 log, which was lower than that of the L-val treatment and the same as that of the AGFK treatment. However, spores treated with *S. thermophilus* and *L. plantarum* supernatants showed the lowest spore germination rate (about 0.2 log; Figure 4). All of these suggested that the supernatants from different microorganisms exhibited different effects, and *B. subtilis*, *E. coli*, and *S. cerevisiae* could derive the substance that exhibited better induction effects for spore germination.

The Relationship Between the Concentration of Supernatant and Spore Germination

As we focused on the effect of supernatants, different concentrations of microbial supernatants derived from *B. subtilis*, *E. coli*, and *S. cerevisiae* were prepared and used to induce spore germination. The results showed that the *B. subtilis* supernatants at concentrations within the range of 0.1–1.0 (1.0 represents the $\text{OD}_{600} = 3$, 0.1 was 10 times the dilution of supernatants with $\text{OD}_{600} = 3$) induced the germination of 0.7 log spore. When the concentration was <0.1 , spore germination decreased (Figure 5A). Moreover, the supernatants from *E. coli* and *S. cerevisiae* exhibited a consistent effect on spore germination, with a 0.7 log (Figures 5B,C). These suggested that three kinds of supernatants with concentrations between 0.1 and 1 exhibited the same effect, whereas concentrations <0.1 inhibited the germination effect (Figures 5A–C). Therefore, these results revealed that three kinds of supernatants from

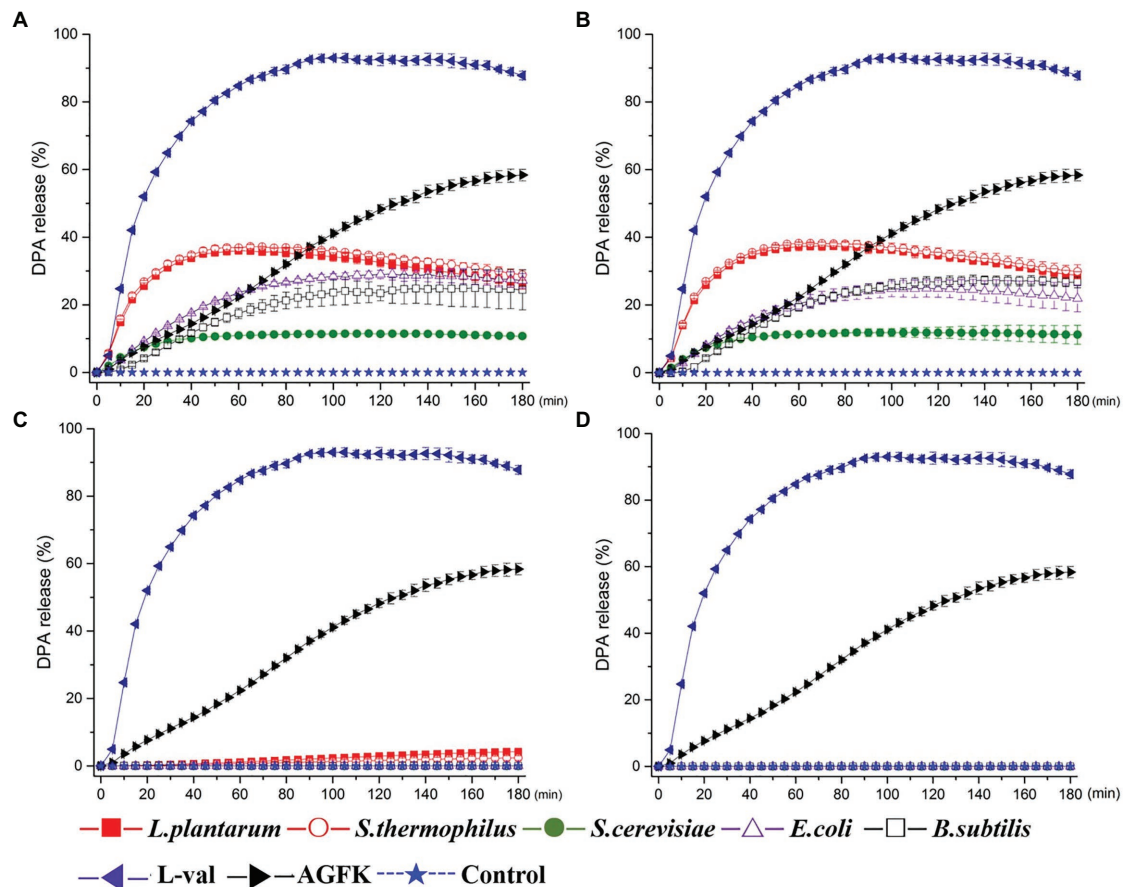


FIGURE 2 | Dipicolinic acid (DPA) release of wild-type *Bacillus subtilis* 168 spores with the treatments of various solutions from *Escherichia coli*, *B. subtilis*, *Saccharomyces cerevisiae*, *Lactiplantibacillus plantarum*, and *Streptococcus thermophilus*. **(A)** The treatment of supernatant from five microorganisms, respectively. **(B)** The treatment of filterable supernatant from five microorganisms, respectively. **(C)** The treatment of sediments solution from five microorganisms, respectively. **(D)** The treatment of ultrasonic sediments solution from five microorganisms, respectively. The treatments of L-val and AGFK were used as the positive control, and untreated spore were control.

B. subtilis, *E. coli*, and *S. cerevisiae* could induce spore germination in a concentration-dependent manner.

The Functional Pathway of Supernatants in Inducing Spore Germination

The previous experiments demonstrated that the substance of supernatants exhibited the effect of inducing spore germination. To further explore the underlying mechanism of supernatants in inducing spore germination, we performed the plate count experiments using GRs or PrkC mutant strains. The supernatants from *B. subtilis*, *E. coli*, and *S. cerevisiae* were used to treat spores, and the germination rates were determined. The results showed that the germination rate of the FB85 spores (GRs mutant) was the lowest (~ 0.15 – 0.2), and that of PB705 spores (PrkC mutant) was intermediate (0.1 – 0.3), although less than 168 spores (0.2 – 0.5 ; **Figure 6**). Moreover, the DPA release experiment showed the same result (data not shown). Therefore, we hypothesize that some substances in supernatants can induce spore germination, mainly through activating the GRs.

Effect of Pressure and Temperature Combined With Supernatants on Spore Germination

To further explore the application of bacterial supernatants in food sterilization, we analyzed the combination of temperature and pressure on spore germination and inactivation. First, the combination analysis of heat-activated ($90^{\circ}\text{C}/10$ min) treatment and various germinating agents showed that, as shown in **Figure 7A**, AGFK and L-val could induce 1.65 and 1.95 log spore germination, respectively, while the supernatant of *B. subtilis* and *S. cerevisiae* could induce 0.67 and 0.81 log spores, which were higher than the control group (0.46 log spores). Moreover, with the treatment of $90^{\circ}\text{C}/10$ min + 200 MPa/ $80^{\circ}\text{C}/20$ min, 6.47 and 5.98 log spores germinated in the AGFK and L-val groups, which were 4.82 and 4.02 log spores more than the heat-activated spores, respectively. The supernatants of *B. subtilis* and *S. cerevisiae* could effectively increase 3 and 4.03 log spores of germination compared with the heat-activated groups, respectively.

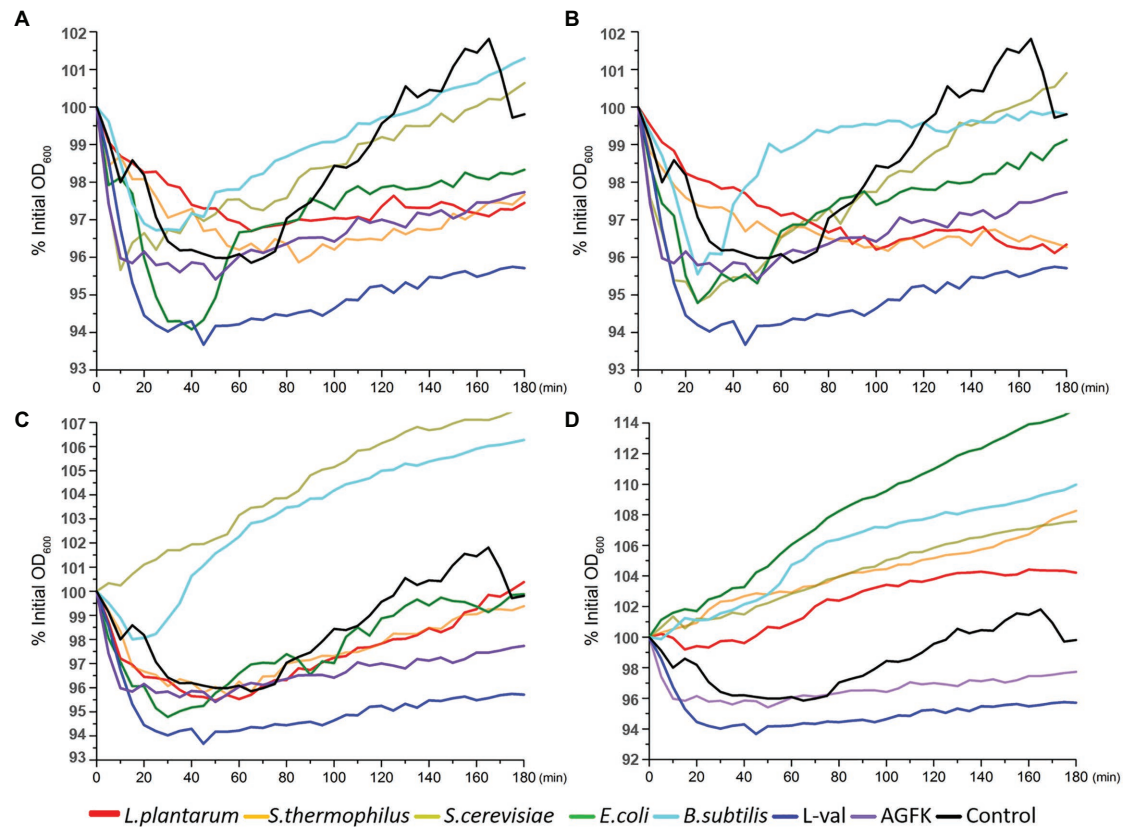


FIGURE 3 | OD₆₀₀ detection of wild-type *B. subtilis* 168 spores with the treatments of various solutions from *E. coli*, *B. subtilis*, *S. cerevisiae*, *L. plantarum*, and *S. thermophilus*. **(A)** The treatment of supernatant from five microorganisms, respectively. **(B)** The treatment of filterable supernatant from five microorganisms, respectively. **(C)** The treatment of sediments solution from five microorganisms, respectively. **(D)** The treatment of ultrasonic sediments solution from five microorganisms, respectively. The treatments of L-val and AGFK were used as the positive control, and untreated spores were control.

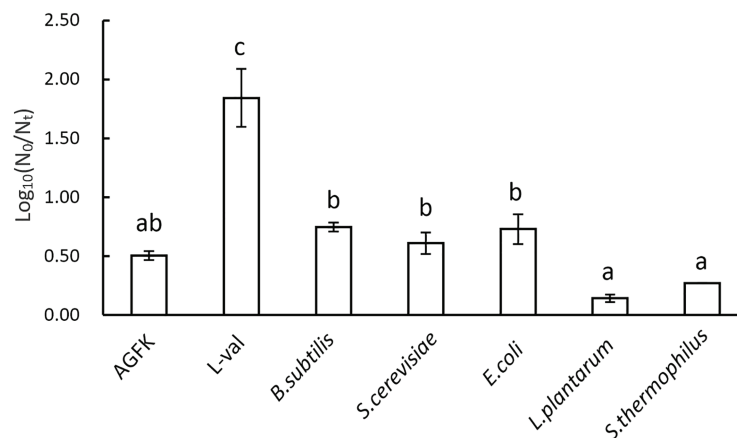


FIGURE 4 | The germination rate of *B. subtilis* 168 spores with various nutrient germinants or microbial supernatants.

Interestingly, the same effective spore germination could also be induced by the synergy of pressure and temperature for a longer time (200 MPa/80°C/30 min), whereas ~1.0 log spore increments were achieved in treatment with supernatants of *B. subtilis*.

In addition, the spore-killing effect under the same conditions was also analyzed. The result (**Figure 7B**) showed that heat activation treatment combined with AGFK, L-val, and the supernatant of *B. subtilis* or *S. cerevisiae* could kill 0.42, 1.05,

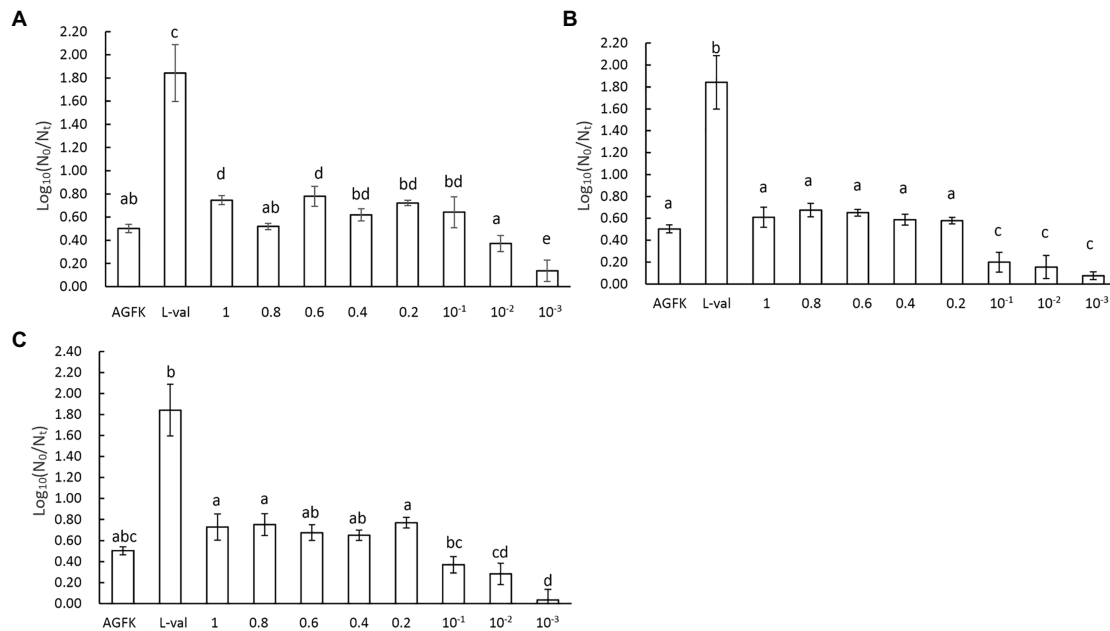


FIGURE 5 | The concentration effect of microbial supernatants on spore germination. **(A)** The treatment of spores with supernatant from *B. subtilis*, **(B)** the treatment of spores with supernatant from *E. coli*, and **(C)** the treatment of spores with supernatant from *S. cerevisiae*. The OD₆₀₀ value of the initial bacterial suspension was 3, the supernatants from which were marked as 1. After diluting 0.8, 0.6, 0.4, 0.2, 10^{-1} , 10^{-2} , and 10^{-3} times, the supernatants were 0.8, 0.6, 0.4, 0.2, 10^{-1} , 10^{-2} , and 10^{-3} , respectively.

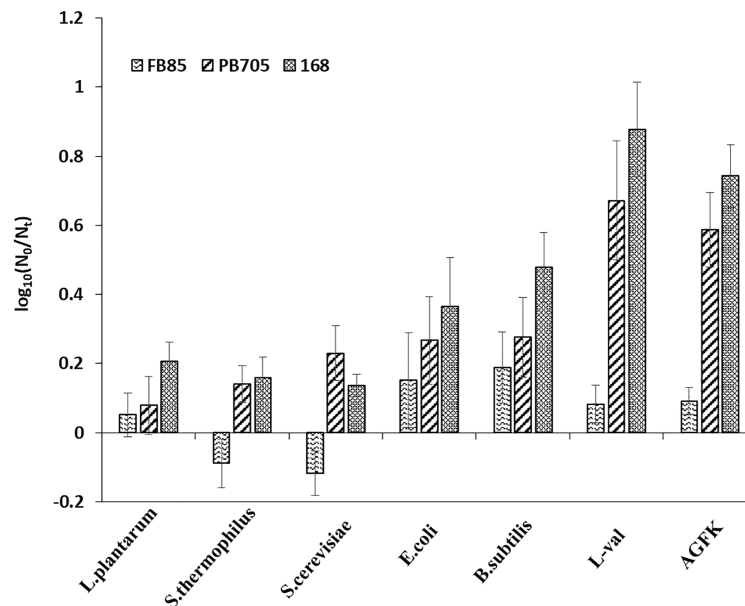


FIGURE 6 | The germination of *B. subtilis* 168, FB85, and PB705 spores with five microbial supernatants and two known germinants (L-val and AGFK). *Bacillus subtilis* FB85 was germination receptors (GRs) mutant strain, and *B. subtilis* PB705 was PrkC mutant.

0.27, and 0.45 log spores, which was much higher than that of the control group (0.07 log). The higher inactivation level was observed in two pressure and temperature treatment combinations: 90°C/10 min + 200 MPa/80°C/20 min and

200 MPa/80°C/30 min. For the treatment of *B. subtilis* and *S. cerevisiae* supernatants, the former could kill 3.35 and 3.47 log spores, respectively, which were significantly higher than 2.38 log spores in the control group ($p > 0.05$), and the latter had

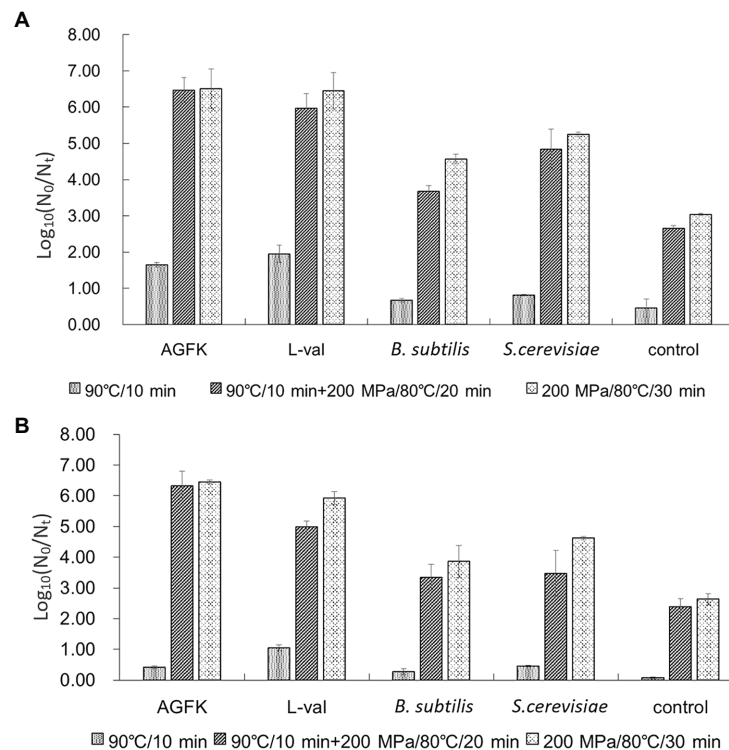


FIGURE 7 | The effect of supernatants from *B. subtilis* and *S. cerevisiae* on spore germination and inactivation. **(A)** The germination of *B. subtilis* 168 spores with different treatments. **(B)** The inactivation of *B. subtilis* 168 spores with different treatments. The supernatants from *B. subtilis* and *S. cerevisiae* combined with temperature and pressure were performed simultaneously.

3.86 and 4.62 log inactive spores. All of these results suggested that the combination of temperature and pressure treatment can increase the effect of *B. subtilis* and *S. cerevisiae* supernatants in inducing spore germination and reducing spore activation.

DISCUSSION

In this study, we developed a strategy to alter spore germination through the use of microbial culture products, which could be developed as a kind of food additive in non-thermal sterilization technology. Our data showed that treatment with various microbial supernatants, including *E. coli*, *B. subtilis*, and *S. cerevisiae*, induced spore germination, but the effects of *S. thermophilus* and *L. plantarum* were not distinct. These results suggested that the stimulus from the microbial supernatants, which only exist in some microorganisms, have the potential to induce spore germination. Further investigation indicated that the induction effects of supernatants depend on their concentration, and the effects were not observed at low concentrations (<0.1). These results indicated that the endogenous factors in microbial supernatants may induce spore germination. Moreover, combined with pressure and temperature, *B. subtilis*, and *S. cerevisiae* supernatants exhibited the effect of killing spores. Collectively, our results not only indicated that microbial supernatants may be potentially used in inducing spore germination, but also may be utilized as an effective germination agent in food processing.

Supernatants have the effect of inducing spore germination, but not the sediments. Microorganisms secrete many kinds of antimicrobial substances that inhibit or trigger the growth of bacteria by directly breaking the membrane structure of bacteria, including bacteriocins, organic acids, and some heat-resistant small peptides (Lash et al., 2005; Song et al., 2014). The antimicrobial activity of *Lactocaseibacillus rhamnosus* was exhibited entirely through secreted cell-free supernatants (He et al., 2017). Moreover, these chemical substances were secreted from bacteria only during the index growth period. The cell-free supernatants from *E. coli* and *B. subtilis* could induce the germination of spores through the PGN derived from the cell wall (Shah et al., 2008). Additionally, the bacteria cell wall was ultrasonically decomposed and various big fragments emerged, but PGN was obtained through zymolysis (Desmarais et al., 2014). Our findings suggested that there may be active components in the bacterial supernatant that impart beneficial effects on spore germination. Moreover, the subtilin produced by *B. subtilis* ATCC 6633 may exhibit antimicrobial effects, which belong to a kind of LAB bacteriocins (Lee and Kim, 2011). Thus, we hypothesized that these germinants can be metabolized by microorganisms during the growth period and are not derived from the damaged bacteria, which will be investigated carefully in future research. In addition, the low concentration of supernatants from microbial species used here did not show better induction effects; however, the moderate concentration of cell-free supernatants induced spore germination

(Figures 5A–C). When OD₆₀₀ of bacterial suspension was 3.0, the microorganism is in the period of stable growth, and a large number of metabolites were produced in catabolism, including PGN fragments from the cell wall, which may contribute to spore germination. To date, many bacteriocins have been exploited in food additives, including nisin and lactacin (Galvez et al., 2007; Gharsallaoui et al., 2016; Castellano et al., 2018; Sanborn et al., 2018). Therefore, screening and application of spore germinants as food additives need to consider their working concentration and edible dosage.

In addition, the five kinds of supernatants could trigger the DPA release, and the levels of DPA release on spores with *S. thermophilus* and *L. plantarum* were higher than the treatment of *B. subtilis*, *E. coli*, and *S. cerevisiae* (Figure 2). The ratio of DPA release indicated that germination commitment and spore germination would ensue (Yi and Setlow, 2010; Zhang et al., 2014). However, *S. thermophilus* and *L. plantarum* did not significantly improve the levels of germination (Figure 4). Various studies have demonstrated that some substances secreted by *S. thermophilus* and *L. plantarum* could inhibit bacteria growth significantly (Rossi et al., 2013; Sanborn et al., 2018). These findings were consistent with the results that substances derived from *S. thermophilus* could inhibit the germination and outgrowth of *C. difficile* spore (Chai et al., 2017; Setlow et al., 2017). In addition, the effects of various bacteriocins, such as nisin, enterocin AS-48, and thurincin H, were unlikely to occur *via* direct induction of dormant spores, but mainly inhibited the germinating spores (Lee and Kim, 2011). The possible reason was that in the early germination period, substances from *S. thermophilus* and *L. plantarum* cell-free supernatants could establish germination commitment and trigger DPA release, and thus spore germination could not be reversed. Then, during the spore outgrowth period, the process could be inhibited by other substances.

The present study shows that supernatants may be potentially utilized in inducing spore germination. However, the specific component of the supernatant that exerts the beneficial effects remains unclear. Supernatants are complex mixtures containing various substances, including organic acids, lipids, proteins, and other small molecules (Lievin-Le Moal and Servin, 2014). Owing to their complexity and uncertainty, it is difficult to ascertain the multiple effects of supernatants. To date, the PGN derived from bacterial cell walls can interact with PrkC kinase and transduce the signal to trigger spore germination (Shah et al., 2008). In our results, the mutant spore germination experiment revealed that the germinants from supernatants mainly interacted with the GRs because GR mutant spore germination was almost inhibited. However, the PrkC mutant spores exhibited a relatively high germination ratio (Figure 6). Thus, the GRs pathway could play a more important role than the PrkC pathway in establishing the effects of supernatants. Interestingly, the log (N_0/N_t) of the GRs mutants was negative with the treatment of *S. thermophilus* and *L. plantarum* cell-free supernatants. A previous study showed that heat shock induced spore germination mainly through GRs (Luu et al., 2015), but it is not clear whether there are other germination pathways. Our results implied that other germination pathways may exist. In subsequent experiments, we will try to explore

the details of cell-free supernatants in inducing spore germination (e.g., the substances that play a role in inducing spore germination and their functional mechanism).

At present, non-thermal sterilization technology has been widely examined, particularly in spore inactivation research, because it can better maintain the flavor and color of food (Olivier et al., 2011). Previous study showed that the mechanism of spore inactivation was different with various pressures and temperatures due to different spore germination receptors. Specifically, 200–500 MPa could activate GRs (Doona et al., 2014; Liang et al., 2019), although >500 MPa could activate the channel proteins of DPA release, SpoVA, resulting in spore germination (Reineke et al., 2013). Although pressure treatment alone could reduce the limited number of spores, the time required was also from 5 to 45 min, resulting in high energy consumption (Reddy et al., 2016). Temperature combined with pressure has been useful technology, and the normal range is 80–100°C, but spores cannot completely be killed (Liang et al., 2019). Therefore, the combination of effective germination agents may be more effective in spore inactivation. We combined pressure and temperature with *B. subtilis* and *S. cerevisiae* supernatants that could inactivate an average of ~4 log spores, especially in the treatment of 200 MPa/80°C/30 min.

In summary, our study revealed that microbial supernatants could induce spore germination mainly by activating nutrient receptors, and combined with pressure and temperature, effectively inactivated spores. Thus, we believe that supernatants may be potentially used as an alternative treatment for preventing spore outgrowth or inducing spore germination. The results also confirmed that supernatants from certain microorganisms can exhibit similar beneficial effects as their anti-bacterial counterparts. Therefore, it is necessary to further identify the active ingredients in supernatants to develop novel antibiotics for use in food processing.

DATA AVAILABILITY STATEMENT

The original contributions presented in the study are included in the article/supplementary material; further inquiries can be directed to the corresponding author.

AUTHOR CONTRIBUTIONS

LD, FC, and XH conceived and designed the experiments. JL and YS performed all the experiments. LD, FC, XH, JL, and YS discussed the results and drafted and revised the manuscript. All authors contributed to the article and approved the submitted version.

FUNDING

This work was supported by National Key Research and Development Program of China (2018YFC1602202), and the National Natural Science Foundation of China (31530058, 31601563, 31872913).

REFERENCES

- Castellano, P., Pena, N., Ibarreche, M. P., Carduza, F., Soteras, T., and Vignolo, G. (2018). Antilisterial efficacy of *Lactobacillus* bacteriocins and organic acids on frankfurters. Impact on sensory characteristics. *J. Food Sci. Technol.* 55, 689–697. doi: 10.1007/s13197-017-2979-8
- Chai, C., Lee, K. S., Imm, G. S., Kim, Y. S., and Oh, S. W. (2017). Inactivation of *Clostridium difficile* spore outgrowth by synergistic effects of nisin and lysozyme. *Can. J. Microbiol.* 63, 638–643. doi: 10.1139/cjm-2016-0550
- Desmarais, S. M., Cava, F., de Pedro, M. A., and Huang, K. C. (2014). Isolation and preparation of bacterial cell walls for compositional analysis by ultra performance liquid chromatography. *J. Vis. Exp.* 83:e51183. doi: 10.3791/51183
- Doona, C. J., Ghosh, S., Feeherry, F. F., Ramirez-Peralta, A., Huang, Y., Chen, H., et al. (2014). High pressure germination of *Bacillus subtilis* spores with alterations in levels and types of germination proteins. *J. Appl. Microbiol.* 117, 711–720. doi: 10.1111/jam.12557
- Drusano, G. L., Okusanya, O. O., Okusanya, A. O., van Scoy, B., Fregeau, B. C., Kulawy, R., et al. (2009). Impact of spore biology on the rate of kill and suppression of resistance in *Bacillus anthracis*. *Antimicrob. Agents Chemother.* 53, 4718–4725. doi: 10.1128/AAC.00802-09
- Galvez, A., Abriouel, H., Lopez, R. L., and Ben Omar, N. (2007). Bacteriocin-based strategies for food biopreservation. *Int. J. Food Microbiol.* 120, 51–70. doi: 10.1016/j.jfoodmicro.2007.06.001
- Gharsallaoui, A., Oulahal, N., Joly, C., and Degraeve, P. (2016). Nisin as a food preservative: part 1: physicochemical properties, antimicrobial activity, and main uses. *Crit. Rev. Food Sci.* 56, 1262–1274. doi: 10.1080/10408398.2013.763765
- Grela, A., Jamrozek, I., Hubisz, M., Iwanicki, A., Hinc, K., Kazmierkiewicz, R., et al. (2018). Positions 299 and 302 of the GerAA subunit are important for function of the GerA spore germination receptor in *Bacillus subtilis*. *PLoS One* 13:e0198561. doi: 10.1371/journal.pone.0198561
- He, X., Zeng, Q., Puthiyakunnon, S., Zeng, Z., Yang, W., Qiu, J., et al. (2017). *Lactobacillus rhamnosus* GG supernatant enhance neonatal resistance to systemic *Escherichia coli* K1 infection by accelerating development of intestinal defense. *Sci. Rep.* 7:43305. doi: 10.1038/srep43305
- Hindle, A. A., and Hall, E. A. (1999). Dipicolinic acid (DPA) assay revisited and appraised for spore detection. *Analyst* 124, 1599–1604. doi: 10.1039/a906846e
- Ishaq, A. R., Manzoor, M., Hussain, A., Altaf, J., Rehman, S. U., Javed, Z., et al. (2021). Prospect of microbial food borne diseases in Pakistan: a review. *Braz. J. Biol.* 81, 940–953. doi: 10.1590/1519-6984.232466
- Kochan, T. J., Shoshiev, M. S., Hastie, J. L., Somers, M. J., Plotnick, Y. M., Gutierrez-Munoz, D. F., et al. (2018). Germinant synergy facilitates *Clostridium difficile* spore germination under physiological conditions. *mSphere* 3, e00335–e00318. doi: 10.1128/mSphere.00335-18
- Lash, B. W., Mysliwiec, T. H., and Gourama, H. (2005). Detection and partial characterization of a broad-range bacteriocin produced by *Lactobacillus plantarum* (ATCC 8014). *Food Microbiol.* 22, 199–204. doi: 10.1016/j.fm.2004.03.006
- Lee, H., and Kim, H. Y. (2011). Lantibiotics, class I bacteriocins from the genus *Bacillus*. *J. Microbiol. Biotechnol.* 21, 229–235. doi: 10.4014/jmb.1010.10017
- Le Lay, C., Dridi, L., Bergeron, M. G., Ouellette, M., and Fliss, I. (2016). Nisin is an effective inhibitor of *Clostridium difficile* vegetative cells and spore germination. *J. Med. Microbiol.* 65, 169–175. doi: 10.1099/jmm.0.000202
- Liang, D., Zhang, L., Wang, X., Wang, P., Liao, X., Wu, X., et al. (2019). Building of pressure-assisted ultra-high temperature system and its inactivation of bacterial spores. *Front. Microbiol.* 10:1275. doi: 10.3389/fmicb.2019.01275
- Lievins-Le Moal, V., and Servin, A. L. (2014). Anti-infective activities of *Lactobacillus* strains in the human intestinal microbiota: from probiotics to gastrointestinal anti-infectious biotherapeutic agents. *Clin. Microbiol. Rev.* 27, 167–199. doi: 10.1128/CMR.00080-13
- Luu, S., Cruz-Mora, J., Setlow, B., Feeherry, F. E., Doona, C. J., and Setlow, P. (2015). The effects of heat activation on *Bacillus* spore germination, with nutrients or under high pressure, with or without various germination proteins. *Appl. Environ. Microbiol.* 81, 2927–2938. doi: 10.1128/AEM.00193-15
- Mathot, A. G., Beliard, E., and Thuault, D. (2003). *Streptococcus thermophilus* 580 produces a bacteriocin potentially suitable for inhibition of *Clostridium tyrobutyricum* in hard cheese. *J. Dairy Sci.* 86, 3068–3074. doi: 10.3168/jds.S0022-0302(03)73906-X
- Modugno, C., Kmiha, S., Simoni, H., Aouadhi, C., Canizares, E. D., Lang, E., et al. (2019). High pressure sensitization of heat-resistant and pathogenic foodborne spores to nisin. *Food Microbiol.* 84:103244. doi: 10.1016/j.fm.2019.103244
- Moir, A., and Smith, D. A. (1990). The genetics of bacterial spore germination. *Annu. Rev. Microbiol.* 44, 531–553. doi: 10.1146/annurev.mi.44.100190.002531
- Nerandzic, M. M., and Donskey, C. J. (2013). Activate to eradicate: inhibition of *Clostridium difficile* spore outgrowth by the synergistic effects of osmotic activation and nisin. *PLoS One* 8:e54740. doi: 10.1371/journal.pone.0054740
- Olivier, S. A., Bull, M. K., Stone, G., van Diepenbeek, R. J., Kormelink, F., Jacobs, L., et al. (2011). Strong and consistently synergistic inactivation of spores of spoilage-associated *Bacillus* and *Geobacillus* spp. by high pressure and heat compared with inactivation by heat alone. *Appl. Environ. Microbiol.* 77, 2317–2324. doi: 10.1128/AEM.01957-10
- Ortiz, S. C., Huang, M., and Hull, C. M. (2019). Spore germination as a target for antifungal therapeutics. *Antimicrob. Agents Chemother.* 63, e00994–e00919. doi: 10.1128/AAC.00994-19
- Paidhungat, M., Ragkousi, K., and Setlow, P. (2001). Genetic requirements for induction of germination of spores of *Bacillus subtilis* by Ca^{2+} -dipicolinate. *J. Bacteriol.* 183, 4886–4893. doi: 10.1128/JB.183.16.4886-4893.2001
- Paidhungat, M., Setlow, B., Daniels, W. B., Hoover, D., Papafragkou, E., and Setlow, P. (2002). Mechanisms of induction of germination of *Bacillus subtilis* spores by high pressure. *Appl. Environ. Microbiol.* 68, 3172–3175. doi: 10.1128/AEM.68.6.3172-3175.2002
- Perez-Valdespino, A., Ghosh, S., Cammett, E. P., Kong, L., Li, Y. Q., and Setlow, P. (2013). Isolation and characterization of *Bacillus subtilis* spores that are superdormant for germination with dodecylamine or Ca^{2+} -dipicolinic acid. *J. Appl. Microbiol.* 114, 1109–1119. doi: 10.1111/jam.12125
- Popham, D. L., Meador-Parton, J., Costello, C. E., and Setlow, P. (1999). Spore peptidoglycan structure in a *cwlD* *dacB* double mutant of *Bacillus subtilis*. *J. Bacteriol.* 181, 6205–6209. doi: 10.1128/JB.181.19.6205-6209.1999
- Reddy, N. R., Patzaca, E., Morrissey, T. R., Skinner, G. E., Loeza, V., Schill, K. M., et al. (2016). Thermal and pressure-assisted thermal destruction kinetics for spores of type A *Clostridium botulinum* and *Clostridium sporogenes* PA3679. *J. Food Prot.* 79, 253–262. doi: 10.4315/0362-028X.JFP-15-310
- Reineke, K., Mathys, A., Heinz, V., and Knorr, D. (2013). Mechanisms of endospore inactivation under high pressure. *Trends Microbiol.* 21, 296–304. doi: 10.1016/j.tim.2013.03.001
- Rossi, F., Marzotto, M., Cremonese, S., Rizzotti, L., and Torriani, S. (2013). Diversity of *Streptococcus thermophilus* in bacteriocin production; inhibitory spectrum and occurrence of thermophilin genes. *Food Microbiol.* 35, 27–33. doi: 10.1016/j.fm.2013.02.006
- Sanborn, V., Azcarate-Peril, M. A., Updegraff, J., Manderino, L. M., and Gunstad, J. (2018). A randomized clinical trial examining the impact of LGG probiotic supplementation on psychological status in middle-aged and older adults. *Contemp. Clin. Trials Commun.* 12, 192–197. doi: 10.1016/j.conctc.2018.11.006
- Setlow, P., Wang, S. W., and Li, Y. Q. (2017). Germination of spores of the orders Bacillales and Clostridiales. *Annu. Rev. Microbiol.* 71, 459–477. doi: 10.1146/annurev-micro-090816-093558
- Shah, I. M., Laaberki, M. H., Popham, D. L., and Dworkin, J. (2008). A eukaryotic-like Ser/Thr kinase signals bacteria to exit dormancy in response to peptidoglycan fragments. *Cell* 135, 486–496. doi: 10.1016/j.cell.2008.08.039
- Song, D. F., Zhu, M. Y., and Gu, Q. (2014). Purification and characterization of plantaricin ZJ5, a new bacteriocin produced by *Lactobacillus plantarum* ZJ5. *PLoS One* 9:e105549. doi: 10.1371/journal.pone.0116455
- Yi, X., and Setlow, P. (2010). Studies of the commitment step in the germination of spores of *Bacillus* species. *J. Bacteriol.* 192, 3424–3433. doi: 10.1128/JB.00326-10
- Zhang, P., Liang, J., Yi, X., Setlow, P., and Li, Y. Q. (2014). Monitoring of commitment, blocking, and continuation of nutrient germination of individual *Bacillus subtilis* spores. *J. Bacteriol.* 196, 2443–2454. doi: 10.1128/JB.01687-14

Conflict of Interest: The authors declare that the research was conducted in the absence of any commercial or financial relationships that could be construed as a potential conflict of interest.

Copyright © 2021 Li, Sun, Chen, Hu and Dong. This is an open-access article distributed under the terms of the Creative Commons Attribution License (CC BY). The use, distribution or reproduction in other forums is permitted, provided the

original author(s) and the copyright owner(s) are credited and that the original publication in this journal is cited, in accordance with accepted academic practice. No use, distribution or reproduction is permitted which does not comply with these terms.



Development of a Direct and Rapid Detection Method for Viable but Non-culturable State of *Pediococcus acidilactici*

Yu Guan^{1†}, Kan Wang^{2†}, Yang Zeng³, Yanrui Ye⁴, Ling Chen⁵ and Tengyi Huang^{6*}

¹ Department of Urology, Beijing Friendship Hospital, Capital Medical University, Beijing, China, ² Center for Translational Medicine, The Second Affiliated Hospital of Shantou University Medical College, Shantou, China, ³ Shantou University Medical College, Shantou, China, ⁴ School of Biological Science and Engineering, South China University of Technology, Guangzhou, China, ⁵ School of Food Science and Engineering, Guangdong Province Key Laboratory for Green Processing of Natural Products and Product Safety, South China University of Technology, Guangzhou, China, ⁶ Department of Laboratory Medicine, The Second Affiliated Hospital of Shantou University Medical College, Shantou, China

OPEN ACCESS

Edited by:

Yang Deng,
Qingdao Agricultural University, China

Reviewed by:

Yuting Tian,
Fujian Agriculture and Forestry
University, China
Wensen Jiang,
Cedars Sinai Medical Center,
United States

*Correspondence:

Yu Guan
guanyu1987.4.19@gmail.com
Tengyi Huang
h-hty@hotmail.com

[†] These authors share first authorship

Specialty section:

This article was submitted to
Food Microbiology,
a section of the journal
Frontiers in Microbiology

Received: 29 March 2021

Accepted: 31 May 2021

Published: 02 July 2021

Citation:

Guan Y, Wang K, Zeng Y, Ye Y, Chen L
and Huang T (2021) Development of a
Direct and Rapid Detection Method
for Viable but Non-culturable State of
Pediococcus acidilactici.
Front. Microbiol. 12:687691.
doi: 10.3389/fmicb.2021.687691

Pediococcus acidilactici may significantly reduce the pH-value, and thus has different influence, including serving as a probiotic in human microbiota but a spoilage in human food as it could change the flavor. *Pediococcus acidilactici* is also capable of entering into the viable but non-culturable (VBNC) state causing false negative results of standard culture-based detection method. Thus, development of detection method for VBNC state *P. acidilactici* is of great significance. In this study, propidium monoazide (PMA) combined with cross priming amplification (CPA) was developed to detect the VBNC cells of *P. acidilactici* and applied on the detection in different systems. With detection limit of 10^4 cells/ml, high sensitivity, and 100% specificity, PMA-CPA can successfully detect VBNC cells of *P. acidilactici* and be applied in with high robustness.

Keywords: *Pediococcus acidilactici*, viable but non-culturable, artificially contaminated food, PMA-CPA, rapid detection, safety control

INTRODUCTION

Pediococcus acidilactici may significantly reduce the pH-value, and thus has different influence, including serving as a probiotic in human microbiota but a spoilage in human food. Most commonly, *P. acidilactici* has been considered to be a probiotic bacteria for human beings, and also a typical type of lactic acid bacteria (LAB), which have been well-documented to be widely existing in human microbiota. Such probiotic bacteria have been well-studied to significantly aid in the microbiota balance, and once altered, various types of human diseases could occur. One important example is the correlation between human microbiota and urinary tract infection, in which microbiota in a few different sites, including intestine and vagina, has been found to play a role in the occurrence of urinary tract infection (Foxman, 2010; Whiteside et al., 2015; Stapleton, 2017; Paalanne et al., 2018; Magruder et al., 2020). Therefore, probiotic LAB is an important type of human probiotic and significantly aids in the prevention of urinary tract infection. In addition, accurate detection of probiotic commensal has significantly raised the public interest as this serves as an important indicator. However, a major concern still remains, as a large proportion of such

probiotic commensal are hard to culture, which has further raised the aim of this study. As a commonly existing human bacteria, *P. acidilactici* is also one of LAB that are frequently used due to their capacity to produce bacteriocin to inhibit the growth of other spoilage bacteria (Salminen et al., 2004; Zhong et al., 2013). However, with improper processing, *P. acidilactici* produces acids including lactic acid, malic acid, citric acid, propionic acid, acetic acid, and short-chain fatty acids through fermentation, resulting in the significant decrease of pH-value, and the change in morphology and flavor (Olaoye et al., 2008; Xu et al., 2009). In consequence, the shelf life of the food would be shorter and the deterioration of the food occurs. Furthermore, it has been proved that *P. acidilactici* is able to enter into the viable but non-culturable (VBNC) state, which causes the false negative detection by the standard culture-based detection methods (Fakruddin et al., 2013; Ramamurthy et al., 2014; Xie et al., 2017a,b; Xu et al., 2017a,b; Li et al., 2020). Thus, accurate detection of *P. acidilactici* cells in the VBNC state is in need (Ding et al., 2017; Truchado et al., 2020).

Nowadays, the detection of the VBNC state is currently based on molecular detection techniques and the fluorescence microscopy with dying kit (Xu et al., 2011a,b,c; Zhao et al., 2018a,b; Dong et al., 2020). In the past few years, PCR based methodologies have been developed for rapid detection of viable bacterial cells, in combination with use of different substances including propidium monoazide (PMA) (Zhong et al., 2016; Bao et al., 2017a,b,c; Jia et al., 2018; Liu et al., 2018b,c; Zhong and Zhao, 2018). However, PCR based methodologies require strict temperature change process and determination step, such as gel electrophoresis or hybridization, which significantly reduces rapidity and simplicity in operation of such methods (Miao et al., 2016, 2017a,b,c; Zhao et al., 2020). In addition, the PMA-PCR has a lower sensitivity compared to the novel isothermal amplification methods with complex procedure and higher cost (Xu et al., 2008a,b; Liu et al., 2019).

Cross priming amplification (CPA) was developed to detect the target DNA with exponential amplification (Xu et al., 2007, 2010; Bai et al., 2015). Cross priming amplification can be completed under constant temperature with the advantages of simplicity, rapidity, high sensitivity, and cost-efficiency (Liu et al., 2015, 2017; Zheng et al., 2020). The expensive heating machine can be replaced by the simple water bath or other heating block. The whole amplification procedure can be completed within 1 h by one pair of primer, which spans three distinct sequences of a target gene (Lin et al., 2016; Zhang et al., 2019). The products of CPA can be measured based on the turbidity, electrophoresis of amplicons, and DNA-specific fluorescent reaction in tubes, such as SYBR Green-I (Xu et al., 2012b,c, 2016a,b,c; Lin et al., 2017).

In a previous study (Li et al., 2020), we had studied the key conditions of VBNC formation of *P. acidilactici*, and then based on the key conditions, we had discovered the reduction of VBNC formation. However, a major concern still remains, as rapid detection of *P. acidilactici* is highly required, especially direct detection and real-time surveillance from food products. Consequently, in this study, first we developed a rapid, sensitive, and specific detection assay on *P. acidilactici* based on CPA methodology. Then, we had further developed a PMA-CPA assay

to directly identify the VBNC cells of *P. acidilactici*. Last, we had applied the established methodology on three different types of food products.

MATERIALS AND METHODS

Strains and Culturing

A total of 20 bacterial strains, which are common foodborne pathogens and spoilage bacteria, were tested in this study, including a *P. acidilactici* strain, and 19 non-target bacteria (Table 2), including *Escherichia coli*, *Salmonella*, *Staphylococcus aureus*, *Listeria monocytogenes*, *Vibrio parahaemolyticus*, *Lactobacillus casei*, *Lactobacillus acetotolerans*, *Lactobacillus plantarum*, and *Pseudomonas aeruginosa*. In brief, after inoculation of single colony on the plate for culturing at 37°C overnight, DNA extraction, VBNC induction, as well as serial dilution were further performed based on the bacterial suspension.

VBNC State Induction

The culture of *P. acidilactici* in the log phase was used to induce into the VBNC state under the freezing condition (−20°C). The changing on the culturable cell number was used as an index to investigate the culturability until the culturable number was below 1 cell/ml; the cells can be regarded as those that entered into the VBNC state (Wang et al., 2011; Miao et al., 2018). The VBNC cells were finally determined by Live/Dead BacLight bacterial viability kit (Thermo Fisher Scientific, USA) (Liu et al., 2018a) in combination with fluorescence microscopy. The growth curves, including total cell numbers, culturable cell numbers, and viable cell numbers, were determined and further analyzed as described previously.

CPA Detection Method Design

The CPA primer was designed to distinguish *P. acidilactici* based on *pheS* gene, which is a housekeeping gene. Primers used in this study were designed using Primer Premier 5 (Table 1) (Singh et al., 2018; Xu et al., 2018). The crude DNA from *P. acidilactici* and other bacterial strains used as templates for CPA amplification was prepared from overnight culture in MRS broth. DNA was extracted using whole genomic DNA extraction kit (Dongsheng Biotech, Guangzhou) according to the manufacturer's instructions. The DNA concentration and quality were measured using a Nano Drop 2000 (Thermo Fisher Scientific Inc., Waltham, MA, USA). The qualified DNA samples were stored at −20°C until further use (Wen et al., 2020).

TABLE 1 | Primer sequences of CPA for detection.

	Primers	Sequence (5'-3')
<i>pheS</i>	4s	GGAGCCATCCGTTGAAGT
	5a	GTCAGGACCAAGGCCAA
	2a/1s	AATGTTGCGTGCCCGTAG CGGTTGGATTGAAGTGTT
	2a	AATGTTGCGTGCCCGTAG
	3a	ACATTGGGATGCACCATGCC

TABLE 2 | Reference strains and results of PCR and CPA assays.

	PCR	CPA
Reference strain no	<i>pheS</i>	<i>pheS</i>
<i>Pediococcus acidilactici</i>	+	+
<i>Salmonella enterica</i> ATCC29629	–	–
<i>Salmonella enterica</i> ATCC14028	–	–
<i>Listeria monocytogenes</i> ATCC19114	–	–
<i>Listeria monocytogenes</i> ATCC19116	–	–
<i>Escherichia coli</i> O157:H7 ATCC43895	–	–
<i>Escherichia coli</i> O157:H7 E019	–	–
<i>Escherichia coli</i> O157:H7 E020	–	–
<i>Escherichia coli</i> O157:H7 E043	–	–
<i>Vibrio parahaemolyticus</i> ATCC27969	–	–
<i>Vibrio parahaemolyticus</i> ATCC17802	–	–
<i>Pseudomonas aeruginosa</i> ATCC27853	–	–
<i>Pseudomonas aeruginosa</i> C9	–	–
<i>Pseudomonas aeruginosa</i> C40	–	–
<i>Staphylococcus aureus</i> ATCC23235	–	–
<i>Staphylococcus aureus</i> 10085	–	–
<i>Staphylococcus aureus</i> 10071	–	–
<i>Lactobacillus casei</i>	–	–
<i>Lactobacillus acetotolerans</i> BM-LA14527	–	–
<i>Lactobacillus plantarum</i> BM-LP14723	–	–

Development of CPA Detection Assay

Cross priming amplification reaction was carried out in a total 26 μ l reaction mixture containing 20 mM Tris-HCl, 10 mM $(\text{NH}_4)_2\text{SO}_4$, 10 mM KCl, 8 mM MgSO_4 , 0.1% Tween 20, 0.7 M betaine (Sigma, USA), 1.4 mM of dNTP mix, 8 U of *Bst* DNA polymerase large fragment (NEB, USA), 1.0 μ M primer of 2a/1s, 0.5 μ M (each) primer of 2a and 3a, 0.6 μ M (each) primer of 4s and 5a, 1 μ l DNA template, and 1 μ l mixed chromogenic agent, and the total reaction mixture was made up of 26 μ l with nuclease free water (Xu et al., 2012a). The mixed chromogenic agent was composed of 0.13 mM calcein and 15.6 mM $\text{MnCl}_2 \cdot 4\text{H}_2\text{O}$. Mixture without DNA template was used as negative control (Xu et al., 2012a). The reaction mixtures are maintained at 63°C for 1 h followed by 80°C for 2 min. The amplified products were detected by electrophoresis on 1.5% agarose gel with ethidium bromide staining.

Evaluation of CPA Methodology

The specificity of CPA assay was evaluated by amplifying genomic DNA extracted from *P. acidilactici* and 19 non-target bacteria (Table 2). Nuclease free water was added instead of DNA template as blank control. The CPA reaction was conducted under the corresponding conditions mentioned above.

Development of PMA-CPA for Detection of VBNC Cells

The evaluation of the CPA assays was conducted by using serially 10-fold diluted genomic DNA and applied in food samples with 10 – 10^8 cells/ml. The CPA products were detected

by electrophoresis on 1.5% agarose gel with ethidium bromide staining (Xu et al., 2019). All the tests were performed in triplicate. The developed CPA assay was used to detect the VBNC cells of *P. acidilactici* combined with the PMA dyeing. Furthermore, the PMA-CPA was applied to detect the VBNC cells in the food samples using *pheS* gene as target. The products were analyzed by 1.5% agarose gel electrophoresis and fluorescent dye (MgCl_2 and calcein). The ladder-like bands were observed under UV light. The color of fluorescent dye that changes reaction system from orange to green indicates positive result (Figure 1).

Formation of VBNC State in Three Types of Artificially Contaminated Food

In this study, three major types of rice/flour products in China were selected, which were mantou, rice noodle, and Cantonese pastry. Mantou, rice noodle, and Cantonese pastry are among the top list of common food in China, with a large consumption market. The sample processing had been performed as follows. Each sample of mantou, rice noodle, and Cantonese pastry weighs 25 g, and a total of 100 μ l with bacterial suspension was added to each sample. All mantou, rice noodle, and Cantonese pastry samples were further stored and subjected to CFU counting at different time points. For the first few days, CFU was performed for each day, and after 3 days, CFU was performed every 3 days.

Application of the PMA-CPA Detection of VBNC Cells in Mantou

In order to further confirm if the established PMA-CPA methodology is capable of detection in the *P. acidilactici* VBNC state, the food samples (mantou, rice noodle, and Cantonese pastry) contaminated with *P. acidilactici* in the VBNC state was used as template. The PMA-treated bacteria suspension was centrifuged at 10,000 r/min for 5 min, and supernatant was removed. DNA was then extracted using a bacterial whole genomic DNA extraction kit (Dongsheng Biotech, Guangzhou). All samples including mantou, rice noodle, and Cantonese pastry were processed according to the standard procedure, and the PMA-CPA was performed accordingly.

RESULTS AND DISCUSSION

Establishment of CPA Assay

A novel and simple nucleic acid isothermal amplification CPA has been developed to detect the species specific gene *pheS*. According to the results, the CPA based assay is capable of detecting *P. acidilactici* cells. According to the evaluation of the CPA assay conducted by series of DNA, the detection limit of CPA was 52 pg/ μ l for *pheS* gene (Figure 2).

Applicability of CPA Assay on the Detection of *P. acidilactici*

The developed CPA assay was utilized in detection of food samples. The bacteria were inoculated into food samples with the concentration of 10 – 10^8 cells/ml. The results showed that the detection limit of application was 10^4 cells/ml (Figure 3). Compared with previously reported PCR based methodologies,



FIGURE 1 | Specificity of CPA detection for different strains with *pheS* genes by 1.5% agarose gel electrophoresis and mixed chromogenic agent; M-DNA marker; lane/tube 1, *P. acidilactici* BM-PA17927; lane/tube 2–20, non-*P. acidilactici* BM-PA17927 strains of *E. coli*, *Salmonella enteric*, *Vibrio parahaemolyticus*, *Pseudomonas aeruginosa*, *Listeria monocytogenes*, *Staphylococcus aureus*, and *Lactobacillus casei*; lane 21, negative control.

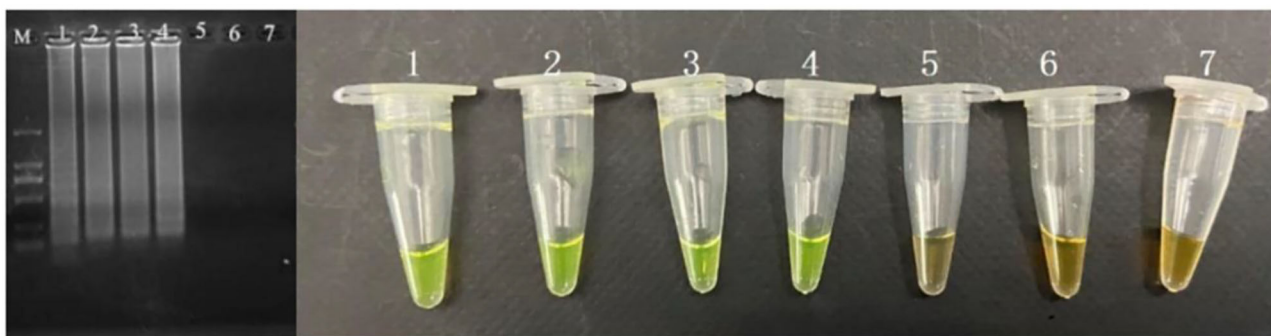


FIGURE 2 | Sensitivity of the CPA assay in genomic DNA of *P. acidilactici* with *pheS* genes by 1.5% agarose gel electrophoresis and mixed chromogenic agent; M-DNA marker; 1–6 refer to 52, 5.2 ng/μl, 520, 52, 5.2 pg/μl, and 520 fg/μl; 7 refers to negative control.

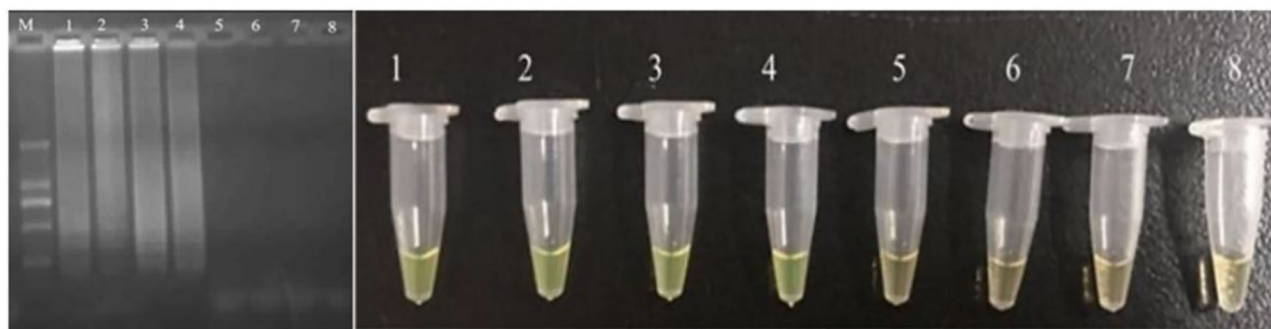


FIGURE 3 | Sensitivity for *pheS* in artificially contaminated food samples. M-DNA marker; 1–7 refer to 10^7 , 10^6 , 10^5 , 10^4 , 10^3 , 10^2 , and 10 cells/ml; 8 refers to negative control.

the CPA assays had shown significant advantages in terms of sensitivity, specificity, rapidity, and simplicity in operation.

Development of PMA-CPA Assay for VBNC *P. acidilactici* Cells

The cells considered may enter into the VBNC state when the culturable cell number in the induction solution is under 1

cell/ml. In order to determine whether *P. acidilactici* cells in the induction solution enter the VBNC state, the LIVE/DEAD[®] BacLight[™] bacterial viability kit (Thermo Fisher Scientific, USA) was used (Berney et al., 2007; You et al., 2012). For these assays, 500 μl of *P. acidilactici* culture sample was obtained and centrifuged at 5,000 r/min for 15 min. Subsequently, the *P. acidilactici* cells were washed twice with PBS. The

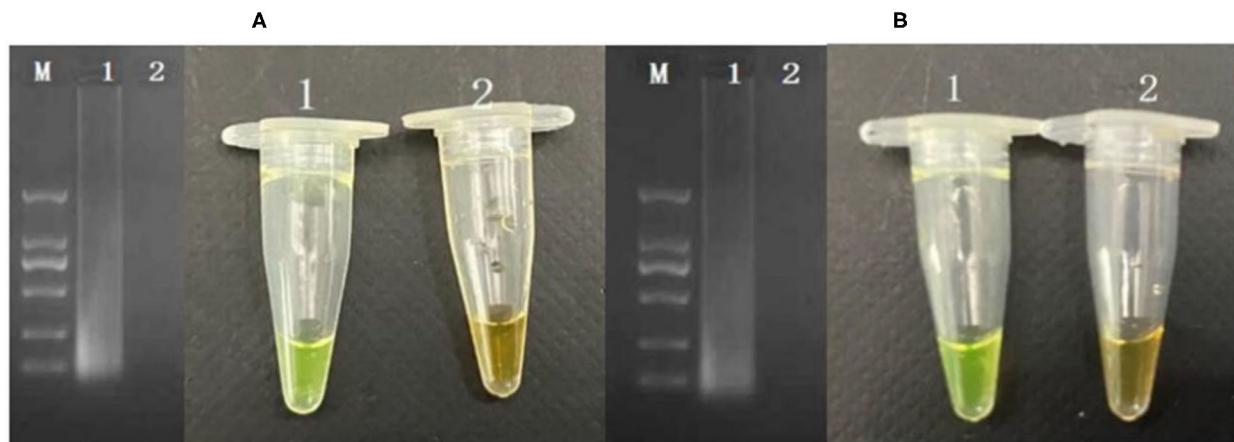


FIGURE 4 | Application of detection of VBNC cells in pure cultures (A) and food samples (B). M-DNA marker; 1: VBNC cells in pure culture; 2: dead cells in pure culture.

supernatant was removed, and the pellet was resuspended in 500 μ l of PBS. The cell suspensions were incubated with 1.5 μ l of dye mixture containing SYTO 9 and PI for 30 min at room temperature in the dark. The mixture (5 μ l) was observed under a fluorescent microscope. The viable cells including normal and VBNC state showed green, and the dead cells are in red. For PMA-CPA assay, the VBNC cells were added to a 1.5 ml centrifuge tube and were thoroughly mixed and left at room temperature for 10 min. Subsequently, the centrifuge tube was placed on a crushed ice box, and light treatment was performed for 15 min at 15 cm from a 650 W halogen lamp for PMA and DNA binding. The PMA molecules remaining after the treatment are passivated. The extracted DNA was detected by CPA. The results showed that the VBNC cells can be detected successfully by PMA-CPA (Figure 4A).

Application of PMA-CPA on Direct Detection of VBNC Cells From Food Products

The developed PMA-CPA assay as above had been further applied to detect VBNC cells of *P. acidilactici* from food samples including mantou, rice noodle, and Cantonese pastry. Firstly, formation of VBNC cells had been performed in artificially contaminated food samples including mantou, rice noodle, and Cantonese pastry. Following a rapid processing method, the samples had been further subjected to PMA-CPA detection. According to the results (Figure 4B), food samples of mantou, rice noodle, and Cantonese pastry containing *P. acidilactici* had yielded positive results. However, samples containing either none of strains (negative control) or non-target microorganisms had yielded negative results. The results demonstrated the fact that the developed method can be used in direct detection of VBNC cells of food samples (Figure 4B).

CONCLUSION

As concluded, from a widely existed human probiotic bacteria and the interest for its accurate detection as an important indicator of the health status of human microbiota, including intestine and vagina, which will be significantly correlated with urinary tract infection, a major concern had been raised as how to accurately detect the probiotic commensal LAB as they are mostly hard to culture. Consequently, in this study, we had firstly developed a rapid, sensitive, and specific detection assay on *P. acidilactici* based on CPA methodology, which had obtained high sensitivity and specificity. Then, we had connected the CPA assay with PMA processing to achieve a PMA-CPA assay to directly identify the VBNC cells of *P. acidilactici*. Thirdly, the developed PMA-CPA method had been further applied for direct detection of VBNC *P. acidilactici* cells to show its robustness.

DATA AVAILABILITY STATEMENT

The raw data supporting the conclusions of this article will be made available by the authors, without undue reservation.

AUTHOR CONTRIBUTIONS

YG conceived the study and participated in its design and coordination. KW and YY performed the experimental work and collected the data. LC organized the database. TH wrote the manuscripts. YZ revised the manuscript. All authors contributed to manuscript revision and read and approved the submitted manuscript.

FUNDING

This work was supported by the National Key Research and Development Program of China (2016YFD04012021) and National Key Research and Development Program of China (No. 2017YFC1601202).

REFERENCES

- Bai, Z., Xie, H., You, Q., Pickerill, S., Zhang, Y., Li, T., et al. (2015). Isothermal cross-priming amplification implementation study. *Lett. Appl. Microbiol.* 60, 205–209. doi: 10.1111/lam.12342
- Bao, X., Jia, X., Chen, L., Peters, B. M., Lin, C., Chen, D., et al. (2017a). Effect of polymyxin resistance (*pmr*) on biofilm formation of *Cronobacter sakazakii*. *Microb. Pathog.* 106, 16–19. doi: 10.1016/j.micpath.2016.12.012
- Bao, X., Yang, L., Chen, L., Li, B., Li, L., Li, Y., et al. (2017b). Virulent and pathogenic features on the *Cronobacter sakazakii* polymyxin resistant *pmr* mutant strain s-3. *Microb. Pathog.* 110, 359–364. doi: 10.1016/j.micpath.2017.07.022
- Bao, X., Yang, L., Chen, L., Li, B., Li, L., Li, Y., et al. (2017c). Analysis on pathogenic and virulent characteristics of the *Cronobacter sakazakii* strain BAA-894 by whole genome sequencing and its demonstration in basic biology science. *Microb. Pathog.* 109, 280–286. doi: 10.1016/j.micpath.2017.05.030
- Berney, M., Hammes, F., Bosshard, F., Weilenmann, H. U., and Egli, T. (2007). Assessment and interpretation of bacterial viability by using the LIVE/DEAD BacLight kit in combination with flow cytometry. *Am. Soc. Microbiol.* 73, 3283–3290. doi: 10.1128/AEM.02750-06
- Ding, T., Suo, Y., Xiang, Q., Zhao, X., Chen, S., Ye, X., et al. (2017). Significance of viable but nonculturable *Escherichia coli*: induction, detection, and control. *J. Microbiol. Biotechnol.* 27, 417–428. doi: 10.4014/jmb.1609.09063
- Dong, K., Pan, H., Yang, D., Rao, L., Zhao, L., Wang, et al. (2020). Induction, detection, formation, and resuscitation of viable but non-culturable state microorganisms. *Comprehen. Rev. Food Sci. Food Saf.* 19, 149–183. doi: 10.1111/1541-4337.12513
- Fakruddin, M. D., Mannan, K. S. B., and Andrews, S. (2013). Viable but nonculturable bacteria: food safety and public health perspective. *ISRN Microbiol.* 2013:703813. doi: 10.1155/2013/703813
- Foxman, B. (2010). The epidemiology of urinary tract infection. *Nat. Rev. Urol.* 7, 653–660. doi: 10.1038/nrurol.2010.190
- Jia, X., Hua, J., Liu, L., Xu, Z., and Li, Y. (2018). Phenotypic characterization of pathogenic *Cronobacter* spp. strains. *Microb. Pathogen.* 121, 232–237. doi: 10.1016/j.micpath.2018.05.033
- Li, Y., Huang, T.-Y., Mao, Y., Chen, Y., Shi, F., Peng, R., et al. (2020). Effect of environmental conditions on the formation of the viable but nonculturable state of *Pediococcus acidilactici* BM-PA17927 and its control and detection in food system. *Front. Microbiol.* 11:586777. doi: 10.3389/fmicb.2020.586777
- Lin, S., Li, L., Li, B., Zhao, X., Lin, C., Deng, Y., et al. (2016). Development and evaluation of quantitative detection of N-epsilon-carboxymethyl-lysine in *Staphylococcus aureus* biofilm by LC-MS method. *Basic Clin. Pharmacol. Toxicol.* 118: 33.
- Lin, S., Yang, L., Chen, G., Li, B., Chen, D., Li, L., et al. (2017). Pathogenic features and characteristics of food borne pathogens biofilm: biomass, viability and matrix. *Microb. Pathog.* 111, 285–291. doi: 10.1016/j.micpath.2017.08.005
- Liu, J., Deng, Y., Soteyome, T., Li, Y., Su, J., Li, L., et al. (2018a). Induction and recovery of the viable but nonculturable state of hop-resistance *Lactobacillus brevis*. *Front. Microbiol.* 9:2076. doi: 10.3389/fmicb.2018.02076
- Liu, J., Zhou, R., Li, L., Peters, B. M., Li, B., Lin, C. W., et al. (2017). Viable but non-culturable state and toxin gene expression of enterohemorrhagic *Escherichia coli* O157 under cryopreservation. *Res. Microbiol.* 168, 188–193. doi: 10.1016/j.resmic.2016.11.002
- Liu, L., Lu, Z., Li, L., Li, B., Zhang, X., Zhang, X., et al. (2018b). Physical relation and mechanism of ultrasonic bactericidal activity on pathogenic *E. coli* with WPI. *Microb. Pathog.* 117, 73–79. doi: 10.1016/j.micpath.2018.02.007
- Liu, L., Xu, R., Li, L., Li, B., Zhang, X., Zhang, X., et al. (2018c). Correlation and *in vitro* mechanism of bactericidal activity on *E. coli* with whey protein isolate during ultrasonic treatment. *Microb. Pathog.* 115, 154–158. doi: 10.1016/j.micpath.2017.12.062
- Liu, L., Ye, C., Soteyome, T., Zhao, X., Xia, J., Xu, W., et al. (2019). Inhibitory effects of two types of food additives on biofilm formation by foodborne pathogens. *Microbiol. Open.* 8:e853. doi: 10.1002/mbo3.853
- Liu, W., Dong, D., Yang, Z., Zou, D., Chen, Z., Yuan, J., et al. (2015). Polymerase Spiral Reaction (PSR): a novel isothermal nucleic acid amplification method. *Sci. Rep.* 5:12723. doi: 10.1038/srep12723
- Magruder, M., Edusei, E., Zhang, L., Albakry, S., Satlin, M. J., et al. (2020). Gut commensal microbiota and decreased risk for *Enterobacteriaceae* bacteriuria and urinary tract infection. *Gut Microbes.* 12:1805281. doi: 10.1080/19490976.2020.1805281
- Miao, J., Chen, L., Wang, J., Wang, W., Chen, D., Li, L., et al. (2017a). Current methodologies on genotyping for nosocomial pathogen methicillin-resistant *Staphylococcus aureus* (MRSA). *Microb. Pathog.* 107, 17–28. doi: 10.1016/j.micpath.2017.03.010
- Miao, J., Chen, L., Wang, J., Wang, W., Chen, D., Li, L., et al. (2017b). Evaluation and application of molecular genotyping on nosocomial pathogen-methicillin-resistant *Staphylococcus aureus* isolates in Guangzhou representative of Southern China. *Microb. Pathog.* 107, 397–403. doi: 10.1016/j.micpath.2017.04.016
- Miao, J., Liang, Y., Chen, L., Wang, W., Wang, J., Li, B., et al. (2017c). Formation and development of *Staphylococcus* biofilm: with focus on food safety. *J. Food Saf.* 7:e12358. doi: 10.1111/jfs.12358
- Miao, J., Peters, B. M., Li, L., Li, B., Zhao, X., Xu, Z., et al. (2016). Evaluation of ERIC-PCR for fingerprinting methicillin-resistant *Staphylococcus aureus* strains. *Basic Clin. Pharmacol. Toxicol.* 118:33.
- Miao, J., Wang, W., Xu, W., Su, J., Li, L., Li, B., et al. (2018). The fingerprint mapping and genotyping systems application on methicillin-resistant *Staphylococcus aureus*. *Microb. Pathog.* 125, 246–251. doi: 10.1016/j.micpath.2018.09.031
- Olaoye, O. A., Onilude, A. A., and Dodd, C. E. R. (2008). Identification of *Pediococcus* spp. from beef and evaluation of their lactic acid production in varying concentrations of different carbon sources. *Adv. Nat. Appl. Sci.* 2, 197–207.
- Paalanne, N., Husso, A., Salo, J., Pieviläinen, O., Tejesviet, M. V., et al. (2018). Intestinal microbiome as a risk factor for urinary tract infections in children. *Eur. J. Clin. Microbiol. Infect. Dis.* 37, 1881–1891. doi: 10.1007/s10096-018-3322-7
- Ramamurthy, T., Ghosh, A., Pazhani, G. P., and Shinoda, S. (2014). Current perspectives on Viable but Non-Culturable (VBNC) pathogenic bacteria. *Front. Publ. Health.* 2:103. doi: 10.3389/fpubh.2014.00103
- Salminen, S., Wright, A. V., and Ouweland, A. (2004). *Lactic Acid Bacteria Microbiological and Functional Aspects, 3rd Edn., Revised and Expanded*. New York, NY: Marcel Dekker. doi: 10.1201/9780824752033
- Singh, V. K., Mangalam, A. K., Dwivedi, S., and Naik, S. (2018). Primer Premier: program for design of degenerate primers from a protein sequence. *Biotechniques* 24, 318–319. doi: 10.2144/98242pf02
- Stapleton, A. E. (2017). “The vaginal microbiota and urinary tract infection,” in *Urinary Tract Infections*, eds M. A. Mulvey, D. J. Klumpp, and A. E. Stapleton (Washington, DC: American Society for Microbiology). doi: 10.1128/9781555817404.ch5
- Truchado, P., Gil, M. I., Larrosa, M., and Allende, A. (2020). Detection and quantification methods for Viable but Non-culturable (VBNC) cells in process wash water of fresh-cut produce: industrial validation. *Front. Microbiol.* 11:673. doi: 10.3389/fmicb.2020.00673
- Wang, L., Zhao, X., Chu, J., Li, Y., Li, Y., Li, C., et al. (2011). Application of an improved loop-mediated isothermal amplification detection of *Vibrio parahaemolyticus* from various seafood samples. *Afr. J. Microbiol. Res.* 5, 5765–5771. doi: 10.5897/AJMR11.1237
- Wen, S., Feng, D., Chen, D., Yang, L., and Xu, Z. (2020). Molecular epidemiology and evolution of *Haemophilus influenzae*. *Infect. Genet. Evolut.* 80:104205. doi: 10.1016/j.meegid.2020.104205
- Whiteside, S. A., Razvi, H., Dave, S., Reid, G., and Burton, J. P. (2015). The microbiome of the urinary tract—a role beyond infection. *Nat. Rev. Urol.* 12, 81–90. doi: 10.1038/nrurol.2014.361
- Xie, J., Peters, B. M., Li, B., Li, L., Yu, G., Xu, Z., et al. (2017a). Clinical features and antimicrobial resistance profiles of important *Enterobacteriaceae* pathogens in Guangzhou representative of Southern China, 2001–2015. *Microb. Pathog.* 107, 206–211. doi: 10.1016/j.micpath.2017.03.038
- Xie, J., Yang, L., Peters, B. M., Chen, L., Chen, D., Li, B., et al. (2017b). A 16-year retrospective surveillance report on the pathogenic features and antimicrobial susceptibility of *Pseudomonas aeruginosa* isolated from Guangzhou representative of Southern China. *Microb. Pathog.* 110:37–41. doi: 10.1016/j.micpath.2017.06.018
- Xu, G., Hu, L., Zhong, H., Wang, H., Yusa, S., Weiss, T. C., et al. (2012a). Cross priming amplification: mechanism and optimization for isothermal DNA amplification. *Sci. Rep.* 2:246. doi: 10.1038/srep00246

- Xu, W., Gao, J., Zheng, H., Yuan, C., Hou, J., Zhang, L., et al. (2019). Establishment and application of polymerase spiral reaction amplification for salmonella detection in food. *J. Microbiol. Biotechnol.* 29, 1543–1552. doi: 10.4014/jmb.1906.06027
- Xu, Z., Gui, Z., Li, L., Li, B., Su, J., Zhao, X., et al. (2012b). Expression and purification of gp41-gp36 fusion protein and application in serological screening assay of HIV-1 and HIV-2. *Afr. J. Microbiol. Res.* 6, 6295–6299. doi: 10.5897/AJMR12.1075
- Xu, Z., Hou, Y., Peters, B. M., Chen, D., Li, B., and Li, L. (2016b). Chromogenic media for MRSA diagnostics. *Mol. Biol. Rep.* 43, 1205–1212. doi: 10.1007/s11033-016-4062-3
- Xu, Z., Hou, Y., Qin, D., Liu, X., Li, B., Li, L., et al. (2016a). Evaluation of current methodologies for rapid identification of methicillin-resistant *Staphylococcus aureus* strains. *Basic Clin. Pharmacol. Toxicol.* 118:33.
- Xu, Z., Li, L., Alam, M. J., Li, L., and Yamasaki, S. (2008a). Integron-bearing methicillin-resistant coagulase-negative *Staphylococci* in South China, 2001–2004. *FEMS Microbiol. Lett.* 278, 223–230. doi: 10.1111/j.1574-6968.2007.00994.x
- Xu, Z., Li, L., Alam, M. J., Zhang, L., Yamasaki, S., and Shi, L. (2008b). First confirmation of integron-bearing methicillin-resistant *Staphylococcus aureus*. *Curr. Microbiol.* 57, 264–268. doi: 10.1007/s00284-008-9187-8
- Xu, Z., Li, L., Chu, J., Peters, B. M., Harris, M. L., Li, B., et al. (2012c). Development and application of loop-mediated isothermal amplification assays on rapid detection of various types of *Staphylococci* strains. *Food Res. Int.* 47, 166–173. doi: 10.1016/j.foodres.2011.04.042
- Xu, Z., Li, L., Shi, L., and Shirliff, M. E. (2011a). Class 1 integron in staphylococci. *Mol. Biol. Rep.* 38, 5261–5279. doi: 10.1007/s11033-011-0676-7
- Xu, Z., Li, L., Shirliff, M. E., Alam, M. J., Yamasaki, S., and Shi, L. (2009). Occurrence and characteristics of class 1 and 2 integrons in *Pseudomonas aeruginosa* isolates from patients in Southern China. *J. Clin. Microbiol.* 47, 230–234. doi: 10.1128/JCM.02027-08
- Xu, Z., Li, L., Shirliff, M. E., Peters, B. M., Li, B., and Peng, Y. (2011b). Resistance class 1 integron in clinical methicillin-resistant *Staphylococcus aureus* strains in southern China, 2001–2006. *Clin. Microbiol. Infect.* 17, 714–718. doi: 10.1111/j.1469-0691.2010.03379.x
- Xu, Z., Li, L., Shirliff, M. E., Peters, B. M., Peng, Y., et al. (2010). First report of class 2 integron in clinical *Enterococcus faecalis* and class 1 integron in *Enterococcus faecium* in South China. *Diagn. Microbiol. Infect. Dis.* 68, 315–317. doi: 10.1016/j.diagmicrobio.2010.05.014
- Xu, Z., Li, L., Zhao, X., Chu, J., Li, B., Shi, L., et al. (2011c). Development and application of a novel multiplex polymerase chain reaction (PCR) assay for rapid detection of various types of *Staphylococci* strains. *Afr. J. Microbiol. Res.* 5, 1869–1873. doi: 10.5897/AJMR11.437
- Xu, Z., Liang, Y., Lin, S., Chen, D., Li, B., Li, L., et al. (2016c). Crystal violet and XTT assays on *Staphylococcus aureus* biofilm quantification. *Curr. Microbiol.* 73, 474–482. doi: 10.1007/s00284-016-1081-1
- Xu, Z., Shi, L., Zhang, C., Zhang, L., Li, X., Cao, Y., et al. (2007). Nosocomial infection caused by class 1 integron-carrying *Staphylococcus aureus* in a hospital in South China. *Clin. Microbiol. Infect.* 13, 980–984. doi: 10.1111/j.1469-0691.2007.01782.x
- Xu, Z., Xie, J., Peters, B. M., Li, B., Li, L., Yu, G., et al. (2017a). Longitudinal surveillance on antibiogram of important gram-positive pathogens in Southern China, 2001 to 2015. *Microb. Pathog.* 103, 80–86. doi: 10.1016/j.micpath.2016.11.013
- Xu, Z., Xie, J., Yang, L., Chen, D., Peters, B. M., and Shirliff, M. E. (2018). Complete sequence of pCY-CTX, a plasmid carrying a phage-like region and ISEcp1-mediated Tn2 element from *Enterobacter cloacae*. *Microb. Drug Resist.* 24, 307–313. doi: 10.1089/mdr.2017.0146
- Xu, Z., Xu, X., Yang, L., Li, B., Li, L., Li, X., et al. (2017b). Effect of aminoglycosides on the pathogenic characteristics of microbiology. *Microb. Pathog.* 113, 357–364. doi: 10.1016/j.micpath.2017.08.053
- You, R., Gui, Z., Xu, Z., Shirliff, M. E., Yu, G., Zhao, X., et al. (2012). Methicillin-resistance *Staphylococcus aureus* detection by an improved rapid PCR assay. *Afr. J. Microbiol. Res.* 6, 7131–7133. doi: 10.5897/AJMR12.708
- Zhang, J., Biao, D. I., Shan, H., Liu, J., Zhou, Y., Chen, H., et al. (2019). Rapid detection of *Bacillus cereus* using cross-priming amplification. *J. Food Prot.* 82, 1744–1750. doi: 10.4315/0362-028X.JFP-19-156
- Zhao, L., Lv, X., Cao, X., Zhang, J., Gu, X., Zeng, X., et al. (2020). Improved quantitative detection of VBNC *Vibrio parahaemolyticus* using immunomagnetic separation and PMAxx-qPCR. *Food Control.* 110:106962. doi: 10.1016/j.foodcont.2019.106962
- Zhao, X., Li, M., and Xu, Z. (2018a). Detection of foodborne pathogens by surface enhanced raman spectroscopy. *Front. Microbiol.* 9:1236. doi: 10.3389/fmicb.2018.01236
- Zhao, X., Yu, Z., and Xu, Z. (2018b). Study the features of 57 confirmed CRISPR loci in 38 strains of *Staphylococcus aureus*. *Front. Microbiol.* 9:1591. doi: 10.3389/fmicb.2018.01591
- Zheng, F., Li, S., Wang, S., Feng, T., Jiang, Z., and Pan, J. (2020). Cross-priming isothermal amplification combined with nucleic acid test strips for detection of meat species. *Anal. Biochem.* 597:113572. doi: 10.1016/j.ab.2020.113672
- Zhong, J., and Zhao, X. (2018). Detection of viable but non-culturable *Escherichia coli* O157:H7 by PCR in combination with propidium monoazide. *3 Biotech.* 8:28. doi: 10.1007/s13205-017-1052-7
- Zhong, N., Gui, Z., Liu, X., Jiangrong, H., and K., Gao, X., et al. (2013). Solvent-free enzymatic synthesis of 1, 3-diacylglycerols by direct esterification of glycerol with saturated fatty acids. *Lipids Health Dis.* 12:65. doi: 10.1186/1476-511X-12-65
- Zhong, Q., Tian, J., Wang, B., and Wang, L. (2016). PMA based real-time fluorescent LAMP for detection of *Vibrio parahaemolyticus* in viable but nonculturable state. *Food Control.* 63, 230–238. doi: 10.1016/j.foodcont.2015.11.043

Conflict of Interest: The authors declare that the research was conducted in the absence of any commercial or financial relationships that could be construed as a potential conflict of interest.

Copyright © 2021 Guan, Wang, Zeng, Ye, Chen and Huang. This is an open-access article distributed under the terms of the Creative Commons Attribution License (CC BY). The use, distribution or reproduction in other forums is permitted, provided the original author(s) and the copyright owner(s) are credited and that the original publication in this journal is cited, in accordance with accepted academic practice. No use, distribution or reproduction is permitted which does not comply with these terms.

Advantages of publishing in Frontiers



OPEN ACCESS

Articles are free to read
for greatest visibility
and readership



FAST PUBLICATION

Around 90 days
from submission
to decision



HIGH QUALITY PEER-REVIEW

Rigorous, collaborative,
and constructive
peer-review



TRANSPARENT PEER-REVIEW

Editors and reviewers
acknowledged by name
on published articles

Frontiers

Avenue du Tribunal-Fédéral 34
1005 Lausanne | Switzerland

Visit us: www.frontiersin.org

Contact us: frontiersin.org/about/contact



REPRODUCIBILITY OF RESEARCH

Support open data
and methods to enhance
research reproducibility



DIGITAL PUBLISHING

Articles designed
for optimal readership
across devices



FOLLOW US

@frontiersin



IMPACT METRICS

Advanced article metrics
track visibility across
digital media



EXTENSIVE PROMOTION

Marketing
and promotion
of impactful research



LOOP RESEARCH NETWORK

Our network
increases your
article's readership